International Journal of Hygiene and Environmental Health 238 (2021) 113826

Contents lists available at ScienceDirect

International Journal of Hygiene and Environmental Health

journal homepage: www.elsevier.com/locate/ijheh

A human biomonitoring (HBM) Global Registry Framework: Further advancement of HBM research following the FAIR principles

Maryam Zare Jeddi [a,*], Ana Virgolino [b], Peter Fantke [c], Nancy B. Hopf [d], Karen S. Galea [e], Sylvie Remy [f], Susana Viegas [g,h,i], Vicente Mustieles [j,k], Mariana F. Fernandez [j,k], Natalie von Goetz [l], Joana Lobo Vicente [m], Jaroslav Slobodnik [n], Loïc Rambaud [o], Sébastien Denys [o], Annie St-Amand [p], Shoji F. Nakayama [q], Tiina Santonen [r], Robert Barouki [s], Robert Pasanen-Kase [t], Hans G.J. Mol [u], Theo Vermeire [a], Kate Jones [v], Maria João Silva [w,x], Henriqueta Louro [w,x], Hilko van der Voet [y], Radu-Corneliu Duca [z,aa], Hans Verhagen [ab,ac], Cristina Canova [ad], Jacob van Klaveren [a], Marike Kolossa-Gehring [ae], Jos Bessems [f]

[a] National Institute for Public Health and the Environment (RIVM), Bilthoven, The Netherlands
[b] Environmental Health Behaviour Lab, Instituto de Saúde Ambiental, Faculdade de Medicina da Universidade de Lisboa, Lisboa, Portugal
[c] Quantitative Sustainability Assessment, Department of Technology, Management and Economics, Technical University of Denmark, Produktionstorvet 424, 2800, Kgs. Lyngby, Denmark
[d] Center for Primary Care and Public Health (Unisanté), University of Lausanne, Lausanne, Epalinges, Switzerland
[e] IOM - Institute of Occupational Medicine, Edinburgh, EH14 4AP, UK
[f] VITO - Flemish Institute for Technological Research, Health Unit, Mol, Belgium
[g] NOVA National School of Public Health, Public Health Research Centre, Universidade NOVA de Lisboa, 1600–560, Lisbon, Portugal
[h] Comprehensive Health Research Center (CHRC), 1169–056, Lisbon, Portugal
[i] H&TRC—Health & Technology Research Center, ESTeSL—Escola Superior de Tecnologia da Saúde, Instituto Politécnico de Lisboa, 1500–310, Lisboa, Portugal
[j] University of Granada, Center for Biomedical Research (CIBM), Granada, Spain
[k] Consortium for Biomedical Research in Epidemiology & Public Health (CIBERESP), Madrid, Spain
[l] Federal Office of Public Health, Bern, Switzerland
[m] EEA - European Environment Agency, Kongens Nytorv 6, 1050, Copenhagen K, Denmark
[n] NORMAN Association, Rue Jacques Taffanel – Parc Technologique ALATA, 60550 Verneuil-en-Halatte, France
[o] SPF - Santé Publique France, Environmental and Occupational Health Division, France
[p] Environmental Health Science and Research Bureau, Health Canada, Ottawa, Ontario, Canada
[q] Japan Environment and Children's Study Programme Office, National Institute for Environmental Studies, Japan
[r] FIOH—Finnish Institute of Occupational Health, P.O. Box 40, FI-00032, Työterveyslaitos, Finland
[s] Université de Paris, Inserm Unit 1124, 45 rue des Saints Pères, 75006, Paris, France
[t] SECO - State Secretariat for Economic Affairs, Labour Directorate Section Chemicals and Work (ABCH), Switzerland
[u] Wageningen Food Safety Research (WFSR) – part of Wageningen University & Research, Wageningen, The Netherlands
[v] HSE - Health and Safety Executive, Harpur Hill, Buxton, SK17 9JN, UK
[w] INSA - National Institute of Health Dr. Ricardo Jorge, Portugal
[x] TOXOMICS - Centre for Toxicogenomics and Human Health, NOVA Medical School, Universidade NOVA de Lisboa, Portugal
[y] Wageningen University & Research, Biometris, Wageningen, the Netherlands
[z] Unit Environmental Hygiene and Human Biological Monitoring, Department of Health Protection, National Health Laboratory, Dudelange, Luxembourg
[aa] Centre Environment and Health, Department of Public Health and Primary Care, KU Leuven, Belgium
[ab] University of Ulster, Coleraine, Northern Ireland, UK
[ac] Technical University of Denmark, Lyngby, Denmark
[ad] Unit of Biostatistics, Epidemiology, and Public Health—University of Padua, Padua, Italy
[ae] UBA – German Environment Agency, Berlin, Germany

ARTICLE INFO

Keywords:
Human biomonitoring
Regulatory risk assessment

ABSTRACT

Data generated by the rapidly evolving human biomonitoring (HBM) programmes are providing invaluable opportunities to support and advance regulatory risk assessment and management of chemicals in occupational and environmental health domains. However, heterogeneity across studies, in terms of design, terminology,

* Corresponding author.
E-mail address: maryam.zare.jeddi@rivm.nl (M. Zare Jeddi).

https://doi.org/10.1016/j.ijheh.2021.113826
Received 7 January 2021; Received in revised form 30 July 2021; Accepted 6 August 2021
Available online 25 September 2021

Data value chain
Data governance
Harmonisation
Registry

biomarker nomenclature, and data formats, limits our capacity to compare and integrate data sets retrospectively (reuse). Registration of HBM studies is common for clinical trials; however, the study designs and resulting data collections cannot be traced easily. We argue that an HBM Global Registry Framework (HBM GRF) could be the solution to several of challenges hampering the (re)use of HBM (meta)data. The aim is to develop a global, host-independent HBM registry framework based on the use of harmonised open-access protocol templates from designing, undertaking of an HBM study to the use and possible reuse of the resulting HBM (meta)data. This framework should apply FAIR (Findable, Accessible, Interoperable and Reusable) principles as a core data management strategy to enable the (re)use of HBM (meta)data to its full potential through the data value chain. Moreover, we believe that implementation of FAIR principles is a fundamental enabler for digital transformation within environmental health.

The HBM GRF would encompass internationally harmonised and agreed open access templates for HBM study protocols, structured web-based functionalities to deposit, find, and access harmonised protocols of HBM studies. Registration of HBM studies using the HBM GRF is anticipated to increase FAIRness of the resulting (meta)data. It is also considered that harmonisation of existing data sets could be performed retrospectively. As a consequence, data wrangling activities to make data ready for analysis will be minimised. In addition, this framework would enable the HBM (inter)national community to trace new HBM studies already in the planning phase and their results once finalised. The HBM GRF could also serve as a platform enhancing communication between scientists, risk assessors, and risk managers/policy makers. The planned European Partnership for the Assessment of Risk from Chemicals (PARC) work along these lines, based on the experience obtained in previous joint European initiatives. Therefore, PARC could very well bring a first demonstration of first essential functionalities within the development of the HBM GRF.

1. Introduction

Human biomonitoring (HBM) is defined as the method for assessing human exposure to chemicals or their effects by measuring chemicals, their metabolites or reaction products (and/or their effects biomarkers) in human specimens (WHO, 2015a). HBM is a valuable tool to support the environment and health policy-making process because it provides quantitative actual distribution of exposures in a population. Environmental pollutants can then be mapped for emerging pollutants, as well as data regarding their resulting health effects, and/or population susceptibility.

HBM has a long history serving health surveys with well-known national programs such as the German Environmental Surveys (GerES), the US National Health and Nutrition Examination Survey (NHANES), the Canadian Health Measures Survey (CHMS), and the Korean National Environmental Health Survey (KoNEHS). (Becker et al., 2003; Choi et al., 2017; Cox, 1992; Haines et al., 2017). However, only recently HBM has become more widely used in risk assessment and management frameworks. HBM is considered the "gold standard" for assessing people's exposure to environmental chemical agents (Sexton et al., 2004). The increased availability of exposure and effect biomarkers is helping HBM to become an even more valuable tool to investigate associations between internal exposures and health outcomes. This approach presents well-known complementary information on and advantages over cell-based and experimental animal studies (Burns et al., 2019; Mustieles and Fernández, 2020). In the current article, we define HBM studies as "all observational studies that apply HBM as a tool to collect data" (WHO, 2015a). These might include studies where the main scope is a health survey, health surveillance, as well as biomonitoring programmes in both general and occupational populations.

HBM research in combination with results from human and/or animal toxicological studies, for example in the form of hypothesized Adverse Outcome Pathway (AOP) networks or the use of biomonitoring equivalents, can provide interpretation tools for human hazard and risk assessment (Baken et al., 2019; Faure et al., 2020; Mustieles et al., 2020; St-Amand et al., 2014; Zare Jeddi et al., 2020). Moreover, HBM provides a holistic perspective, enabling an integrative measurement of combined exposures from all routes (ingestion, inhalation, and dermal uptake) and all environmental sources (air, water, soil, dust, food), the results of toxicokinetic processes and individual differences in combination with signs of (early) responses with effect biomarkers (Mustieles et al., 2020; Zare Jeddi et al., 2020). If combined with health surveys and cohorts, HBM (meta)data can also provide opportunities to investigate the relationship between internal exposure and health effects, promote risk-reduction measures, monitor exposure trends, and evaluate the effectiveness of implemented national and global policies (e.g., (Eykelbosh et al., 2018; Romano et al., 2020)). Overall, the use of HBM (meta) data increases the value of exposure information in risk assessment and management context (Wilhelm, 2020).

Given the multiple benefits of using HBM at national and global levels, the use of HBM is a recognized priority in chemical safety. HBM can increase the robustness of regulatory long-term decisions for marketed chemicals, and in particular, the increased importance of mixture risk assessment of chemicals and grouping approaches, as echoed at national, supranational, and intergovernmental level such as UN, WHO, OECD and EU (EC, 2020a; OECD, 2018; SAICM, 2013; WHO, 2015b). To serve this role, methodologies should be harmonised and HBM (meta) data should be easily findable, accessible, interoperable, secure, shared and reused by default (EC, 2020a).

Regrettably, HBM has received little regulatory application to date which is partly due to a lack of sufficient, reliable, quality-assured, and well-structured (meta)data. HBM is an important and useful tool, yet quite complicated in terms of its design, application, and interpretation. The existing legislative frameworks on chemicals do not currently provide clear harmonised guidance for developing a comprehensive and integrated assessment of (combined) internal exposures to chemicals from different sources and routes. Any available guidance has evolved separately in different regulatory frameworks (Bopp et al., 2018; Drakvik et al., 2020; Evans et al., 2016; Fantke et al., 2020a; Louro et al., 2019).

This article aims to describe the challenges and needs to drastically increase the use and possible reuse of HBM data. It describes requirements to make HBM study information (metadata as wells as measurement data) more FAIR (Findable, Accessible, Interoperable, and Reusable) (Wilkinson et al., 2016). In this article, these four principles are grouped in the coupled cornerstones of findability/accessibility and interoperability/reusability. Findability/accessibility is a system to store HBM (meta)data. Interoperability/reusability is how the (meta)data themselves should be expressed (and stored in HBM data repositories). For both cornerstones, harmonisation is critical. Harmonisation of storage systems for HBM (meta)data helps to find and better access HBM (meta)data (better findability and quicker access) where harmonisation of the HBM (meta)data generation itself enables reuse and interoperability. This article attempts to scrutinise whether a framework for harmonised, web-based HBM study registries, as so called HBM Global

Registry Framework (HBM GRF), could accommodate existing needs.

2. Harmonisation and FAIRification of HBM studies, needs, challenges and opportunities

Systematic harmonisation and FAIRification of HBM (meta)data production through the data value chain can improve all aspects of HBM. First, results from several HBM studies could be compared easier to delineate e.g., exposure patterns. This refers to challenges for instance regarding differences in the definition of age groups (teenagers e.g., 10–18 years old or 13–19 years old), lifestyle parameters measured, biological matrices used, and of sampling methods, storage conditions as well as analytical procedures (Ågerstrand et al., 2018; Bocato et al., 2019; Joas et al., 2012). Moreover, the metadata including information about the studies are not always readily available. Even when such data are accessible, data are often scattered and/or incomplete thereby undermining the proper understanding, interpretation, and final use of the HBM data collected to support chemical risk assessment. Second, it could facilitate performing combined (meta)analyses of data from different HBM studies, aiming for increased statistical power, to find e.g., correlations between exposure biomarkers and effect biomarkers to support exposure to outcome assessments (Boyden and Walnicki, 2021). The use of systematic reviews and (meta)analyses is gaining acceptance in exposure science to transparently synthesize and evaluate a body of scientific evidence to answer research or policy questions (Hubal, 2019; Wikoff et al., 2020; Wolffe et al., 2019). Nevertheless, handling and comparing heterogeneous data generated across multiple scientific disciplines is challenging. This is especially true when a high degree of variability across studies is expected in terms of study aims and designs, population characteristics, exposure assessment procedures, data analysis and reporting (Burns et al., 2019; Goodman et al., 2019; Hubal, 2019). Third, it would also enable data sharing and data integration which are of particular relevance for decision making in environmental and occupational health policies (Kromerová and Bencko, 2019; Louro et al., 2019). It is clear that there is an increasing use purpose for HBM data in compliance to the FAIR (Findable, Accessible, Interoperable, Reusable) data principles.

Currently, the abovementioned opportunities are unfortunately hindered by problems with data comparability due to lack of harmonisation. Based on a survey regarding national practices in risk assessment and risk assessors' views on HBM use in Europe (Louro et al., 2019), the European Human Biomonitoring Initiative HBM4EU[1] recognized that regulatory practices related to HBM still vary across different countries. HBM data should be collected using harmonised study protocols to a significant extent to facilitate data interpretation (Fiddicke et al., 2021). In addition, the need for harmonised coding of substances and metabolites measured and the statistical analysis such as aggregation of individual data to percentiles of a distribution of HBM levels has received particular attention under recent HBM research projects. Harmonised study designs and structured study registries could counter these problems.

The HBM community would profit from global sharing of information of existing, new, and planned HBM studies. The authors envisage that any registry system should be globally useable and legislative framework independent, be it national legislation such as in the USA, Canada, Japan, Korea, Germany, France, or regional legislations in the EU or a framework like the OECD. Given that, we hereby present the concept for a web-based system based on modern IT-technology and independent of any website host requirements as part of an overarching HBM GRF.

The HBM GRF would facilitate and promote prospective (a priori) harmonisation of HBM study designs and thus the resulting HBM data would follow the FAIR data principals. As a consequence, data wrangling activities to make data ready for analysis will be minimised. Therefore, prospective (a priori) harmonisation of foreseen or already planned HBM studies is recommended rather than focusing on retrospective (post-hoc) harmonisation. The prospective (a priori) harmonisation leads to a higher degree of data homogeneity in an effective way. It should be noted that aligning in terms of harmonisation is essential but is different from standardization. HBM is not science in the sense of duplicating experiments based on standardised methods. It is a tool for field studies where some parts obviously could be standardised in the future, such as analytical chemical methods while the process of defining study population and the sampling process can be harmonised but not standardised. The HBM GRF should facilitate a step-by-step harmonisation process but not necessarily standardization using a scientifically and technically sound and viable system. Fig. 1 provides a general overview of the HBM GRF concepts and potentials.

3. Existing initiatives towards verification of HBM data

Comparability and combination of results and interoperability of data are often difficult due to a lack of harmonisation, even when different HBM studies have investigated similar research questions (Joas et al., 2012; Lermen et al., 2020). In the last 10–15 years, significant efforts have been made towards harmonising HBM studies prospectively such as in the European Commission funded projects COPHES, DEMO-COPHES and HBM4EU (Ganzleben et al., 2017) as well as the European Cooperation in Science and Technology (COST) Action DiMoPEx (DiMoPEx, 2015). Codebooks were developed for both the HBM exposure data as well as accompanying variables important for interpretation (age, sex, gender, NUTS [Nomenclature of Territorial Units for Statistics] codes, season of sampling, etc.) in a harmonised structure and format. Statistical analysis protocols scripted in R were used to extract comparable and machine-readable summary statistics or "aggregated data" that can be compared across data collections of the HBM4EU aligned studies and also across existing studies that share similarities in design. This has allowed the development of an interactive dashboard to display the data of the HBM4EU project (https://www.hbm4eu.eu/eu-hbm-dashboard/). Work on occupational exposure under the HBM4EU project is also directed to harmonise methodologies and data collection by developing standard operating procedures (SOPs), that can be used in multiple countries and analysed in an integrative approach (Santonen et al., 2019).

Registries containing some (meta)data on HBM studies or studies containing an HBM part exist such as the WHO International Clinical Trials Registry Platform[2], the US Clinical Trials database[3]. In addition, registries exist in which planned work is registered before the execution of the study. PROSPERO[4] is an example of such an international database of prospectively registered systematic reviews with a health-related outcome. Others such as the EU Clinical Trials Register[5], already contains human intervention studies.

Moreover, there are several initiatives as listed in Table 1 regarding data collections containing mainly environmental monitoring and external exposure monitoring data. The Information Platform for Chemical Monitoring (IPCHEM[6]), the NORMAN network[7], the Elixir community (ELIXIR, 2017), the BBMRI-ERIC[8] and the Hazchem@work for occupational exposure data have been created to tackle the lack of harmonised information (EU, 2016). Most of these portals have their own challenges, some of which are highlighted in Table 1. In addition,

[1] https://www.hbm4eu.eu/.

[2] https://www.who.int/clinical-trials-registry-platform.
[3] https://clinicaltrials.gov/.
[4] https://www.crd.york.ac.uk/prospero/.
[5] https://www.clinicaltrialsregister.eu/.
[6] https://ipchem.jrc.ec.europa.eu/.
[7] https://www.norman-network.net.
[8] https://www.bbmri-eric.eu.

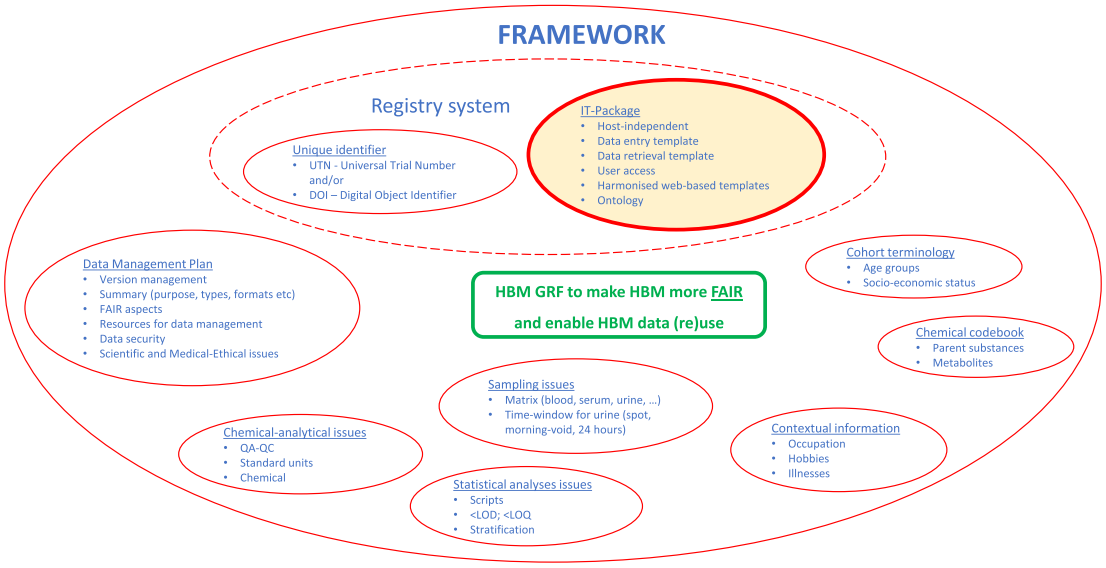

Fig. 1. HBM Global Registry Framework (HBM GRF).

there are many health surveys and HBM studies at national, regional and/or international levels which are not typically integrated into these platforms despite their potential for enhancing informed decision making in environment, public and occupational health.

IPCHEM was established by the European Commission (EC) to support a coordinated approach for collecting, storing, sharing, and assessing data on the occurrence of chemicals and chemical mixtures in humans and the environment. It is structured in four thematic modules: 'environmental monitoring', 'human biomonitoring', 'food and feed' and 'products and indoor air.' IPCHEM is designed to specifically provide access to chemical monitoring data and underlying (meta)data currently not readily accessible, making them findable and accessible and to a certain extent interoperable and reusable (Comero et al., 2020; Knetsch and Ruether, 2016; Wilkinson et al., 2016). IPCHEM is intended to assist scientists and risk managers/policy makers to discover and access chemical monitoring data on existing, new, emerging and less-investigated chemicals, covering a wide range of matrices and media (Comero et al., 2020). It is however not intended to register study designs ex ante. IPCHEM is the European Commission's reference access point for searching, accessing and retrieving chemical occurrence data collected and managed in Europe. IPCHEM is a distributed infrastructure. Data owners/data providers can decide on the level of detail to which the different IPCHEM user groups can access their data. As shown in Fig. 2, the volume of HBM datasets uploaded to the IPCHEM platform has increased by over 400% in the last two years. It includes now more than 100 (meta)data for HBM data collections gathered under the HBM4EU project (EC, 2020b).

The platform already includes particularly useful (meta)data, containing crucial information concerning study design, population size and age, sampling, analytics, and substances/biomarkers monitored, etc., amongst others. However, it is not able (yet) to quickly upload new data from data collections as the data collections themselves and the preceding study designs are lacking sufficient harmonisation. This limits easy and wider reuse and meta-analyses. There is for example currently not yet an optimal use of ontologies to facilitate linking different biomarker metabolites measured in different data collections but originating from the same parent substance to that parent substance.

4. Remaining challenges to be addressed by development of the HBM registry system under the HBM GRF

The current absence of harmonised study design templates makes searching HBM studies and their (meta)data cumbersome, and retrospective information validation processes time-consuming and often subject to errors. Data and metadata data harmonisation, at least from a retrospective point of view, requires access to a lot of information on each study including objectives, measured biomarkers and biological matrices, sampling methods, protocols, questionnaires, etc., which needs to be validated. Moreover, retrospective harmonisation processes are, to some extent, subjective processes and can thus present an inherent risk of biased (meta)data in a 'post-hoc harmonised' repository.

In addition, researchers typically provide the data, including the (meta)data, quite some time after study completion. This can be problematic as other researchers and regulatory risk assessors, providing scientific advice to risk managers/policy makers, are often looking for fast and user-friendly access to information as well as protocols regarding planned and ongoing studies. Early-on registration of the plan for an HBM study, even in draft form, would enable other researchers to prepare for (re)using the new data once available.

Another main issue is the lack of harmonisation in reporting of the chemical compounds investigated in HBM studies. Hundreds of non-endogenous compounds are found in HBM samples, some of them being known chemicals with a Chemical Abstract Services Registry Number (CAS RN), but many are unknown. Even known metabolites do not have CAS RNs as usually only the parent substance has been registered. Beyond this, even the use of a CAS RN for known compounds can be ambiguous (Williams and Yerin, 2013). Therefore, it is essential to harmonise how chemical compounds (parents and metabolites) are identified and findable (fulfil the FAIR criteria) in HBM studies. The InChI/InChIKey framework of IUPAC (IUPAC, 2018) is, to our knowledge, the only system for unique identification of chemical substances with a known structure (including stereochemistry). Ontologies based on fragmentation in molecular structure might help in linking metabolites to parent compounds.

Although several environmental exposure studies have been registered in existing platforms (e.g., Study number NCT03440307 in the US ClinicalTrials database[9]), these platforms currently lack the design to enhance and optimize the dialogue between the scientific disciplines of epidemiology, HBM, toxicology and risk assessment. Most of these platforms merely make HBM-related studies findable. The harmonisation of HBM would also be useful for prospective cohorts. Indeed,

[9] https://www.bbmri-eric.eu.

Table 1
Examples of existing platforms related to chemical monitoring data.

Platform	Coverage	Funding	Main aim(s)	Limitation(s)
IPCHEM (Information Platform for Chemical Monitoring) https://ipchem.jrc.ec.europa.eu/	Europe	EC	• Assisting policy makers and scientists to discover and access chemical monitoring data on chemicals covering a range of matrices and media (environment, food and feed, human biomonitoring, indoor air, and products) • Hosting data currently not readily accessible (e.g., outcomes of research projects, off-line stored monitoring data) • Providing chemical monitoring data and information of defined quality in terms of spatial, temporal, methodological and metrological traceability	• Differences in data quality • Differences in representativeness of populations[a] • Discrepancies in reporting formats (harmonised for the essential fields but leaving room for data collection specific fields) • Only occurrence data from targeted, quantitative analyses
Canada Open Government, 2020 Canadian Health Measures Survey (CHMS) Human Biomonitoring Data for Environmental Chemicals Health Canada, Ottawa, ON (2020) http://open.canada.ca/data/en/dataset/8cc88229-8132-4ccd-a3dd-b456579158c6	Canada	Canada government	• Present HBM results of the 5 cycles of the Canadian Health Measures Survey (2007–2017). • Tabulated CSV-downloadable results	• Metadata not directly available in the app
NORMAN Association https://www.norman-network.com/	Europe, North America, and Asia	Not for profit network; self-funded by its members	• Enhancing the exchange of information and collection of data on emerging environmental substances • Encouraging the validation and harmonisation of common measurement methods and monitoring tools • Ensuring that knowledge on emerging pollutants is maintained and developed by stimulating coordinated, interdisciplinary projects on problem-oriented research and knowledge transfer to address identified needs	• Focus only on environment • Absence of information regarding human data
BBMRI-ERIC (Biobanking and Biomolecular Resources Research Infrastructure) https://www.bbmri-eric.eu/	Europe	European Research Infrastructure Consortium funded by its members	• Collecting and making available information about biobanks throughout Europe that are willing to share their data and/or samples, and to collaborate with other research groups	• Only puts in contact people who search information on biobanks • Sample query processing missing
Elixir community https://elixir-europe.org/	Europe	National funding in each country (hubs)	Managing and safeguarding the increasing volume of data being generated by publicly funded life sciences research	• Currently mostly focussed on human endogenous compounds (DNA, proteins, small molecules)
HazChem@work https://www.certifico.com/sicurezza-lavoro/documenti-sicurezza/68-documenti-ue/3859-hazchem-work-project-to-estimate-occupational-exposure-chemicals	Europe	European Commission (DG Employment)	Create a database and developing a model to estimate the occupational exposure for a list of hazardous chemicals in EU countries and in the EFTA/EEA countries.	• Discontinued • Dedicated only to specific chemicals

EC-European Commission; EFTA - European Free Trade Association; EEA – European Economic Area.
[a] E.g., samples in one 'national' HBM cohort might be taken in 50 different locations in that country where another cohort in the same country might be taken at only 10 different locations.

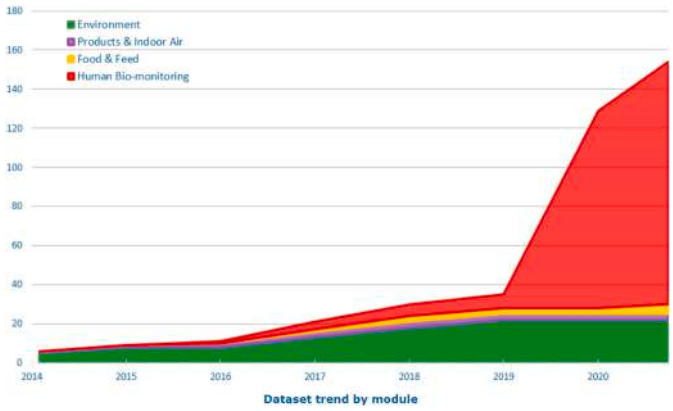

Fig. 2. Time trend of monitoring data included in IPCHEM.

the proposed HBM GRF should promote a dialogue between organisers of HBM surveys and cohort studies since cohort data add a longitudinal component to better investigate exposure-effect-outcome relationships. Beyond this, a dialogue with the fields of toxicology and risk assessment must also be fostered. Toxicological data, preferably organized through AOPs (Adverse Outcome Pathways), help prioritise the most relevant effect biomarkers and adverse health outcomes to be investigated. Effect biomarkers are at the intersection of toxicology, epidemiology and HBM, and a more systematic use of effect biomarkers in HBM studies has been proposed (Zare Jeddi et al., 2020). Notwithstanding, given the complexity and diversity of effect biomarkers, a prospective harmonisation of the type of biological samples collected (e.g., blood, urine), their processing (e.g., whole blood with or without RNA preservation, DNA isolation, serum, plasma, red blood cells, white blood cells) and their storage and biobanking are crucial for an optimal evaluation.

Pourchet et al. (2020) in their recent publication on suspect and non-targeted screening of biomarkers in human matrices highlighted that harmonisation of quality assurance/quality control (QA/QC)

criteria and structure of reporting results appear necessary for better comparability of results produced by different laboratories (Pourchet et al., 2020). In addition, Galea et al. highlighted in their lessons learned from undertaking the HBM4EU chromates study that users must receive training and instruction to ensure that harmonised templates used to collect study data are populated correctly (Galea et al., 2021). A rigorous structure for reporting of screening-level monitoring data in environmental matrices is already incorporated in the NORMAN Database System in the EMPODAT (Environmental Monitoring of POllutants DATabase) module (Dulio et al., 2020) and the first prototype for structured collection of non-target and suspect screening data has been developed in its Digital Sample Freezing Platform module (DSFP (Alygizakis et al., 2019)). Another critical issue is how to deal with observations below the LOD (limit of determination) or LOQ (limit of quantification) in the statistical analyses and aggregation of the individual data. Obviously, these are issues that could be included in the harmonisation efforts as part of the HBM GRF.

In addition, policy support is not a strong component of existing platforms, which tend to function primarily as a repository of scientific information for researchers and not as an easily useable source of information for regulatory risk assessors, providing advice to risk managers/policy makers.

Existing platforms should be scrutinized for their strengths and weaknesses when developing the HBM GRF. Overall, user friendly web-based platforms would be key to facilitate further use of HBM (meta) data available or accessible via HBM GRF for regulatory risk assessment of chemicals and their mixtures.

5. Aim and objectives of the HBM Global Registry Framework (HBM GRF)

The aim of the HBM GRF is to make HBM research FAIR (Fig. 1). Only by doing so, the ethical imperative to make the most out of human volunteer data would be met.

Based on crucial needs, a series of underlying objectives can be defined that, when accomplished, will increase wider use of HBM (meta) data. An HBM GRF is expected to be able to contribute to the following objectives:

1. Creating an open-access web-based registry system that allows researchers to register HBM studies.
2. Improving data management infrastructure that will meet the FAIR principles by facilitating registrations of HBM studies. For example, assigning a unique reference ID for each study, which can be referred to in any research using data from that study. This would simplify the identification of studies generating new data or reusing data (original study).
3. Harmonising identifiers for chemical substances, including parent substances, metabolites, and effect biomarkers. Examples of effect biomarkers are hormones, specific DNA methylation, markers for gene expression of specific nuclear receptor, cholesterol, liver enzymes.
4. Facilitating multidisciplinary interaction among research scientists, regulatory risk assessors and risk managers/policy makers in the domain of HBM, epidemiology, toxicology, and risk assessment.

As an HBM GRF would benefit many stakeholders (national, EU, international), Table 2 summarises suggested intended audiences for the proposed HBM GRF including other regulatory frameworks and risk assessment processes, as well as for demonstrating regulatory efficacy (Louro et al., 2019). In addition, policy initiatives foreseen under the European Green Deal might benefit from an HBM GRF. A tabulated overview as prepared by the HBM4EU project indicates where HBM data could support directly and indirectly the European Green Deal (see Annex A, unpublished HBM4EU deliverable).

Table 2
Description of potential users and foreseen advantages of the HBM Global Registry Framework (HBM GRF).

Users/Regulatory Frameworks	More specific data/ information to be provided by the registries[a]	Advantages
HBM and epidemiological researchers/REACH[b], OSH[c], Food safety	Questionnaires; Informed consent templates; Sampling templates; Analytical methods, QC/QA; Guidelines for ethics, monitoring and reporting; Methods description; Harmonised Standard Operating Procedures (SOPs) describing some of the above; Statistical analysis plan; Biological sample processing and biobanking.	Harmonised approaches; Comparability of the data; Awareness of data requirements, Identification of gaps and needs for further research; Discovery of chemical analytical methods available; Use of HBM data for building and evaluating exposure models.
Exposure researchers and regulatory exposure assessors/ REACH, OSH, Food safety	Harmonised SOPs; Methods description; Guidelines for ethics, monitoring and reporting; Statistical analysis plan.	Harmonised approaches; Comparability of the data; Data available to support modelling; Awareness for data requirements; Support for defining new HBM campaigns/ programmes.
Regulatory risk assessors and competent authorities/REACH, OSH, Food safety	Access to planned HBM-related studies (measuring exposure as well as effect biomarkers) also pointing at contextual data of studies; HBM results might enable setting of HBM guidance and limit values.	Definition of priorities for RMMs (risk management measures) implementation; identification of new RMMs; Risk assessment options; Identification of needs for further regulatory actions to be supported by robust and available scientific knowledge.
Industry and trade associations/REACH and OSH	Access to planned HBM-related studies also pointing at contextual data of studies.	Definition of priorities for RMMs implementation; identification of new RMMs.

[a] The registries aimed at are not about results, but about the contextual data, and information on the study (sampling plan, study population, QC/QA, research hypotheses etc).
[b] EU Regulation on Registration, Evaluation and Authorisation of CHemicals.
[c] Occupational Safety and Health.

6. How to make the HBM Global Registry Framework (HBM GRF) happen?

In Europe there is an opportunity to bring the outlined concepts to fruition. In the coming years, the EU-wide research and innovation program PARC (Partnership for the Assessment of Risks from Chemicals) will run (see intermezzo overleaf). We think that this provides an excellent opportunity to investigate feasibility and options for development of such a registry framework. The current organisations involved in the preparation of the Partnership represent 28 EU and non-EU countries and include ministries (for research, health, and environment), national and EU agencies and research organisations as well as academia and research institutions. We believe that this broad set-up is very well suited and capable of developing further the HBM GRF as advocated by the authors of in this article from various parts of the world. The stimulus could very well come from Europe under PARC. Global input during the process could be processed through the international PARC Advisory Board. Global contributions where possible along the process would be essential to ensure worldwide use of the HBM GRF to enhance registration of new and ongoing HBM studies e.g.,

NHANES in the USA, the CHMS in Canada, KNEHS in Korea and JECS in Japan. Additionally, support from and cooperation with UN, WHO and OECD would help global implementation of this initiative.

PARC – Partnership for the Assessment of Risks from Chemicals

PARC is an EU-wide research and innovation programme that will run 2022–2028. The Partnership will promote harmonisation of data and exchange between different actors (scientific community, health agencies, regulators, policymakers etc.) and disciplines (e.g., exposure science, toxicology) to promote transparency, support risk assessment, and facilitate wider reuse of obtained data. To achieve this, it will build on existing data platforms included in or collaborating with the Partnership and contribute to extend their usability for risk assessors and managers. It will ensure data and associated information is FAIR and addresses the GDPR (EU General Data Protection Regulation) related challenges for data exchange. Important will be that all relevant EU Agencies can duly contribute to and access relevant PARC activities and outputs, and the most relevant European Commission Directorates General will be involved as well.

The Partnership will strive towards fostering European leadership at the international level for research and innovation in chemical risk assessment and will promote cooperation and collaboration across Europe and internationally. The Partnership will contribute to international fora, dealing with chemicals, pollution, and the SDGs (UN Sustainable Development Goals), such as the World Health Organisation (WHO) (e.g., International Programme on Chemical Safety IPCS Chemical Risk Assessment Network) and Strategic Approach to International Chemicals Management (SAICM), UN Environment Programme (UNEP) and OECD, dealing with chemicals, pollution, and the SDGs. Bilateral relations with major international risk assessment agencies (e.g., U. S. Environmental Protection Agency) and research institutions (e. g., U.S. National Toxicology Program) will also be envisaged. Member States are already contributing as single entity to many of these networks. Collaboration of MS in the Partnership will strengthen the influence of the EU in addressing global challenges associated with chemical risk assessment and place the EU as the front runner of the international community in this area.

Dialogue and collaboration with the international community is essential for mutual support and for the identification of needs and opportunities for harmonisation actions and development of tools that support the collaboration. Connecting this Partnership with the international community will foster the dissemination of results and will promote the importance of data and knowledge sharing among international networks. An international board consisting of experts from other international chemical risk assessment platforms, scientific advisory boards or scientific societies, or experts in related EU or international activities will contribute to ensuring the Partnership establishes links and dialogue with relevant international activities.

7. Summary and conclusion

Overall, we propose to develop an HBM Global Registry Framework (HBM GRF) aiming at harmonising the design and structuring the registration of HBM studies and by such, making the ultimate HBM (meta)data more FAIR (Findable, Accessible, Interoperable and Reusable). Consequently, this will improve the assessment, comparability and combination, reuse, and interpretation of HBM-study results. Preparing HBM study protocols would be facilitated with such a web-based system as they would be based on digitised and harmonised templates. This would result in harmonised data entries into registries.

The ultimate objective could be to make HBM (meta)data accessible in a virtual, federated, infrastructure, so that data with the right credentials become instantaneously accessible for human and machine interactions. Implementing the FAIR principles in the HBM domain could act as fundamental enabler for digital transformation in the environment and health domain.

HBM GRF would facilitate the process of data creation and use to its final use and reuse (the data value chain). This is expected to better channel knowledge on the internal exposure of chemicals (exposure biomarkers) and early warnings of effects (effects biomarkers) in human samples into regulatory risk assessment and risk management (Burns et al., 2019).

The HBM GRF would help to close the science to policy interface gap between scientific ambitions and regulatory and policy requirements resulting in an added value in protecting human health (Burns et al., 2019).This knowledge transfer is of particular relevance for the European Chemicals Sustainability Strategy, which needs more and better exposure data, as well as in the scope of international conventions aiming to protect human health from chemical exposures. Creating the HBM GRF as proposed here would advance exposure science and would ultimately support a better protection of citizen's health throughout the world (Fantke et al., 2020b).

Disclaimer

The contents, including any opinions and/or conclusions expressed of this manuscript, are those of the authors alone and do not necessarily reflect the opinions or policy of the organisations to which they are employed.

Acknowledgements

Stephanie Bopp (European Commission, DG Joint Research Centre) is acknowledged to provide valuable information regarding the IPCHEM Platform. The VITO HBM data management team is acknowledged for providing specific input. The HBM expert working group of the European Chapter of the International Society for Exposure Science (ISES Europe) is acknowledged for their great support.

Appendix A. Supplementary data

Supplementary data to this article can be found online at https://doi.org/10.1016/j.ijheh.2021.113826.

References

Ågerstrand, M., Christiansen, S., Hanberg, A., Rudén, C., Andersson, L., Andersen, S., Appelgren, H., Bjørge, C., Clausen, I.H., Eide, D.M., 2018. A call for action: improve reporting of research studies to increase the scientific basis for regulatory decision-making. J. Appl. Toxicol. 38, 783–785.

Alygizakis, N.A., Oswald, P., Thomaidis, N.S., Schymanski, E.L., Aalizadeh, R., Schulze, T., Oswaldova, M., Slobodnik, J., 2019. NORMAN digital sample freezing platform: a European virtual platform to exchange liquid chromatography high resolution-mass spectrometry data and screen suspects in "digitally frozen" environmental samples. Trac. Trends Anal. Chem. 115, 129–137.

Baken, K.A., Lambrechts, N., Remy, S., Mustieles, V., Rodríguez-Carrillo, A., Neophytou, C.M., Olea, N., Schoeters, G., 2019. A strategy to validate a selection of human effect biomarkers using adverse outcome pathways: proof of concept for phthalates and reproductive effects. Environ. Res. 175, 235–256.

Boyden J., and Walnicki D., Leveraging the Power of Longitudinal Data: Insights on Data Harmonisation and Linkage from Young Lives. (2021).

Becker, K., Schulz, C., Kaus, S., Seiwert, M., Seifert, B., 2003. German Environmental Survey 1998 (GerES III): environmental pollutants in the urine of the German population. Int. J. Hyg Environ. Health 206, 15–24.

Bocato, M.Z., Bianchi Ximenez, J.P., Hoffmann, C., Barbosa, F., 2019. An overview of the current progress, challenges, and prospects of human biomonitoring and exposome studies. J. Toxicol. Environ. Health, Part B 22, 131–156.

Bopp, S.K., Barouki, R., Brack, W., Dalla Costa, S., Dorne, J.-L.C., Drakvik, P.E., Faust, M., Karjalainen, T.K., Kephalopoulos, S., van Klaveren, J., 2018. Current EU research activities on combined exposure to multiple chemicals. Environ. Int. 120, 544–562.

Burns, C.J., LaKind, J.S., Mattison, D.R., Alcala, C.S., Branch, F., Castillo, J., Clark, A., Clougherty, J.E., Darney, S.P., Erickson, H., 2019. A matrix for bridging the epidemiology and risk assessment gap. Global Epidemiology 1, 100005.

Choi, W., Kim, S., Baek, Y.-W., Choi, K., Lee, K., Kim, S., Do Yu, S., Choi, K., 2017. Exposure to environmental chemicals among Korean adults-updates from the second Korean National Environmental Health Survey (2012–2014). Int. J. Hyg Environ. Health 220, 29–35.

Comero, S., Dalla Costa, S., Cusinato, A., Korytar, P., Kephalopoulos, S., Bopp, S., Gawlik, B.M., 2020. A conceptual data quality framework for IPCHEM–the European commission information platform of chemical monitoring. Trac. Trends Anal. Chem. 115879.

Cox, C.S., 1992. Plan and Operation of the NHANES I Epidemiologic Followup Study, 1987. US Department of Health and Human Services, Public Health Service, Centers.

DiMoPEx, 2015. Diagnosis, Monitoring and Prevention of Exposure Related Non-communicable Diseases, DiMoPEx (CA 15129). http://dimopex.eu/.

Drakvik, E., Altenburger, R., Aoki, Y., Backhaus, T., Bahadori, T., Barouki, R., Brack, W., Cronin, M.T., Demeneix, B., Bennekou, S.H., 2020. Statement on advancing the assessment of chemical mixtures and their risks for human health and the environment. Environ. Int. 134, 105267.

Dulio, V., Koschorreck, J., van Bavel, B., van den Brink, P., Hollender, J., Munthe, J., Schlabach, M., Aalizadeh, R., Agerstrand, M., Ahrens, L., 2020. The NORMAN association and the European partnership for chemicals risk assessment (PARC): let's cooperate! Environ. Sci. Eur. 32, 1–11.

Ec, 2020a. European Comission Chemicals Strategy for Sustainability-Towards a Toxic-free Environment. Brussels, COM(2020) 667 Final.

Ec, 2020b. European Commission, Information Platform for Chemical Monitoring (IPCHEM) Data Integration.

ELIXIR, 2017. Position Paper on FAIR Data Management in Life Sciences.

EU, 2016. Service Contract to Create a Database and Develop a Model to Estimate the Occupational Exposure for a List of Hazardous Chemicals in the Member States of the European Union and in the EFTA/EEA Countries No VT/2013/079. Publications Office of the European Union, Luxembourg, ISBN 978-92-79-45435-6.

Evans, R.M., Martin, O.V., Faust, M., Kortenkamp, A., 2016. Should the scope of human mixture risk assessment span legislative/regulatory silos for chemicals? Sci. Total Environ. 543, 757–764.

Eykelbosh, A., Werry, K., Kosatsky, T., 2018. Leveraging the Canadian health measures survey for environmental health research. Environ. Int. 119, 536–543.

Fantke, P., Aurisano, N., Provoost, J., Karamertzanis, P.G., Hauschild, M.Z., 2020a. Toward effective use of REACH data for science and policy. Environ. Int. 135.

Fantke, P., Von Goetz, N., Schlüter, U., Bessems, J., Connolly, A., Dudzina, T., Ahrens, A., Bridges, J., Coggins, M.A., Conrad, A., 2020b. Building a European exposure science strategy. J. Expo. Sci. Environ. Epidemiol. 30, 917–924.

Faure, S., Noisel, N., Werry, K., Karthikeyan, S., Aylward, L.L., St-Amand, A., 2020. Evaluation of human biomonitoring data in a health risk based context: an updated analysis of population level data from the Canadian Health Measures Survey. Int. J. Hyg Environ. Health 223, 267–280.

Fiddicke, U., Pack, L.K., Tolonen, H., Sepai, O., López, M.E., Castaño, A., Schoeters, G., Kolossa-Gehring, M., 2021. A Phased Approach for preparation and organization of human biomonitoring studies. Int. J. Hyg Environ. Health 232, 113684.

Galea, K.S., Porras, S.P., Viegas, S., Bocca, B., Bousoumah, R., Duca, R.C., Godderis, L., Iavicoli, I., Janasik, B., Jones, K., 2021. HBM4EU chromates study-Reflection and lessons learnt from designing and undertaking a collaborative European biomonitoring study on occupational exposure to hexavalent chromium. Int. J. Hyg Environ. Health 234, 113725.

Ganzleben, C., Antignac, J.-P., Barouki, R., Castaño, A., Fiddicke, U., Klánová, J., Lebret, E., Olea, N., Sarigiannis, D., Schoeters, G.R., 2017. Human biomonitoring as a tool to support chemicals regulation in the European Union. Int. J. Hyg Environ. Health 220, 94–97.

Goodman, K.J., Geary, J., Walker, E., Fagan-Garcia, K., Archie, B., Lennie, C., Munday, R., McAlpine, L., Colquhoun, A., Chang, H.-J., 2019. Community-driven epidemiologic research: guiding principles. Global Epidemiology 1, 100013.

Haines, D.A., Saravanabhavan, G., Werry, K., Khoury, C., 2017. An overview of human biomonitoring of environmental chemicals in the Canadian Health Measures Survey: 2007–2019. Int. J. Hyg Environ. Health 220, 13–28.

Hubal, E.A.C., 2019. PFAS: Insights from Past Actions to Inform Today's Decisions. Nature Publishing Group.

IUPAC, 2018. What on Earth Is InChI?.

Joas, R., Casteleyn, L., Biot, P., Kolossa-Gehring, M., Castano, A., Angerer, J., Schoeters, G., Sepai, O., Knudsen, L.E., Joas, A., 2012. Harmonised human biomonitoring in Europe: activities towards an EU HBM framework. Int. J. Hyg Environ. Health 215, 172–175.

Knetsch, G., Ruether, M., 2016. The European Information Platform for Chemical Monitoring (IPCheM)-How Can You Realize Interoperability?.

Kromerová, K., Bencko, V., 2019. Added value of human biomonitoring in assessment of general population exposure to xenobiotics. Cent. Eur. J. Publ. Health 27, 68–72.

Lermen, D., Gwinner, F., Bartel-Steinbach, M., Mueller, S.C., Habermann, J.K., Balwir, M.-B., Smits, E., Virgolino, A., Fiddicke, U., Berglund, M., 2020. Towards harmonized biobanking for biomonitoring: a comparison of human biomonitoring-related and clinical biorepositories. Biopreserv. Biobanking 18, 122–135.

Louro, H., Heinälä, M., Bessems, J., Buekers, J., Vermeire, T., Woutersen, M., Van Engelen, J., Borges, T., Rousselle, C., Ougier, E., 2019. Human biomonitoring in health risk assessment in Europe: current practices and recommendations for the future. Int. J. Hyg Environ. Health 222, 727–737.

Mustieles, V., d'Cruz, S.C., Couderq, S., Rodríguez-Carrillo, A., Fini, J.-B., Hofer, T., Steffensen, I.-L., Dirven, H., Barouki, R., Olea, N., 2020. Bisphenol A and its analogues: a comprehensive review to identify and prioritize effect biomarkers for human biomonitoring. Environ. Int. 144, 105811.

Mustieles, V., Fernández, M.F., 2020. Bisphenol A shapes children's brain and behavior: towards an integrated neurotoxicity assessment including human data. Environ. Health 19, 1–8.

OECD, 2018. Consideration for Assessing the Risk of Combined Exposure to Multiple Chemicals, Series on Testing and Assessment, No. 296. Environment, Health and Safety Division, Environment Directorate.

Pourchet, M., Debrauwer, L., Klanova, J., Price, E.J., Covaci, A., Caballero-Casero, N., Oberacher, H., Lamoree, M., Damont, A., Fenaille, F., 2020. Suspect and non-targeted screening of chemicals of emerging concern for human biomonitoring, environmental health studies and support to risk assessment: from promises to challenges and harmonisation issues. Environ. Int. 139, 105545.

Romano, M.E., Gallagher, L.G., Eliot, M.N., Calafat, A.M., Chen, A., Yolton, K., Lanphear, B., Braun, J.M., 2020. Per-and polyfluoroalkyl substance mixtures and gestational weight gain among mothers in the Health Outcomes and Measures of the Environment study. Int. J. Hyg Environ. Health 231, 113660.

SAICM, 2013. Strategic Approach to International Chemical Management.

Santonen, T., Alimonti, A., Bocca, B., Duca, R.C., Galea, K.S., Godderis, L., Göen, T., Gomes, B., Hanser, O., Iavicoli, I., 2019. Setting up a collaborative European human biological monitoring study on occupational exposure to hexavalent chromium. Environ. Res. 177, 108583.

Sexton, K.L., Needham, L.L., Pirkle, J., 2004. Human Biomonitoring of Environmental Chemicals: measuring chemicals in human tissues is the" gold standard" for assessing people's exposure to pollution. Am. Sci. 92, 38–45.

St-Amand, A., Werry, K., Aylward, L.L., Hays, S.M., Nong, A., 2014. Screening of population level biomonitoring data from the Canadian Health Measures Survey in a risk-based context. Toxicol. Lett. 231, 126–134.

Who, 2015a. Human Biomonitoring: Facts and Figures. WHO Regional Office for Europe, Copenhagen.

Who, 2015b. Human Biomonitoring: Facts and Figures. WHO Regional Office for Europe Copenhagen.

Wikoff, D., Lewis, R.J., Erraguntla, N., Franzen, A., Foreman, J., 2020. Facilitation of risk assessment with evidence-based methods–A framework for use of systematic mapping and systematic reviews in determining hazard, developing toxicity values, and characterizing uncertainty. Regul. Toxicol. Pharmacol. 118, 104790.

Wilhelm, M., 2020. Human biomonitoring: its importance in toxicological regulation. Regulatory Toxicology 1–20.

Wilkinson, M.D., Dumontier, M., Aalbersberg, I.J., Appleton, G., Axton, M., Baak, A., Blomberg, N., Boiten, J.-W., da Silva Santos, L.B., Bourne, P.E., 2016. The FAIR Guiding Principles for scientific data management and stewardship. Scientific data 3, 1–9.

Williams, A.J., Yerin, A., 2013. Automated systematic nomenclature generation for organic compounds. Wiley Interdisciplinary Reviews: Computational Molecular Science 3, 150–160.

Wolffe, T.A., Whaley, P., Halsall, C., Rooney, A.A., Walker, V.R., 2019. Systematic evidence maps as a novel tool to support evidence-based decision-making in chemicals policy and risk management. Environ. Int. 130, 104871.

Zare Jeddi, M., Hopf, N.B., Viegas, S., Price, A.B., Paini, A., van Thriel, C., Benfenati, E., Ndaw, S., Bessems, J., Behnisch, P.A., 2020. Towards a systematic use of effect biomarkers in population and occupational biomonitoring. Environ. Int. 146, 106257.

International Journal of Hygiene and Environmental Health 238 (2021) 113860

Contents lists available at ScienceDirect

International Journal of Hygiene and Environmental Health

journal homepage: www.elsevier.com/locate/ijheh

Analytical uncertainties in a longitudinal study – A case study assessing serum levels of per- and poly-fluoroalkyl substances (PFAS)

Sandra Nilsson [a,*], Jochen F. Mueller [a], Anna Rotander [b], Jennifer Bräunig [a]

[a] Queensland Alliance for Environmental Health Sciences (QAEHS), The University of Queensland, 20 Cornwall Street, Woolloongabba, 4102, QLD, Australia
[b] Man-Technology-Environment Research Centre (MTM), Örebro University, 701 82, Örebro, Sweden

ARTICLE INFO

Keywords:
Storing
Analytical uncertainty
Quality assurance/quality control
Human biomonitoring
Study design

ABSTRACT

Per- and poly-fluoroalkyl substances (PFAS) are a range of persistent organofluorine contaminants, some of which have been found to accumulate in humans and have long half-lives. In longitudinal studies, when relying on measurements obtained at different points in time, it is critical to understand the associated analytical uncertainties when interpreting the data. In this manuscript we assess precision measurements of serum PFAS analysis in a follow-up study undertaken approximately 5 years after the initial study. These measurements included intra-(n = 58) and inter-batch duplicates (n = 57), inter-batch replicates (n = 58), inter-laboratory replicates (n = 10) and a re-analysis of 120 archived serum samples from the initial study. Average coefficients of variation (CV) for perfluorooctanoic acid (PFOA), perfluorohexane sulfonate (PFHxS) and perfluorooctane sulfonate (PFOS) associated with the reanalysis of archived samples ranged from 4 to 8%, which was greater than the inter- and intra -batch duplicates (<3%), but lower than the inter-laboratory comparison (CV ≥ 10%). Multi-centre analytical capacity in studies increases the variance within the dataset and implementation of variability-measures are useful to refine and maintain comparability. Due to long PFAS half-lives, this variance is an important consideration when deciding appropriate time intervals for sample collections in longitudinal studies, to ensure the difference is greater than the analytical uncertainty.

1. Introduction

Per- and polyfluoroalkyl substances (PFASs) are a group of manmade fluorinated organic compounds used in applications and products such as stain repellents, cookware and aqueous film forming foam (AFFF). Due to the high production and use, as well as the persistency of these compounds, PFASs are ubiquitously detected in the environment, in wildlife and in humans globally (Lindstrom et al., 2011).

The most frequently studied PFASs, belonging to the group of perfluoroalkyl acids (PFAAs), are perfluorooctane sulfonate (PFOS), perfluorohexane sulfonate (PFHxS) and perfluorooctanoic acid (PFOA). Worldwide, biomonitoring studies estimate exposure to these PFASs through measuring the blood serum concentrations (Calafat et al., 2007; Eriksson et al., 2017; Ingelido et al., 2018; Li et al., 2018; Zhou et al., 2014). Studies have suggested that PFAS exposure may be associated with adverse health effects. PFAS serum concentrations have been found to associate with biomarkers for several health outcomes such as cardiovascular disease, liver and kidney function, and have been discussed in several recent reviews (Ballesteros et al., 2017; Kirk et al., 2018; Zhao et al., 2020). However, studies have not always been consistent, and longitudinal studies are needed to reduce the risk of bias, uncontrolled confounding and reverse causality (Buckley et al., 2018). Additionally, longitudinal studies are necessary to estimate temporal exposure trends and are of special importance after exposure control attempts, when evaluating the success of intervention and estimating the apparent elimination half-lives.

Notwithstanding, longitudinal study designs implicit numerous challenges such as increased temporal and financial demands and the possibility of incomplete follow-up of individuals. The loss to follow up may be especially apparent in studies using invasive sample collections, such as blood collection, due to increased time-commitment, intrusiveness and burden to the study participants (Boyle et al., 2020; Galea and Tracy, 2007). Minimizing the degree and frequency of sampling can limit the burden on study participants, as well as shorten the study duration and deliver faster outcomes. Planning and interpretation of such a study, will need to consider the associated uncertainties. It is critical to relate the precision and accuracy of PFAS analysis to the long half-life of PFASs (>several years for longer chained PFAAs) (Li et al.,

* Corresponding author.
E-mail address: s.nilsson@uq.edu.au (S. Nilsson).

https://doi.org/10.1016/j.ijheh.2021.113860
Received 29 June 2021; Received in revised form 2 September 2021; Accepted 5 October 2021
Available online 11 October 2021

2019; Olsen et al., 2007). Consideration of appropriate temporal distance between sample collections is critical to be able to detect PFAS concentration trends and differentiate them from the variability of PFAS analysis.

In the last two decades PFAS analysis has substantially advanced. Standard methods using isotopically labelled standards have been developed and reference materials have become available (Martin et al., 2004). Inter-laboratory studies are available on an annual basis for PFAS serum analysis, and have shown that experienced laboratories can quantify several PFAAs, including PFOA, PFHxS and PFOS, in human serum, with precision and accuracy, using validated sample preparation methods, labelled and native standards and appropriate instrumentation (Kaiser et al., 2021; Keller et al., 2010; Lindström et al., 2009).

However, the development of PFAS analysis over time needs to be considered in longitudinal studies. For example, if samples are obtained and analysed over the course of several years, potential changes of analytical methods may also influence the uncertainty when comparing data from the different years, and this has been discussed as a major limitation in previous studies investigating half-lives in individuals followed over time (Li et al., 2018; Olsen et al., 2012).

The overall aim of this manuscript is to assess uncertainties in a longitudinal biomonitoring study. We evaluate the uncertainty associated with the use of analytical data obtained approximately five years apart versus the reanalysis of archived samples. We compare this to the uncertainties associated with other aspects of analysis, such as the analytical variation within a batch, between batches and between laboratories.

2. Methods

2.1. Overview

This manuscript focuses on a range of samples that were included as quality assurance and quality control (QA/QC) in an exposure study, and a flowchart of the methodology is presented in Fig. 1. The study was approved by the Human research ethics committee (number 2014000614 and 2018001790), and consent from participants was recorded verbally. The study was first undertaken in 2013–2014, where serum from airport firefighters was analysed for PFASs (Rotander et al., 2015)(Fig. 1(a)). After analysis, serum samples of consenting participants were archived in a −20° freezer. In 2018–2019, airport firefighters were recruited again, including both new and previous study participants (Fig. 1(b)). A total of 130 participants had two longitudinally collected samples (2013–2014 and 2018–2019), while 671 had a single sample from 2018 to 2019. Archived serum samples (n = 120) from 2013 to 2014 were re-extracted and analysed together with all samples collected in the 2018–2019 study to assess the agreement between the two analysis years. PFOA, PFHxS and PFOS were the dominant PFASs in the 2013–2014 study, with the highest detection frequency and greatest concentration and are therefore the compounds of main interest in the longitudinal study. Likewise, these three compounds are generally the dominant PFASs in both exposed communities and the general populations. The longitudinal dataset is limited to PFOA, PFHxS, PFOS and is the main focus in this manuscript. However, other variability measurements include an extended suite of PFASs, and are presented in the

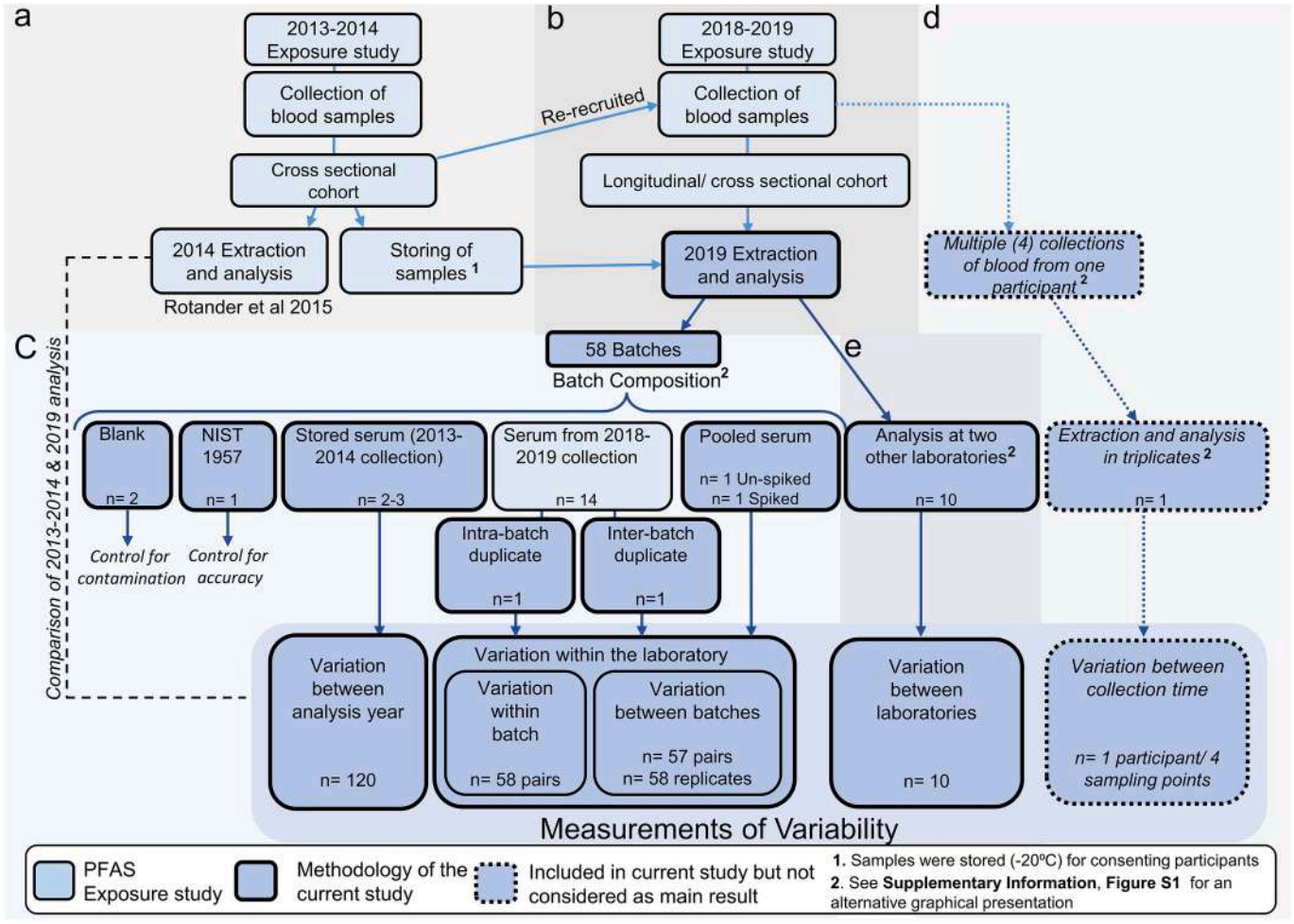

Fig. 1. Flowchart of the methodology and measurements of variability performed in the current study. The current study focuses on a range of quality assurance/quality control measurements (c–e), which were included in an 2018–2019 exposure study(b), as a follow up to a 2013–2014 exposure study(a).

SI.

Serum samples were extracted and analysed in 58 batches during a period of 5 months (June–November 2019) (Fig. 1(c)). Each batch consisted of 14 individual serum samples from the 2018–2019 study, as well as 1–3 of the archived serum samples. In each batch, one serum sample was extracted and analysed as an intra-batch duplicate, and one sample as an inter-batch duplicate. Additionally, two aliquots (spiked and un-spiked) of a pooled serum sample were included as inter-batch replicates (aliquots from the same pooled serum sample were included in all batches). In total, the following QA/QC measurements were obtained for the assessment of precision/variability within the laboratory; intra-batch duplicate samples (n = 58 pairs), inter-batch duplicate samples (n = 57 pairs) and two inter-batch replicates (spiked (n-58), and un-spiked (n = 58). The variability associated with storage and long term variance within our laboratory is assessed by the 120 stored samples that were reanalysed, by comparing the measurements to what was measured in the 2013–2014 study. Additionally, one participant provided multiple blood samples on several different days and times of the day, including fasting and non-fasting samples (Fig. 1(d)). These samples were extracted as triplicates and used to investigate potential daily variability of serum PFAS levels and consequently assess sample collection time as a factor of variability. However, as only one participant was used for this assessment, this is not considered a main result, and any further details of this assessment are presented in the SI. In addition to the variation that could be assessed within our laboratory, inter-laboratory variation was assessed with ten randomly selected serum samples which were extracted and analysed at two other laboratories that are accredited for serum PFAS analysis (National Association of Testing Authorities accredited) (Fig. 1(e)). Each measurement of variability, as well as a graphical presentation of the analytical batch construction and QA/QC measurements are explained in detail in the SI.

2.2. Extraction and instrumental analysis

Serum samples were extracted according to previously described methods (Rotander et al., 2015; Toms et al., 2019) with some minor modifications. Briefly, serum samples (1 mL), spiked with labelled PFAS mix, were vortex mixed and sonicated with acetonitrile, centrifuged, filtered and concentrated before they were spiked with recovery mix. PFASs were analysed using a high-performance liquid chromatograph (HPLC, Nexera, Shimadzu Corp., Kyoto Japan), coupled to a tandem mass spectrometer (SCIEX Triple Quad 6500+, Concord, Ontario, Canada) equipped with an electrospray ionisation source and run on negative ionisation mode and scheduled multiple reaction monitoring mode (MRM). Separation was achieved by gradient elution on a Kinetex EVO C18 column (2.6 μm, 100 Å, 100 × 2.1 mm, Phenomenex). Reported concentrations are for linear isomers, with the exception of PFOS where the total concentration of both linear and branched isomers is presented. Further details of the solvents, PFAS mixes, and extraction and analysis methods are presented in the SI.

2.3. General QA/QC

During the extraction, two blanks (acetonitrile and MilliQ) and a standard reference material (SRM, NIST 1957) from the National Institute of Standards and Technology, were extracted and analysed in each batch (National Institute of Standards and Technology, 2016). Native spike recovery was assessed by comparing a serum sample that was spiked with native PFAS mix before and after extraction. Our laboratory participates in two external quality assessment schemes (AMAP and G-EQUAS) and passed acceptable criteria. Concurrently to this study, one round of each study was conducted (AMAP 2020-01, and G-EQUAS 64) (Tables S5 and SI). Method detection limits (MDLs) were determined using EPA guidelines (40 CFR 136 Appendix B, detailed in SI) and set as 3.14 times the standard deviation of seven spiked replicates. MDLs ranged from 0.06 to 0.08 ng/mL for PFOA, PFHxS and PFOS, and all MDLs are presented in the SI (Table S4).

2.4. Statistical analysis

Statistical analysis were performed in GraphPad Prism 8.3.1. The assessments of uncertainty consisted of comparisons between two samples (the re-extracted archived samples, the intra and inter batch duplicates), as well as comparisons across several measurements (the inter batch replicate, inter-laboratory comparisons). The coefficient of variation (CV) was calculated for all of these measurements, to be able to compare them to each other. Additionally, Pearson correlation was used to assess the association between mean ln-transformed PFAS concentration and CV. To further assess if there was a systematic difference when re-analysing the archived serum samples, the agreement between respective PFAS measurements(M) in the 2018–2019 re-analysis ($M_{re\text{-}analysis}$) and 2013–2014 analysis ($M_{original}$) was assessed using Bland-Altman (B&A) plots (Bland and Altman, 1999). This method is used to calculate the mean difference between the two analysis years (the bias), as well as the 95% limits of agreement (1.96 SD of the mean difference). Systematic difference between the methods was considered if the 95% of agreements do not include the line of equity (0%). The B&A plots present the mean PFAS concentration (($M_{re\text{-}analysis} + M_{original}$)/2), used as reference (the x-axis), plotted against the percentage difference between each paired measurement ($M_{re\text{-}analysis}$ - $M_{original}$)/Average). Linear regression was used to assess the relationship between mean percentage difference and mean PFAS concentration. Only measurements which were greater than the MDLs were included in the assessments. An overview of all statistical methods used for each measurement of uncertainty is presented in the SI.

3. Results & discussion

3.1. General QA/QC

The mean PFASs concentrations of NIST 1957, included in all batches, were within acceptable limits of reference values (Z-score $-2<x>2$), and the CV of PFOA, PFHxS and PFOS were 7.8%, 6.1% and 6.1% respectively. Average recovery of mass labelled internal standards, and spiked native standards were 97% and 95% respectively.

3.2. Variation within and between batches

The detection frequency and concentration ranges of all PFAAs analysed in the 2018–2019 exposure study are presented in Table S6, in the SI. PFOA, PFHxS and PFOS were detected in all assessed samples in concentrations ranging from 0.08 to 15 ng/mL, 0.08–168 ng/mL and 0.12–185 ng/mL, respectively. The average CV of the duplicates within and between batches respectively were 1.9% and 2.6% for PFOA, 1.8% and 2.4% for PFHxS and 1.8% and 2.6% for PFOS. The CVs between batch replicates were 5.8% for PFOA, 6.9% for PFHxS, and 6.4% for PFOS (Table 1, Fig. 2), which is comparable to the CV of NIST 1957 replicates. No significant correlation between CV and PFAS concentrations was found (Table 1, Figs. S1 and SI).

3.3. Variation between laboratories

PFOA, PFHxS and PFOS were detected in all ten inter-laboratory samples in our laboratory with concentrations ranging from 0.51 to 2.8 ng/mL, 0.93–45 ng/mL and 4–78 ng/mL, respectively. PFOS was detected in all of the samples by the two other laboratories, however, due to a greater MDL (1 ng/mL), PFOA and PFHxS were only reported in nine of the ten samples, and thus assessment is only based on nine samples for these two compounds. The mean CV% between the laboratories for PFOA, PFHxS and PFOS were 12%, 10% and 15% respectively (Table 1, Fig. 2). This variation is consistent with results of the inter-laboratory comparison included in the external quality assessment

Table 1
Outcomes of all uncertainty assessments. For other compounds, see SI.

Uncertainty		CV (%) Mean (SD)/(p95)[a]			Pearson Correlation[b] r			B&A Bias (95% CI)		
		PFOA	PFHxS	PFOS	PFOA	PFHxS	PFOS	PFOA	PFHxS	PFOS
Within batches	Duplicates	1.9 (1.6)/4.7	1.8 (1.6)/5.2	1.8 (1.7)/4.9	−0.17	0.16	0.23			
Between batches	Duplicates	2.6(2.2)/7.6	2.4(2.0)/7.2	2.6(1.7)/6.2	−0.25	0.17	−0.15			
	Replicates	5.8	6.9	6.6						
Inter-laboratory		12	10	15	0.51	0.11	0.21			
Re-analysis of archived samples		4.3(2.9)/9.2	5.0 (3.9)/13	5.5 (3.7)/13	−0.01	0.29*	0.13	−2.4(4.2,−0.51)	0.77 (−1.5, 3.1)	−5.8 (−8.0, −3.7)
Collection time[c]	Within triplicates	1.7	3.2	3.5						
	Fast vs non fast	1.6	8.4	6.7						
	All collection times	5.4	5.2	4.3						

CV (%); coefficient of variance.
B&A; Bland-Altman analysis.
SD; Standard Deviation.
p95; 95th percentile.
r: Correlation coefficient.
CI: Confidence interval.
*. p-value <0.05.
[a] Where CV is calculated from paired measurements (Duplicates, replicates, re-analysis), the mean CV is presented, as well as the SD and p95.
[b] Correlation between CV and PFAS concentration.
[c] Collection time (Representative sampling) is presented and discussed further in SI.

scheme conducted concurrently to this study (SI, Table S6), as well as other published inter-laboratory comparisons (Kaiser et al., 2021; Lindström et al., 2009). No significant correlation between CV% and PFAS concentration was found (Figs. S2 and SI).

3.4. Re-analysis of archived 2013–2014 serum samples

The 120 serum-samples that were archived and reanalysed, the original measurements ranged from 0.30 to 18 ng/mL (PFOA), 0.59–277 ng/mL (PFHxS) and 3.3–391 ng/mL (PFOS). Comparing to each respective re-analysed measurement, the mean CV was 4.3%, 5.0% and 5.5% respectively for PFOA, PFHxS and PFOS (Table 1, Fig. 2). B&A analyses were performed to assess the mean difference and define the limits of agreement between the original PFAS measurements and the re-analysis (Fig. 3) (Giavarina, 2015). Calculated mean difference(bias) for PFOA, PFHxS and PFOS were −2.4%, 0.77% and −5.8% respectively. The negative bias for PFOA and PFOS, indicate lower reported results in the re-analysis compared to the original analysis. However, the 95% limits of agreement overlapped the line of equity (0%) for all three PFASs, suggesting there is no systematic difference (visually shown in Fig. 3). Linear regression analysis indicated no significant relationship between average difference and magnitude of concentration. This is in agreement with all other variation measurements, indicating no relationship between analytical variance and the measured concentrations. However, although a broad range of concentrations was assessed, it should be noted that no samples had PFOA, PFHxS or PFOS concentrations close to the MDL, where interferences may be more noticeable and consequently analytical uncertainty greater.

Due to the wide range of PFHxS and PFOS concentrations of the dataset that was assessed in the B&A analysis, the relationship between bias and magnitude of concentrations was further assessed separately for lower and higher concentrations respectively (SI, Fig. S3). No apparent difference was observed for PFOS, while the bias in PFHxS concentrations was negative (-3.7%) in the subset of datapoints with low concentration (<15 ng/mL), and positive (3.6%) for datapoints >15 ng/mL. However, the 95% limits of agreement overlapped the line of equity (0%) in both subsets. Thus, no systematic difference can be assumed. Due to the stable chemical structures of these PFAAs, degradation of these compounds while storing is not likely, and unchanged PFAS concentrations have previously also been reported after storage at various temperatures and times (Buck et al., 2011; Kato et al., 2013), indicating that there is no apparent degradation or adsorption to storage tubes that is affected by the time of storage. It is likely that the variability observed is a result of improved/modified analytical methods. However, the storage of samples as well as the increased number of freeze-thaw cycles, could possibly also affect the homogeneity/physical integrity or the samples differently and contribute to the variation observed between the analysis years. By storage of replicate samples, this hypothesis could be assessed in future studies. Evidence of reliable PFAS analysis after long term storing is of great importance to biomonitoring studies that are relying on samples from biobanks that have been stored for a long time, making it possible to accurately assess historical PFAS exposure retrospectively.

The mean CV associated with the re-analysis of the archived samples (10–15%), was lower compared to the variation observed between laboratories (CVs; 12% (PFOA), 10% (PFHxS) and 15% (PFOS)). Compared to the original analysis in 2013–2014, the laboratory has moved, a different laboratory technician performed the analysis, and a different instrument was used. However, the extraction and analysis methodology were only modified slightly compared to the methodologies used in 2014. In contrast, the extraction procedure between the three different labs in the inter-laboratory assessment varied considerably (Tables S2 and SI), possibly explaining the greater CV.

The variation associated with re-analysis of the archived samples, were greater than the mean CV of the duplicates both within batches (CV <2.00%) and between batches (CV% <2.70%), but in line with the CV

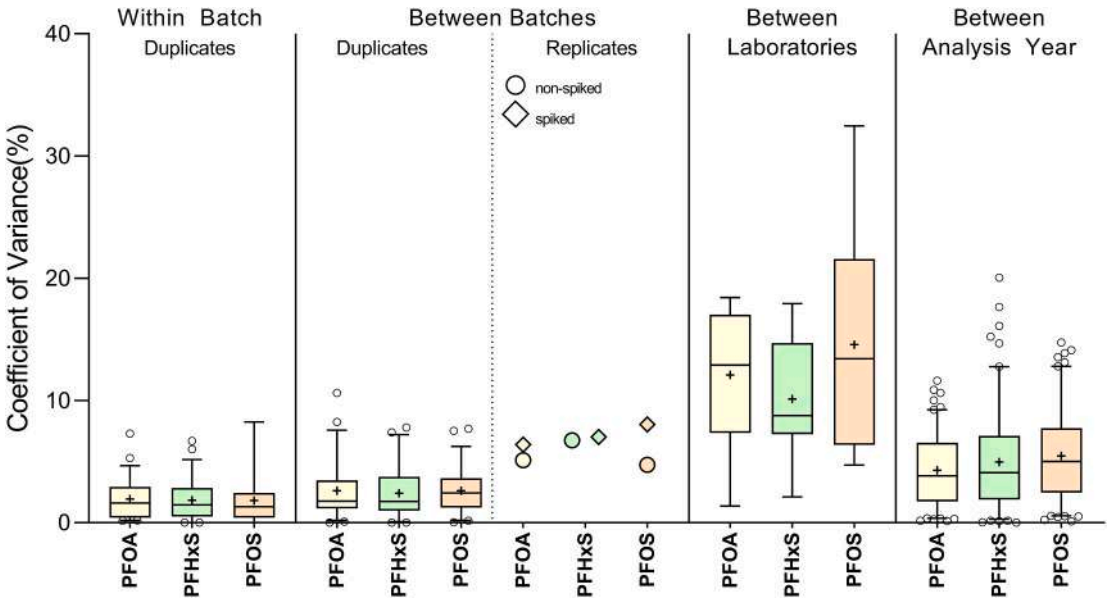

Fig. 2. The Coefficient of Variance (%) of PFOA (yellow), PFHxS (green) and PFOS (orange) for the measurements of variation in the current study; within batch variation (duplicates n = 58), between batch variation (duplicates n = 57 and replicates n = 58 × 2), inter-laboratory variation (n = 10) and the variation of the re-analysis of archived samples (n = 120). Where several duplicate measurements are used to represent the variation, CV% of all pairs are presented as box and whiskers, where whiskers present the 5–95 percentiles and the + represents the mean. (For interpretation of the references to colour in this figure legend, the reader is referred to the Web version of this article.)

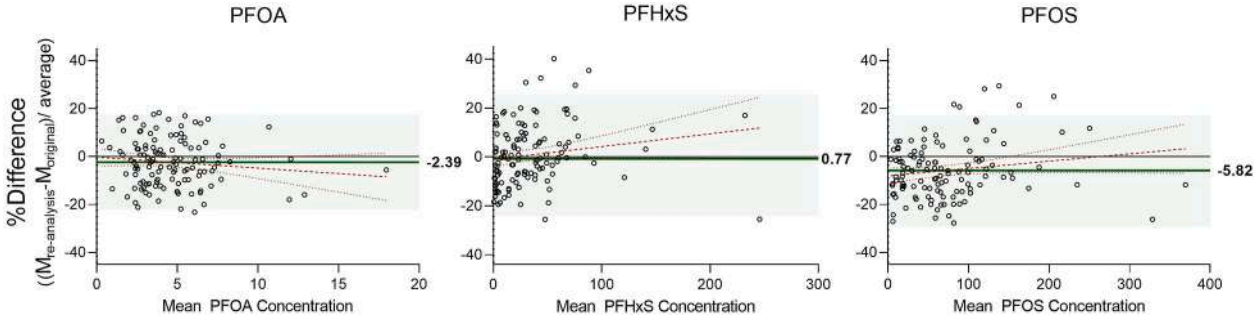

Fig. 3. Bland Altman plot for PFOA, PFHxS and PFOS showing the percent (%) difference between the re-analysis (in 2018–2019) and original analysis (in 2013–2014). Average difference (bias) shown as a green line and 95% limits of agreement shown by the shaded green area. The regression-line shows the relationship (and 95%CI) between the difference and the magnitude of concentration. (For interpretation of the references to colour in this figure legend, the reader is referred to the Web version of this article.)

between batch replicates.

Knowledge of uncertainties associated with the analysis is essential for detecting significant differences between samples and needs to be considered in both the interpretation of already published studies, as well as when designing future studies. When designing longitudinal studies, the analytical uncertainty has implications for defining sampling frequency (time between collection of two serum samples longitudinally). Here we showed that archiving and reanalysing samples in the same batch, reduces the uncertainty more than two-fold. This means that we can determine differences between two samples more accurately, which is important for elimination studies and half-life estimations. Additionally, we can distinguish trends with smaller concentration differences, expected from samples collected within shorter time periods. Consequently, less data will be required to assess PFAS concentration trends over time and the duration of a study can be minimized, decreasing the temporal and financial costs. A shorter study can also deliver faster outcomes, especially important when assessing the outcomes of exposure control attempts.

In addition to physical health effects that may be associated with PFAS exposure, communities affected by elevated PFAS exposure are also affected by physiological health effects such as elevated stress (Calloway et al., 2020). In such communities, it is critical to design intervention studies that can report results back to the community as fast as possible.

While storing and reanalysing samples may not always be possible, understanding the uncertainties with sampling and analysis combined with a prior estimate of the long half-lives of the compounds investigated, is critical for choosing an appropriate time interval between the

sample collections. As an example, for PFHxS, with an estimated half-life of 8.5 years (representing a decrease of 8%/year assuming successful exposure control), 11 months between two sample collections would be enough, to be able to measure a reliable difference between two samples that is greater than our within-batch variation (>95th percentile of the CV; 5.2%). If relying on previously reported data, 2.5 years would be required to overcome the variability associated with our re-analysis (>95th percentile of the CV; 13%).

In this study, we found the greatest analytical variation between laboratories. In studies that are aiming to assess differences between samples that are analysed at different laboratories, it may be worth including an interlaboratory comparison to define the specific uncertainty. In such a longitudinal study, a longer time between sampling may be needed to be able to detect a trend with greater confidence.

Although this study assessed the uncertainty of the analysis of PFAS concentrations in serum, the overall concept is applicable to any study assessing longitudinal trends of chemicals with long half-lives in blood. By defining the magnitude of difference aimed to be detected, knowing the expected analytical variation is crucial when deciding on the sampling frequency and number of samples needed in a study to accurately assess trends. In regard to participants of a longitudinal exposure study, minimizing the number of samples required and providing timely information lowers the burden and time commitment needed from participants. These are factors that may increase the willingness to participate in a study (Boyle et al., 2020; Galea and Tracy, 2007).

4. Conclusion

Using multi-centre analytical capacity in studies can impose a risk of high variance within the study data set. Thus, implementation of special measures is important for refining and maintaining comparability between analysis years and inter- and intra-laboratory analysis. This study shows that retrospective analysis of archived serum samples for PFAS improves precision when measuring longitudinal exposure trends. Consequently, such a study will require less sampling and allowing much faster outcomes, which is especially important when assessing the success of exposure control. The outcome of this study highlights the need to understand the uncertainties associated with longitudinal studies for both data interpretation and study design. By considering the analytical uncertainties associated with study design, the accuracy of PFAS exposure analysis can be improved in longitudinal epidemiological studies and risk assessments.

Declarations of interest

This study was undertaken as part of a larger biomonitoring study, funded by Airservices Australia. Sample and data analysis was performed at the Queensland Alliance for Environmental Health Sciences at the University of Queensland, which is co-funded by Queensland Health. The PhD of the corresponding author is supported by a UQ Scholarship.

Declaration of competing interest

None.

Acknowledgements

This study was undertaken as a part of a larger biomonitoring study, funded by Airservices Australia. We want to acknowledge the assistance, involvement and contribution of all current and former firefighter staff for participating in the biomonitoring study. We also want to thank Sullivan and Nicolaides Pathology and Paula Gscheidel for access to, and pooling of QA/QC samples. Sample and data analysis was performed at the Queensland Alliance for Environmental Health Sciences at the University of Queensland, which is co-funded by Queensland Health. The PhD of the corresponding author is supported by a UQ Scholarship.

Appendix A. Supplementary data

Supplementary data to this article can be found online at https://doi.org/10.1016/j.ijheh.2021.113860.

References

Ballesteros, V., Costa, O., Iñiguez, C., Fletcher, T., Ballester, F., Lopez-Espinosa, M.-J., 2017. Exposure to perfluoroalkyl substances and thyroid function in pregnant women and children: a systematic review of epidemiologic studies. Environ. Int. 99, 15–28.

Bland, J.M., Altman, D.G., 1999. Measuring agreement in method comparison studies. Stat. Methods Med. Res. 8, 135–160.

Boyle, J., Berman, L., Dayton, J., Iachan, R., Jans, M., ZuWallack, R., 2020. Physical measures and biomarker collection in health surveys: propensity to participate. In: Research in Social and Administrative Pharmacy, vol. 17.

Buck, R.C., Franklin, J., Berger, U., Conder, J.M., Cousins, I.T., de Voogt, P., Jensen, A.A., Kannan, K., Mabury, S.A., van Leeuwen, S.P.J., 2011. Perfluoroalkyl and polyfluoroalkyl substances in the environment: terminology, classification, and origins. Integrated Environ. Assess. Manag. 7, 513–541.

Buckley, N., Sim, M., Douglas, K., Håkansson, H., 2018. Expert Health Panel for Per- and Poly-Fluoroalkyl Substances (PFAS) Report to. the Department of Health.

Calafat, A.M., Wong, L.-Y., Kuklenyik, Z., Reidy, J.A., Needham Larry, L., 2007. Polyfluoroalkyl chemicals in the U.S. Population: data from the National health and nutrition examination survey (NHANES) 2003–2004 and comparisons with NHANES 1999–2000. Environ. Health Perspect. 115, 1596–1602.

Calloway, E.E., Chiappone, A.L., Schmitt, H.J., Sullivan, D., Gerhardstein, B., Tucker, P. G., Rayman, J., Yaroch, A.L., 2020. Exploring community psychosocial stress related to per- and poly-fluoroalkyl substances (PFAS) contamination: lessons learned from a qualitative study. Int. J. Environ. Res. Publ. Health 17.

Eriksson, U., Mueller, J.F., Toms, L.-M.L., Hobson, P., Kärrman, A., 2017. Temporal trends of PFSAs, PFCAs and selected precursors in Australian serum from 2002 to 2013. Environ. Pollut. 220, 168–177.

Galea, S., Tracy, M., 2007. Participation rates in epidemiologic studies. Ann. Epidemiol. 17, 643–653.

Giavarina, D., 2015. Understanding Bland Altman analysis. Biochem. Med. 25, 141–151.

Ingelido, A.M., Abballe, A., Gemma, S., Dellatte, E., Iacovella, N., De Angelis, G., Zampaglioni, F., Marra, V., Miniero, R., Valentini, S., Russo, F., Vazzoler, M., Testai, E., De Felip, E., 2018. Biomonitoring of perfluorinated compounds in adults exposed to contaminated drinking water in the Veneto Region. Italy Environ. Int. 110, 149–159.

Kaiser, A.-M., Aro, R., Kärrman, A., Weiss, S., Hartmann, C., Uhl, M., Forsthuber, M., Gundacker, C., Yeung, L.W.Y., 2021. Comparison of extraction methods for per- and polyfluoroalkyl substances (PFAS) in human serum and placenta samples—insights into extractable organic fluorine (EOF). Anal. Bioanal. Chem. 413, 865–876.

Kato, K., Wong, L.-Y., Basden, B.J., Calafat, A.M., 2013. Effect of temperature and duration of storage on the stability of polyfluoroalkyl chemicals in human serum. Chemosphere 91, 115–117.

Keller, J.M., Calafat, A.M., Kato, K., Ellefson, M.E., Reagen, W.K., Strynar, M., O'Connell, S., Butt, C.M., Mabury, S.A., Small, J., Muir, D.C.G., Leigh, S.D., Schantz, M.M., 2010. Determination of perfluorinated alkyl acid concentrations in human serum and milk standard reference materials. Anal. Bioanal. Chem. 397, 439–451.

Kirk, M., Smurthwaite, K., Bräunig, J., Trevenar, S., D', E., Cate, Lucas, R., Lal, A., Korda, R., Clements, A., Mueller, J., Armstrong, B., 2018. The PFAS Health Study: Systematic Literature Review. The Australian National University, Canberra.

Li, Y., Fletcher, T., Mucs, D., Scott, K., Lindh, C.H., Tallving, P., Jakobsson, K., 2018. Half-lives of PFOS, PFHxS and PFOA after end of exposure to contaminated drinking water. Occup. Environ. Med. 75, 46.

Li, Y., Xu, Y., Scott, K., Lindh, C., Jakobsson, K., Fletcher, T., 2019. Half-lives of PFOA, PFPeS, PFHxS, PFHpS and PFOS after end of exposure to contaminated drinking water, 3, 237.

Lindstrom, A.B., Strynar, M.J., Libelo, E.L., 2011. Polyfluorinated compounds: past, present, and future. Environ. Sci. Technol. 45, 7954–7961.

Lindström, G., Kärrman, A., van Bavel, B., 2009. Accuracy and precision in the determination of perfluorinated chemicals in human blood verified by interlaboratory comparisons. J. Chromatogr. A 1216, 394–400.

Martin, J.W., Kannan, K., Berger, U., De Voogt, P., Field, J., Franklin, J., Giesy, J.P., Harner, T., Muir, D.C.G., Scott, B., Kaiser, M., Järnberg, U., Jones, K.C., Mabury, S. A., Schroeder, H., Simcik, M., Sottani, C., Van Bavel, B., Kärrman, A., 2004. Analytical challenges hamper perfluoroalkyl research: researchers need better tools to get to the bottom of the contamination mystery. Environ. Sci. Technol. 38, 248a–255a.

Olsen, G.W., Burris, J.M., Butenhoff, J.L., Zobel, L.R., 2007. Half-life of serum elimination of perfluorooctanesulfonate, perfluorohexanesulfonate, and perfluorooctanoate in retired fluorochemical production workers. Environ. Health Perspect. 115, 1298–1305.

Olsen, G.W., Lange, C.C., Ellefson, M.E., Mair, D.C., Church, T.R., Goldberg, C.L., Herron, R.M., Medhdizadehkashi, Z., Nobiletti, J.B., Rios, J.A., Reagen, W.K., Zobel, L.R., 2012. Temporal trends of perfluoroalkyl concentrations in American red cross Adult blood donors, 2000–2010. Environ. Sci. Technol. 46, 6330–6338.

Rotander, A., Toms, L.-M.L., Aylward, L., Kay, M., Mueller, J.F., 2015. Elevated levels of PFOS and PFHxS in firefighters exposed to aqueous film forming foam (AFFF). Environ. Int. 82, 28–34.

SRM 1957, 26 January 2016. Human serum; National Institute of Standards and Technology; U.S. Department of Commerce: Gaithersburg, MD.
Toms, L.M.L., Braunig, J., Vijayasarathy, S., Phillips, S., Hobson, P., Aylward, L.L., Kirk, M.D., Mueller, J.F., 2019. Per- and polyfluoroalkyl substances (PFAS) in Australia: current levels and estimated population reference values for selected compounds. Int. J. Hyg Environ. Health 222, 387–394.
Zhao, J., Hinton, P., Chen, J., Jiang, J., 2020. Causal inference for the effect of environmental chemicals on chronic kidney disease. Comput. Struct. Biotechnol. J. 93–99.
Zhou, Z., Shi, Y., Vestergren, R., Wang, T., Liang, Y., Cai, Y., 2014. Highly elevated serum concentrations of perfluoroalkyl substances in fishery employees from tangxun lake, China. Environ. Sci. Technol. 48, 3864–3874.

International Journal of Hygiene and Environmental Health 238 (2021) 113863

Contents lists available at ScienceDirect

International Journal of Hygiene and Environmental Health

journal homepage: www.elsevier.com/locate/ijheh

Antibiotic resistance patterns of *Escherichia coli* isolates from the clinic through the wastewater pathway

Brandon Bojar [a], Jennifer Sheridan [a], Rachelle Beattie [b], Caitlin Cahak [c], Elizabeth Liedhegner [a], L. Silvia Munoz-Price [d], Krassimira R. Hristova [b], Troy Skwor [a,*]

[a] Department of Biomedical Sciences, College of Health Sciences, University of Wisconsin - Milwaukee, Milwaukee, WI, 53211, USA
[b] Department of Biological Sciences, Marquette University, Milwaukee, WI, 53233, USA
[c] Wisconsin Diagnostic Laboratories, Milwaukee, WI, 53226, USA
[d] Department of Medicine, Medical College of Wisconsin, Milwaukee, WI, 53226, USA

ARTICLE INFO

Keywords:
CTX-M
ESBL
Phylogroup
Uropathogenic
Wastewater
SXT

ABSTRACT

Antimicrobial resistance (AMR) remains one of the leading global health threats. This study compared antimicrobial resistance patterns among *E. coli* isolates from clinical uropathogenic *Escherichia coli* (UPEC) to hospital wastewater populations and throughout an urban wastewater treatment facility – influent, pre- and post-chlorinated effluents. Antibiotic susceptibility of 201 isolates were analyzed against eleven different antibiotics, and the presence of twelve antibiotic resistant genes and type 1 integrase were identified. AMR exhibited the following pattern: UPEC (46.8%) > hospital wastewater (37.8%) > urban post-chlorinated effluent (27.6%) > pre-chlorinated effluent (21.4%) > urban influent wastewater (13.3%). However, multi-drug resistance against three or more antimicrobial classes was more prevalent among hospital wastewater populations (29.7%) compared to other sources. *E. coli* from wastewaters disinfected with chlorine were significantly correlated with increased trimethoprim-sulfamethoxazole resistance in *E. coli* compared to raw and treated wastewater populations. $bla_{\text{CTX-M-1}}$ group was the most common extended spectrum beta-lactamase in *E. coli* from hospital wastewater (90%), although UPEC strains also encoded $bla_{\text{CTX-M-1}}$ group (50%) and bla_{TEM} (100%) genes. Among tetracycline-resistant populations, *tetA* and *tetB* were the only resistance genes identified throughout wastewater populations that were associated with increased phenotypic resistance. Further characterization of the *E. coli* populations identified phylogroup B2 predominating among clinical UPEC populations and correlated with the highest AMR, whereas the elevated rate of multi-drug resistance among hospital wastewater was mostly phylogroup A. Together, our findings highlight hospital wastewater as a rich source of AMR and multi-drug resistant bacterial populations.

1. Introduction

Antimicrobial resistance (AMR) poses one of the largest global public health threats claiming up to 700,000 deaths worldwide annually (WHO, 2019). A major driver of AMR is the prevalent use of antibiotics throughout healthcare and agriculture (Kummerer, 2009), which leads to increased antibiotic deposition in wastewater. This widespread antibiotic use contributes to selective pressure for the transfer and acquisition of antibiotic resistant genes (ARGs) (Karkman et al., 2018; Rizzo et al., 2013). In particular, hospital wastewater remains a hotspot of antibiotic resistant bacterial populations due to contaminating levels of sub-inhibitory concentrations of antibiotics (Verburg et al., 2019) and pathogenic organisms (Paulshus et al., 2019; Sib et al., 2019). In addition, wastewater, from both hospital and urban sources, contains other stressors such as heavy metals and biocides, which have been implicated in accelerated mutation rates and horizontal gene transfer (HGT) among bacterial populations, including *Escherichia coli* (Pal et al., 2015; Seiler and Berendonk, 2012). Thus, when hospital wastewater merges with municipal streams, favorable niches for the acquisition, retention, and transfer of ARGs are created due to the high concentration of bacteria, sub-inhibitory concentrations of antibiotics, and the presence of other stressors (i.e. heavy metals) resulting in antibiotic resistant bacterial populations (Karkman et al., 2018; Lorenzo et al., 2018). Importantly, these antibiotic resistant bacterial populations are capable of surviving

* Corresponding author.
E-mail address: skwor@uwm.edu (T. Skwor).

https://doi.org/10.1016/j.ijheh.2021.113863
Received 10 May 2021; Received in revised form 13 October 2021; Accepted 13 October 2021
Available online 16 October 2021

the wastewater treatment process and are commonly found in receiving bodies of water (Kappell et al., 2015; Skwor et al., 2020) where they can further cause recreational waterborne illnesses (Dorevitch et al., 2012; Graciaa et al., 2018a; Søraas et al., 2013).

One bacterial population prevalent in wastewater is *Escherichia coli*, which is commonly used as a fecal pollution indicator in environmental waters (Brechet et al., 2014; Lenart-Boron et al., 2020). Due to an abundance of genetic diversity, *E. coli* populations can be phylogenetically clustered into phylogroups partially coincide different ecological niches and propensities to cause disease. For example, commensal populations residing in a symbiotic relationship in warm-blooded animals are typically comprised of phylogroup A (Stoppe et al., 2017), whereby other phylogroups can cause clinical manifestations ranging from mild gastroenteritis to life-threatening sepsis caused by extra-intestinal pathogenic *E. coli* (ExPEC) (Jang et al., 2017). Most ExPEC strains belong to phylogroups B2 and D, whereby intestinal pathogenic strains typically belong to phylogroups B1, D or A (Sarowska et al., 2019). Phylogrouping *E. coli* populations in wastewater allows for improved understanding of the bacterial source and can further predict linkages between source and resistance patterns.

Coliforms, such as *E. coli*, are prevalent in both warm-blooded animals, including humans, and the environment and can be used in AMR monitoring programs to assess antibiotic resistance patterns (Schrijver et al., 2018; Stelling et al., 2005). One rationale for the use of *E. coli* to monitor resistance is its identification as both a major donor and recipient of ARGs mediated through horizontal gene transfer (Young, 1993). Thus, assessing the antimicrobial resistance profiles of *E. coli* populations allows comparison between sources to aid in identifying potential hot spots of antibiotic resistance acquisition, like hospital and urban wastewater. Identifying these resistance profiles also aids in determining if clinical resistance patterns survive throughout the wastewater process which can lead to environmental release of resistant bacteria into receiving aquatic ecosystems. Given that heterogeneity of resistance patterns globally are influenced by geographic region and the Human Development Index (Hendriksen et al., 2019a), it is critical to identify AMR patterns within connected sites. To address this, our study compared AMR profiles among clinical uropathogenic *E. coli* (UPEC), hospital wastewater, and throughout different stages of wastewater treatment plant in an urban city. We also compared phylogroups to resistance profiles to identify a potential common source for the resistant populations.

2. Material and methods

2.1. Isolation of E. coli strains

Wastewater samples were acquired weekly for three straight weeks (October 5th, 12th, and 18th) from Jones Island Water Reclamation Facility (Supplemental Figure 1; Milwaukee, WI, USA: 43.02044, −87.89905) and two continuous weeks from two separate outflow locations (October 2nd and 11th) at the Medical College of Wisconsin (Supplemental Figure 1; Milwaukee, WI, USA: 43.04355, −88.02139) in October 2018 by plant technicians. Water samples were immediately placed on ice until further processed in the laboratory; all water samples were processed within 8 h of collection. To acquire *E. coli* isolates, various dilutions and volumes of water were passed over a 0.45 μm filter and placed on modified mTEC (Hardy Diagnostics, Santa Maria, CA, USA) agar to acquire red or magenta colored *E. coli* isolates following the Environmental Protection Agency Method 1603 (EPA, 2014). More specifically, 5–20 mL of raw or 1:10 diluted hospital wastewater, 5–50 mL of raw or 1:10–1:1000 diluted urban wastewater influent, and 20–300 mL of raw urban wastewater pre-chlorinated effluent and post-chlorinated effluent were filtered for *E. coli* colonies. Five to ten colonies were selected at random from each source per date and further isolated using a four-quadrant streak over TSA to ensure isolation. From these plates, a total of 124 isolates were acquired from hospital wastewater (n = 37), as well as urban wastewater influents (n = 30), pre-chlorinated (n = 28) and post-chlorinated effluents (POC; n = 29).

Uropathogenic *E. coli* (UPEC) patient isolates were obtained from the hospital used for wastewater samples. Briefly, urine specimens were inoculated onto 5% sheep blood and MacConkey agar with subsequent incubation for 18–24 h at 35 °C in ambient air. Presumptive *E. coli* colonies were further isolated by sub-culturing onto sheep blood agar plates if needed and confirmed as *E. coli* using MALDI-TOF mass spectrometry (Bruker, Bremen, Germany) following a spot extraction method used for the identification of aerobic bacterial isolates. The suspected colonies were applied to a stainless-steel target chip (Bruker) with the sample spot overlaid with 70% formic acid to extract the proteins. Once dry, a matrix solution was applied to the sample spot and allowed to again dry, resulting in a homogeneous mixture of sample and matrix crystals. This target chip was then placed inside the MALDI-TOF for analysis. The protein spectrum detected by the analyzer was then compared to the Bruker MTB Compass Library (Revision E, 7854 MSP) to determine the identification. Frozen glycerol stocks were made of all cultures for further analysis.

2.2. Determining antibiotic susceptibility

Kirby-Bauer disk diffusion assay were used to examine antibiotic resistance of wastewater isolates. Briefly, overnight cultures were diluted to obtain a 0.5 McFarland standard in phosphate buffered saline (PBS). Isolates from wastewater samples were then cultured on to Mueller Hinton plates (BD Biosciences, San Jose, CA, USA) and stamped with the following eleven antibiotic disks (BD Biosciences) from seven different antibiotic classes (Magiorakos et al., 2012): chloramphenicol (30 mcg) – phenicol class; sulfamethoxazole-trimethoprim (SXT; 23.75/1.25 mcg) – folate pathways inhibitors class; ciprofloxacin (5 mcg) – fluoroquinolone class; gentamicin (10 mcg) – aminoglycosides class; tetracycline (30 mcg) – tetracyclines class; ceftriaxone (30mcg), cefotaxime (30 mcg), and ceftazidime (30 mcg) – extended-spectrum cephalosporins class; meropenem (10 mcg), imipenem (10 mcg), and ertapenem (10 mcg) – carbapenem class. After an 18–24h incubation at 35 °C, zones of inhibition were measured, and antibiotic susceptibility determined following the Clinical and Laboratory Standards Institute (CLSI) susceptibility standards (CLSI, 2015b). UPEC isolate susceptibility was determined using minimum inhibitory concentration (MIC) methods following CLSI protocol (CLSI, 2015a). MIC results and the detection of resistance markers were identified by the BD Phoenix susceptibility system which utilizes self-inoculating panels and doubling dilutions to determine susceptibility. The Phoenix system is interfaced with the BD EpiCenter System V6.41 where CLSI guidelines and customized rules were implemented to determine the SIR interpretations from the MIC results given from the Phoenix. Isolates exhibiting intermediate levels of resistance were categorized with susceptible populations. Multi-drug resistance (MDR) was determined by any isolate demonstrating resistance to three or more classes of antibiotics (Magiorakos et al., 2012) and MAR index was calculated by the number of resistant phenotypes against different antibiotic classes divided by the seven (the total number of antibiotic classes).

2.3. Phylotyping

E. coli populations were characterized by their phylogenetic group using the revised Clermont phylotyping method (Clermont et al., 2013). Briefly, multiplex PCR was used to amplify the following targets: *chuA* (288bp), *yjaA* (211bp), TspE4.C2 (152bp) and *arpA* (400). Further characterization of phylogroups C (*trp*), D, E (*arpAgpE*), and clades were performed using additional sets of primers (Supplemental Table 1). If an isolate displayed a genotype that did not match a phylogroup, they were listed as unknown.

2.4. Determination of ARGs

Bacterial genomic DNA was isolated using Promega Genomic DNA Purification kit. DNA was amplified using 2x GoTaq Green PCR Master Mix (Promega Corp., Madison, WI, USA) and 0.1 μM of ARG primers (Supplemental Table 1). *TetA* and *tetB* PCR reactions were amplified using the following protocol: initial denaturation at 95 °C for 60 s, followed by 30 cycles at 96 °C for 30s, 60 °C for 30 s, and 72 °C for 30 s, and a final elongation at 72 °C for 10 min. *TetC, E, M, O*, and *Int1* PCR reactions followed a similar PCR protocol except the annealing temperature was 55 °C for 30 s, and *TetD* had an annealing of 57 °C. *CTX-M, SHV, TEM*, and *sul1* PCR reactions were amplified using the following protocol: initial denaturation at 95 °C for 5 min, followed by 35 cycles at 94°c for 30 s, 60 °C for 30 s, and 72 °C for 2 min, and a final elongation at 72 °C for 7 min *Sul1* PCR reactions followed similar PCR protocol except the annealing temperature was 55.6 °C for 30 s. PCR products were analyzed using agarose gel electrophoresis.

2.5. MIC to determine the level of antibiotic resistance

To assess the correlation of ARGs with the level of resistance, MICs were further determined following a previous method (Baron et al., 2017). Briefly, overnight cultures were diluted in PBS to make a 0.5 McFarland standard. 96-well microplates were prepared with 50 mcl of serial two-fold antibiotic dilutions: tetracycline (4–256 mcg/mL) or ceftazidime (7.8–500 mcg/mL). Bacterial isolates were further diluted 1:100 in Mueller-Hinton broth and 50 mcl added to the appropriate wells. MIC value was determined by identifying the well with the lowest antibiotic concentration without turbidity after 18–24 h.

2.6. Plasmid isolation and transformation

Overnight antibiotic resistant *E. coli* cultures were grown in tryptic soy broth. Isolation of plasmids was performed using Zymo Research mini prep kit (Zymo Research, Irvine, CA, USA) following manufacturer's instructions. Plasmids were characterized via electrophoresis using a 0.7% agarose gel at 80 V for 3 h. The gel was subsequently stained with ethidium bromide and banding patterns analyzed with UV transillumination. Kodak software was used to determine nucleotide sizes of plasmids.

Transformation experiments were performed with E. cloni® 10G chemically competent cells (Lucigen, Middleton, WI, USA). Briefly, 5 mcl of plasmid DNA was combined with 40 mcl of competent cells and incubated on ice for 30 min. Heat shock was performed for 90 s at 42 °C followed by 1 h incubation at 37 °C at 175 rpm. The reaction was plated on tetracycline or cefotaxime-containing plates based on the initial susceptibility and incubated overnight at 37 °C. Plasmids were isolated as discussed above and transformants further tested for antibiotic susceptibility by Kirby-Bauer disk diffusion assay and interpreted according to CLSI susceptibility standards.

2.7. Statistical analysis

Comparison of antibiotic susceptibility between water sources, as well as among phylogroups, were performed using a one-way ANOVA followed by a Tukey's post-hoc test using GraphPad Prism version 9.1.0 (GraphPad Software, San Diego, CA, USA). Differences among antibiotic susceptibility rates between different water sources was analyzed using a two-tailed Fisher's exact test. PERMANOVA was performed on the phylotype and antibiotic resistance phenotype of each of the isolates to assess *E. coli* populations variation from different sources.

3. Results

3.1. Comparing antimicrobial resistance of E. coli UPEC, and isolates from hospital and urban wastewater

To aid in assessing the health risk associated with wastewater, we compared antibiotic resistance patterns among UPEC isolates (n = 77) to both hospital (n = 37) and combined (both stormwater runoff and sanitary sewage) urban wastewater (n = 30) *E. coli* isolates. All isolates were acquired from the Milwaukee, WI metropolitan area (population of 1,572,245). Total *E. coli* colonies acquired from hospital wastewater over the period of the study ranged from 4.0×10^1–5.5×10^5 CFU/100 ml compared to urban influent 4.0×10^3–7.6×10^7 CFU/100 ml. AMR was most prevalent among UPEC strains, followed by hospital wastewater; combined urban influent had the lowest AMR (Table 1: 46.8% vs 37.8% vs 13.3%; $P < 0.01$). Interestingly, when analyzing resistance to multiple antibiotics, hospital wastewater exhibited the highest MDR prevalence (29.7%) and multiple antibiotic resistance (MAR) index (0.22) compared to UPEC populations (Table 1: 6.5% and 0.102 respectively; $P = 0.001$ and $P < 0.05$) followed by urban influent isolates (Table 1: 0% and 0.029 respectively; $P < 0.001$ and $P < 0.005$). Importantly, we observed that only the hospital wastewater contained isolates with resistance to five of seven different antibiotic classes (Fig. 1: 24%). When comparing resistance patterns between UPEC strains and hospital wastewater sources, isolates from hospital wastewater were significantly more resistant to SXT, gentamicin, ceftazidime, and ceftriaxone (Table 1, $P < 0.05$). For six of eleven antibiotics tested, hospital wastewater exhibited greater resistance to SXT, gentamicin, ciprofloxacin, ceftriaxone, ceftazidime, and cefotaxime compared to urban wastewater influents (Table 1, $P < 0.05$). No hospital or urban wastewater isolates demonstrated resistance to carbapenems, although one UPEC isolate was resistant to ertapenem (Table 1). In contrast to other antibiotic patterns, tetracycline resistance was a common phenotype among UPEC, hospital, and urban wastewater populations (Table 1: 18.2%–32.4% to 13.3% respectively), although UPEC and hospital wastewater isolates exhibited resistance to higher concentrations (Fig. 2A).

Table 1
Prevalence of resistance in hospital wastewater compared to urban wastewater influents.

Resistance % (n)					
Antibiotic	UPEC (77)	Hospital WW (37)	WW Influent (30)	WW Effluent (28)	WW POC Effluent (29)
CHL	1.3 (1)	2.7 (1)	6.7 (2)	3.6 (1)	0
SXT	15.6 (12)	35.1 (13)	0	3.6 (1)	24.1 (7)
GEN	5.2 (4)	29.7 (11)	0	3.6 (1)	0
CIP	26.0 (20)	29.7 (11)	0	3.6 (1)	0
TET	18.2 (14)	32.4 (12)	13.3 (4)	17.9 (5)	13.8 (4)
CRO	3.9 (3)	24.3 (9)	0	3.6 (1)	3.4 (1)
CAZ	1.3 (1)	16.2 (6)	0	3.6 (1)	3.4 (1)
ETP	1.3 (1)	0	0	0	3.4 (1)
AMR	46.8 (36)[a]	37.8 (14)	13.3 (4)	21.4 (6)	27.6 (8)
MDR	6.5 (5)	29.7 (11)[b]	0.0 (0)	3.6 (1)	0.0 (0)
MAR Index	0.102	0.220[b]	0.029	0.050	0.059

CHL: chloramphenicol; SXT: trimethoprim/sulfamethoxazole; GEN: gentamicin; CIP: ciprofloxacin; TET: tetracycline; CRO: ceftriaxone; CAZ: ceftazidime; ETP: ertapenem; AMR: antimicrobial resistance; MDR: multi-drug resistance; MAR: multiple antibiotic resistance; UPEC: uropathogenic *E. coli;* WW: wastewater; Influent: combined urban stormwater and sanitary wastewater; Effluent: pre-chlorinated; POC: post-chlorinated; [a] $P < 0.05$ compared to WW influent; [b] $P < 0.05$ compared to all other water sources.

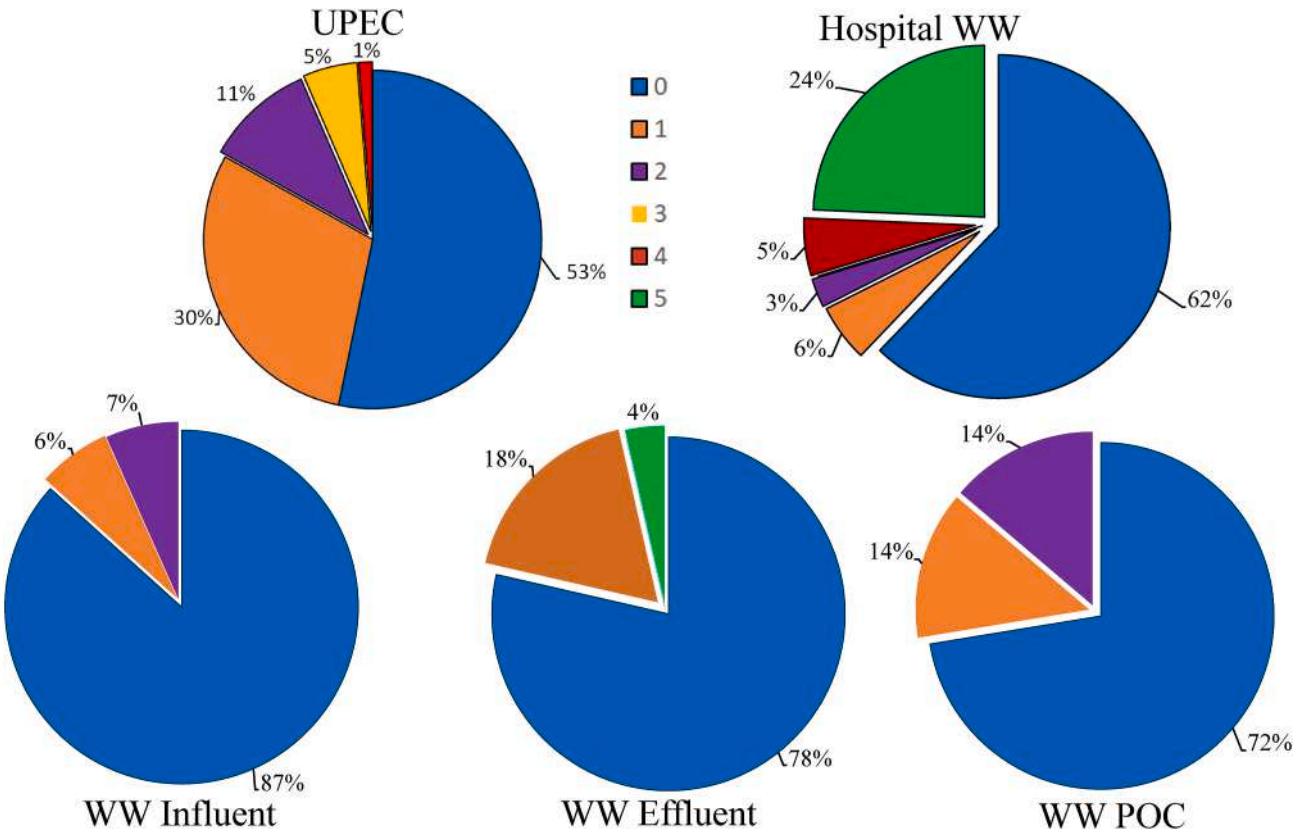

Fig. 1. Prevalence of antibiotic resistance among *E. coli* isolates. Each isolate was tested against seven different classes of antibiotics from five different environments: UPEC (n = 77), hospital WW (n = 37), urban influent WW (n = 30), pre-chlorinated effluent WW (n = 28), and POC WW (n = 29). Pie charts represent the prevalence of isolates in each source exhibiting resistance to different number of antibiotic classes represented by various colors (0–5). WW: wastewater; POC: post-chlorinated. (For interpretation of the references to color in this figure legend, the reader is referred to the Web version of this article.)

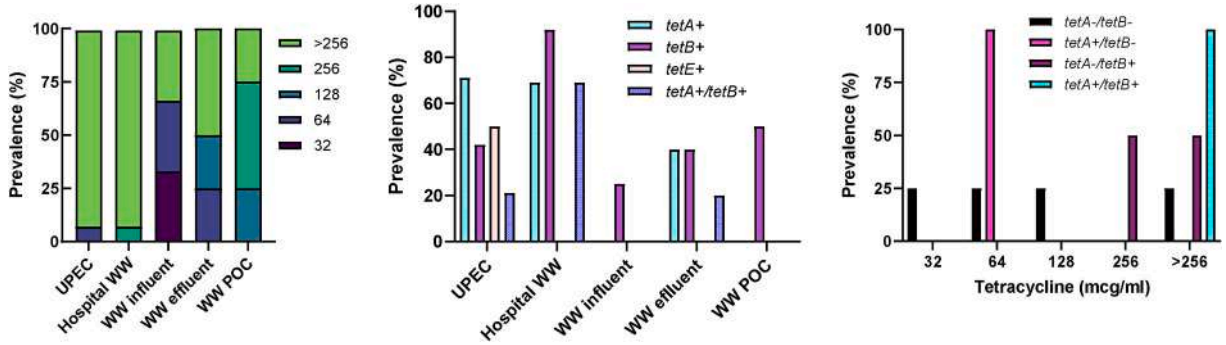

Fig. 2. Tetracycline resistance among *E. coli* populations. A) The MIC was performed among all *E. coli* tetracycline resistant isolates. Data illustrates the percentage of isolates with varying degrees of resistance in each class. B) Out of seven different tetracycline genes, only three were detected amongst the *E. coli* isolates. The prevalence of ARGs was determined amongst tetracycline resistant populations. The number of isolates resistant in each class is provided in parentheses. C) Illustrates the tetracycline MIC values according to genotype. Clinical UPEC (n = 14), hospital WW (n = 13), influent WW (n = 4), pre-chlorinated WW (n = 5), and POC WW (n = 4). WW: wastewater.

3.2. Prevalence of antibiotic resistance throughout the urban wastewater treatment process

Wastewater treatment plants typically focus on reducing the overall levels of microbial populations to minimize health risk as assessed by fecal indicators, like *E. coli*. Some wastewater reclamation facilities utilize additional disinfection steps through chlorination or ultraviolet light to further reduce bacterial loads. In this study, we assessed antibiotic susceptibility levels at different treatment stages – influent; pre-chlorinated effluents (water has passed through the primary and secondary treatment); post-chlorinated effluents (final treated water entering recipient aquatic reservoir). Initially, the untreated combined urban influent contained a mean of $1.49x10^7 \pm 2.11 \times 10^7$ CFU/100 ml of *E. coli*, which was reduced, on average, by over five logs to $6.33x10^1 \pm 8.66 \times 10^1$ CFUs/100 ml at the pre-chlorinated effluent stage. Following chlorine disinfection, the *E. coli* abundance was reduced an additional 86.3% to 8.64 ± 9.41 CFUs/100 ml (data not shown). To identify the potential impact wastewater treatment has on the development of antibiotic resistance, the prevalence of antibiotic resistance among *E. coli* populations was determined from different stages of the treatment process: influent (30 isolates), pre-chlorinated (28 isolates) and post-chlorinated effluents (29 isolates). There were minimal differences

among antibiotic resistance patterns of *E. coli* throughout the treatment process for most antibiotics; however, there was a 7-fold increase of SXT resistance after chlorination (Table 1: Influent 0%, Effluent 3.6%, POC 24.1%; $P < 0.05$), which appeared to be plasmid-mediated (Table 2 and Supplemental Figure 4). All combined urban wastewater *E. coli* isolates were susceptible to carbapenems (Table 1), although 3% of both pre- and post-chlorinated effluent populations displayed resistance to third-generation cephalosporins (Table 1 and Supplemental Table 2). Unlike the hospital isolates, multidrug resistance was only found in 1.1% of the total isolates throughout the urban wastewater samples (Fig. 1 and Table 1).

Considering the high prevalence of tetracycline resistance throughout wastewater sources, we next analyzed if there was a difference in the level of resistance to this antibiotic. Prevalence of tetracycline resistance (≥128 mcg/ml) continually increased throughout the wastewater treatment process with the highest resistance levels (100%) apparent in post-chlorinated effluents (Fig. 2A: influent 33% and pre-chlorinated effluent 80%).

3.3. ARG association with resistance phenotypes

After determining the resistant phenotypes, we identified the associated ARGs to assess if UPEC ARGs were the predominant molecular mechanism associated with resistance among wastewater populations. The most common resistance phenotype was tetracycline with all wastewater sources exhibiting greater than 13% resistance. Of seven different *tet* genes tested, *tetA* and *tetB* were the predominant ARGs among resistant isolates, although only UPEC populations encoded *tetE* as well (Fig. 2B and Supplemental Figure 2). *TetA* positive isolates were more common among hospital wastewater and UPEC isolates than urban wastewater populations (Fig. 2B: 69.2% vs 71.4% vs 15.3% respectively). Almost all hospital wastewater isolates carried *tetB* (Fig. 2B: 92.3%), which was associated with a high-degree of tetracycline resistance (Fig. 2C: ≥ 256 mcg/ml). In addition, the co-occurrence of both *tetA* and *tetB* exhibited the strongest resistance to tetracycline (Fig. 2C). Similar to resistance to SXT, resistance to tetracycline also appeared plasmid-mediated (Table 2 and Supplemental Figure 4).

Resistance to trimethoprim and sulfonamides was primarily associated with *sul1* and *sul2*. All UPEC and hospital wastewater populations carried both *sul1* and *sul2* (Supplemental Table 2 and Supplement Figure 2). SXT resistance increased after chlorine disinfection of the wastewater treatment process with 24.1% of isolates exhibiting resistance and the majority of isolates encoding *sul1* and/or *sul2* (Supplemental Figure 2: 86% vs. 57%), though only 43% had both ARG genes (Supplemental Table 2 and data not shown).

Among ESBL-carrying isolates, TEM was only identified among UPEC strains (Suppl. Figure 1: 100%). Hospital wastewater and pre-chlorinated effluent isolates all carried CTX-M-15/23 (Supplemental Figure 2 and data not shown). Among the eleven wastewater ESBL-isolates, CTX-M positive strains were more resistant than the non-CTX-M strain (Supplemental Figure 3). Resistance to third-generation cephalosporins was at least partially mediated through ESBLs encoded on plasmids (Table 2 and Supplemental Figure 4).

Class 1 integrons can contain and express resistant gene cassettes and are found on mobile genetic elements, like transposons or plasmids, aiding the widespread dissemination of ARGs (Deng et al., 2015). They are commonly found in Gram-negative bacterial populations, especially clinical strains (Deng et al., 2015). Among our samples, we identified a higher prevalence of class 1 integrases among UPEC (99%) and hospital wastewater (84%) AMR *E. coli* isolates compared to urban influents (0%), pre- (40%) and post-chlorinated effluents (33%) (Supplemental Figure 3). Molecular characterization of the variable regions of class 1 integrons identified the majority of hospital WW isolates encoded dihydrofolate reductase *dfrA17*, aminoglycoside modifying enzymes *aadA5*, *aac(3)-Ib*, and *ant(3')-IIB* (Supplemental Table 2), whereby more diversity was evident among isolates throughout the WW treatment process (Supplemental Table 2).

3.4. Phylogrouping E. coli populations from different water sources

The *E. coli sensu stricto* population is genetically quite diverse but can be categorized into seven main phylogroups (Clermont et al., 2013). These genetic substructures are not random and suggest a common bacterial host or geographical origin. In our study, phylotyping was performed to aid in assessing the potential source of *E. coli* in each sample type (Fig. 3), as well as to determine a potential correlation with various antibiotic resistant phenotypes or ARGs. Amongst UPEC strains, phylogroup B2 (72.7%) predominated, whereas phylogroup A (62.9%) and B2 (17.1%) were more common amongst hospital wastewater populations. This polarization contrasts with the heterogeneity in water sources within the wastewater treatment facility. Urban influents were populated with phylogroups E (28.6%), B1 and B2 (21.4% each), and A (14.3%), whereby the majority of treated pre-chlorinated effluents were unknown (34.5%) or A (26.9%) and B1 (21.1%). Post-chlorinated *E. coli* populations were more similar to urban influent with phylogroups E (42.9%), B2 (21.4%) and B1 (17.9%) comprising the majority.

Table 2
Resistant profiles associated with plasmids.

Strain	CHL	SXT	GEN	CIP	TET	CRO	CAZ
Hospital Effluent							
HEC-11	S	R	R	R	R	R	R
T-HEC-11	S	S	S	S	S	R	R
WW Pre-chlorinated Effluent							
EEC-3	S	S	S	S	R	S	S
T-EEC-3	S	S	S	S	R	S	S
EEC-27	S	S	S	S	R	S	S
T-EEC-27	S	S	S	S	R	S	S
WW Post-chlorinated effluent							
PEC-4	S	R	S	S	R	S	S
T-PEC-4	S	R	S	S	R	S	S

T- : transformed *E. coli* with plasmid from parental strain. Blue shading represents resistance patterns not encoded on the plasmid in the transformed cell. Orange shading represents antibiotic resistance patterns that are plasmid-mediated.

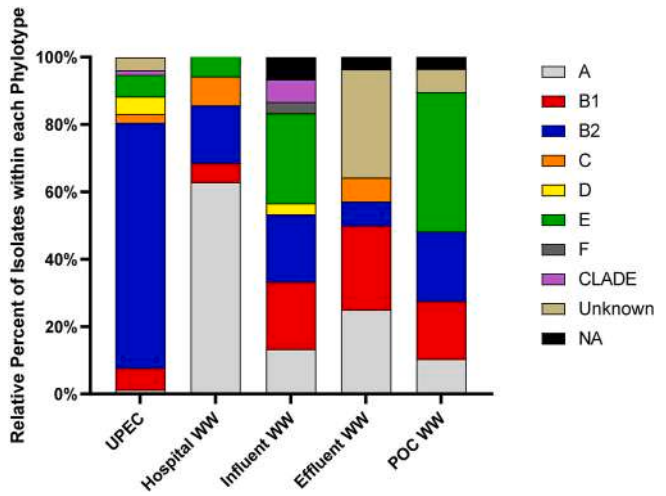

Fig. 3. Phylotyping of *E. coli* isolates from various sources. Phylogroups were determined from isolates in each class: Clinical UPEC (n = 77), hospital WW (n = 35), influent WW (n = 28), effluent WW (n = 26), and post-chlorinated effluent WW (n = 28). UPEC: uropathogenic *E. coli;* WW: wastewater; POC: post-chlorinated effluent.

Considering phylogroups of *E. coli* are associated with similar origins, we next analyzed their association with antimicrobial susceptibility patterns. All phylogroup D strains exhibited AMR, which was significantly higher than both phylogroups B1 and E (Fig. 4A, $P < 0.05$ and 0.005 respectively). However, when comparing the mean MAR indices of each phylotype population, phylotype A strains had significantly higher MAR indices than both phylotype B2 and E (Fig. 4B, $P < 0.05$ and 0.005 respectively). Considering the chlorinated effluent is entering the environment, it is notable that phylogroup B2 had the highest AMR rate compared to other phylogroups within this water source (B2: 67%; A: 33%; B1: 0%; E: 25%, data not shown). Further analyses of phylotypes and antibiotic resistance phenotypes together identified UPEC and hospital wastewater communities as significantly different from each other and most wastewater sources (Supplemental Table 3, $P < 0.05$). However, there was not a significant difference among *E. coli* populations from within the various stages of treatment (e.g. influent, pre- and post-chlorinated effluents).

4. Discussion

AMR is a leading public health concern and both municipal and hospital wastewaters have been identified as point sources of ARGs and AMR bacterial contaminants to the recipient aquatic environments. Global metagenomics analysis of wastewater has not only highlighted the diversity of ARGs associated with AMR, but also highlighted the variability between geographical regions, dependent on the Human Development Index (Hendriksen et al., 2019b). Additionally, the gut microbiomes of urban industrialized populations exhibit elevated HGT frequencies, including for ARGs (Groussin et al., 2021). Thus, there is an urgent need to perform antimicrobial susceptibility testing within defined geographic regions to better understand how ARGs are spread within urban communities, therefore highlighting the importance of this study. The novelty of our study is that it compared antibiotic resistant profiles of *E. coli* in directionally connected sites from clinical to hospital wastewater and throughout the wastewater process into the environment. We identified the highest prevalence of AMR in *E. coli* in the following order: Clinical UPEC > hospital wastewater > post-chlorinated effluents > pre-chlorinated effluents > urban wastewater influents, although, MDR and MAR index were higher in hospital wastewater populations compared to all other water sources.

The UPEC population in our study had the highest prevalence of AMR including clinically important classes of antibiotics, like fluoroquinolones, third-generation cephalosporins, aminoglycosides, and last resort antibiotics like carbapenems. Globally, AMR continues to pose significant health risks amongst both nosocomial and community-acquired infections. Both SXT and fluoroquinolones are commonly prescribed antibiotics for community-acquired urinary tract infections caused by UPEC (Yelin et al., 2019). From 1999 to 2017, Yamaji et al. identified minimal changes in SXT resistance (16.9–17.1%); however, ciprofloxacin resistance significantly increased from 0.9 to 5.1% in the United States (Yamaji et al., 2018). Our findings support the moderate level of SXT resistance (15.6%), although we observed a sharp increase in resistance to ciprofloxacin (26%) in comparison to previous reports. Considering nosocomial and community acquired urinary tract infections (UTI) are the most common healthcare-acquired and outpatient infections in the United States (Medina and Castillo-Pino, 2019), the

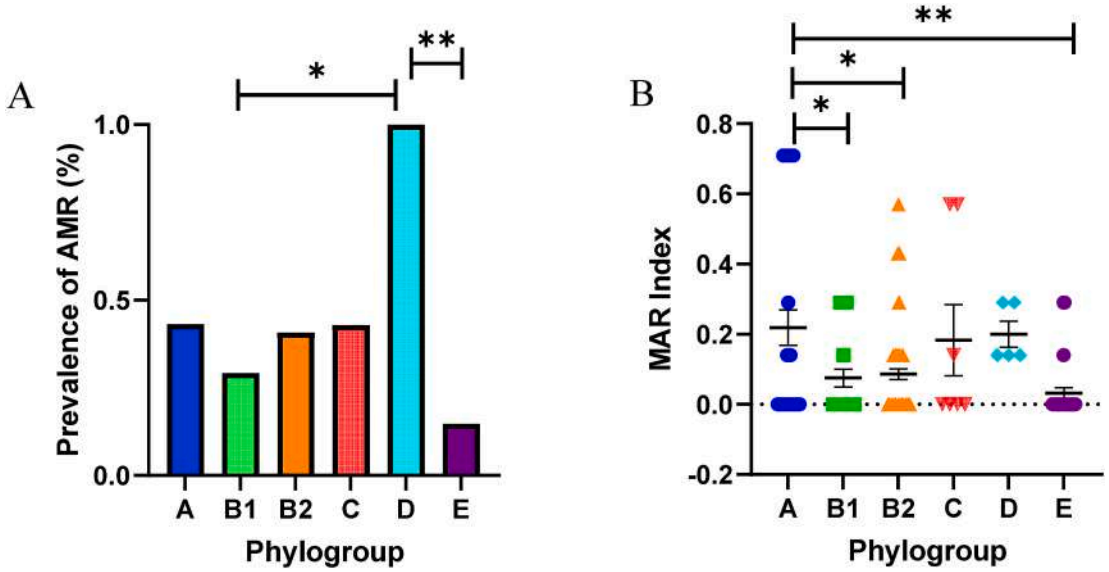

Fig. 4. Comparing antibiotic resistance between phylogroups. Data represent the mean AMR (A) and MAR index (B) among isolates within each phylogroup ± standard deviation for MAR index. The number of isolates in each phylogroup are as follows: A (n = 37), B1 (n = 25), B2 (n = 76), C (n = 7), D (n = 5), E (n = 27); *$P < 0.05$; **$P < 0.005$.

increased prevalence of AMR among UTIs (Simmering et al., 2017) contributes a significant impact on public health. Furthermore, our findings and others of ESBL- and carbapenemase-producing UPEC along with multi-drug resistant populations present serious challenges to healthcare (Mughini-Gras et al., 2019; Yelin et al., 2019).

AMR bacteria entering wastewater not only can act as a reservoir of ARGs but also can mutate or acquire more ARGs. Importantly, UPEC strains are capable of surviving wastewater treatment processes including chlorination (Anastasi et al., 2010). Indeed, 10% of chlorine-tolerant *E. coli* strains isolated from wastewater effluents contained at least two UPEC-related virulence genes (Zhi et al., 2020). Similarly to the report that the B2 phylotype predominates among UPEC strains (Yazdanpour et al., 2020), our findings demonstrates a nearly three-fold increase in B2 phylotype between wastewater pre- and post-chlorinated wastewater supports the alarming resilience of this *E. coli* population. Additionally, the MAR index and AMR rates were comparable between UPEC and post-chlorinated phylotype B2 populations.

Hospital wastewater provides a reservoir of antibiotic residues, ARGs and multi-drug resistant microbial populations, including pathogenic species (Kaur et al., 2020). Our study found *E. coli* isolates from hospital wastewater with the greatest prevalence of resistance to five of seven different antibiotic classes and over four-fold higher levels of MDR than any other tested microbial source. MAR index were 7.6 -fold higher in hospital wastewater compared to urban wastewater as well. Our findings correspond with other studies recognizing elevated resistance among hospital wastewater compared to raw urban influent (Kwak et al., 2015). The majority of the hospital wastewater strains were phylogroup A, which predominantly is associated with human commensals (Stoppe et al., 2017). Our data supports previous studies exhibiting increased prevalence of $bla_{\text{CTX-M}}$ ESBL-producing *E. coli* (Korzeniewska et al., 2013) among hospital wastewater isolates compared to urban wastewater (Paulshus et al., 2019). Multi-drug resistant patterns of ceftazidime-resistant hospital wastewater isolates were similar to other studies where they also co-occurred with gentamicin and ciprofloxacin resistance (Calhau et al., 2014), though our isolates were also co-resistant to tetracycline and SXT. These resistant populations comprise a more biochemically diverse population than susceptible populations (Kwak et al., 2015). Hospital wastewater remains a hot spot of multi-drug resistance with its origin deriving from patient populations, as well as within biofilms residing in shower heads, medical devices, plumbing systems and other surfaces (Sib et al., 2019; Soto-Giron et al., 2016).

In contrast to the high level of AMR and MDR among hospital wastewater isolates, *E. coli* from the urban wastewater treatment process exhibited antimicrobial susceptibility to most therapeutics except a consistent low-level resistance to tetracycline (13–18%). This finding might be explained with the high dilution rate of hospital wastewater into urban influent wastewater (Raven et al., 2019). Once inside the treatment facility, naturalized wastewater strains predominate (Zhi et al., 2019). Minimal differences in susceptibility patterns were observed among *E. coli* populations inside wastewater treatment pathways, except SXT resistance which peaked in post-chlorinated populations. One explanation for the low-level variation throughout the wastewater process is due to the smaller sample size (~30 isolates per source). The increase in SXT resistance in sewage *E. coli* populations is in agreement with others which identified it specifically among phylogenetic group A (Boczek et al., 2007). Our study found 57% of SXT resistant post-chlorinated effluent populations were phylogroup B2 with only 14% comprised of phylogroup A. Potential reasons for the rise in SXT resistance could be correlated with the increased resilience of the B2 phylogroup to chlorination. Although wastewater treatment processes remove greater than 99.99% of *E. coli* populations, UPEC strains appear more adapted to wastewater environments surviving throughout even chlorine disinfection (Anastasi et al., 2010; Zhi et al., 2020). The surviving population appears to be among a less diverse phylogenetic group, unlike *E. coli* populations that remain post-disinfection with ultraviolet light (Anastasi et al., 2013). Another explanation for the increased SXT-resistance in post-chlorination effluents is an increased rate of HGT. Among wastewater bacterial populations, particle-attachment is associated with increased prevalence of *sul1* and *sul2* genes (Lorenzo et al., 2018). This close proximity for extended periods favors conjugation as the HGT mechanism, which was further supported by the plasmid-mediated resistance and high prevalence of *sul1* and *sul2* among post-chlorinated isolates observed in our study. Furthermore, *sul1* is commonly found on the 3′-conserved segment of class 1 integrons (Engelstädter et al., 2016), which are linked to mobile genetic elements. Our findings support previous reports of class 1 integrons residing predominantly in clinical isolates (Deng et al., 2015) and presence in treated wastewater (Kotlarska et al., 2015), thus increasing its abundance in anthropogenic-impacted aquatic reservoirs (Koczura et al., 2016). Additionally, chlorine disinfection can damage cell-membranes releasing their genomic DNA. Together, the extracellular DNA in proximity with chlorine-damaged cells, heavy metal exposure, and elevated oxidative stress can provide ideal environments for increased cell permeability of ARGs (Jin et al., 2020) supporting natural transformation as another mechanism of HGT. Indeed, mercury concentrations have correlated positively with resistance to both tetracycline and SXT (Ferreira da Silva et al., 2007). Resistance to tetracycline and SXT were the most prevalent form of antibiotic resistance in our study and co-existed on the same plasmid. The continual presence of sub-inhibitory SXT concentrations in wastewater (Lorenzo et al., 2018; Nelson et al., 2011) provides fitness benefits for the retention and acquisition of these genes.

Wastewater is a point source of antimicrobial populations and ARGs with its release into the environment. In a different study, we found that *E. coli* from urban waterways impacted by wastewater showed a greater incidence of resistance to higher numbers of antibiotics compared to the human derived isolates (Kappell et al., 2015). The One Health approach recognizes the interconnectedness of humans, animals, and the environment. Our previous work also compared the AMR of *E. coli* sourced from these three environments and identified a greater similarity among manure and environmental populations than clinical (Beattie et al., 2020a). The current study focused on the impact of anthropogenic activity on the environment considering we characterized hospital and urban wastewater *E. coli* populations entering the aquatic environment (e.g. post-chlorinated effluents). These populations can become part of recreational surface water and sediments (Beattie et al., 2020b; Chávez-Díaz et al., 2020; Kappell et al., 2015), as well as beaches (Beversdorf et al., 2007; Shrestha et al., 2020) where they comprise even higher concentrations than nearshore waters (Palmer et al., 2020). Swimming in recreational freshwater containing *E. coli* has been linked to increased risk in acquiring AMR bacteria, including ESBL-producers (Søraas et al., 2013), UTIs (Soraas et al., 2013), as well as Shiga-toxin producing *E. coli* outbreaks (Graciaa et al., 2018b; Vanden Esschert et al., 2020). Once in surface water, they can continue to circulate through the ecosystem through aerosolized droplets (Salazar et al., 2020) and birds (Bueno et al., 2020).

5. Conclusions

This study analyzed antimicrobial resistance patterns from directionally connected sites from clinical strains (UPEC) to hospital wastewater through an urban wastewater treatment processes concluding with the final effluent entering the recipient aquatic ecosystem. Our findings identify hospital wastewater effluent *E. coli* populations with the highest MDR patterns, as well as encoding similar ARGs and *int1* compared to UPEC populations. The highest prevalence of AMR existed within UPEC populations that are predominately characterized as phylogroup B2. This phylotype was enriched among post-chlorinated effluents and contained similarly high-levels of AMR contributing to the potential health risk associated with wastewater effluents entering the

recipient aquatic environments. Longitudinal studies utilizing quantitative microbiological risk assessment tools (Derx et al., 2016) are needed to track resistance patterns and ARGs throughout connected sites to help indicate the origin posing the greatest public health impact.050.

Funding

This study was supported by funds from Department of Biomedical Sciences at the University of Wisconsin – Milwaukee, WI, USA (Skwor) and Marquette University Explorer Challenge Grant, Milwaukee, WI, USA (Hristova).

Declaration of competing interest

The authors declare no actual or potential conflict of interest with other people or organizations that might influence the associated research.

Acknowledgments

The authors would like to thank the staff of Milwaukee Metropolitan Sewage District and Jones Island Water Reclamation Facility for their assistance and cooperation in acquiring wastewater samples for the above study. Graphical abstract was created with BioRender.com.

Appendix A. Supplementary data

Supplementary data to this article can be found online at https://doi.org/10.1016/j.ijheh.2021.113863.

References

Anastasi, E.M., Matthews, B., Gundogdu, A., Vollmerhausen, T.L., Ramos, N.L., Stratton, H., Ahmed, W., Katouli, M., 2010. Prevalence and persistence of *Escherichia coli* strains with uropathogenic virulence characteristics in sewage treatment plants. Appl. Environ. Microbiol. 76, 5882–5886.

Anastasi, E.M., Wohlsen, T.D., Stratton, H.M., Katouli, M., 2013. Survival of *Escherichia coli* in two sewage treatment plants using UV irradiation and chlorination for disinfection. Water Res. 47, 6670–6679.

Baron, S., Granier, S.A., Larvor, E., Jouy, E., Cineux, M., Wilhelm, A., Gassilloud, B., Le Bouquin, S., Kempf, I., Chauvin, C., 2017. Aeromonas diversity and antimicrobial susceptibility in freshwater-an attempt to set generic epidemiological cut-off values. Front. Microbiol. 8, 9.

Beattie, R.E., Bakke, E., Konopek, N., Thill, R., Munson, E., Hristova, K.R., 2020a. Antimicrobial resistance traits of *Escherichia coli* isolated from dairy manure and freshwater ecosystems are similar to one another but differ from associated clinical isolates. Microorganisms 8.

Beattie, R.E., Skwor, T., Hristova, K.R., 2020b. Survivor microbial populations in post-chlorinated wastewater are strongly associated with untreated hospital sewage and include ceftazidime and meropenem resistant populations. Sci. Total Environ. 740, 140186.

Beversdorf, L.J., Bornstein-Forst, S.M., McLellan, S.L., 2007. The potential for beach sand to serve as a reservoir for *Escherichia coli* and the physical influences on cell die-off. J. Appl. Microbiol. 102, 1372–1381.

Boczek, L.A., Rice, E.W., Johnston, B., Johnson, J.R., 2007. Occurrence of antibiotic-resistant uropathogenic *Escherichia coli* clonal group A in wastewater effluents. Appl. Environ. Microbiol. 73, 4180–4184.

Brechet, C., Plantin, J., Sauget, M., Thouverez, M., Talon, D., Cholley, P., Guyeux, C., Hocquet, D., Bertrand, X., 2014. Wastewater treatment plants release large amounts of extended-spectrum beta-lactamase-producing *Escherichia coli* into the environment. Clin. Infect. Dis. 58, 1658–1665.

Bueno, I., Verdugo, C., Jimenez-Lopez, O., Alvarez, P.P., Gonzalez-Rocha, G., Lima, C.A., Travis, D.A., Wass, B., Zhang, Q., Ishii, S., Singer, R.S., 2020. Role of wastewater treatment plants on environmental abundance of antimicrobial resistance genes in Chilean rivers. Int. J. Hyg Environ. Health 223, 56–64.

Calhau, V., Mendes, C., Pena, A., Mendonça, N., Da Silva, G.J., 2014. Virulence and plasmidic resistance determinants of *Escherichia coli* isolated from municipal and hospital wastewater treatment plants. J. Water Health 13, 311–318.

Chávez-Díaz, L.V., Gutiérrez-Cacciabue, D., Poma, H.R., Rajal, V.B., 2020. Sediments quality must be considered when evaluating freshwater aquatic environments used for recreational activities. Int. J. Hyg Environ. Health 223, 159–170.

Clermont, O., Christenson, J.K., Denamur, E., Gordon, D.M., 2013. The Clermont *Escherichia coli* phylo-typing method revisited: improvement of specificity and detection of new phylo-groups. Environ Microbiol Rep 5, 58–65.

CLSI, 2015a. Methods for Dilution Antimicrobial Susceptibility Tests for Bacteria that Grow Aerobically; Approved Standard. CLSI Document M07-A10, tenth ed. Clinical and Laboratory Standards Institute, Wayne, PA.

CLSI, 2015b. Performance Standards for Antimicrobial Susceptibility Testing; Twenty-Fifth Informational Supplement. CLSI Document M100-S25. Clinical and Laboratory Standards Insititute, Wayne, PA.

Deng, Y., Bao, X., Ji, L., Chen, L., Liu, J., Miao, J., Chen, D., Bian, H., Li, Y., Yu, G., 2015. Resistance integrons: class 1, 2 and 3 integrons. Ann. Clin. Microbiol. Antimicrob. 14, 45.

Derx, J., Schijven, J., Sommer, R., Zoufal-Hruza, C.M., van Driezum, I.H., Reischer, G., Ixenmaier, S., Kirschner, A., Frick, C., de Roda Husman, A.M., Farnleitner, A.H., Blaschke, A.P., 2016. QMRAcatch: human-associated fecal pollution and infection risk modeling for a river/floodplain environment. J. Environ. Qual. 45, 1205–1214.

Dorevitch, S., Pratap, P., Wroblewski, M., Hryhorczuk, D.O., Li, H., Liu, L.C., Scheff, P.A., 2012. Health risks of limited-contact water recreation. Environ. Health Perspect. 120, 192–197.

Engelstädter, J., Harms, K., Johnsen, P.J., 2016. The evolutionary dynamics of integrons in changing environments. ISME J. 10, 1296–1307.

EPA, U.S.A, 2014. Method 1603: *Escherichia coli (E. coli)* in Water by Membrane Filtration Using Modified Membrane-Thermotolerant Escherichia coli Agar (Modified mTEC). United States Environmental Protection Agency, Office of Water Reference no. EPA-821-R-14-010.

Ferreira da Silva, M., Vaz-Moreira, I., Gonzalez-Pajuelo, M., Nunes, O.C., Manaia, C.M., 2007. Antimicrobial resistance patterns in Enterobacteriaceae isolated from an urban wastewater treatment plant. FEMS Microbiol. Ecol. 60, 166–176.

Graciaa, D.S., Cope, J.R., Roberts, V.A., Cikesh, B.L., Kahler, A.M., Vigar, M., Hilborn, E. D., Wade, T.J., Backer, L.C., Montgomery, S.P., Secor, W.E., Hill, V.R., Beach, M.J., Fullerton, K.E., Yoder, J.S., Hlavsa, M.C., 2018a. Outbreaks associated with untreated recreational water - United States, 2000-2014. MMWR Morb. Mortal. Wkly. Rep. 67, 701–706.

Graciaa, D.S., Cope, J.R., Roberts, V.A., Cikesh, B.L., Kahler, A.M., Vigar, M., Hilborn, E. D., Wade, T.J., Backer, L.C., Secor, E., Hill, V.R., Beach, M.J., Fullerton, K.E., Yoder, J.S., Hlavsa, M.C., 2018b. Outbreaks associated with untreated recreational water - United States, 2000-2014. MMWR Morb. Mortal. Wkly. Rep. 67, 701–706.

Hendriksen, R.S., Munk, P., Njage, P., van Bunnik, B., McNally, L., Lukjancenko, O., Roder, T., Nieuwenhuijse, D., Pedersen, S.K., Kjeldgaard, J., Kaas, R.S., Clausen, P., Vogt, J.K., Leekitcharoenphon, P., van de Schans, M.G.M., Zuidema, T., de Roda Husman, A.M., Rasmussen, S., Petersen, B., , Global Sewage Surveillance project, c, Amid, C., Cochrane, G., Sicheritz-Ponten, T., Schmitt, H., Alvarez, J.R.M., Aidara-Kane, A., Pamp, S.J., Lund, O., Hald, T., Woolhouse, M., Koopmans, M.P., Vigre, H., Petersen, T.N., Aarestrup, F.M., 2019a. Global monitoring of antimicrobial resistance based on metagenomics analyses of urban sewage. Nat. Commun. 10, 1124.

Groussin, M., Poyet, M, Sistiaga, A, Kearney, S.M., Moniz, K., Noel, M., Hooker, J., Gibbons, S.M., Segurel, L., Froment, A., Mohamed, R.S., Fezeu, A., Juimo, V.A., Lafosse, S., Tabe, F.E., Girard, C., Iqaluk, D., Nguyen, L.T.T., Shapiro, B.J., Lehtimaki, J., Ruokolainen, L., Kettunen, P.P., Vatanen, T., Sigwazi, S., Mabulla, A., Dominguez-Rodrigo, M., Nartey, Y.A., Agyei-Nkansah, A., Duah, A., Awuku, Y.A., Valles, K.A., Asibey, S.O., Afihene, M.Y., Roberts, L.R., Plymoth, A., Onyekwere, C. A., Summons, R.E., Xavier, R.J., Alm, E.J., 2021. Elevated rates of horizontal gene transfer in the industrialized human microbiome. Cell 184, 2053–2067 e2018.

Hendriksen, R.S., Munk, P., Njage, P., van Bunnik, B., McNally, L., Lukjancenko, O., Röder, T., Nieuwenhuijse, D., Pedersen, S.K., Kjeldgaard, J., Kaas, R.S., Clausen, P.T. L.C., Vogt, J.K., Leekitcharoenphon, P., van de Schans, M.G.M., Zuidema, T., de Roda Husman, A.M., Rasmussen, S., Petersen, B., Bego, A., Rees, C., Cassar, S., Coventry, K., Collignon, P., Allerberger, F., Rahube, T.O., Oliveira, G., Ivanov, I., Vuthy, Y., Sopheak, T., Yost, C.K., Ke, C., Zheng, H., Baisheng, L., Jiao, X., Donado-Godoy, P., Coulibaly, K.J., Jergović, M., Hrenovic, J., Karpíšková, R., Villacis, J.E., Legesse, M., Eguale, T., Heikinheimo, A., Malania, L., Nitsche, A., Brinkmann, A., Saba, C.K.S., Kocsis, B., Solymosi, N., Thorsteinsdottir, T.R., Hatha, A.M., Alebouyeh, M., Morris, D., Cormican, M., O'Connor, L., Moran-Gilad, J., Alba, P., Battisti, A., Shakenova, Z., Kiiyukia, C., Ng'eno, E., Raka, L., Avsejenko, J., Bērziņš, A., Bartkevics, V., Penny, C., Rajandas, H., Parimannan, S., Haber, M.V., Pal, P., Jeunen, G.-J., Gemmell, N., Fashae, K., Holmstad, R., Hasan, R., Shakoor, S., Rojas, M.L.Z., Wasyl, D., Bosevska, G., Kochubovski, M., Radu, C., Gassama, A., Radosavljevic, V., Wuertz, S., Zuniga-Montanez, R., Tay, M.Y.F., Gavačová, D., Pastuchova, K., Truska, P., Trkov, M., Esterhuyse, K., Keddy, K., Cerdà-Cuéllar, M., Pathirage, S., Norrgren, L., Örn, S., Larsson, D.G.J., Heijden, T.V.d., Kumburu, H.H., Sanneh, B., Bidjada, P., Njanpop-Lafourcade, B.-M., Nikiema-Pessinaba, S.C., Levent, B., Meschke, J.S., Beck, N.K., Van, C.D., Phuc, N.D., Tran, D.M.N., Kwenda, G., Tabo, D.-a., Wester, A.L., Cuadros-Orellana, S., Amid, C., Cochrane, G., Sicheritz-Ponten, T., Schmitt, H., Alvarez, J.R.M., Aidara-Kane, A., Pamp, S.J., Lund, O., Hald, T., Woolhouse, M., Koopmans, M.P., Vigre, H., Petersen, T.N., Aarestrup, F.M., The Global Sewage Surveillance project, c, 2019b. Global monitoring of antimicrobial resistance based on metagenomics analyses of urban sewage. Nat. Commun. 10, 1124.

Jang, J., Hur, H.G., Sadowsky, M.J., Byappanahalli, M.N., Yan, T., Ishii, S., 2017. Environmental *Escherichia coli:* ecology and public health implications-a review. J. Appl. Microbiol. 123, 570–581.

Jin, M., Liu, L., Wang, D.N., Yang, D., Liu, W.L., Yin, J., Yang, Z.W., Wang, H.R., Qiu, Z. G., Shen, Z.Q., Shi, D.Y., Li, H.B., Guo, J.H., Li, J.W., 2020. Chlorine disinfection promotes the exchange of antibiotic resistance genes across bacterial genera by natural transformation. ISME J. 14, 1847–1856.

Kappell, A.D., DeNies, M.S., Ahuja, N.H., Ledeboer, N.A., Newton, R.J., Hristova, K.R., 2015. Detection of multi-drug resistant *Escherichia coli* in the urban waterways of Milwaukee, WI. Front. Microbiol. 6, 336.

Karkman, A., Do, T.T., Walsh, F., Virta, M.P.J., 2018. Antibiotic-resistance genes in waste water. Trends Microbiol. 26, 220–228.
Kaur, R., Yadav, B., Tyagi, R.D., 2020. Microbiology of hospital wastewater. Current Developments in Biotechnology and Bioengineering 103–148.
Koczura, R., Mokracka, J., Taraszewska, A., Łopacinska, N., 2016. Abundance of class 1 integron-integrase and sulfonamide resistance genes in river water and sediment is affected by anthropogenic pressure and environmental factors. Microb. Ecol. 72, 909–916.
Korzeniewska, E., Korzeniewska, A., Harnisz, M., 2013. Antibiotic resistant *Escherichia coli* in hospital and municipal sewage and their emission to the environment. Ecotoxicol. Environ. Saf. 91, 96–102.
Kotlarska, E., Łuczkiewicz, A., Pisowacka, M., Burzyński, A., 2015. Antibiotic resistance and prevalence of class 1 and 2 integrons in *Escherichia coli* isolated from two wastewater treatment plants, and their receiving waters (Gulf of Gdansk, Baltic Sea, Poland). Environ. Sci. Pollut. Res. 22, 2018–2030.
Kummerer, K., 2009. Antibiotics in the aquatic environment–a review–part II. Chemosphere 75, 435–441.
Kwak, Y.K., Colque, P., Byfors, S., Giske, C.G., Mollby, R., Kuhn, I., 2015. Surveillance of antimicrobial resistance among *Escherichia coli* in wastewater in Stockholm during 1 year: does it reflect the resistance trends in the society? Int. J. Antimicrob. Agents 45, 25–32.
Lenart-Boron, A., Prajsnar, J., Guzik, M., Boron, P., Chmiel, M., 2020. How much of antibiotics can enter surface water with treated wastewater and how it affects the resistance of waterborne bacteria: a case study of the Bialka river sewage treatment plant. Environ. Res. 191, 11.
Lorenzo, P., Adriana, A., Jessica, S., Carles, B., Marinella, F., Marta, L., Luis, B.J., Pierre, S., 2018. Antibiotic resistance in urban and hospital wastewaters and their impact on a receiving freshwater ecosystem. Chemosphere 206, 70–82.
Magiorakos, A.P., Srinivasan, A., Carey, R.B., Carmeli, Y., Falagas, M.E., Giske, C.G., Harbarth, S., Hindler, J.F., Kahlmeter, G., Olsson-Liljequist, B., Paterson, D.L., Rice, L.B., Stelling, J., Struelens, M.J., Vatopoulos, A., Weber, J.T., Monnet, D.L., 2012. Multidrug-resistant, extensively drug-resistant and pandrug-resistant bacteria: an international expert proposal for interim standard definitions for acquired resistance. Clin. Microbiol. Infect. 18, 268–281.
Medina, M., Castillo-Pino, E., 2019. An introduction to the epidemiology and burden of urinary tract infections. Therapeutic advances in urology 11, 1756287219832172.
Mughini-Gras, L., Dorado-Garcia, A., van Duijkeren, E., van den Bunt, G., Dierikx, C.M., Bonten, M.J.M., Bootsma, M.C.J., Schmitt, H., Hald, T., Evers, E.G., de Koeijer, A., van Pelt, W., Franz, E., Mevius, D.J., Heederik, D.J.J., Consortium, E.A., 2019. Attributable sources of community-acquired carriage of *Escherichia coli* containing beta-lactam antibiotic resistance genes: a population-based modelling study. Lancet Planet Health 3, e357–e369.
Nelson, E.D., Do, H., Lewis, R.S., Carr, S.A., 2011. Diurnal variability of pharmaceutical, personal care product, estrogen and alkylphenol concentrations in effluent from a tertiary wastewater treatment facility. Environ. Sci. Technol. 45, 1228–1234.
Pal, C., Bengtsson-Palme, J., Kristiansson, E., Larsson, D.G., 2015. Co-occurrence of resistance genes to antibiotics, biocides and metals reveals novel insights into their co-selection potential. BMC Genom. 16, 964.
Palmer, J.A., Law, J.Y., Soupir, M.L., 2020. Spatial and temporal distribution of *E. coli* contamination on three inland lake and recreational beach systems in the upper Midwestern United States. Sci. Total Environ. 722, 9.
Paulshus, E., Kuhn, I., Mollby, R., Colque, P., O'Sullivan, K., Midtvedt, T., Lingaas, E., Holmstad, R., Sorum, H., 2019. Diversity and antibiotic resistance among *Escherichia coli* populations in hospital and community wastewater compared to wastewater at the receiving urban treatment plant. Water Res. 161, 232–241.
Raven, K.E., Ludden, C., Gouliouris, T., Blane, B., Naydenova, P., Brown, N.M., Parkhill, J., Peacock, S.J., 2019. Genomic surveillance of *Escherichia coli* in municipal wastewater treatment plants as an indicator of clinically relevant pathogens and their resistance genes. Microb. Genom. 5.
Rizzo, L., Manaia, C., Merlin, C., Schwartz, T., Dagot, C., Ploy, M.C., Michael, I., Fatta-Kassinos, D., 2013. Urban wastewater treatment plants as hotspots for antibiotic resistant bacteria and genes spread into the environment: a review. Sci. Total Environ. 447, 345–360.
Salazar, D., Ginn, O., Brown, J., Soria, F., Garvizu, C., 2020. Assessment of antibiotic resistant coliforms from bioaerosol samples collected above a sewage-polluted river in La Paz, Bolivia. Int. J. Hyg Environ. Health 228, 113494.
Sarowska, J., Futoma-Koloch, B., Jama-Kmiecik, A., Frej-Madrzak, M., Ksiazczyk, M., Bugla-Ploskonska, G., Choroszy-Krol, I., 2019. Virulence factors, prevalence and potential transmission of extraintestinal pathogenic *Escherichia coli* isolated from different sources: recent reports. Gut Pathog. 11, 10.
Schrijver, R., Stijntjes, M., Rodriguez-Bano, J., Tacconelli, E., Babu Rajendran, N., Voss, A., 2018. Review of antimicrobial resistance surveillance programmes in livestock and meat in EU with focus on humans. Clin. Microbiol. Infect. 24, 577–590.
Seiler, C., Berendonk, T., 2012. Heavy metal driven co-selection of antibiotic resistance in soil and water bodies impacted by agriculture and aquaculture. Front. Microbiol. 3.
Shrestha, A., Kelty, C.A., Sivaganesan, M., Shanks, O.C., Dorevitch, S., 2020. Fecal pollution source characterization at non-point source impacted beaches under dry and wet weather conditions. Water Res. 182, 10.
Sib, E., Voigt, A.M., Wilbring, G., Schreiber, C., Faerber, H.A., Skutlarek, D., Parcina, M., Mahn, R., Wolf, D., Brossart, P., Geiser, F., Engelhart, S., Exner, M., Bierbaum, G., Schmithausen, R.M., 2019. Antibiotic resistant bacteria and resistance genes in biofilms in clinical wastewater networks. Int. J. Hyg Environ. Health 222, 655–662.
Simmering, J.E., Tang, F., Cavanaugh, J.E., Polgreen, L.A., Polgreen, P.M., 2017. The increase in hospitalizations for urinary tract infections and the associated costs in the United States, 1998–2011. Open Forum Infectious Diseases 4.
Skwor, T., Stringer, S., Haggerty, J., Johnson, J., Duhr, S., Johnson, M., Seckinger, M., Stemme, M., 2020. Prevalence of potentially pathogenic antibiotic-resistant aeromonas spp. in treated urban wastewater effluents versus recipient riverine populations: a 3-year comparative study. Appl. Environ. Microbiol. 86.
Soraas, A., Sundsfjord, A., Sandven, I., Brunborg, C., Jenum, P.A., 2013. Risk factors for community-acquired urinary tract infections caused by ESBL-producing enterobacteriaceae–a case-control study in a low prevalence country. PLoS One 8, e69581.
Søraas, A., Sundsfjord, A., Sandven, I., Brunborg, C., Jenum, P.A., 2013. Risk factors for community-acquired urinary tract infections caused by ESBL-producing enterobacteriaceae –A case–control study in a low prevalence country. PLoS One 8, e69581.
Soto-Giron, M.J., Rodriguez-R, L.M., Luo, C., Elk, M., Ryu, H., Hoelle, J., Santo Domingo, J.W., Konstantinidis, K.T., 2016. Biofilms on hospital shower hoses: characterization and implications for nosocomial infections. Appl. Environ. Microbiol. 82, 2872–2883.
Stelling, J.M., Travers, K., Jones, R.N., Turner, P.J., O'Brien, T.F., Levy, S.B., 2005. Integrating *Escherichia coli* antimicrobial susceptibility data from multiple surveillance programs. Emerg. Infect. Dis. 11, 873–882.
Stoppe, N.C., Silva, J.S., Carlos, C., Sato, M.I.Z., Saraiva, A.M., Ottoboni, L.M.M., Torres, T.T., 2017. Worldwide phylogenetic group patterns of *Escherichia coli* from commensal human and wastewater treatment plant isolates. Front. Microbiol. 8, 2512.
Vanden Esschert, K.L., Mattioli, M.C., Hilborn, E.D., Roberts, V.A., Yu, A.T., Lamba, K., Arzaga, G., Zahn, M., Marsh, Z., Combes, S.M., Smith, E.S., Robinson, T.J., Gretsch, S.R., Laco, J.P., Wikswo, M.E., Miller, A.D., Tack, D.M., Wade, T.J., Hlavsa, M.C., 2020. Outbreaks associated with untreated recreational water - California, Maine, and Minnesota, 2018-2019. MMWR Morb. Mortal. Wkly. Rep. 69, 781–783.
Verburg, I., Garcia-Cobos, S., Hernandez Leal, L., Waar, K., Friedrich, A.W., Schmitt, H., 2019. Abundance and antimicrobial resistance of three bacterial species along a complete wastewater pathway. Microorganisms 7.
WHO, 2019. New Report Calls for Urgent Action to Avert Antimicrobial Resistance Crisis. World Health Organization.
Yamaji, R., Rubin, J., Thys, E., Friedman, C.R., Riley, L.W., 2018. Persistent pandemic lineages of uropathogenic *Escherichia coli* in a College community from 1999 to 2017. J. Clin. Microbiol. 56.
Yazdanpour, Z., Tadjrobehkar, O., Shahkhah, M., 2020. Significant association between genes encoding virulence factors with antibiotic resistance and phylogenetic groups in community acquired uropathogenic *Escherichia coli* isolates. BMC Microbiol. 20, 241.
Yelin, I., Snitser, O., Novich, G., Katz, R., Tal, O., Parizade, M., Chodick, G., Koren, G., Shalev, V., Kishony, R., 2019. Personal clinical history predicts antibiotic resistance of urinary tract infections. Nat. Med. 25, 1143–1152.
Young, H.K., 1993. Antimicrobial resistance spread in aquatic environments. J. Antimicrob. Chemother. 31, 627–635.
Zhi, S., Banting, G., Stothard, P., Ashbolt, N.J., Checkley, S., Meyer, K., Otto, S., Neumann, N.F., 2019. Evidence for the evolution, clonal expansion and global dissemination of water treatment-resistant naturalized strains of *Escherichia coli* in wastewater. Water Res. 156, 208–222.
Zhi, S., Stothard, P., Banting, G., Scott, C., Huntley, K., Ryu, K., Otto, S., Ashbolt, N., Checkley, S., Dong, T., Ruecker, N.J., Neumann, N.F., 2020. Characterization of water treatment-resistant and multidrug-resistant urinary pathogenic *Escherichia coli* in treated wastewater. Water Res. 182, 115827.

International Journal of Hygiene and Environmental Health 238 (2021) 113852

Contents lists available at ScienceDirect

International Journal of Hygiene and Environmental Health

journal homepage: www.elsevier.com/locate/ijheh

Are carbon water filters safe for private wells? Evaluating the occurrence of microbial indicator organisms in private well water treated by point-of-use activated carbon block filters

Riley Mulhern [a,*,1], Megan Stallard [a], Hania Zanib [a], Jill Stewart [a], Emanuele Sozzi [a], Jacqueline MacDonald Gibson [b]

[a] University of North Carolina at Chapel Hill, Gillings School of Global Public Health, Department of Environmental Science & Engineering, 135 Dauer Drive, Chapel Hill, NC, 27599, USA

[b] Indiana University, School of Public Health, Department of Environmental and Occupational Health, 1025 E. 7th Street, Bloomington, IN, 47405, USA

ARTICLE INFO

Keywords:
Private wells
Drinking water
Point-of-use
Activated carbon
Microbial risk assessment

ABSTRACT

Point-of-use (POU) water treatment is highly relevant to private well users vulnerable to chemical contamination, but uncertainty remains around the effects of activated carbon based POU devices on the microbial quality of the treated water. In this study, under-sink activated carbon block water filters were installed in 17 homes relying on private well water in North Carolina. The influent and effluent water in each home was evaluated for bacterial and viral microbial indicator organisms monthly for five months. Multiple logistic regression was used to identify water quality and water usage variables that were significant predictors of each indicator organism occurring in the filter effluent. The odds of total coliforms occurring in the effluent decreased by 84% with each 1-$\log_{10}$ increase in the influent HPC ($p < 0.05$), suggesting a protective effect by native heterotrophic bacteria, but increased by over 50 times with low cumulative water use ($p < 0.05$). The filters were not protective against coliphages in the influent and viral shedding may occur after periods of increased virus concentrations in the raw well water. Specific bacteria were also found to increase in the effluent, causing a shift in the bacterial community composition, although potential opportunistic pathogens were detected in both the influent and the effluent. Overall, under normal conditions of use, the filters tested in this study did not represent a significant additional risk for well users beyond the existing exposures from undisinfected well water alone.

1. Introduction

Private wells serve the domestic water needs of 42.5 million U.S. (Dieter et al., 2018) and over 4 million Canadian (Statistics Canada, 2017) residents. These wells are vulnerable to a range of chemical and microbial contaminants (DeSimone et al., 2009; Lesage, 2005), but neither the U.S. nor Canada has federal drinking water standards or monitoring and treatment requirements for private well water. Thus, ensuring and maintaining safe drinking water quality is the responsibility of individual well owners. In this situation, private well users may turn to activated carbon point-of-use (AC-POU) water treatment devices as a potential solution. Many consumer AC-POU treatment products advertise the removal of dozens of chemical contaminants, such as lead, volatile organic compounds, and perfluoroalkyl substances, and public information sheets provided by the U.S. Environmental Protection Agency (USEPA) and the National Ground Water Association recommend AC-POU filters as a possible treatment option for well users addressing chemical contaminants (NGWA, 2017; USEPA, 2009, 2002). Previous studies have also been dedicated to testing AC-POU devices to remove chemical contaminants from well water (Mulhern and MacDonald Gibson, 2020; Tomlinson et al., 2019).

AC-POU filters are not designed to removed microbial contaminants, however. Despite their widespread use, the USEPA and World Health Organization recommend that AC-POU filters should not be used with water of poor or unknown microbiological quality (USEPA, 2006; WHO, 2003), which includes many private wells. In a survey of 400 domestic

* Corresponding author.
E-mail address: rmulhern@rti.org (R. Mulhern).

[1] Present address: Center for Environmental Health, Risk, and Sustainability, RTI International, 3040 East Cornwallis Road, P.O. Box 12194, Research Triangle Park, NC 27709-2194 USA.

https://doi.org/10.1016/j.ijheh.2021.113852
Received 21 May 2021; Received in revised form 9 September 2021; Accepted 28 September 2021
Available online 6 October 2021

wells across the U.S., 34% were contaminated with total coliforms, a group of bacteria that can indicate potential contamination from human or animal waste (DeSimone et al., 2009). In Virginia, the prevalence of total coliforms was found to be as high as 41% ($n = 538$) (Allevi et al., 2013). Following USEPA recommendations, the manuals of consumer AC-POU devices often make explicit warnings about microbial risks and recommend not using them without disinfection or restricting use to municipally treated water.

These warnings are based on studies—mostly from the 1970s and 1980s—reporting inconsistent and sometimes contradictory results, with wide variability in influent and effluent microbial water quality. These studies found that microbial growth within AC filter cartridges and the consequent effects on effluent water quality are difficult to predict and depend on a wide range of factors, including time in operation, influent microbial population, water and ambient temperatures, seasonal trends, stagnation time, rate and frequency of faucet flushing, device design, carbon volume, pre-filter and housing material, influent nutrient load, organic content, and more (Table 1). This prior research was largely conducted on older technologies that used packed granular carbon columns, whereas most modern in-line AC-POU filters use molded or extruded carbon blocks with smaller pore sizes than granular carbon systems and less surface area for microbial growth (CBTech, 2019). More recent studies have shown that even modern AC-POU filters can be colonized by certain bacteria in municipal tap water and that preferential flow paths exist through which bacteria can pass directly from the influent to the effluent (Wu et al, 2017, 2021). Only two studies have tested AC-POU filters on private well water (Fiore and Babineau, 1977; Snyder et al., 1995), and none have assessed the occurrence of coliphages in these systems as a viral indicator of groundwater contamination and health risk (Jofre et al., 2016). As a result, uncertainty remains around whether modern AC-POU treatment products are safe to use with private wells where the influent water is not guaranteed to be microbiologically safe. This knowledge gap generates considerable confusion around best management practices for private well water and likely deters well users from adopting treatment for chemical risks. Recommendations around private well stewardship are focused on encouraging the adoption of testing, treatment, and mitigation behaviors (Flanagan et al., 2018; Malecki et al., 2017; Mulhern et al., 2022),

Table 1
Review of selected studies conducted on the microbial effects of activated carbon point-of-use filters.

Study	Water source	Filter type	Study setting	Length of test	# of designs tested	# of filters tested per design	Influent HPC (CFU/mL)	Max effluent HPC (CFU/mL)	Factors affecting filter colonization
Wallis et al. (1974)	Municipally treated tap	Tap-mounted	Lab	6 days	1	1	1	70,000	Time in operation, concentration of assimilable organic carbon within filter
Fiore and Babineau (1977)	Municipally treated tap and 1 private well	Under-sink	Lab and Household	11 weeks	1	6	10 - 300,000	300 - 35,000	Stagnation time, faucet flushing
Taylor et al. (1979)	Municipally treated tap	Under-sink	Lab	24 weeks	4	1	<100	>10,000	Temperature, carbon surface area, flow volume and velocity, time of sampling, influent bacterial population, chlorine removal efficiency of the filter
Tobin et al. (1981)	Municipally treated tap	Under-sink and tap-mounted	Lab	55 days	3	2	First-draw: 9,500 Flushed: 160	First draw: 162,000 Flushed: 8,000	Time in operation (flow rate not significant)
Regunathan et al. (1983)	Municipally treated tap	Under-sink	Lab	30 days	1	2	<1–330,000	66,000	Stagnation time (no relation between influent and effluent plate counts)
Bell et al. (1984)	Municipally treated tap and untreated groundwater	Various	Lab	5 days	10	Variable, 29 total	10-14,000	350,000	Stagnation time
Geldreich et al. (1985)	Municipally treated tap, dechlorinated	Under-sink	Lab	12 months	4	1	49 - 17,000	84 - 530,000	Time in operation, filter design, time of day, water temperature, competition/inhibition from other bacteria
Reasoner et al. (1987)	Municipally treated tap, dechlorinated	Under-sink	Lab	12 months	7	1	<10,000	260,000	Time of day, faucet flushing, season, temperature, disinfectant residual, unit design, carbon volume, prefilter/cartridge composition, influent bacteria
Snyder et al. (1995)	Private wells and springs	Under-sink	Household	12 months	1	24	<500	First draw: 5,000 Flushed: 300	Influent bacteria, faucet flushing, stagnation time, nutrient load
Chaidez and Gerba (2004)	Municipally treated tap	Under-sink	Household	6 weeks	1	10	$10–5 \times 10^4$	$100–4 \times 10^7$	Organic content, influent water quality, distribution system contamination
Su et al. (2009)	Municipally treated tap	Tap-mounted	Lab	37 days	1	3	20	205	Flow rate, temperature, volume treated per day
Wu et al. (2017)	Municipally treated tap	Tap-mounted	Lab	67 days	1	6	>1,000	>100,000	Presence of chlorinated phenol-based disinfection by-products, presence of pre-filter fabric, operation mode
Wu et al. (2021)	Municipally treated tap	Tap-mounted	Lab	29 days	2	2	N/A	N/A	Filter design (flow path diameter, hydraulic shear, carbon block permeability), bacterial species-specific adaptations

yet in the relative absence of targeted studies to characterize the microbial risks of AC-POU treatment on non-municipally treated water, current knowledge is insufficient to adequately inform health-protective best practice for private well users.

Thus, the goal of this research was to compare the occurrence of bacterial and viral indicator organisms in the influent and effluent of AC-POU water filters installed in households on private wells and to evaluate significant water usage and water quality predictors of indicator organism occurrence in the filter effluent. This improved understanding of factors influencing microbial risk provides actionable information for well users, public health practitioners, and policymakers regarding best practices for the safety of POU treatment for private well water.

2. Materials and methods

2.1. Study area and recruitment

This study was conducted under real-world conditions in 17 homes with private wells. Participant recruitment for this study has been described previously (Mulhern and MacDonald Gibson, 2020). Briefly, households were recruited from neighborhoods in Orange County and Robeson County, North Carolina, located in three geographic clusters (A, B, and C; Fig. S1). Cluster A is a non-agricultural, suburban area 1–2 km southwest from the Orange County landfill. Clusters B and C in Robeson County are peri-urban, mixed-use areas near agricultural activities and confined swine and poultry feeding operations. These areas are also flood-prone and were heavily impacted by hurricanes Matthew in 2016 and Florence in 2018. All wells were within 150 feet of a septic system, and five had surface elevations downgradient of the septic tank (household-specific information is available in Table S1). Households were recruited by e-mail, word-of-mouth, and outreach by community partners. This study was approved by the University of North Carolina at Chapel Hill (UNC) Institutional Review Board (IRB Study No. 19–1015).

2.2. POU treatment system design

As described previously, an AC-POU water filter was installed in-line below the primary kitchen sink in each household in October–November 2019 (Mulhern and MacDonald Gibson, 2020). The selected filter (A.O. Smith, AO-MF-ADV) is widely available at national hardware stores for $100 and is certified to reduce aesthetic impurities under NSF/ANSI 42 and certain contaminants of health concern, including lead, under NSF/ANSI 53, and two perfluoroalkyl substances under NSF P473. The device is composed of an extruded AC block without a prefilter membrane or fabric and is designed to treat the full flow of cold water at the tap, up to 5.67 L per minute. The manufacturer recommends that the filter cartridge be replaced every six months. Sample ports were installed at the filter influent and effluent underneath the sink such that the effluent sample had no interaction with the faucet fixture or aerator (Fig. S2). A flow sensor (Sea YF-S201 or Gredia GR-301) and data logger (Onset Hobo State Logger) were integrated into each system to capture water usage patterns.

2.3. Monthly sampling

Water samples were collected at the filter influent and effluent monthly from October 2019 to March 2020. Samples were collected in 500 mL sterile HDPE or polypropylene bottles. Before sampling, the sample ports were disinfected with 70% isopropyl alcohol and allowed to dry for a minimum of 30 s. Influent and effluent ports were then flushed for 10 s prior to sample collection to clear the tubing leading to the sample port and ensure the sample was representative of the true influent and effluent. To ensure proper aseptic procedures, samples were collected at the time of the researcher's visit, meaning that each filter was sampled at a different time of day with varying levels of use and stagnation before sampling. Influent and effluent pH, temperature, and electrical conductivity were measured at the time of sample collection using a handheld probe calibrated daily (Hanna Instruments, HI98219). After sample collection, all bottles were placed on ice and transported to UNC–Chapel Hill within six to 8 h and stored at 4 °C until analysis. Most samples were processed within 24 h, with some samples held for up to 48 h based on USEPA guidelines (USEPA, 2001).

2.4. Water quality analyses

2.4.1. Culture-based indicator organisms

Bacterial indicator tests included general indicators of sanitary quality including heterotrophic plate count (HPC) and total coliforms, as well as presumptive *E. coli* as a fecal-specific indicator. Total coliforms and *E. coli* were measured by a USEPA approved enzyme substrate test (Colilert IDEXX, Westbrook, ME) according to Standard Method 9223 (APHA et al., 2018a). Concentrations were recorded as most probable number (MPN) per 100 mL. HPC testing was performed in duplicate via spread-plate using R2A agar according to Standard Method 9215C (APHA et al., 2018b). Volumes of 0.1 mL were aseptically spread on R2A, and Petri dishes were then covered and incubated at room temperature for 5–7 days. R2A plates were counted manually and reported as CFU per mL. According to the method, high results (>10 colonies/cm^2) were estimated by counting four representative 1 cm^2 squares, taking the average count per square, and multiplying by the plate area. HPC results were analyzed for quantitative variations in plate count and qualitative changes in morphology and color according to Standard Method 9215C (APHA et al., 2018b) and previous assessments of HPC changes in drinking water (Oguma et al., 2018). The number of different colony colors on each plate was quantified as an estimate of the sample richness to characterize changes in alpha-diversity after treatment.

For viruses, F-specific coliphages were selected as the indicator of choice as they can be shed in human feces, are similar in size and morphology to human enteric pathogens, and exhibit similar mechanisms of transport and survival in soils and groundwater (Jofre et al., 2016; Leclerc et al., 2000). Viruses can also be more persistent and migrate further than bacterial pathogens in groundwater and thus may occur in the absence of bacterial indicators (Borchardt et al., 2003; Leclerc et al., 2000; Ogorzaly et al., 2010). F-specific coliphage were enumerated using a single-agar layer assay adapted from USEPA Method 1602 (USEPA, 2001). Briefly, the male-specific coliphage host (*E. coli* Famp, ATCC#700891) was incubated until it reached exponential-phase growth and added to 100 mL of sample pre-mixed with 0.5% magnesium chloride. The sample/host mixture was then combined with 100 mL of 2X tryptic soy agar (TSA) containing ampicillin/streptomycin antibiotic to minimize contamination risks. The sample was mixed and divided into approximately equivalent volumes on five sterile 150 × 15 mm Petri dishes and incubated at 36.5 ± 0.5 °C for 18–24 h before enumeration. The number of plaques in each plate was summed to give the total number of plaque forming units (PFU) per 100 mL of sample. A method blank using 100 mL of sterile deionized water was included in each batch for quality control. Low levels were detected in the method blanks of some batches (<5 PFU/100 mL) and the blank values were subtracted from the sample result.

2.4.2. Bacterial speciation

Ten colonies occurring on R2A plates that were representative of the dominant colors and morphologies were selected for speciation from six different samples (three influent and three effluent samples). Briefly, colonies were streaked to isolation on TSA, then inoculated into 1X tryptic soy broth (TSB) and incubated at 36.5 ± 0.5 °C. A 500-μL aliquot of the inoculated TSB was mixed with 500 μL of 40% glycerol and sterile water (to achieve a 20% glycerol concentration in the frozen sample), vortexed, and stored at −80 ± 10 °C before sequencing. In some cases, colonies did not grow on TSA and were picked from the R2A plates and inoculated into TSB as above. Glycerol stock solutions were sent to a

commercial laboratory for DNA sequencing and taxonomical identification (MR DNA, Shallowater, Texas). The Supporting Information (SI) provides details on the sequencing method.

2.5. Data analysis

Differences between paired influent and effluent samples for each microbial indicator were analyzed using Wilcoxon signed rank tests (McDonald, 2014). The appropriateness of the Wilcoxon signed rank test was determined by visually inspecting the histogram of the differences between paired sample points for each microbial analyte for approximate symmetry and verified by the Shapiro-Wilk test. To calculate log-removals, households with no detectable indicator organisms for any of the assays were assigned a value of one-half the theoretical detection limit (0.5 MPN/100 mL for total coliforms, 5 CFU/mL for HPC, and 0.5 PFU/100 mL for coliphages).

Multiple logistic regression models were constructed to identify predictors of the odds of each microbial indicator organism occurring in the filter effluent. All models were developed in the software RStudio (R version 4.0.3). Table S2 lists the predictor variables evaluated. A searching algorithm was used to select the best models according to the Akaike information criterion (Calcagno, 2020). Significance of predictor variables selected by the algorithm was assessed using Wald tests. Insignificant predictors ($p > 0.05$) were removed in a stepwise fashion to reduce model complexity. Predictor variables included in the final model were assessed for multicollinearity using the variance inflation factor and for approximate linearity with the logit of the outcome variable. The random effects of the clustering of data points by household and geographic area were also tested in mixed-effects logistic regression models (Bates et al., 2015). Mixed-effects models were found to result in a zero variance for the household and geographic cluster variables, with negligible effects on the model coefficients, and the structure of the model was reduced to drop the random effects.

3. Results and discussion

3.1. Occurrence of microbial indicator organisms in filter effluent samples

3.1.1. Total coliforms

Of 66 filter effluent samples collected over the course of the study, five (7.5%) tested positive for total coliforms, representing three of 17 (17.6%) AC-POU filters with a positive total coliform result in the effluent at any time during the study (Table 2). No influent or effluent samples tested positive for *E. coli*. The five positive total coliform results in effluent samples ranged 1–2,203 MPN/100 mL. Of these five samples, none of the paired influent samples were positive for total coliform. Six influent samples (9.1%) also tested positive for total coliform (ranging 1–101 MPN/100 mL) during the study, but none of the paired effluent samples had detectable coliform bacteria, potentially due to removal of particle-associated bacteria by size exclusion.

Table 2
Summary of influent and effluent water quality across all 17 households over the course of the study.

Sample location	Analyte	All households *n* households = 17, *n* paired samples = 66			
		mean	*sd*	*range*	*% positive*
Influent	pH	4.93	1.18	3.53–7.35	–
	Temp (°C)	16.7	3.39	9.9–23.4	–
	Electrical Conductivity (μS/cm)	172	128	43–485	–
	HPC (CFU/mL)	1498	4258	<10–25792	82%
	Total Coliforms (MPN/100 mL)	3.40	15.6	<1–101	9.1%
	F+ coliphage (PFU/100 mL)	4.5	6.4	<1–33	55%
Effluent	pH	5.9	1.2	3.6–8.4	–
	Temperature (°C)	18.0	4.3	9.5–28.7	–
	Electrical Conductivity (μS/cm)	166	121	47–461	–
	HPC (CFU/mL)	924	1342	5–9760	97%
	Total Coliforms (MPN/100 mL)	39.6	273	<1-2203	7.5%
	F+ coliphage (PFU/100 mL)	3.5	5.4	<1-30	53%

3.1.2. Heterotrophic plate count

Heterotrophic bacteria were nearly ubiquitous in both the filter influent and effluent throughout the study; 82% of all influent samples and 97% of all effluent samples had detectable HPC (Table 2). HPCs showed wide variability between households and time points. Influent HPCs ranged <10–25,792 CFU/mL (median = 108). Mean influent HPC was notably greater in households in cluster A (mean = 5,307 CFU/mL) than in B (mean = 536 CFU/mL, unpaired Wilcoxon $p < 0.0005$) or C (mean = 353 CFU/mL, unpaired Wilcoxon $p = 0.057$; Table S3). Two households consistently had no detectable influent HPC but had detectable HPC in the effluent (ranging 15–1,850 CFU/mL). Overall, HPC bacteria in the effluent ranged 5–9,760 CFU/mL (median = 653). By comparison, effluent HPCs from AC-POU filters treating municipally treated tap water have been recorded 2–3 orders of magnitude greater than these levels (Bell et al., 1984; Chaidez and Gerba, 2004; Geldreich et al., 1985; Wallis et al., 1974; Wu et al., 2017). This may be a function of older filter technologies using granular AC media rather than AC blocks and/or whether the device contains a cloth pre-filter providing additional surfaces for microbial growth. Effluent concentrations were not significantly different between geographic clusters ($p > 0.05$) despite significant differences in the influent concentrations. A statistically significant increase in effluent HPCs was observed in cluster C where influent HPCs were lower ($p < 0.001$), but not in clusters A or B (Fig. 1).

3.1.3. F-specific coliphages

In contrast to the infrequent detections of total coliforms in the filter effluents, 35 of 66 effluent samples (53%) tested positive for F-specific coliphage (concentration range of 1–30 PFU/100 mL; Table 2). Prevalence in the filter influent was similar, with 35 of 64 samples (55%) having detectable coliphage. These viruses were detected in 16 of 17 homes (94%) at least once during the study, indicating that nearly all wells were vulnerable to some form of microbial contamination (Stallard et al., 2021). The small size of virus particles (<100 nm (Lute et al., 2004)) also allows them to easily pass through filter pores. When paired samples from all households and time points were aggregated, a statistically significant reduction in the effluent concentrations was detected ($p < 0.05$), but the effect size was small (Fig. S3). The mean concentration decreased by only 1 PFU/100 mL after treatment (0.11-$\log_{10}$ reduction), and the median influent and effluent concentrations were equivalent (1 PFU/100 mL). Of the cases with coliphages in the influent, 83% had a lower effluent concentration, with removals ranging from 0.04- to 1.25-$\log_{10}$. However, effluent concentrations increased in 22% of paired samples, representing negative log reductions from −0.22- to −1.45-$\log_{10}$. Thus, a slight attenuation of influent viral coliphage was observed overall, but removal was generally not meaningful to health protection and was highly variable across settings.

3.2. Changes in bacterial diversity

The type and diversity of colonies on R2A plates in the effluent were generally distinct from those in the influent. Among all 66 influent samples, white and cream-colored colonies were the most frequently observed on the R2A plates across all three clusters, with 76% ($n = 50$) of all influent plates containing at least one white or cream colored colony (Fig. 2, panel A). White and cream-colored colonies isolated from three separate influent plates were identified as *Ralstonia picketti*

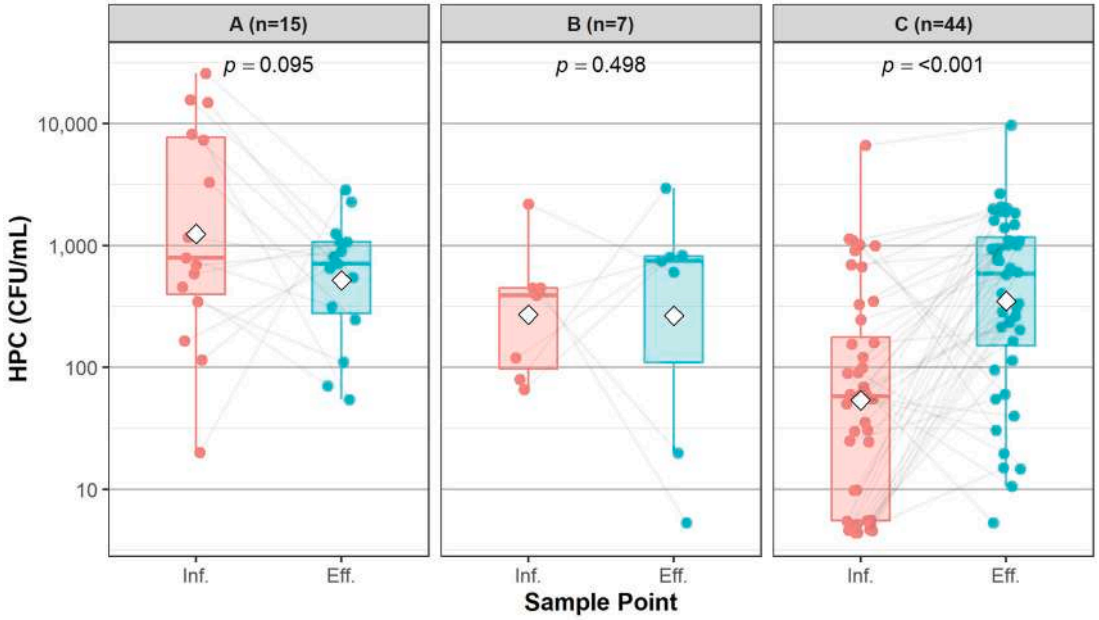

Fig. 1. Paired influent and effluent HPCs (CFU/mL) in each geographic cluster showing a significant increase in effluent HPC in cluster C but not in clusters A or B. *p* values represent the result of paired, non-parametric Wilcoxon signed rank tests.

(previously Pseudomonas pickettii) and *Bacillus circulans*, respectively. *R. picketti* and *Bacillus* spp. Have been implicated in drinking water biofilm formation in diverse environments ranging from industrial and laboratory-based ultrapure water systems to the space shuttle (Adley et al., 2005; Gardner and Shulman, 1984; Koenig and Pierson, 1997; Kulakov et al., 2002). These species have also been recognized as opportunistic pathogens associated with nosocomial infections (Alebouyeh et al., 2011; Logan et al., 1985; Ryan et al., 2006). Transparent colonies on influent plates were most likely *Aquabacterium commune*, a bacteria found in biofilms in drinking water utility distribution systems, but not known to be a human pathogen (Kalmbach et al., 1999). Table S4 provides DNA sequence BLAST results.

In contrast, yellow colonies were most frequently observed in the 66 effluent plates, with 35% ($n = 23$) of plates having at least one yellow colony (compared to only 14% of influent plates with yellow colonies), followed by white and cream-colored colonies (Fig. 2, panel B). Four yellow colonies, selected from three effluent plates, were separately isolated. Two of the four were identified as *Sphingomonas paucimobilis,* and the other two were *Cellulomonas xylanilytica,* and *Staphylococcus capitis*. *Sphingomonas* spp. (also previously included in the genus Pseudomonas) are found in a wide range of aqueous and terrestrial environments with a unique ability to survive in low-nutrient environments and biodegrade organic contaminants (White et al., 1996). *S. paucimobilis* has been identified in biofilms in household settings (such as on shower curtains) and in drinking water in diverse scenarios together with *R. picketti* (Adley et al., 2005; Kelley et al., 2004; Koenig and Pierson, 1997; Kulakov et al., 2002). It has been detected in water supplies in clinical settings and is considered an emerging opportunistic pathogen (Ryan and Adley, 2010). *Staphylococcus* spp. Have also been detected in water supplies, including household taps served by private wells (Lamka et al., 1980; Lechevallier and Seidler, 1980), and as human pathogens in clinical settings (Cameron et al., 2015).

Other species, producing pink, red, and orange colonies, also appeared in some effluent plates (pink colonies were observed in 6% of effluent plates, while red and orange were each observed in 5% of effluent plates) even when they were not present in any of the paired influent samples (Fig. 2). Pink colonies were identified as *Paenibacillus provencensis*, and orange colonies were *Rhodococcus corynebacterioides*, both occurring in a wide range of aqueous and terrestrial environments (Carrasco et al., 2017; Kitamura et al., 2012). Overall, the median number of distinct colors identified on effluent plates increased significantly compared to influent plates (2 in influent vs. 3 in effluent, $p < 0.0001$; Fig. S4). This increase in diversity (richness) was independent of whether the overall HPC increased or decreased in the effluent (Fig. 2).

3.3. Potential factors influencing the occurrence of microbial indicator organisms in filter effluent

3.3.1. Total coliforms

3.3.1.1. Low influent HPC. Low influent HPC appears to have been a factor in allowing total coliform bacteria to proliferate within the filter media in certain households. Four of the five effluent samples that were positive for total coliforms were from filters treating well water with less than the HPC sample median (100 CFU/mL), and all were below the sample mean (1,571 CFU/mL). Evidence from previous research supports the hypothesis that HPC bacteria play a role in preventing the colonization of AC by total coliforms. Camper et al. (1985) demonstrated that when the human enteric pathogens *Yersinia entercolitica*, *Salmonella typhimurium*, and *Escherichia coli* were introduced to virgin granular AC columns in sterile water, all three organisms could form stable biofilms on the AC surface. When the pathogens were introduced to the sterile AC columns together with HPC bacteria, however, the pathogens attached to the carbon surface as before but then rapidly decreased. Similarly, Reasoner et al. (1987) showed that, among AC-POU devices inoculated with bacterial pathogens, including *Klebsiella pneumoniae* and *Aeromonas hydrophila*, the device with the greatest HPC growth demonstrated the most resistance to pathogenic colonization. In more recent experiments using modern AC-POU filters challenged by tap water spiked with *E. coli* and *Pseudomonas aeruginosa*, Wu et al. (2021) demonstrated that *E. coli* was less able to adapt to the filter environment than *P. aeruginosa* and was likely outcompeted by other microorganisms in the filter influent.

Similar behavior was observed in household #16 in this study, which had no detectable HPC bacteria in the influent (<10 CFU/mL) and total coliform concentrations as high as 2,203 MPN/100 mL in the effluent after 10 days of use. As a suspected biofilm formed on the carbon surface, shown by the elevated effluent HPCs, the total coliform

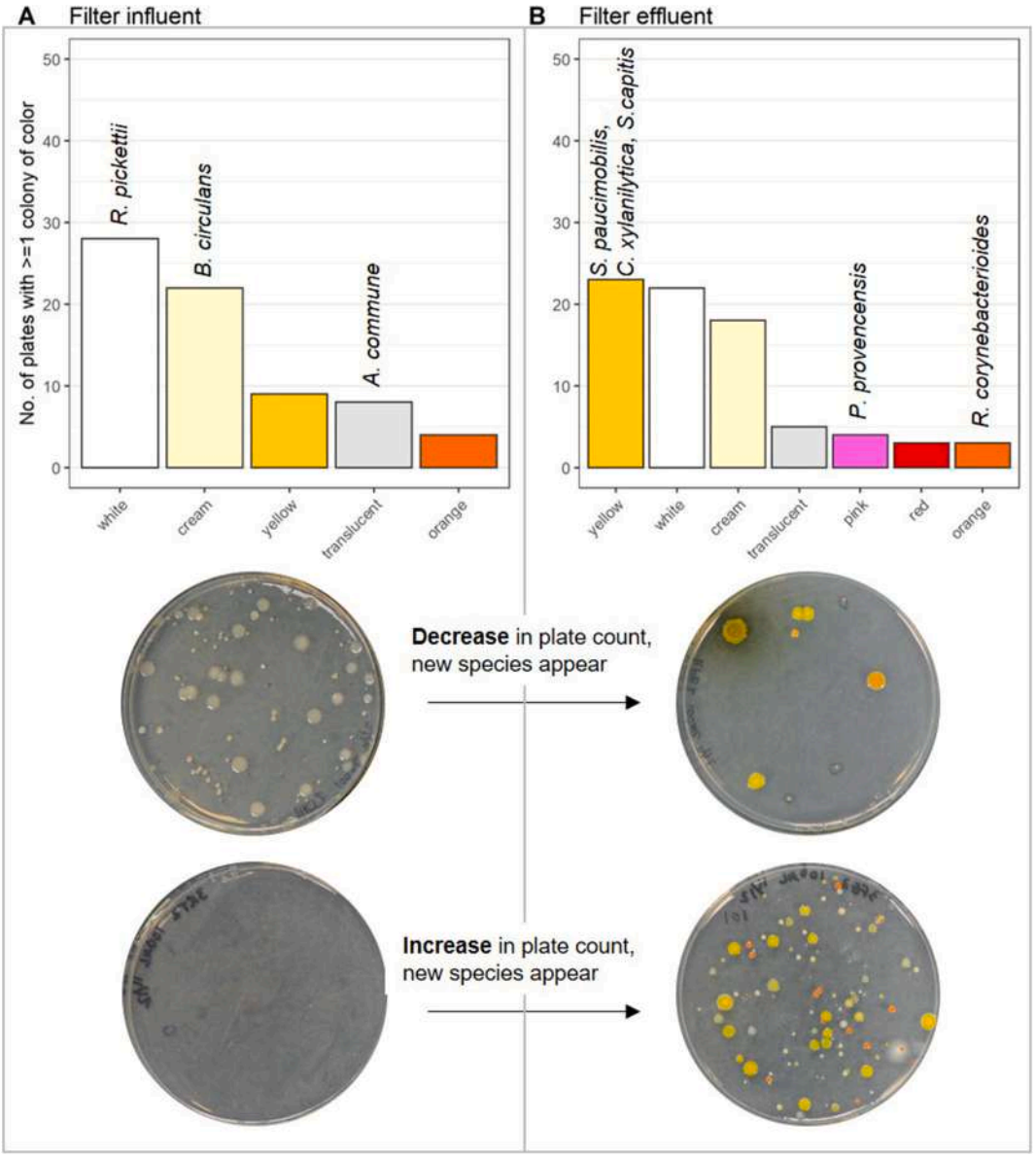

Fig. 2. Frequency of color descriptions of colonies on HPC plates in all filter influent and effluent samples over the course of the study. Increases in diversity (richness) were observed in cases where the overall effluent HPC both increased and decreased. (For interpretation of the references to color in this figure legend, the reader is referred to the Web version of this article.)

concentration in the effluent declined exponentially while the effluent HPC remained elevated (Fig. 3). Thus, colonization of the filter by native heterotrophic bacteria may be protective against the proliferation of coliforms and potential enteric pathogens in the filter media. The multiple logistic regression results from all households confirmed that the influent HPC concentration influenced the risk of total coliforms appearing in the effluent such that each 1-$\log_{10}$ increase in the influent HPC decreased the odds of total coliforms appearing in the effluent by 84% (OR = 0.16, 95% CI: 0.01–0.67, $p < 0.05$) after controlling for cumulative water use (Model 1, Table 3).

3.3.1.2. Low water use. In all three households with coliforms in the effluent, positive samples were only detected in the first few weeks after the filter was installed. In household #16, the total coliform concentration was highest after 10 days (35 L) of use and decreased exponentially (Fig. 3), while in the other two households (#15 and #9), concentrations of 6 and 1 MPN/100 mL were detected after 11 and 18 days (34 and 62 L) of use, respectively, and were not detected again thereafter, suggesting that the risk of coliform bacteria may be highest in the absence of a significant autochthonous bacterial community soon after filter start-up. This risk may be exacerbated by low water use. Household #16, for example, demonstrated an extremely low rate of water use from the cold water tap in the first 10 days (1 L/day after the initial flushing at start-up, compared to the study average of 7.6 L/day) due to the household's primary reliance on bottled water for most domestic needs, which likely allowed for excessive proliferation of bacteria in the first few days. As a result, the filter in household #16 clogged prematurely, after just 150 L (approximately 40 days) of use (5% of the filter's stated capacity). The maximum flow rate dropped from 3.2 L/min at start-up to 1.3 L/min after 10 days of low use and became unusable after 40 days.

Under laboratory-controlled conditions, Su et al. (2009) showed that low daily use rate and low flow rate both increased the amount of bacterial growth in faucet-mounted AC-POU filters and decreased the filter's lifespan. A use rate as low as 6 L/day reduced the filter's capacity by 26%, and flow rates below 1 L/min increased HPCs in the effluent by

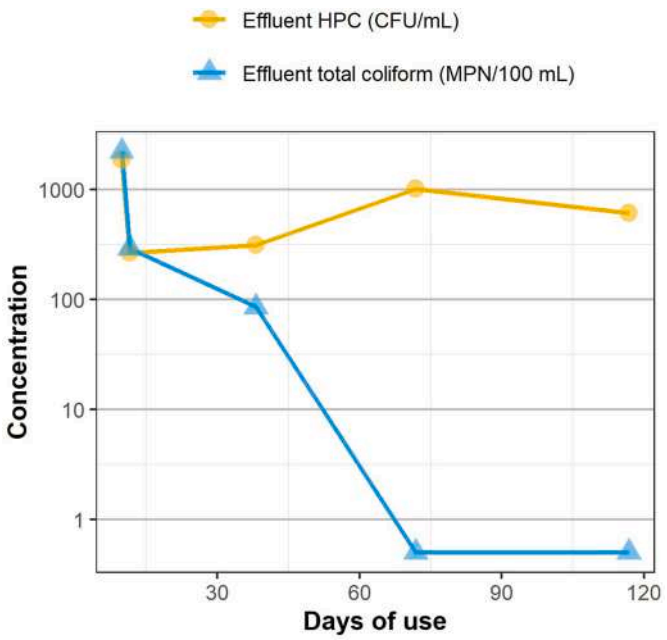

Fig. 3. Effluent concentrations of total coliform bacteria (CFU/100 mL) and HPC (CFU/mL) over four months of use from the filter in household #16.

Table 3
Summary of logistic regression results identifying significant predictors of microbial indicator organisms occurring in the filter effluent.

	OR	95% CI	*p*-value
Model 1: Presence of total coliforms in effluent			
Log_{10} Influent HPC	0.16	0.01 - 0.67	<0.05
Cumulative water usage less than 50 L	51	4–3788	<0.05
Model 2: Increase in effluent HPC			
Log10 Influent HPC	0.17	0.06 - 0.38	<0.001
Cumulative water use (L)	1.00	0.99 - 1.00	0.32
Model 3: Presence of coliphage in effluent			
Duration of filter use (weeks)	1.18	1.05 - 1.36	<0.01
Influent coliphage concentration	1.28	1.07 - 1.66	<0.05
Cumulative water use (L)	0.99	0.99 - 1.00	0.73

up to a factor of 3.5. Coliforms may have been introduced to the filter in household #16 during installation or from unsanitary conditions within the household plumbing and allowed to multiply rapidly due to the lack of use and low influent HPC to prevent their initial growth. Across all households, cumulative water use at the time of sampling influenced the risk of total coliforms in the effluent such that early in the filter's life (less than 50 L of water treated), the odds of total coliform occurrence in the effluent increased by 50 times (OR = 51, 95% CI: 3.8–3788, $p < 0.05$) after controlling for influent HPC (Model 1, Table 3). No other water usage or water quality variables, including maximum flow rate, average daily flow rate, influent pH, temperature, or presence of F-specific coliphages and total coliforms in the influent, were significant predictors of coliform detection in the effluent.

3.3.2. Heterotrophic bacteria

3.3.2.1. Bacterial selection. The filters in this study were selective for species that form suspected biofilms on the carbon surface and outcompete other bacteria for nutrients and attachment sites. Oligotrophic species that are capable of surviving in the low-nutrient environments that may occur during long stagnation periods may persist or increase in the effluent, while other species that are inhibited by competing species may decrease (see Wu et al., 2021). Although it is now generally assumed that AC-based devices increase HPCs in the filter effluent (USEPA, 2006), the results of this study suggest that it may be more accurate to consider microbial growth within AC-POU filters treating private well water as a shift in the composition of the microbial flora, depending on myriad environmental and design factors, rather than as a strict increase or decrease in the microbial load.

In this study, the bacterial diversity (richness) of R2A plates increased in the filter effluent (Fig. S4), but in other AC-POU filter tests conducted with municipally treated tap water, the overall bacterial richness decreased (Wu et al., 2017). Thus, diversity changes across the filter may also be a function of source water type and the presence of a disinfectant residual. Regardless, the proliferation of heterotrophic bacteria within AC-POU filters is a highly unpredictable process with complex effects on microbial diversity. Depending on the autochthonous bacterial community in the raw well water, other influent water quality parameters, and household usage patterns, the overall effluent plate count may change significantly in either direction, even after flushing. In cluster C, where influent plate counts were lower, there was a 926% increase in the median effluent concentrations (median influent = 58 CFU/mL compared to median effluent = 590 CFU/mL; $p < 0.001$; Fig. 1). Under different groundwater quality conditions in cluster A, median influent HPCs decreased by 11% (median influent = 795 CFU/mL compared to median effluent = 710 CFU/mL in cluster A; $p = 0.095$; Fig. 1). After controlling for cumulative water usage, the odds of an increase in HPC in the filter effluent across all households and geographic clusters decreased by 83% with each 1-log_{10} increase in the influent HPC (OR = 0.17, 95% CI: 0.06–0.38, $p < 0.001$; Model 2, Table 3).

3.3.3. F-specific coliphages

3.3.3.1. Influent groundwater quality. Effluent coliphage concentrations were highly correlated with the influent concentrations ($p < 0.001$; Fig. S5). Although AC has been shown to be capable of virus removal in flow-through column tests (Powell et al., 2000), the optimized conditions necessary for effective removal are difficult to replicate in decentralized water treatment scenarios. Viral adsorption depends on the virus type, carbon surface properties, and water quality parameters, such as pH and ionic strength (Cookson, 1969; Gerba, 1984). Considering that the isoelectric point of F-specific coliphages in water is generally low (e.g., 3.9 for the male-specific bacteriophage MS2 (Dowd et al., 1998) compared to mean influent pH values of 4.3–6.9; Table 2), most phages in the filter influent in this study were likely negatively charged. The carbon in the filters in this study also likely had a high concentration of negatively charged hydroxyl groups on the surface since a significant increase in the effluent pH was observed (median influent pH of 5.2 to a median effluent of 9.1 at start-up). Thus, a repulsive interaction between like charges on the phage and carbon surface probably prevented significant adsorption from occurring in these waters (Gerba, 1984). Additionally, the influent groundwaters in this study had low ionic strength ($6.9x10^{-4}$–7.8×10^{-3} M), thus increasing the distance of the electrical double layer around viral particles and increasing these repulsive forces. By comparison, Cookson (1969) showed that optimal virus adsorption kinetics occurred in solutions with ionic strengths of 0.04–0.12 M.

3.3.3.2. Seasonal effects and duration of use. Coliphages were more prevalent in both the filter influent and effluent over time (Fig. 4). Thus, the longer each filter was in use, the more likely it was to be challenged by coliphage spikes. One possible explanation of these spikes is increased rainfall causing infiltration of virus-laden surface water through cracks and leaks at the wellhead in poorly maintained wells. Indeed, Stallard et al. (2021) have shown that coliphage concentrations in the wells in this study and others across Robeson County were significantly associated with rainfall during the winter months. Another explanation is that viral adsorption is a reversible reaction (Cookson and

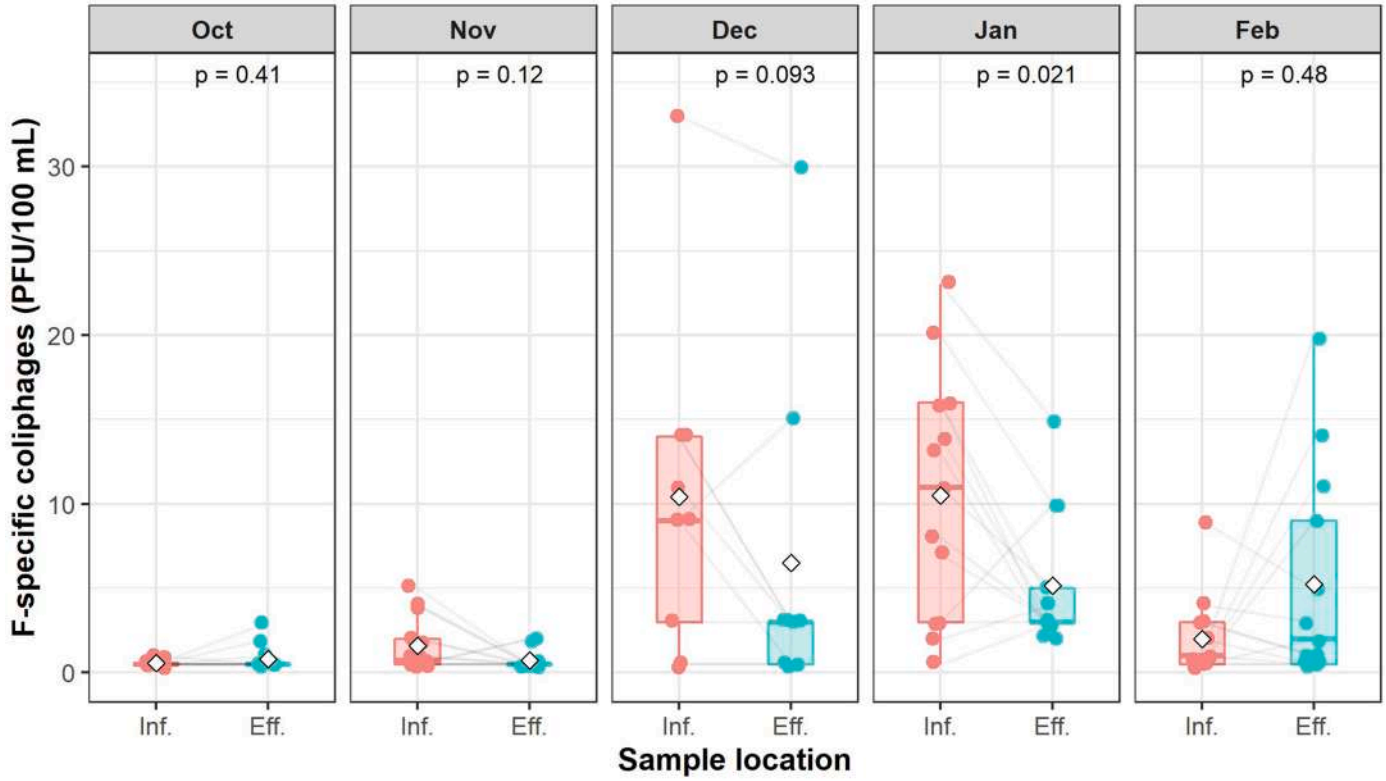

Fig. 4. Monthly paired influent-effluent F-specific coliphage concentrations reveal seasonal nature of coliphage concentrations in filter influent and possible viral shedding in effluent after influent concentrations subside.

North, 1967), thus allowing for possible viral shedding from the filter cartridge after periods of increased occurrence in raw well water. This behavior may explain the trend observed in later months where effluent concentrations were slightly higher than influent concentrations (Feb 2020 influent mean = 2 PFU/100 mL; effluent mean = 5.2 PFU/100 mL) following an increase in the influent concentrations the month before (Jan 2020 influent mean = 10.5 PFU/100 mL; Fig. 4). As a result of these mechanisms, each week of filter use led to an 18% increase in the odds of coliphages occurring in the effluent when controlling for the influent concentration and cumulative water usage (OR = 1.18, 95% CI: 1.05–1.36, $p < 0.01$). Each 1 PFU/mL increase in the filter influent also increased the odds of a positive coliphage result in the effluent by 28% (OR = 1.28, 95% CI: 1.07–1.66, $p < 0.05$; Model 3, Table 3).

3.4. Significance for private well users

The POU water treatment industry has largely developed around controlling chemical contaminants in public water systems, such as lead and disinfection byproducts, but is highly relevant to the needs of private well users. This study provides insight into whether AC-POU water filters may be safely used for private well water treatment in the absence of disinfection. Notably, with one exception, the microbial quality of the effluent of the 17 AC-POU devices tested in this study was not significantly worse than the influent water quality when considering indicator organisms representing gastrointestinal health risk. Indeed, total coliforms were removed from the influent more often than they were detected in the effluent. Effluent HPCs increased in some cases but decreased in others and were similar to or less than the levels in the effluent of AC-POU filter studies conducted on municipally treated tap water. In addition, effluent coliphage concentrations were directly related to influent concentrations. Certain bacterial isolates identified as potential opportunistic pathogens were detected in both the influent and effluent, demonstrating that well users are exposed to these bacteria with or without implementing AC-POU treatment. The results of this study thus emphasize the already poor microbial water quality that exists in many private wells, which AC-POU treatment does not significantly improve or exacerbate.

Similarly, Fiore and Babineau (1977) found that AC-POU devices caused both upward and downward fluctuations in HPC and did not affect total coliform levels when tested on five municipal waters and one private well, concluding that AC-POU devices were "microbiologically neutral." Snyder et al. (1995) also showed that total coliforms did not increase in the effluent of any of 24 AC-POU filters installed in homes connected to private wells over one year of use. In fact, the total coliform detection rate in the filter effluent in this study (7.5%) was significantly less than that reported by Chaidez and Gerba (2004) for 10 filters connected to a municipal water system, where 82.4% of effluent samples contained total coliforms. These results demonstrate that the potential for colonization of AC-POU filters by total coliforms is not unique to private wells and that choosing to implement household water treatment can alter the microbial quality of both public and private drinking water. The limited studies that exist on private well water suggest that the risk may even be lower for private wells due to the abundance of natural heterotrophic bacteria in most wells that may help prevent colonization by unwanted bacteria. Although further study is warranted, these findings suggest that, under normal conditions of use, AC-POU filters treating private well water do not represent a significant additional risk beyond the existing exposures users may experience from well water alone. The added health benefits of AC-POU filters to alleviate chemical hazards from private well water, such as high lead levels, likely outweigh concerns around microbial changes across the filter.

The results of this study do not indicate an absence of microbial risks associated with AC-POU treatment for private wells, however. In one instance of extremely low water use and low influent HPC, total coliforms rapidly colonized the filter leading to high effluent concentrations (2,203 MPN/100 mL) for a short time. Additionally, influent coliphages passed through the filter and were potentially shed from the carbon media into the effluent after influent levels subsided, suggesting

that these filters provide limited protection from potential viral pathogens. Finally, AC-POU filters may alter and, in some cases, increase the occurrence of HPC bacteria and potential opportunistic pathogens in the treated water. Epidemiological evidence is conclusive that increased ingestion of HPC bacteria in drinking water from AC-POU devices is not a gastrointestinal health risk due to the extremely high infective dose of these species (Allen et al., 2004; Calderon and Wood, 1987; Calderon, 1990; Dufour, 1988; Edberg and Allen, 2004; Mena and Gerba, 2009; WHO, 2003). Severely immunocompromised individuals could develop higher risk of gastrointestinal illness from ingestion of heterotrophic bacteria in drinking water, but such conditions are specific and normally require hospitalization (Edberg and Allen, 2004). Certain species, however, such as *Pseudomonas*, *Klebsiella* and *Aeromonas*, as well as *Sphingomonas* and *Ralstonia* which were isolated in both the filter influent and effluent of this study, can be opportunistic pathogens through exposure pathways other than oral ingestion, like cleaning of large wounds, inhalation of water droplets, or cleansing of contacts lenses (Allen et al., 2004; Edberg, 1996; Mena and Gerba, 2009; Rasheduzzaman et al., 2019). Although private well users are likely exposed to these potential opportunistic pathogens with or without an AC-POU filter, the relative bacterial virulence and infectivity of opportunistic pathogens in raw well water compared to AC-POU effluent remains to be studied.

Thus, private well users who choose to install AC-POU filters to remove chemical contaminants or improve the water's aesthetic quality should be aware of these possible microbial risks and take precautions to minimize them. Recommendations for private well users based on this study include:

- Avoid using AC-POU filtered water for purposes other than drinking, cooking, and washing. For more sensitive needs, such as for large wound irrigation or nasal cleansing (e.g., with a Neti Pot), AC-POU filtered water should be boiled, or an alternative source, such as distilled water or sterile saline, should be used.
- Ensure frequent and consistent use, especially during the first 1–2 weeks after installation and after each successive filter replacement, to allow a healthy biofilm to develop on the filter's surface and prevent any coliform bacteria and/or potential enteric pathogens from excessively colonizing the filter.
- Flush the system frequently, especially after the filter has been stagnant overnight or after extended periods of non-use.
- Consider using full-flow, under-sink filters that have higher use rates and flow rates than third-faucet and refrigerator filters, thus providing more frequent flushing and less opportunity for excessive bacterial growth.
- Ensure the microbial safety of private well water through regular testing for total and fecal coliforms and coliphages, well inspections and regular maintenance (see Simpson, 2004), shock chlorination and/or household ultraviolet disinfection technologies if necessary.

3.5. Limitations and future study

Recommendations around POU treatment for private well users may be improved through future study of AC devices on a wider range of water quality and use conditions across the U.S. and Canada, as well as across Europe where there are also large populations of private well users (UBA, 2013). The results presented here suggest that AC-POU devices do not represent an added drinking water health risk with respect to bacterial and viral indicators, but follow-up study regarding other microbes such as fungi and protozoa may be informative. Targeted research into the risk of infection from specific bacterial species identified in the influent and effluent using quantitative microbial risk assessment could also inform future decision-making regarding AC-POU devices. Although it was not evaluated in this study, particle association of influent coliform bacteria in groundwater may be another possible factor determining whether coliform bacteria appear in the filter effluent. Finally, the filters tested were designed to be replaced every six months but microbial testing of the filter effluents was ended after five months due to the COVID-19 pandemic, so possible microbial changes in the water quality at or beyond the filter's recommended lifetime could not be evaluated here.

4. Conclusions

This study evaluated the occurrence of microbial indicator organisms in the influent and effluent of AC-POU filters treating private well water. Under normal conditions of use, the microbial water quality in the filter effluents was comparable to that of the raw well water at each household and did not represent a significant additional health risk. Colonization of filter media by heterotrophic bacteria may provide a protective effect against colonization by enteric pathogens, but filters were not protective against coliphages and opportunistic pathogens in both the filter influent and effluent may represent an infection risk through non-ingestion exposure pathways for private well users. Thus, well users should not rely on AC-POU to protect against microbial contaminants in their well water and should first take measures to protect the microbial quality of their well before installing any AC-POU treatment for chemical concerns. State and federal health agencies ought to promote adoption of AC-POU treatment for well users in conjunction with continued efforts to ensure good well stewardship behaviors by caring for "upstream" risks that influence general well water safety and quality (Kreutzwiser et al., 2011; Simpson, 2004). Such behaviors include regularly inspecting the well cap and seal to prevent leaks from the surface, ensuring adequate separation between the well and all neighboring waste systems, testing annually for total and fecal coliforms and (ideally) coliphages, and disinfection if microbial contamination is detected. Additionally, efforts should be made by POU device manufacturers and public health agencies alike to promote a multi-barrier approach to household drinking water treatment among private well users, with improved source protection and/or an additional disinfection step before or after AC-POU filters to reduce the inherent microbial risks associated with well water.

Funding sources

This research was supported by funding from the North Carolina Policy Collaboratory at the University of North Carolina Chapel Hill.

Declarations of competing interest

None.

Acknowledgments

The authors would like to acknowledge Bill Smith, Melissa Packer, Michele Fanning, and Cedric Locklear at the Robeson County Health Department and Rev. Robert Campbell at the Rogers Eubanks Neighborhood Association for support during recruitment. Tejas Pruthi, Jared Peck, and April Desclos at UNC Chapel Hill assisted in the filter installation and sampling. Brad Gibson and Glenn Walters advised on the design and installation of the treatment system. Alyssa Grube provided valuable feedback on the manuscript.

Appendix A. Supplementary data

Supplementary data to this article can be found online at https://doi.org/10.1016/j.ijheh.2021.113852.

References

Adley, C., Ryan, M., Pembroke, J., Saieb, F., 2005. Ralstonia picketii: biofilm formation in high purity water. In: McBain, A., Allison, D., Pratten, J., Spratt, D., Upton, M., Verran, J. (Eds.), Biofilms: Persistence and Ubiquity. BioFilm Club, pp. 151–162.

Alebouyeh, M., Gooran Orimi, P., Azimi-rad, M., Tajbakhsh, M., Tajeddin, E., Jahani Sherafat, S., Nazemalhosseini, E., Zali, M., 2011. Fatal sepsis by Bacillus circulans in an immunocompromised patient. Iran. J. Microbiol. 3, 156–158.

Allen, M.J., Edberg, S.C., Reasoner, D.J., 2004. Heterotrophic plate count bacteria - what is their significance in drinking water? Int. J. Food Microbiol. 92, 265–274. https://doi.org/10.1016/j.ijfoodmicro.2003.08.017.

Allevi, R.P., Krometis, L.A.H., Hagedorn, C., Benham, B., Lawrence, A.H., Ling, E.J., Ziegler, P.E., 2013. Quantitative analysis of microbial contamination in private drinking water supply systems. J. Water Health 11, 244–255. https://doi.org/10.2166/wh.2013.152.

APHA, AWWA, WEF, 2018a. 9223 enzyme substrate coliform test. In: Standard Methods for the Examination of Water and Wastewater. American Public Health Association, American Water Works Association, Water Environment Federation. https://doi.org/10.2105/SMWW.2882.194.

APHA, AWWA, WEF, 2018b. 9215 heterotrophic plate count. In: Standard Methods for the Examination of Water and Wastewater. American Public Health Association, American Water Works Association, Water Environment Federation. https://doi.org/10.2105/SMWW.2882.188.

Bates, D., Maechler, M., Bolker, B., Walker, S., 2015. Fitting linear mixed-effects models using lme4. J. Stat. Software 67, 1–48. https://doi.org/10.18637/jss.v067.i01.

Bell, F.A., Perry, D.L., Smith, J.K., Lynch, S.C., 1984. Studies on home water treatment systems. J. Am. Water Works Assoc. 76, 126–130. https://doi.org/10.1002/j.1551-8833.1984.tb05312.x.

Borchardt, M.A., Bertz, P.D., Spencer, S.K., Battigelli, D.A., 2003. Incidence of enteric viruses in groundwater from household wells in Wisconsin. Appl. Environ. Microbiol. 69, 1172–1180. https://doi.org/10.1128/AEM.69.2.1172-1180.2003.

Calcagno, V., 2020. Glmulti: Model Selection and Multimodel Inference Made Easy. R package version 1.0.8. [WWW Document]. https://cran.r-project.org/package=glmulti.

Calderon, R., Wood, E., 1987. Bacteria Colonizing Point-Of-Use, Granular Activated Carbon Filters and Their Relationship to Human Health, CR-911904-01-0. U.S. Environmental Protection Agency, Cincinatti, Ohio.

Calderon, R.L., 1990. Bacteria Colonizing Point-Of-Entry Granular Activated Carbon Filters and Their Relationship to Human Health, CR-911904-01-0. U.S. Environmental Protection Agency, Cincinatti, Ohio.

Cameron, D.R., Jiang, J., Hassan, K.A., Elbourne, L.D.H., Tuck, K.L., Paulsen, I.T., Peleg, A.Y., 2015. Insights on Virulence from the Complete Genome of Staphylococcus Capitis, vol. 6, pp. 1–12. https://doi.org/10.3389/fmicb.2015.00980.

Camper, A.K., LeChevallier, M.W., Broadaway, S.C., McFeters, G.A., 1985. Growth and persistence of pathogens on granular activated carbon filters. Appl. Environ. Microbiol. 50, 1378–1382. https://doi.org/10.1128/aem.50.6.1378-1382.1985.

Carrasco, G., Garrido, N., Villalón, P., Valdezate, S., 2017. Paenibacillus spp . isolated from human and environmental samples in Spain : detection of 11 new species. New Microbes New Infect 19, 19–27. https://doi.org/10.1016/j.nmni.2017.05.006.

CBTech, 2019. Carbon block buyer's guide [WWW Document]. https://www.carbonblocktech.com/carbon-filter-buyer-guide/.

Chaidez, C., Gerba, C.P., 2004. Comparison of the microbiologic quality of point- of-use (POU) -treated water and tap water. Int. J. Environ. Health Res. 14, 253–260. https://doi.org/10.1080/09603120410001725595.

Cookson, J.T., 1969. Mechanism of virus adsorption on activated carbon. J. Am. Water Works Assoc. 61, 52–56. https://doi.org/10.1002/j.1551-8833.1969.tb03702.x.

Cookson, J.T., North, W.J., 1967. Adsorption of viruses on activated carbon: equilibria and kinetics of the attachment of Escherichia coli bacteriophage T4 on activated carbon. Environ. Sci. Technol. 1, 46–52. https://doi.org/10.1021/es60001a002.

DeSimone, L.A., Hamilton, P.A., Gilliom, R.J., 2009. The Quality of Our Nation's Waters: Quality of Water from Domestic Wells in Principal Aquifers of the United States, 1991–2004: Overview of Major Findings. USGS Circular 1332. United States Geological Society, Reston, vol. A.

Dieter, C.A., Maupin, M.A., Caldwell, R.R., Harris, M.A., Ivahnenko, T.I., Lovelace, J.K., Barber, N.L., Linsey, K.S., 2018. Estimated Use of Water in the United States in 2015: U.S. Geological Survey Circular 1441. United States Geological Survey, Reston, VA. https://doi.org/10.3133/cir1441.

Dowd, S.E., Pillai, S.D., Wang, S., 1998. Delineating the specific influence of virus isoelectric point and size on virus adsorption and transport through sandy soils. Appl. Environ. Microbiol. 64, 405–410.

Dufour, A.P., 1988. Health studies of aerobic heterotrophic bacteria colonizing granular activated carbon systems. In: Proceedings: Conference on Point-of-Use Treatment of Drinking Water EPA/600/9-88/012. U.S. Environmental Protection Agency, Washington, D.C., pp. 84–87

Edberg, S.C., 1996. Assessing health risk in drinking water from naturally occurring microbes. J. Environ. Health 58, 18–24.

Edberg, S.C., Allen, M.J., 2004. Virulence and risk from drinking water of heterotrophic plate count bacteria in human population groups. Int. J. Food Microbiol. 92, 255–263. https://doi.org/10.1016/j.ijfoodmicro.2003.08.012.

Fiore, J.V., Babineau, R.A., 1977. Effect of an activated carbon filter on the microbial quality of water. Appl. Environ. Microbiol. 34, 541–546.

Flanagan, S.V., Gleason, J.A., Spayd, S.E., Procopio, N.A., Rockafellow-Baldoni, M., Braman, S., Chillrud, S.N., Zheng, Y., 2018. Health protective behavior following required arsenic testing under the New Jersey Private Well Testing Act. Int. J. Hyg Environ. Health 221, 929–940. https://doi.org/10.1016/j.ijheh.2018.05.008.

Gardner, S., Shulman, S.T., 1984. A nosocomial common source outbreak caused by pseudomonas pickettii. Pediatr. Infect. Dis. 3 https://doi.org/10.1097/00006454-198409000-00006.

Geldreich, E.E., Taylor, R.H., Blannon, J.C., Reasoner, D.J., 1985. Bacterial colonization of point-of-use water treatment devices. J. Am. Water Works Assoc. 77, 72–80. https://doi.org/10.1002/j.1551-8833.1985.tb05495.x.

Gerba, C.P., 1984. Applied and theoretical aspects of virus adsorption to surfaces. Adv. Appl. Microbiol. 30, 133–168.

Jofre, J., Lucena, F., Blanch, A.R., Muniesa, M., 2016. Coliphages as model organisms in the characterization and management of water resources. Water 8, 1–21. https://doi.org/10.3390/w8050199.

Kalmbach, S., Manz, W., Wecke, J., Szewzyk, U., 1999. Aquabacterium gen. nov., with description of Aquabacterium citratiphilum sp. nov., Aquabacterium parvum sp. nov. and Aquabacterium commune sp. nov., three in situ dominant bacterial species from the Berlin drinking water system. Int. J. Syst. Bacteriol. 49, 769–777. https://doi.org/10.1099/00207713-49-2-769.

Kelley, S.T., Theisen, U., Angenent, L.T., Amand, A.S., Pace, N.R., Al, K.E.T., Icrobiol, A. P.P.L.E.N.M., 2004. Molecular Analysis of Shower Curtain Biofilm Microbes 70, 4187–4192. https://doi.org/10.1128/AEM.70.7.4187.

Kitamura, Y., Sawabe, E., Ohkusu, K., Tojo, N., Tohda, S., 2012. First Report of Sepsis Caused by Rhodococcus Corynebacterioides in a Patient with Myelodysplastic Syndrome, pp. 1089–1091. https://doi.org/10.1128/JCM.06279-11.

Koenig, D., Pierson, D., 1997. Microbiology of the space shuttle system. Water Sci. Technol. 35, 59–64.

Kreutzwiser, R., De Loë, R., Imgrund, K., Conboy, M.J., Simpson, H., Plummer, R., 2011. Understanding stewardship behaviour: factors facilitating and constraining private water well stewardship. J. Environ. Manag. 92, 1104–1114. https://doi.org/10.1016/j.jenvman.2010.11.017.

Kulakov, L.A., Mcalister, M.B., Ogden, K.L., Larkin, M.J., O'Hanlon, J.F., 2002. Analysis of bacteria contaminating ultrapure water in industrial systems. Appl. Environ. Microbiol. 68, 1548–1555. https://doi.org/10.1128/AEM.68.4.1548.

Lamka, K.G., LeChevallier, M.W., Seidler, R.J., 1980. Bacterial contamination of drinking water supplies in a modern rural neighborhood. Appl. Environ. Microbiol. 39, 734–738.

Lechevallier, M.W., Seidler, R.J., 1980. Staphylococcus aureus in rural drinking water. Appl. Environ. Microbiol. 30, 739–742.

Leclerc, H., Edberg, S., Pierzo, V., Delattre, J.M., 2000. Bacteriophages as indicators of enteric viruses and public health risk in groundwaters. J. Appl. Microbiol. 88, 5–21. https://doi.org/10.1046/j.1365-2672.2000.00949.x.

Lesage, S., 2005. Groundwater quality in Canada: a national overview. In: Thomson, N.R. (Ed.), Bringing Groundwater Quality Research to the Watershed Scale. IAHS Press, Wallingford, UK, pp. 11–18.

Logan, N.A., Old, D.C., Dick, H.M., 1985. Isolation of Bacillus circulans from a wound infection. J. Clin. Pathol. 38, 838–839. https://doi.org/10.1136/jcp.38.7.838.

Lute, S., Aranha, H., Tremblay, D., Liang, D., Ackermann, H.W., Chu, B., Moineau, S., Brorson, K., 2004. Characterization of coliphage PR772 and evaluation of its use for virus filter performance testing. Appl. Environ. Microbiol. 70, 4864–4871. https://doi.org/10.1128/AEM.70.8.4864-4871.2004.

Malecki, K.M.C., Schultz, A.A., Severtson, D.J., Anderson, H.A., VanDerslice, J.A., 2017. Private-well stewardship among a general population based sample of private well-owners. Sci. Total Environ. 601–602, 1533–1543. https://doi.org/10.1016/j.scitotenv.2017.05.284.

McDonald, J.H., 2014. Wilcoxon signed-rank test. In: Handbook of Biological Statistics. Sparky House Publishing, Baltimore, MD, pp. 186–189.

Mena, K.D., Gerba, C.P., 2009. Risk assessment of Pseudomonas aeruginosa in water. In: Whitacre, D.M. (Ed.), Reviews of Environmental Contamination and Toxicology. Springer, New York, NY, pp. 71–107. https://doi.org/10.1007/978-1-4419-0032-6.

Mulhern, R.E., Grubbs, B., Gray, K., MacDonald Gibson, J., 2022. User experience of point-of-use water treatment for private wells in North Carolina: implications for outreach and well stewardship. Sci. Total Environ. 806 (1), 150448 https://doi.org/10.1016/j.scitotenv.2021.150448.

Mulhern, R., MacDonald Gibson, J., 2020. Under-sink activated carbon water filters effectively remove lead from private well water for over six months. Water 12, 3584. https://doi.org/10.3390/w12123584.

NGWA, 2017. Well Owners Guide. National Ground Water Association, Westerville, OH.

Ogorzaly, L., Bertrand, I., Paris, M., Maul, A., Gantzer, C., 2010. Occurrence, survival, and persistence of human adenoviruses and F-specific RNA phages in raw groundwater. Appl. Environ. Microbiol. 76, 8019–8025. https://doi.org/10.1128/AEM.00917-10.

Oguma, K., Kanazawa, K., Kasuga, I., Takizawa, S., 2018. Effects of UV irradiation by light emitting diodes on heterotrophic bacteria in tap water. Photochem. Photobiol. 94, 570–576. https://doi.org/10.1111/php.12891.

Powell, T., Brion, G.M., Jagtoyen, M., Derbyshire, F., 2000. Investigating the effect of carbon shape on virus adsorption. Environ. Sci. Technol. 34, 2779–2783. https://doi.org/10.1021/es991097w.

Rasheduzzaman, M., Singh, R., Haas, C.N., Tolofari, D., Yassaghi, H., Hamilton, K.A., Yang, Z., Gurian, P.L., 2019. Reverse QMRA as a decision support tool: setting acceptable concentration limits for Pseudomonas aeruginosa and Naegleria fowleri. Water 11, 1–15. https://doi.org/10.3390/w11091850.

Reasoner, D.J., Blannon, J.C., Geldreich, E.E., 1987. Microbiological characteristics of third-faucet point-of-use devices. J. Am. Water Works Assoc. 79, 60–66.

Regunathan, P., Beauman, W.H., Kreusch, E.G., 1983. Efficiency of point-of-use treatment devices. J. Am. Water Works Assoc. 75, 42–50. https://doi.org/10.1002/j.1551-8833.1983.tb05057.x.

Ryan, M.P., Adley, C.C., 2010. Sphingomonas paucimobilis: a persistent Gram-negative nosocomial infectious organism. J. Hosp. Infect. 75, 153–157. https://doi.org/10.1016/j.jhin.2010.03.007.

Ryan, M.P., Pembroke, J.T., Adley, C.C., 2006. Ralstonia pickettii: a persistent Gram-negative nosocomial infectious organism, 2006 J. Hosp. Infect. 278–284. https://doi.org/10.1016/j.jhin.2005.08.015.

Simpson, H., 2004. Promoting the management and protection of private water wells. J. Toxicol. Environ. Health Part A 67, 1679–1704. https://doi.org/10.1080/15287390490492296.

Snyder, J.W., Mains, C.N., Anderson, R.E., Bissonnette, G.K., 1995. Effect of point-of-use, activated carbon filters on the bacteriological quality of rural groundwater supplies. Appl. Environ. Microbiol. 61, 4291–4295.

Stallard, M., Mulhern, R., Greenwood, E., Franklin, T., Engel, L.S., Fisher, M.B., Sobsey, M.D., Zanib, H., Noble, R., Stewart, J.R., Sozzi, E., 2021. Occurrence of male-specific and somatic coliphages and relationship with rainfall in privately-owned wells from peri-urban and rural households. Water Res. X 12. https://doi.org/10.1016/j.wroa.2021.100102.

Statistics Canada, 2017. Households and the Environment Survey, Dwelling's Main Source of Water. https://doi.org/10.25318/3810027401-eng. Table 38-10-0274-01.

Su, F., Luo, M., Zhang, F., Li, P., Lou, K., Xing, X., 2009. Performance of microbiological control by a point-of-use filter system for drinking water purification. J. Environ. Sci. 21, 1237–1246. https://doi.org/10.1016/S1001-0742(08)62410-9.

Taylor, R.H., Alien, M.J., Geldreich, E.E., 1979. Testing of home use carbon filters. J. Am. Water Works Assoc. 577–579. https://doi.org/10.1002/j.1551-8833.1979.tb04423.x.

Tobin, R.S., Smith, D.K., Lindsay, J.A., 1981. Effects of activated carbon and bacteriostatic filters on microbiological quality of drinking water. Appl. Environ. Microbiol. 41, 646–651.

Tomlinson, M.S., Bommarito, P., George, A., Yelton, S., Cable, P., Coyte, R., Karr, J., Vengosh, A., Gray, K.M., Fry, R.C., 2019. Assessment of inorganic contamination of private wells and demonstration of effective filter-based reduction: a pilot-study in Stokes County, North Carolina. Environ. Res. 177, 108618 https://doi.org/10.1016/j.envres.2019.108618.

UBA, 2013. Gesundes trinkwasser aus eigenen burnnen und quellen: Empfehlungen für betrieb und nutzung. Umwelt Bundesamt, Bonn, Germany.

USEPA, 2009. Water on Tap: what You Need to Know - EPA 816-K-09-002. U.S. Environmental Protection Agency - Office of Water, Washington D.C.

USEPA, 2006. Point-of-Use or Point-of- Entry Treatment Options for Small Drinking Water Systems: EPA 815-R-06-010. U.S. Environmental Protection Agency, Arlington, VA.

USEPA, 2002. Drinking Water from Household Wells - EPA 816-K-02-003. US Environmental Protection Agency, Office of Water, Washington D.C.

USEPA, 2001. Method 1602: Male-specific (F+) and Somatic Coliphage in Water by Single Agar Layer (SAL) Procedure. EPA 821-R-01-029. U.S. Environmental Protection Agency, Washington, D.C.

Wallis, C., Stagg, C.H., Melnick, J.L., 1974. The hazards of incorporating charcoal filters into domestic water systems. Water Res. 8, 111–113.

White, D.C., Suttont, S.D., Ringelberg, D.B., 1996. The Genus Sphingomonas: Physiology and Ecology, pp. 301–306.

WHO, 2003. Heterotrophic Plate Counts and Drinking-Water Safety: the Significance of HPCs for Water Quality and Human Health. IWA Publishing, Cornwall, UK. https://doi.org/10.2166/9781780405940.

Wu, C.C., Ghosh, S., Martin, K.J., Pinto, A.J., Denef, V.J., Olson, T.M., Love, N.G., 2017. The microbial colonization of activated carbon block point-of-use (PoU) filters with and without chlorinated phenol disinfection by-products. Environ. Sci. Water Res. Technol. 3, 830–843. https://doi.org/10.1039/c7ew00134g.

Wu, C.C., Love, N.G., Olson, T.M., 2021. Bacterial transmission and colonization in activated carbon block (ACB) point-of-use (PoU) filters. Environ. Sci. Water Res. Technol. 7, 1114–1124. https://doi.org/10.1039/d0ew00982b.

International Journal of Hygiene and Environmental Health 238 (2021) 113857

Contents lists available at ScienceDirect

International Journal of Hygiene and Environmental Health

journal homepage: www.elsevier.com/locate/ijheh

Association between environmental exposure to phthalates and allergic disorders in Korean children: Korean National Environmental Health Survey (KoNEHS) 2015–2017

Ju-Yeon Lee [a,b], Jiyun Lee [a,b], Da-An Huh [c], Kyong Whan Moon [b,d,*]

[a] Department of Health and Safety Convergence Science, Korea University, Seoul, Republic of Korea
[b] BK21 FOUR R&E Center for Learning Health System, Korea University, Seoul, Republic of Korea
[c] Institute of Health Sciences, Korea University, Seoul, Republic of Korea
[d] Department of Health and Environmental Science, Korea University, Seoul, Republic of Korea

ARTICLE INFO

Keywords:
Atopic dermatitis
Asthma
Allergic rhinitis
Allergic multimorbidity
Total immunoglobulin E
Phthalates

ABSTRACT

Background: Phthalates are common industrial chemicals that are used as plasticizers in plastics, personal care products, and building materials. Although these chemicals have been suspected as risk factors for allergic outcomes among children, inconsistent associations between environmental exposure to phthalates and allergic disorders have been found across different populations. Therefore, this study aimed to assess whether environmental phthalate exposure was associated with parent-reported current allergic symptoms (atopic dermatitis, AD; asthma; and allergic rhinitis, AR) and the index of allergic response (levels of serum total immunoglobulin E, IgE) in a nationally representative sample of children.

Methods: In this study, children aged 3–17 years (n = 2208) were recruited from the Korean National Environmental Health Survey (KoNEHS) 2015–2017 to conduct an analysis of their current allergic symptoms. Among this number of children, the total IgE analysis included 806 participants because total IgE levels were only measured in children aged 12–17 years.

Results: After adjusting for all covariates, mono-benzyl phthalate (MBzP) [OR (95% CI) = 1.15 (1.01, 1.30)], mono-(carboxyoctyl) phthalate (MCOP) [OR (95% CI) = 1.35 (1.02, 1.78)], and the sum of di-(2-ethylhexyl) phthalate metabolites (∑DEHP) [OR (95% CI) = 1.39 (1.09, 1.79)] were associated with increased odds of current AD. MCOP [OR (95% CI) = 1.19 (1.01, 1.40)], mono-(carboxynonyl) phthalate (MCNP) [OR (95% CI) = 1.24 (1.05, 1.45)], and ∑DEHP [OR (95% CI) = 1.22 (1.02, 1.44)] were also associated with increased odds of current AR. Individual DEHP metabolites showed similar associations with current AD and AR. In addition, MCNP was positively related to IgE levels [β (95% CI) = 0.26 (0.12, 0.40)]. MBzP [OR (95% CI) = 1.17 (1.01, 1.35)], MCOP [OR (95% CI) = 1.62 (1.12, 2.32)], and mono-(2-ethyl-5-oxohexyl) phthalate (MEOHP) [OR (95% CI) = 1.36 (1.06, 1.76)] showed positive relationships with allergic multimorbidity. Moreover, higher concentrations of MCNP were related to increased odds of experiencing both current AR and total IgE levels [OR (95% CI) = 1.98 (1.29, 3.04)], and children with elevated IgE levels (>100IU/mL) were more likely to have current AR associated with MCNP than those without elevated IgE levels ($p = 0.007$). Specifically, the relationship between MCNP and current AR was significantly mediated through alterations in IgE levels (14.7%), and MCNP also showed the positive association with current AR, independent of IgE (85.3%).

Conclusion: These results suggest that environmental exposure to phthalates may affect the immune system and increase the occurrence of allergic symptoms in children.

1. Introduction

The prevalence of allergic diseases has dramatically increased worldwide in recent decades (Ha et al., 2020). In particular, children are known to have a higher prevalence of major allergic diseases such as atopic dermatitis (AD), asthma, and allergic rhinitis (AR) than adults (Bousquet et al., 2015; Lee, 2020). The increased prevalence of allergic diseases is severely impacting the lives of individuals and is also a

* Corresponding author. Department of Health and Environmental Science, Korea University, 145 Anam-ro, Seongbuk-gu, Seoul, 02841, Republic of Korea.
E-mail address: kwmoon@korea.ac.kr (K.W. Moon).

https://doi.org/10.1016/j.ijheh.2021.113857
Received 20 April 2021; Received in revised form 12 September 2021; Accepted 4 October 2021
Available online 10 October 2021

socioeconomic burden; therefore, it is important to determine and manage the factors affecting the induction of allergic disorders (Maio et al., 2012).

Known risk factors for the development of allergic symptoms include environmental pollution, climate change, and exposure to endocrine disrupting chemicals, such as parabens and phthalates (D'Amato et al., 2017; Ha et al., 2020; Park et al., 2013). Among such risk factors, a growing body of evidence has reported that phthalate exposure was associated with allergic outcomes (Bolling et al., 2020). Phthalates are ubiquitous environmental chemicals used primarily in plastics, building materials, food packaging, toys, cosmetics, and personal care products (Wang et al., 2019; Wittassek et al., 2011). Because of their ability to leach out of the source and move into the environment, humans are frequently exposed to these chemicals through various exposure pathways (Benjamin et al., 2017; Tsai et al., 2012). Compared to adults, infants and children are more vulnerable to phthalate exposure due to their hand-to-mouth activity, immaturity of their organs, their comparatively higher food/water intake per unit body mass, and ventilation rate (Braun et al., 2013; Kimber and Dearman, 2010; Wang et al., 2016). Multiple studies have revealed that exposure to phthalates decreases with age (Frederiksen et al., 2011; Tran and Kannan, 2015; Wang et al., 2019; Zota et al., 2014).

Increasing numbers of in vitro, animal, and human epidemiological studies have reported that phthalate exposure may have a detrimental effect on immune function. It has been determined that phthalates can affect various cell types, such as macrophages, dendritic cells, and lymphocytes (including T cells) (Bolling et al., 2020; Yang et al., 2014); act as allergens or adjuvants leading to alterations in airways remodeling or allergen response (Benjamin et al., 2017; Kimber and Dearman, 2010); and cause changes in immunoglobulin E (IgE), which is an initial mediator that may activate an inflammatory cascade which could lead to allergic diseases (Benjamin et al., 2017; Bousquet et al., 2015; Wang et al., 2014). It has also been found that phthalate exposure was positively associated with allergic symptoms such as AD (Ait Bamai et al., 2014; Beko et al., 2015; Bornehag et al., 2004; Callesen et al., 2014a; Hsu et al., 2012; Kim et al., 2017; Shi et al., 2018; Wang et al., 2014), asthma (Beko et al., 2015; Bertelsen et al., 2013; Bornehag et al., 2004; Franken et al., 2017; Ku et al., 2015; Odebeatu et al., 2019; Wang and Karmaus, 2017; Wang et al., 2015), and AR (Ait Bamai et al., 2014; Beko et al., 2015; Bornehag et al., 2004; Hsu et al., 2012; Shi et al., 2018). However, several epidemiological studies have observed inconsistent relationships between phthalate exposure and the prevalence of allergic diseases in nationally representative samples of children (Ait Bamai et al., 2016; Callesen et al., 2014a, 2014b; Choi et al., 2014; Hoppin et al., 2013; Hsu et al., 2012; Kolarik et al., 2008; Wang et al., 2014; Wu et al., 2020). Therefore, these inconsistencies need to be addressed with more studies in support of the significant associations between exposure to phthalates and allergic disorders in children using a large representative sample.

Because European regulations on the use of phthalate were imposed prior to those in Asia, the sum of urinary phthalate metabolite concentrations in Asian children is generally known to be higher than that in the general population of several European countries (Tranfo et al., 2018; Wang et al., 2019). Multiple studies have been conducted on the association between environmental exposure to phthalates and allergic disorders in general populations of Asian children (Ait Bamai et al., 2014, 2016; Choi et al., 2014; Hsu et al., 2012; Kim et al., 2017; Ku et al., 2015; Shi et al., 2018; Wang and Karmaus, 2017; Wang et al., 2014, 2015). However, to our knowledge, only two studies have attempted to assess the effect of phthalate exposure on the occurrence of allergic disorders in Korean children (Choi et al., 2014; Kim et al., 2017). These previous studies were conducted in relation to only one allergic disease, AD, and reported the effects of only a few phthalate metabolites. Moreover, they used limited age ranges and small populations (n = 448 and n = 18).

It is thus necessary to focus on more than one allergic disorder and larger numbers of phthalates. In addition, it is necessary to expand the age range used to conduct research on the association between exposure to phthalates and overall allergic outcomes in Korean children. Therefore, this study aimed to examine the association of environmental exposure to several phthalates with current allergic symptoms of AD, asthma, and AR and the indicator of allergic response (total IgE levels) using data from the Korean National Environmental Health Survey (KoNEHS), which is representative of Korean children aged between three and 17 years.

2. Methods

2.1. Study population

The Korean National Environmental Health Survey (KoNEHS) is an ongoing three-year cycle cross-sectional survey which began since 2009 to monitor the current level of exposure to environmental chemicals in the general Korean population (Lee et al., 2020). This national survey is comprised of questionnaires, physical examinations, and biospecimen collection and analysis. The survey collects information about demographic, socioeconomic, and behavioral characteristics using a questionnaire administered to a household reference person responsible for completing the interview on behalf of children to assess environmental chemical exposure routes. In the case of children aged twelve to 17 years, additional surveys are conducted on several factors such as transportation and lifestyle. Blood and spot urine samples are collected for biospecimen collection (NIER, 2019a).

Of the KoNEHS data sets, the KoNEHS cycle 3 (2015–2017) was the only one to include questions about current symptoms of allergic diseases. In addition, it was conducted exclusively on participants under the age of 18 years. Therefore, we used the data from KoNEHS 2015–2017 to examine the association between urinary phthalate metabolites and parent-reported current allergic symptoms (AD, asthma, and AR) and total IgE levels in children aged between three and 17 years.

A total of 2380 children were included in the 2015–2017 survey, comprising 571 infants aged 3–5, 922 elementary school students aged 6–11, and 887 middle and high school students aged 12–17 years. Of these participants, we excluded individuals who had not been measured for urinary phthalate metabolite concentrations (n = 23) and those with missing information on any other covariates (n = 149). A total of 2208 children thus remained in the analysis of the current allergic symptoms. In the analysis used to determine the association between urinary phthalate metabolites and total IgE levels, we excluded children aged 3–11 years because they had not undergone a total IgE examination (n = 1402). In KoNEHS, the level of total IgE was only measured in children aged 12 years and older. Therefore, a total of 806 children aged 12–17 years were selected for this part of the analysis (Fig. 1).

2.2. Measurement of phthalate metabolites

Urinary phthalate metabolite concentrations were measured using liquid-liquid extraction (LLE) and ultra-performance liquid chromatography mass spectrometry (UPLC-MS) separation, followed by electrospray ionization (ESI) and tandem mass spectrometry (MS/MS). Details of the extraction and analytical procedures are described elsewhere (NIER, 2018). During KoNEHS 2015–2017, eight phthalate metabolites were measured: a metabolite of di-n-butyl phthalate (DBP), [i.e., mono-n-butyl phthalate (MnBP)]; a metabolite of benzylbutyl phthalate (BzBP) [i.e., mono-benzyl phthalate (MBzP)]; a metabolite of di-isononyl phthalate (DNP) [i.e., mono-(carboxyoctyl) phthalate (MCOP)]; a metabolite of di-isodecyl phthalate (DDP) [i.e., mono-(-carboxynonyl) phthalate (MCNP)]; a metabolite of di-n-octyl phthalate (DOP) [mono-(3-carboxylpropyl) phthalate (MCPP)]; and metabolites of di-(2-ethylhexyl) phthalate (DEHP) [i.e., mono-(2--ethyl-5-hydroxyhexyl) phthalate (MEHHP), mono-(2-ethyl-5-oxohexyl)

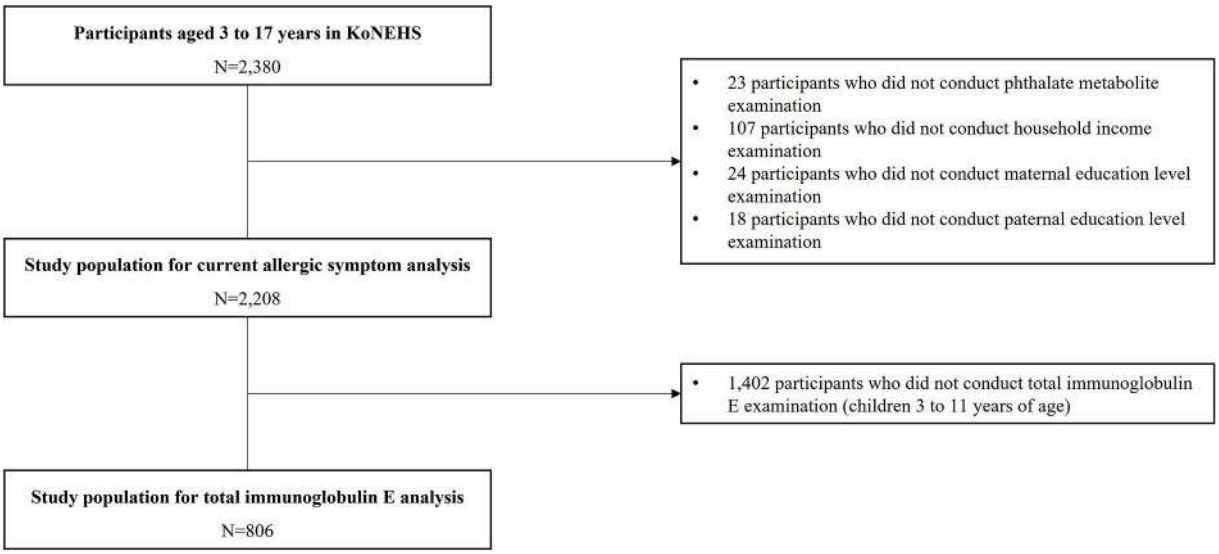

Fig. 1. Exclusion criteria of study participants in the 2015–2017 Korean National Environmental Health Survey.

phthalate (MEOHP), mono-(2-ethyl-5-carboxypentayl) phthalate (MECPP)]. As the concentrations of MEHHP, MEOHP, and MECPP were measured among the major secondary oxidized metabolites of DEHP, the urinary DEHP concentrations were calculated by summing the concentrations of these three metabolites for analysis, and they were denoted as ∑DEHP (Lee et al., 2020). The limit of detection (LOD) values for MnBP, MBzP, MCOP, MCNP, MCPP, MEHHP, MEOHP, and MECPP were determined at 0.040 μg/dL, 0.066 μg/dL, 0.048, μg/dL, 0.139 μg/dL, 0.078 μg/dL, 0.056 μg/dL, 0.048 μg/dL, and 0.141 μg/L, respectively. Concentrations below the LOD of each phthalate metabolite were replaced by the value of the LOD divided by the square root of 2 (Choi et al., 2012).

2.3. Allergic symptoms

Information about current allergic symptoms relating to AD, asthma, or AR was collected using the questionnaire (NIER, 2019a). Current allergic symptoms were defined as a positive response to the question "Do you currently have an allergic symptom relating to …. ?" for each allergic symptom. As these three allergic disorders tend to coexist in patients (a phenomenon known as multimorbidity) (Bousquet et al., 2015), we defined allergic multimorbidity as the coexistence of at least two current allergic symptoms (AD, asthma, or AR) in one individual (Koh et al., 2019).

2.4. Total IgE analysis

We analyzed total IgE levels of participants because serum total IgE level is a good predictor of allergy in children (Satwani et al., 2009). The level of serum total IgE is used as a reference value to predict allergic skin diseases (such as childhood atopy), and it is also used as a marker of airway inflammation in patients with allergic diseases, such as asthma and AR (Cardinale et al., 2005; Liu et al., 2003; NIER, 2019b). Serum samples were analyzed for total IgE levels by IMMULITE 2000 XPi (Siemens Medical Sol., USA) using a chemiluminescent immunoassay (CLIA) (NIER, 2019b). Serum Total IgE levels were considered increased at values > 100 IU/mL (Karli et al., 2013; Liu et al., 2003).

2.5. Covariates

The potential confounders considered in the analyses were demographic information (age, sex, household income, and maternal and paternal education levels), physical measurements (height and weight), and laboratory examinations (urinary creatinine and cotinine levels). Urinary cotinine is a biomarker of exposure to cigarette smoking (Odebeatu et al., 2019). Age, sex, household income, and the maternal and paternal education levels of participants were ascertained via questionnaires. The body mass index (BMI) was calculated as weight (in kilograms) divided by the square of height (in square meters) using the height and weight data obtained from KoNEHS data.

Household income was classified by quartiles. Maternal and paternal education levels were classified into three categories: < high school, high school, and > high school (Baiz et al., 2014; Gruber et al., 2010; Wen et al., 2009). Models were adjusted for urinary creatinine levels to account for urinary dilution and the urinary flow rate (James-Todd et al., 2016).

2.6. Statistical analysis

The KoNEHS data were analyzed in consideration of a stratified two-stage cluster sampling design, and stratum and cluster weights were included in regression models to provide a sample of participants representing the general population of Korea.

BMI and urinary creatinine levels were normally distributed, and urinary phthalate metabolite, serum total IgE, and urinary cotinine levels were normalized by log-transformation prior to analysis due to their skewed distribution. The concentrations of urinary phthalate metabolites were used as continuous variables.

We used a logistic regression analysis to estimate the odds ratios (ORs) and their 95% confidence intervals (CI) for current allergic symptoms. Furthermore, the association between urinary phthalate metabolites and the number of current allergic symptoms was analyzed to explore allergic multimorbidity. This was done by grouping the number of allergic symptoms into "no symptoms", "one symptom", and "two or more symptoms" categories in multinomial logistic regression models. All models were adjusted for age, sex, household income, maternal and paternal education levels, BMI, urinary creatinine level, and urinary cotinine level.

In a subgroup analysis conducted among children aged 12–17 years for whom information on serum total IgE level was available, the relationship between urinary phthalate metabolites and total IgE levels was analyzed by linear regression analyses. We also expanded logistic regression models to multinomial logistic regression models to evaluate whether the associations between urinary phthalate metabolites and allergic symptoms differed according to IgE levels. Concentrations of serum total IgE ≤100 IU/ml were defined as "low IgE", and those of

serum total IgE >100 IU/ml were defined as "high IgE" (Wang et al., 2014). We used a combination of two categorical variables to classify individuals into the following four groups: "no symptoms and low IgE", "symptoms with low IgE", "high IgE without symptoms", and "symptoms and high IgE". To test whether the ORs differed across the groups, we used the Sidak correction test, which is known to be a conservative and exact method, and a p-value for the difference was based on the results of this test (Abdi, 2007; Blakesley et al., 2009).

In addition, a mediation analysis was conducted to assess how much odds of allergic symptoms in relation to phthalate exposure could be explained by alterations in IgE levels (Ditlevsen et al., 2005). We used both logistic and linear regressions after adjusting for all covariates (Wang et al., 2016). The mediation proportion [(indirect effect/total effect) × 100%] was calculated by integrating the different regression coefficients (exposure: urinary phthalate metabolite, mediator: IgE, and outcome: current allergic symptom) (Ditlevsen et al., 2005).

All statistical analyses were performed using SPSS version 25.0, and the statistical significance level was considered $p < 0.05$.

3. Results

Table 1 demonstrates the characteristics of the study participants in KoNEHS 2015–2017 according to demographic and clinical conditions. A total number of 2208 Korean children were included in our study: 25.2% (n = 557) of the total number of participants were infants, 38.0% (n = 840) were elementary school students, and 36.7% (n = 811) were middle and high school students. Among these children, the prevalence of AD, asthma, and AR symptoms was 9.4% (n = 207), 1.1% (n = 24), and 29.5% (n = 651), respectively. Of the total subjects, 5.2% (n = 115) were identified as having allergic multimorbidity (having multiple allergic symptoms at the same time). More than 50% of the participants aged 12–17 years also had elevated serum total IgE levels that exceeded 100 IU/mL. In addition, the characteristics of children excluded due to missing information on any other covariates were not significantly different from those of children included in the analysis (Table S1).

The distribution of urinary phthalate metabolite concentrations (μg/L) among participants in this study is shown in Table 2. All phthalate metabolites were detected in the majority of the samples (detection frequency >95%). MCNP and MnBP were present at the lowest and highest median concentrations, respectively. In addition, urinary phthalate metabolite concentrations of excluded children were similar to those of children included in the analysis (Table S2).

Significant associations of current allergic symptoms and total IgE levels appeared with higher phthalate metabolite concentrations (Table 3). The analysis for current allergic symptoms was performed among all children (N = 2208). After adjusting for all covariates, MBzP [OR (95% CI) = 1.15 (1.01, 1.30)], MCOP [OR (95% CI) = 1.35 (1.02, 1.78)], and ∑DEHP [OR (95% CI) = 1.39 (1.09, 1.79)] were associated with increased odds of current AD. In addition, MCOP [OR (95% CI) = 1.19 (1.01, 1.40)], MCNP [OR (95% CI) = 1.24 (1.05, 1.45)], and ∑DEHP [OR (95% CI) = 1.22 (1.02, 1.44)] were associated with increased odds of current AR. Among the phthalate metabolites, MCOP and ∑DEHP showed significant positive associations with both current AD and AR in children. Individual DEHP metabolites showed similar relationships with current AD and AR. However, no phthalate metabolites were significantly associated with current asthma in children. In the subgroup of children aged 12–17 years (N = 806), the analysis for total IgE levels was performed. MCNP was positively related to total IgE levels [β (95% CI) = 0.26 (0.12, 0.40)].

The relationship between concentrations of urinary phthalate metabolites and the number of current allergic symptoms was identified to determine whether the prevalence of at least one of the current allergic symptoms increased in relation to phthalate exposure (and whether allergic multimorbidity occurred) (Table 4). After adjusting for confounders, MCNP [OR (95% CI) = 1.27 (1.06, 1.51)] and ∑DEHP [OR (95% CI) = 1.27 (1.06, 1.53)] were positively associated with the odds of occurrence of any current allergic symptom. Individual DEHP metabolites showed similar positive associations with any current allergic symptom. In addition, MBzP [OR (95% CI) = 1.17 (1.01, 1.35)], MCOP [OR (95% CI) = 1.62 (1.12, 2.32)], and MEOHP [OR (95% CI) = 1.36 (1.06, 1.76)] were positively related to the odds of occurrence of two or more current allergic symptoms. This implies that allergic multimorbidity occurred in association with elevations of these phthalate metabolite concentrations.

Fig. 2 presents the proportion of children with elevated IgE levels (>100IU/mL) according to current allergic symptoms. Among children with current allergic symptoms (AD, asthma, or AR), more than 65% of the participants aged 12–17 years had serum total IgE levels that exceeded 100 IU/mL. In particular, 85.7% of children with current asthma (six of seven) also had elevated IgE levels.

There was a significant association between urinary phthalate

Table 1
Demographic and clinical characteristics of study participants (unweighted).

Characteristics	All participants	Male	Female
N (%)	2208 (100)	1092 (49.5)	1116 (50.5)
Age (years)			
Infants (3–5)	557 (25.2)	279 (25.5)	278 (24.9)
Elementary school students (6–11)	840 (38.0)	429 (39.3)	411 (36.8)
Middle and high school students (12–17)	811 (36.7)	384 (35.2)	427 (38.3)
Household income (million won)			
<1	29 (1.3)	18 (1.6)	11 (1.0)
1–3	496 (22.5)	251 (23.0)	245 (22.0)
3–5	1381 (62.5)	669 (61.3)	712 (63.8)
>5	302 (13.7)	154 (14.1)	148 (13.3)
Maternal education level			
< High school	31 (1.4)	11 (1.0)	20 (1.8)
High school	732 (33.2)	351 (32.1)	381 (34.1)
> High school	1445 (65.4)	730 (66.8)	715 (64.1)
Paternal education level			
< High school	38 (1.7)	17 (1.6)	21 (1.9)
High school	628 (28.4)	298 (27.3)	330 (29.6)
> High school	1542 (69.8)	777 (71.2)	765 (68.5)
Urinary cotinine level (μg/L)			
< LOD (<0.030)	334 (15.1)	147 (13.5)	187 (16.8)
Low (0.030–10)	1795 (81.3)	886 (81.1)	909 (81.5)
High (≥10)	79 (3.6)	59 (5.4)	20 (1.8)
Body mass index (kg/m^2)[a]			
Underweight/Normal	1877 (85.0)	894 (81.9)	983 (88.1)
Overweight	221 (10.0)	126 (11.5)	95 (8.5)
Obese	110 (5.0)	72 (6.6)	38 (3.4)
Current status of allergic symptoms (Parent-reported)			
Atopic Dermatitis	207 (9.4)	97 (8.9)	110 (9.9)
Asthma	24 (1.1)	14 (1.3)	10 (0.9)
Allergic Rhinitis	651 (29.5)	390 (35.7)	261 (23.4)
Allergic multimorbidity	115 (5.2)	59 (5.4)	56 (5.0)
Elevated serum total IgE level[b] (in 12–17 years old)	434 (53.8)	220 (57.3)	214 (50.7)

Abbreviations: IgE, immunoglobulin E.

[a] Body mass index was classified into three categories: underweight or normal (<85th percentile), overweight (85–95th percentile), and obese (≥95th percentile) (Krebs et al., 2007).

[b] Elevated serum total IgE level was defined as > 100 IU/mL.

Table 2
Distribution of urinary phthalate metabolite concentrations (μg/L) for KoNEHS 2015–2017 children aged 3–17 years (N = 2208).

Phthalate metabolite		LOD	> LOD (%)	GM (SE)	Percentile				
					5th	25th	50th	75th	95th
Mono-n-butyl phthalate	MnBP	0.040	99.8	41.42 (1.05)	10.15	25.15	43.33	72.93	152.75
Mono-benzyl phthalate	MBzP	0.066	95.4	2.82 (1.05)	0.18	1.35	3.14	7.01	25.38
Mono-(carboxyoctyl) phthalate	MCOP	0.048	99.2	1.87 (1.03)	0.55	1.07	1.78	3.18	7.57
Mono-(carboxynonyl) phthalate	MCNP	0.139	96.9	0.49 (1.03)	0.19	0.34	0.50	0.64	1.33
Mono-(3-carboxypropyl) phthalate	MCPP	0.078	99.7	1.58 (1.02)	0.70	1.07	1.46	2.14	4.45
∑Di-(2-ethylhexyl) phthalate	∑DEHP			78.69 (1.04)	20.54	48.41	79.16	137.57	278.55
Mono-(2-ethyl-5-hydroxyhexyl) phthalate	MEHHP	0.056	100	22.62 (1.05)	4.63	13.49	24.38	43.03	84.49
Mono-(2-ethyl-5-oxohexyl) phthalate	MEOHP	0.048	99.9	15.60 (1.05)	2.75	9.10	16.32	29.87	66.31
Mono-(2-ethyl-5-carboxypentyl) phthalate	MECPP	0.141	100	37.63 (1.04)	10.27	22.71	37.78	64.92	137.18

Abbreviations: GM, geometric mean; SE, geometric standard error of the mean.
The values below the LOD were determined as LOD divided by the square root of 2; imputed values were used in the calculation of GM (SE).
Restricted to participants with all covariates in logistic regression model such as age, sex, household income, maternal and paternal education levels, body mass index, urinary creatinine level, and urinary cotinine level.

Table 3
Association of urinary phthalate metabolites with current allergic symptoms and total IgE levels using logistic and linear regressions.

Metabolite	Atopic dermatitis[a]	Asthma[a]	Allergic rhinitis[a]	total IgE levels[b]
MnBP	1.08 (0.89, 1.31)	1.46 (0.92, 2.31)	1.04 (0.90, 1.21)	0.07 (−0.07, 0.21)
MBzP	**1.15 (1.01, 1.30)**	0.96 (0.79, 1.17)	1.03 (0.96, 1.11)	0.04 (−0.05, 0.12)
MCOP	**1.35 (1.02, 1.78)**	1.19 (0.76, 1.86)	**1.19 (1.01, 1.40)**	−0.02 (−0.20, 0.16)
MCNP	1.20 (0.95, 1.52)	0.46 (0.20, 1.05)	**1.24 (1.05, 1.45)**	**0.26 (0.12, 0.40)**
MCPP	1.01 (0.79, 1.31)	0.74 (0.33, 1.69)	0.99 (0.81, 1.22)	0.04 (−0.20, 0.28)
∑DEHP	**1.39 (1.09, 1.79)**	0.90 (0.53, 1.53)	**1.22 (1.02, 1.44)**	0.12 (−0.11, 0.35)
MEHHP	**1.26 (1.01, 1.59)**	1.01 (0.66, 1.57)	**1.21 (1.04, 1.41)**	0.13 (−0.04, 0.30)
MEOHP	**1.38 (1.14, 1.67)**	1.13 (0.72, 1.78)	**1.18 (1.04, 1.35)**	0.09 (−0.03, 0.22)
MECPP	1.26 (0.96, 1.65)	0.85 (0.51, 1.40)	1.15 (0.97, 1.35)	0.08 (−0.17, 0.32)

Abbreviations: IgE, immunoglobulin E.
Adjusted for age, sex, household income, maternal and paternal education levels, body mass index, urinary creatinine level, and urinary cotinine level.
[a] All 2208 children were analyzed, and ORs (95% CI) for current allergic symptoms were estimated using logistic regression.
[b] Children aged 12–17 years (N = 806) were analyzed, and β (95% CI) for total IgE levels was estimated using linear regression.

Table 4
Associations [ORs (95% CI)] of urinary phthalate metabolites and the number of current allergic symptoms using weighted multinomial logistic regression (N = 2208).

Metabolite	Number of symptoms[a]	n	OR (95% CI)	p-value[b]
MnBP	0	1442	1.00	
	1	648	1.00 (0.84, 1.18)	
	2 or 3	115	1.22 (0.94, 1.59)	0.250
MBzP	0	1444	1.00	
	1	649	1.02 (0.95, 1.10)	
	2 or 3	115	**1.17 (1.01, 1.35)**	0.075
MCOP	0	1444	1.00	
	1	649	1.12 (0.96, 1.30)	
	2 or 3	115	**1.62 (1.12, 2.32)**	**0.020**
MCNP	0	1444	1.00	
	1	649	**1.27 (1.06, 1.51)**	
	2 or 3	115	1.07 (0.76, 1.51)	**0.016**
MCPP	0	1444	1.00	
	1	649	0.98 (0.79, 1.21)	
	2 or 3	115	0.97 (0.72, 1.33)	0.979
∑DEHP	0	1444	1.00	
	1	649	**1.27 (1.06, 1.53)**	
	2 or 3	115	1.33 (0.96, 1.83)	**0.018**
MEHHP	0	1444	1.00	
	1	649	**1.28 (1.09, 1.51)**	
	2 or 3	115	1.20 (0.91, 1.58)	**0.006**
MEOHP	0	1444	1.00	
	1	649	**1.23 (1.07, 1.42)**	
	2 or 3	115	**1.36 (1.06, 1.76)**	**0.010**
MECPP	0	1444	1.00	
	1	649	**1.19 (1.00, 1.42)**	
	2 or 3	115	1.18 (0.86, 1.61)	0.099

Adjusted for age, sex, household income, maternal and paternal education levels, body mass index, urinary creatinine level, and urinary cotinine level.
Allergic multimorbidity was defined as a significant OR for 2 or 3 allergic symptoms.
[a] 0: no current allergic symptoms, 1: one of any current allergic symptoms, 2 or 3: two or three of allergic symptoms.
[b] p-value for the difference of ORs using Sidak correction test in multinomial logistic regression models.

metabolites and the increased odds of having allergic symptoms and higher IgE levels, and an increase in IgE levels was associated with allergic symptoms. Therefore, multinomial logistic regression models were used to evaluate whether the associations between urinary phthalate metabolites and allergic symptoms differed according to IgE levels (Table 5). We stratified each of the three symptoms (AD, asthma, and AR) based on total IgE levels ("no symptoms and low IgE", "symptoms with low IgE", "high IgE without symptoms", and "symptoms and high IgE"). As only MCNP was positively associated with both allergic symptoms and total IgE levels, we selected urinary MCNP for this analysis. With respect to current AD and asthma, there were no statistically significant differences in the ORs of each group. For current AR, the OR of the AR and high IgE group increased 1.98 times (95% CI: 1.29, 3.04), compared to the reference group (no symptoms and low IgE), as the concentration of urinary MCNP in the log-transformation increased. In addition, individuals with AR and high IgE had the highest OR of exposure ($p = 0.007$). This implies that the OR for AR and high IgE was higher than that OR for high IgE without AR, and children with high IgE were more likely to have AR symptoms associated with MCNP than those with low IgE.

We conducted a mediation analysis to estimate the odds of AR symptoms in relation to MCNP that could be explained by changes in IgE (Fig. 3). This analysis incorporated various regression coefficients (exposure: urinary MCNP, mediator: IgE, and outcome: current AR). We found that the mediation effect was partial, and the relationship between MCNP and current AR was significantly mediated through alterations in IgE levels (14.7%). After adjusting the effect of total IgE, we observed that the positive association between MCNP and current AR remained stable, and the ratio of the direct effect to the total effect of MCNP on AR reached 85.3%.

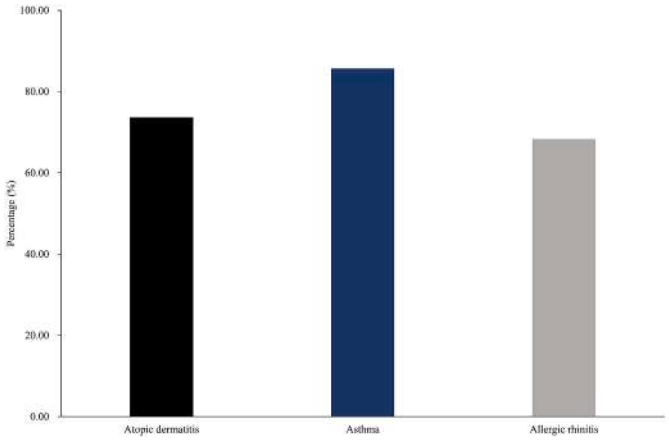

Fig. 2. Proportion of children with elevated total immunoglobulin E levels (>100IU/mL) according to current allergic symptoms.

Table 5
ORs (95% CI) for urinary MCNP and current allergic symptoms, stratified based on total IgE levels in children 12–17 years of age using weighted multinomial logistic regression (N = 806).

Symptom/outcome	n	OR (95% CI)	p-value[a]
Atopic dermatitis			
No atopic dermatitis and low IgE	347	1.00	
Atopic dermatitis with low IgE	25	1.19 (0.50, 2.84)	
High IgE without atopic dermatitis	364	**1.44 (1.01, 2.03)**	
Atopic dermatitis and high IgE	70	1.52 (0.87, 2.64)	0.123
Asthma			
No asthma and low IgE	371	1.00	
Asthma with low IgE	1	-	
High IgE without asthma	428	**1.40 (1.04, 1.88)**	
Asthma and high IgE	6	2.23 (0.58, 8.54)	0.052
Allergic rhinitis			
No allergic rhinitis and low IgE	296	1.00	
Allergic rhinitis with low IgE	76	1.29 (0.75, 2.23)	
High IgE without allergic rhinitis	270	1.30 (0.92, 1.83)	
Allergic rhinitis and high IgE	164	**1.98 (1.29, 3.04)**	**0.007**

Abbreviations: IgE, immunoglobulin E.
Adjusted for age, sex, household income, maternal and paternal education levels, body mass index, urinary creatinine level, and urinary cotinine level.
[a] p-value for the difference of ORs using Sidak correction test in multinomial logistic regression models.

4. Discussion

In this study, we determined the positive associations of urinary phthalate metabolites with parent-reported current allergic symptoms and serum total IgE levels in a large nationally representative sample of Korean children. After adjusting for all covariates, elevated levels of MBzP, MCOP, ∑DEHP, MEHHP, and MEOHP in urine were positively associated with the prevalence of current AD. In addition, the prevalence of current AR was higher in individuals with increased urinary phthalate metabolite concentrations (MCOP, MCNP, ∑DEHP, MEHHP, and MEOHP). We also found that MCNP was positively associated with serum total IgE levels. Evaluating the association between phthalate exposure and the number of allergic symptoms, urinary phthalate metabolites (except for MnBP and MCPP) were positively associated with at least one current allergic symptom, and the phenomenon of allergic multimorbidity occurred in the context of increased levels of urinary MBzP, MCOP, and MEOHP. Although MCNP was found at the lowest concentration among all phthalate metabolites, we consistently observed significant associations between MCNP and allergic outcomes. Higher MCNP concentrations were associated with increased odds of having both current AR and elevated IgE levels, and AR symptoms were partly caused by an increase in IgE levels, which was related to an increase in MCNP. These results imply that there was a certain interplay between IgE and current AR in response to MCNP. Furthermore, MCNP showed the positive association with AR symptoms, despite adjusting for the effect of IgE on current AR. In summary, significant relationships were determined between most phthalate metabolites (except for MnBP and MCPP) and the occurrence of at least one of the allergic outcomes.

Phthalates from various exposure routes can act as allergens or adjuvants to promote allergic reactions and inflammation by perturbing the immunologic system (Benjamin et al., 2017; Kimber and Dearman, 2010; Wang et al., 2019). These chemicals bind with and activate peroxisome proliferator-activated receptors (PPARs), which are mainly involved in anti-inflammatory effects occurring in the lungs and immune systems, thus leading to changes in airway remodeling and the development and exacerbation of hypersensitivity (Bolling et al., 2013; Cocci et al., 2015). In addition, they interfere with immunity against infections and cause changes in the balance of overall T helper type 1 (Th1) and T helper type 2 (Th2) cells (Benjamin et al., 2017; Yang et al., 2014). They also suppress CpG-induced interferon (IFN) -α/IFN-β expression and regulate the ability to stimulate T-cell reactions, which leads to a reduction in Th2 reactions and exacerbates the allergic response (Yang et al., 2014). Th2 differentiation and the secretion of Th2-promoted immunoglobulins (such as IgE) are enhanced by these chemicals (Jepsen et al., 2004; Larsen et al., 2002; Qin et al., 2018; Yang et al., 2014). Furthermore, they provoke the synthesis of proinflammatory Th2 cytokines (such as IL-6 and IL-8) in human lung epithelial cells and macrophage production of inflammatory cytokines and chemokines (Jepsen et al., 2004; Nishioka et al., 2012; Qin et al., 2018).

Consequently, phthalate exposure is likely to have adverse effects throughout the different steps of the immune response as well as alterations in IgE and enhance allergic disorders. Allergy is mediated by multiple immune cell types, including T-cells, cytokines, and chemokines, and is driven mainly by an allergen-specific Th2 immune response (Kuo et al., 2013). In the context of IgE-mediated allergic diseases, after an allergen-IgE antibody response has been developed, any subsequent exposure to the inducing allergen reacts with IgE, and this encounter causes the release of cytokines and chemokines, which amplify allergic inflammation (Kimber and Dearman, 2010). Eventually, this inflammation induces allergic symptoms, which may be observed as AD in the skin and asthma and AR in the respiratory tract (Kimber and Dearman, 2010). Based on this process of allergic disease development, a strong and consistent association has been reported between AD, asthma, AR, and IgE levels (Ballardini et al., 2016; Wang et al., 2016). In addition, allergic multimorbidity (the co-occurrence of at least two allergic symptoms in one individual) has been observed with respect to these allergic diseases (Bousquet et al., 2015). AD, asthma, and AR are underlying disorders with similar immunological (including allergen-IgE antibody response) and non-immunological traits, and these phenomena of multimorbidity are induced by common causal mechanisms between these diseases that are partly IgE-mediated (Bousquet et al., 2015). Thus, patients tend to have concomitant or continuous allergic diseases (Bousquet et al., 2012; Spergel and Paller, 2003).

Based on this biological evidence, we found that urinary biomarkers of phthalate exposure were related to allergic symptoms and total IgE levels, and other multiple population-based epidemiological studies have shown similar results. Several prior studies have observed a positive association between HMW metabolites and the risk of AD (including eczema) in children: exposure to BBzP and DEHP was positively related to the development of AD (Ait Bamai et al., 2014; Beko et al., 2015; Bornehag et al., 2004; Hsu et al., 2012); MBzP, MEHHP, and MEOHP concentrations were positively associated with AD (Kim et al., 2017; Shi et al., 2018; Wang et al., 2014); and prenatal MBzP, MCOP, MCNP, and ∑DEHP levels were associated with the increased odds of AD in children (Just et al., 2012; Soomro et al., 2018). With respect to AR (including rhinoconjunctivitis), multiple studies have found an increased risk of the development AR in relation to DEHP exposure (Ait Bamai et al., 2016; Beko et al., 2015). For total IgE levels, very limited information has been

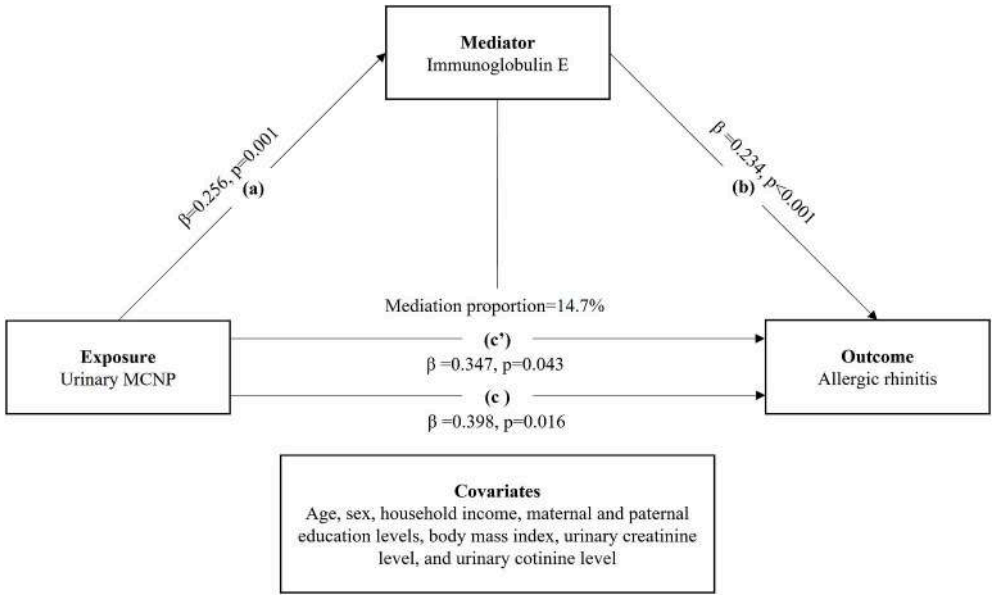

Fig. 3. Diagram of the research model demonstrating the relationship between exposure and outcome variables: (a) association between urinary MCNP and total immunoglobulin E levels; (b) association between total immunoglobulin E levels and current allergic rhinitis; (c) association between urinary MCNP and current allergic rhinitis; (c') association between urinary MCNP concentrations and current allergic rhinitis considering the effect of total immunoglobulin E levels.

reported on the concentrations of urinary phthalate metabolites in relation to total IgE levels in children. Wang et al. (2014) showed the positive association between urinary mono-(2-ethylhexyl phthalate (MEHP) and total IgE levels, but exposure to only four phthalates (di-ethyl phthalate, DBP, BBzP, and DEHP) was addressed.

Previous studies have found that exposure to phthalates such as DEHP, BBzP, and DBP, or the concentrations of urinary phthalate metabolites such as MnBP, MBzP, MCOP, MCNP, and ∑DEHP may affect the occurrence of asthma (Beko et al., 2015; Bertelsen et al., 2013; Bornehag et al., 2004; Franken et al., 2017; Ku et al., 2015; Odebeatu et al., 2019). However, we found no positive association between phthalate exposure and current asthma. This disparity may be attributed to the differences in specimen collection, ∑DEHP calculation, asthma definition, or to the matrix examined. With respect to specimen collection, Bertelsen et al. (2013) used first-morning voids, whereas the present study used spot urine samples for the analysis, which may have influenced the concentrations of phthalate metabolites measured. For the ∑DEHP calculation method, we defined ∑DEHP as the sum of the concentrations of MEHHP, MEOHP, and MECPP, whereas Ku et al. (2015) calculated ∑DEHP by summing the concentrations of MEHP, MEOHP, and MECPP. With respect to the definition of asthma, asthma in the present study was defined as a parent-reported current asthma symptom, while Odebeatu et al. (2019) combined a diagnosis of a doctor or another health professional and self-reported current asthma and wheeze. Another possible explanation could be related to the matrix assessed [i.e., dust in other studies (Beko et al., 2015; Bornehag et al., 2004; Callesen et al., 2014b) as opposed to urine in this study]. It is also possible that the reason for the lack of association in this study is due to the small number of participants that had current asthma symptoms (n = 24). Lee (2020) suggested that the reason for the decrease in asthma prevalence is the Korean central and local governments' active policies against allergic diseases.

Comparing this study population to data of children in the United States (U.S) obtained from the National Health and Nutrition Examination Survey (NHANES) 2007–2012, the concentrations of urinary MnBP and metabolites of DEHP (MEHHP, MEOHP, and MECPP) of children in the present study were higher than those of children in the U.S., but the levels of urinary MBzP, MCNP, and MCPP in this study population were lower than those of children in the U.S.(Odebeatu et al., 2019). Urinary MCOP concentrations of Korean children in this study were also lower than those of U.S. children (from NHANES, 2005–2006 data) (Hoppin et al., 2013). Although the concentrations of urinary MBzP, MCNP, and MCOP in Korean children were lower than those of children in the U.S., this study revealed a significant association between urinary phthalate metabolite concentrations and allergic outcomes in a representative sample of Korean children. Therefore, our results suggest that a lower dose of environmental exposure to phthalates could be a risk factor for allergic response and symptoms.

The main strength of this study is that we revealed significant associations between urinary biomarkers of phthalate exposure, allergic symptoms, and total IgE levels in a large representative sample of Korean children while considering the various potential confounders. This is the first study to verify a positive association between urinary phthalate metabolites and AR in Korean children. Moreover, the present study is the only study to determine the following in children: a positive association between urinary biomarkers of phthalate exposure and multimorbidity of allergic symptoms, a significant association between urinary MCNP and higher total IgE levels, and a positive relationship between urinary MCNP and AR considering the effect of total IgE levels.

However, our study has certain limitations. First, as KoNEHS data are cross-sectional survey data, the associations that we demonstrated cannot represent a causal relationship. Second, we were unable to find an association between exposure to phthalates and asthma. Although evidence for a potential relationship between exposure to DEHP and BBzP and asthma in children has increased (Beko et al., 2015; Ku et al., 2015; Wu et al., 2020), we failed to show a significant association between urinary phthalate metabolites and current asthma, and it is considered that this could be related to the small population that had current asthma symptoms at the time of survey (n = 24) in this study. Third, we restricted the study population to children aged three to 17 years because the KoNEHS data did not include information on allergic symptoms in adults. Finally, it is acknowledged that the use of specific IgE may be more objective than total IgE as an index for diagnosing allergic diseases (Chang et al., 2015), but we used serum total IgE levels because the serum levels of specific IgE were not measured in the KoNEHS. However, specific IgE are included in total IgE, and the level of serum total IgE is used as a predictive marker of allergic skin diseases (such as AD) and allergic airway diseases (such as asthma or AR); therefore, it could also be used as an indicator of AD, asthma, and AR (Cardinale et al., 2005; Liu et al., 2003; NIER, 2019b).

5. Conclusion

We analyzed data for a nationally representative population of children in South Korea and demonstrated that urinary biomarkers of phthalate exposure were positively associated with both current allergic symptoms and total IgE levels. We also determined that the multimorbidity of AD, asthma, and AR symptoms was associated with increased concentrations of urinary phthalate metabolites. Furthermore, consistently significant relationships between MCNP and allergic outcomes were observed. Our observations suggest that environmental phthalates could act as allergens or adjuvants to affect the immune system and increase the occurrence of allergic symptoms in children. Further studies involving a longitudinal follow-up analysis of children are required to establish a causal relationship between environmental exposure to phthalates and allergic outcomes.

Declaration of competing interest

The authors declare no conflict of interest.

Appendix A. Supplementary data

Supplementary data to this article can be found online at https://doi.org/10.1016/j.ijheh.2021.113857.

References

Abdi, H., 2007. Bonferroni and Šidák corrections for multiple comparisons. Encyclopedia of measurement statistics 3, 103–107.

Ait Bamai, Y., Shibata, E., Saito, I., Araki, A., Kanazawa, A., Morimoto, K., Nakayama, K., Tanaka, M., Takigawa, T., Yoshimura, T., Chikara, H., Saijo, Y., Kishi, R., 2014. Exposure to house dust phthalates in relation to asthma and allergies in both children and adults. Sci. Total Environ. 485–486, 153–163.

Ait Bamai, Y., Araki, A., Kawai, T., Tsuboi, T., Saito, I., Yoshioka, E., Cong, S., Kishi, R., 2016. Exposure to phthalates in house dust and associated allergies in children aged 6-12years. Environ. Int. 96, 16–23.

Baiz, N., Dargent-Molina, P., Wark, J.D., Souberbielle, J.C., Annesi-Maesano, I., Group, EDEN Mother-Child Cohort Study Group., 2014. Cord serum 25-hydroxyvitamin D and risk of early childhood transient wheezing and atopic dermatitis. J. Allergy Clin. Immunol. 133, 147–153.

Ballardini, N., Bergstrom, A., Wahlgren, C.F., van Hage, M., Hallner, E., Kull, I., Melen, E., Anto, J.M., Bousquet, J., Wickman, M., 2016. IgE antibodies in relation to prevalence and multimorbidity of eczema, asthma, and rhinitis from birth to adolescence. Allergy 71, 342–349.

Beko, G., Callesen, M., Weschler, C.J., Toftum, J., Langer, S., Sigsgaard, T., Host, A., Kold Jensen, T., Clausen, G., 2015. Phthalate exposure through different pathways and allergic sensitization in preschool children with asthma, allergic rhinoconjunctivitis and atopic dermatitis. Environ. Res. 137, 432–439.

Benjamin, S., Masai, E., Kamimura, N., Takahashi, K., Anderson, R.C., Faisal, P.A., 2017. Phthalates impact human health: epidemiological evidences and plausible mechanism of action. J. Hazard Mater. 340, 360–383.

Bertelsen, R.J., Carlsen, K.C., Calafat, A.M., Hoppin, J.A., Haland, G., Mowinckel, P., Carlsen, K.H., Lovik, M., 2013. Urinary biomarkers for phthalates associated with asthma in Norwegian children. Environ. Health Perspect. 121, 251–256.

Blakesley, R.E., Mazumdar, S., Dew, M.A., Houck, P.R., Tang, G., Reynolds 3rd, C.F., Butters, M.A., 2009. Comparisons of methods for multiple hypothesis testing in neuropsychological research. Neuropsychology 23, 255–264.

Bolling, A.K., Holme, J.A., Bornehag, C.G., Nygaard, U.C., Bertelsen, R.J., Nånberg, E., Bodin, J., Sakhi, A.K., Thomsen, C., Becher, R., 2013. Pulmonary phthalate exposure and asthma is PPAR plausible mechanistic link? EXCLI Journal 12, 733–759.

Bolling, A.K., Sripada, K., Becher, R., Beko, G., 2020. Phthalate exposure and allergic diseases: review of epidemiological and experimental evidence. Environ. Int. 139, 105706.

Bornehag, C.G., Sundell, J., Weschler, C.J., Sigsgaard, T., Lundgren, B., Hasselgren, M., Hagerhed-Engman, L., 2004. The association between asthma and allergic symptoms in children and phthalates in house dust: a nested case-control study. Environ. Health Perspect. 112, 1393–1397.

Bousquet, J., Anto, J.M., Wickman, M., Keil, T., Valenta, R., Haahtela, T., Lodrup Carlsen, K., van Hage, M., Akdis, C., Bachert, C., Akdis, M., Auffray, C., Annesi-Maesano, I., Bindslev-Jensen, C., Cambon-Thomsen, A., Carlsen, K.H., Chatzi, L., Forastiere, F., Garcia-Aymerich, J., Gehrig, U., Guerra, S., Heinrich, J., Koppelman, G.H., Kowalski, M.L., Lambrecht, B., Lupinek, C., Maier, D., Melen, E., Momas, I., Palkonen, S., Pinart, M., Postma, D., Siroux, V., Smit, H.A., Sunyer, J., Wright, J., Zuberbier, T., Arshad, S.H., Nadif, R., Thijs, C., Andersson, N., Asarnoj, A., Ballardini, N., Ballereau, S., Bedbrook, A., Benet, M., Bergstrom, A., Brunekreef, B., Burte, E., Calderon, M., De Carlo, G., Demoly, P., Eller, E., Fantini, M. P., Hammad, H., Hohman, C., Just, J., Kerkhof, M., Kogevinas, M., Kull, I., Lau, S., Lemonnier, N., Mommers, M., Nawijn, M., Neubauer, A., Oddie, S., Pellet, J., Pin, I., Porta, D., Saes, Y., Skrindo, I., Tischer, C.G., Torrent, M., von Hertzen, L., 2015. Are allergic multimorbidities and IgE polysensitization associated with the persistence or re-occurrence of foetal type 2 signalling? The MeDALL hypothesis. Allergy 70, 1062–1078.

Bousquet, J., Schunemann, H.J., Samolinski, B., Demoly, P., Baena-Cagnani, C.E., Bachert, C., Bonini, S., Boulet, L.P., Bousquet, P.J., Brozek, J.L., Canonica, G.W., Casale, T.B., Cruz, A.A., Fokkens, W.J., Fonseca, J.A., van Wijk, R.G., Grouse, L., Haahtela, T., Khaltaev, N., Kuna, P., Lockey, R.F., Lodrup Carlsen, K.C., Mullol, J., Naclerio, R., O'Hehir, R.E., Ohta, K., Palkonen, S., Papadopoulos, N.G., Passalacqua, G., Pawankar, R., Price, D., Ryan, D., Simons, F.E., Togias, A., Williams, D., Yorgancioglu, A., Yusuf, O.M., Aberer, W., Adachi, M., Agache, I., Ait-Khaled, N., Akdis, C.A., Andrianarisoa, A., Annesi-Maesano, I., Ansotegui, I.J., Baiardini, I., Bateman, E.D., Bedbrook, A., Beghe, B., Beji, M., Bel, E.H., Ben Kheder, A., Bennoor, K.S., Bergmann, K.C., Berrissoul, F., Bieber, T., Bindslev Jensen, C., Blaiss, M.S., Boner, A.L., Bouchard, J., Braido, F., Brightling, C.E., Bush, A., Caballero, F., Calderon, M.A., Calvo, M.A., Camargos, P.A., Caraballo, L.R., Carlsen, K.H., Carr, W., Cepeda, A.M., Cesario, A., Chavannes, N.H., Chen, Y.Z., Chiriac, A.M., Chivato Perez, T., Chkhartishvili, E., Ciprandi, G., Costa, D.J., Cox, L., Custovic, A., Dahl, R., Darsow, U., De Blay, F., Deleanu, D., Denburg, J.A., Devillier, P., Didi, T., Dokic, D., Dolen, W.K., Douagui, H., Dubakiene, R., Durham, S. R., Dykewicz, M.S., El-Gamal, Y., El-Meziane, A., Emuzyte, R., Fiocchi, A., Fletcher, M., Fukuda, T., Gamkrelidze, A., Gereda, J.E., Gonzalez Diaz, S., Gotua, M., Guzman, M.A., Hellings, P.W., Hellquist-Dahl, B., Horak, F., Hourihane, J.O., Howarth, P., Humbert, M., Ivancevich, J.C., Jackson, C., Just, J., Kalayci, O., Kaliner, M.A., Kalyoncu, A.F., Keil, T., Keith, P.K., Khayat, G., Kim, Y.Y., Koffi N'goran, B., Koppelman, G.H., Kowalski, M.L., Kull, I., Kvedariene, V., Larenas-Linnemann, D., Le, L.T., Lemiere, C., Li, J., Lieberman, P., Lipworth, B., Mahboub, B., Makela, M.J., Martin, F., Marshall, G.D., Martinez, F.D., Masjedi, M.R., Maurer, M., Mavale-Manuel, S., Mazon, A., Melen, E., Meltzer, E.O., Mendez, N.H., Merk, H., Mihaltan, F., Mohammad, Y., Morais-Almeida, M., Muraro, A., Nafti, S., Namazova-Baranova, L., Nekam, K., Neou, A., Niggemann, B., Nizankowska-Mogilnicka, E., Nyembue, T.D., Okamoto, Y., Okubo, K., Orru, M.P., Ouedraogo, S., Ozdemir, C., Panzner, P., Pali-Scholl, I., Park, H.S., Pigearias, B., Pohl, W., Popov, T.A., Postma, D. S., Potter, P., Rabe, K.F., Ratomaharo, J., Reitamo, S., Ring, J., Roberts, R., Rogala, B., Romano, A., Roman Rodriguez, M., Rosado-Pinto, J., Rosenwasser, L., Rottem, M., Sanchez-Borges, M., Scadding, G.K., Schmid-Grendelmeier, P., Sheikh, A., Sisul, J.C., Sole, D., Sooronbaev, T., Spicak, V., Spranger, O., Stein, R.T., Stoloff, S.W., Sunyer, J., Szczeklik, A., Todo-Bom, A., Toskala, E., Tremblay, Y., Valenta, R., Valero, A.L., Valeyre, D., Valiulis, A., Valovirta, E., Van Cauwenberge, P., Vandenplas, O., van Weel, C., Vichyanond, P., Viegi, G., Wang, D. Y., Wickman, M., Wohrl, S., Wright, J., Yawn, B.P., Yiallouros, P.K., Zar, H.J., Zernotti, M.E., Zhong, N., Zidarn, M., Zuberbier, T., Burney, P.G., Johnston, S.L., Warner, J.O., World Health Organization Collaborating Center for Asthma and Rhinitis, 2012. Allergic rhinitis and its impact on asthma (ARIA): achievements in 10 years and future needs. J. Allergy Clin. Immunol. 130, 1049–1062.

Braun, J.M., Sathyanarayana, S., Hauser, R., 2013. Phthalate exposure and children's health. Curr. Opin. Pediatr. 25, 247–254.

Callesen, M., Beko, G., Weschler, C.J., Langer, S., Brive, L., Clausen, G., Toftum, J., Sigsgaard, T., Host, A., Jensen, T.K., 2014a. Phthalate metabolites in urine and asthma, allergic rhinoconjunctivitis and atopic dermatitis in preschool children. Int. J. Hyg Environ. Health 217, 645–652.

Callesen, M., Beko, G., Weschler, C.J., Sigsgaard, T., Jensen, T.K., Clausen, G., Toftum, J., Norberg, L.A., Host, A., 2014b. Associations between selected allergens, phthalates, nicotine, polycyclic aromatic hydrocarbons, and bedroom ventilation and clinically confirmed asthma, rhinoconjunctivitis, and atopic dermatitis in preschool children. Indoor Air 24, 136–147.

Cardinale, F., de Benedictis, F.M., Muggeo, V., Giordano, P., Loffredo, M.S., Iacoviello, G., Armenio, L., 2005. Exhaled nitric oxide, total serum IgE and allergic sensitization in childhood asthma and allergic rhinitis. Pediatr. Allergy Immunol. 16, 236–242.

Chang, M.L., Cui, C., Liu, Y.H., Pei, L.C., Shao, B., 2015. Analysis of total immunoglobulin E and specific immunoglobulin E of 3,721 patients with allergic disease. Biomed Rep 3, 573–577.

Choi, W.J., Kwon, H.J., Hong, S., Lim, W.R., Kim, H., Kim, J., Kim, C., Kim, K.S., 2014. Potential nonmonotonous association between di(2-ethylhexyl) phthalate exposure and atopic dermatitis in Korean children. Br. J. Dermatol. 171, 854–860.

Choi, Y.H., Hu, H., Mukherjee, B., Miller, J., Park, S.K., 2012. Environmental cadmium and lead exposures and hearing loss in U.S. adults: the National Health and Nutrition Examination Survey, 1999 to 2004. Environ. Health Perspect. 120, 1544–1550.

Cocci, P., Mosconi, G., Arukwe, A., Mozzicafreddo, M., Angeletti, M., Aretusi, G., Palermo, F.A., 2015. Effects of diisodecyl phthalate on PPAR: RXR-dependent gene expression pathways in sea bream hepatocytes. Chem. Res. Toxicol. 28, 935–947.

D'Amato, G., Vitale, C., Rosario, N., Neto, H.J.C., Chong-Silva, D.C., Mendonca, F., Perini, J., Landgraf, L., Sole, D., Sanchez-Borges, M., Ansotegui, I., D'Amato, M., 2017. Climate change, allergy and asthma, and the role of tropical forests. World Allergy Organ J 10, 11.

Ditlevsen, S., Keiding, N., Christensen, U., Damsgaard, M.T., Lynch, J., 2005. Mediation proportion. Epidemiology-Baltimore 16, 114–120.

Franken, C., Lambrechts, N., Govarts, E., Koppen, G., Den Hond, E., Ooms, D., Voorspoels, S., Bruckers, L., Loots, I., Nelen, V., Sioen, I., Nawrot, T.S., Baeyens, W., Van Larebeke, N., Schoeters, G., 2017. Phthalate-induced oxidative stress and association with asthma-related airway inflammation in adolescents. Int. J. Hyg Environ. Health 220, 468–477.

Frederiksen, H., Aksglaede, L., Sorensen, K., Skakkebaek, N.E., Juul, A., Andersson, A.M., 2011. Urinary excretion of phthalate metabolites in 129 healthy Danish children and adolescents: estimation of daily phthalate intake. Environ. Res. 111, 656–663.

Gruber, C., van Stuijvenberg, M., Mosca, F., Moro, G., Chirico, G., Braegger, C.P., Riedler, J., Boehm, G., Wahn, U., Group, M.W., 2010. Reduced occurrence of early atopic dermatitis because of immunoactive prebiotics among low-atopy-risk infants. J. Allergy Clin. Immunol. 126, 791–797.
Ha, J., Lee, S.W., Yon, D.K., 2020. Ten-Year trends and prevalence of asthma, allergic rhinitis, and atopic dermatitis among the Korean population, 2008-2017. Clin Exp Pediatr 63, 278–283.
Hoppin, J.A., Jaramillo, R., London, S.J., Bertelsen, R.J., Salo, P.M., Sandler, D.P., Zeldin, D.C., 2013. Phthalate exposure and allergy in the U.S. population: results from NHANES 2005-2006. Environ. Health Perspect. 121, 1129–1134.
Hsu, N.Y., Lee, C.C., Wang, J.Y., Li, Y.C., Chang, H.W., Chen, C.Y., Bornehag, C.G., Wu, P. C., Sundell, J., Su, H.J., 2012. Predicted risk of childhood allergy, asthma, and reported symptoms using measured phthalate exposure in dust and urine. Indoor Air 22, 186–199.
James-Todd, T.M., Huang, T., Seely, E.W., Saxena, A.R., 2016. The association between phthalates and metabolic syndrome: the national health and nutrition examination survey 2001-2010. Environ. Health 15, 52.
Jepsen, K.F., Abildtrup, A., Larsen, S.T., 2004. Monophthalates promote IL-6 and IL-8 production in the human epithelial cell line A549. Toxicol. Vitro 18, 265–269.
Just, A.C., Whyatt, R.M., Perzanowski, M.S., Calafat, A.M., Perera, F.P., Goldstein, I.F., Chen, Q., Rundle, A.G., Miller, R.L., 2012. Prenatal exposure to butylbenzyl phthalate and early eczema in an urban cohort. Environ. Health Perspect. 120, 1475–1480.
Karli, R., Balbaloglu, E., Uzun, L., Cinar, F., Ugur, M.B., 2013. Correlation of symptoms with total IgE and specific IgE levels in patients presenting with allergic rhinitis. Ther. Adv. Respir. Dis. 7, 75–79.
Kim, E.H., Jeon, B.H., Kim, J., Kim, Y.M., Han, Y., Ahn, K., Cheong, H.K., 2017. Exposure to phthalates and bisphenol A are associated with atopic dermatitis symptoms in children: a time-series analysis. Environ. Health 16, 24.
Kimber, I., Dearman, R.J., 2010. An assessment of the ability of phthalates to influence immune and allergic responses. Toxicology 271, 73–82.
Koh, H.Y., Kim, T.H., Sheen, Y.H., Lee, S.W., An, J., Kim, M.A., Han, M.Y., Yon, D.K., 2019. Serum heavy metal levels are associated with asthma, allergic rhinitis, atopic dermatitis, allergic multimorbidity, and airflow obstruction. J Allergy Clin Immunol Pract 7, 2912–2915 e2.
Kolarik, B., Naydenov, K., Larsson, M., Bornehag, C.G., Sundell, J., 2008. The association between phthalates in dust and allergic diseases among Bulgarian children. Environ. Health Perspect. 116, 98–103.
Krebs, N.F., Himes, J.H., Jacobson, D., Nicklas, T.A., Guilday, P., Styne, D., 2007. Assessment of child and adolescent overweight and obesity. Pediatrics 120, S193–S228.
Ku, H.Y., Su, P.H., Wen, H.J., Sun, H.L., Wang, C.J., Chen, H.Y., Jaakkola, J.J., Wang, S. L., Group, T., 2015. Prenatal and postnatal exposure to phthalate esters and asthma: a 9-year follow-up study of a taiwanese birth cohort. PLoS One 10, e0123309.
Kuo, C.H., Hsieh, C.C., Kuo, H.F., Huang, M.Y., Yang, S.N., Chen, L.C., Huang, S.K., Hung, C.H., 2013. Phthalates suppress type I interferon in human plasmacytoid dendritic cells via epigenetic regulation. Allergy 68, 870–879.
Larsen, S.T., Lund, R.M., Nielsen, G.D., Thygesen, P., Poulsen, O.M., 2002. Adjuvant effect of di-n-butyl-, di-n-octyl-, di-iso-nonyl-and di-iso-decyl phthalate in a subcutaneous injection model using BALB/c mice. Pharmacol. Toxicol. 91, 264–272.
Lee, K.S., 2020. Trends in prevalence of allergic diseases in Korean children: how and why? Clin Exp Pediatr 63, 263–264.
Lee, I., Park, J.Y., Kim, S., An, J.N., Lee, J., Park, H., Jung, S.K., Kim, S.Y., Lee, J.P., Choi, K., 2020. Association of exposure to phthalates and environmental phenolics with markers of kidney function: Korean National Environmental Health Survey (KoNEHS) 2015-2017. Environ. Int. 143, 105877.
Liu, C.-A., Wang, C.-L., Chuang, H., Ou, C.-Y., Hsu, T.-Y., Yang, K.D., 2003. Prediction of elevated cord blood IgE levels by maternal IgE levels, and the neonate's gender and gestational age. Chang Gung Med. J. 26, 561–569.
Maio, S., Baldacci, S., Simoni, M., Angino, A., Martini, F., Cerrai, S., Sarno, G., Pala, A., Bresciani, M., Paggiaro, P., Viegi, G., Group, A.S., 2012. Impact of asthma and comorbid allergic rhinitis on quality of life and control in patients of Italian general practitioners. J. Asthma 49, 854–861.
NIER, 2018. The 3rd Korean Natioanl Environmental Health Survey. Manual for Analysis of Environmental Pollutants in Biological Samples (Organic Chemicals) (National Institute of Environmental Research). Korea Ministry of Environment.
NIER, 2019a. The 3rd Korean Natioanl Environmental Health Survey. Instruction for Use of Data (National Institute of Environmental Research). Korea Ministry of Environment.
NIER, 2019b. The 3rd Korean natioanl environmental health survey (National Institute of Environmental Research). Manual for Clinical Examination. Korea Ministry of Environment.
Nishioka, J., Iwahara, C., Kawasaki, M., Yoshizaki, F., Nakayama, H., Takamori, K., Ogawa, H., Iwabuchi, K., 2012. Di-(2-ethylhexyl) phthalate induces production of inflammatory molecules in human macrophages. Inflamm. Res. 61, 69–78.
Odebeatu, C.C., Taylor, T., Fleming, L.E., N, J.O., 2019. Phthalates and asthma in children and adults: US NHANES 2007-2012. Environ. Sci. Pollut. Res. Int. 26, 28256–28269.
Park, M., Luo, S., Kwon, J., Stock, T.H., Delclos, G., Kim, H., Yun-Chul, H., 2013. Effects of air pollution on asthma hospitalization rates in different age groups in metropolitan cities of Korea. Air Qual Atmos Health 6.
Qin, W., Deng, T., Cui, H., Zhang, Q., Liu, X., Yang, X., Chen, M., 2018. Exposure to diisodecyl phthalate exacerbated Th2 and Th17-mediated asthma through aggravating oxidative stress and the activation of p38 MAPK. Food Chem. Toxicol. 114, 78–87.
Satwani, H., Rehman, A., Ashraf, S., Hassan, A., 2009. Is serum total IgE levels a good predictor of allergies in children. J Pak Med Assoc 59.
Shi, W., Lin, Z., Liao, C., Zhang, J., Liu, W., Wang, X., Cai, J., Zou, Z., Wang, H., Norback, D., Kan, H., Huang, C., Zhao, Z., 2018. Urinary phthalate metabolites in relation to childhood asthmatic and allergic symptoms in Shanghai. Environ. Int. 121, 276–286.
Soomro, M.H., Baiz, N., Philippat, C., Vernet, C., Siroux, V., Nichole Maesano, C., Sanyal, S., Slama, R., Bornehag, C.G., Annesi-Maesano, I., 2018. Prenatal exposure to phthalates and the development of eczema phenotypes in male children: results from the EDEN mother-child cohort study. Environ. Health Perspect. 126, 027002.
Spergel, J.M., Paller, A.S., 2003. Atopic dermatitis and the atopic march. J. Allergy Clin. Immunol. 112, S118–S127.
Tran, T.M., Kannan, K., 2015. Occurrence of phthalate diesters in particulate and vapor phases in indoor air and implications for human exposure in Albany, New York, USA. Arch. Environ. Contam. Toxicol. 68, 489–499.
Tranfo, G., Caporossi, L., Pigini, D., Capanna, S., Papaleo, B., Paci, E., 2018. Temporal trends of urinary phthalate concentrations in two populations: effects of REACH authorization after five years. Int. J. Environ. Res. Publ. Health 15.
Tsai, M.J., Kuo, P.L., Ko, Y.C., 2012. The association between phthalate exposure and asthma. Kaohsiung J. Med. Sci. 28, S28–S36.
Wang, I.J., Lin, C.C., Lin, Y.J., Hsieh, W.S., Chen, P.C., 2014. Early life phthalate exposure and atopic disorders in children: a prospective birth cohort study. Environ. Int. 62, 48–54.
Wang, I.J., Karmaus, W.J., Chen, S.L., Holloway, J.W., Ewart, S., 2015. Effects of phthalate exposure on asthma may be mediated through alterations in DNA methylation. Clin. Epigenet. 7, 27.
Wang, I.J., Chen, C.Y., Bornehag, C.G., 2016. Bisphenol A exposure may increase the risk of development of atopic disorders in children. Int. J. Hyg Environ. Health 219, 311–316.
Wang, I.J., Karmaus, W.J., 2017. Oxidative stress-related genetic variants may modify associations of phthalate exposures with asthma. Int. J. Environ. Res. Publ. Health 14.
Wang, Y., Zhu, H., Kannan, K., 2019. A review of biomonitoring of phthalate exposures. Toxics 7.
Wen, H.J., Chen, P.C., Chiang, T.L., Lin, S.J., Chuang, Y.L., Guo, Y.L., 2009. Predicting risk for early infantile atopic dermatitis by hereditary and environmental factors. Br. J. Dermatol. 161, 1166–1172.
Wittassek, M., Koch, H.M., Angerer, J., Bruning, T., 2011. Assessing exposure to phthalates - the human biomonitoring approach. Mol. Nutr. Food Res. 55, 7–31.
Wu, W., Wu, C., Ji, C., Diao, F., Peng, J., Luo, D., Mu, X., Ruan, X., 2020. Association between phthalate exposure and asthma risk: a meta-analysis of observational studies. Int. J. Hyg Environ. Health 228, 113539.
Yang, S.N., Hsieh, C.C., Kuo, H.F., Lee, M.S., Huang, M.Y., Kuo, C.H., Hung, C.H., 2014. The effects of environmental toxins on allergic inflammation. Allergy Asthma Immunol Res 6, 478–484.
Zota, A.R., Calafat, A.M., Woodruff, T.J., 2014. Temporal trends in phthalate exposures: findings from the national health and nutrition examination survey, 2001-2010. Environ. Health Perspect. 122, 235–241.

International Journal of Hygiene and Environmental Health 238 (2021) 113849

Contents lists available at ScienceDirect

International Journal of Hygiene and Environmental Health

journal homepage: www.elsevier.com/locate/ijheh

Combined chemical exposure using exposure loads on human biomonitoring data of the 4th Flemish Environment and Health Study (FLEHS-4)

Jurgen Buekers [a,*], Veerle Verheyen [a], Sylvie Remy [a], Adrian Covaci [b], Ann Colles [a], Gudrun Koppen [a], Eva Govarts [a], Liesbeth Bruckers [c], Martine Leermakers [d], Annie St-Amand [e], Greet Schoeters [a,f]

[a] VITO, Flemish Institute for Technological Research, Unit Health, Boeretang 200, 2400, Mol, Belgium
[b] Toxicological Center, University of Antwerp, 2610, Wilrijk, Belgium
[c] Hasselt University, Data Science Institute, Interuniversity Institute for Biostatistics and Statistical Bioinformatics, Diepenbeek, Belgium
[d] Department of Analytical, Environmental and Geochemistry (AMGC), Vrije Universiteit Brussel (VUB), Brussels, Belgium
[e] Health Canada, Ottawa, Canada
[f] Department of Biomedical Sciences, University of Antwerp, 2610, Wilrijk, Belgium

ARTICLE INFO

Keywords:
Exposure load
HBM
FLEHS
Combined chemical exposure
Relatively high exposed subpopulation
Exposure determinants

ABSTRACT

To improve our understanding of internal exposure to multiple chemicals, the concept exposure load (EL) was used on human biomonitoring (HBM) data of the 4th FLEHS (Flemish Environment and Health Study; 2016–2020). The investigated chemicals were per- and polyfluoroalkyl substances (PFASs), bisphenols, phthalates and alternative plasticizers, flame retardants, pesticides, toxic metals, organochlorine compounds and polycyclic aromatic hydrocarbons (PAHs). The EL calculates "the number of chemicals to which individuals are internally exposed above a predefined threshold". In this study, the 50th and 90th percentile of each of the 45 chemicals were applied as thresholds for the EL calculations for 387 study participants. Around 20% of the participants were exposed to >27 chemicals above the P50 and to >6 chemicals above the P90 level. This shows that participants can be internally exposed to multiple chemicals in relatively high concentrations. When the chemical composition of the EL was considered, the variability between individuals was driven by some chemicals more than others. The variability of the chemical profiles at high exposure loads (EL-P90) was somewhat dominated by e.g. organochlorine chemicals, PFASs, phthalates, PAHs, organophosphate flame retardants, bisphenols (A & F), pesticides, metals, but to a lesser extent by brominated flame retardants, the organophosphorus flame retardants TCIPP & TBOEP, naphthalene and benzene, bisphenols S, B & Z, the pesticide 2,4-D, the phthalate DEP and alternative plasticizer DINCH. Associations between the EL and exposure determinants suggested determinants formerly associated with fat soluble chemicals, PFASs, bisphenols, and PAHs. This information adds to the knowledge needed to reduce the exposure by policymakers and citizens. However, a more in depth study is necessary to explore in detail the causes for the higher EL in some individuals. Some limitations in the EL concept are that a binary number is used for exposure above or below a threshold, while toxicity and residence time in the body are not accounted for and the sequence of exposure in different life stages is unknown. However, EL is a first useful step to get more insight in multiple chemical exposure in higher exposed subpopulations (relative to the rest of the sampled population).

1. Introduction

There are few data on combined human internal exposure for the majority of the >100,000 chemicals available on the European market (ECHA, 2020). A considerable fraction of these chemicals is found in personal care products, electronics, food packaging, pharmaceuticals, building materials and home furnishings which leads to widespread human exposure (UN, 2020). There is also chemical exposure of humans

* Corresponding author.
E-mail address: jurgen.buekers@vito.be (J. Buekers).

https://doi.org/10.1016/j.ijheh.2021.113849
Received 8 July 2021; Received in revised form 13 September 2021; Accepted 13 September 2021
Available online 20 September 2021

via the environment, e.g. chemicals emitted during burning processes and through contamination of water and soil. People are typically not exposed to one chemical at a time, but to a mixture of chemicals and, due to the long half-life of many chemicals in humans, past external exposure can still be detected in the internal exposure. A paradigm shift from the chemical-by-chemical assessment towards an assessment of combined exposure to multiple chemicals is therefore imperiously necessary, together with an expansion of the exposure concepts towards mixtures. Unfortunately, the number of mixtures that can be formed from the thousands of environmental chemicals is enormous. It can be assumed that exposure to multiple chemicals in the environment is often not random, but related to e.g. identical sources or exposure pathways, comparable personal characteristics or lifestyle factors.

To investigate the uniqueness of the combination of chemicals to which a person is internally exposed at a given point in time and whether we can distinguish subpopulations that are highly exposed to many chemicals, the concept of exposure load (EL) was used. It was slightly adapted from the Canadian Health Measurement Survey (CHMS) (St-Amand, 2019; Willey et al., 2021) and applied on HBM data from adolescents monitored in the 4th Flemish Environment and Health Study (FLEHS-4). Human biomonitoring studies measure concentrations of chemicals or their metabolites in body fluids or tissues (Angerer et al., 2007). Measurements of different exposure biomarkers in individual urine and/or blood samples provide an aggregated picture of the chemical internal exposure of an individual resulting from different exposure routes and from various sources.

The EL is based as first on establishing whether a person is exposed (assigned a value of 1) or non-exposed (assigned a value of 0) above a predefined concentration threshold of a given biomonitored chemical, and then summing the exposure counts. Yet, EL does not take toxicity into account. The technique finds its origin in frequent itemset mining (FIM), initially developed by marketing researchers to identify items that are frequently purchased together (Borgelt, 2016). It was already applied by Kapraun et al. (2017) to the 2009–2010 NHANES (National Health And Nutrition Examination Survey) dataset. FIM is also used to identify relationships between chemicals, health biomarkers and disease (Bell and Edwards, 2015). Other applications of FIM are the evaluation of the presence of chemicals in food (Krishan et al., 2017) and the identification and quantification of associations between environmental and social stressors (Huang et al., 2017). This adapted approach of the CHMS exposure load was then tested on HBM data of Flemish adolescents (Belgium) participating in the 4th FLEHS campaign.

The study had three goals: a) calculate the EL and study the distribution across the FLEHS-4 population, b) study the chemical composition of the EL and c) identify determinants of EL variability, which could lead to the identification of disproportionally exposed subpopulations.

The present study was a proof of concept for the H2020 HBM4EU (Human Biomonitoring for Europe) project, which aims to develop a sustainable European wide HBM network (2017–2021). HBM4EU will also provide better evidence of the actual exposure of citizens to chemicals and the possible health effects to support policy making (https://www.hbm4eu.eu/about-hbm4eu/).

2. Methodology

2.1. Population

The 4th cycle of the Flemish Environment and Health study, FLEHS-4, gives a snapshot of exposure to chemicals in a general population of adolescents (14-15y). The FLEHS-4 study was running in 2016–2020. Collection of biological samples was done over a 1-year period from September 2017 until September 2018. Adolescents were not occupationally exposed and serve as a sentinel for the environment where they grew up in. Details of the recruitment protocols have been reported before (Den Hond et al., 2009; Baeyens et al., 2014; De Craemer et al., 2016). In FLEHS-4, a Flemish study population of 428 participants background exposed was recruited. The aim was to enrol equal numbers of girls and boys and to reflect the proportion of Flemish adolescents in all educational levels. In order to obtain a geographically representative sample, adolescents were recruited through schools in the five Flemish provinces, proportional to the number of inhabitants per province. To account for seasonal variation, recruitment was spread over one year with no recruitment during examination periods and summer holidays (June, July, August, September). Inclusion criteria were: informed consent signed by participants and parents (no cases where legal guardians needed to sign), living in Flanders for at least 5 years, the ability to fill out extensive questionnaires in Dutch. Exclusion criteria were: pregnancy, more than 1 out of 3 questionnaires missing, blood and urine sample missing, being held back in school for more than 1 year, attending boarding school.

Study participants and their parents filled in questionnaires in Dutch with information needed for interpretation of biomarkers of exposure and of effect. The questionnaires covered information on health status, dietary habits, home environment, lifestyle and socio-economic status (SES). The HBM study was approved by the Ethical committee of the Antwerp University Hospital (registration number B300201732753).

2.2. Chemicals and exposure biomarkers

Chemicals of interest to measure during the FLEHS-4 campaign were selected in a transparent and participatory way involving scientists, policy makers and other stakeholders, based on technical criteria, health and exposure-related criteria and policy relevance (Schoeters et al., 2012b). The involved laboratories had to fulfil standard quality assurance and quality control (QA/QC). Validation dossiers were required and participation in international ring tests was desired (Esteban López et al., 2021). A broad range of chemicals from various potential sources were included in the EL analysis including several emerging chemicals: polyaromatic hydrocarbons (PAHs), benzene (Bz), metals, pesticides, organochlorine compounds (OC), brominated – and organophosphate flame retardants, bisphenols, per- and polyfluoroalkyl substances (PFASs) and phthalates and their alternatives. An overview is given in Table 1.

For the EL analysis, concentrations in blood were expressed per volume unit (μg/L) for PFASs and lead and were normalized by blood fat for organochlorine compounds and brominated diphenyl ethers, while urinary concentrations were standardised by specific gravity. Only those biomarkers for which at least 30% of the values were above the LOD or LOQ reported by the laboratories were considered for the EL calculation. The value of 30% was chosen as cut-off (or threshold), as it was not the intention to focus on chemicals detected only in a small part of the studied population (<30%). The total number of chemicals considered for the EL analysis was 45.

Biomarkers for which less than 30% of measurements was above LOD or LOQ were: 4-hydroxyphenanthrene (4-OH-PHE), perfluoroheptane sulfonate (PFHpS), perfluorobutane sulfonate (PFBS), perfluorododecanoic acid (PFDoDA), perfluoroundecanoic acid (PFUnDA), perfluorohexanesulfonic acid (PFHxA), perfluoropentanoic acid (PFPeA), perfluoroheptanoic acid (PFHPA), bisphenol-AF (BP-AF), mono-isononyl-cyclohexane-1,2-dicarboxylate (MINCH), mono-2-ethylhexyl terephthalate (MEHTP), mono(2-ethylhexyl) adipate (MEHA), mono(2-ethyl-5-hydroxyhexyl) adipate (OH-MEHA), 1,2-di(2-ethylhexyl) trimellitate (DEHTM), BDE28, BDE100, BDE153, BDE183, gamma-hexachlorocyclohexane (γ-HCH), 4-hydroxyphenyl diphenyl phosphate (4-OH-TPHP), 4-hydroxyphenyl phenyl phosphate (4-OH-DPHP), bis(1-chloro-2-propyl) phosphate (BCIPP), tris(chloroethyl) phosphate (TCEP), bis(2-butoxyethyl) phosphate (BBOEP), bis(2-butoxyethyl) 3′-hydroxy-2-butoxyethyl phosphate (3-OH-TBOEP), di-n-butyl phosphate (DNBP).

Details of the sampling and an overview of biomarkers measured in previous FLEHS campaigns have been previously reported (Schoeters et al., 2012a; Schoeters et al., 2012b; Schoeters et al., 2017; Steunpunt

Table 1
List of chemicals & biomarkers considered in the EL (exposure load) analysis.

Chemical group	Nr	Chemical	Biomarker	Grouping[a]
PAHs in urine	1	Pyrene (PYR)	1-Hydroxypyrene (1-OH-PYR)	
	2	Naphthalene (NAP)	2-Hydroxynaphthalene (2-OH-NAP)	
	3	Fluorene (FLU)	Sum of 2- and 3-Hydroxyfluorene (2&3-OH-FLU)	
	4	Phenanthrene (PHE)	2-Hydroxyphenanthrene (2-OH-PHE) 3-Hydroxyphenanthrene (3-OH-PHE) Sum of 1- and 9-Hydroxyphenanthrene (1&9-OH-PHE)	Considered as group in analysis
Benzene in urine	5	Benzene (Bz)	T,t'-muconic acid (t,t'-MA)	
Metals in urine[b]	6	Cadmium (Cd)	Cadmium (Cd)	
	7	Thallium (TI)	Thallium (TI)	
Metals in blood	8	Lead (Pb)	Lead (Pb)	
Pesticides in urine	9	Pyrethroïd pesticides 3-PBA	3-Phenoxybenzoic acid (3-PBA)	
	10	Chlorpyrifos (CPS)	3,5,6-Trichloro-2-pyridinol (TCPY)	
	11	Phenoxy herbicide 2,4-D	2,4-dichlorophenoxy acetic acid (2,4-D)	
	12	Glyphosate herbicide (GLY)	Glyphosate (GLY) Aminomethylphosphonic acid (AMPA)	Considered as group in analysis
Persistent Organic Pollutants (POPs) in serum: Organochlorine Compounds (OC)	13	Sum polychlorinated biphenyls (Sum PCBs) (138,153,180)	Sum PCBs 138,153,180	
	14	Hexachlorobenzene (HCB)	Hexachlorobenzene (HCB)	
	15	Dichloro-diphenyl-trichloroethane (DDT)	DDT DDT metabolite: p,p'-DDE	Considered as group in analysis
	16	Oxychlordane (OXC)	Oxychlordane (OXC)	
	17	Trans-nonachlor (TN)	Trans-nonachlor (TN)	
	18	Beta-hexachlorocyclohexane (HCH)	Beta-hexachlorocyclohexane (HCH)	
POPs: Brominated diphenyl ethers (BDEs) in serum	19	Brominated diphenyl ether (BDE)47	BDE47	
	20	BDE99	BDE99	
	21	BDE154	BDE154	
Organophosphate flame retardants in urine	22	Diphenyl phosphate (DPHP)	Diphenyl phosphate (DPHP)	
	23	2-Ethylhexyl diphenyl phosphate (EHDPHP)	2-Ethylhexyl phenyl phosphate (EHPHP) 2-Ethyl-5-hydroxyhexyl diphenyl phosphate (5-OH-EHDPHP)	Considered as group in analysis
	24	Tris(2-chloroisopropyl) phosphate (TCIPP)	1-Hydroxy-2-propyl bis(1-chloro-2-propyl) phosphate (BCIPHIPP)	
	25	Tris(2-butoxyethyl) phosphate (TBOEP)	2-Hydroxyethyl bis(2-butoxyethyl) phosphate (BBOEHEP)	
	26	Tris(1,3-dichloro-2-propyl) phosphate (TDCIPP)	Bis(1,3-dichloro-2-propyl) phosphate (BDCIPP)	
POPs: Per- and polyfluoroalkyl substances (PFAS) in serum	27	Perfluorooctane sulfonate (PFOS)	Perfluorooctane sulfonate (PFOS)	
	28	Perfluorohexane sulfonate (PFHxS)	Perfluorohexane sulfonate (PFHxS)	
	29	Perfluorodecanoic acid (PFDA)	Perfluorodecanoic acid (PFDA)	
	30	Perfluorononanoic acid (PFNA)	Perfluorononanoic acid (PFNA)	
	31	Perfluorooctanoic acid (PFOA)	Perfluorooctanoic acid (PFOA)	
Bisphenols (BP) in urine	32	Bisphenol-Z (BPZ)	Bisphenol-Z (BPZ)	
	33	Bisphenol-B (BPB)	Bisphenol-B (BPB)	
	34	Bisphenol-S (BPS)	Bisphenol-S (BPS)	
	35	Bisphenol-F (BPF)	Bisphenol-F (BPF)	
	36	Bisphenol-A (BPA)	Bisphenol-A (BPA)	
Phthalates and alternatives in urine	37	Diisodecyl phthalate (DIDP)	Mono-oxo-isodecyl phthalate (OXO-MiDP) Mono-carboxy-isononyl phthalate (CX-MiDP) Mono-hydroxy-isodecyl phthalate (OH-MiDP)	Considered as group in analysis
	38	1,2-Cyclohexane dicarboxylic acid, diisononyl ester (DINCH)	Cyclohexane-1,2-dicarboxylic acid, mono (carboxyoctyl) ester (MCOCH) Cyclohexane-1,2-dicarboxylic acid, mono(cis-hydroxy-isononyl) ester (MHNCH)	Considered as group in analysis
	39	Di-isononyl phthalate (DINP)	Monocarboxyoctyl phthalate (MCOP) Mono-hydroxy-isononyl phthalate (MHNP)	Considered as group in analysis
	40	di-2-ethylhexyl terephthalate (DEHTP)	mono(2-ethyl-5-hydroxyhexyl) terephthalate (OH-MEHTP)	
	41	Di-2-ethylhexyl phthalate (DEHP)	Mono(2-Ethylhexyl) phthalate (MEHP) Mono(2-ethyl-5-hydroxyhexyl) phthalate (MEHHP) Mono(2-ethyl-5-oxohexyl) phthalate (MEOHP) Mono-(2-ethyl-5-carboxypentyl) phthalate (CX-MEPP)	Considered as group in analysis
	42	Benzylbutyl phthalate (BzBP)	Monobenzyl phthalate (MBzP)	
	43	Di-*n*-butyl phthalate (DBP)	Monobutyl phthalate (MBP)	
	44	Di-isobutyl phthalate (DiBP)	Monoisobutyl phthalate (MiBP)	
	45	Diethyl phthalate (DEP)	Monoethyl phthalate (MEP)	

[a] Grouping process applied in exposure load analysis is explained further (see section 2.3.1).
[b] Arsenic was only measured in half of the participants and is thus not considered here.

Milieu en Gezondheid, 2020). Organophosphate flame retardants were measured extensively for the first time in FLEHS-4 (Bastiaensen et al., 2021b).

In short, metals were measured in urine and blood by high resolution ICP-MS (Baeyens et al., 2014). The benzene metabolite, t,t'-muconic acid, was measured according to Ducos et al. (1990). Urine was purified with solid-phase extraction (SPE) using a strong anionic-exchange cartridge and retained components were eluted with acetic acid. Analysis was with an ultra-performance liquid chromatography (UPLC) system coupled with a (Photodiode Array) PDA detector (Waters USA). Metabolites of polyaromatic hydrocarbons (PAHs) were analysed according to Onyemauwa et al. (2009) and Ramsauer et al. (2011). They were enzymatically released overnight, followed by an ultra-performance liquid chromatography tandem mass spectrometry analysis (UPLC-MS/MS) (Waters Xevo TQ-S). POPs (organochlorine compounds and PBDEs) were measured in serum using SPE and gas chromatography-electron capture negative ionization mass spectrometry (Dirtu et al., 2013). Metabolites of organophosphate flame retardants were extracted from urine by SPE on C18 cartridges and eluted with methanol. The analytes were separated by liquid chromatography on a biphenyl column and detected by triple quadrupole mass spectrometry (Bastiaensen et al., 2018, 2021b). The herbicide glyphosate and its main metabolite aminomethylphosphonic acid (AMPA) were analysed by gas chromatography with tandem mass spectrometry (GC-MS-MS), according to the procedure of Alferness and Iwata (1994) with some modifications (Hoppe, 2013). TCPY, a metabolite of the organophosphorus pesticide chlorpyrifos (CPS), 3-PBA, a shared metabolite of several synthetic pyrethroid pesticides, and the herbicide 2,4-Dichlorophenoxyacetic acid (2,4-D) were measured in urine. The analytical method comprised an SPE extraction of the deconjugated urine sample and analysis by liquid chromatography and triple-quadrupole mass spectrometry (Davis et al., 2013). Phthalates and alternative metabolites were extracted from urine by SPE on Oasis Max cartridges and thereafter eluted and concentrated. The analytes were separated by liquid chromatography on a biphenyl column and detected by triple quadrupole mass spectrometry (Bastiaensen et al., 2021a). PFAS were analysed via a dilute-and-shoot technique, measured with LC-MS/MS. Bisphenols were extracted from urine by SPE on Oasis Wax cartridges and thereafter eluted and concentrated. Analytes were further separated by gas chromatography using a DB-5MS capillary column and analysed by triple quadrupole mass spectrometry (Gys et al., 2021).

2.3. Exposure load (EL)

Detailed information about FIM, which serves as a as basis for the EL, can be found in Kapraun et al. (2017). Briefly, for "biomarker b", the concentration distribution is generated and descriptive statistics P50 (50th percentile) and P90 were derived. These values serve as discretization threshold. To further illustrate this approach, P50 is used. For each participant, it was checked whether the concentration for biomarker b was higher, equal or lower than the P50 value. If the concentration was higher or equal, the participant was assigned a value of 1 for biomarker b, in case the concentration was lower a value of 0 was assigned. In case the P50 was lower than the LOD or LOQ, then LOD or LOQ was used as threshold (this was the case for 4 chemicals). This discretization was repeated for all biomarkers considered (actually a binary 0 1 matrix was made). For some biomarkers, a grouping process was first performed before applying the discretization process (see next paragraph). Eventually, the total sum of all values (0 and 1) was taken as the exposure load for each participant (Willey et al., 2021). For the analysis, a valid value (0 or 1) for every single chemical involved was required for all participants.

Participants with missing data for one of the chemicals were excluded from the analysis. This means that all participants have theoretically the same maximal EL. A similar calculation can be made for discretization thresholds other than the P50. In this study, we applied the P50 and the P90 as thresholds. Exposure load were abbreviated as EL-P50 when P50 was used as threshold and EL-P90 when P90 was used as threshold.

2.4. Grouping process prior to EL determination

Some chemicals in the analysis were assessed by more than one biomarker (see Table 1): phenanthrene, DDT, glyphosate, 2-ethylhexyl diphenyl phosphate (EHDPHP), diisodecyl phthalate (DIDP), 1,2-cyclohexane dicarboxylic acid diisononyl ester (DINCH), di-isononyl phthalate (DINP) and di-2-ethylhexyl phthalate (DEHP). For calculating the EL, biomarkers representing the same chemical were first grouped, i.e. biomarkers were expressed as molar mass and summed. In this way, each chemical involved can have a 0 or 1 value, which brings the maximum exposure load for a participant equal to 45.

This grouping process deviates somewhat from the one of CHMS. They considered groups of chemicals and for chemical groups with more than 1 biomarker (e.g. for the benzene chemical group: benzene in blood, S-phenylmercapturic acid (S-PMA) in urine, t,t'-muconic acid (t, t'-MA) in urine), if one or more biomarker had a concentration > predefined threshold, then +1 was assigned for that chemical group. More information can be found in the publication of Willey et al., (2021).

2.5. Statistical analysis

In a first step, to assess how strong each internal exposure to a chemical was associated with the EL, Pearson biserial correlation coefficients were calculated between the EL and the scores for each chemical (0 or 1) by which the EL was formulated. To analyse the chemical composition further into detail, a dendrogram was created with the heatmap function in R statistical analysis software package using default settings (Euclidian distance; clustering = complete linkage method) (R Core Team, 2018). Clusters were generated based on similarities between the chemical internal exposure of the individuals (based on binary 0 1 matrix).

Determinants of variability in EL were analysed. Negative binomial regression analysis (no fixed effects) was performed with SPSS Statistics 26. Variables considered were among others personal factors as sex and blood fat, questions related to the living environment as exposure to groundwater and use of a heating stove inside, questions related to food consumption, use of consumer products, information on socio-economic status (SES; categories for equivalent household income and highest education in household), information on degree of urbanization at the home address and lifestyle factors (e.g. sports). The Benjamini-Hochberg method was used to check for false discovery rates (FDR). A backward negative binomial multiple regression analysis was performed starting from variables having a significant association ($p < 0.05$) in the univariate analysis.

3. Results and discussion

The exposure to multiple chemicals from various sources is a major concern, and up to now there are few attempts to describe and deal with the diversity of environmental chemicals in humans. However questions such as whether there are subpopuIations that are highly exposed to a lot of chemicals, whether these are the same chemicals or chemical clusters and whether these are related to specific lifestyle and environmental factors are key questions for prevention. The exposure load concept is a unique way to identify individuals that are higher exposed to a combination of chemicals.

3.1. Adolescents

Of the 428 adolescents in the FLEHS-4 study population background exposed, 387 participants had no missing data for all chemicals involved. This means 387 participants (Male: 185; Female: 202) were

included in the exposure load analysis.

3.2. Exposure load (EL)

Exposure load is reported for discretization thresholds P50 in Fig. 1 and P90 in Fig. 2. It is shown that 80% of the participants are exposed to ≤27 out of 45 chemicals above the P50 and ≤ 6 chemicals above the P90. Ten percent of the participants are exposed to ≤15 out of 45 chemicals above the P50 and ≤ 1 chemical above the P90 level.

Looking from another perspective, it also means for example that 20% of the participants are exposed to >27 chemicals out of 45 above the P50 and to >6 chemicals above the P90 level. This shows that participants can be internally exposed to multiple chemicals in relatively high concentrations. Keep in mind that an equal EL value does not necessarily imply exactly the same composition of chemicals present, neither the same concentration levels for these chemicals. More information on the composition is described below.

3.3. Chemical composition EL

A biserial correlation analysis between the EL and its constituents lead to following results (Table 2). Largest significant ($p < 0.001$) Pearson biserial correlation coefficients between EL-P90 and chemical scores (0 or 1) were observed for TN ($r = 0.38$), DBP ($r = 0.35$), sum PCBs ($r = 0.31$), OXC ($r = 0.30$) and EHDPHP ($r = 0.30$). Remaining coefficients can be found in Table 2. For the EL with threshold P50, more chemicals had a significant correlation coefficient above 0.30. In general, coefficients were larger for the EL-P50. Also DBP, sum PCBs, DEHP and DiBP are ranked relatively high for both EL-P50 and EL-P90. Chemicals which did not significantly contributed to the EL-P50 were NAP and BDE47. For BDE154, there was a significant negative correlation with the EL-P50. For the EL-P90, there was no significant correlation with Bz, NAP, DEP, BPB and BPZ.

From a participants' individual point of view, the combination of chemicals or itemsets (combination of 0 and 1) may be almost unique. A cluster analysis was performed and dendrograms were created to assess possible similar clustering of chemicals within individuals (see Fig. 3 and Fig. 4). For 4 chemicals (BPZ, PFDA, BDE99, BDE154), the P50 was equal to the LOD or LOQ. Therefore LOD or LOQ values were used instead of the P50 as threshold and slightly less than the half of the 387participants got a score of +1 for these chemicals.

From the dendrograms for both EL-P50 and EL-P90, it can be observed that similar clusters occur. Indeed, several organochlorine compounds (TN, OXC, sum PCBs, HCB, HCH) measured in serum were clustered close to PFAS. Both PFAS and PCBs bind to e.g. albumin, but PCBs also to lipids (Guo et al., 1987; Jones et al., 2003). They are

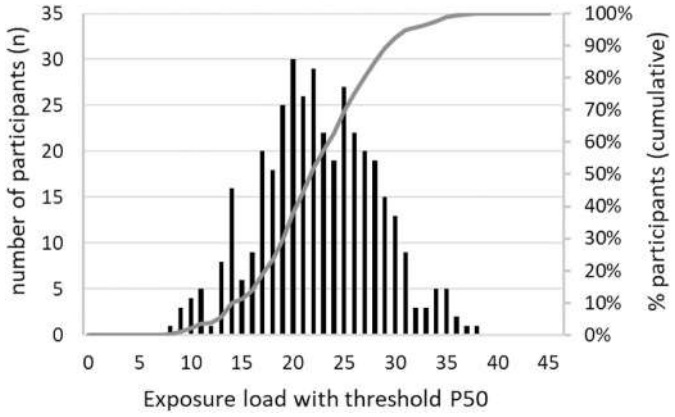

Fig. 1. Distribution of exposure load (EL) with discretization threshold P50-value. Maximum level of exposure load is 45. The line in the figure present the % of participants (cumulative).

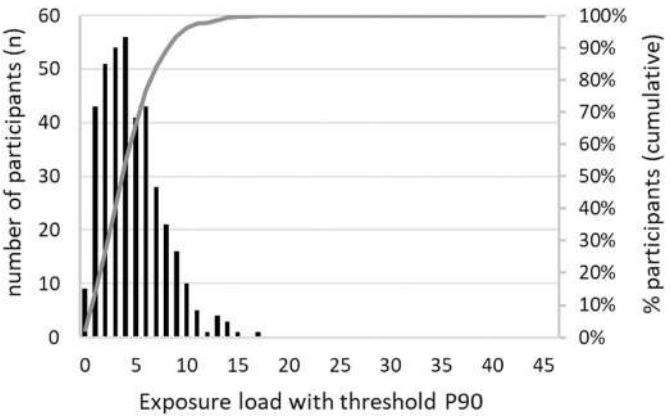

Fig. 2. Distribution of exposure load (EL) with discretization threshold P90-value. Maximum value of exposure load is 45. The line in the figure present the % of participants (cumulative).

Table 2
Biserial correlation between the exposure loads and their constituents.

EL-P50			EL-P90		
Chemical	Biserial Pearson correlation coefficient(r)[a]	p	Chemical	Biserial Pearson correlation coefficient (r)[a]	p
DBP	0.44	***	TN	0.38	***
DiBP	0.35	***	DBP	0.35	***
FLU	0.35	***	SumPCBs	0.31	***
PFOA	0.34	***	OXC	0.30	***
DPHP	0.34	***	EHDPHP	0.30	***
BzBP	0.34	***	PFOS	0.29	***
DEHP	0.34	***	DEHP	0.29	***
SumPCBs	0.34	***	DiBP	0.28	***
PFDA	0.33	***	PYR	0.28	***
HCB	0.33	***	PFNA	0.28	***
EHDPHP	0.32	***	HCB	0.27	***
DDT	0.32	***	PHE	0.27	***
3-PBA	0.32	***	PFOA	0.27	***
BPA	0.31	***	DIDP	0.26	***
PYR	0.31	***	DPHP	0.26	***
PFNA	0.31	***	Pb	0.26	***
PHE	0.30	***	DDT	0.25	***
DINCH	0.30	***	BzBP	0.24	***
DEHTP	0.29	***	FLU	0.24	***
TN	0.29	***	Cd	0.23	***
PFOS	0.29	***	DINP	0.23	***
OXC	0.28	***	PFDA	0.23	***
TCIPP	0.28	***	3-PBA	0.22	***
DINP	0.28	***	TDCIPP	0.22	***
Pb	0.27	***	PFHxS	0.21	***
GLY	0.27	***	DEHTP	0.21	***
PFHxS	0.26	***	HCH	0.21	***
TDCIPP	0.26	***	CPS	0.20	***
CPS	0.25	***	BPA	0.20	***
HCH	0.25	***	TI	0.19	***
Cd	0.24	***	BPF	0.19	***
DIDP	0.23	***	GLY	0.18	***
BPB	0.22	***	TCIPP	0.17	**
2,4-D	0.21	***	BDE99	0.17	**
TBOEP	0.21	***	2,4-D	0.17	**
DEP	0.19	***	BDE47	0.17	**
BDE99	0.18	***	DINCH	0.16	**
BPF	0.17	**	BDE154	0.15	**
TI	0.16	**	TBOEP	0.15	**
BPS	0.16	**	BPS	0.12	*
Bz	0.15	**	Bz	0.10	NS
BPZ	0.15	**	NAP	0.10	NS
BDE47	0.06	NS	DEP	0.09	NS
NAP	−0.04	NS	BPB	0.08	NS
BDE154	−0.10	*	BPZ	0.06	NS

[a]: ranked by value of correlation coefficient.
*:0.01 < p ≤ 0.05; **:0.001 < p ≤ 0.01; ***: p ≤ 0.001.

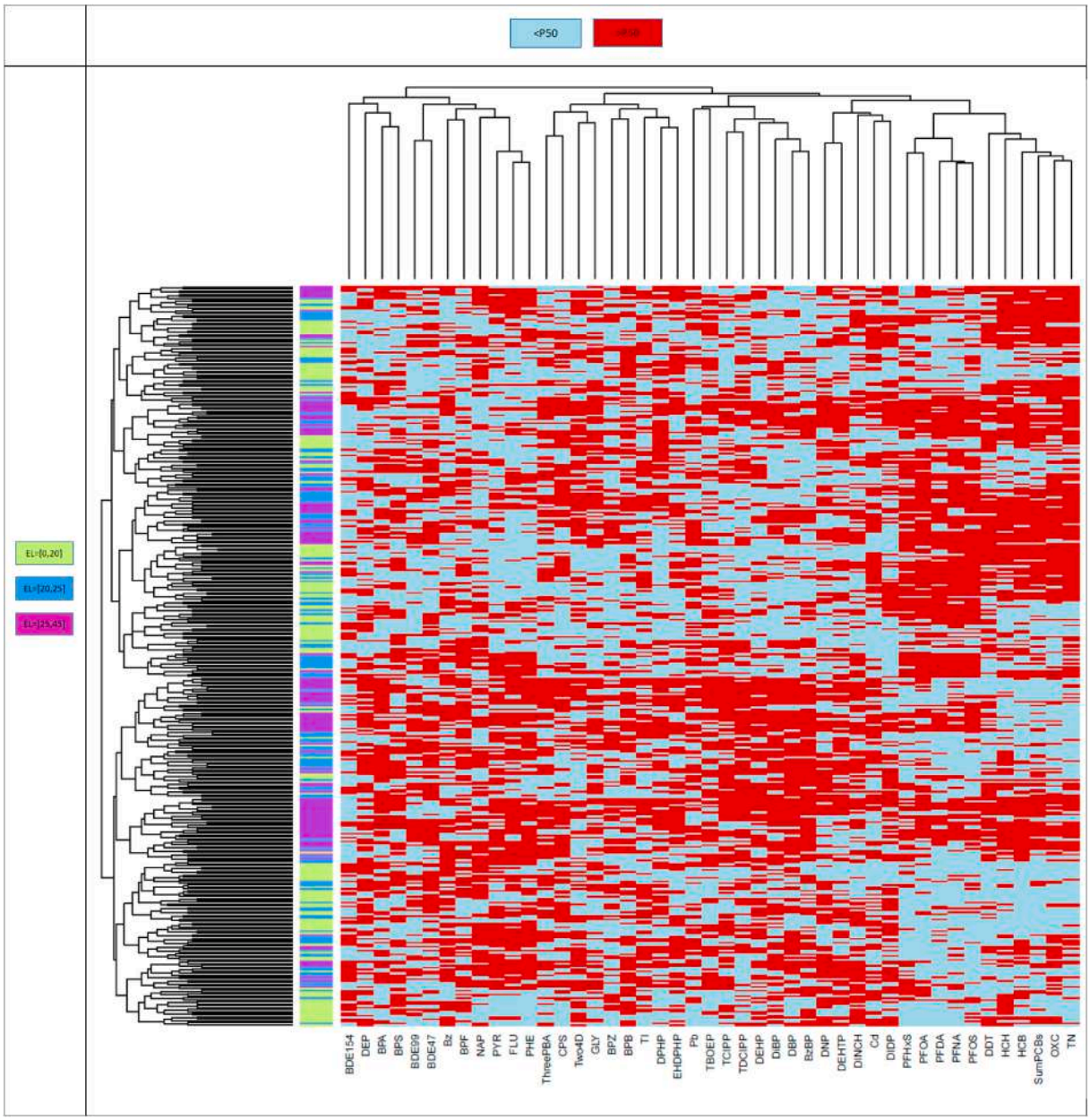

Fig. 3. Dendrogram for internal chemical exposure of 387 individuals using a threshold of P50. Each row presents an individual and each column represents a chemical. Red colour means that for the considered chemical the concentration was equal to or above the threshold. The colours of the bar at the left represent the value of the EL (green ≤20, blue >20 and ≤ 25, purple >25). ThreePBA = 3-PBA; Two4D = 2,4D. (For interpretation of the references to colour in this figure legend, the reader is referred to the Web version of this article.)

persistent and have a longer half-life than most of the short-term biomarkers measured in urine in this study.

Furthermore, similar clusters based on EL-P50 as well as EL-P90 were observed, e.g. pesticides 3-PBA, 2,4-D, CPS and GLY were closely related (GLY only based on EL-P50 and not on EL-P90). Polyaromatic hydrocarbons NAP, PYR, FLU and PHE were clustered for both EL-P50 and EL-P90. Organophosphorus flame retardants TCIPP, TDCIPP, TBOEP, DPHP, EHDPHP were clustered (DPHP and EHDPHP not in the cluster based on EL-P90 data). Brominated flame retardants BDE47 & BDE99 were clustered. Bisphenols BPB and BPZ were clustered (BPA and BPS were clustered only for the EL-P50). Phthalates and alternatives DEHP, DiBP, DBP, BzBP, DINP, DEHTP, DINCH and DIDP were clustered for the EL-P50. For the EL-P90, this group fell into two separate groups: (a) DEHP, DEHTP, DINP and DIDP and (b) DiBP, DBP, BzBP, DINCH. The phthalate DEP was not aggregated with other phthalates or alternatives. The phthalate DEP is mainly used in cosmetics, whereas the other phthalates mainly occur in clothing, household products, food or food contact materials (Tranfo et al., 2018).

The dendrogram EL-P50 (Fig. 3) shows that some individuals are more exposed to POPs, such as PFAS and PCBs, which are displayed in right side in the x-axis and upper part in Y-axis, and they are less exposed to non-persistent compounds (left side). And the other way around, some individuals who are displayed on the left side in the x-axis and bottom part in y-axis, are more exposed to non-persistent compounds and less exposed to POPs.

From the dendrogram EL-P90 (Fig. 4), it can be seen that TN, OXC, sum PCBs and PFAS are marginally present at EL ≤ 2 (green), while they are more present at EL between 2 and 5 (blue) and at EL > 5 (purple). This is observed also for other biomarkers like PAHs (FLU, PYR, PHE).

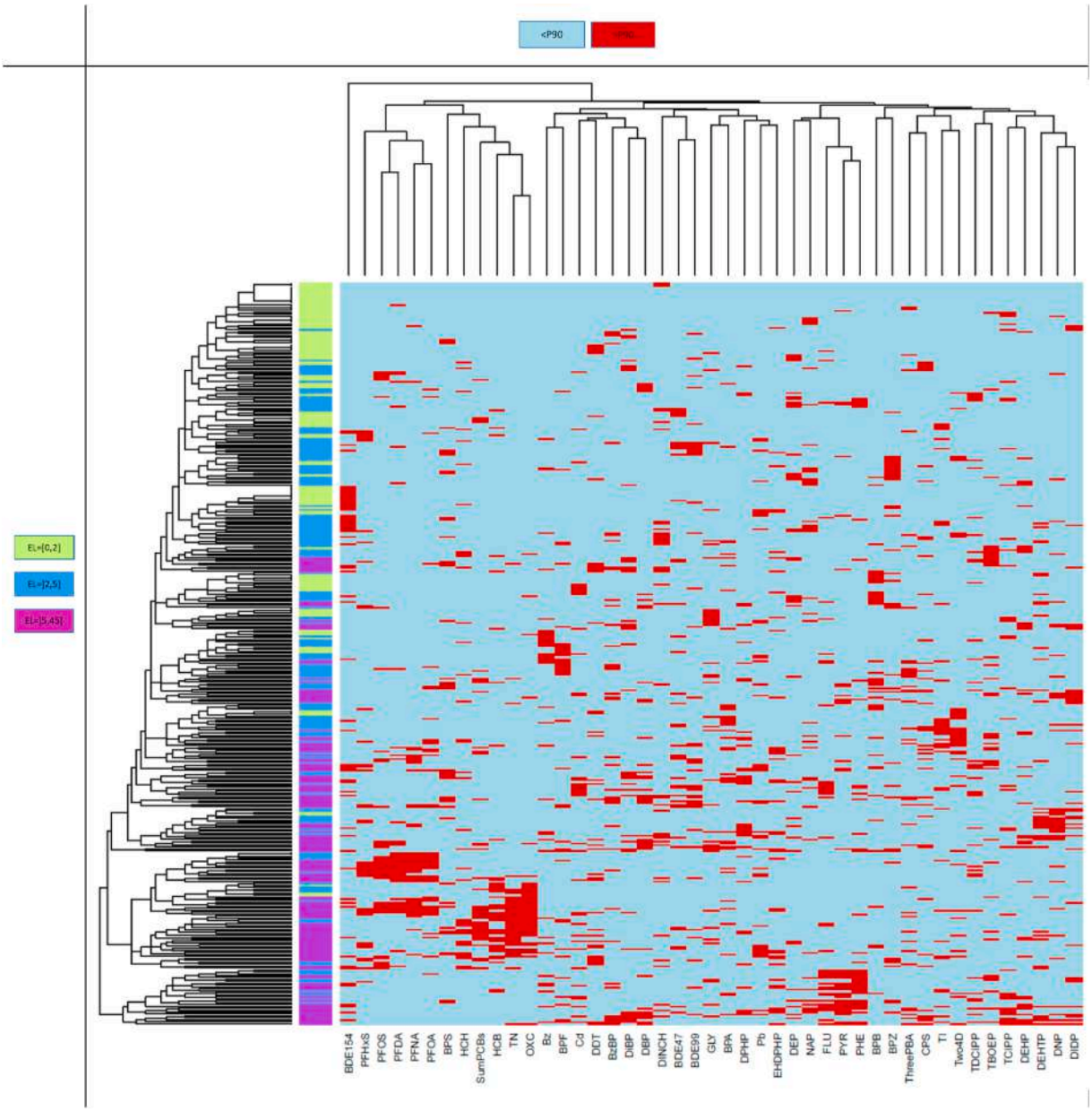

Fig. 4. Dendrogram for internal chemical exposure of 387 individuals using a threshold of P90. Each row presents an individual. Each column a chemical. Red colour means that for the considered chemical the concentration was equal to or above the threshold. The colours of the bar at the left represent the value of the EL (green $\leq$2, blue >2 and $\leq$ 5, purple >5). ThreePBA = 3-PBA; Two4D = 2,4D. (For interpretation of the references to colour in this figure legend, the reader is referred to the Web version of this article.)

3.4. Determinants of variability in EL

We included some common determinants of exposure in the analysis of determinants in EL variability. The determinants considered here are only a fraction of the questions in the questionnaires or a fraction of the gathered information. Results of the univariate analysis are given in detail in Appendix (Table A1). Based on univariate regression results, the following observations can be reported. Mean EL values were significantly ($p < 0.05$) higher for boys compared to girls, certainly for the EL-P50 (boys: 23.37 vs girls: 21.66). A possible explanation is the inverse association between EL and BMI (underweight: 24.16, normal weight: 22.70, overweight: 20.63) and the fact that girls usually have higher BMI than boys (Agentschap Zorg en Gezondheid, 2016) (data FLEHS-4). Associations between biomarker concentrations and BMI were earlier observed for fat soluble chemicals, e.g. PCBs (Agudo et al., 2009; Dirinck et al., 2011). A possible explanation for this observation (lower EL with higher BMI) can be found in the dilution capabilities of these chemicals: as these contaminants are preferably stored in adipose tissue, a higher percentage of body fat leads to faster and more efficient storage of these compounds, with lower serum concentrations as a consequence (Dirinck et al., 2011). Having lower serum concentrations of fat soluble chemicals does not mean that the total amount of fat soluble chemicals in the body is lower. In addition to the difference in BMI between girls and boys, also other variables may influence the difference in EL, such as hormonal differences which may influence toxicokinetics, different hobbies, use of cosmetics, which may result in differences in exposure etc.

A positive association between mean EL-P50 and playing sports was observed (never or seldom: 20.39, 1–2 times per week: 22.46, >3 times per week: 23.14). This was not found for the EL-P90. It was checked if BMI could influence this association with the EL-P50, but there was no significant trend between the BMI class and playing sports. During sport

activities, higher ventilation rates could lead to a higher intake of some volatile chemicals (Dong et al., 2018), however there is only a very limited amount of volatile chemicals considered here so main reasons for this observation of a higher EL-P50 with increased sport activities remain unclear.

Having been breastfed in infancy was significantly positive associated with the EL-P50 (breastmilk no: 21.07, yes: 23.19) and EL-P90 (breastmilk no: 4.06, yes: 4.87). Human milk as a source of exposure for children has been reported earlier for POPs (a.o. PCBs) (Lancz et al., 2015) and for PFAS (Mogensen et al., 2015).

Indoor use of a heating stove was significantly positive associated with the EL-P50 (stove no: 21.96, yes: 23.35). Emissions of residential woodstoves are primarily related to PAHs, but to some extent also to dioxins and PCBs (Gullett et al., 2003). The construction year of the house was significantly associated with the EL-P90 with higher values for the EL with relatively older houses (<1960: 5.07, 1961–1980: 4.96, 1981–2000: 4.31, 2001–2006: 4.22, >2006: 3.77). In the US NHANES, higher urinary cadmium, cobalt, platinum, mercury, 2,5-dichlorophenol and 2,4-dichlorophenol concentrations and mono-cyclohexyl phthalate and mono-isobutyl phthalate metabolites were shown in occupants of houses built before 1990 (Shiue and Bramley, 2015). Also increased concentrations of blood lead were found in persons of relatively older houses (Dixon et al., 2008).

Other significant determinants for the variability in EL were the use of compost in the vegetable garden, consumption of locally-produced eggs and, to some extent, consumption of locally-produced vegetables, fruit and smoked fish. EL values varied significantly for the use of compost (EL-P50: never: 22.18, sometimes: 21.73, often: 24.72; EL-P90: never: 4.43, sometimes: 4.56, often: 5.87), the consumption of locally-produced eggs (EL-P50: never: 21.57, 1 egg/month: 22, 1–4 eggs/month: 22.15, 1 egg/week: 24.74; EL-P90: never: 4.48, 1 egg/month: 4.28, 1–4 eggs/month: 4.36, 1 egg/week: 5.47), consumption of locally produced vegetables (EL-P50: never: 21.84, < once/week: 22.46, ≥ once/week: 23.70; EL-P90: never: 4.38, < once/week: 4.33, ≥ once/week: 5.39), consumption of locally produced fruit (EL-P50: never: 22.23, < once/week: 22, ≥ once/week: 24.35) and the consumption of smoked fish (EL-P50: never: 21.49, < once/week: 23.18, ≥ once/week: 22.70).

The consumption of locally-produced eggs and use of compost in the vegetable garden are determinants for increased serum levels of organochlorine compounds (such as PCBs, DDT), but also PFAS like PFOS and PFNA (data not shown). The consumption of locally-produced fruit and vegetables is also associated with increased PFAS levels (e.g. PFNA; data not shown). For PFASs, similar results were found in FLEHS-3 (Colles et al., 2020). The association with smoked fish may be related to the possible presence of PAHs, however this depends on the smoking process. Finally, the consumption of canned food in the past 3 days was associated here with an increase in the EL-P50 (no: 22.17 vs yes:23.76). Bisphenols are typically used in the lining (Russo et al., 2019) but also appear along the food production chain (González et al., 2020).

For educational level based on highest education within the household, significantly higher mean EL-P50 values were found with higher education categories (ISCED), indicating exposure to more chemicals above P50-levels with increasing level of attained education (ISCED0-2: 20.83, ISCED3-4: 21.79; ISCED≥5: 23.11). Analysis for the EL-P90 showed no clear results. Previous FLEHS studies reported social inequalities in exposure in both directions: for some chemicals (POPs, PFASs) higher exposure levels were observed with increasing ISCED scores, while an opposite trend was observed for other chemicals (e.g. metals) (Morrens et al., 2012; Buekers et al., 2018, 2019). It should be kept in mind, that education level is a proxy for many variables, that cannot always easily be captured using a questionnaire.

In general, there were more associations with determinants for the EL-P50 than for the EL-P90 and they were more strongly pronounced for the EL-P50 than for the EL-P90 except for smoking and construction year of the house where there was only an association for the EL-P90. The EL-P90 increased substantially with smoking but the total of smokers in the studied population of young teenagers was limited. For all determinants, trends for the EL-P50 and EL-P90 go in the same direction. A reason why in general associations were stronger with the EL-P50 than the EL-P90 is that the distribution was wider for the EL-P50 whereas for the EL-P90 it became increasingly tightly packed, and as such less variability to be explained by possible determinants. For the EL-P50, the following associations remained significant after correction for FDR using the Benjamini-Hochberg method (BH): sex, BMI, received breastmilk, use of compost in the vegetable garden, consumption of local eggs and sports. These are also the determinants that were detected in the negative binomial multiple regression analysis (see next paragraph). For the EL-P90 no univariate significant regressions were found following the BH method. However, for the multiple regression analysis the raw data (without BH correction) were applied.

The negative binomial multiple regression analysis showed for the EL-P50 that sex, BMI, having been breastfed, local egg consumption, use of compost in the vegetable garden and playing sports were significant in the final model ($p < 0.05$) (Table 3). For the EL-P90, sex, local egg consumption, use of compost in vegetable garden and smoking remained significant in the model. Next to sex, the consumption of local eggs and use of compost in the vegetable garden were found back in both EL-P50 and EL-P90. Pseudo regressions coefficients were low, i.e. 0.09 for the EL-P50 and 0.04 for the EL-P90, however these should be interpreted with caution. Take into account that for the univariate analysis, no significant associations were found for the EL-P90 according to the BH method.

Interpretation exp(B): for example for sex the ELP50 is 5.8% higher for males than for females. Exponent is taken seeing the negative binomial multiple regression analysis.

These results clearly illustrate the usefulness of the EL-approach to identify variables associated with high exposure load. Changes in these variables, where possible, can result in lowering exposure to multiple pollutants. This can help policymakers to gather knowledge about possibilities to reduce the exposure and make citizens more aware of their possibilities to act themselves. Examples are: reduce smoking, gather more info on the chemical composition of the soil in the chicken run, check which type of compost is used in the vegetable garden. Based on other studies in Flanders, similar suggestions are already in place (https://www.gezonduiteigengrond.be/home).

Current analysis included a biserial correlation test between EL and its biomarkers, cluster analysis of biomarkers and individuals with indication of the EL and regression analysis between EL and determinants of variability based on questionnaire data. Information was thus gathered on variation of the chemical composition by the EL value and separately on determinants of variability of the EL based on questionnaire data. Combining data of the cluster analysis directly with data of the questionnaire to discern patterns and identify chemicals associated with the determinants would also be an option.

3.5. Limitations

The ultimate goal for applying techniques taking into account exposure to multiple chemicals is advancing our understanding of main drivers for the health impact. For the moment, this study focused solely on exposure and the toxicity of the chemicals was not taken into account. Also the itemsets are limited by the available chemicals measured in the study. Not all chemicals to which a person is exposed to, are measured. Further, to truly understand the impact of chemical mixtures itself on health, one needs to account for the chemical concentration, the toxic potential of the chemical, the residence time in the body but also the sequence of the exposure. Therefore, the exposome concept defined as the totality of all human environmental exposures from conception to death is more appropriate (Wild, 2005), although more complicated. To tackle the toxic potential of chemicals and bring it into the EL concept, instead of choosing a threshold within the data itself (i.e. P50 or P90),

Table 3
Negative binomial multiple regression analyses.

Parameter		ELP50				ELP90			
		Exp(B)	95% CI		P	Exp(B)	95% CI		p
			LL	UL			LL	UL	
Intercept		24.966	22.719	27.480	<0.001	9.516	6.708	13.498	<0.001
Sex	M	1.058	1.008	1.110	0.021	1.189	1.044	1.1.353	0.009
	F	Ref				Ref			
BMI	Underweight	1.174	1.063	1.296	0.002				
	Normal weight	1.094	1.025	1.167	0.006				
	Overweight	Ref							
Received breastmilk	No	0.928	0.881	0.976	0.004				
	Yes	Ref							
Consumption of local eggs	Never	0.872	0.819	0.928	<0.001	0.736	0.621	0.873	<0.001
	1 egg/month	0.894	0.829	0.963	0.003	0.794	0.651	0.969	0.023
	1-4 eggs/month	0.901	0.839	0.967	0.004	0.789	0.653	0.953	0.014
	>1 egg/week	Ref				Ref			
Use of compost in vegetable garden	Never	0.917	0.857	0.981	0.012	0.748	0.626	0.895	0.001
	Sometimes	0.857	0.783	0.938	0.001	0.739	0.586	0.933	0.011
	Often	Ref				Ref			
Sports (sweating or breathless)	Never or seldom	0.882	0.818	0.950	0.001				
	1-2 times per week	1.019	0.966	1.074	0.489				
	≥3 times per week	Ref							
Smoking	Never or once					0.671	0.501	0.899	0.008
	Yes					Ref			
Model Pseudo R2 (=1-L1/L0)		0.09			<0.001	0.04			<0.001

LL: lower limit; UL: upper limit; Ref: reference or Exp(B) = 1.
L1: likelihood model.
L0: likelihood intercept.

the threshold can be set equal to HBM guidance values like the biomonitoring equivalents (BE), German HBM-I values or guidance values derived within the HBM4EU project. These values do not exists for all chemicals.

The exposure load (EL) combines exposure to multiple chemicals in one measure. Groups which are disproportionally exposed can be revealed. It would be worth to see how the EL concept may be applied in health outcome studies as it is a different exposure metric that may rank individuals by aggregating their exposure levels to multiple chemicals. In addition, an EL can be calculated for a large series of chemicals, but also for a component based-approach, in which chemicals are grouped by e.g. functionality or based on adverse outcome pathways, and for which several different ELs are calculated. Associations between these ELs and biomarkers of effect or health outcomes can then be examined. As discussed above toxicity can be brought into the EL by setting the threshold to HBM guidance values or take into account potency factors when considering a component based-approach.

The exposure load concept is just one part of the puzzle of combined exposure. While it is a simple concept, it can help pushing our understanding on combined exposure to multiple chemicals. On the other hand, information about the concentration levels is lost due to the discretization process. Comparison of ELs between different studies is difficult seeing differences in studied chemicals, population characteristics, differences in the established cut-offs, etc.

For the calculation of the EL, a threshold (cut-off concentration value) was used. Persons exposed just above the threshold get a value of 1, while persons just below, a zero, however the exposure does not differ that much between these persons. A more correct way to address the EL in future could be to use a continuous variable, e.g. distance function instead of a cut-off or threshold value.

For the associations reported here between variability in EL and possible determinants, no statements can be made about causality in this context. Also other determinants for the relatively higher EL of some participants should be added to the considered questionnaire data in our dataset.

4. Conclusions

We found that 20% of the study population had for 27 out of 45 chemicals biomarker levels above the 50th percentile. The exact profile of biomarkers in these exposed individuals was rather unique. We found also that 20% of the 387 Flemish adolescents had for 6 out of 45 chemicals, exposure biomarkers with levels above the 90th percentile. Chemical profiles showed some dominance of organochlorine chemicals, PFASs, phthalates, PAHs, organophosphate flame retardants, bisphenols (A & F), pesticides, metals, but to a lesser extent brominated flame retardants, the organophosphorus flame retardants TCIPP & TBOEP, naphthalene and benzene, bisphenols S, B & Z, the pesticide 2,4-D, phthalate DEP and alternative plasticizer DINCH. Associations between the EL and exposure determinants pointed in the direction of determinants formerly associated with fat soluble chemicals, PFASs, bisphenols and PAHs. This analysis adds information on possibilities to reduce exposure and is helpful for policymakers and citizens themselves e.g. reduce smoking, gather information on chemical composition of soil in chicken run and check which type of compost is used in the vegetable garden etc.

Acknowledgements

The FLEHS-4 was carried out by the Flemish Centre of Expertise on Environment and Health. The study of the Centre was commissioned, financed and steered by the Flemish Department of Environment and Spatial Development (DOMG), Ministry of the Flemish Community.

Appendix A. Supplementary data

Supplementary data to this article can be found online at https://doi.org/10.1016/j.ijheh.2021.113849.

References

Agentschap Zorg en Gezondheid, 2016. Zorg en gezondheid BMI bij schoolkinderen 2012-2013.
Agudo, A., Goñi, F., Etxeandia, A., Vives, A., Millán, E., López, R., Amiano, P., Ardanaz, E., Barricarte, A., Dolores Chirlaque, M., Dorronsoro, M., Jakszyn, P.,

Larrañaga, N., Martínez, C., Navarro, C., Rodríguez, L., José Sánchez, M., José Tormo, M., González, C.A., 2009. Polychlorinated biphenyls in Spanish adults: determinants of serum concentrations. Environ. Res. 109, 620–628. https://doi.org/10.1016/j.envres.2009.03.009.

Alferness, P.L., Iwata, Y., 1994. Determination of glyphosate and (Aminomethyl) phosphonic acid in soil, plant and animal matrixes, and water by capillary gas chromatography with mass-selective detection. J. Agric. Food Chem. 42, 2751–2759. https://doi.org/10.1021/jf00048a020.

Angerer, J., Ewers, U., Wilhelm, M., 2007. Human biomonitoring: state of the art. Int. J. Hyg Environ. Health 210, 201–228. https://doi.org/10.1016/j.ijheh.2007.01.024.

Baeyens, W., Vrijens, J., Gao, Y., Croes, K., Schoeters, G., Den Hond, E., Sioen, I., Bruckers, L., Nawrot, T., Nelen, V., Van Den Mieroop, E., Morrens, B., Loots, I., Van Larebeke, N., Leermakers, M., 2014. Trace metals in blood and urine of newborn/mother pairs, adolescents and adults of the Flemish population (2007-2011). Int. J. Hyg Environ. Health 217, 878–890. https://doi.org/10.1016/j.ijheh.2014.06.007.

Bastiaensen, M., Gys, C., Colles, A., Malarvannan, G., Verheyen, V., Koppen, G., Govarts, E., Bruckers, L., Morrens, B., Francken, C., Den Hond, E., Schoeters, G., Covaci, A., 2021a. Biomarkers of phthalates and alternative plasticizers in the Flemish Environment and Health Study (FLEHS IV): time trends and exposure assessment. Environ. Pollut. 276 https://doi.org/10.1016/j.envpol.2021.116724.

Bastiaensen, M., Gys, C., Colles, A., Verheyen, V., Koppen, G., Govarts, E., Bruckers, L., Morrens, B., Loots, I., De Decker, A., Nelen, V., Nawrot, T., De Henauw, S., Van Larebeke, N., Schoeters, G., Covaci, A., 2021b. Exposure levels, determinants and risk assessment of organophosphate flame retardants and plasticizers in adolescents (14–15 years) from the Flemish Environment and Health Study. Environ. Int. 147 https://doi.org/10.1016/j.envint.2020.106368.

Bastiaensen, M., Xu, F., Been, F., Van den Eede, N., Covaci, A., 2018. Simultaneous determination of 14 urinary biomarkers of exposure to organophosphate flame retardants and plasticizers by LC-MS/MS. Anal. Bioanal. Chem. 410, 7871–7880. https://doi.org/10.1007/s00216-018-1402-2.

Bell, S.M., Edwards, S.W., 2015. Identification and prioritization of relationships between environmental stressors and adverse human health impacts. Environ. Health Perspect. 123, 1193–1199. https://doi.org/10.1289/ehp.1409138.

Borgelt, C., 2016. Frequent Itemset Mining for Python.

Buekers, J., Colles, A., Cornelis, C., Morrens, B., Govarts, E., Schoeters, G., 2018. Socio-economic status and health: evaluation of human biomonitored chemical exposure to per- and polyfluorinated substances across status. Int. J. Environ. Res. Publ. Health 15, 2818. https://doi.org/10.3390/ijerph15122818.

Buekers, J., Morrens, B., Loots, I., Ganzleben, C., Schoeters, G., 2019. Inequalities in chemical exposure. Environmental Health Inequalities in Europe: Second Assessment Report. WHO, Regional Office for Europe, Copenhagen, WHO, pp. 84–89.

Colles, A., Bruckers, L., Den Hond, E., Govarts, E., Morrens, B., Schettgen, T., Buekers, J., Coertjens, D., Nawrot, T., Loots, I., Nelen, V., De Henauw, S., Schoeters, G., Baeyens, W., van Larebeke, N., 2020. Perfluorinated substances in the Flemish population (Belgium): levels and determinants of variability in exposure. Chemosphere 242. https://doi.org/10.1016/j.chemosphere.2019.125250.

Davis, M.D., Wade, E.L., Restrepo, P.R., Roman-Esteva, W., Bravo, R., Kuklenyik, P., Calafat, A.M., 2013. Semi-automated solid phase extraction method for the mass spectrometric quantification of 12 specific metabolites of organophosphorus pesticides, synthetic pyrethroids, and select herbicides in human urine. J. Chromatogr. B Anal. Technol. Biomed. Life Sci. 929, 18–26. https://doi.org/10.1016/j.jchromb.2013.04.005.

De Craemer, S., Croes, K., van Larebeke, N., Sioen, I., Schoeters, G., Loots, I., Nawrot, T., Nelen, V., Campo, L., Fustinoni, S., Baeyens, W., 2016. Investigating unmetabolized polycyclic aromatic hydrocarbons in adolescents' urine as biomarkers of environmental exposure. Chemosphere 155, 48–56. https://doi.org/10.1016/j.chemosphere.2016.04.017.

Den Hond, E., Govarts, E., Bruckers, L., Schoeters, G., 2009. Determinants of polychlorinated aromatic hydrocarbons in serum in three age classes-Methodological implications for human biomonitoring. Environ. Res. 109, 495–502. https://doi.org/10.1016/j.envres.2009.02.007.

Dirinck, E., Jorens, P.G., Covaci, A., Geens, T., Roosens, L., Neels, H., Mertens, I., Van Gaal, L., 2011. Obesity and persistent organic pollutants: possible obesogenic effect of organochlorine pesticides and polychlorinated biphenyls. Obesity 19, 709–714. https://doi.org/10.1038/oby.2010.133.

Dirtu, A.C., Dirinck, E., Malarvannan, G., Neels, H., Van Gaal, L., Jorens, P.G., Covaci, A., 2013. Dynamics of organohalogenated contaminants in human serum from obese individuals during one year of weight loss treatment. Environ. Sci. Technol. 47, 12441–12449. https://doi.org/10.1021/es400657t.

Dixon, S., Wilson, J., Kawecki, C., Green, R., Phoenix, J., Galke*, W., Clark, S., Breysse, J., 2008. Selecting a lead hazard control strategy based on dust lead loading and housing condition: I. Methods and results. J. Occup. Environ. Hyg. 5, 530–539. https://doi.org/10.1080/15459620802219799.

Dong, J., Zhang, S., Xia, L., Yu, Y., Hu, S., Sun, J., Zhou, P., Chen, P., 2018. Physical activity, a critical exposure factor of environmental pollution in children and adolescents health risk assessment. Int. J. Environ. Res. Publ. Health 15, 1–16. https://doi.org/10.3390/ijerph15020176.

Ducos, P., Gaudin, R., Robert, A., Francin, J.M., Maire, C., 1990. Improvement in HPLC analysis of urinary trans, trans-muconic acid, a promising substitute for phenol in the assessment of benzene exposure. Int. Arch. Occup. Environ. Health 62, 529–534. https://doi.org/10.1007/BF00381185.

ECHA, 2020. EC inventory [WWW document]. accessed 1.14.20. https://echa.europa.eu/nl/information-on-chemicals/ec-inventory.

Esteban López, M., Göen, T., Mol, H., Nübler, S., Haji-Abbas-Zarrabi, K., Koch, H.M., Kasper-Sonnenberg, M., Dvorakova, D., Hajslova, J., Antignac, J.P., Vaccher, V., Elbers, I., Thomsen, C., Vorkamp, K., Pedraza – Díaz, S., Kolossa-Gehring, M., Castaño, A., 2021. The European human biomonitoring platform - design and implementation of a laboratory quality assurance/quality control (QA/QC) programme for selected priority chemicals. Int. J. Hyg Environ. Health 234, 113740. https://doi.org/10.1016/j.ijheh.2021.113740.

González, N., Cunha, S.C., Ferreira, R., Fernandes, J.O., Marquès, M., Nadal, M., Domingo, J.L., 2020. Concentrations of nine bisphenol analogues in food purchased from Catalonia (Spain): comparison of canned and non-canned foodstuffs. Food Chem. Toxicol. 136 https://doi.org/10.1016/j.fct.2019.110992.

Gullett, B.K., Touati, A., Hays, M.D., 2003. PCDD/F, PCB, HxCBz, PAH, and PM emission factors for fireplace and woodstove combustion in the san francisco bay region. Environ. Sci. Technol. 37, 1758–1765. https://doi.org/10.1021/es026373c.

Guo, Y.L., Emmett, E.A., Pellizzari, E.D., Rohde, C.A., 1987. Influence of serum cholesterol and albumin on partitioning of PCB congeners between human serum and adipose tissue. Toxicol. Appl. Pharmacol. 87, 48–56. https://doi.org/10.1016/0041-008X(87)90083-4.

Gys, C., Bastiaensen, M., Bruckers, L., Colles, A., Govarts, E., Martin, L.R., Verheyen, V., Koppen, G., Morrens, B., Den Hond, E., De Decker, A., Schoeters, G., Covaci, A., 2021. Determinants of exposure levels of bisphenols in flemish adolescents. Environ. Res. 193 https://doi.org/10.1016/j.envres.2020.110567.

Hoppe, H., 2013. Determination of Glyphosate Residues in Human Urine Samples from 18 European Countries. Bremen.

Huang, H., Tornero-Velez, R., Barzyk, T.M., 2017. Associations between socio-demographic characteristics and chemical concentrations contributing to cumulative exposures in the United States. - PubMed - NCBI. J. Expo. Sci. Environ. Epidemiol. 27, 544–550.

Jones, P.D., Hu, W., De Coen, W., Newsted, J.L., Giesy, J.P., 2003. Binding of perfluorinated fatty acids to serum proteins. Environ. Toxicol. Chem. 22, 2639–2649. https://doi.org/10.1897/02-553.

Kapraun, D.F., Wambaugh, J.F., Ring, C.L., Tornero-Velez, R., Woodrow Setzer, R., 2017. A method for identifying prevalent chemical combinations in the U.S. population. Environ. Health Perspect. 125 https://doi.org/10.1289/EHP1265.

Krishan, M., Trautman, T., Kapraun, D., Fix, L., Karmaus, A., 2017. Identification, Curation, and Prioritization of Food-Use Chemicals in ToxCast (SOT) | SOT Annual Meeting. https://doi.org/10.23645/epacomptox.5176930.

Lancz, K., Hertz-Picciotto, I., Jusko, T.A., Murínová, Ľ., Wimmerová, S., Šovčíková, E., Dedík, L., Strémy, M., Drobná, B., Farkašová, D., Trnovec, T., 2015. Duration of breastfeeding and serum PCB 153 concentrations in children. Environ. Res. 136, 35–39. https://doi.org/10.1016/j.envres.2014.09.036.

Mogensen, U.B., Grandjean, P., Nielsen, F., Weihe, P., Budtz-Jørgensen, E., 2015. Breastfeeding as an exposure pathway for perfluorinated alkylates. Environ. Sci. Technol. 49, 10466–10473. https://doi.org/10.1021/acs.est.5b02237.

Morrens, B., Bruckers, L., Hond, E. Den, Nelen, V., Schoeters, G., Baeyens, W., Van Larebeke, N., Keune, H., Bilau, M., Loots, I., 2012. Social distribution of internal exposure to environmental pollution in Flemish adolescents. Int. J. Hyg Environ. Health 215, 474–481. https://doi.org/10.1016/j.ijheh.2011.10.008.

Onyemauwa, F., Rappaport, S.M., Sobus, J.R., Gajdošová, D., Wu, R., Waidyanatha, S., 2009. Using liquid chromatography-tandem mass spectrometry to quantify monohydroxylated metabolites of polycyclic aromatic hydrocarbons in urine. J. Chromatogr. B Anal. Technol. Biomed. Life Sci. 877, 1117–1125. https://doi.org/10.1016/j.jchromb.2009.02.067.

R Core Team, 2018. R: A Language and Environment for Statistical Computing. R Foundation for Statistical Computing, Vienna, Austria.

Ramsauer, B., Sterz, K., Hagedorn, H.W., Engl, J., Scherer, G., McEwan, M., Errington, G., Shepperd, J., Cheung, F., 2011. A liquid chromatography/tandem mass spectrometry (LC-MS/MS) method for the determination of phenolic polycyclic aromatic hydrocarbons (OH-PAH) in urine of non-smokers and smokers. Anal. Bioanal. Chem. 399, 877–889. https://doi.org/10.1007/s00216-010-4355-7.

Russo, G., Varriale, F., Barbato, F., Grumetto, L., 2019. Are canned beverages industries progressively switching to bisphenol AF? J. Food Sci. 84, 3303–3311. https://doi.org/10.1111/1750-3841.14833.

Schoeters, G., Colles, A., Den Hond, E., Croes, K., Vrijens, J., Baeyens, W., Nelen, V., Van De Mieroop, E., Covaci, A., Bruckers, L., Van Larebeke, N., Sioen, I., Morrens, B., Loots, I., 2012a. Chapter 2 F the flemish environment and health study (FLEHS) - second survey (2007-2011): establishing reference values for biomarkers of exposure in the Flemish population. Biomarkers and Human Biomonitoring. https://doi.org/10.1039/9781849733373-00135.

Schoeters, G., Den Hond, E., Colles, A., Loots, I., Morrens, B., Keune, H., Bruckers, L., Nawrot, T., Sioen, I., De Coster, S., Van Larebeke, N., Nelen, V., Van de Mieroop, E., Vrijens, J., Croes, K., Goeyens, K., Baeyens, W., 2012b. Concept of the Flemish human biomonitoring programme. Int. J. Hyg Environ. Health 215, 102–108. https://doi.org/10.1016/j.ijheh.2011.11.006.

Schoeters, G., Govarts, E., Bruckers, L., Den Hond, E., Nelen, V., De Henauw, S., Sioen, I., Nawrot, T.S., Plusquin, M., Vriens, A., Covaci, A., Loots, I., Morrens, B., Coertjens, D., Van Larebeke, N., De Craemer, S., Croes, K., Lambrechts, N., Colles, A., Baeyens, W., 2017. Three cycles of human biomonitoring in Flanders – time trends observed in the flemish environment and health study. Int. J. Hyg Environ. Health 220, 36–45. https://doi.org/10.1016/j.ijheh.2016.11.006.

Shiue, I., Bramley, G., 2015. Environmental chemicals mediated the effect of old housing on adult health problems: US NHANES, 2009–2010. Environ. Sci. Pollut. Res. 22, 1299–1308. https://doi.org/10.1007/s11356-014-3468-5.

St-Amand, A., 2019. Using biomonitoring data to understand multipollutant exposure burden in Canada. ISES/ISIAQ Conference. Kaunas.

Steunpunt Milieu en Gezondheid, 2020. VLAAMS HUMANE-BIOMONITORINGSPROGRAMMA 2016-2020 REFERENTIEWAARDEN BIJ JONGEREN VERSIE 2 - MEI 2020.

Tranfo, G., Caporossi, L., Pigini, D., Capanna, S., Papaleo, B., Paci, E., 2018. Temporal trends of urinary phthalate concentrations in two populations: effects of REACH authorization after five years. Int. J. Environ. Res. Publ. Health 15, 1950. https://doi.org/10.3390/ijerph15091950.

UN, 2020. An Assessment Report on Issues of Concern: Chemicals and Waste Issues Posing Risks to Human Health and the Environment.

Wild, C.P., 2005. Complementing the genome with an "exposome": the outstanding challenge of environmental exposure measurement in molecular epidemiology. Canc. Epidemiol. Biomarkers Prev. 14, 1847–1850. https://doi.org/10.1158/1055-9965.EPI-05-0456.

Willey, J.B., Pollock, T., Thomson, E.M., Liang, C.L., Maquiling, A., Walker, M., St-Amand, A., 2021. Exposure Load: using biomonitoring data to quantify multi-chemical exposure burden in a population. Int. J. Hyg Environ. Health 234. https://doi.org/10.1016/j.ijheh.2021.113704.

International Journal of Hygiene and Environmental Health 238 (2021) 113833

Contents lists available at ScienceDirect

International Journal of Hygiene and Environmental Health

journal homepage: www.elsevier.com/locate/ijheh

Distinct weather conditions and human mobility impacts on the SARS-CoV-2 outbreak in Colombia: Application of an artificial neural network approach

Santiago Gómez-Herrera [a], Erik Sartori Jeunon Gontijo [a], Sandra M. Enríquez-Delgado [b], André H. Rosa [a,*]

[a] São Paulo State University (UNESP), Institute of Science and Technology, Av. Três de Marco, 511, Alto da Boa Vista, CEP: 18087-180, Sorocaba, SP, Brazil
[b] School of Science, Department of Earth Sciences, EAFIT University, Medellin, Colombia

ARTICLE INFO

Keywords:
COVID-19
Artificial neural network
Biome
Temperature
Humidity
Human mobility

ABSTRACT

The coronavirus disease 2019 (COVID-19) is still spreading fast in several tropical countries after more than one year of pandemic. In this scenario, the effects of weather conditions that can influence the spread of the virus are not clearly understood. This study aimed to analyse the influence of meteorological (temperature, wind speed, humidity and specific enthalpy) and human mobility variables in six cities (Barranquilla, Bogota, Cali, Cartagena, Leticia and Medellin) from different biomes in Colombia on the coronavirus dissemination from March 25, 2020, to January 15, 2021. Rank correlation tests and a neural network named self-organising map (SOM) were used to investigate similarities in the dynamics of the disease in the cities and check possible relationships among the variables. Two periods were analysed (quarantine and post-quarantine) for all cities together and individually. The data were classified in seven groups based on city, date and biome using SOM. The virus transmission was most affected by mobility variables, especially in the post-quarantine. The meteorological variables presented different behaviours on the virus transmission in different biogeographical regions. The wind speed was one of the factors connected with the highest contamination rate recorded in Leticia. The highest new daily cases were recorded in Bogota where cold/dry conditions (average temperature <14 °C and absolute humidity >9 g/m^3) favoured the contagions. In contrast, Barranquilla, Cartagena and Leticia presented an opposite trend, especially with the absolute humidity >22 g/m^3. The results support the implementation of better local control measures based on the particularities of tropical regions.

1. Introduction

The respiratory illness named Coronavirus Disease 2019 (COVID-19) induced by the Severe Acute Respiratory Syndrome Coronavirus 2 (SARS-CoV-2) has rapidly increased its presence across the world since its first occurrence in Wuhan, China, in December of 2019 (Zhou et al., 2020). Based on the magnitude of the emergency, the World Health Organisation (WHO) declared the outbreak a Public Health Emergency of International Concern (PHEIC) in January 2020 and officially a pandemic on March 11th (WHO 2020a, 2020b). This new virus is highly contagious, and the transmission ways include direct contact by secretions of an infected person and indirect contamination via contact with contaminated surfaces (Dhand and Li, 2020; Guarner, 2020; Mouchtouri et al., 2020). The dispersion of this virus depends on social factors (affected by human mobility) and extra-human factors such as environmental conditions that have effects on its inactivation and persistence (Aboubakr et al., 2020; Kubota et al., 2020).

Recent epidemiological studies have shown evidence of significant correlations between the weather conditions and the SARS-CoV-2 cases (Briz-Redón and Serrano-Aroca, 2020a; Fernández-Ahúja and Martínez, 2021; Islam et al., 2021; Kulkarni et al., 2021; Nottmeyer and Sera, 2021; Pan et al., 2021; Rosario et al., 2020; Sanchez-Lorenzo et al., 2021). Temperature, for instance, has apparently two main effects: inhibiting the virus replication under warm conditions or favouring its stability under cold or temperate conditions (Araújo and Naimi, 2020; Bukhari and Jameel, 2020; Notari, 2021; Wu et al., 2020). Other authors highlighted the relevant role of variables such as wind speed and humidity (Coşkun et al., 2021; Diao et al., 2021; Farkas et al., 2021; Wei

* Corresponding author. São Paulo State University (UNESP), Institute of Science and Technology, Sorocaba, SP, Brazil.
E-mail address: andre.rosa@unesp.br (A.H. Rosa).

https://doi.org/10.1016/j.ijheh.2021.113833
Received 27 January 2021; Received in revised form 12 August 2021; Accepted 23 August 2021
Available online 25 August 2021

et al., 2020). Results indicated that the severity of the disease in terms of infections presented marked differences between temperate and tropical countries (Battineni et al., 2020; Tushabe, 2020). This makes the stability of SARS-CoV-2 under different meteorological conditions an important area of study, particularly in tropical countries such as Brazil, Bangladesh, Singapore, Philippines or Indonesia where several outbreaks have been recorded (Auler et al., 2020; He et al., 2021; Hridoy et al., 2021; Pani et al., 2020; Seposo et al., 2021; Tosepu et al., 2020).

The current scenario of the pandemic and the presence of large amounts of data turns essential the use of good tools to cluster and visualise relationships among variables involved in the virus transmission to support control strategies (Yahya et al., 2021). Artificial neural network (ANN) techniques are examples of tools that can be used to perform exploratory analysis of these data and model the spread of the disease to predict future outbreaks (Car et al., 2020; Mollalo et al., 2020; Niazkar and Niazkar, 2020). They are mathematic models and algorithms used to mimic some characteristics of the human brain such as the capacity of learning by examples (Terfloth and Gasteiger, 2001). ANN is formed by basic units named neurons that collect input data, converting them by using a function in output data (Terfloth and Gasteiger, 2001).

Self-organising map (SOM, also known as Kohonen neural network) is an example of ANN that is based on unsupervised learning (Kohonen, 2001; Vesanto, 1999). This technique projects high-dimensional data into a lower-dimensional space with the purpose of grouping samples with similar characteristics and finding possible patterns (Brereton, 2012; Doan et al., 2020). It has outstanding visualisation capabilities, it is ease to implement and robust to missing data (Asan and Ercan, 2012; Vesanto, 1999). In the context of the COVID-19 pandemic, SOM has been used to find similarities in the transmission dynamics among cities, regions or countries worldwide (Galvan et al., 2021; Hartono, 2020; Melin et al., 2020). Other authors focused on evaluating the influence of demographic, socio-economic, and health conditions in the virus spread (Galvan et al., 2020; Khan et al., 2021). Leichtweis et al. (2021) considered the relationship between the virus dissemination rate and some meteorological variables such as environmental temperature, relative humidity and solar radiations with SOM. The study was limited to clustering countries that displayed similar predictor variables.

Colombia is an equatorial country dominated by tropical conditions with climatic variations connected to elevation differences across its territory (Raines et al., 2020). This makes it an ideal place to study the spread of SARS- CoV-2, since the behaviour of the virus under warm climates is still debatable and the country is one of the worst affected countries worldwide (He et al., 2021; Prata et al., 2021; Islam et al., 2020). From July 2020 to January 2021, Colombia was positioned within the 11 countries with the most confirmed cases in the world according to Johns Hopkins University; in September, the country reached the 5th position (Johns Hopkins, 2021). This knowledge would help to implement local health policies and predict when to expect the worst outbreaks in tropical areas where several poorer countries are located (Islam et al., 2020). Furthermore, information about the changes in the meteorological variables in Colombia and the direct relation with the virus spread is still limited, and this investigation intends to fill this gap (De la Hoz-Restrepo et al., 2020)

This paper aims to assess if the weather conditions of different geographical regions in Colombia affect the dissemination of SARS-CoV-2. Mobility variables were included because human contact has an important role in the virus transmission (Marcu, 2021; Shao et al., 2021). Since the results from this type of study are difficult to interpret because of their complexity (due to large amounts of data and variables) and spatial-temporal variability (Khan et al., 2021), we selected the SOM technique because of its visualisation and clustering capabilities. This investigation has the potential to contribute to the development of site-specific public health policies for controlling COVID-19 in Colombia and other tropical countries, where the pandemic is still out of control. We intend to demonstrate the applicability of SOM in this type of study for exploratory analysis that was not performed in Colombia so far.

2. Methodology

2.1. Study area

Colombia is a transcontinental country in Latin America with a population of fewer than 50 million inhabitants. It is formed by 33 administrative regions distributed in a total area of 2.07 million km^2 (Departamento Administrativo Nacional de Estadística, 2018). Since the beginning of the outbreak, the development of the pandemic has been concentrated in the main cities that acted as sources of the disease to other regions of the country (De la Hoz-Restrepo et al., 2020).

Six cities located in five different biomes (humid montane forest, pre-mountain rainforest, subtropical dry forest, tropical dry forest and tropical rainforest) in Colombia were selected to analyse the dissemination of COVID-19: Bogota (BOG), Medellin (MED), Cali (CAL), Barranquilla (BAR), Cartagena (CAR), and Leticia (LET). The main demographic and geographical information of the cities are presented in Table S1 (Appendix A). The localisation of the cities with their respective biomes is shown in Fig. 1. The data was obtained from the Institute of Hydrology, Meteorology and Environmental Studies of Colombia (IDEAM) (http://www.ideam.gov.co/, accessed in April 2021). The classification of the biomes was based on the Holdridge's scheme (Holdridge and Grenke, 1971) and the map was created using ArcGis pro software (v.2.2.4 ESRI, USA).

2.2. Data collection

The first case of coronavirus in Colombia was confirmed on March 6th' 2020 in its capital Bogota. As a result of a fast raise in number of the new cases and the spread of the virus in most of the departments, the

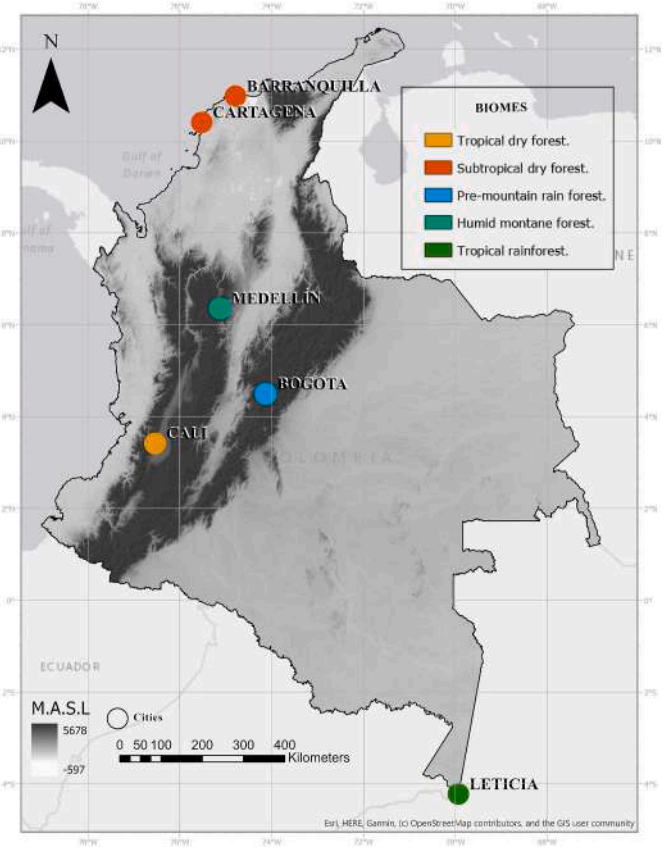

Fig. 1. Map showing the localisation and biome of each studied city.

government decreed a total quarantine with the intent to contain the growing emergence on March 25th (Ramírez et al., 2020). Nevertheless, due to the imminent economic crisis, the state was forced to ease the restrictions in May for some commercial sectors and the end of the mandatory isolation since September 1st, but continuing with the biosafety protocols (Arellana et al., 2020). In January 2021, some restrictions were promulgated aiming to control a new wave of the virus after December festivities.

Data of COVID-19 cases were downloaded from the *Instituto Nacional de Salud* (https://www.ins.gov.co/Noticias/Paginas/Coronavirus.aspx, accessed in April 2021). The epidemiological variables selected in this study for the period from March 25th, 2020, to January 15th, 2021, were new daily cases (NDC) and contamination rate (CR). CR was calculated dividing the number of new daily reported cases by the total population of the city, and then multiplying the result by 100 thousand inhabitants.

The weather data were obtained from the online database archives of the Weather Underground (http://wunderground.com/, accessed in April 2021). This website has as information sources typical weather stations from countries around the world. The meteorological variables evaluated were daily average temperature (T_{avg}), minimum temperature (T_{min}), maximum temperature (T_{max}), relative humidity (RH), absolute humidity (AH), specific enthalpy (h) and wind speed (WS). AH was calculated as per the Clausius Clapeyron equation (1) presented below (Bukhari and Jameel, 2020):

$$AH = \frac{6.112 \times e^{\frac{17.67 \times T_{avg}}{T_{avg}+243.5}} \times RH \times 2.1674}{273.15 + T_{avg}} \quad (1)$$

where AH is the absolute humidity in g/m^3 and T_{avg} is the average temperature in °C.

Average temperature and relative humidity were used to calculate specific enthalpy (h) based on the following psychrometric parameters: saturated vapour pressure (P_{WS}), vapour pressure (P_W), total ambient pressure (P_{tot}) and mixing ratio (X). Specific enthalpy represents the total heat of a mass air (latent heat energy of the water vapour + specific heat of the dry air) and consequently the amount of energy required to change the psychrometric conditions of the air (de Castro Júnior and da Silva, 2021; Spena et al., 2020a, 2020b).The empirical equations of these parameters are presented below:

a) Saturated vapour pressure (Alduchov and Eskridge, 1996):

$$P_{WS} = 6.116441 \times 10^{\frac{7.591386 \times T}{T+240.7263}} \quad (2)$$

where P_{WS} is the saturated vapour pressure in hPa and T is the average temperature in °C.

b) Vapour pressure (Lawrence, 2005):

$$P_W = P_{WS} \times \frac{RH}{100} \quad (3)$$

where P_W is the vapour pressure in hPa and RH is the relative humidity (%).

c) Total ambient pressure (Berberan-Santos et al., 1997):

$$P_{tot} = 1013.25 \times e^{-0.000118 \times E} \quad (4)$$

where P_{tot} is the total ambient pressure and E is the elevation above sea level of each city (BAR: 20 m.a.s.l; BOG: 2630 m.a.s.l; CAL: 1018 m.a.s.l; CAR: 14 m.a.s.l; LET: 96 m.a.s.l; MED: 1495 m.a.s.l).

d) Mixing ratio (Marquet and Geleyn, 2015):

$$X = \frac{621.9907 \times P_W}{P_{tot} - P_W} \quad (5)$$

where X is the mixing ratio in g/kg.

e) Specific enthalpy (Marquet and Geleyn, 2015):

$$h = T \times (1.01 + 0.00189\,X) + 2.5\,(X) \quad (6)$$

where h is specific enthalpy in kJ/kg.

The mobility data was acquired from the Community Mobility Reports provided by Google (https://www.google.com/covid19/mobility/, accessed in April 2021). It was used to assess the influence of human mobility on the spread of the virus (Bochenek et al., 2021). The indices show changes (%) in the number of visitors across different category of places collected by Google applications: retail and recreation (RR), grocery and pharmacy (GP), parks (PK), transport or transit stations (TS), workplaces (WP) and residential (RS). The results were calculated by comparing the mobility values from a given day during the pandemic with a pre-pandemic baseline value of mobility (January 3rd - February 6th, 2020) (Sulyok and Walker, 2021). For the city of LET, only GP and PK variables were available. Furthermore, two weeks of September were not available.

The meteorological and mobility data used for each city in the analysis corresponded to the average of 7–14 days before the reported day. Previous studies have pointed out the relevance of considering the lag effect based on the latency period of COVID-19 from the infected day to the confirmed day (Chen et al., 2020; Dhouib et al., 2021; N. Islam et al., 2020; Xie and Zhu, 2020).

2.3. Statistical analysis

As a result of a non-normal distribution (asymmetry and kurtosis out of range), the Spearman rank correlation (r_s) was selected to evaluate relevant association coefficients (>0.4) among the epidemiological, meteorological and mobility variables in two different periods: quarantine (March/2020–August/2020) and post-quarantine (September/2020–January/2021). The data were standardised by the z-scores method to perform the statistical tests. The software PAST 2.7 was used for all calculations (Hammer et al., 2001).

2.4. Self-organising maps

SOM technique was used to identity relationships between the epidemiological variables (NDC and CR) and the meteorological (AH, h, RH, T_{max}, T_{avg}, T_{min}, WS) and mobility variables (GP, PK, RR, RS, TS and WP) in the six selected cities from Colombia. Similarities in the spreading of the infections among the cities were also evaluated.

The technique consists of neurons arranged in a two-dimensional grid. Each input sample is represented by a vector whose elements correspond to the variables from data collected in each day (epidemiological, meteorological and mobility variables; dimension was 15). The neurons in the output maps have hexagonal lattice and the same dimension of the input vectors. The number of neurons in these maps are defined by the user. The input and output layers in the technique are connected by weight vectors. Initially, the weight vectors are initialised with small random numbers and the algorithm calculates the Euclidian distance between an input vector and the weight vector of each output neuron. The neuron with the smallest distance (best-matching unit, BMU) is then selected and the weights from this BMU and the neighbours are updated according to a Gaussian function (Çinar and Merdun, 2009). Nearby neurons in the output layer represents similar properties and neurons located farther away from each other have dissimilar properties (Asan and Ercan, 2012).

The batch training algorithm was used for training the SOM. Firstly, a matrix was organised with the data collect from all cities from March/2020 to January/2021, including the analysed variables. The data set was normalised before the analysis via z-score. Since the discrimination capabilities of the SOM depends on the number of neurons (hexagonal

units) in the maps, several architectures (35 × 35 to 50 × 50) were tested and the most informative one (with the highest discrimination capability) was selected. A summary of the method is displayed in Fig. 2. Maps with a small number of neurons would have the samples clustered together. On the other hand, too big maps would have sample too far apart. Therefore, both high and low number of neurons in the maps would prevent to extraction information and were avoided (Garcia et al., 2007). The software MatLab 2017b (MathWorks, Natick, MA) and the SOM toolbox 2.1 (freely available on http://research.ics.aalto.fi/software/somtoolbox/, accessed in April 2021) were used to perform all analysis (Alhoniemi et al., 2000). The method was also applied to each city separately, testing architectures from 15 × 15 to 25 × 25.

3. Results

Fig. 3 shows the daily variations of the epidemiological and meteorological variables in the studied cities. A descriptive statistical analysis of the epidemiological and meteorological data is presented in Table 1. The results indicate that spatial fluctuations of the meteorological variables were greater than temporal ones (Fig. 3). The T_{avg} for BOG, for instance, varied between 12.9 °C and 15.6 °C (difference of 2.7 °C) from March 2020 to January 2021 (average in the period was 14.1 °C, the lowest among the cities). The difference was much larger (15.0 °C) if BOG is compared with CAR, which presented the highest average of T_{avg} in the study period (29.1 °C) among the cities.

The highest AH values were recorded in the Amazonian (LET) and north coastal cities (BAR and CAR) that presented daily records above 18 g/m^3. In contrast, the capital (BOG) recorded the lowest daily values (maximum AH was 10.2 g/m^3). Regarding WS, the highest values were recorded in the north coastal cities (daily records above 6.8 km/h) and the lowest in LET (maximum WS was 5.9 g/m^3) (Table 1). The h reached the highest daily value (88 kJ/kg) in CAR and the lowest daily value (30.4 kJ/kg) in BOG (Table 1).

A descriptive statistical analysis of the mobility data is presented in Table 2. Moreover, Fig. 4 shows the human mobility data in six place categories in the six cities from Colombia during the analysed period (March 2020–January 2021). The graphs show that these variables were strongly affected by the restriction measures, especially BOG, MED, and BAR. The quarantine appeared to increase the mobility in residential places (RS) in all the cities, standing out BOG that presented average increase of 27.2% (quarantine) when compared to the pre-pandemic period. Conversely, other locations presented a drastic reduction in the number of visitors as a result of the restrictions implemented. While the lowest values for GP, PK, RR, TS and WP were recorded in April 2020, the highest values were in December, exceeding the number of visitors before the quarantine for places such as GP in BOG, MED, CAL and BAR (Fig. 4).

Based on the trends depicted in Fig. 3, the disease dissemination in the country reflected a fast-growing rise from its first detection in March until August 2020. Afterwards, there was downward trend until November. New pronounced peaks occurred in December, likely associated with the year-end celebrations. This motivated the government to implement some restrictions in January again. For our study period, a total of 970,383 confirmed cases were registered in the six cities. BOG was the city with the highest number of NDC (maximum record of 7471 cases in January 2021), followed by CAL and MED (Table 1). Regarding CR, LET had the highest record (396.7 contagions/per 100 thousand people) in May 2020. This city has the lowest urban population density compared to the other assessed cities (Table S1, Appendix A).

3.1. Correlations

The correlations among the epidemiological, meteorological and mobility variables are presented in Table S2 (Appendix A). The results showed that the variables NDC and CR had the same correlations with meteorological and mobility variables. The following relationships were found in the period of quarantine: high correlation correlations involving epidemiological and meteorological variables were obtained between NDC/CR and h, especially in CAL ($r_s = -0.46$, $p < 0.01$) and MED ($r_s = -0.58$, $p < 0.01$). Furthermore, significant negative correlations were found between $T_{max}/T_{min}/T_{avg}$/AH and NDC/CR in some cities, for example in BOG (T_{max} and T_{avg}: $r_s = -0.62$, $p < 0.01$; AH: $r_s = -0.54$, $p < 0.01$) and CAL (AH: $r_s = -0.53$, $p < 0.01$). In contrast, humidity variables were positively and significantly correlated with NDC/CR in CAR (e.g., AH: $r_s = 0.59$, $p < 0.01$) and BAR (e.g., RH: $r_s = 0.70$, $p < 0.01$). Moreover, the north coastal cities had the highest negative

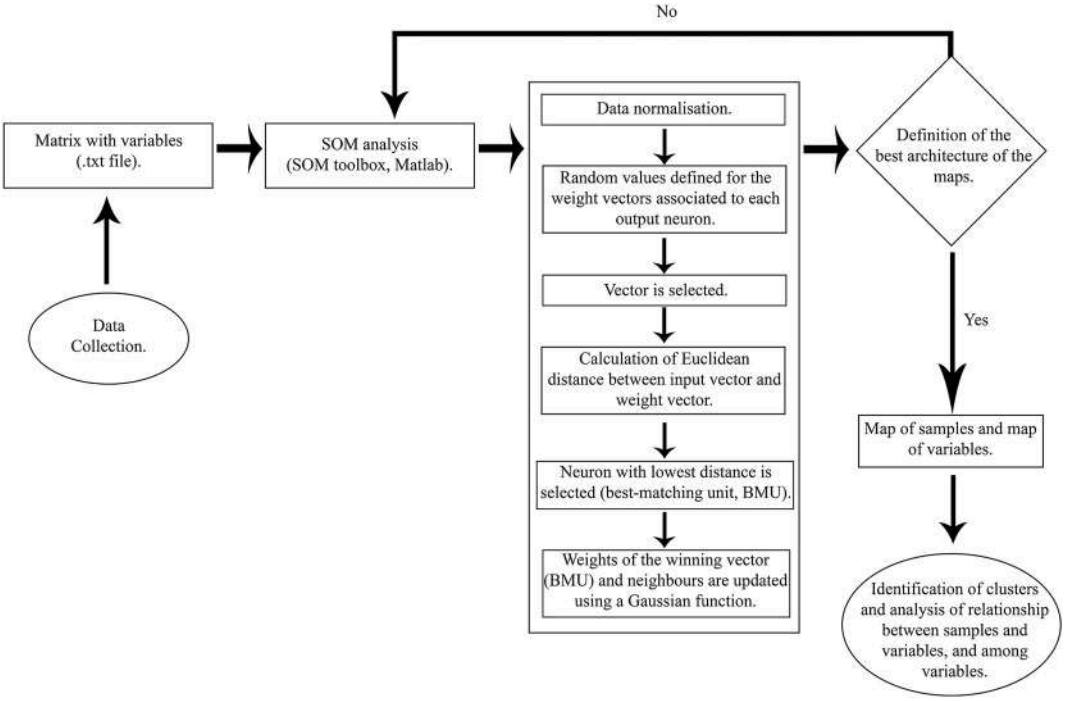

Fig. 2. Flowchart of SOM algorithm application.

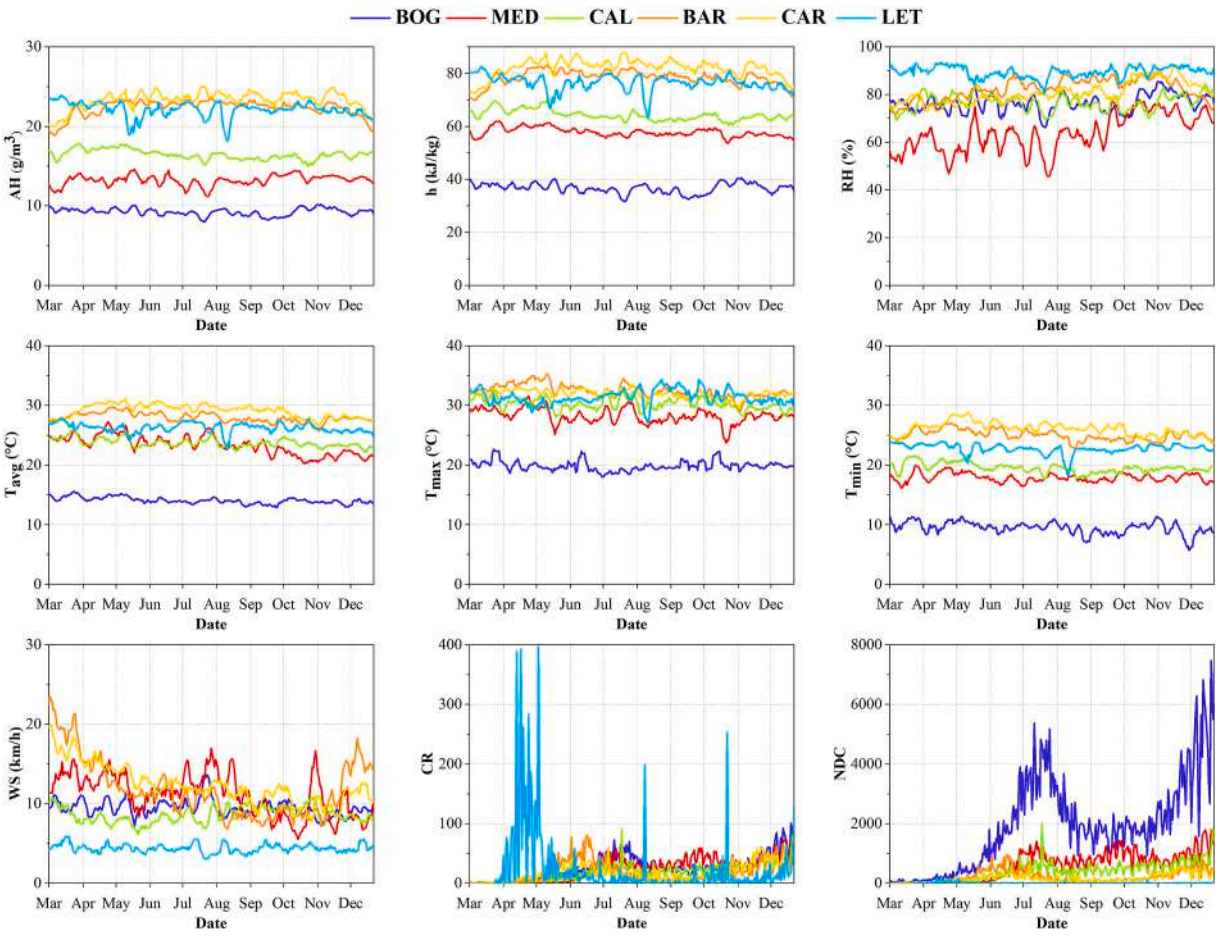

Fig. 3. Meteorological (Average Temperature, Minimum Temperature, Maximum Temperature, Relative Humidity, Absolute Humidity, Wind Speed and Specific Enthalpy) and epidemiological variables (New Daily Cases and Contamination Rate) from March/2020 to January/2021.

coefficients between WS and the epidemiological variables, especially CAR with coefficients (r_s) of −0.70 ($p < 0.01$). Regarding the mobility variables, GP, PK, RR, TS, and WP presented significant positive correlations (except LET) with the epidemiological variables in all the cities. In BOG, MED, and CAL these coefficients (r_s) were higher than the obtained for the meteorological variables. The highest correlations were observed between NDC/CR and PK ($r_s = 0.71$, $p < 0.01$) in CAL and between NDC/CR and RR ($r_s = 0.64$, $p < 0.01$) in BOG. In LET, the mobility variables presented negative coefficients with the epidemiological variables, probably linked with the high caseloads registered in this period.

The period of post-quarantine in cities such as BAR, CAR, and LET presented higher coefficients between the mobility variables and NDC/CR than in the quarantine period (in LET just for PK). Some examples are RR ($r_s = 0.82$, $p < 0.01$) and GP ($r_s = 0.81$, $p < 0.01$) in BAR. In contrast, the most populated cities (BOG, MED and CAL) presented lower coefficients between these variables in post-quarantine than in the quarantine period.

3.2. Self-organising maps

3.2.1. Whole data set

The SOM analysis resulted in 7 groups (I-VI) as shown in the map of samples (Fig. 5). The map architecture 45 × 45 neurons was selected as the most informative one. The neurons were coloured based on the date of the reported confirmed cases (Fig. 5a), the city from where the cases were reported (Fig. 5b), the biome from where the cases were reported (Fig. 5c) and if the data belong to quarantine or post-quarantine period (Fig. 5d). From the figure, it is clear that the data can be clustered using any of these four classifications. The data from the quarantine period (March–August), for instance, were clustered in the bottom-left region, while the data from the post-quarantine period (September–January) were clustered in the upper-right part of the map (Fig. 5d).

Samples located in the same or neighbouring neurons in the map are very similar to each other considering the analysed variables. Conversely, samples in neurons farther from each other are less similar (Brereton, 2012). Therefore, one can say that the data from Bogota (group VII, Fig. 5), for example, are more similar to samples from Medellin (group IV) than data from north coastal cities (BAR and CAR; group I) and Leticia (group III). In contrast, samples from BAR and CAR are very similar because they are very close from each other in the map, belonging to the same groups (groups I and V). This may be linked to the geographical proximity between the cities that share the same biome (subtropical dry forest; Fig. 1). Inside each group, clusters based on the date of the records can also be seen (Fig. 5a). These clusters correspond to temporal stages of the pandemic in each city regarding the analysed variables.

The maps of variables (component planes) are shown in Fig. 6. They are like "hidden" layers behind the map of samples (Fig. 5) and represent the variables used to create the SOM (Brereton, 2012). The colour bars located beside each map represent the intensity of respective variable: the red colour indicates higher intensity and the blue colour lower intensity (Kowalski et al., 2013). From the maps, it is also possible to visualise possible correlations between two variables. GP and RR, for instance, have similar pattern in their maps, indicating a positive correlation. On the other hand, GP and RS have opposite patterns indicating

Table 1
Descriptive statistical analysis of the epidemiological and meteorological variables for each city.

	NDC	CR	T_{max} (°C)	T_{avg} (°C)	T_{min} (°C)	RH (%)	AH (g/m^3)	WS (km/h)	h (kJ/kg)
Bogotá									
Mean	1893.2	25.5	19.9	14.1	9.5	76.4	9.2	9.5	36.7
SD	1533.6	20.7	0.8	0.5	1.0	3.7	0.5	1.0	1.9
CV (%)	81.0	81.0	4.2	3.8	10.9	4.9	4.9	11.0	5.1
Min	9.0	0.1	18.0	12.9	5.7	66.1	8.0	7.2	31.7
Max	7471.0	100.8	22.6	15.6	11.5	85.5	10.2	13.6	41.0
Asym	6.4	6.4	6.5	2.8	−5.4	−0.1	−2.3	7.4	−2.3
Kurt	2.5	2.5	5.2	0.0	4.2	−0.7	−1.8	9.8	−1.0
Medellín									
Mean	582.5	23.2	28.2	23.3	17.9	63.6	13.2	11.2	57.8
SD	480.6	19.8	1.2	1.6	0.5	7.8	0.7	2.6	1.7
CV (%)	82.5	82.5	4.4	6.9	4.0	12.3	5.0	23.5	3.0
Min	0.0	0.0	23.6	20.2	16.1	45.7	11.2	5.5	53.7
Max	1790.0	73.8	31.6	27.3	19.9	77.9	14.6	17.0	61.8
Asym	1.6	1.6	−2.7	0.4	2.5	−0.6	−4.9	−0.9	2.5
Kurt	−3.5	−3.5	4.0	−2.6	−0.3	−2.7	2.1	−3.1	−0.9
Cali									
Mean	393.9	17.7	30.3	23.7	19.5	76.8	16.5	8.6	64.2
SD	314.2	14.1	1.0	0.7	0.8	3.4	0.6	1.0	2.0
CV (%)	79.8	79.8	3.3	3.0	4.2	4.5	3.7	11.7	3.0
Min	0.0	0.0	28.1	22.1	17.7	69.0	15.0	6.1	60.4
Max	2026.0	91.0	32.7	26.0	21.6	84.5	17.9	10.8	70.0
Asym	8.1	8.1	0.6	4.8	2.1	−0.5	1.1	0.9	5.6
Kurt	11.1	11.1	−1.7	1.1	0.0	−2.6	−1.3	−2.6	0.8
Barranquilla									
Mean	217.8	18.1	32.5	28.0	25.0	82.2	22.3	11.8	78.4
SD	216.7	17.9	1.1	0.8	0.9	4.4	1.0	3.7	2.8
CV (%)	99.5	99.5	3.3	2.8	3.5	5.4	4.6	31.3	3.5
Min	0.0	0.0	29.0	25.7	22.7	71.8	18.9	6.8	69.9
Max	972.0	80.6	35.3	29.7	27.0	90.5	23.5	23.5	83.0
Asym	8.8	8.8	0.5	0.2	1.4	−2.8	−11.3	7.2	−7.3
Kurt	3.4	3.4	2.3	−0.8	−1.2	−2.8	7.5	1.7	3.8
Cartagena									
Mean	169.4	17.4	31.9	29.1	26.1	80.6	23.3	12.4	82.0
SD	144.6	14.9	0.7	1.1	1.1	4.5	1.1	2.4	3.3
CV (%)	85.4	85.4	2.2	3.6	4.2	5.6	4.6	19.6	4.0
Min	0.0	0.0	29.7	26.6	23.6	72.8	20.0	7.7	72.6
Max	585.0	60.1	33.6	31.2	28.8	92.7	25.1	19.9	88.0
Asym	7.1	7.1	−3.4	−2.0	1.2	4.6	−8.7	4.6	−7.5
Kurt	0.9	0.9	0.1	−3.8	−0.8	−1.1	5.3	1.1	3.6
Leticia									
Mean	11.4	23.7	31.4	26.2	22.8	89.5	22.1	4.4	76.4
SD	27.2	56.5	1.2	0.8	0.8	2.3	1.0	0.5	3.0
CV (%)	228.8	238.8	3.9	3.1	3.7	2.6	4.4	12.2	3.9
Min	0.0	0.0	27.0	22.6	18.1	80.5	18.1	3.1	63.2
Max	191.0	396.7	34.3	27.9	24.0	93.5	23.9	5.9	83.0
Asym	30.1	30.1	−0.2	−6.8	−15.1	−4.6	−9.8	2.5	−9.1
Kurt	76.4	76.4	1.5	9.2	27.0	1.3	10.4	0.8	11.0

Asym: asymmetry; CV: coefficient of variation; Kurt: kurtosis; Max: maximum value; Min: minimum value; SD: standard deviation.

a negative correlation. Possible associations between epidemiological and meteorological variables can also be found by comparing different variable maps. The neurons with high intensity for CR at the corresponding neurons with lower WS, for instance, indicate that lower WS may favour the virus infections.

The characteristics of each cluster in the map and the similarities and differences among the data can be visualised by simultaneously analysing the map of samples and its component planes. The differences between the quarantine and post-quarantine periods, for instance, can be attributed to the mobility variables GP, PK, RR, TS and WP that presented high intensity for the data from the post-quarantine period (cf. intensity of these variables in Fig. 6 at the position of neurons from post quarantine period as marked in Fig. 5d). The variable RS that presented low intensity during the post-quarantine period also contributed to the formation of both clusters.

Differences among groups can also be explained by visualising the maps of samples and variables. The group VII (BOG samples; Fig. 5), for example, is characterised by low intensities of the meteorological variables AH, h, T_{avg}, T_{max} and T_{min}. Furthermore, the data in this group had the highest NDC. In contrast, groups I, III and V that contains samples from BAR, CAR and LET had high intensities for AH, h, RH, T_{avg}, T_{max} and T_{min}. The main distinction between LET (group III) and the other analysed cities was the lower WS. In addition, the highest CR was recorded for samples from LET.

The SOM analysis indicated that BAR and CAR were the cities that presented the largest differences between quarantine and post-quarantine periods. This is because a substantial amount of data from each period were in different groups (cf. group I with most samples in quarantine period and group V with all samples in post-quarantine period; Fig. 5). The mobility variables (GP, PK, RR, RS, TS and WP) were responsible for the separation of the data in two groups since they presented different intensities in each analysed group. In the same way, these variables were also responsible for dividing CAL data into two groups (II and VI, Fig. 5).

3.2.2. SOM by city

The maps of samples of each city individually were coloured and grouped based on the date of the reported infections (Fig. S1, Appendix

Table 2
Descriptive statistical analysis of the mobility variables for each city.

	PK	WP	TS	RR	GP	RS
	(Δ%)	(Δ%)	(Δ%)	(Δ%)	(Δ%)	(Δ%)
Bogotá						
Mean	−40.8	−40.2	−45.2	−51.9	−23.0	22.9
SD	15.3	16.6	21.8	16.1	18.1	8.7
CV (%)	−37.6	−41.2	−48.3	−31.1	−78.7	37.9
Min	−77.9	−70.9	−81.9	−85.1	−62.0	3.0
Max	−7.0	5.1	0.4	10.4	18.9	40.1
Asym	−5.2	3.8	1.5	−1.4	−1.7	1.9
Kurt	0.1	0.4	−3.4	−1.3	−1.2	−2.9
Medellín						
Mean	−41.9	−35.9	−48.4	−49.7	−26.9	18.3
SD	16.8	18.4	18.2	19.9	21.2	8.0
CV (%)	−40.1	−51.1	−37.6	−40.0	−78.9	43.8
Min	−80.1	−77.3	−82.7	−87.7	−68.0	2.7
Max	−11.4	1.7	7.4	10.3	19.3	35.0
Asym	−5.3	−5.0	−0.8	−1.4	−1.3	3.6
Kurt	−1.1	−0.8	−2.3	−2.7	−2.6	−2.3
Cali						
Mean	−42.0	−30.9	−36.5	−43.5	−19.6	16.2
SD	17.3	18.1	18.6	19.3	19.8	7.6
CV (%)	−41.2	−58.8	−50.8	−44.4	−101.4	46.8
Min	−82.0	−74.0	−76.6	−84.4	−63.3	−1.6
Max	8.9	5.0	3.3	9.7	17.3	33.0
Asym	−7.3	−6.6	−3.8	−4.4	−4.4	5.2
Kurt	−0.3	0.3	−1.4	−2.0	−1.6	−1.5
Barranquilla						
Mean	−48.6	−38.9	−51.2	−54.2	−28.0	19.1
SD	20.1	18.6	22.1	19.6	25.2	6.8
CV (%)	−41.3	−46.5	−43.2	−36.1	−90.2	35.6
Min	−81.9	−76.1	−81.3	−85.0	−67.1	1.3
Max	−5.0	5.7	0.1	−9.3	29.0	30.9
Asym	0.5	−0.9	2.9	1.4	1.5	−0.3
Kurt	−4.0	−3.4	−3.8	−4.1	−4.7	−4.3
Cartagena						
Mean	−68.1	−42.7	−71.1	−62.6	−38.7	19.0
SD	14.8	17.0	16.7	16.2	22.2	6.2
CV (%)	−21.7	−39.9	−23.5	−25.9	−57.3	32.4
Min	−88.9	−74.3	−91.3	−86.6	−72.6	2.9
Max	−30.6	1.7	−17.0	−19.0	7.1	29.6
Asym	3.1	−1.0	5.2	2.9	1.6	−0.2
Kurt	−3.5	−3.5	−2.3	−3.4	−4.4	−4.2
Leticia						
Mean	−55.9	−20.4	NA	NA	NA	NA
SD	13.6	16.4	NA	NA	NA	NA
CV (%)	−24.3	−80.3	NA	NA	NA	NA
Min	−80.3	−49.6	NA	NA	NA	NA
Max	−12.0	8.0	NA	NA	NA	NA
Asym	1.8	−2.0	NA	NA	NA	NA
Kurt	0.6	−3.6	NA	NA	NA	NA

Asym: asymmetry; CV: coefficient of variation; Kurt: kurtosis; NA: not available; Max: maximum value; Min: minimum value; SD: standard deviation.

A). They were classified in 4 (I-IV) or 5 (I–V) groups, from where it is possible to visualise the influence of restriction measures: the groups from March to August/2020 (quarantine) are in one side of the maps and the groups from September/2020 to January/2021 (post-quarantine) are in the other sited of the maps. From the component planes of each city (Fig. S2-27, Appendix A), the mobility variables (GP, PK, RR, RS, TS and WP) were responsible for the distinctions between these two periods in all cities individually. Apart from RS, these variables presented higher intensities in the post-quarantine, indicating that they had higher importance during this period. In contrast, RS presented the highest intensity and importance during the quarantine months.

The analysis of the component planes (Figs. S2–S7, Appendix A) showed that the relationship between epidemiological and meteorological variables presented distinct trends during quarantine. The maps from BAR, CAR and LET (Fig. S2, S5 and S6, Appendix A), for instance, revealed that days with higher number of new cases (high NDC and CR) had higher intensities for AH and h. WS presented the opposite trend (higher WS, lower number of cases), except for LET where this association is not clear. The maps from CAL and MED (Figs. S4 and S7, Appendix A) showed that low records of T_{min} were related to high NDC/CR values. On the other hand, high NDC/CR was related in BOG to lower T_{avg} and T_{max} (Fig. S3, Appendix A). In BOG and CAL (Figs. S3 and S4, Appendix A) days with high intensities for NDC/CR had lower values of AH, RH and h.

No clear patterns could be visualised in the post-quarantine period between epidemiological and meteorological variables in most component planes (Fig. S2 – Fig. S7, Appendix A). In CAL, for example, the highest number of NDC/CR was related to a lower T_{avg} and T_{max}. These maps also show that mobility variables in post-quarantine were dominant and well correlated with epidemiological variable in most of the cities (e.g., the neurons with highest intensity for GP, PK, RR, TS and WP in CAR maps were related to neurons with highest intensity for NDC/CR. Fig. S5, Appendix A).

4. Discussion

The dynamics of SARS-CoV-2 in Colombia appear to be affected by the different biomes in the country as revealed by the clusters visualised in SOM analysis (Fig. 5c). This is supported by Kubota et al. (2020) who speculated that specific factors (e.g., weather) from different biogeographic regions affect partially the development of the pandemic. Since the weather is considered a modulator of the stability or inhibition of SARS-CoV-2, the particular meteorological conditions of each city may have influenced the differences in the outbreaks (Briz-Redón and Serrano-Aroca, 2020a; Oliveiros et al., 2020; Paraskevis et al., 2021). Although, environmental conditions are not the single driver of the COVID-19 spread and other important factors (e.g., socioeconomic conditions, immunity, etc.) that were not considered in this study could have had a relevant role in the mechanism of transmission (Kubota et al., 2020; Wei et al., 2020). Furthermore, the samples were clearly divided by period (quarantine and post-quarantine, Fig. 5d) which support the effects of the containment measures. Indeed, independently of the climate of each city, isolation restrictions decrease the impact of the COVID-19 outbreaks (Maier and Brockmann, 2020).

In the quarantine period, the meteorological variables reflected clearer relationships with the caseloads than in the post-quarantine period. The lower effect of weather in the post-quarantine may be related to the increment of human mobility, since social contact rises the probability of contracting COVID-19 (Fazio et al., 2021). In addition, the increase of contagions in our study may be explained by different combinations of two or more meteorological conditions (e.g., higher NDC/CR were associated with lower AH, h and T_{min} in CAL). This is supported by other studies which reported that the analysis of just a single variable is not enough to explain the dynamics of the virus (Bannister-Tyrrell et al., 2020; Beggs and Avital, 2021; Chen et al., 2020). Auler et al. (2020), for instance, found that a combination of RH around 80% and T_{avg} of 27.5 °C may explain the evolution of COVID-19 in some cities in Brazil.

Our findings revealed distinct effects of temperature (T_{avg}, T_{max} and T_{min}) and humidity (AH and RH) variables on the COVID-19 spread in the assessed cities. It corroborates the adaptability of this new coronavirus to different environmental conditions (Bhardwaj and Agrawal, 2020; Yang et al., 2021). In MED and CAL, when T_{min} was lower (<18 °C and <17 °C, respectively) the number of contagions increased in quarantine (Figs. S4 and S7, Appendix A). This trend was also verified in other countries as Spain or China (Fernández-Ahúja and Martínez, 2021; Yang et al., 2021). In the case of T_{max}, this variable has been negatively correlated with the COVID-19 infections in cities as Wuhan (China) (Yang et al., 2021). In our study, BOG registered an increase of cases when T_{max} was below 20 °C in quarantine (Fig. S3, Appendix A). Other negative associations in this city were related to T_{avg} and AH with the contagions, especially when these variables were lower than 14 °C and 9 g/m^3, respectively (Fig. S3, Appendix A). This agrees with other epidemiological studies with this novel coronavirus and its predecessors

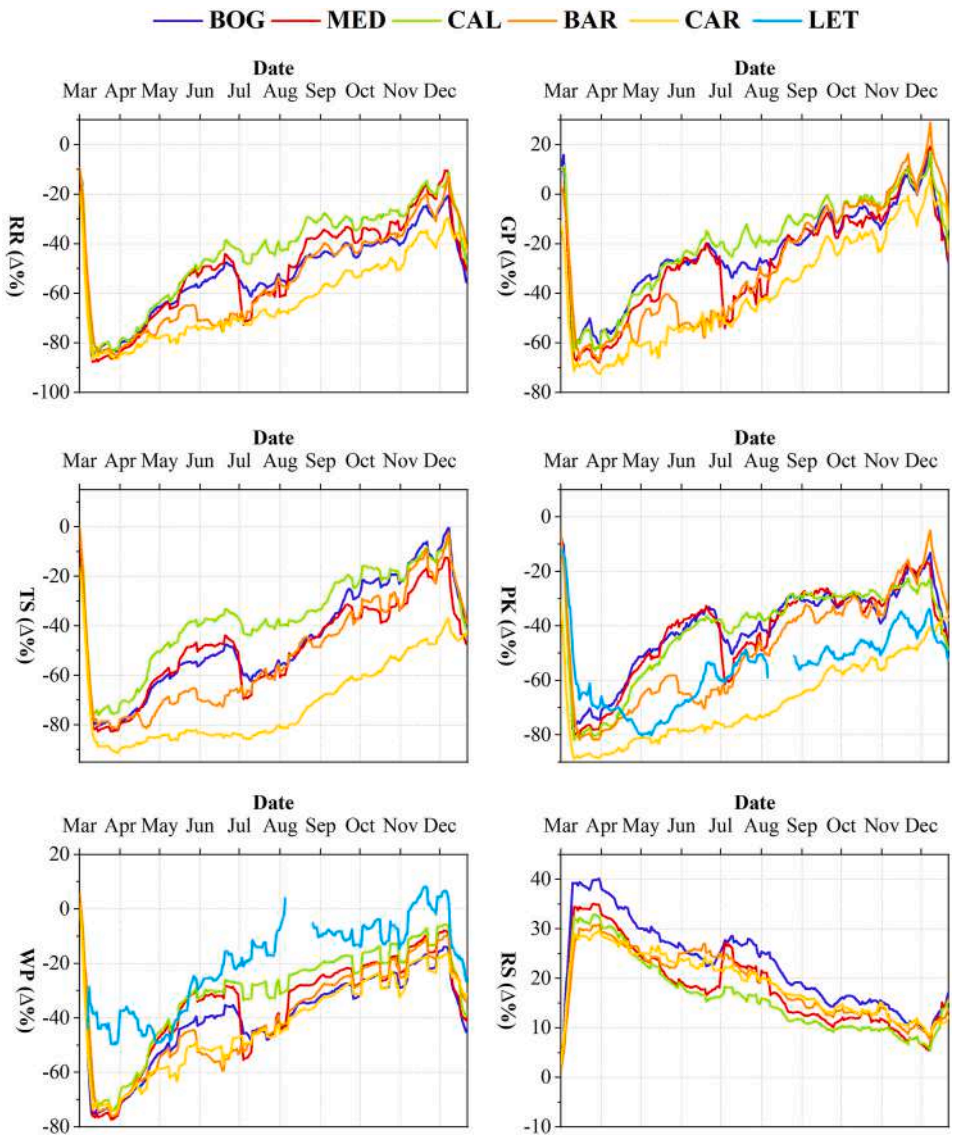

Fig. 4. Mobility variables (Retail and Recreation, Grocery and Pharmacy, Parks, Transport Stations, Workplaces, and Residential) from March/2020 to January/2021.

suggesting a higher transmission when temperature and humidity decrease (Briz-Redón and Serrano-Aroca, 2020a; Chan et al., 2011; Fernández-Ahúja and Martínez, 2021; Gardner et al., 2019; Nottmeyer and Sera, 2021). The stability of the virus in cold temperatures is associated to its heat intolerance (Beggs and Avital, 2021). Furthermore, colder/drier conditions such as the ones observed in BOG may promote that the respiratory droplets with the virus continue suspended for more time (Wang et al., 2021). These settings dry out the human mucous membrane, reducing the function of cilia and supporting the transmission of the disease (Qi et al., 2020; Sun et al., 2020). Some BOG records for T_{avg} (12.9–15.6 °C; Table 1) and AH (8–10.2 g/m^3; Table 1) corresponded with the vulnerable ranges to the virus spread reported in the literature: 4–9 g/m^3 and 3–17 °C (Bukhari and Jameel, 2020), 3–8 g/m^3 and 5–11 °C (Sajadi et al., 2020), 4–6 g/m^3 and 4–11 °C (Gupta et al., 2020). However, other demographic factors (Table S1, Appendix A) must be taking into consideration, for instance, the high population density may increase the frequency of direct contact (Diao et al., 2021; Lin et al., 2020). This is relevant if it is considered that BOG and MED have been listed as cities with the most higher and concentrated densities in the world (Brodie, 2017; Burdett, 2015; Wheeler, 2015).

In the case of the hottest (average $T_{avg} > 26$ °C) and wettest (average AH > 22 g/m^3) cities of the study, the increase of AH (BAR, CAR and LET) and T_{avg} (CAR) were related to higher NDC/CR records (Fig. S2, S5 and S6, Appendix A). Although high T_{avg} favour the instability of the virus in suspended droplets, it increments the amount of virus settled on surfaces (Magurano et al., 2021). Moreover, the likelihood of SARS-CoV-2 survival is approximately five times higher under humid conditions than under dry conditions, which may have influenced the contagions in these cities (Bhardwaj and Agrawal, 2020). The mechanisms of transmission of respiratory viruses in hot-wet settings seems to be related to: (i.) fomites, due to the faster deposition of virus-laden droplets on surfaces and their slow evaporation (Paynter, 2015; Rodó et al., 2021); (ii.) direct contact through small virus-laden particles produced by air conditioner systems (Ahlawat et al., 2020).

Humid-rainy conditions in Colombia have been associated with outbreaks of other respiratory viruses such as influenza and respiratory syncytial virus (RSV) (Gamba-Sanchez et al., 2016; Rodriguez-Martinez et al., 2015; Tamerius et al., 2013). This agrees with our data that show that COVID-19 outbreaks occurred in BAR, CAR and LET under wet conditions (average AH > 22 g/m^3). Moreover, our results accord with the hypothesis proposed by Auler et al. (2020): the reduction in CR associated with high temperature and humidity is not entirely reliable

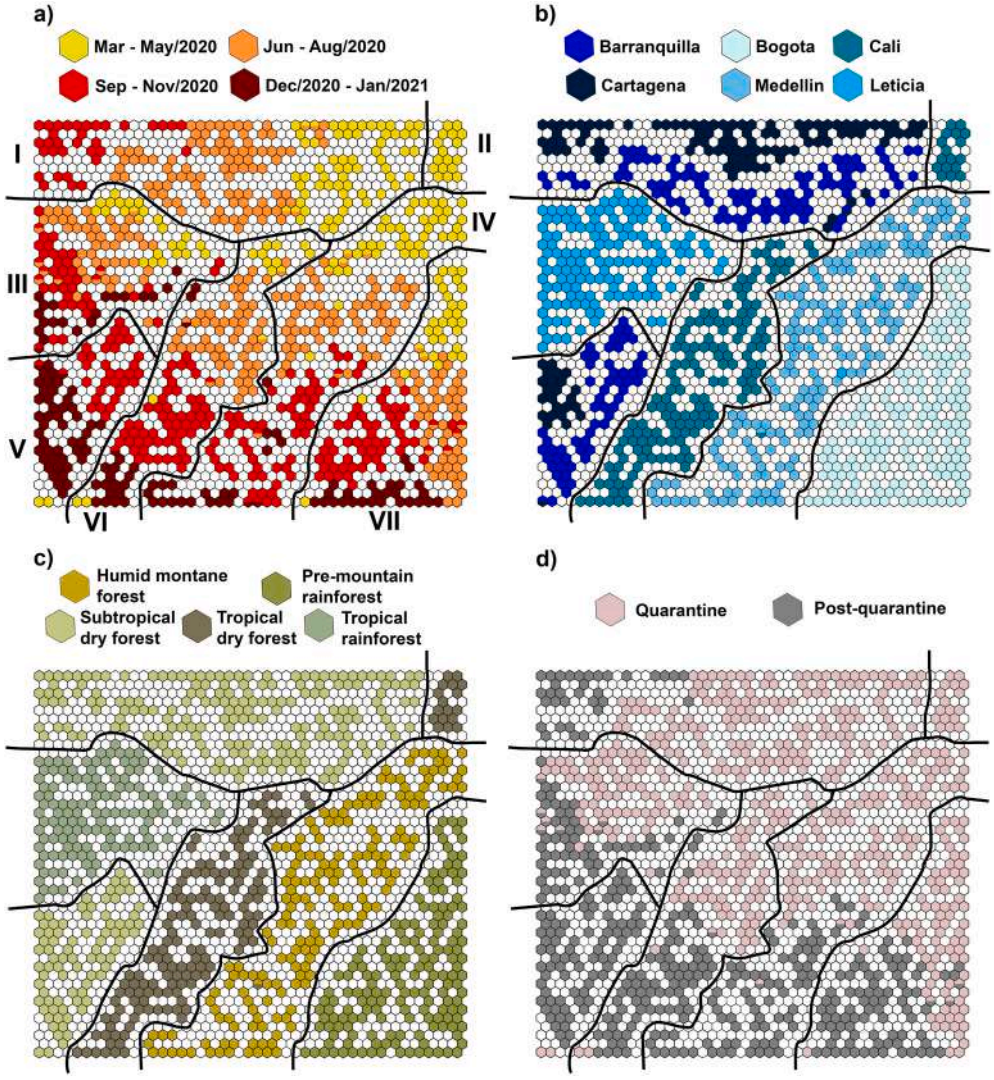

Fig. 5. Map of samples of the whole dataset classified by date of the reported cases (a), the city from where the cases were reported (b), the biome from where the cases where reported (c), and the period to which the data belongs (d). The samples were divided in 7 distinct groups (I-VII) based on the proximity between samples in the neurons (hexagonal units) and the different classifications.

for cities in tropical and subtropical regions. This conclusion is supported by other authors as Raines et al. (2020), who also identified in CAR a considerable increment of NDC in quarantine that was correlated with a RH above 78%. Likewise, Prata et al. (2021) found in Brazil that each 1% rise of the daily RH is associated with increments in COVID-19 cases of 2.26% in tropical regions and 2.35% in subtropical regions.

Special attention deserves h because it includes the effect of two variables at the same time (T_{avg} and RH). Some studies have listed h as a significant predictor variable of the SARS-CoV-2 survival (Beggs and Avital, 2021; Spena et al., 2020a). In our case, this variable for cities such as BOG, MED and CAL presented even higher correlation coefficients (Table S2, Appendix A) and clearer patterns with NDC/CR (e.g., Figs. S2 and S3, Appendix A) than temperature (T_{avg}, T_{max} and T_{min}) or humidity (AH and RH) variables, particularly in the quarantine period. Spena and collaborators (2020b) proposed a seasonal virulence risk scale based on the incidence rate of COVID-19 and h. This scale set a negligible risk when $h < 9$ kJ/kg and when $h > 33$ kJ/kg; low-to-average risk when h is between 9 and 12 kJ/kg and when h is between 23 and 33 kJ/kg; and average-to-high risk when h is between 12 and 23 kJ/kg. In our study, all assessed cities were classified as negligible risk, except BOG that presented potential risk (low-to-average risk) considering its h records (h between 30.4 and 36.4 kJ/kg, Table 1). It is consistent with our findings since BOG presented the highest NDC records throughout the study (maximum value of 7471 cases). However, cities that registered high CR values (BAR, CAR and LET) were not classified as average-to-high potential risk in the scale. Consequently, it is necessary to include the conditions of cities in (sub)tropical regions and the possible effect of other modulator variables (e.g., WS in LET) in this type of scale (which is based on temperate regions).

Regarding WS, it can modulate the dynamics of SARS-CoV-2 by reducing the suspending time of the virus in the air due to dilution and consequent removal (Ahmadi et al., 2020; N. Islam et al., 2020; Wang et al., 2021). This can be seen in the north coastal cities where the high WS records were related to diminutions in the caseloads (especially in the quarantine period, Figs. S2 and S5, Appendix A). The potential of WS to gradually reduce the effects of the pandemic also has been observed in other tropical coastal cities like Rio de Janeiro (Brazil) (Rosario et al., 2020). On the other hand, some studies determined higher contagion rates when the WS values were below 5.4 km/h in China (Wei et al., 2020) and 7.2 km/h in Italy (Coccia, 2020). In this investigation, the city (LET) with more records below these limits presented the highest CRs (Fig. 3; Table 1). This suggests that this variable may be an important factor controlling the virus transmission across Colombia.

Concerning the mobility variables, when people spent more time at

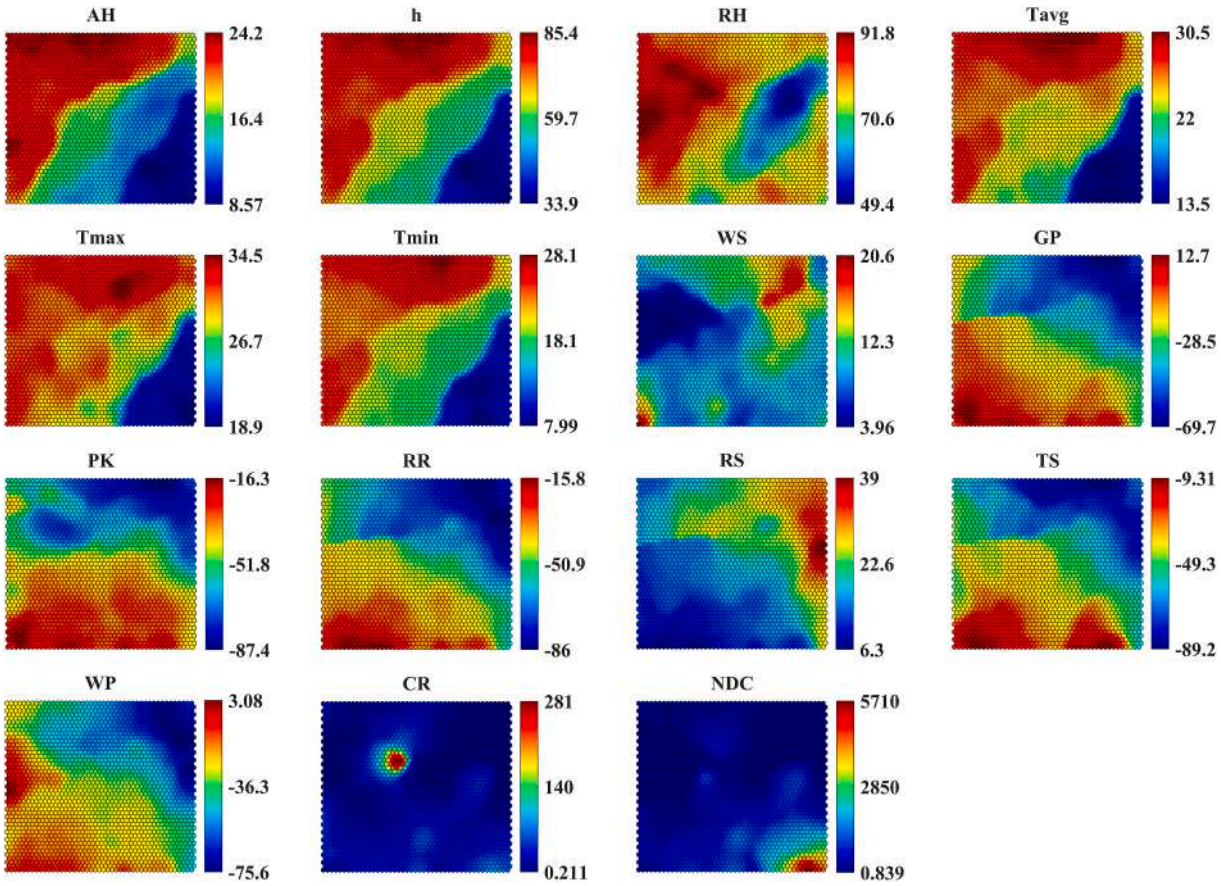

Fig. 6. Maps of variables of the whole dataset (component planes). The colour bar beside each map indicates the intensity of the variable: the red colour indicates high intensity and blue colour indicates low intensity. (For interpretation of the references to colour in this figure legend, the reader is referred to the Web version of this article.)

home (residential mobility), the transmission of SARS-CoV-2 was lower compared to the other variables (GP, PK, RR, TS, and WP). Previous studies stressed on the implications of weather on human interactions, for instance, warmed days may be associated with outdoor activities (e.g., visits to parks or public places) and more exposure to the virus (Damette et al., 2021; Shao et al., 2021). This is evident in our study in cities as BAR and CAR with clear patterns in post-quarantine between the mobility and epidemiological variables. A study developed at Johns Hopkins University revealed significant associations among the SARS-CoV-2 infections, the use of public transport, gatherings with more than 10 people and more than 100 people, and visits to indoor or outdoor places with crowds (Clipman et al., 2020). Finally, the role of mobility variables on the increment of cases in the post-quarantine period mirrored that the lockdown is a sensible alternative but an effective way to control the transmission of SARS-CoV-2. It has been evidenced in studies carried out in China, England or Italy (Cartenì et al., 2020; Chinazzi et al., 2020; Sartorius et al., 2021; Vollmer et al., 2020; Y. Zhou et al., 2020).

Our findings are limited by the socioeconomic conditions of the country, e.g., Colombia has a Human Development Index of 0.74 (http://hdr.undp.org, accessed in April 2021) with serious gaps in the provision of health and food services that could easily counteract any potential climatic effect at local scales (Coelho et al., 2020). In addition, this investigation did not take into consideration other possible predictors as the number of tests applied, general health policies, transportation or cultural aspects (Oliveiros et al., 2020). However, we considered that our results may contribute to a better understanding of how SARS-CoV-2 is sustained in tropical countries such as Colombia. In addition, other strengths are: (i.) the evaluation of 15 different variables using a dataset of 10 months, unlike several studies that assessed narrower periods (Sanchez-Lorenzo et al., 2021; Yang et al., 2021); (ii). This study about the influence of multiple variables (meteorological and mobility) on the SARS-CoV-2 transmission in Colombia could be carried out using other methods such as Principal Component Analysis (PCA) or Partial Least Squares (PLS). Nevertheless, the use of SOM technique presents several advantages related to its highlighted visualisation capabilities with different graphical representation options, its good performance in clustering and pattern recognition, efficient use of space in the maps and its robustness to missing data or noise (Brereton, 2012; Gontijo et al., 2021).

5. Conclusions

This study has shown that different biogeographical regions in Colombia had distinct dynamics regarding the virus spread. This was attributed to both restriction measures that affected human mobility and larger spatial than temporal variations of the analysed meteorological variables. Hence, our outcomes may contribute to the implementation of measures to preserve public health and the formulation of site-specific policies to prevent disease dissemination.

The highest CR occurred in LET, where the lowest WS may have an important influence on the virus transmission. In MED and CAL, T_{min} had an important role in the increment of NDC/CR. Furthermore, the highest NDC recorded in BOG appeared to be linked to a decrease in T_{avg} (<14 °C) and AH (<9 g/m^3), besides its largest population, higher population density and importance. The increase of AH and T_{avg} also seemed to favour the virus spread in warmer and wetter cities with an average $T_{avg} > 26.2$ °C and AH > 22.1 g/m^3 (BAR, CAR and LET) that

achieved higher CR records. The different impact of meteorological variables on the virus transmission may be connected to local characteristics such as sociodemographic aspects and combined factors.

The human mobility variables influenced the development of the pandemic in most of the analysed cities, especially in the post-quarantine period. The higher amount of time spent at home was more important when quarantine was in place. This supported the efficacy of the restriction measures during quarantine, when meteorological variables seem to have grown in importance These measures did not avoid a fast spread of the virus (e.g., in LET), supporting the need for well-ventilated spaces, stricter hygiene and restriction measures, and investigation of other variables (e.g., solar radiation, air pollutants or vaccination rate).

The SOM analysis was suitable to show the distinctions between quarantine and post-quarantine periods, differences related to local biomes (e.g., humidity effects) and the development of the pandemic considering all analysed variables combined. This technique can be applied in other regions based on its ability to spatially or temporally group samples. Future investigations using SOM should focus on (i.) comparing the specific conditions (e.g., weather or mobility) of regions located in other latitudes and their implemented strategies to cope with the pandemic; (ii.) assessing the dynamic of the new virus variants and whether the meteorological conditions have the same influence; (iii.) (sub)tropical regions, especially in Latin America or Africa, where the influence of particular environmental (e.g., high humidity did not prevent the increase of contagions in this study), socioeconomic (e.g., access to healthcare or migration) or sanitary (e.g., drinking water) conditions on the pandemic needing more attention (Briz-Redón and Serrano-Aroca, 2020b).

Declaration of competing interest

The authors declared no conflict of interests.

Acknowledgements

S. Gómez-Herrera and S. Enríquez-Delgado thank the support of the government of Nariño (Colombia) and Ceiba Foundation for the scholarships granted. E. S. J Gontijo and A. H Rosa would like to thank the São Paulo Research Foundation (FAPESP, grant number 19/06800–5) and the Coordination for the Improvement of Higher Education Personnel (CAPES, grant number 99999.008107/2015–07) for financial support.

Appendix A. Supplementary data

Supplementary data to this article can be found online at https://doi.org/10.1016/j.ijheh.2021.113833.

References

Aboubakr, H.A., Sharafeldin, T.A., Goyal, S.M., 2020. Stability of SARS-CoV-2 and other coronaviruses in the environment and on common touch surfaces and the influence of climatic conditions: a review. Transbound Emerg. Dis. 68, 296–312. https://doi.org/10.1111/tbed.13707.

Ahlawat, A., Wiedensohler, A., Mishra, S.K., 2020. An overview on the role of relative humidity in airborne transmission of SARS-CoV-2 in indoor environments. Aerosol. Air Qual. Res. 20, 1856–1861. https://doi.org/10.4209/aaqr.2020.06.0302.

Ahmadi, M., Sharifi, A., Dorosti, S., Jafarzadeh Ghoushchi, S., Ghanbari, N., 2020. Investigation of effective climatology parameters on COVID-19 outbreak in Iran. Sci. Total Environ. 729, 138705. https://doi.org/10.1016/j.scitotenv.2020.138705.

Alduchov, O.A., Eskridge, R.E., 1996. Improved magnus form approximation of saturation vapor pressure. J. Appl. Meteorol. Climatol. 35, 601–609. https://doi.org/10.1175/1520-0450(1996)035<0601:IMFAOS>2.0.CO, 2.

Alhoniemi, E., Himberg, J., Parhankangas, J., Vesanto, J., 2000. SOM Toolbox for Matlab. SOM Toolbox Team. Helsinki University, Espoo.

Araújo, M.B., Naimi, B., 2020. Spread of SARS-CoV-2 Coronavirus likely constrained by climate. medRxiv. https://doi.org/10.1101/2020.03.12.20034728, 03.12.20034728.

Arellana, J., Márquez, L., Cantillo, V., 2020. COVID-19 outbreak in Colombia: an analysis of its impacts on transport systems [WWW Document]. Journal of Advanced Transportation. https://doi.org/10.1155/2020/8867316.

Asan, U., Ercan, S., 2012. An introduction to self-organizing maps. Computational Intelligence Systems in Industrial Engineering. Springer, pp. 295–315.

Auler, A.C., Cássaro, F.A.M., da Silva, V.O., Pires, L.F., 2020. Evidence that high temperatures and intermediate relative humidity might favor the spread of COVID-19 in tropical climate: a case study for the most affected Brazilian cities. Sci. Total Environ. 729, 139090. https://doi.org/10.1016/j.scitotenv.2020.139090.

Bannister-Tyrrell, M., Meyer, A., Faverjon, C., Cameron, A., 2020. Preliminary evidence that higher temperatures are associated with lower incidence of COVID-19, for cases reported globally up to 29th February 2020. medRxiv. https://doi.org/10.1101/2020.03.18.20036731, 03.18.20036731.

Battineni, G., Chintalapudi, N., Amenta, F., 2020. Tropical Conditions and Outbreak of COVID-19. Pharmaceutical and Biomedical Research.

Beggs, C.B., Avital, E.J., 2021. A psychrometric model to assess the biological decay of the SARS-CoV-2 virus in aerosols. PeerJ 9, e11024.

Berberan-Santos, M.N., Bodunov, E.N., Pogliani, L., 1997. On the barometric formula. Am. J. Phys. 65, 404–412. https://doi.org/10.1119/1.18555.

Bhardwaj, R., Agrawal, A., 2020. Likelihood of survival of coronavirus in a respiratory droplet deposited on a solid surface. Phys. Fluids 32, 061704. https://doi.org/10.1063/5.0012009.

Bochenek, B., Jankowski, M., Gruszczynska, M., Nykiel, G., Gruszczynski, M., Jaczewski, A., Ziemianski, M., Pyrc, R., Figurski, M., Pinkas, J., 2021. Impact of meteorological conditions on the dynamics of the COVID-19 pandemic in Poland. Int. J. Environ. Res. Publ. Health 18, 3951.

Brereton, R.G., 2012. Self organising maps for visualising and modelling. Chem. Cent. J. 6, S1. https://doi.org/10.1186/1752-153X-6-S2-S1.

Briz-Redón, Á., Serrano-Aroca, Á., 2020a. The effect of climate on the spread of the COVID-19 pandemic: a review of findings, and statistical and modelling techniques. Prog. Phys. Geogr.: Earth Environ. 44, 591–604.

Briz-Redón, Á., Serrano-Aroca, Á., 2020b. A spatio-temporal analysis for exploring the effect of temperature on COVID-19 early evolution in Spain. Sci. Total Environ. 728, 138811. https://doi.org/10.1016/j.scitotenv.2020.138811.

Brodie, C., 2017. These Are the World's Most Crowded Cities. Presented at the World Economic Forum.

Bukhari, Q., Jameel, Y., 2020. Will coronavirus pandemic diminish by summer? SSRN J. https://doi.org/10.2139/ssrn.3556998.

Burdett, R., 2015. A Tale of Four World cities–London, Delhi, Tokyo and Bogotá Compared, vol. 11. The Guardian.

Car, Z., Baressi Šegota, S., Anđelić, N., Lorencin, I., Mrzljak, V., 2020. Modeling the spread of COVID-19 infection using a multilayer perceptron. Comput. Math. Methods Med. 2020, 1–10. https://doi.org/10.1155/2020/5714714.

Cartenì, A., Di Francesco, L., Martino, M., 2020. How mobility habits influenced the spread of the COVID-19 pandemic: results from the Italian case study. Sci. Total Environ. 741, 140489.

Chan, K.H., Peiris, J.S.M., Lam, S.Y., Poon, L.L.M., Yuen, K.Y., Seto, W.H., 2011. The effects of temperature and relative humidity on the viability of the SARS coronavirus. Adv. Virol. 734690. https://doi.org/10.1155/2011/734690.

Chen, B., Liang, H., Yuan, X., Hu, Y., Xu, M., Zhao, Y., Zhang, B., Tian, F., Zhu, X., 2020. Roles of Meteorological Conditions in COVID-19 Transmission on a Worldwide Scale (Preprint). Infectious Diseases (Except HIV/AIDS). https://doi.org/10.1101/2020.03.16.20037168.

Chinazzi, M., Davis, J.T., Ajelli, M., Gioannini, C., Litvinova, M., Merler, S., Piontti, A.P. y, Mu, K., Rossi, L., Sun, K., Viboud, C., Xiong, X., Yu, H., Halloran, M.E., Longini, I. M., Vespignani, A., 2020. The effect of travel restrictions on the spread of the 2019 novel coronavirus (COVID-19) outbreak. Science 368, 395–400. https://doi.org/10.1126/science.aba9757.

Çinar, Ö., Merdun, H., 2009. Application of an unsupervised artificial neural network technique to multivariant surface water quality data. Ecol. Res. 24, 163–173.

Clipman, S.J., Wesolowski, A.P., Gibson, D.G., Agarwal, S., Lambrou, A.S., Kirk, G.D., Labrique, A.B., Mehta, S.H., Solomon, S.S., 2020. Rapid Real-Time Tracking of Nonpharmaceutical Interventions and Their Association with Severe Acute Respiratory Syndrome Coronavirus 2 (SARS-CoV-2) Positivity: the Coronavirus Disease 2019 (COVID-19) Pandemic Pulse Study. Clinical Infectious Diseases. https://doi.org/10.1093/cid/ciaa1313.

Coccia, M., 2020. Factors determining the diffusion of COVID-19 and suggested strategy to prevent future accelerated viral infectivity similar to COVID. Sci. Total Environ. 729, 138474. https://doi.org/10.1016/j.scitotenv.2020.138474.

Coelho, M.T.P., Rodrigues, J.F.M., Medina, A.M., Scalco, P., Terribile, L.C., Vilela, B., Diniz-Filho, J.A.F., Dobrovolski, R., 2020. Global expansion of COVID-19 pandemic is driven by population size and airport connections. PeerJ 8, e9708. https://doi.org/10.7717/peerj.9708.

Coşkun, H., Yıldırım, N., Gündüz, S., 2021. The spread of COVID-19 virus through population density and wind in Turkey cities. Sci. Total Environ. 751, 141663. https://doi.org/10.1016/j.scitotenv.2020.141663.

Damette, O., Mathonnat, C., Goutte, S., 2021. Meteorological factors against COVID-19 and the role of human mobility. PloS One 16, e0252405. https://doi.org/10.1371/journal.pone.0252405.

de Castro Júnior, S.L., da Silva, I.J.O., 2021. The specific enthalpy of air as an indicator of heat stress in livestock animals. Int. J. Biometeorol. 65, 149–161. https://doi.org/10.1007/s00484-020-02022-8.

De la Hoz-Restrepo, F., Alvis-Zakzuk, N.J., De la Hoz-Gomez, J.F., De la Hoz, A., Gómez Del Corral, L., Alvis-Guzmán, N., 2020. Is Colombia an example of successful containment of the 2020 COVID-19 pandemic? A critical analysis of the epidemiological data, March to July 2020. International Journal of Infectious Diseases 99, 522–529. https://doi.org/10.1016/j.ijid.2020.08.017.

Departamento Administrativo Nacional de Estadistica, 2018. Censo nacional de Población y vivienda 2018 [WWW Document]. URL. https://www.dane.gov.co/in

dex.php/estadisticas-por-tema/demografia-y-poblacion/censo-nacional-de-poblacion-y-vivenda-2018, 11,22,20.
Dhand, R., Li, J., 2020. Coughs and sneezes: their role in transmission of respiratory viral infections, including SARS-CoV-2. Am. J. Respir. Crit. Care Med. 202, 651–659. https://doi.org/10.1164/rccm.202004-1263PP.
Dhouib, W., Maatoug, J., Ayouni, I., Zammit, N., Ghammem, R., Fredj, S.B., Ghannem, H., 2021. The incubation period during the pandemic of COVID-19: a systematic review and meta-analysis. Syst. Rev. 10, 101. https://doi.org/10.1186/s13643-021-01648-y.
Diao, Y., Kodera, S., Anzai, D., Gomez-Tames, J., Rashed, E.A., Hirata, A., 2021. Influence of population density, temperature, and absolute humidity on spread and decay durations of COVID-19: a comparative study of scenarios in China, England, Germany, and Japan. One Health 12, 100203. https://doi.org/10.1016/j.onehlt.2020.100203.
Doan, Q.-V., Kusaka, H., Sato, T., Chen, F., 2020. A structural self-organizing map (S-SOM) algorithm for weather typing. Geosci. Model Dev. Discuss. (GMDD) 1–27.
Farkas, C., Iclanzan, D., Olteán-Péter, B., Vekov, G., 2021. Estimation of parameters for a humidity-dependent compartmental model of the COVID-19 outbreak. PeerJ 9, e10790. https://doi.org/10.7717/peerj.10790.
Fazio, R.H., Ruisch, B.C., Moore, C.A., Samayoa, J.A.G., Boggs, S.T., Ladanyi, J.T., 2021. Social distancing decreases an individual's likelihood of contracting COVID-19. Proc. Natl. Acad. Sci. Unit. States Am. 118 https://doi.org/10.1073/pnas.2023131118.
Fernández-Ahúja, J.M.L., Martínez, J.L.F., 2021. Effects of climate variables on the COVID-19 outbreak in Spain. Int. J. Hyg Environ. Health 234, 113723.
Galvan, D., Effting, L., Cremasco, H., Adam Conte-Junior, C., 2020. Can socioeconomic, health, and safety data explain the spread of COVID-19 outbreak on Brazilian federative units? Int. J. Environ. Res. Publ. Health 17, 8921.
Galvan, D., Effting, L., Cremasco, H., Conte-Junior, C.A., 2021. The spread of the COVID-19 outbreak in Brazil: an overview by kohonen self-organizing map networks. Medicina 57, 235. https://doi.org/10.3390/medicina57030235.
Gamba-Sanchez, N., Rodriguez-Martinez, C., Sossa-Briceño, M., 2016. Epidemic activity of respiratory syncytial virus is related to temperature and rainfall in equatorial tropical countries. Epidemiol. Infect. 144, 2057–2063.
Garcia, J.S., da Silva, G.A., Arruda, M.A., Poppi, R.J., 2007. Application of Kohonen neural network to exploratory analyses of synchroton radiation x-ray fluorescence measurements of sunflower metalloproteins. X Ray Spectrom.: Int. J. 36, 122–129.
Gardner, E.G., Kelton, D., Poljak, Z., Van Kerkhove, M., von Dobschuetz, S., Greer, A.L., 2019. A case-crossover analysis of the impact of weather on primary cases of Middle East respiratory syndrome. BMC Infect. Dis. 19, 113. https://doi.org/10.1186/s12879-019-3729-5.
Gontijo, E.S.J., Herzsprung, P., Lechtenfeld, O.J., de Castro Bueno, C., Barth, A.C., Rosa, A.H., Friese, K., 2021. Multi-proxy approach involving ultrahigh resolution mass spectrometry and self-organising maps to investigate the origin and quality of sedimentary organic matter across a subtropical reservoir. Org. Geochem. 151, 104165. https://doi.org/10.1016/j.orggeochem.2020.104165.
Guarner, J., 2020. Three emerging coronaviruses in two Decades. Am. J. Clin. Pathol. 153, 420–421. https://doi.org/10.1093/ajcp/aqaa029.
Gupta, S., Raghuwanshi, G.S., Chanda, A., 2020. Effect of weather on COVID-19 spread in the US: a prediction model for India in 2020. Sci. Total Environ. 728, 138860. https://doi.org/10.1016/j.scitotenv.2020.138860.
Hammer, Ø., Harper, D.A., Ryan, P.D., 2001. PAST: paleontological statistics software package for education and data analysis. Palaeontol. Electron. 4, 9.
Hartono, P., 2020. Generating Similarity Map for COVID-19 Transmission Dynamics with Topological Autoencoder arXiv preprint arXiv:2004.01481.
He, Z., Chin, Y., Yu, S., Huang, J., Zhang, C.J., Zhu, K., Azarakhsh, N., Sheng, J., He, Y., Jayavanth, P., 2021. The influence of average temperature and relative humidity on new cases of COVID-19: time-series analysis. JMIR Public Health Surveillance 7, e20495.
Holdridge, L.R., Grenke, W.C., 1971. Forest Environments in Tropical Life Zones: a Pilot Study. Forest Environments in Tropical Life Zones: a Pilot Study.
Hopkins, Johns, 2021. Track Reported Cases of COVID-19 Coronavirus Resource Center. WWW Document, online).
Hridoy, A.-E.E., Mohiman, M.A., Tusher, S.M.S.H., Nowraj, S.Z.A., Rahman, M.A., 2021. Impact of meteorological parameters on COVID-19 transmission in Bangladesh: a spatiotemporal approach. Theor. Appl. Climatol. 144, 273–285.
Islam, A.R.M.T., Hasanuzzaman, M., Azad, M.A.K., Salam, R., Toshi, F.Z., Khan, M.S.I., Alam, G.M., Ibrahim, S.M., 2020. Effect of meteorological factors on COVID-19 cases in Bangladesh. Environ. Dev. Sustain. 1–24.
Islam, N., Shabnam, S., Erzurumluoglu, A.M., 2020. Meteorological factors and Covid-19 incidence in 310 regions across the world (preprint). Infectious Diseases (except HIV/AIDS). https://doi.org/10.1101/2020.03.27.20045658.
Islam, N., Bukhari, Q., Jameel, Y., Shabnam, S., Erzurumluoglu, A.M., Siddique, M.A., Massaro, J.M., D'Agostino, R.B., 2021. COVID-19 and climatic factors: a global analysis. Environ. Res. 193, 110355. https://doi.org/10.1016/j.envres.2020.110355.
Khan, W., Hussain, A., Khan, S.A., Al-Jumailey, M., Nawaz, R., Liatsis, P., 2021. Analysing the impact of global demographic characteristics over the COVID-19 spread using class rule mining and pattern matching, 8. Royal Society Open Science, p. 201823. https://doi.org/10.1098/rsos.201823.
Kohonen, T., 2001. Self-Organizing Maps, third ed. Springer Series in Information Sciences. Springer-Verlag, Berlin Heidelberg. https://doi.org/10.1007/978-3-642-56927-2.
Kowalski, C.H., da Silva, G.A., Godoy, H.T., Poppi, R.J., Augusto, F., 2013. Application of Kohonen neural network for evaluation of the contamination of Brazilian breast milk with polychlorinated biphenyls. Talanta 116, 315–321. https://doi.org/10.1016/j.talanta.2013.05.033.
Kubota, Y., Shiono, T., Kusumoto, B., Fujinuma, J., 2020. Multiple drivers of the COVID-19 spread: the roles of climate, international mobility, and region-specific conditions. PloS One 15, e0239385.
Kulkarni, H., Khandait, H., Narlawar, U.W., Rathod, P., Mamtani, M., 2021. Independent association of meteorological characteristics with initial spread of Covid-19 in India. Sci. Total Environ. 764, 142801. https://doi.org/10.1016/j.scitotenv.2020.142801.
Lawrence, M.G., 2005. The relationship between relative humidity and the dewpoint temperature in moist air: a simple conversion and applications. Bull. Am. Meteorol. Soc. 86, 225–234.
Leichtweis, B.G., de Faria Silva, L., da Silva, F.L., Peternelli, L.A., 2021. How the global health security index and environment factor influence the spread of COVID-19: a country level analysis. One Health 12, 100235. https://doi.org/10.1016/j.onehlt.2021.100235.
Lin, C., Lau, A.K.H., Fung, J.C.H., Guo, C., Chan, J.W.M., Yeung, D.W., Zhang, Y., Bo, Y., Hossain, M.S., Zeng, Y., Lao, X.Q., 2020. A mechanism-based parameterisation scheme to investigate the association between transmission rate of COVID-19 and meteorological factors on plains in China. Sci. Total Environ. 737, 140348. https://doi.org/10.1016/j.scitotenv.2020.140348.
Magurano, F., Baggieri, M., Marchi, A., Rezza, G., Nicoletti, L., Eleonora, B., Concetta, F., Stefano, F., Maedeh, K., Paola, B., Emilio, D., Silvia, G., 2021. SARS-CoV-2 infection: the environmental endurance of the virus can be influenced by the increase of temperature. Clin. Microbiol. Infect. 27, 289. https://doi.org/10.1016/j.cmi.2020.10.034 e5-289.e7.
Maier, B.F., Brockmann, D., 2020. Effective containment explains subexponential growth in recent confirmed COVID-19 cases in China. Science 368, 742–746.
Marcu, S., 2021. Towards sustainable mobility? The influence of the COVID-19 pandemic on Romanian mobile citizens in Spain. Sustainability 13, 4023.
Marquet, P., Geleyn, J.-F., 2015. Formulations of Moist Thermodynamics for Atmospheric Modelling arXiv preprint arXiv:1510.03239.
Melin, P., Monica, J.C., Sanchez, D., Castillo, O., 2020. Analysis of spatial spread relationships of coronavirus (COVID-19) pandemic in the world using self organizing maps. Chaos, Solit. Fractals 138, 109917. https://doi.org/10.1016/j.chaos.2020.109917.
Mollalo, A., Rivera, K.M., Vahedi, B., 2020. Artificial neural network modeling of novel coronavirus (COVID-19) incidence rates across the continental United States. Int. J. Environ. Res. Publ. Health 17, 4204.
Mouchtouri, V.A., Koureas, M., Kyritsi, M., Vontas, A., Kourentis, L., Sapounas, S., Rigakos, G., Petinaki, E., Tsiodras, S., Hadjichristodoulou, C., 2020. Environmental contamination of SARS-CoV-2 on surfaces, air-conditioner and ventilation systems. Int. J. Hyg Environ. Health 230, 113599.
Niazkar, H.R., Niazkar, M., 2020. Application of artificial neural networks to predict the COVID-19 outbreak. Glob. Health Research Pol. 5, 50. https://doi.org/10.1186/s41256-020-00175-y.
Notari, A., 2021. Temperature dependence of COVID-19 transmission. Sci. Total Environ. 763, 144390. https://doi.org/10.1016/j.scitotenv.2020.144390.
Nottmeyer, L.N., Sera, F., 2021. Influence of temperature, and of relative and absolute humidity on COVID-19 incidence in England - a multi-city time-series study. Environ. Res. 196, 110977. https://doi.org/10.1016/j.envres.2021.110977.
Oliveiros, B., Caramelo, L., Ferreira, N.C., Caramelo, F., 2020. Role of temperature and humidity in the modulation of the doubling time of COVID-19 cases (preprint). Public and Global Health. https://doi.org/10.1101/2020.03.05.20031872.
Pan, J., Yao, Y., Liu, Z., Meng, X., Ji, J.S., Qiu, Y., Wang, Weidong, Zhang, L., Wang, Weibing, Kan, H., 2021. Warmer weather unlikely to reduce the COVID-19 transmission: an ecological study in 202 locations in 8 countries. Sci. Total Environ. 753, 142272. https://doi.org/10.1016/j.scitotenv.2020.142272.
Pani, S.K., Lin, N.-H., RavindraBabu, S., 2020. Association of COVID-19 pandemic with meteorological parameters over Singapore. Sci. Total Environ. 740, 140112. https://doi.org/10.1016/j.scitotenv.2020.140112.
Paraskevis, D., Kostaki, E.G., Alygizakis, Nikiforos, Thomaidis, N.S., Cartalis, C., Tsiodras, S., Dimopoulos, M.A., 2021. A review of the impact of weather and climate variables to COVID-19: in the absence of public health measures high temperatures cannot probably mitigate outbreaks. Sci. Total Environ. 768, 144578. https://doi.org/10.1016/j.scitotenv.2020.144578.
Paynter, S., 2015. Humidity and respiratory virus transmission in tropical and temperate settings. Epidemiol. Infect. 143, 1110–1118. https://doi.org/10.1017/S0950268814002702.
Prata, D., Rodrigues, W., Bermejo, P.H.D.S., Moreira, M., Camargo, W., Lisboa, M., Reis, G.R., de Araujo, H.X., 2021. The relationship between (sub) tropical climates and the incidence of COVID-19. PeerJ 9, e10655.
Qi, H., Xiao, S., Shi, R., Ward, M.P., Chen, Y., Tu, W., Su, Q., Wang, W., Wang, X., Zhang, Z., 2020. COVID-19 transmission in Mainland China is associated with temperature and humidity: a time-series analysis. Sci. Total Environ. 728, 138778. https://doi.org/10.1016/j.scitotenv.2020.138778.
Raines, K.S., Doniach, S., Bhanot, G., 2020. The transmission of SARS-CoV-2 is likely comodulated by temperature and by relative humidity (preprint). Epidemiology. https://doi.org/10.1101/2020.05.23.20111278.
Ramírez, J.D., Florez, C., Muñoz, M., Hernández, C., Castillo, A., Gomez, S., Rico, A., Pardo, L., Barros, E.C., Castañeda, S., Ballesteros, N., Martínez, D., Vega, L., Jaimes, J.E., Cruz-Saavedra, L., Herrera, G., Patiño, L.H., Teherán, A.A., Gonzalez-Reiche, A.S., Hernandez, M.M., Sordillo, E.M., Simon, V., van Bakel, H., Paniz-Mondolfi, A., 2020. The arrival and spread of SARS-CoV-2 in Colombia. J. Med. Virol. 93, 1158–1163. https://doi.org/10.1002/jmv.26393.
Rodó, X., San-José, A., Kirchgatter, K., López, L., 2021. Changing climate and the COVID-19 pandemic: more than just heads or tails. Nat. Med. 27, 576–579. https://doi.org/10.1038/s41591-021-01303-y.

Rodriguez-Martinez, C., Sossa-Briceño, M., Acuña-Cordero, R., 2015. Relationship between meteorological conditions and respiratory syncytial virus in a tropical country. Epidemiol. Infect. 143, 2679–2686.
Rosario, D.K.A., Mutz, Y.S., Bernardes, P.C., Conte-Junior, C.A., 2020. Relationship between COVID-19 and weather: case study in a tropical country. Int. J. Hyg Environ. Health 229, 113587. https://doi.org/10.1016/j.ijheh.2020.113587.
Sajadi, M.M., Habibzadeh, P., Vintzileos, A., Shokouhi, S., Miralles-Wilhelm, F., Amoroso, A., 2020. Temperature, Humidity and Latitude Analysis to Predict Potential Spread and Seasonality for COVID-19 (SSRN Scholarly Paper No. ID 3550308). Social Science Research Network, Rochester, NY. https://doi.org/10.2139/ssrn.3550308.
Sanchez-Lorenzo, A., Vaquero-Martínez, J., Calbó, J., Wild, M., Santurtún, A., Lopez-Bustins, J.A., Vaquero, J.M., Folini, D., Antón, M., 2021. Did anomalous atmospheric circulation favor the spread of COVID-19 in Europe? Environ. Res. 194, 110626. https://doi.org/10.1016/j.envres.2020.110626.
Sartorius, B., Lawson, A., Pullan, R., 2021. Modelling and predicting the spatio-temporal spread of COVID-19, associated deaths and impact of key risk factors in England. Sci. Rep. 11, 1–11.
Seposo, X., Ng, C.F.S., Madaniyazi, L., 2021. Immediate and Delayed meteorological effects on COVID-19 time-varying infectiousness in tropical cities. Atmosphere 12, 513.
Shao, W., Xie, J., Zhu, Y., 2021. Mediation by human mobility of the association between temperature and COVID-19 transmission rate. Environ. Res. 194, 110608.
Spena, A., Palombi, L., Corcione, M., Carestia, M., Spena, V.A., 2020a. On the optimal indoor air conditions for SARS-CoV-2 inactivation. An enthalpy-based approach. Int. J. Environ. Res. Publ. Health 17, 6083.
Spena, A., Palombi, L., Corcione, M., Quintino, A., Carestia, M., Spena, V.A., 2020b. Predicting SARS-CoV-2 weather-induced seasonal virulence from atmospheric air enthalpy. Int. J. Environ. Res. Publ. Health 17, 9059.
Sulyok, M., Walker, M.D., 2021. Mobility and COVID-19 mortality across Scandinavia: a modeling study. Trav. Med. Infect. Dis. 41, 102039.
Sun, Z., Thilakavathy, K., Kumar, S.S., He, G., Liu, S.V., 2020. Potential factors influencing repeated SARS outbreaks in China. Int. J. Environ. Res. Publ. Health 17, 1633. https://doi.org/10.3390/ijerph17051633.
Tamerius, J.D., Shaman, J., Alonso, W.J., Bloom-Feshbach, K., Uejio, C.K., Comrie, A., Viboud, C., 2013. Environmental predictors of seasonal influenza epidemics across temperate and tropical climates. PLoS Pathog. 9, e1003194 https://doi.org/10.1371/journal.ppat.1003194.
Terfloth, L., Gasteiger, J., 2001. Neural networks and genetic algorithms in drug design. Drug Discov. Today 6, 102–108. https://doi.org/10.1016/S1359-6446(01)00173-8.
Tosepu, R., Gunawan, J., Effendy, D.S., Ahmad, L.O.A.I., Lestari, H., Bahar, H., Asfian, P., 2020. Correlation between weather and covid-19 pandemic in jakarta, Indonesia. Sci. Total Environ. 725, 138436. https://doi.org/10.1016/j.scitotenv.2020.138436.
Tushabe, F., 2020. Comparison of COVID-19 severity between tropical and non-tropical countries. Int. J. Infect. 7 https://doi.org/10.5812/iji.104142.
Vesanto, J., 1999. SOM-based data visualization methods. Intell. Data Anal. 3, 111–126.
Vollmer, M.A., Mishra, S., Unwin, H.J.T., Gandy, A., Mellan, T.A., Bradley, V., Zhu, H., Coupland, H., Hawryluk, I., Hutchinson, M., 2020. Report 20: Using Mobility to Estimate the Transmission Intensity of COVID-19 in Italy: a Subnational Analysis with Future Scenarios. medRxiv.
Wang, J., Tang, K., Feng, K., Lin, X., Lv, W., Chen, K., Wang, F., 2021. Impact of temperature and relative humidity on the transmission of COVID-19: a modelling study in China and the United States. BMJ open 11, e043863. https://doi.org/10.1136/bmjopen-2020-043863.
Wei, J.-T., Liu, Y.-X., Zhu, Y.-C., Qian, J., Ye, R.-Z., Li, C.-Y., Ji, X.-K., Li, H.-K., Qi, C., Wang, Y., 2020. Impacts of transportation and meteorological factors on the transmission of COVID-19. Int. J. Hyg Environ. Health 230, 113610.
Wheeler, S.M., 2015. Built landscapes of metropolitan regions: an international typology. J. Am. Plann. Assoc. 81, 167–190. https://doi.org/10.1080/01944363.2015.1081567.
WHO, 2020a. COVID 19 Public Health Emergency of International Concern (PHEIC). Global research and innovation forum: towards a research roadmap.
WHO, 2020b. WHO announces COVID-19 outbreak a pandemic [WWW Document]. URL https://www.euro.who.int/en/health-topics/health-emergencies/coronavirus-covid-19/news/news/2020/3/who-announces-covid-19-outbreak-a-pandemic (accessed 12.14.20).
Wu, Y., Jing, W., Liu, J., Ma, Q., Yuan, J., Wang, Y., Du, M., Liu, M., 2020. Effects of temperature and humidity on the daily new cases and new deaths of COVID-19 in 166 countries. Sci. Total Environ. 729, 139051. https://doi.org/10.1016/j.scitotenv.2020.139051.
Xie, J., Zhu, Y., 2020. Association between ambient temperature and COVID-19 infection in 122 cities from China. Sci. Total Environ. 724, 138201. https://doi.org/10.1016/j.scitotenv.2020.138201.
Yahya, B.M., Yahya, F.S., Thannoun, R.G., 2021. COVID-19 prediction analysis using artificial intelligence procedures and GIS spatial analyst: a case study for Iraq. Appl. Geomat. 13, 481–491. https://doi.org/10.1007/s12518-021-00365-4.
Yang, X.-D., Li, H.-L., Cao, Y.-E., 2021. Influence of meteorological factors on the COVID-19 transmission with season and geographic location. Int. J. Environ. Res. Publ. Health 18, 484.
Zhou, P., Yang, X.-L., Wang, X.-G., Hu, B., Zhang, L., Zhang, W., Si, H.-R., Zhu, Y., Li, B., Huang, C.-L., Chen, H.-D., Chen, J., Luo, Y., Guo, H., Jiang, R.-D., Liu, M.-Q., Chen, Y., Shen, X.-R., Wang, X., Zheng, X.-S., Zhao, K., Chen, Q.-J., Deng, F., Liu, L.-L., Yan, B., Zhan, F.-X., Wang, Y.-Y., Xiao, G.-F., Shi, Z.-L., 2020. A pneumonia outbreak associated with a new coronavirus of probable bat origin. Nature 579, 270–273. https://doi.org/10.1038/s41586-020-2012-7.
Zhou, Y., Xu, R., Hu, D., Yue, Y., Li, Q., Xia, J., 2020. Effects of human mobility restrictions on the spread of COVID-19 in Shenzhen, China: a modelling study using mobile phone data. Lancet Dig. Health 2, e417–e424.

International Journal of Hygiene and Environmental Health

doi: 10.1016/S1438-4639(21)00187-5

International Journal of Hygiene and Environmental Health 238 (2021) 113838

Contents lists available at ScienceDirect

International Journal of Hygiene and Environmental Health

journal homepage: www.elsevier.com/locate/ijheh

Estimating nickel exposure in respirable dust from nickel in inhalable dust

Cornelia Wippich *, Dorothea Koppisch, Katrin Pitzke, Dietmar Breuer

Institute for Occupational Safety and Health of the German Social Accident Insurance, Alte Heerstraße 111, 53757, Sankt Augustin, Germany

ARTICLE INFO

Keywords:
Nickel
Respirable dust
Inhalable dust
Aerosol
Exposure assessment
Regression analysis

ABSTRACT

The conversion of dust components is of high importance for retrospective evaluations of exposure levels, of occupational diseases or the time trend of occupational dust exposure. For this purpose, possibilities to convert nickel concentrations from inhalable to respirable dust are discussed in this study. Therefore, 551 parallel measurements of nickel concentrations in inhalable and respirable dust fractions were extracted from the exposure database MEGA (maintained at the Institute for Occupational Safety and Health of the German Social Accident Insurance) and investigated by linear regression analysis of ln-transformed concentrations. Inhalable dust is the most important predictor variable, showing an adjusted coefficient of determination (*adj.* R^2) of 0.767 (R^2 adjusted to sample size). Since multilinear regression analysis, cannot be applied, further description of data is gained by splitting the whole dataset into working activity groups (e. g. '*high temperature processing*', *adj.* R^2 = *0.628,*' *filling/transport/storage*' *adj.* R^2 = *0.741*, '*machining/abrasive techniques*', *adj.* R^2 = 0.777). From these groups, four task restrictive subgroups, so-called *'heuristic groups'*, can be derived by pooling similar working tasks with similar regression coefficients and enhanced quality measures (*adj.* R^2 between 0.724 and 0.924): '*welding (grinding time fraction [GTF] < 5%)*', '*welding (grinding time fraction [GTF] > 5%)*', '*high temperature cutting*' and '*grinding*'. For the working activity group '*high temperature processing*' and the heuristic group '*welding*' the determination of the grinding time fraction and its inclusion or exclusion from a dataset has a huge impact on the description of data and whether a transformation of nickel concentrations using the natural logarithm (ln) is necessary or not. In case of *GTF* < 5%, the conversions functions are linear, all other conversion functions are power functions with exponents between 0.713 and 0.986. It is possible to develop conversion functions for estimating the nickel concentration in the respirable dust fraction ($c_{R(Ni)}$) out of the nickel concentration in the inhalable dust fraction ($c_{I(Ni)}$). For the estimation of Nickel in respirable dust other studies, it is recommend to use the conversion functions of the heuristic trial and error groups. Limitations of the possibility to use the conversion functions are discussed.

1. Introduction

Nickel is one of the most commonly used elements in metal industry. Due to its physical and chemical properties, it has a wide field of application. The element is mainly used as an alloy to form chemical resistant materials, for nickel-cadmium batteries and as a catalyst in chemical and food industry (Genchi et al., 2020; Kasprzak et al., 2003). The exposure of workers through the inhalation of metal particles or fumes can be quite high. Nickel can cause allergic reactions, but it is also known to cause cancer in parts of the respiratory tract, like the lungs and the nose (Tsai et al., 1995; Andersen et al., 1996; Rahilly and Price, 2003).

In 1985, the International Committee on Nickel Carcinogenesis in man (ICNCM) was initiated, where the nickel forms causing cancer were determined and a dose-response relation was derived (Doll, 1990). This was the start of the nickel exposure evaluation, firstly based on the measurement of nickel and its compounds (Tsai et al., 1995; Andersen et al., 1996) in total dust. During the following years the carcinogenicity and toxicity of nickel was tested in various experiments and studies (Andersen et al., 1996; Grimsrud et al., 2002). Nickel and its compounds have been categorized as 'carcinogenic for humans' group 1 (IARC) (IARC, 2012) or group 1A (CLP) (ECHA, 2021), whereas metallic nickel and nickel alloys are categorized as 'possibly carcinogenic for humans' group 2B (IARC) (IARC, 1990) or Carc 2 (CLP) (ECHA, 2021) (Hughson et al., 2010; IARC, 2012).

Nickel was mainly measured in the inhalable dust fraction, based on

* Corresponding author.
E-mail addresses: cornelia.wippich@dguv.de (C. Wippich), dorothea.koppisch@dguv.de (D. Koppisch), katrin.pitzke@dguv.de (K. Pitzke), dietmar.breuer@dguv.de (D. Breuer).

https://doi.org/10.1016/j.ijheh.2021.113838
Received 8 March 2021; Received in revised form 1 September 2021; Accepted 1 September 2021
Available online 6 September 2021

a technical guide concentration [TRK], which was firstly established 1977 in Germany (BMAS, 1977). These legal values were adopted to the technical state of the art over the years. In 2004, a TRK of 0.05 mg m^{-3} (in inhalable dust) in droplets and for nickel and its compounds 0.5 mg m^{-3} (in inhalable dust) was valid. In 2005, all TRKs for carcinogenics were suspended. After several years, new limit values for nickel compounds due to its carcinogenic effects in respirable dust were established at 0.006 mg m^{-3} as exposure-risk-relationship (ERB) (AGS, 2021). Furthermore, nickel and nickel compounds are toxic and highly sensitizing; regarding these non-carcinogenic effects an occupational exposure limit value of 0.03 mg m^{-3} in inhalable dust was established. For nickel metal, additional an occupational exposure limit value of 0.006 mg m^{-3} in respirable dust has been valid since 2017 (AGS, 2020). Subsequently the number of parallel measurements of nickel in respirable and inhalable dust increased in the recent years. Apart from air monitoring, measurements of individual nickel concentrations in workers is also a common tool for assessing occupational health risks of workers. For biomonitoring of nickel in Germany, no threshold values in biological material was established so far, besides a reference value [BAR] of 3 µg Nickel/L urine (DFG, 2012). Since this study focusses on air monitoring, with respect to the legal limit values, biomonitoring will not be discussed in further detail.

The increase of measurements targeting respirable dust and its components was not unique in Germany but it was also an international trend to focus on the dust fraction with an associated limit value. When it comes to retrospective assessment, monitoring the development of nickel exposure and investigation of occupational diseases, it remains problematic if only data from inhalable dust is available. In order to be able to use the historical data, e.g. in epidemiological evaluations, a mathematically conversion of nickel concentrations in inhalable dust to nickel concentrations in respirable dust is desirable.

Other studies mainly focused on the ratio of “inhalable” to “total” dust (Tsai et al., 1995; Tsai and Vincent, 2001). Only a few studies target nickel in respirable dust (Tanaka et al., 1985; Roels et al., 1993).

In our recently published study, we offered a mathematical solution for converting inhalable dust into respirable dust and vice versa (Wippich et al., 2020) by using the exposure data from the nonpublic database MEGA. Using further data from the same database, we developed a method to determine a possible relation between nickel in inhalable dust and nickel in respirable dust depending on working environments, using similar methods and assumptions as in our past study.

2. Materials and methods

2.1. Exposure database MEGA

The data were obtained by the surveillance activity of the German Social Accident Insurance (Gabriel et al., 2010). The database MEGA holds over 3 million dataset with exposure data from over 870 hazardous substances, including additional information about the measurement procedure, the used equipment and the analytical method. It was established in 1972 and it is designed for the evaluation of occupational diseases, hazard and exposure analysis in specific types of industry, as well as time-dependent analysis of exposure to hazardous substances at work places.

2.2. Sampling systems

The most measurements in this study were performed using the samplers GSP and FSP. The FSP sampler is used to collect respirable dust, where a cyclone is used as a pre-separator for coarse particles. Smaller particles (with an aerodynamic diameter less than 10 µm) are separated on a cellulose nitrate filter (0.8 µm pore size) (Siekmann, 1998). In case of the GSP, inhalable dust is collected through a cone on a filter, directly without pre-separation (Riediger, 2001). Both, FSP and GSP can be used for personal and stationary sampling (Mattenklott and Möhlmann, 2011). Besides FSP and GSP, also the systems Gravikon PM4 and Gravikon VC-25 are used for the stationary measurement of inhalable and respirable dust. The system PM4 for respirable dust also uses a cyclone as a pre-separator for coarse particles. For the collection of inhalable dust, the sampling volume is drawn into a filter cassette with an annular gap nozzle onto a filter (Siekmann, 1998; Riediger, 2001). The Gravikon VC-25 system also uses two different sampling heads to collect both dust fractions. For respirable dust, an additional impactor is used. Similar to the PM4, the inhalable fraction is measured with the VC-25 by drawing the sampling volume through an annular gap onto a filter (Coenen, 1981) (Siekmann, 1998) (Riediger, 2001). The most common combination of sampling systems in this study is GSP (inhalable dust, sampling rate: 3.5 L/min) and FSP-10 (respirable dust, sampling rate: 10 L/min), providing 274 pairs of parallel personal measurements. The second highest abundance can be seen for the combination GSP-10 (inhalable dust, sampling rate: 10 L/min) and FSP-10 with 197 personal parallel measurements. For the complete list of used sampling systems, the sampling rate and the type of sampling, see Table 1.

All samplers used in this study are validated according to the international standards EN 13205, EN 1540 and comply with ISO 7708.

2.3. Analytical methods

The sampling systems were equipped with cellulose nitrate filters (0.8 µm pore size). These filters were shipped to the Institute for Occupational Safety and Health of the German Social Accident Insurance for gravimetric and quantitative metal analysis. The filters were conditioned for at least one day in the laboratory atmosphere at a fixed temperature and humidity.

Nickel was determined by inductively coupled plasma mass spectrometry (ICP-MS) after digestion with a mixture of nitric and hydrochloric acid. A detailed method description was recently published (Pitzke et al., 2020).

2.4. Data selection

The method of pair formation of inhalable and respirable dust follows mainly the same scheme, as in our previous study (Wippich et al. (2020)). However, in this work the pairs are formed from nickel in respirable and inhalable dust, which was measured in parallel.

Firstly, the datasets are extracted from the database MEGA. Between the years 1989 and September 2020, a total of 234 202 respirable fraction measurements, 123 118 inhalable fraction measurements and 32 882 nickel measurements were collected in total.

For the formation of parallel measured pairs of nickel in inhalable and nickel in respirable dust, first, measurements are excluded, if the concentration is below the limit of quantification. With this restriction 169 458 measurements of the respirable fraction, 95 328 measurements of the inhalable fraction and 22 941 total nickel measurements remain

Table 1
Measurement systems and sampling rates used for both dust fractions in parallel measurements.

sampler inhalable dust (sampling rate)	sampler respirable dust (sampling rate)	*n*	type of sampling
GSP (3.5 L/min)	FSP-10 (10 L/min)	274	Personal
GSP-10 (10 L/min)	FSP-10 (10 L/min)	197	Personal
GSP-10 (10 L/min)	FSP-10 (10 L/min)	31	Stationary
GSP (3.5 L/min)	FSP-10 (10 L/min)	28	Stationary
PM4-G (66.7 L/min)	PM4-F (66.7 L/min)	6	Stationary
VC-25 G (375 L/min)	VC-25 F (375 L/min)	5	Stationary
VC-25 G (375 L/min)	PM4-F (66.7 L/min)	4	Stationary
GSP (3.5 L/min)	PM4-F (66.7 L/min)	3	Stationary
GSP (3.5 L/min)	FSP-2 (2 L/min)	2	Personal
GSP-10 (10 L/min)	PM4-F (66.7 L/min)	1	Stationary

for the formation of pairs.

Parallel pairs are formed if:

- the nickel concentration ($c_{I(Ni)}$) and the concentration of inhalable dust (c_I), and the nickel concentration ($c_{R(Ni)}$)and the concentration of respirable dust (c_R) respectively, were analyzed from the same sample carrier (filter) and
- the measurements have the same report number, industrial sector, working activity, type of sampling and were executed at the same day (remaining pairs: $n = 1117$),
- the measurements were executed at the same time (starting and ending times of both measurements do not differ by more than 5 min) and the sampling duration was $\geq$ 2 h ($n = 1011$),
- the measurement procedure and the analytical process are standardized methods in the Measurement system for exposure assessment of the German Social Accident Insurance Institutions (MGU) ($n = 598$).

The industrial sector describes the type of industry where the measurement was executed, as *metalworking* or *electronic waste recycling* for example. With the parameter *working activity,* the task and the process were combined. The *type of sampling* consists of the two subgroups: *personal* and *stationary sampling.* It was considered necessary, that all these variables were concordant within a pair.

In Germany according to the Technical Guidance 402, the minimum number of samples which have to be taken during a work shift with constant exposure is dependent on the sampling duration. When the sampling duration is higher or equal 2 h, one measurement is sufficient (AGS, 2017). Therefore, only measurements with a sampling duration of higher or equal 2 h have been included.

One further restriction is placed on the dataset: Samples have been excluded if c_R was higher than c_I or c_{Ni} in the respirable fraction was higher than c_{Ni} in the inhalable fraction. Physically it is not possible, that $c_{R(Ni)}$ or c_R exceed $c_{I(Ni)}$ or c_I, respectively, because respirable dust is a subset of inhalable dust, but at work places, these cases can be observed occasionally. Measurements like that can result from incorrect sampling, particle movement, thermal effects or inhomogeneous materials. This criterion affects only 45 pairs of measurement. Further discussion on these values will be done later in this study.

After merging the datasets of nickel/inhalable fraction and nickel/respirable fraction and considering all previous described restrictions, a dataset of 553 pairs, gathered between the years 2011 and 2020 can be formed. The data has been collected in 105 different working activities and the majority of dust concentrations was recorded during 2 h-measurements. As described in section 'Statistical and mathematical methods', two leverage points have been eliminated, so the whole dataset (group 0, see Table 3) consist of 551 pairs of parallel measured nickel concentrations.

According to the approach in our prior study, the whole dataset is divided into activity groups (Wippich et al., 2020). For nickel, we found measurement pairs for the groups *'high temperature processing', 'filling/-transport/storage'* and *'machining/abrasive techniques'*. From these groups more restrictive subgroups, 'heuristic groups' are formed as well. The formation of these groups is described in section 'Statistical and mathematical methods'.

At the work place, there is often no spatial separation of welding and grinding. In many cases a mixture of dusts, produced through the same worker, who is grinding for a certain time-share of the shift, e.g. when smoothing the welding seam cannot be excluded. In such cases, as additional information '< 5 % grinding time fraction (GTF)' or '> 5 % grinding time fraction (GTF)' can be added to each measured dataset at welding workplaces. This also has been considered in the group formation.

2.5. Statistical and mathematical methods

All statistical analyses were performed using the statistical software IBM SPSS statistics, version 26 (IBM Corp.). For all tests, the significance level is fixed at $\alpha = 0.05$, equaling a confidence interval of 95 %.

The assumption of a normal or lognormal distribution had to be rejected at the significance level of 0.05, using the Lilliefors-corrected Kolmogorov-Smirnov test (Sachs, 2004) for nickel in both dust fractions. This is mainly caused by the heterogeneous working activities, which are included in the total dataset. To identify the effects of the *type*

Table 2
Descriptive statistics of respirable and inhalable nickel samples used in the study, with the amount of paired nickel concentrations (n) arithmetic mean (AM), standard deviation (SD), median, minimum measured concentration (Min), maximum measured concentration (Max).

ID	Group	Dust fraction	n	AM [mg m^{-3}]	SD [mg m^{-3}]	Median [mg m^{-3}]	Min [mg m^{-3}]	Max [mg m^{-3}]
0	*Entire dataset*	$c_{I(Ni)}$	551	0.079	0.303	0.005	$1.6*10^{-5}$	4.700
		$c_{R(Ni)}$	551	0.008	0.019	0.001	$5.8*10^{-7}$	0.190
1	*High temperature processing*	$c_{I(Ni)}$	250	0.021	0.050	0.003	$2.3*10^{-4}$	0.350
		$c_{R(Ni)}$	250	0.008	0.022	0.001	$5.8*10^{-7}$	0.190
1a	*High temperature processing (incl. welding GTF < 5%)*	$c_{I(Ni)}$	159	0.022	0.054	0.003	$2.3*10^{-4}$	0.350
		$c_{R(Ni)}$	159	0.010	0.026	0.001	$5.8*10^{-7}$	0.190
1b	*High temperature processing (incl. welding GTF > 5%)*	$c_{I(Ni)}$	159	0.022	0.054	0.003	$2.3*10^{-4}$	0.350
		$c_{R(Ni)}$	159	0.007	0.021	0.001	$1.2*10^{-4}$	0.190
2	*Filling/transport/storage*	$c_{I(Ni)}$	42	0.048	0.167	0.004	$3.0*10^{-4}$	1.000
		$c_{R(Ni)}$	42	0.004	0.008	0.001	$6.7*10^{-5}$	0.049
3	*Machining/abrasive techniques*	$c_{I(Ni)}$	198	0.133	0.326	0.012	$6.7*10^{-5}$	2.300
		$c_{R(Ni)}$	198	0.013	0.027	0.003	$5.4*10^{-5}$	0.190
α	*Welding*	$c_{I(Ni)}$	198	0.021	0.050	0.003	$2.3*10^{-4}$	0.350
		$c_{R(Ni)}$	198	0.007	0.021	0.001	$5.8*10^{-7}$	0.190
α1/ α2	*Welding (GTF < 5%)*	$c_{I(Ni)}$	91	0.018	0.041	0.003	$3.3*10^{-4}$	0.230
		$c_{R(Ni)}$	91	0.008	0.022	0.001	$5.8*10^{-7}$	0.170
α3/ α4	*Welding (GTF > 5%)*	$c_{I(Ni)}$	91	0.018	0.041	0.003	$2.3*10^{-4}$	0.250
		$c_{R(Ni)}$	91	0.004	0.007	0.001	$1.2*10^{-4}$	0.049
ß	*High temperature cutting*	$c_{I(Ni)}$	48	0.011	0.021	0.002	$4.7*10^{-4}$	0.100
		$c_{R(Ni)}$	48	0.005	0.012	0.001	$1.8*10^{-4}$	0.073
γ	*Grinding*	$c_{I(Ni)}$	156	0.196	0.641	0.015	$6.7*10^{-5}$	2.300
		$c_{R(Ni)}$	156	0.017	0.059	0.003	$5.4*10^{-5}$	0.190

Table 3
Regression coefficients k, C_0 with standard errors for Equation (2) or (4), range of standard errors for regression function $s_{Fit}(\ln(c_{R(Ni)}))$ within groups 1–3 for working activity and heuristic groups α - γ including group names as defined in Table 3; GTF = Grinding time fraction. To use the conversion functions concentrations have to be inserted in mg m^{-3}.

ID	Group	*n*	*R*	adj. R^2	C_0	k	$s_{Fit}(\ln(c_{R(Ni)}))$	conversion function
0	*Entire dataset*	551	0.876	0.767	−2.835 ± 0.090	0.726 ± 0.017	0.085–0.220	$c_{R(Ni)} = c_{I(Ni)}^{0.726} * e^{-2.835}$
	Working activities							
1	*High temperature processing*	250	0.793	0.628	−1.801 ± 0.239	0.870 ± 0.042	0.113–0.237	$c_{R(Ni)} = c_{I(Ni)}^{0.870} * e^{-1.801}$
1a	*High temperature processing (incl. welding GTF < 5%)*	159	0.759	0.573	−1.599 ± 0.348	0.906 ± 0.062	0.132–0.275	$c_{R(Ni)} = c_{I(Ni)}^{0.906} * e^{-1.599}$
1b	*High temperature processing (incl. welding GTF > 5%)*	159	0.922	0.851	−1.685 ± 0.165	0.881 ± 0.029	0.130–0,273	$c_{R(Ni)} = c_{I(Ni)}^{0.881} * e^{-1.685}$
2	*Filling/transport/storage*	42	0.864	0.741	−3.290 ± 0.368	0.746 ± 0.068	0.301–0.536	$c_{R(Ni)} = c_{I(Ni)}^{0.746} * e^{-3.290}$
3	*Machining/abrasive techniques*	198	0.822	0.777	−2.956 ± 0.124	0.713 ± 0.027	0.161–0.692	$c_{R(Ni)} = c_{I(Ni)}^{0.713} * e^{-2.956}$
	Heuristic groups							
α	*Heuristic groupsWelding*	198	0.758	0.573	−2.039 ± 0.286	0.834 ± 0.051	0.116–0.246	$c_{R(Ni)} = c_{I(Ni)}^{0.834} * e^{-2.039}$
α1	*Welding (GTF < 5%) ln-transformed*	91	0.620	0.377	−2.189 ± 0.628	0.820 ± 0.111	0.164–0.317	$c_{R(Ni)} = c_{I(Ni)}^{0.820} * e^{-2.189}$
α2	*Welding (GTF < 5%) not transformed*	91	0.852	0.724	0.001 ± 0.001	0.347 ± 0.023	0.004–0.021	$c_{R(Ni)} = c_{I(Ni)} * 0.347 + 0.001$
α3	*Welding (GTF > 5%) ln-transformed*	91	0.912	0.830	−2.094 ± 0.223	0.816 ± 0.039	0.159–0.345	$c_{R(Ni)} = c_{I(Ni)}^{0.816} * e^{-2.094}$
α4	*Welding (GTF > 5%) not transformed*	91	0.679	0.455	0.002 ± 0.001	0.143 ± 0.016	0.002–0.143	$c_{R(Ni)} = c_{I(Ni)} * 0.143 + 0.002$
ß	*High temperature cutting*	48	0.962	0.924	−0.829 ± 0.247	0.986 ± 0.042	0.210–0.350	$c_{R(Ni)} = c_{I(Ni)}^{0.986} * e^{-0.829}$
γ	*Grinding*	156	0.894	0.798	−2.997 ± 0.128	0.705 ± 0.028	0.182–0.493	$c_{R(Ni)} = c_{I(Ni)}^{0.705} * e^{-2.997}$

of sampling, of *working activity* and possible interactions between these two variables, a two-factor ANOVA was performed. Following our prior study (Wippich et al., 2020), for further evaluation of the variable *working activity*, the total dataset was split into working activity groups. The criterions to form these groups mainly base on the technical information, which also can be found in the database. For nickel, these groups are: *'high temperature processing'*, *'filling/transport/storage'* and *'machining/abrasive techniques'*. The ratio $c_{R(Ni)}/c_{I(Ni)}$ was calculated for

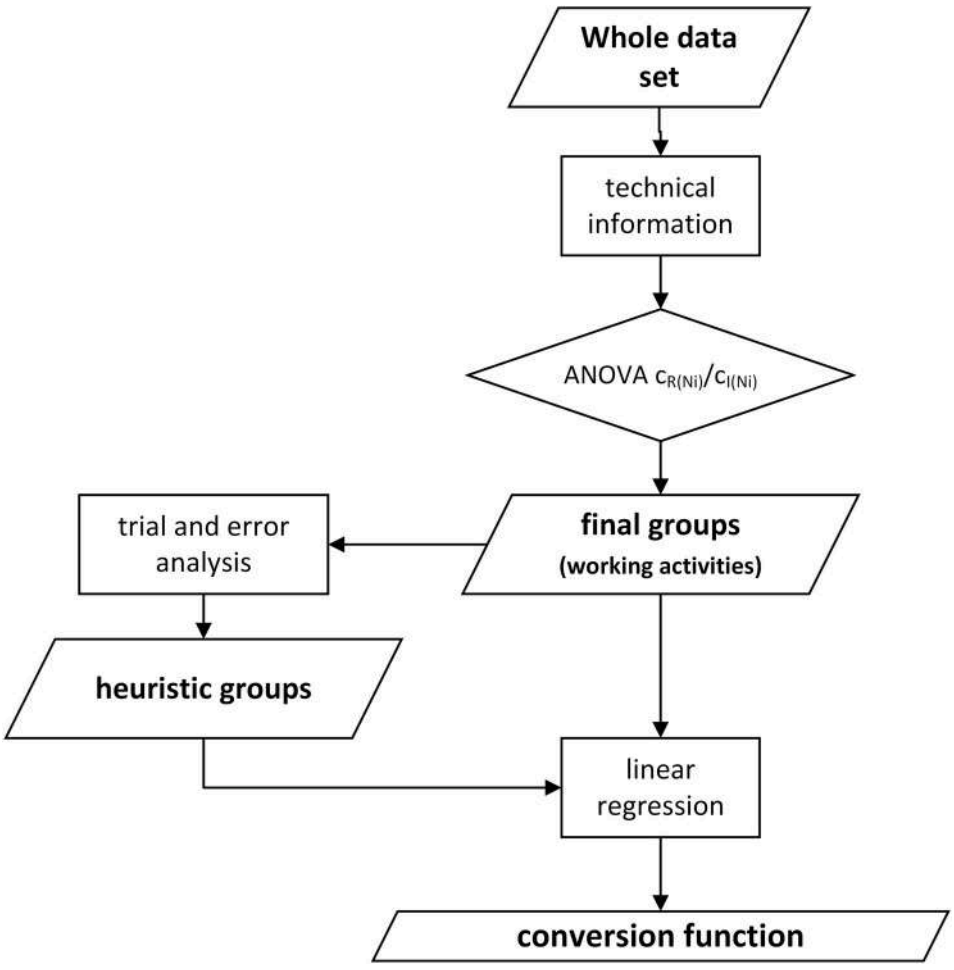

Fig. 1. Flowchart of the group formation steps and statistical tests (for each group distribution: Kolmogoroff-Smirnov, ANOVA: F-Test, Kruskal-Wallis test, variance homogeneity: Levene-test and graphical evaluation, post hoc tests: Games-Howell).

each group and homogeneity of variance was confirmed applying the Levene-Test ((Janssen and Laatz, 2017). To determine differences between the working activity groups, ANOVA, the non-parametric Kruskal-Wallis test and pair-by-pair comparisons using the Games-Howell post-hoc test (Sachs, 2004; Hilton and Armstrong, 2006) were conducted. The formation steps and statistical tests are shown in the flowchart (Fig. 1). This systematic approach leads to groups of parallel measured nickel concentrations in inhalable and respirable dust.

Similar, to evaluate the impact of the *type of sampling,* the total dataset was divided into the two subgroups *'stationary'* and *'personal'*. In the next step, the ratio of $c_{R(Ni)}$ and $c_{I(Ni)}$ was calculated for each pair in the two subgroups. Differences in both groups were compared by Median tests (with correction after Yates) and the non-parametric Mann-Whitney-U-Test for independent samples (Sachs, 2004; MacFarland and Yates, 2016; Haviland, 1990).

In each group the residuals of all analyses have been checked graphically (histograms) for normality and the absence of trends: There are no patterns discernible apart from the omission $c_{R(Ni)} > c_{I(Ni)}$ and all residuals are approximately normally distributed. Additionally each group has been checked for autocorrelation by performing a Durbin-Watson test (Sachs, 2004). These are prerequisites to perform a regression analysis. Before calculating the regression equations, possible leverage points are identified, and eliminated using the Cook's measure (Cook and Weisberg, 1982; Chatterjee and Hadi, 1989; Kleinbaum et al., 2014). In a next step, the groups are subjected to a linear regression analysis. The quality of regression parameters is evaluated using the correlation coefficient R and the adjusted coefficient of determination *adj.* R^2 (Janssen and Laatz, 2017):

$$adj.\ R^2 = R^2 - \frac{m}{n-m-1} * \left(1 - R^2\right) \tag{1}$$

This accounts for the number of variables m and the number of paired data n. Since in our case $n \gg m$, *adj.* $R^2 \approx R^2$.

This study describes in most cases a linear relationship between $ln(c_{R(Ni)})$ (natural logarithm of the nickel concentration in respirable dust) and $ln(c_{I(Ni)})$ (natural logarithm of the nickel concentration in inhalable dust):

$$ln\left(c_{R(Ni)}\right) = k \cdot ln\left(c_{I(Ni)}\right) + C_0 \tag{2}$$

where k is the slope and C_0 the intercept, which can be determined by regression analysis. C_0 and k are given with their standard errors (compare Table 3). We also calculated the range of the standard errors of the fitted regression function $s_{Fit}(ln(c_{R(Ni)}))$, for calculating the confidence intervals for the regression function at a given $ln(c_{I(Ni)})$ (Draper and Smith, 1998). Equation (2) can be transformed back into a function with the original concentrations:

$$c_{R(Ni)} = {c_{I(Ni)}}^{k} \cdot e^{C_0}. \tag{3}$$

From equation (3) two things can be derived: First, when $c_{I(Ni)}$ tends to zero, $c_{R(Ni)}$ also tends to zero. This is a necessary condition, since $c_{R(Ni)} \leq c_{I(Ni)}$. Second, the linear relation of $c_{R(Ni)}$ and $c_{I(Ni)}$ is included in equations (2) and (3) if the value 1 is included in the 95 % confidence interval of k. The worst-case assumption $c_{R(Ni)} = c_{I(Ni)}$ is included, if $C_0 = 0$ and $k = 1$.

In some cases, the correlation coefficient was better for untransformed data. In this cases a correlation between $c_{R(Ni)}$ and $c_{I(Ni)}$ was calculated:

$$c_{R(Ni)} = c_{I(Ni)} \cdot k + C_0 \tag{4}$$

In general it is possible to expand equation (2) or (4) with further covariates, such as *working activity* or *measurement system*, and perform a multilinear regression analysis. One prerequisite of a multilinear regression analysis is that all covariates have to be independent. In case of this study, $c_{I(Ni)}$ is influenced by all other possible covariates. Therefore, the prerequisite would be violated and this method cannot be applied.

From the working activity groups, more restrictive subgroups, so-called 'heuristic groups' (*'welding', 'high temperature cutting'* and *'grinding'*) were derived. These groups cannot be formed systematically. The working activity groups contain many subgroups which describe similar working tasks, such as *'wet grinding'* and *'dry grinding'* (from working activity group *'machining/abrasive techniques'*) or *'tungsten inert gas welding', 'metal active gas welding'* and *'arc welding'* (in working group *'high temperature processing'*) for example. These subgroups were pooled, when they showed similar regression coefficients and enhanced quality measures (higher R and *adj.* R^2) compared to their associating working activity group in order to form the so-called 'heuristic groups'.

3. Results

3.1. Nickel in inhalable and respirable dust: Description of the whole dataset

After two leverage points have been eliminated, simple linear regression analysis is performed on the whole dataset of 551 pairs of parallel nickel measurements. When only $c_{I(Ni)}$ is considered as predictor variable, one obtains $k = 0.726$ and $C_0 = -2.835$ in equation (2). The adjusted coefficient of determination *adj.* R^2 and correlation coefficient R are 0.767 and 0.876, respectively.

Fig. 2 shows a scatterplot of the log-transformed, parallel measured nickel concentrations in inhalable versus respirable dust and the 95% confidence interval. The cutoff values, resulting from the data selection for $c_{R(Ni)} > c_{I(Ni)}$ are clearly visible.

The arithmetic mean (*AM*) for nickel in inhalable dust is 0.07933 mg m^{-3}, for nickel in respirable dust 0.0077 mg m^{-3} respectively (Table 2). The lowest observed concentration of nickel in inhalable dust was $1.6*10^{-5}$ mg m^{-3} and for nickel in respirable dust $5.8*10^{-7}$ mg m^{-3}. The highest observed concentrations were 4.7 mg m^{-3} (Ni in inhalable dust) and 0.19 mg m^{-3} (Ni in respirable dust).

3.2. Exclusion of 'unphysical' nickel concentrations

With the restriction ($c_{R(Ni)}$ cannot be higher than $c_{I(Ni)}$), 45 parallel measurements were excluded. If one considers these measurements for linear regression, the quality measures for the whole dataset decrease slightly ($\Delta R = -0.038$; $\Delta adj.\ R^2 = -0.065$) in comparison to group 0. The regression coefficients vary by -0.069 (Δk) and -0.224 (ΔC_0), resulting in lower nickel concentrations in respirable dust with increasing amount of nickel in the inhalable dust fraction.

3.3. Type of sampling

For this study, 473 personal and 78 stationary measurements are considered. The high amount of personal measurements results from the requirements of the Technical Guidance 402, where exposure measurements should mainly be performed personally and stationary measurements only in exceptional cases, when a personal measurement is not possible (AGS, 2017). In the whole dataset, the median in both groups '*stationary*' (median = 0.322) and '*personal*' (median = 0.245), as well as the distribution of the ratio $c_{R(Ni)}/c_{I(Ni)}$ are not identical. The tests show significant differences (median test: $p = 0.036$; Mann-Whitney-U test: $p = 0.007$). In order to prove, if the differences actually result from the type of sampling, a two-factor ANOVA was done on the whole dataset. This ANOVA showed that the differences in the ratio $c_{R(Ni)}/c_{I(Ni)}$ result from the different working activities included in the whole dataset ($p = 0.007$), and do not result from the type of sampling ($p = 0.273$). The ANOVA also showed no interactions between *working activity* and *type of sampling* ($p = 0.308$).

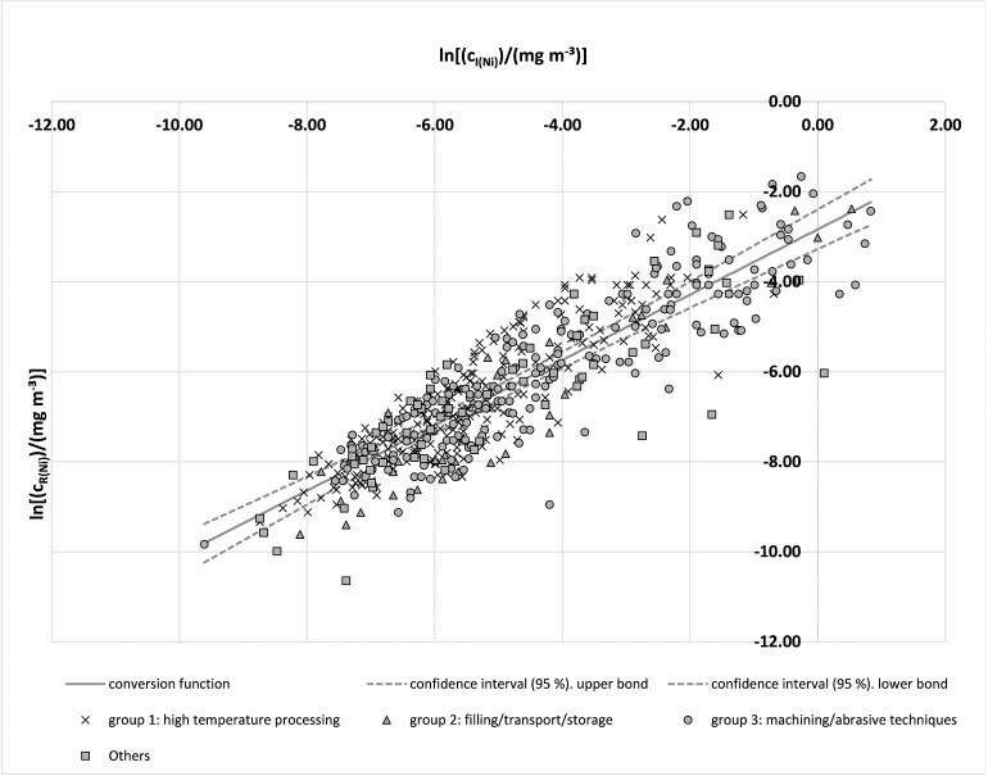

Fig. 2. Scatterplot $y = ln(c_{R(Ni)})$ versus $x = ln(c_{I(Ni)})$ for parallel measurements with their relating working activity group, the linear regression line and 95thconficence interval (equation (2)).

3.4. Working activity

In this study, three working activity groups are formed (Tables 2 and 3):

- *Group 1: high temperature processing* (such as welding, foundry, soldering)
- Group 2: *filling/transport/storage*
- Group 3: *machining/abrasive techniques* (such as grinding, milling, polishing)

As group 1 also contains all welding processes, as an additional information the Grinding time fraction (GTF) is given in most of the datasets concerning welding. Group 1 was divided into group 1a (high temperature processing *(incl. welding GTF < 5%)*) and group 1b (*high temperature processing (incl. welding GTF > 5%)*). These groups both contain 16 measurement pairs with no GTF information, and 52 datasets of further high temperature processes excluding welding, which is the reason for their similar AM, SD and median (Table 2). The purpose of group 1a and 1b is to highlight the impact of abrasive techniques during welding measurements. Comparing the minimum concentrations of group 1a and group 1b, lower concentrations of nickel in respirable dust were measured in group 1a ($5.8*10^{-7}$ mg m^{-3} for nickel in respirable and $1.2*10^{-4}$ mg m^{-3} for nickel in inhalable dust).

The highest concentrations of nickel in inhalable and respirable dust can be determined in group 3 *'machining/abrasive techniques'* ($c_{I(Ni)}$ = 2.300 mg m^{-3} and $c_{R(Ni)}$ = 0.1900 mg m^{-3}). The lowest concentrations of nickel in respirable dust can be found in group 1 *'high temperature processes'* ($c_{R(Ni)}$ = $5.8*10^{-7}$ mg m^{-3}) and of nickel in inhalable dust in group 3 *'machining/abrasive techniques'* ($c_{I(Ni)} = 6.7*10^{-5}$ mg m^{-3}). No significant difference of the ratio $c_{R(Ni)}/c_{I(Ni)}$ between group 2 (*'filling/transport/storage'*) and 3 (*'machining/abrasive techniques'*) can be determined ($p = 0.385$), whereas the ANOVA shows, that group 1 (*'high temperature processing'*) differs highly from the other two groups (in both cases: $p < 0.001$). In the next step, the groups 1–3 (Tables 2 and 3) are subjected to a linear regression analysis. The biggest dataset is group 1 *'high temperature processing'*. The regression coefficients, $k = 0.870$ and $C_0 = -1.801$, differ strongly from the other two groups and the differences are larger than the respective standard errors (Table 3).

Comparing *'high temperature processing'* to the whole dataset (group 0), the quality measures are lower in group 1 ($\Delta R = 0.083$; $\Delta adj.\ R^2 = 0.139$). This is caused by the GTF, as it can be seen in group 1a and 1b. Our model, using the ln-transformation and the linear regression analysis, results in high quality measures ($R = 0.922$; $adj.\ R^2 = 0.850$), for group 1b *'high temperature processing (incl. welding GTF > 5%)'*, exceeding the measures of group 0 (compare Table 3). Whereas high temperature processing datasets describing a GTF <5% show weaker quality measures than the entire dataset (group 0) ($R = 0.759$, $adj.\ R^2 = 0.573$, group 1a, Table 3).

The other working activity groups (*'filling/transport/storage'* and *'machining/abrasive techniques'*) show similar quality measures compared to the entire dataset (group 0, compare Table 3).

3.5. Heuristic groups

Apart from the systematic approach, three so-called heuristic groups were formed. These groups were formed from similar working task subgroups (see Table 4) to bigger groups, describing the same activity. The groups α *'welding'* and β *'high temperature cutting'* are subgroups of group 1 and γ *'grinding'* is a subgroup of group 3. Because of the small number of data pairs, it was not possible to form more heuristic groups.

Similar to working activity group 1 *'high temperature processing'*, the heuristic group α *'welding'* was divided according to the GTF. The groups α1 and α2 contain parallel nickel measurements during welding processes with a GTF < 5% (n = 91). For this dataset, a transformation with the natural logarithm results in a poor correlation of $c_{R(Ni)}$ and $c_{I(Ni)}$ ($R = 0.620$, $adj.\ R^2 = 0.377$, group α1 *'welding (GTF < 5%) ln-transformed'*). If one applies a linear regression to the non-transformed dataset (group α2

Table 4
Heuristic groups with listed special activities, materials and number of data pairs (*n*).

ID	Group name	Originating group no.	Working activities	n
α	Welding	1	gas-melt welding, laser welding/ manual arc welding with coated rod electrode/ arc welding, mixed arc process/ metal inert gas welding/ metal active gas welding/ metal welding, mixed welding processes/ plasma welding/ submerged arc welding/ mesh welding machines tungsten inert gas welding	198
β	High temperature cutting	1	flame cutting/ plasma cutting/ laser cutting	48
γ	Grinding	3	wet grinding dry grinding abrasive grinding sanding block grinding	156

'welding (GTF < 5%) not transformed'), a better description of the data can be achieved with $R = 0.852$ and *adj.* $R^2 = 0.724$. The groups α3 and α4 contain parallel nickel measurements during welding processes with a GTF > 5% (n = 91). Linear regression results in higher quality measures for the ln-transformed data (*adj* $R^2 = 0.830$ and $R = 0.912$ (group α3 '*welding (GTF > 5%) ln-transformed*'), in comparison to the untransformed data (*adj* $R^2 = 0.455$, $R = 0.679$; group α4 '*welding (GTF > 5%) not transformed*'). Group α 'welding' itself should be used in cases, where no information about the GTF during welding processes is known, since this group also contains 16 parallel measured pairs of nickel without information about the GTF.

The regression models of the heuristic groups α3 '*welding (GTF > 5%) ln-transformed*', β '*high temperature cutting*' and γ '*grinding*', show a better description of the data than those with the systematic approach (Table 3). The *adj.* R^2 are 0.830, 0.924 and 0.798 respectively. The standard errors of s_{Fit} increase with decreasing group size.

Although transformed data were used, a plot of the regression curve for the group β '*high temperature cutting*' shows a nearly linear relationship (Fig. 3). This corresponds to the fact that the value 1 lays within $k \pm$ standard error from this group. Applying linear regression on the untransformed concentrations in this group leads to a smaller correlation coefficient ($R = 0.565$). In addition to that, the relating working activity group 1 '*high temperature processing*' shows no linear relationship or more specifically, the value 1 does not lay within $k \pm$ standard error from this group. Therefore, no linear conversion function for group β is presumed and in Table 3 only equation (2) is described for this group.

Comparing just the heuristic groups with transformed nickel concentrations (groups α1, α3, β and γ, Table 3), the regression coefficients show a variety for both k ($0.705 \leq k \leq 0.986$) and C_0 ($-2.997 \leq C_0 \leq -0.829$). Figs. 3 and 4 show the regression functions with their relating 95 % confidence intervals in their valid working range. It can be seen from these figures, that each heuristic group shows a different conversion function. If one measures for example $c_{I(Ni)} = 0.03$ mg m^{-3}, the result for $c_{R(Ni)}$ is different in each group, such as $c_{R(Ni)} \approx 0.014$ mg m^{-3} for '*high temperature cutting*' or $c_{R(Ni} \approx 0.004$ mg m^{-3} for '*grinding*'.

4. Discussion

4.1. Identification of groups

Describing the whole dataset by means of equation (2) or (3), reveals that the most important variable is inhalable dust, already explaining 76 % of the variation in the dataset (Table 3, group 0) and, resulting in $k = 0.726$ and $C_0 = -2.835$. Considering working activity as an additional variable, it leads especially to the group '*high temperature processing*', which is described by $k = 0.870$ and $C_0 = -1.801$. All other working activity groups in this systematic approach combine many different dust-generating processes and lead to coefficients similar to those of the

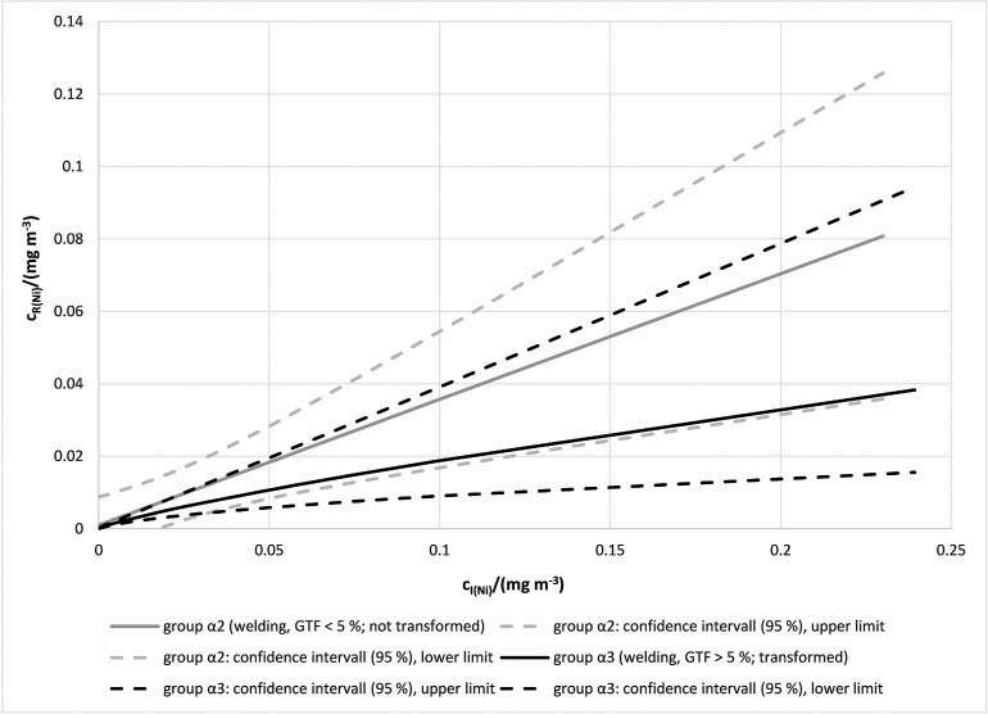

Fig. 3. Comparison of the determined conversion functions for the heuristic groups α2 *'welding, GTF < 5 %; not transformed'* and α3 *'welding, GTF > 5%; transformed'* with their 95 % confidence intervals.

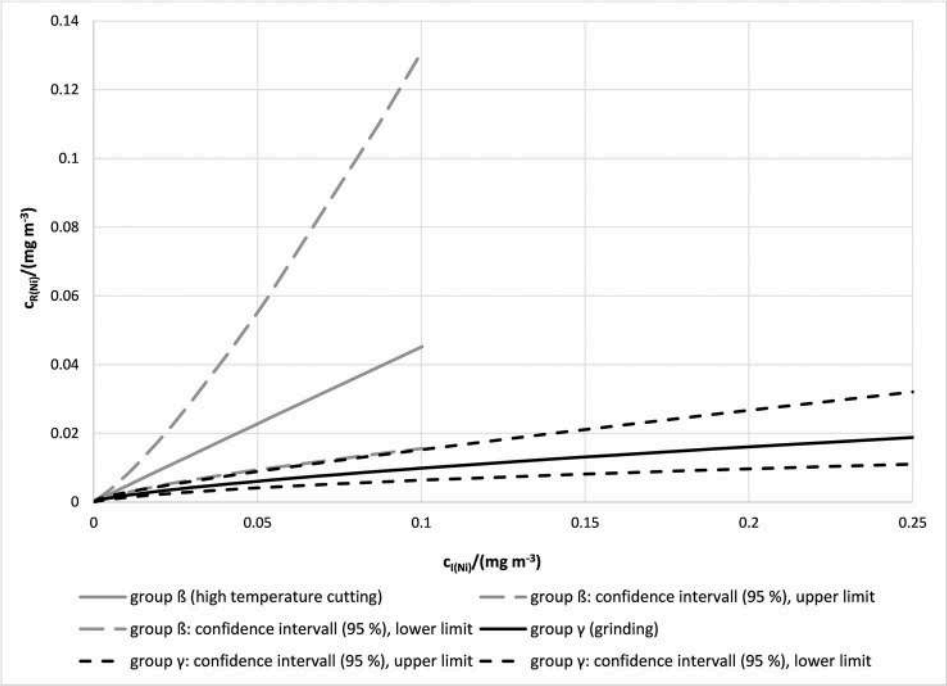

Fig. 4. Comparison of the determined conversion functions for the heuristic groups *ß 'high temperature cutting'* and *γ 'grinding'* with their 95% confidence intervals.

total dataset (Table 3).

The working activity groups *'high temperature processing'* and *'machining/abrasive techniques'* are mainly characterized by some large, specific subgroups. Group 1 is characterized by the subgroup *'welding'*, which represents 79 % of the data. 70 % of the presented data in group 3 contribute to the subgroup *'dry grinding'*. This shows that group 1 and 3 might not be representative for the whole working activity group which they are supposed to describe. In contrast to that, group 2 (*'filling/transport/storage'*) consists of heterogeneous data pairs with no dominant subgroup. However, this group consists of only 42 parallel measurements and we have limited information about the type of products that are transported or stored. Therefore, its validity is limited.

Since group 1 *'high temperature processing'* mainly consists of welding measurements, many datapoints contain additional information about the GTF. The groups 1a *'high temperature processing (incl. welding GTF < 5%)'* and 1b *'high temperature processing (incl. welding GTF < 5%)'* show similar descriptive statistics, at least for $c_{I(Ni)}$ (Table 2) because in both cases also data points without further information on GTF and other processes than welding are included. These two groups were created to highlight the impact of the GTF, when risk assessment is performed for workplaces with high temperature processes and other processes, such as abrasive techniques influence the measurements. The GTF is only given for welding processes, so the process specific groups α1 and α2 (*'welding GTF < 5%'*), as well as groups α3 and α4 (*'welding GTF > 5%'*) were formed.

4.2. Application of equations (2) and (3) or (4)

There are two limiting cases of equation (2):

- The worst-case assumption $c_{R(Ni)} = c_{I(Ni)}$, equivalent to $C_0 = 0$ and $k = 1$.
- The linear assumption for $c_{R(Ni)} > c_{I(Ni)}$, equivalent to $C_0 < 0$ and $k = 1$.

The worst-case assumption has not been observed in our dataset. Additionally all C_0 values for equation (2) throughout this study are negative ($-3.290 \leq C_0 \leq -0.829$).

All k values of this study are smaller than 1 ($0.347 \leq k \leq 0.986$), although the regression analysis does not prohibit $k > 1$. For equation (2), this indicates that $k < 1$ is a systematic effect. Which means, that the resulting function is not linear. The ratio $c_{R(Ni)}/c_{I(Ni)}$ is declining with increasing values of $c_{I(Ni)}$.

Table 3 shows that the concentrations of nickel in respirable dust are strongly dependent on the grinding time fraction. In the special case, that the GTF is lower than 5 %, the regression function shows a better description for untransformed data using equation (4). In contrast to that, if the GTF is higher than 5 %, a better description of the data can be achieved when the data is transformed. By this observation, we strongly recommend, to consider the GTF at the workplace when welding dust exposure is about to be evaluated.

A linear relation with $k = 1$ implies, that a single process is responsible for a constant ratio of emission for both dust fractions. One possible explanation for the finding of $k < 1$ in this study are agglomeration effects, which become more important with increasing concentrations (Rumpf et al., 1976; Koch et al., 1999). In addition, one can speculate that similar processes, which emit different concentrations of dust at different ratios, are coded as to the same working activity in the database.

4.3. Exclusion of 'unphysical' nickel concentrations

For this study pairs of nickel concentration are excluded when $c_{R(Ni)}$ is higher than $c_{I(Ni)}$. In fact, in some cases higher nickel concentrations are measured in respirable dust. This is possible as independent sampling systems for both dust fractions are used. Therefore, inhomogeneous materials, particle movement, thermal effects, incorrect sampling, wall deposits in FSP cyclones or the distance of the sampling systems to the source of emission can lead to higher nickel concentrations in respirable dust samples. In the result section, it was shown, that the exclusion of these data pairs does not have a large impact on the analysis at this stage, regarding the nickel concentration ranges of interest. However, to include these samples would introduce a bias the analysis toward a physically uncommon situation. Therefore, these values remain excluded.

4.4. Type of sampling

As ANOVA shows, the significant differences of $c_{R(Ni)}/c_{I(Ni)}$ found for the whole dataset (group 0) with the median and distribution tests, are caused by the different working activities which are included in the whole dataset and are not an effect of using different types of sampling.

However, one cannot exclude, that the type of sampling has an impact on the concentration, as it has been observed in various studies (Lillienberg and Brisman, 1994; Esmen and Hall, 2000; Lee et al., 2006; Klasson et al., 2016). Personal sampling systems collect occupational dusts in reduced distance to the source of exposure, while stationary systems can only be directed to the source. Personal sampling systems might collect larger, heavier particles directly after the source of emission, while the amount of those particles decreases with increasing distance and thus are collected to a lesser extend using stationary sampling systems. This cannot be proved using the technical information in the database MEGA, as it contains no information about the distance from the source of emission.

4.5. Application and limitations of results

Especially for the group welding, it cannot be excluded, that the nickel content of the welding material might influence the nickel concentration in inhalable and respirable dust, and therefore the conversion function resulting for welding (Kendzia et al., 2017). When different forms of welding are pooled it is possible, that the effect of different nickel contents is concealed.

The considered measurements in this study have to be representative for a whole 8-h shift with regard to the German limit values. This is a prerequisite for analyses and the data storage in the exposure database MEGA. According to the German Technical Guidance 402, one measurement during a 2-h measurement is sufficient, to report a representative exposure during the shift of a worker. It remains problematic, if the 2 h during which the measurements were executed, are not representative for the whole work shift, but monitors a part of a work shift (Kendzia et al., 2017). The restriction of 2 h-measurements is also a limitation, because at workplaces with high exposures, the sampler could be loaded with particles in a shorter time.

The given groups are heterogeneous considering the different working activities and subgroups. One has to be careful to use the model parameters in toxicological or epidemiological analyses without a careful check of applicability. The results in this study were derived for nickel dust-generating processes in the German industry between 2011 and 2020 and the working conditions described in the previous sections.

For the estimation of Nickel in respirable dust, we recommend to use the conversion functions of the heuristic groups if the concerning working activity matches to these groups. Special attention should be paid, if there is no spatial separation between welding and grinding at the evaluated work place. When welding processes with GTF < 5% are evaluated, we recommend to use the conversion function of group α2 (*'welding (GTF < 5%) not transformed'*). When the GTF is supposed to exceed 5 % at welding processes, we recommend to use the formula of group α3 (*'welding (GTF > 5 %) ln-transformed'*). When the GTF of a welding process is unknown, it is recommended to use function α (*'welding'*). In all cases, where other high temperature processes than welding (or high temperature cutting, group β) are to be evaluated, one should use the conversion function of group 1 *'high temperature processing'*. If the concerning working activity does not match the heuristic groups, the functions of the working activity groups could be used (group 1–3). If they are also not applicable, the use of group 0 is not recommended.

If one calculates $ln(c_{R(Ni)})$ using the regression coefficients in Table 3 for a given group and a given $ln(c_{I(Ni)})$, then the result has the confidence interval of $\pm 1.96 \cdot s_{Fit} ln(c_{R(Ni)})$. The smaller value of s_{Fit} (Table 3) is only valid around the mean value of $ln(c_{I(Ni)})$ (Table 3). This variance has to be added to the measurement uncertainty, which should be calculated for the dust sampling process, as well as the analytical process. The measurement uncertainty (u) for the overall process (sampling and analytics) of nickel is about 6.05 % (expanded measurement uncertainty (U): 12.1 %) for concentrations up to 0.003 mg m^{-3} and $u = 12.1$ % ($U =$ 24.2 %) for concentrations up to 0.012 mg m^{-3}. The calculations and estimation of measurement uncertainties comply with the demands and requirements in the international standards EN 482, ISO 21832 and ISO/IEC Guide 98–3:2008 (GUM).

The uncertainty of the measured concentrations is in this study limited to several percent of the measured value (European Committee for Standardization, 2010; Deutsches Institut für Normung, 2021). The concentrations themselves, on the other hand, cover up to an order of magnitude due to other influences such as the type of work and inter or intra worker effects. The difference of these two scales suggest that the estimates of the slope parameter are not severely biased (Draper and Smith, 1998). If such a bias existed, it would decrease the size of the slope parameter. However, a rigorous treatment of the effect of uncertainty in the concentrations is beyond the scope of this study, as it includes the transfer from the natural to a logarithmic scale in combination with non-constant uncertainties.

The conversion functions were calculated from measurements performed with the sampling systems listed in Table 1. Applying the functions on data associated with other sampling systems, other measurement uncertainties have to be taken into account and the overall uncertainty might differ. The applicability of the functions on such data can be assumed, when the sampling systems were validated by the same international standards.

4.6. Comparison with literature

In a study of Kendzia et al. (2017), the average occupational exposure to inhalable nickel was estimated, also using the exposure database MEGA. In this study a total of 8 052 personal measurements of Nickel, collected between the years 1990 and 2009 were evaluated and a median of $c_{I(Ni)} = 0.009$ mg m^{-3} was determined (Kendzia et al., 2017). In our study, for 551 measurements a median of $c_{I(Ni)} = 0.0047$ mg m^{-3} was calculated, although both studies used the same database. In our study, only nickel concentrations of inhalable dust were considered, when a relating nickel concentration of respirable dust was measured as well. Additional to that, in our study more requirements and restrictions were demanded for the dataset, such as the sampling time should be equal or higher than 2 h or the restriction of not using samples with measured concentrations below the limit of quantification and a restriction to the used sampling systems. Kendzia et al. (2017) evaluated different occupations, such as welders and metalworkers. The median for nine different welding processes ranged between 0.004 mg $m^{-3}$and 0.022 mg m^{-3} ($c_{I(Ni)}$). In our study, we pooled ten different welding processes, forming the heuristic group α *'welding'*, determining a median of 0.0034 mg m^{-3}. In the study of Kendiza et al. (2017) also the effect of different nickel content of the welding material is evaluated, in our study this was not possible due to insufficient data.

In a study of Weiss et al. (2013) the correlation of parallel measured nickel concentrations ($n = 228$) in respirable and inhalable dust during different welding processes were evaluated. In contrast to our study, values < LOQ have been included and were imputed with values randomly selected from a log-normal distribution using a bootstrap algorithm with 100 runs. A transformation of nickel concentrations with log_{10} was done instead of ln (natural logarithm). The study distinguishes between metals with a nickel content lower or higher 5 %, whereas the grinding time fraction in the measurements is neglected (Weiss et al., 2013). In our study the correlation coefficient is smaller for the heuristic group *welding* ($R = 0.758$ vs. $R = 0.850$). Considering the influence of the GTF on the correlation of $c_{I(Ni)}$ and $c_{R(Ni)}$, the correlation in group α2 ($R = 0.852$) is close to the one of Weiss et al. (2013) and in group α3 the correlation coefficient is even higher ($R = 0.912$). If one uses the conversion function of Weiss et al. (2013), considering $c_{I(Ni)} = 0.03$ mg m^{-3},

the resulting $c_{R(Ni)}$ is ≈ 0.016 mg m^{-3}. If one uses the functions from our study for group α or α3, $c_{R(Ni)}$ ≈ 0.007 mg m^{-3} is estimated and if one uses the function of group α2 0.011 mg m^{-3} respectively. The differences of the regression functions in the two studies and thus the estimated $c_{R(Ni)}$, increase with higher $c_{I(Ni)}$. Weiss et al. (2013) performed additionally multiple linear regression models to determine predictor variables for internal and external exposure. In our study, it was not possible to correlate such variables, as the exposure database MEGA does not contain biomonitoring measurements and these are not part of this study.

The study of Berlinger et al. (2019) describes workplace exposures during different hot work processes. In two different facilities inhalable and respirable dust measurements were performed, and among other elements also analyzed for the nickel content. Their study contains measurements for flame cutting and plasma cutting (Berlinger et al., 2019), which can be compared to our group β *'high temperature cutting'*, since this heuristic group contains both subgroups (see Table 4). A further group which can be compared is their group 'surface grinding' and our group γ *'grinding'*. The measurements of the two facilities in the study of Berliner et al. (2019) showed big differences in the measured concentrations, resulting in broad median ranges. The median range for nickel in inhalable dust in the groups 'flame cutting' and 'plasma cutting' is 0.038–0.180 mg m^{-3} and in respirable dust 0.025–0.140 mg m^{-3}. In our study the median is lower, for $c_{I(Ni)}$ it is 0.0021 mg m^{-3} and $c_{R(Ni)}$ 0.0012 mg m^{-3}, respectively. The maximum concentrations (Max) of $c_{I(Ni)}$ of the cutting groups vary between 0.051 and 0.480 mg m^{-3} ($c_{R(Ni)}$ = 0.030–0.550 mg m^{-3}), and the minimum concentrations (Min) of $c_{I(Ni)}$ between 0.023 and 0.100 mg m^{-3} ($c_{R(Ni)}$ = 0.015–0.060 mg m^{-3}). In our group β, $c_{I(Ni)}$ Max is 0.100 mg m^{-3} ($c_{R(Ni)}$ Max = 0.73 mg m^{-3}) and $c_{I(Ni)}$ Min is 0.00047 ($c_{R(Ni)}$ Min = 0.00018 mg m^{-3}). In our study, we cover a broader range of concentrations as it can be seen for our Min and Max concentrations. The different medians comparing both studies might result from the different number of measurements. Berlinger et al. (2019) calculated their parameters on the basis of 5–7 pairs of measurement (dependent on facility and cutting group), whereas we were able to use 48 parallel measured nickel concentrations. In case of grinding, the study of Berlinger et al. (2019) showed also big differences between the two facilities, medians of nickel in inhalable dust are 0.016 mg m^{-3} (facility 1) and 0.190 mg m^{-3} (facility 2). The median of facility 1 matches the median of our group γ *'grinding'* (0.015 mg m^{-3}). Berlinger et al. (2019) did not use linear regression to correlate nickel in respirable and inhalable dust, but calculated the ratio $c_{R(Ni)}/c_{I(Ni)}$ by 0.64 ± 0.14 (flame cutting), 0.75 ± 0.34(plasma cutting) and 1.22 ± 0.36 (surface grinding). As we cannot assume a linear correlation for these concentrations, we did not calculate any ratios. In addition, a ratio of 1.22 cannot result from our study, because of the restriction $c_{R(Ni)} > c_{I(Ni)}$.

5. Summary and conclusion

In summary, it is possible to develop conversion functions for estimating the nickel concentration in the respirable dust fraction out of the nickel concentration in the inhalable dust fraction. 551 data pairs were analyzed including different working activities. The given conversion functions can help occupational hygienists and risk assessors to estimate missing nickel concentrations for retrospective analyses which are often required for the assessment of occupational diseases or for epidemiological studies. The used data represents nickel exposure at work places in Germany and therefore, the conversion functions might be more applicable for German exposure data. The application of the conversion functions for data measured in other countries should be done with caution.

The study suggests that the data should generally be evaluated using linear regression of the log-transformed data shown in equation (2) or (3) with $k \leq 1$ and $C_0 < 0$, except for welding with a grinding time fraction (GTF) < 5 %, where a linear regression of the untransformed, original concentrations is feasible, using equation (4). With specific working conditions, it is possible to identify heuristic groups (α2, α3, β, γ) where 72 – 92 % of the variance in the data is accounted for by the regression functions. The bigger working activity groups 1 – 3 are less specific and the regression explains only 63 – 85 % of the variance.

For the estimation of Nickel in respirable dust, it is recommend to use the conversion functions of the heuristic groups if the concerning working activity matches these groups. When welding processes with GTF < 5 % are evaluated, we recommend to use the conversion function of group α2 (*'welding (GTF < 5 %) not transformed'*). When the GTF exceeds 5 %, we recommend to use the formula of group α3 (*'welding (GTF > 5%) ln-transformed'*). When the GTF of a welding process is unknown, function α (*'welding'*) should be used. In all cases, where other high temperature processes than welding (or high temperature cutting, group β) are to be evaluated, one should use the conversion function of group 1 *'high temperature processing'*. If the concerning working activity does not match the heuristic groups, the functions of the working activity groups could be used (group 1 – 3). In the next years, more measurements of nickel in respirable and inhalable dust will be performed and these new measurements will be used for further verification of the conversion functions found in this study. This study is the starting point for investigating further health related dust components, such as Cobalt and Manganese.

Declaration of competing interest

The authors declare no conflict of interest relating to the material presented in this article its contents, including any opinions and/or conclusions expressed, are solely those of the authors.

Acknowledgments

The authors thank the German Social Accident Insurance institutions for the provision of the data. All authors contributed substantially to the work and approved the final version of the manuscript. They also agree to take responsibility for the work.

References

AGS, 2020. Technische Regeln für Gefahrstoffe: arbeitsplatzgrenzwerte (TRGS 900). GMBl 1–69.
AGS, 2017. Technische Regeln für Gefahrstoffe: ermitteln und Beurteilen der Gefährdungen bei Tätigkeiten mit Gefahrstoffen: inhalative Exposition (TRGS 402). GMBl 43, 843–846.
AGS, 2021. Technische Regeln für Gefahrstoffe: risikobezogenes Maßnahmenkonzept für Tätigkeiten mit krebserzeugenden Gefahrstoffen (TRGS 910). GMBl 1–165.
Andersen, A., Berge, S.R., Engeland, A., Norseth, T., 1996. Exposure to nickel compounds and smoking in relation to incidence of lung and nasal cancer among nickel refinery workers. Occup. Environ. Med. 13, 708. https://doi.org/10.1136/oem.53.10.708.
Berlinger, B., Skogen, U., Meijer, C., Thomassen, Y., 2019. Workplace exposure to particulate matter bioaccessible and non-soluble metal compounds during hot work processes. J. Occup. Environ. Hyg. 16, 378. https://doi.org/10.1080/15459624, 2019.1594841, 86.
BMAS, 1977. Arbeitsschutz. BArbBl 128.
Chatterjee, S., Hadi, A.S., 1989. Influential observations, high leverage points, and outliers in linear regression. Stat. Sci. 379–416. https://doi.org/10.1214/ss/1177013622.
Coenen, W., 1981. Beschreibung der Erfassungs- und Durchgangsfunktion von Partikeln bei der Atmung - messtechnische Realisierung. Staub Reinhalt. Luft 41, 472–479.
Cook, R.D., Weisberg, S., 1982. Residuals and Influence in Regression. Chapman and Hall, New York, 0-412-24280-0.
Deutsches Institut für Normung, 2021. Exposition am Arbeitsplatz – Verfahren zur Bestimmung der Konzentration von chemischen Arbeitsstoffen – Grundlegende Anforderungen an die Leistungsfähigkeit. Deutsches Insitut für Normung, Berlin. https://doi.org/10.31030/3211072. DIN 482:2021-05.
DFG, 2012. Stoffliste. MAK- und BAT-Werte-Liste 2012.
Doll, R., 1990. Report of the international committee on nickel carcinogenesis in man. Report of the international committee on nickel carcinogenesis in man. Scandinavian J. Work. https://doi.org/10.5271/sjweh.1813. Environment & Health. Oxford.
Draper, N., Smith, H., 1998. Applied Regression Analysis. Wiley & Sons, New York, ISBN 978-0-471-17082-2.
ECHA, E.C.A., 2021. Nickel. 2021 Feb. Available from: URL: https://echa.europa.eu/de/substance-information/-/substanceinfo/100.028.283. (Accessed 11 February 2021). accessed.

Esmen, N.A., Hall, T.A., 2000. Theoretical investigation of the interrelationship between stationary and personal sampling in exposure estimation. Appl. Occup. Environ. Hyg 19, 114. https://doi.org/10.1080/104732200301935.

European Committee for Standardization, 2010. ISO 15767:2010-10. Workplace Atomospheres – Controlling and Characterizing Uncertainty in Weighing Collected Aerosols. European Commettee for Standardization, Brussels. https://doi.org/10.31030/1709485.

Gabriel, S., Koppisch, D., Range, D., 2010. The MGU - a monitoring system for the collection and documentation of valid workplace exposure data. Gefahrst. Reinhalt. Luft 43–49.

Genchi, G., Carocci, A., Lauria, G., Sinicropi, M.S., Catalano, A., 2020. Nickel: human health and environmental toxicology. Int. J. Environ. Res. Publ. Health 21, 1. https://doi.org/10.3390/2Fijerph17030679.

Grimsrud, T.K., Berge, S.R., Haldorsen, T., Andersen, A., 2002. Exposure to different forms of nickel and risk of lung cancer. Am. J. Epidemiol. 1123–1132. https://doi.org/10.1093/aje/kwf165.

Haviland, M.G., 1990. Yates's correction for continuity and the analysis of 2 x 2 contingency tables. Stat. Med. 9, 363–367. https://doi.org/10.1002/sim.4780090403.

Hilton, A., Armstrong, R., 2006. Post hoc ANOVA tests. Microbiologist 34–36, 09.

Hughson, G.W., Galea, K.S., Heim, K.E., 2010. Characterization and assessment of dermal and inhalable nickel exposures in nickel production and primary user industries. Ann. Occup. Hyg. 8–22. https://doi.org/10.1093/annhyg/mep068.

IARC, 1990. IARC monographs on the evaluation of carcinogenic risks to humans. Int. Agency Res. Canc. 49 (7). Chromium, Nickel and Welding, 978-92-832-1249-2.

IARC, 2012. Nickel and nickel compounds Chemical Agents and related occupations. In: IARC Monographs on the Evaluation of Carcinogenic Risks of Chemicals to Humans 100 C.

Janssen, J., Laatz, W., 2017. Statistsiche Datenanalyse mit SPSS: Eine anwendungsorientierte Einführung in das Basissystem und das Modul Exakte Tests. Springer Gabler Verlag, Berlin, ISBN 978-3-662-53477-9.

Kasprzak, K.S., Sunderman Jr., F.W., Salnikow, K., 2003. Nickel carcinogenesis. In: Mutation Research/Fundamental and Molecular Mechanisms of Mutagenesis, pp. 67–97. https://doi.org/10.1016/j.mrfmmm.2003.08.021.

Kendzia, B., Pesch, B., Koppisch, D., Van Gelder, R., Pitzke, K., Zschiesche, W., Behrens, T., Weiss, T., Siemiatycki, J., Lavoué, J., et al., 2017. Modelling of occupational exposure to inhalable nickel compounds. J. Expo. Sci. Environ. Epidemiol. 27, 427–433. https://doi.org/10.1038/jes.2016.80.

Klasson, M., Bryngelsson, I.-L., Pettersson, C., Husby, B., Arvidsson, H., Westberg, H., 2016. Occupational exposure to Cobalt and tungsten in the Swedish hard metal industry: air concentrations of particle mass, number, and surface area. The Annals of Occupational Hygiene 684–699. https://doi.org/10.1093/annhyg/mew023.

Kleinbaum, D.G., Kupper, L.L., Nizam, A., Rosenberg, E.S., 2014. Applied Regression Analysis - and Other Multivariable Methods. Cengage Learning, Boston, ISBN 978-128-505108-6.

Koch, W., Dunkhorst, W., Lodding, H., 1999. Design and performance of a new personal aerosol monitor. Aerosol. Sci. Technol. 231–246. https://doi.org/10.1080/027868299304282; 2-3.

Lee, S.-A., Adhikari, A., Grinshpun, S.A., KcKay, R., Shukla RR, T., 2006. Personal exposure to airborne dust and microogranisms in agricultural environments. J. Occup. Environ. Hyg. 30, 118. https://doi.org/10.1080/15459620500524607.

Lillienberg, L., Brisman, J., 1994. Flour dust in bakeries - a comparison between methods. Ann. Occup. Hyg. 75, 571. https://doi.org/10.1093/annhyg/38.inhaled_particles_VII.571.

Mattenklott, M., Möhlmann, C., 2011. Probenahme und analytische Bestimmung von granulären biobeständigen Stäuben (GBS). Gefahrst. Reinhalt. Luft 425–428.

MacFarland, T.W., Yates, J.M., 2016. Mann-Whintney U Test. Introduction to Nonparametric Statistics for the Biological Sciences Using R. Springer Interantional Publishing Switzerland, Basel, ISBN 978-3-319-30634-6.

Pitzke, K., Schwank, T., Wippich, C., 2020. Krebserzeugende Metalle (Arsen, Beryllium, Cadmium, Cobalt, Nickel) und ihre Verbindungen (ICP-Massenspektrometrie) (Loseblattsammlung Kennzahl: 7808). Deutsche Gesetzliche Unfallversicherung e. V. Berlin: Erich Schmidt. Available from: URL: https://www.ifa-arbeitsmappedigital.de/IFA-AM_7808. (Accessed 26 February 2021). accessed.

Rahilly, G., Price, N., 2003. Nickel allergy and orthodontics. J. Orthod. 74, 171. https://doi.org/10.1093/2Fortho.30.2.171.

Riediger, G., 2001. Geräte zur Probenahme der einatembaren Staubfraktion (E-Staub) (Loseblattsammlung Kennzahl 3010). Deutsche Gesetzliche Unfallversicherung e. V. Berlin: Erich Schmidt. Available from: URL: www.ifa-arbeitsmappedigital.de/3010. (Accessed 26 February 2021). accessed.

Roels, H., Van de Voorde, R., Vargas, V.M.M., Lauwerys, R., 1993. Relationship between atmospheric and urinary nickel in workers manufacturing electrical restistances using nickel oxide: role of the bioavailability of nickel. Occup. Med. 95–104. https://doi.org/10.1093/occmed/43.2.95.

Rumpf, H., Sommer, K., Steier, K., 1976. Mechanismen der Haftverstärkung bei der Partikelhaftung durch plastisches Verformen, Sintern und viskoelastisches Fließen. Chem. Ing. Tech. 4, 300. https://doi.org/10.1002/cite.330480408, 07.

Sachs, L., 2004. Angewandte Statistik. Springer Verlag, Berlin-Heidelberg-New York, ISBN 978-3-662-05744-5.

Siekmann, H., 1998. Geräte zur Probenahme der alveolengängigen Staubfraktion (A-Staub) (Loseblattsammlung Kennzahl 3020). Deutsche Gesetzliche Unfallversicherung e. V. Berlin: Erich Schmidt Verlag. Available from: URL: www.ifa-arbeitsmappedigital.de/3020. (Accessed 26 February 2021). accessed.

Tanaka, I., Ishimatsu, S., Matsuno, K., Kodama, Y., Tsuchiya, K., 1985. Biological half time of deposited nickel oxide aerosol in rat lung by inhalation. Trace Element Res. 10, 203. https://doi.org/10.1007/BF02917459.

Tsai, P.-J., Werner, M.A., Vincent, J.H., Maldonando, G., 1996. Worker exposure to nickel-containing aerosol in two electroplating shops: comparison between inhalable and total aerosol. Appl. Occup. Environ. Hyg 11, 484–492. https://doi.org/10.1080/1047322X, 1996.10389360.

Tsai, Perng-Jy, Vincent, James H., 2001. A Study of Workers' Exposures to the Inhalable and'Total' Aerosol Fractions in the Primary NickelProduction Industry using Mannequins to Simulate Personal Sampling. Annal. Occup. Hyg. 45 (5), 385–394. https://doi.org/10.1093/annhyg/45.5.385. In press.

Tsai, P.J., Vincent, J.H., Wahl, G., Maldonado, G., 1995. Occupational exposure to inhalable and total aerosol in the primary nickel production industry. Occup. Environ. Med. 99, 793. https://doi.org/10.1136/2Foem.52.12.793.

Weiss, T., Pesch, B., Lotz, A., Gutwinski, E., Van Gelder, R., Punkenburg, E., Kendzia, B., Gawrych, K., Lehnert, M., Heinze, E., et al., 2013. Levels and predictors of airborne and internal exposure to chromium and nickel among welders—results of the WELDOX study. Int. J. Hyg Environ. Health 216, 175–183. https://doi.org/10.1016/j.ijheh.2012.07.003.

Wippich, C., Rissler, J., Koppisch, D., Breuer, D., 2020. Estimating respirable dust exposure from inhalable dust exposure. Ann. Work Expos. Health 44, 430. https://doi.org/10.1093/annweh/wxaa016.

International Journal of Hygiene and Environmental Health 238 (2021) 113854

Contents lists available at ScienceDirect

International Journal of Hygiene and Environmental Health

journal homepage: www.elsevier.com/locate/ijheh

Human urinary biomonitoring in Western Kenya for micronutrients and potentially harmful elements

Michael J. Watts [a,*], Diana Menya [b,**], Olivier S. Humphrey [a], DanielR.S. Middleton [c], Elliott Hamilton [a], Andrew Marriott [a], Valerie McCormack [c], Odipo Osano [d]

[a] Inorganic Geochemistry, Centre for Environmental Geochemistry, British Geological Survey, Nottingham, UK
[b] School of Public Health, Moi University, Eldoret, Kenya
[c] Environment and Lifestyle Epidemiology Branch, International Agency for Research on Cancer, Lyon, France
[d] School of Environmental Sciences, University of Eldoret, Eldoret, Kenya

ARTICLE INFO

Keywords:
Urinary biomonitoring
Micronutrients
Potentially harmful elements
Reference values
Creatinine
Hydration correction
Kenya

ABSTRACT

Spot urinary elemental concentrations are presented for 357 adults from Western Kenya collected between 2016 and 2019 as part of a wider environmental geochemical survey. The aim of this study was to establish population level urinary elemental concentrations in Western Kenya for micronutrients and potentially harmful elements for inference of health status against established thresholds. For elements where thresholds inferring health status were not established in the literature using urine as a non-invasive matrix, this study generated reference values with a 95% confidence interval (RV_{95}s) to contextualise urinary elemental data for this population group.

Data are presented with outliers removed based upon creatinine measurements leaving 322 individuals, for sub-categories (e.g. age, gender) and by county public health administrative area. For Western Kenya, reference values with a 95% confidence interval (RV_{95}s) were calculated as follows (μg/L): 717 (I), 89 (Se), 1753 (Zn), 336 (Mo), 24 (Cu), 15.6 (Ni), 22.1 (As), 0.34 (Cd), 0.47 (Sn), 0.46 (Sb), 7.0 (Cs), 13.4 (Ba and 1.9 (Pb).

Urinary concentrations at the 25th/75th percentiles were as follows (μg/L): 149/368 (I), 15/42 (Se), 281/845 (Zn), 30/128 (Mo), 6/13 (Cu), 1.7/6.1 (Ni), 2.0/8.2 (As). 0.1/0.3 (Cd), 0.05/0.22 (Sn), 0.04/0.18 (Sb), 1.2/3.6 (Cs), 0.8/4.0 (Ba) and 0.2/0.9 (Pb). Urinary concentrations at a population level inferred excess intake of micronutrients I, Se, Zn and Mo in 38, 6, 57 and 14% of individuals, respectively, versus a bioequivalent (BE) upper threshold limit, whilst rates of deficiency were relatively low at 15, 15, 9 and 18%, respectively. Each of the administrative counties showed a broadly similar range of urinary elemental concentrations, with some exceptions for counties bordering Lake Victoria where food consumption habits may differ significantly to other counties e.g. I, Se, Zn.

Corrections for urinary dilution using creatinine, specific gravity and osmolality provided a general reduction in RV_{95}s for I, Mo, Se, As and Sn compared to uncorrected data, with consistency between the three correction methods.

1. Introduction

Human biomonitoring is a routine tool for the estimation of chemical exposures and dietary intakes. Urine has increasingly been employed as a non-invasive biomarker in biomonitoring studies to measure both potentially harmful elements (PHEs) and beneficial micronutrients as an integrated quantitative marker of human exposure from multiple pathways. Such information can inform public health, hazard assessments and subsequent mitigation strategies (NRC, 2012) to address excessive or deficient intakes of various environmental and dietary chemicals.

National scale biomonitoring programmes are common in many countries worldwide, particularly in North America (e.g. NHANES, 2021), Europe (HBM4EU, 2021; GHBC, 2021), and South East Asia (Kim and Baek, 2016), with fewer programmes in Africa outside of the occupational setting (Phiri et al. 2020, 2021). More commonly in Africa, single event studies in the range of 100–500 individuals have been

* Corresponding author.
** Corresponding author.
E-mail addresses: mwatts@bgs.ac.uk (M.J. Watts), dianamenya@gmail.com (D. Menya).

https://doi.org/10.1016/j.ijheh.2021.113854
Received 11 August 2021; Received in revised form 20 September 2021; Accepted 30 September 2021
Available online 5 October 2021

reported in the Democratic Republic of Congo-DRC (Tuakila et al., 2015), Ethiopia (Godebo et al., 2019), Malawi, Kenya (Watts 2019b) and Tanzania (Middleton et al., 2018) and on rare occasions on a much larger scale up to 5000 (Farebrother et al., 2018). The complexities of interpreting biomonitoring data were discussed in depth by Saravanabhavan et al. (2017), in which common approaches using descriptive statistics (geometric/arithmetic mean, percentiles) are often compared with reference intervals using appropriate statistical methodologies to account for baseline exposure in a reference population for a health-risk based context (Legrand et al., 2010). A large body of work has accumulated in the scientific literature to establish biomonitoring equivalents (BE) to assist in contextualising biomonitoring data from a reference value based on toxicokinetic data into a biomonitoring concentration (Angerer et al., 2011; Boogaard et al., 2011). For example, Hays et al. (2014, 2016) reported biomonitoring equivalents (BE) for trace elements without established thresholds using external reference doses to relate to urine or blood concentrations. This followed efforts at a Biomonitoring Equivalents Expert Workshop in 2008 to harmonise an approach to interpreting HBM data and to provide guidance in a public health context (Hays & Aylward 2009, 2012) including transparency of discussions of confidence and uncertainty (LaKind et al., 2008).

Increasingly a reference value of background exposure in a population has been reported in the literature using a 95th percentile (RV_{95}s) rather than a geometric mean, providing an upper margin of the current background exposure (i.e. environmental, dietary sources) of a general population to a given substance at a given point in time (Saravanabhavan et al., 2017). The establishment of reference values can be a useful snapshot of population level status, for which a database can be revised and refined with new data. A powerful combination of reference values and BEs can provide a broad comparison to a relatively non-invasive and inexpensive biomonitoring use of urine to reflect human dietary or exposure status to an appropriate range of potentially harmful elements or micronutrients essential for human health. An exceedance of the RV_{95}s may indicate a need to re-test and investigate further, and does not take into account toxicological information to inform clinical intervention, but are a useful starting point in the absence of population level data for comparison against or in the absence of upper or lower thresholds for exceedance or deficiency of exposure/intake.

Urinary biomonitoring offers a route to supporting public health professionals, with fewer logistical requirements compared to blood or in settings where resources and infrastructure are challenging for sample collection and storage, alongside capacity for sensitive analyses of trace elements with appropriate quality control measures. Therefore, the aim of this paper was to establish urinary biomonitoring reference values for Western Kenya covering both micronutrients and potentially harmful elements by: (1) presentation of a community based urinary biomonitoring dataset; (2) calculation of population level urinary reference values (RV_{95}s) for Western Kenya, and (3) examine the influence of hydration corrections on the calculated RV_{95}s for each element using creatinine, osmolality and specific gravity compared to commonly used uncorrected data.

2. Methods

Ethical approval

Ethical approval was obtained from the Institutional Research and Ethics Committee of Moi University (000921). Permission and assistance was then requested from the Ministry of Health office for each County before proceeding to the field areas and subsequent engagement with participants via community health workers. Additional research permission granted in Kenya NACOSTI/P/19/43659/29731.

2.1. Study setting

Sample collection between October 2016 and November 2019 was part of a wider project as described in Watts et al. (2019a,b), which collected residential samples of soil, crops, drinking water and a urine sample from households. Each sampled household is shown in Fig. 1, spanning administrative areas in the 'n' Western Kenyan counties of Bomet, Bungoma, Busia, Elgeyo Marakwet, Kericho, Kakamega, Kisumu, Nandi, Siaya, Uasin Gishu, Kisii, Nyamira, Homa Bay and Vihaga. Few sample points are shown in Uasin Gishu and Nandi counties owing to urine samples not being collected in the first field survey when field collections were focussed solely on geochemical samples and when the majority of visits were made for these counties.

2.2. Recruitment methods and collection of urine

With the need to collect these samples from the home of each participating house, households were approached through an in-person visit of the study team (often by local community health workers or village leaders) which was travelling by vehicle and stopping at homes in close proximity to a pre-determined sampling location set out for each field team using Maps.me™. These pre-determined sampling locations were selected according to geochemistry, determined by soil parameters and geology of each county, but also considering an appropriate spatial distribution across the county where logistical access was feasible. Upon approaching a house, an adult member (>18 years) of the household was informed about the study and invited to participate. Consenting participants were confirmed by Kenyan counterparts/community practitioners verbally for ages 18 years and older at each site, where urinary samples alongside other environmental samples were requested following an explanation of the study and its rationale. In general, we attempted to collect from a minimum of 30 different sites that were spread out evenly across each county, representing rural land-use, although the geographic size and accessibility resulted in a slight variation in numbers per county. One sample was generally collected from each household, a second adult participant provided a sample in <10% of households. Participants urinated into a 30 mL nalgene LDPE bottle, which was transported in a coolbox (~4 °C) and filtered into an 8 mL nalgene LDPE bottle using a nylon 0.45 μm syringe filter at the end of each day, followed by storage in a coolbox and freezing at −20 °C on return to the University of Eldoret laboratory in Kenya. Urine samples were transported frozen to the UK for immediate elemental analyses and urinary dilution measurements for subsequent corrections.

2.3. ICP-MS elemental analyses

Urine samples were analysed for a general suite of trace and major elements. Samples were diluted ×10 with 1% nitric acid/0.5% hydrochloric acid prior to total element determination by Inductively Coupled Plasma Mass Spectrometry (ICP-QQQ-MS, Agilent 8900), with Sn in no gas mode; Zn, Mo, Cu, Ni, Cd, Sn, Sb, Cs, Ba, Pb in He mode; Se in H_2 mode; and As in O_2 mode and Sc, Ge, Rh, In, Te and Ir elements used as internal standards. Iodine was measured separately as described in Watts et al. (2019b) with a ×20 dilution of urine samples in 0.5% Tetramethyl ammonium hydroxide (TMAH) solution prior to analyses by ICP-MS with the reaction/collision cell in no gas mode. Tellurium was used as an internal standard to correct for minor signal drift. Calibration standards, quality control solutions and certified reference material were matrix matched with either 1% nitric acid/0.5% hydrochloric acid or 0.5% TMAH. Performance characteristics for the limit of detection and accuracy measured for the Seronorm™ Trace Elements Urine L-1, produced by SERO AS is presented in full in Supplementary Table 1. Seronorm solutions were analysed on a ratio of 1 for every 15 urine samples. Calibration standards were analysed at the beginning and end of each analytical batch and analytical run quality was verified using a series of chemical quality control standards prepared on the day of

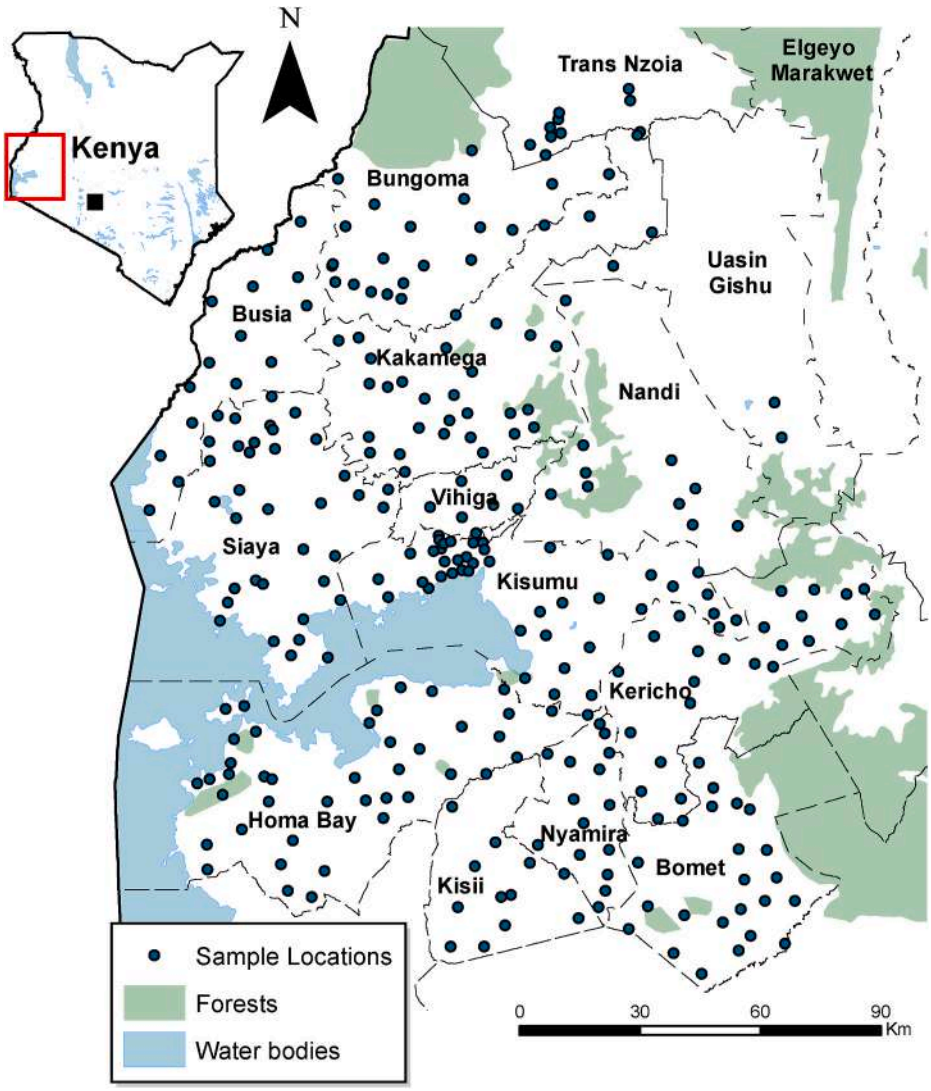

Fig. 1. Location map for collection points and county administrative areas in Western Kenya.

analysis (Ni, Cu, Zn, As, Se, Mo, Sb, Ba, Pb at 5 μg/L, Cd, Sn, Cs at 1 μg/L, I at 50 μg/L), produced from an independent source to the calibration standards (SCP Science, UK and Sigma Aldrich for I).Analytical trends were monitored via charting in SPC for Microsoft Excel™ version 5 as described in Abellanosa et al. (2018).

2.4. Statistical analyses

Urinary element concentrations that were below their respective limit of detection (LOD) were assigned a value of LOD/2. Information on age and sex were obtained from household questionnaires. Element data from participants with urinary creatinine values < 0.3 g/L or >3.0 g/L were excluded from statistical analysis following guidelines from the Human Biomonitoring Commission (2007) before testing exclusion variables (WHO, 1996; Wilhelm et al., 2008). Summary statistics were then calculated for each element: arithmetic mean, SD, median, median absolute deviation, minimum and maximum values, percentiles (P25, P75, and P90), skewness, and kurtosis. Summary statistics were also calculated based on sex and age groups. Human biomonitoring reference values (RV_{95}s) aim to represent current background exposure; therefore, extreme values were removed, as they may disproportionately influence the final values. The data were natural log-transformed, and the normality of the data distributions evaluated using the Kolmogorov-Smirnov test. Extreme values were identified and removed using Tukey's approach (Tukey, 1977) if the data were not skewed, or a modified Tukey's approach (Hubert and Van der Veeken, 2008) if the data remained skewed after log-transformation. After extreme value removal, RV_{95}s were estimated statistically as the rounded 95th percentile and its corresponding 95% confidence interval (95%CI). Statistical analysis was conducted using R version 4.0.3 (R Core Team 2020).

2.5. Urinary dilution corrections

Urinary creatinine was determined using a Randox liquid assay kit and a Randox RX Imola chemistry analyser. Osmolality was measured by freezing-point osmometry using an Osmomat 030 (Gonotec, Germany). Specific gravity (SG) was measured with a PAL-10-S digital refractometer (Atago, Japan) prior to filtration. Creatinine, SG and osmolality corrections were performed using Equation (1):

$$UC_{cor} = UC_{vol} \times D_{ref}/D_{meas} \quad (1)$$

where UC_{cor} is dilution corrected urinary concentration; UC_{vol} is the measured, volume-based urinary concentration (in μg/L); D_{ref} is the reference value to which UC concentrations are scaled to and D_{meas} is that measured in the given specimen (note: D_{ref} −1 and D_{meas}-1 are used for SG correction). D_{ref} was 1 g/L for creatinine – synonymous with the

conventional division-based correction and yielding results in μg per g creatinine; and, for both SG and osmolality, the study group medians (n = 357) were selected: 1.017 (unitless) and 585 mOsm/kg, respectively (Middleton et al., 2016).

3. Results & discussion

3.1. Urinary elemental concentrations

Urinary elemental concentrations for 322 adults with outliers removed are summarised in Table 1, along with descriptive summary statistics and the calculated RV_{95}s values for each element. The full dataset is reported in Supplementary Table 2 (including outliers – 357 individuals) and 3 (outliers removed). Descriptive statistics for each county administrative area are presented in Supplementary Table 4 and for age and gender in Supplementary Tables 5 and 6 Supplementary Table 6 includes an individual male/female RV_{95}s gender, to allow for the imbalance in female/male participants (207/112). Comparisons of data will be discussed in detail for each selected micronutrient and PHEs. Elemental concentrations are presented without hydration correction for comparison to the literature, although correction values (creatinine, osmolality, specific gravity) are presented in the supplementary tables for additional information.

The discussion of urinary elemental concentrations will be organised into three sections: micronutrients essential to health with comparative published threshold values (I, Se, Zn, Mo), potentially harmful elements with published threshold values (As, Cd, Sn, Ba) and other elements for which there are no published threshold values (Cu, Ni, Sb, Cs, Pb), but where alternative RV_{95}s values are available in the literature. The range of concentrations for each element are illustrated in Fig. 2a–c.

3.2. Micronutrients with threshold values (I, Se, Zn, Mo)

Median urinary iodine was 243 μg/L - slightly lower than the 261 μg/L reported by Watts et al. (2019b), which comprised of a smaller component of this same dataset and without outliers removed. Urinary iodine concentrations were between 9 and 3146 μg/L, P25 and P75 were 149 and 368 μg/L, respectively. Approximately 15% were considered to represent a status that was moderately deficient (<100 μg/L), whilst 38% of samples were considered to represent an excess of iodine intake (>300 μg/L) (WHO/UNICEF/ICCIDD, 2007). In comparison, the calculated RV_{95}s of 740 and 663 μg/L (female/male) are both considerably higher than the threshold associated with excess iodine intake, and is high when comparing to biomonitoring equivalent (BE) values calculated by Hayes et al. (2018) using Estimated Average Requirement (EAR), Recommended Dietary Allowance (RDA) and for toxicity, Tolerable Upper Intake Level (UL) and Minimal Risk Level (MRL). For example, the BE values derived for adults by Hays et al. (2018) were; 60, 100, 730 and 450 μg/L, respectively.

These urinary iodine data are comparable to other African studies reporting the prevalence of excess iodine intake. For example, Farebrother et al. (2018) reported uncorrected median urinary iodine in women across central Kenya of 289 μg/L (IQR 173, 458 μg/L). Median uncorrected urinary iodine reported in Malawi (Watts et al., 2015) were 221 μg/L (141–344 μg/L); in Port Sudan 464 and 561 μg/L, Medani et al. (2012) and Hussein et al. (2012), respectively. In Sadami, Ethiopia, women of reproductive age (WRA) and school age children (SAC) presented median urinary iodine of 143 and 187 μg/L, respectively, 10 months after a salt iodisation campaign commenced, although inconsistent iodine content of salt was found in this study (Tafere and Stoecker, 2020). In Somalia, WRA provided a median urinary iodine of 329 μg/L (Kassim et al., 2014) and in Lesotho, a median urinary iodine of 280 μg/L (Sebotsa et al., 2005). Tanzanian SAC in Kindoni presented a very high median urinary iodine at 400 μg/L, with one third >500 μg/L (Venance et al., 2020). The Iodine Global Scorecard (IGN, 2021) summarised median uncorrected urinary iodine in Kenyan SAC as 208 μg/L, although this summary of global progress used data from a 2011 national survey (Kenya Ministry of Health, 2011) – underlining the need for timely and relevant data. Food supply calculations previously suggested a 100% risk of iodine deficiency for this same study area in Western Kenya from dietary source sampling reported in Watts et al. (2019a), although did not include iodised salt reported to be present in 98% of Kenyan households (Joy et al., 2014). Fig. 3a illustrates the range of urinary iodine within each County administrative area with little variation in the median values, although some examples of excess values as outliers at concentrations >1000 μg/L are clearly illustrated in Fig. 1 for Homa Bay, Kisumu and Saiya Counties bordering Lake Victoria, possibly representing elevated fish consumption (Watts et al., 2015) as the main source of protein or possible salt-preserved fish (personal observation).

The median urinary selenium concentration was 26 μg/L, with P25 and P75 of 15 and 42 μg/L, respectively. These values are comparable to Middleton et al. (2018) reported median urinary selenium of 24 μg/L for 45 individuals in Kenya and 29 μg/L for 200 individuals in Tanzania. Fourteen percent of individuals were below the lower threshold of 10 μg/L using a BE estimation (Hays et al., 2014), below which could infer a status of deficiency. As Fig. 2a shows, just 15% indicated deficiency using a 10 μg/L (BE) low threshold, but with still 6% of samples above an upper/excess threshold of 90–100 μg/L (BE). The calculated RV_{95}s for females of 78 μg/L was slightly below the upper threshold, whereas the male RV_{95}s was significantly different from females and above the threshold at 103 μg/L. The urinary selenium concentrations contrasts

Table 1
Descriptive statistics for uncorrected urinary elemental concentrations (μg/L) with calculated RV_{95}s values.

	I	Se	Zn	Mo	Cu	Ni	As	Cd	Sn	Sb	Cs	Ba	Pb
mean	297	36	636	101	11	5.7	7.1	0.20	1.70	0.16	2.9	6.6	0.7
sd	261	38	473	109	7	9.1	10.4	0.23	6.56	0.33	2.9	19.8	0.9
median	**243**	**26**	**529**	**64**	**9**	**3.5**	**3.9**	**0.20**	**0.09**	**0.08**	**2.1**	**1.7**	**0.50**
P .25	149	15	281	30	6	1.7	2.0	0.10	0.05	0.04	1.2	0.8	0.2
P.75	368	42	845	128	13	6.1	8.2	0.30	0.22	0.18	3.6	4.0	0.9
P.90	544	68	1261	229	20	10.4	16.8	0.40	4.23	0.38	6.3	12.9	1.4
RV_{95}s	**717**	**89**	**1753**	**336**	**24**	**15.6**	**22.1**	**0.34**	**0.47**	**0.46**	**7.9**	**13.4**	**1.9**
Lower 95% CI	64	79	1549	286	22	13.4	18.8	0.31	0.37	0.39	6.9	11.0	1.7
Upper 95% CI	811	103	2016	403	27	18.6	26.6	0.38	0.58	0.55	9.1	16.9	2.2
Comparative values													
[a]RV_{95}s value Canada	300	120	1100	170	25	4.4	27	1.3	20	0.17	12		1.9
[b]EAR - BE (NHANES)	100	10	159	22									
[c]Excess BE (NHANES)	300	90–100	439–3489	200–7500			6.4	2.5–6.38*	20			190	

[a] Saravanabhavan et al. (2017) RV_{95}s comparative values for NHANES data.
[b] Estimated Average Requirement (EAR) for minimum intake: I (WHO, 1996, 2004); Se (Hays et al., 2014), Zn (Poddolgoda et al., 2019); Mo (Hays et al., 2016).
[c] Threshold for excess intake using Bioequivalence (BE): for I, Se, Zn, Mo same references as for EAR; As (Hays et al., 2010); Cd (Hays et al., 2008); Sn (Poddalgoda et al., 2016); Ba (Poddalgoda et al., 2017).

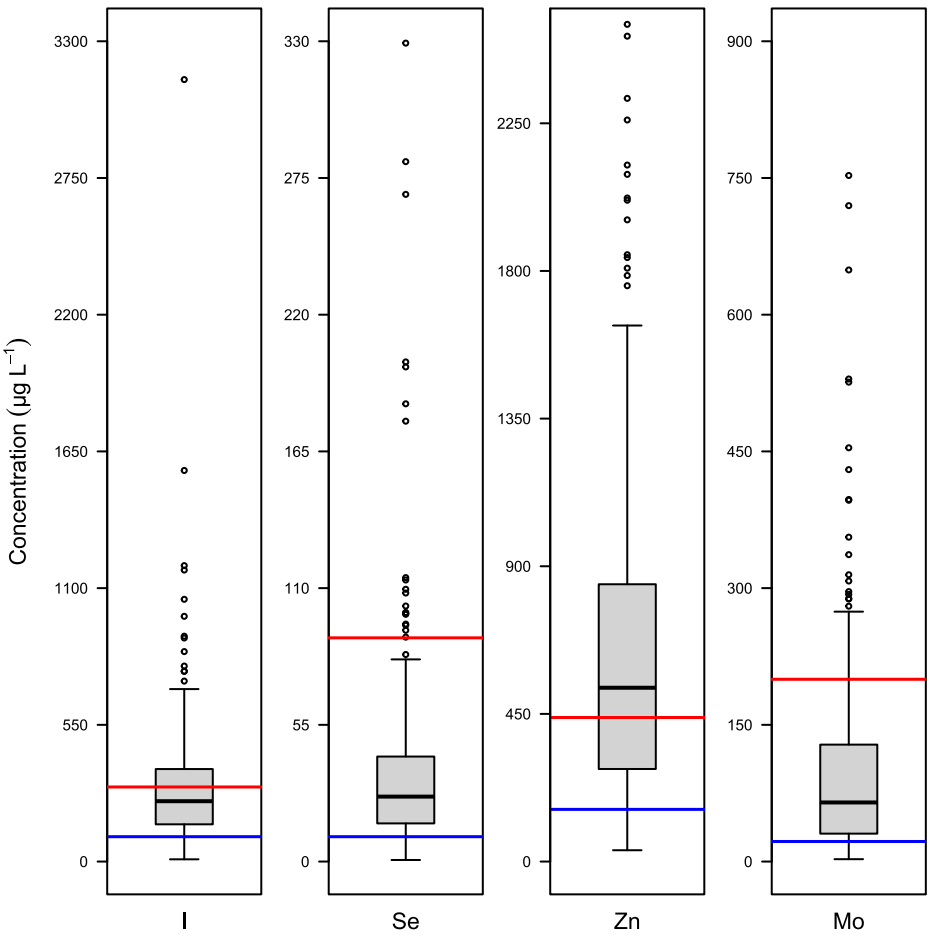

Fig. 2. Distribution of urinary elemental concentrations (uncorrected) in groups of (a) micronutrients - above red line denotes excess biomonitoring equivalent from NHANES most conservative value, blue line below which deficiency based on the estimated average requirement-EAR bioequivalent from NHANES most conservative value, (b) potentially harmful elements - (above red line denotes excess biomonitoring equivalent from NHANES most conservative value, and (c) elements with comparable published reference values (RV_{95}s) - red line denotes calculated RV_{95}s value. (For interpretation of the references to colour in this figure legend, the reader is referred to the Web version of this article.)

with the calculated risk of deficiency for male and females of 100 and 93%, respectively for dietary supply data and measured food items from the same households in Western Kenya as the urine collections. Median urinary selenium for male (n = 111) and female (n = 204) were 30 µg/L and 25 µg/L, respectively. Phiri et al. (2020) reported a greater potential deficiency in Malawi indicated by urinary selenium in ~35% of the study (n = 1618) and similar ~5% exhibiting an excess status. The median urinary selenium from this national survey was relatively lower at 16.2 and 15.0 µg/L in women of reproductive age and school age children, respectively. In contrast, Joy et al. (2015) calculated a risk of deficiency for Se intake of 74% from dietary supply calculations in Malawi. Fig. 3a shows a similar range of urinary selenium across each of the County administrative areas, with the exception of outlier values in Homa Bay and Kakamega counties and in particular, Vihaga county where the median urinary selenium of 42 µg/L is represented by a very small number of samples. Phiri et al. (2019) also demonstrated geographical variation for urinary selenium in Malawi.

The median urinary zinc concentration was 529 µg/L, with P25 and P75 of 281 and 845 µg/L and median urinary zinc of 700 and 448 µg/L for male and females, in comparison to a BE for nutritional requirement reported by Poddalgoda et al. (2019) of 206 and 159 µg/L for male and female, respectively. In general, urinary zinc suggests a status of deficiency in 9% of volunteers (Fig. 2a) in contrast to 57% of urinary zinc exhibiting an excess status when using the lower exposure guideline value for North America of 439 µg/L, yet no exceedances when using the more conservative European value of 3489 µg/L (Poddalgoda et al., 2019). The RV_{95}s for this study was 2030 µg/L for males and 1551 µg/L for females, both between the two proposed upper BE thresholds. In general, Fig. 3a shows that each of the County administrative areas were similarly above minimum nutritional requirements for Zn. This contrasts with food supply calculations in the same area by Watts et al. (2019a) that suggested a risk of deficiency for Zn status of 85–100% for males and females and equivalent published data of 100% risk, suggesting greater food diversity for this region of Kenya or perhaps greater consumption of dairy, meat and fish deriving a higher Zn status than national survey data would suggest (FAOSTAT, 2019).

Urinary zinc data for this study were generally much higher than other African studies. For example, a national survey in Malawi (Phiri et al., 2021) presented a median urinary zinc of 322 µg/L for women of reproductive age (n = 741) and 346 µg/L in school age children (n = 645). Similarly, Godeboa et al. (2019) presented urinary zinc for the Ethiopian Rift valley with a median of 287 µg/L (P25 167; P75 502) (n = 386). However, Middleton et al. (2018) broadly similar median urinary zinc of 479 and 427 µg/L for Kenya and Tanzania, respectively.

The median urinary molybdenum concentration was 64 µg/L, with P25 and P75 of 30 and 128 µg/L, respectively. Median urinary molybdenum were broadly similar for male and females at 68 and 64 µg/L, respectively. These values were relatively high in comparison to a BE for nutritional requirement reported by Hays et al. (2016) of 21.7 µg/L using an estimated average requirement (EAR) assumption or recommended daily allowance (RDA) of 28.4 µg/L. Upper thresholds ranged from 206 µg/L for North American and 7516 µg/L for OECD values. Using the lower EAR threshold, 18% were considered deficient using urinary molybdenum BE, whilst 14% exceeded the upper BE threshold (Fig. 2a). The calculated RV_{95}s of 379 µg/L for males and 314 µg/L for females both exceeded the lower of the published BE upper threshold values of 206 µg/L. Middleton et al. (2018) reported a slightly higher exceedance rate of 25 and 18% for Kenya and Tanzania, respectively. In

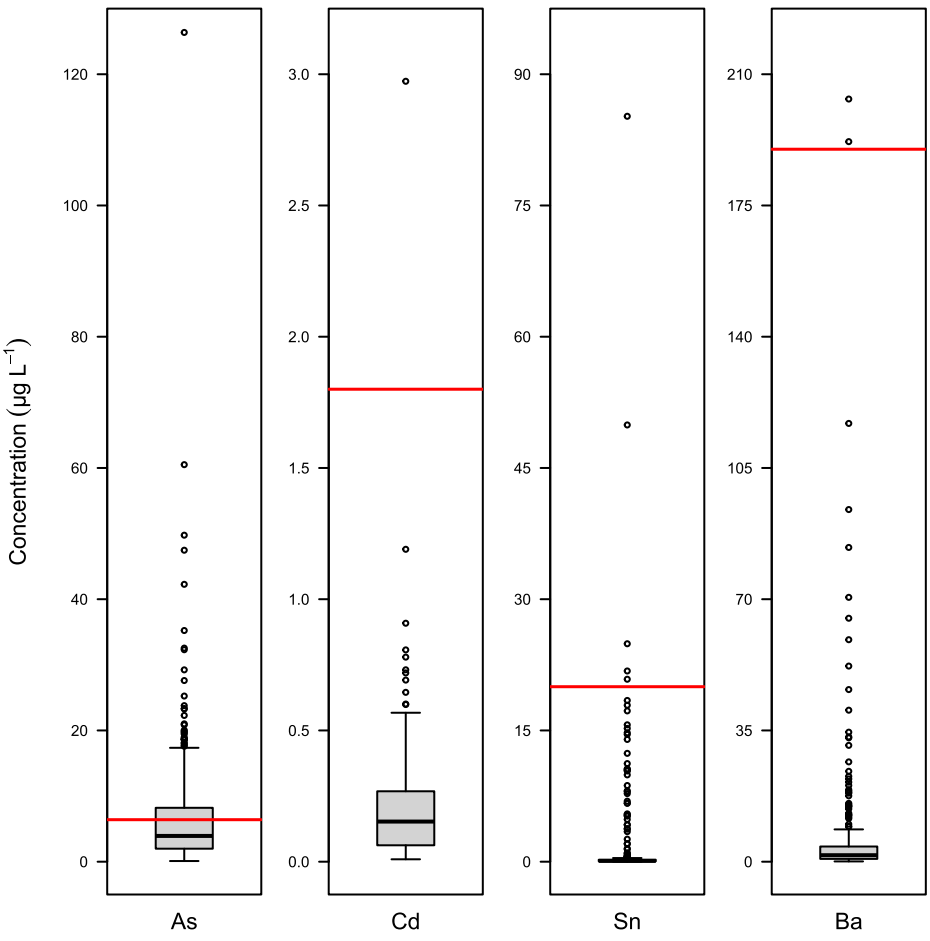

Fig. 2. (*continued*).

general, each of the county administrative areas demonstrated a level of Mo sufficiency, with notable exceptions illustrated in Fig. 3a for Homa Bay and Kisumu bordering Lake Victoria, although not for Saiya which also borders the lake. The general Mo sufficiency derived from urinary molybdenum agrees with the predicted risk of deficiency close to zero calculated for this area by Watts et al. (2019a) in which vegetable groups, seeds and pulses were reported to be a significant contributor of Mo to the daily dietary intake. Godeboa et al. (2019) reported significantly higher urinary molybdenum values for the Ethiopian Rift valley, with a median of 367 µg/L and P25 and P75 of 197 and 614 µg/L (n = 386).

3.3. Potentially harmful elements (PHEs) with published threshold values (As, Cd, Sn, Ba)

Median urinary arsenic concentrations were 3.9 µg/L, with P25 and P75 of 2.0 and 8.2 µg/L, with median UAsC for male and females showing no contrast at 3.9 and 4.2 µg/L, respectively. The median values were below the biomonitoring equivalent upper threshold representing toxicity of 6.4 µg/L for inorganic As published by Hays et al. (2010). It should be noted that urinary arsenic values in this study (Fig. 2b) represent total As, which incorporates both inorganic and organic As, the latter most likely derived from dietary sources. Therefore, care should be taken in interpreting that 34% of participants had total urinary inorganic arsenic values that exceeded 6.4 µg/L. The calculated RV_{95}s of 23.6 µg/L for males and 22.1 µg/L for females in this study fall midway between studies for adults in Germany, Belgium and South Korea with RV_{95}s reported as 15, 49 and 106 µg/L (Wilhelm et al., 2004; Hoet et al., 2013; Lee et al., 2012). Further investigation is required to understand the higher measurement of urinary arsenic, using arsenic speciation to derive inorganic and organic As species to provide additional interpretation and to support differentiation between occupational, environmental or dietary sources (Hays et al., 2010; Middleton et al., 2016). In general, the majority of administrative county areas as illustrated in Fig. 3b were below Hays et al. (2010) upper threshold for urinary arsenic, or at least with few outliers, with the exception of Homa Bay, and Saiya in particular and to a lesser extent Kisumu county, all bordering Lake Victoria. In these instances, greater fish consumption may contribute to elevated As dietary intake, represented as organic-arsenic (Middleton et al., 2016). Godeboa et al. (2019) reported higher urinary arsenic in the Ethiopian Rift Valley, with a median of 18.9 µg/L and 25/75th percentiles of 11.4 and 38.9 µg/L (n = 386). Tuakila et al. (2015) also reported significantly higher urinary arsenic in the Democratic Republic of Congo (DRC) with a median of 171 µg/L (n = 60) in the age group of 6–14 years old, although these volunteers represented occupational exposure from artisanal mining. Middleton et al. (2018) reported exceedances of 25 and 16% in Kenya and Tanzania, respectively, when considering inorganic-As.

Median urinary cadmium concentrations were 0.2 µg/L, with P25 and P75 of 0.1 and 0.3 µg/L in comparison to a BE upper threshold of 2.5 µg/L using underlying kidney and urinary Cd concentration data (Hays et al., 2008). No individuals were above this threshold as shown in Fig. 2b, whilst the calculated RV_{95}s was 0.22 µg/L for males and 0.35 µg/L for females. Fig. 3b shows a similarly low status using UCdC for all county administrative areas. The urinary cadmium were low in comparison to Godeboa et al. (2019) study in Ethiopia with a median of 0.61 µg/L, P25 and P75 of 0.27 and 1.05 µg/L (n = 386). Al-Saleh et al. (2020) reported a similarly low median urinary cadmium of 0.4 µg/L for non-occupationally exposed women in Saudi Arabia, but with an RV_{95}s of 1.2 µg/L, which was significantly higher than this study. Wilhelm

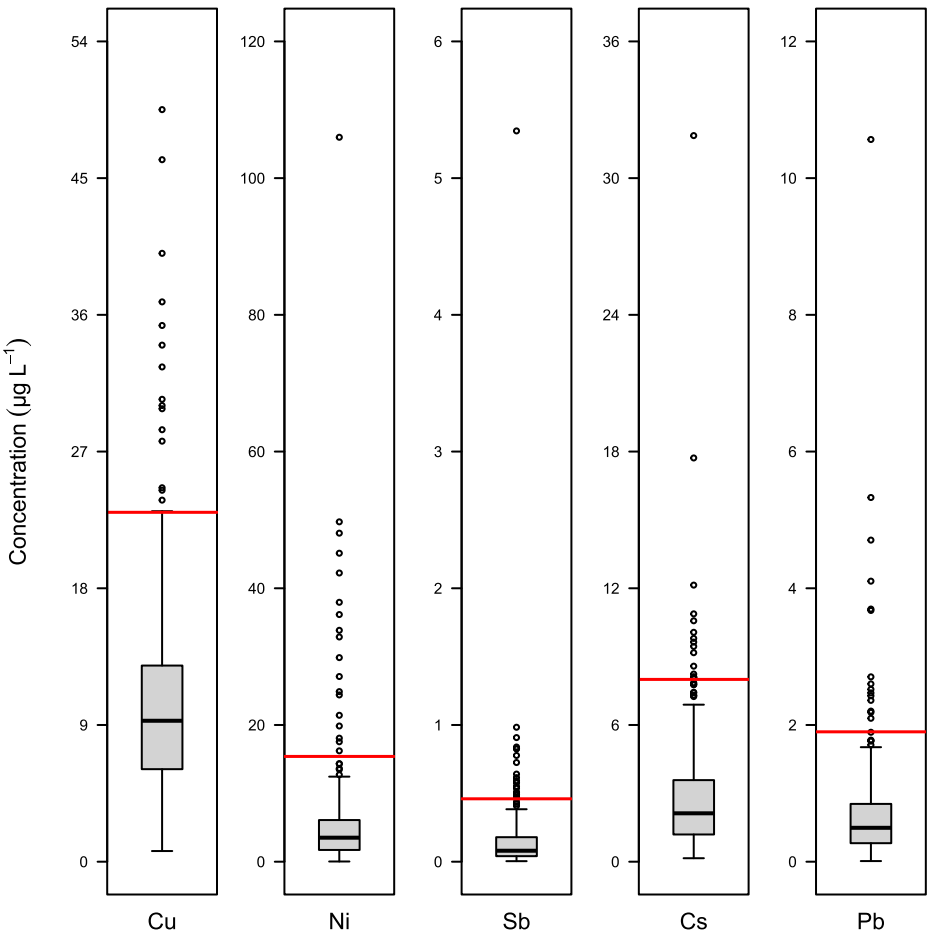

Fig. 2. (*continued*).

et al. (2004) reported a median urinary cadmium value of 0.2 µg/L and an RV_{95}s of 0.8 µg/L. For an African comparison, Tuakila et al. (2015) reported a much higher median urinary cadmium in the DRC of 1.7 µg/L than this study for children occupationally exposed to mining activities, albeit below the BE threshold. Similarly, Middleton et al. (2018) reported no exceedances for urinary cadmium in Kenya or Tanzania for non-occupationally exposed individuals.

Median urinary tin concentrations were 0.09 µg/L, with P25 and P75 of 0.05 and 0.22 µg/L, respectively, were very low in comparison to a BE of 20 µg/L for inorganic tin (Poddalgoda et al., 2016). Just 2% of volunteers exceeded this threshold and can be seen as outliers in Figs. 2b and 3b. The majority of administrative counties exhibited low urinary tin ranges with the notable exception of Bomet and Vihaga counties and to a lesser extent Bungoma, albeit with the majority of their urinary tin below the upper threshold, confirmed with the RV_{95}s calculated as 1.3 µg/L for males and much lower at 0.4.µg/L for females. Few non-occupationally derived studies exist for urinary tin, particularly for Africa.

Median urinary barium concentrations were 1.7 µg/L, with P25 and P75 of 0.8 and 4.0 µg/L, were generally low with just 1% of individuals exceeding the BE upper threshold of 190 µg/L (Poddalgoda et al., 2017) largely representing outliers in this study as illustrated in Figs. 2b and 3b. This contrasts with relative exceedances reported by Middleton et al. (2018) of 16 and 14% for Kenya and Tanzania. The RV_{95}s calculated for this study was 8.2 µg/L for males and a much higher value of 17.2 µg/L for females. Median urinary barium for male and females were 1.9 and 1.4 µg/L, respectively. All counties exhibited a similarly low urinary barium, with a slight difference in Saiya, albeit well below the upper threshold. There is a paucity of data for UBaC in the literature, particularly for Africa. Therefore, the NHANES survey for North America from which the BE value was derived is an exceptional resource for a range of biomonitoring matrices and elements, particularly for elements such as barium for which the health consequences are less certain (Poddalgoda et al., 2017).

3.4. *Elements with no published thresholds, but comparative RV_{95}s values (Cu, Ni, Sb, Cs, Pb)*

Median urinary copper concentrations were 9 µg/L, with P25 and P75 of 6 and 13 µg/L (Fig. 2c). Male and female median urinary copper were 9.6 and 8.8 µg/L, respectively. There are currently no thresholds or BE values reported in the literature for copper, although the calculated RV_{95}s value of 29 and 21 µg/L for male and females, respectively for this study can be compared to RV_{95}s values for population groups reported in other countries for some context, although should not be interpreted in depth. For example, Hoet el al. (2013) reported that non-occupationally exposed individuals in Belgium had an RV_{95}s value of 19.6 µg/L (n = 1001), and Saravanabhavan et al. (2017) 25 µg/L for a Canadian study (n = 1513), both of a similar magnitude to this study. Godeboa et al. (2019) reported a broader range of urinary copper data, with a median urinary copper of 5.6 µg/L, with P25 and P75 of 2.2 and 9.1 µg/L in the Ethiopian Rift valley. Middleton et al. (2018) reported similar median urinary copper of 10 and 8.9 µg/L for Kenya and Tanzania, respectively. There were no marked differences in the range of urinary copper across the County administrative areas as illustrated in Fig. 3c.

Median urinary nickel concentrations were 3.5 µg/L, with P25 and P75 of 1.7 and 6.1 µg/L (Fig. 2c), with male and female median values of 2.7 and 3.6 µg/L, respectively. There are no thresholds or BE values reported in the literature for Ni, although similarly to Cu, the calculated RV_{95}s value of 15.4 µg/L for this study can be compared to RV_{95}s values

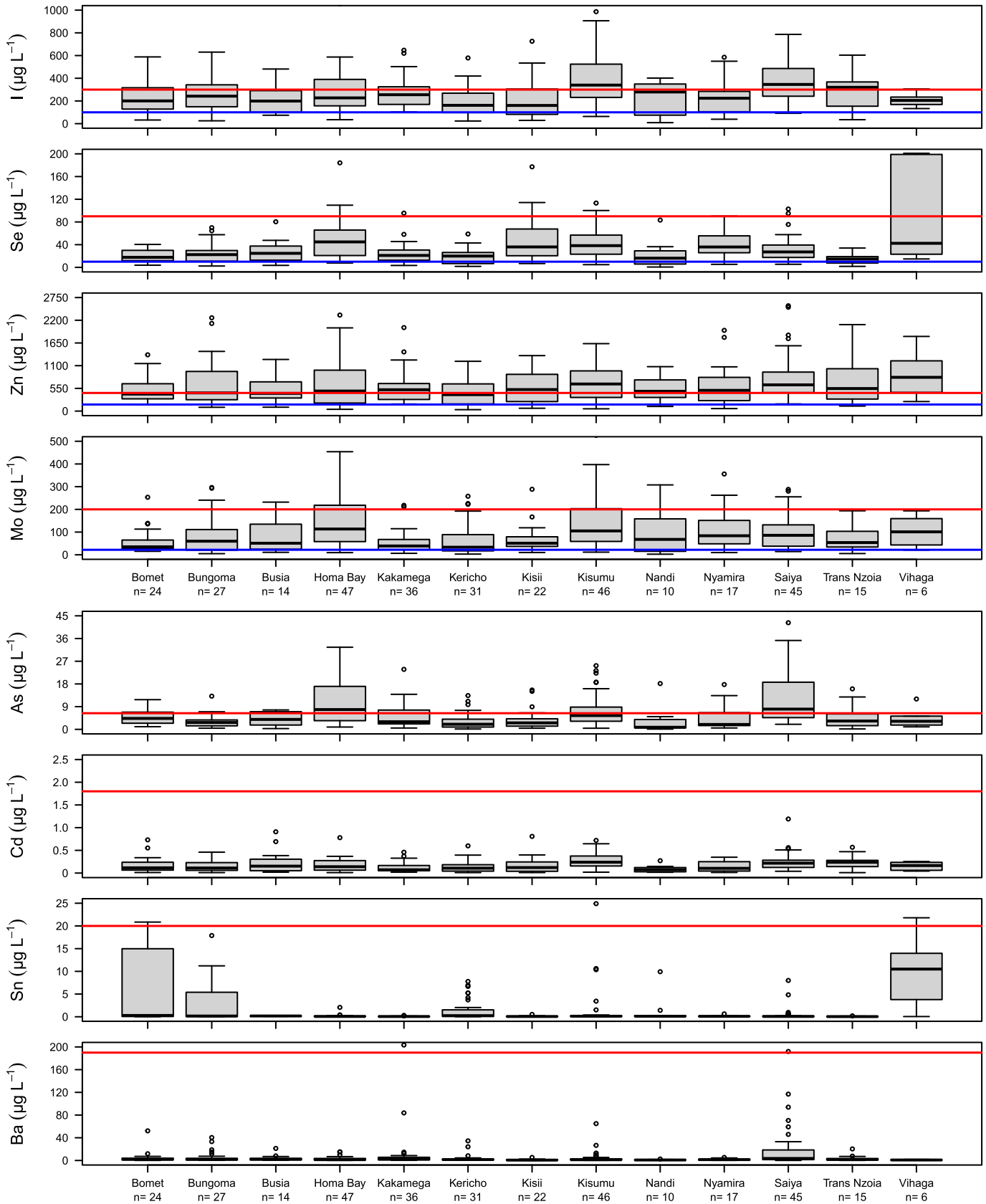

Fig. 3. Distribution of urinary elemental concentrations (uncorrected) by county administrative areas in groups of (a) micronutrients - above red line denotes excess biomonitoring equivalent from NHANES most conservative value, blue line below which deficiency based on the estimated average requirement-EAR bioequivalent from NHANES most conservative value, (b) potentially harmful elements - above red line denotes excess biomonitoring equivalent from NHANES most conservative value, and (c) elements with comparable published reference values (**RV_{95}s**) - red line denotes calculated RV_{95}s value. (For interpretation of the references to colour in this figure legend, the reader is referred to the Web version of this article.)

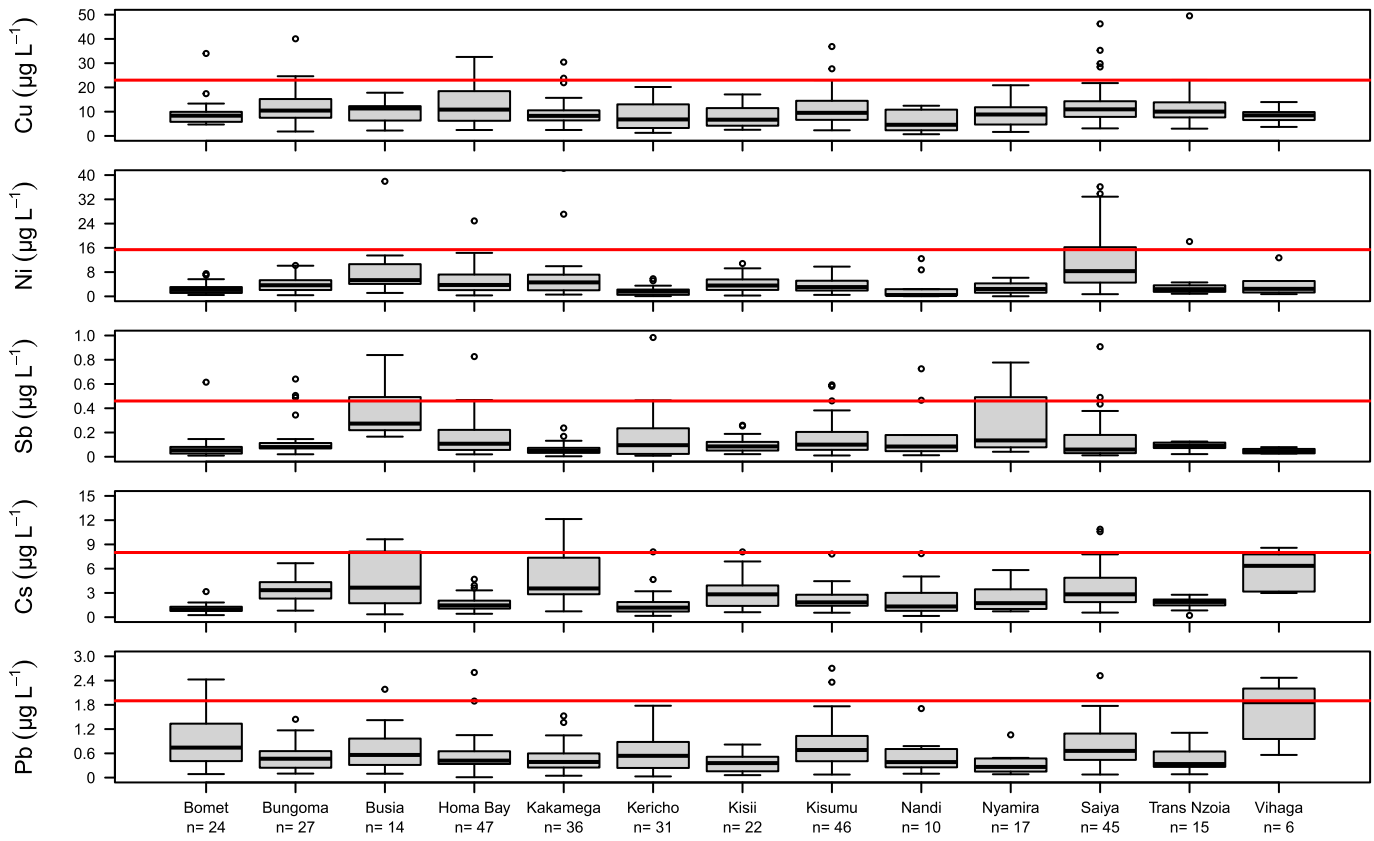

Fig. 3. (*continued*).

for population groups reported in other countries for some context, although should not be interpreted in depth. For example, Hoet el al. (2013) reported that non-occupationally exposed individuals in Belgium had an RV_{95}s value of 4.7 µg/L (n = 1001), Wilhelm et al. (2004) reported an RV_{95}s for adults in a German study of 3.0 and Saravanabhavan et al. (2017) 4.4 µg/L for a Canadian study (n = 5602), each of them of a similar magnitude to this study. Very few studies have reported urinary nickel, with Godeboa et al. (2019) also reporting Ni in a broad elemental suite with a broader range of urinary nickel data, with a median of 7.4 µg/L, with 25/75th percentiles of 3.5 and 11.6 µg/L in the Ethiopian Rift valley. There were no marked differences in the range of urinary nickel across the County administrative areas as illustrated in Fig. 3c.

Median urinary antimony concentrations were 0.08 µg/L, with P25 and P75 of 0.04 and 0.18 µg/L (Fig. 2c). There are no thresholds or BE values reported in the literature for Sb, although similarly to Ni and Cu, the calculated RV_{95}s value of 0.43 and 0.48 µg/L for male and females, respectively, in this study can be compared to RV_{95}s values for population groups reported in other countries for some context, although this should not be interpreted in depth. For example, Hoet et al. (2013) for adults in Belgium reported a much lower RV_{95}s of 0.24 µg/L in Germany, whilst a Canadian study reported 0.17 µg/L (Saravanabhavan et al., 2017). No African comparison is available, as urinary antimony measurements in the Ethiopian Rift valley were below the limit of detection (Godeboa et al. (2019). The urinary antimony were generally similar across county administrative areas (Fig. 3c), with the exception of Busia and Nyamira.

Median urinary caesium concentrations were 2.1 µg/L, with P25 and P75 of 1.2 and 3.6 µg/L (Fig. 2c). The calculated RV_{95}s was 7.4 and 8.2 µg/L were for male and females, respectively, in comparison to a Canadian RV_{95}s of 12 µg/L (Saravanabhavan et al., 2017). No other studies exist for non-occupationally exposed populations, particularly in Africa. Across county administrative areas, urinary caesium were generally within a similar range, with the exception of Busia, Kakamega and Vihaga (Fig. 3c).

Median urinary lead concentrations were 0.5 µg/L, with P25 and P75 of 0.2 and 0.9 µg/L (Fig. 2c). The calculated RV_{95}s was 2.2 and 1.8 µg/L for male and females, respectively, which compared closely to a Canadian study also 1.9 µg/L (Saravanabhavan et al., 2017) and a Belgian study at 2.8 µg/L (Hoet et al., 2013). Godeboa et al. (2019) reported lower median 0.14 µg/L and P25 to be less than the lower limit of detection and P75 at 0.36 µg/L in Ethiopia, yet Al Saleh et al. (2020) reported a much a higher median of 14 µg/L in non-occupationally exposed women, which was comparable to a group of occupationally exposed miners in DRC at 19.3 µg/L (Tuakila et al., 2015). In general, county administrative areas presented a similar range of urinary lead (Fig. 3c), although Bomet and Vihaga exhibited a broader and higher range of concentrations in comparison to other counties.

3.5. *Influence of urinary hydration corrections*

Data in this study was presented without hydration corrections for comparison with literature values, where such corrections are inconsistently presented or where they are present, presented with and without correction. This study employed hydration corrections using creatinine, osmolality and specific gravity (SG). Only occasionally, published data includes both corrected and uncorrected data. For example, Tuakila et al. (2015) usefully presented differing RV_{95}s values with and without creatinine corrections, ranging from a −31% reduction following correction for urinary arsenic, −113% for urinary cadmium and +20% for urinary lead. The employment of the appropriate correction factor to each urinary elemental concentration should be considered, with significant differences in individual values possible with and without correction or even between correction methods. For example, urinary iodine (Watts et al. 2015, 2019b) exhibited greater uncertainty when deploying creatinine compared to osmolality and SG, whilst Middleton et al. (2016) observed a similar pattern for urinary

arsenic. Phiri et al. (2020) presented a comparison of hydration factors for urinary selenium in women of reproductive age (WRA) and school age children (SAC) groups and subsequently employed SG corrections for urinary zinc (Phiri et al., 2021) in a national Malawian survey. For urinary selenium, mean corrected concentrations were similar, yet lower than uncorrected values, explained as a consequence of protein energy malnutrition, particularly for SAC.

For this study, urinary elemental concentrations and associated RV_{95}s values are summarised as uncorrected or with one of the three hydration correction methods in Table 2. The urinary iodine, urinary selenium, urinary molybdenum, urinary arsenic, urinary tin RV_{95}s values show a significant difference between uncorrected and corrected data, but with general agreement for the three correction methods. It is likely that the removal of outliers for creatinine as suggested by Saravanabhavan et al. (2017) has improved the comparison with SG and Osmolality against previously reported UIC in Watts et al. (2019b).

3.6. Application of urinary biomonitoring data

In general, most biomonitoring studies are reported with descriptive statistics for aggregated data, with comparison to a reference or population value to establish a public health context. As Morrens et al. (2021) pointed out, there is no universal consensus to communicate individual results to study participants, where most surveillance studies, including this study are designed to communicate aggregated results. For this study, aggregated data has been communicated with public health administrators for onward public health contextual interpretation with community workers, alongside individual data for follow-up on exceedances or where specifically requested by the participants. The latter often involved individuals sensitised and with an interest in health conditions in their local areas (e.g. iodine deficiency-goitre; fluorosis). The majority of participants wanted to contribute to research, with a small proportion curious about their own results. The RV_{95}s values provide some context and aid to explaining results, particularly for elements where there are no established bioequivalent thresholds that can infer health status, but can be used as a reference point against the rest of the study participants. However, care should be used where health-based/bioequivalent guidance values are not available and the RV_{95}s values used as a comparison with other population groups to generate a body of evidence/requirement for investment in bioequivalent calculations.

4. Conclusion

Health studies will benefit from a dual approach to deconvolute and design mitigation strategies to deficiencies of micronutrients essential to health and reduce exposure to potentially harmful elements using food consumption surveys alongside human biomonitoring. Biomonitoring through the use of urinary elemental concentrations does provide a cost effective approach compared to accurate food dietary survey/analyses for population background exposure albeit with a snapshot in time. The increasing literature providing comparative reference values (RV_{95}s) for study organisers and participants where health-based guidelines are lacking may assist in building evidence and targeting of resources towards the development of bioequivalent calculations to better infer health outcomes and subsequent design of mitigation strategies. For biomonitoring data to be used to inform health interventions, it must have sufficient quality assurance controls and levels of reliability, including consideration of hydration correction factors to derive reference values for a range of elements appropriate to urinary measurements. Further studies should consider targeted hydration corrections for each of the urinary elemental concentration versus uncorrected data for transparent comparison with published studies and building of confidence in the appropriate correction strategy. This will have significance in challenging environments where lower cost measurements such as SG may be more appropriate or in a low-income nation setting where low protein intake may render creatinine a poor method.

Table 2
Influence of hydration adjustment methods on urinary elemental concentrations (μg/L).

Element	Correction Method	Mean	SD	Median	RV_{95}s (95% CI)
I	Uncorrected	297	361	243	717 (643–811)
	Osmolality	299	253	262	539 (502–585)
	Creatinine	255	257	207	530 (482–588)
	Specific gravity	302	259	246	548 (508–596)
Se	Uncorrected	36	38	26	89 (79–103)
	Osmolality	36	34	27	70 (64–78)
	Creatinine	31	38	21	50 (46–56)
	Specific gravity	34	31	26	63 (58–70)
Zn	Uncorrected	636	473	529	1753 (1549–2016)
	Osmolality	678	442	570	1628 (1469–1829)
	Creatinine	530	386	429	1226 (1109–1374)
	Specific gravity	654	400	572	1509 (1370–1683)
Mo	Uncorrected	101	109	64	336 (286–403)
	Osmolality	98	88	70	268 (235–310)
	Creatinine	80	79	57	222 (194–258)
	Specific gravity	93	80	70	248 (220–285)
Cu	Uncorrected	11	7	9	24 (22–27)
	Osmolality	11	7	10	20 (19–22)
	Creatinine	9	7	7	16 (15–17)
	Specific gravity	11	7	9	18 (17–19)
Ni	Uncorrected	5.7	9.1	3.5	15.6 (13.4–18.6)
	Osmolality	5.5	7.8	3.4	14.4 (12.6–16.8)
	Creatinine	4.5	6.8	2.7	11.9 (10.4–14.0)
	Specific gravity	5.5	7.8	3.4	14.4 (12.6–16.8)
As	Uncorrected	7.1	10.4	3.9	22.1 (18.8–26.6)
	Osmolality	6.7	8.0	4.2	18.1 (15.9–21.1)
	Creatinine	5.6	6.7	3.6	16.7 (14.5–19.8)
	Specific gravity	6.6	7.7	4.2	18.1 (15.8–21.1)
Cd	Uncorrected	0.20	0.23	0.20	0.34 (0.31–0.38)
	Osmolality	0.20	0.19	0.16	0.55 (0.48–0.64)
	Creatinine	0.16	0.17	0.11	0.46 (0.40–0.54)
	Specific gravity	0.20	0.20	0.16	0.51 (0.45–0.58)
Sn	Uncorrected	1.70	6.56	0.09	0.47 (0.37–0.58)
	Osmolality	2.24	7.71	0.11	0.51 (0.43–0.63)
	Creatinine	2.02	7.44	0.08	0.76 (0.61–0.98)
	Specific gravity	2.30	8.35	0.10	0.81 (0.65–0.98)
Sb	Uncorrected	0.16	0.33	0.08	0.46 (0.39–0.55)
	Osmolality	0.17	0.31	0.09	0.50 (0.43–0.60)
	Creatinine	0.14	0.22	0.06	0.42 (0.36–0.50)
	Specific gravity	0.16	0.26	0.09	0.46 (0.40–0.55)
Cs	Uncorrected	2.9	2.9	2.1	7.9 (6.9–9.1)
	Osmolality	3.0	2.6	2.2	6.9 (6.2–7.8)
	Creatinine	2.4	2.1	1.8	5.8 (5.1–6.6)
	Specific gravity	3.0	2.6	2.2	7.3 (6.6–8.3)
Ba	Uncorrected	6.6	19.8	1.7	13.4 (11.0–16.9)
	Osmolality	6.4	17.0	2.0	14.1 (11.7–17.6)
	Creatinine	6.1	26.8	1.6	13.4 (11.0–17.0)
	Specific gravity	6.4	16.3	2.0	14.8 (12.1–18.5)
Pb	Uncorrected	0.7	0.9	0.5	1.9 (1.6–2.2)
	Osmolality	0.9	1.8	0.5	1.6 (1.5–1.9)
	Creatinine	0.7	1.1	0.4	1.3 (1.2–1.5)
	Specific gravity	0.9	1.8	0.5	1.4 (1.3–1.6)

Acknowledgements

This research was supported by the BGS-NERC grant NE/R000069/1 entitled Geoscience for Sustainable Futures and BGS Centre for Environmental Geochemistry programmes for financial support. It was delivered via the BGS Eastern Africa Official Development Assistance (ODA) Research Platform. We would like to thank the many people who assisted in the collection of samples, including the Public Health Officers from each county administrative area and in particular the field and laboratory staff from the University of Eldoret (UoE), Moi University (Moi U) and BGS. David Samoie, Doreen Meso, Charles Owano (UoE), Esilaba Anabwani, Amimo Anabwani (Moi U), Nicholas Porter, Sophia Dowell (BGS). Thanks also to David Gardner at the University of Nottingham School of Veterinary Sciences for creatinine and osmolality measurements. This manuscript is published with the permission of the

Executive Director of the British Geological Survey.

Appendix A. Supplementary data

Supplementary data to this article can be found online at https://doi.org/10.1016/j.ijheh.2021.113854.

Declarations

The authors declare that there is no financial/personal interest or belief that could affect their objectivity.

Data statement

All data is included in Supplementary information, but without compromising the anonymity of study participants.

References

Abellanosa, C.I.D.G., Ander, E.L., Gowing, C.J.B., 2018. Validation for the Transition of SPSS QI Analyst to the SPC for Excel Program for Quality Control Charting, British Geological Survey Report. CR/18/044N, Free to access online - Validation for the transition of SPSS QI Analyst to the SPC for Excel program for quality control charting | NERC Library Service (worldcat.org) [Accessed online 20/09/21].

Al-Saleh, I., 2020. Reference values for heavy metals in the urine and blood of Saudi women derived from two human biomonitoring studies. Int. J. Hyg Environ. Health 225, 113473.

Angerer, J., Aylward, L.L., Hays, S.M., Heinzow, B., Wilhelm, M., 2011. Human biomonitoring assessment values: approaches and data requirements. Int. J. Hyg Environ. Health 214, 348–360.

Boogaard, P.J., Hays, S.M., Aylward, L.L., 2011. Human biomonitoring as a pragmatic tool to support health risk management of chemicals - examples under the EU REACH programme. Regul. Toxicol. Pharmacol. 59 (1), 125–132.

Farebrother, J., Zimmermann, M.B., Abdallah, F., Assey, V., Fingerhut, R., Gichohi-WainainaIzzeldin, H., Makokha, A., Sagno, K., Untoro, J., Watts, M.J., Andersson, M., 2018. The effect of excess iodine intake from iodized salt and/or groundwater iodine on thyroid function in non-pregnant and pregnant women, infants and children: a multicenter study in East Africa. Thyroid 28, 9.

FAO (Food and Agriculture Organisation), 2019. FBS Data for Kenya. Accessed April 2021. https://faostat.fai.org.

GHBC, 2021. Human Biomonitoring Commission (HBM Commission). Accessed on 19th May 2021. https://www.umweltbundesamt.de/en/topics/health/commissions-working-groups/human-biomonitoring-commission-hbm-commission.

Godeboa, T.R., Paul, C.J., Jeuland, M.A., Tekle-Haimanot, R., 2019. Biomonitoring of metals and trace elements in urine of central Ethiopian populations. Int. J. Hyg Environ. Health 222, 410–418.

Hays, S.M., Nordberg, M., Yager, J.W., Aylward, L.L., 2008. Biomonitoring Equivalents (BE) dossier for cadmium (Cd) (CAS No. 7440-43-9). Regul. Toxicol. Pharmacol. 51, S49–S56.

Hays, S.M., Aylward, L.L., 2009. Using Biomonitoring Equivalents to interpret human biomonitoring data in a public health risk context. J Appl Toxicol 29 (4), 275–288.

Hays, S.M., Aylward, L.L., Gagné, M., Nong, A., Krishnan, K., 2010. Biomonitoring Equivalents for inorganic arsenic. Regul. Toxicol. Pharmacol. 58, 1–9.

Hays, S.M., Aylward, L.L., 2012. Interpreting human biomonitoring data in a public health risk context using Biomonitoring Equivalents. Int. J. Hyg Environ. Health 215 (2), 145–148.

Hays, S.M., Macey, K., Nong, A., Aylward, L.L., 2014. Biomonitoring equivalents for selenium. Regul. Toxicol. Pharmacol. 70, 333–339.

Hays, S.M., Macey, K., Poddalgoda, D., Lu, M., Nong, A., Aylward, L.L., 2016. Biomonitoring equivalents for molybdenum. Regul. Toxicol. Pharmacol. 77, 223–229.

Hays, S.M., Poddalgoda, D., Macey, K., Aylward, L., Nong, A., 2018. Biomonitoring Equivalents for interpretation of urinary iodine. Regul. Toxicol. Pharmacol. 94, 40–46.

HBM4EU, 2021. The European Human Biomonitoring Project, 19th May 2021. https://www.hbm4eu.eu/.

Hoet, P., Jacquerye, C., Deumer, G., Lison, D., Haufroid, V., 2013. Reference values and upper reference limits for 26 trace elements in the urine of adults living in Belgium. Clin. Chem. Lab. Med. 51 (4), 839–849.

Hubert, M., Van der Veeken, S., 2008. Outlier detection for skewed data. J. Chemometr.: J. Chemometr. Soc. 22 (3-4), 235–246.

Human Biomonitoring Commission, 2007. (Kommission “Human-Biomonitoring” des Umweltbundesamtes) Naphthalin/Naphthole und Human-Biomonitoring. Stellungnahme der Kommission “Human-Biomonitoring” des Umweltbundesamtes. Bundesgesundheitsblatt - Gesundheitsforsch. - Gesundheitsschutz 50, 1357–1364.

Hussein, I.S., Min, Y., Ghebremeskel, K., Gaffar, A.M., 2012. Iodine status and fish intake of Sudanese schoolchildren living in the Red Sea and White Nile regions. Publ. Health Nutr. 15, 2265–2271.

IGN Iodine Global Network, 2021. estimates state that 19 countries remain at risk of ID and 10 of iodine excess (SAC data), but that certain population groups e.g. pregnant women, are more at risk. Thirty-nine countries report inadequate intakes in PW. Accessed online 09/06/2021. https://www.ign.org/cm_data/IGN_Global_Scorecard_2021_7_May_2021.pdf.

Joy, E.J.M., Ander, E.L., Young, S.D., Black, C., Watts, M.J., Chilimba, A.D.C., Chilima, B., Siyame, E., Kalimbira, A.A., Hurst, R., Fairweather-Tait, S.J., Stein, A., Gibson, R.S., White, P., Broadley, M., 2014. Dietary mineral micronutrient supplies in Africa. Physiol. Plantarum 151, 208–229.

Kassim, I.A.R., Moloney, G., Busili, A., Nur, A.Y., Paron, P., Jooste, P., Gadain, H., Seal, A.J., 2014. Iodine intake in Somalia is excessive and associated with the source of household drinking water. J. Nutr. 144, 281–375.

Kenya Ministry of Health, 2011. Kenya National Micronutrient Survey 2011, Nutrition and Dietetics Unit. Ministry of Health, Kenya.

Kim, S., Baek, Y.-W., 2016. Korean National Environment Health Survey (KoNEHS), the Past, Present and Future of Human Biomonitoring in Korea, 2nd International conference on Human Biomonitoring, Berlin, 2016. Access April 2021. https://www.umweltbundesamt.de/sites/default/files/medien/378/dokumente/suejin_kim_korean_national_environmental_health_survey_konehs.pdf.

LaKind, J.S., Aylward, L.L., Brunk, C., DiZio, S., Dourson, M., Goldstein, D.A., Kilpatrick, M.E., Krewski, D., Bartels, M.J., Barton, H.A., Boogaard, P.J., Lipscomb, J., Krishnan, K., Nordberg, M., Okino, M., Tan, Y.M., Viau, C., Yager, J.W., Hays, S.M., 2008. Biomonitoring equivalents Expert Workshop. Guidelines for the communication of biomonitoring equivalents: report from the biomonitoring equivalents Expert Workshop. Regul. Toxicol. Pharmacol. 51 (3), S16–S26.

Lee, J.W., Lee, C.K., Moon, C.S., Choi, I.J., Lee, K.J., Yi, S.-K., Jang, B.-K., Yoon, B.J., Kim, D.S., Peak, D., Sul, D., Oh, E., Im, H., Kang, H.S., Kim, J.-H., Lee, J.-T., Kim, K., Park, K.L., Ahn, R., Park, S.H., Kim, S.C., Park, C.-H., Lee, J.H., 2012. Korea national survey for environmental pollutants in the human body 2008: heavy metals in the blood or urine of the Korean population. Int. J. Hyg Environ. Health 215 (4), 449–457.

Legrand, M., Feeley, M., Tikhonov, C., Schoen, D., Li-Muller, A., 2010. Methylmercury blood guidance values for Canada. Can. J. Public Health 101, 28–31.

Medani, A.M.M.H., Elnour, A.A., Saeed, A.M., 2012. Excessive iodine intake, water chemicals and endemic goitre in a Sudanese coastal area. Publ. Health Nutr. 16 (9), 1586–1592.

Middleton, D.R.S., Watts, M.J., Hamilton, E.M., Ander, E.L., Close, R.M., Exley, K.S., Crabbe, H., Leonardi, G.S., Fletcher, T., Polya, D.A., 2016. Urinary arsenic profiles reveal exposures to inorganic arsenic from private drinking water supplies in Cornwall, UK. Sci. Rep. 6, 25656.

Middleton, D.R.S., Munishi, M.O., Menya, D., Marriott, A.L., Mwasamwaja, A.O., Mmbaga, B.T., Samoei, D., Osano, O., Schüz, J., McCormack, V.A., Watts, M.J., 2018. Intra-household agreement of urinary elemental concentrations in Tanzania and Kenya: potential surrogates in case-control studies. J. Expo. Sci. Environ. Epidemiol. 29, 335–343.

Morrens, B., Jonker, H., Hond, E.D., Coertjens, D., Colles, A., Schoeters, G., Van Larebeke, N.V., Nawrot, T., Covaci, A., Nelen, V., Vandermoere, F., Loots, I., 2021. Participant experiences in a human biomonitoring study: follow-up interviews with participants of the Flemish environment and health study. Toxics 9, 69.

NHANES, 2021. National health center for health statistics accessed on May 19th 2021. https://www.cdc.gov/nchs/nhanes/index.htm.

NRC (National Research Council), 2012. Exposure Science in the 21st Century: A Vision and a Strategy. National Academies Press, Washington, DC.

Phiri, F.P., Ander, E.L., Bailey, E.H., Chilima, B., Chilimba, A.D.C., Gondwe, J., Joy, E.M. J., Kalimbira, A.A., Kumssa, D.B., Lark, R.M., Phuka, J.C., Salter, A., Suchdev, P.S., Watts, M.J., Young, S.D., Broadley, M.R., 2019. The risk of selenium deficiency in Malawi is large and varies over multiple spatial scales. Sci. Rep. 9, 6566. https://doi.org/10.1038/s41598-019-43013-z.

Phiri, P., Ander, E.L., Lark, M., Bailey, E., Chilima, B., Gondwe, J., Joy, E., Kalimbira, A., Phuka, J., Suchdev, P., Middleton, D., Hamilton, E.M., Watts, M.J., Young, S.D., 2020. Urine selenium concentration is a useful biomarker for assessing population level selenium status. Environ. Int. 134, 105218.

Phiri, F., Ander, E.L., Lark, R.M., Joy, E.J.M., Kalimbira, A.A., Suchdev, P.S., Gondwe, J., Hamilton, E.M., Watts, M.J., Broadley, M.R., 2021. Spatial analysis of urine zinc (Zn) concentration in Malawi. Environ. Geochem. Health 43, 259–271.

Poddalgoda, D., Macey, K., Jayawardene, I., Krishnan, K., 2016. Derivation of biomonitoring equivalent for inorganic tin for interpreting population-level urinary biomonitoring data. Regul. Toxicol. Pharmacol. 81, 430–436.

Poddalgoda, D., Macey, K., Assad, H., Krishnan, K., 2017. Development of biomonitoring equivalents for barium in urine and plasma for interpreting human biomonitoring data. Regul. Toxicol. Pharmacol. 86, 303–311.

Poddalgoda, D., Macey, K., Hancock, S., 2019. Derivation of biomonitoring equivalents (BE values) for zinc. Regul. Toxicol. Pharmacol. 106, 178–186.

R Core Team, 2020. R: A Language and Environment for Statistical Computing. R Foundation for Statistical Computing, Vienna, Austria. URL. https://www.R-project.org/.

Saravanabhavan, G., Werry, K., Walker, M., Haines, D., Malowany, M., Khoury, C., 2017. Human biomonitoring reference values for metals and trace elements in blood and urine derived from the Canadian Health Measures Survey 2007–2013. Int. J. Hyg Environ. Health 220, 189–200.

Sebotsa, M.L.D., Dannhauser, A., Jooste, P.L., Joubert, G., 2005. Iodine status as determined by urinary iodine excretion in Lesotho two years after introducing legislation on universal salt iodisation. Nutrition 21, 20–24.

Tafere, G., 2020. High variability of iodine in iodised salt and urine from rural households in Sidama zone, Southern Ethiopia: a cross-sectional study. Afr. J. Food Nutr. Sci. 20 (1), 15235–15251.

Tuakila, J., Kabamba, M., Mata, H., Mbuyi, F., 2015. Tentative reference values for environmental pollutants in blood of urine from the children of Kinshasha. Chemosphere 139, 326–333.
Tukey, J.W., 1977. Exploratory Data Analysis, vol. 2, pp. 131–160.
Venance, M.S., Martin, H.D., Kimiye, J., 2020. Iodine status and discretionary choices consumption among primary school children, Kinondoni Tanzania. Pediatr. Health Med. Therapeut. 11, 359–368.
Watts, M.J., Joy, E.J.M., Broadley, M.R., Young, S.D., Ander, E.L., Chilimba, A.D.C., Gibson, R.S., Siyame, E.W.P., Kalimbira, Chilima, B., 2015. Iodine source apportionment in the Malawian diet. Sci. Rep. 5, 1521.
Watts, M.J., Middleton, D.R.S., Marriott, A.L., Humphrey, O.S., Hamilton, E.M., Gardner, A., Smith, M., McCormack, V.A., Menya, D., Munishi, M.O., Mmbaga, B.T., Osano, O., 2019a. Source apportionment of micronutrients in the diets of Kilimanjaro-Tanzania and counties of western Kenya. Sci. Rep. 9, 14447.
Watts, M.J., Middleton, D.R.S., Marriott, A., Humphrey, O.S., Hamilton, E., McCormack, V., Menya, D., Farebrother, J., Osano, O., 2019b. Iodine status in western Kenya: a community-based cross-sectional survey of urinary and drinking water iodine concentrations. Environ. Geochem. Health 42, 1141–1151. https://doi.org/10.1007/s10653-019-00352-0.
Wilhelm, M., Ewers, U., Schulz, C., 2004. Revised and new reference values for some trace elements in blood and urine for human biomonitoring in environmental medicine. Int. J. Hyg Environ. Health 207 (1), 69–73.
Wilhelm, M., Hardt, J., Schulz, C., Angerer, J., 2008. New reference value and the background exposure for the PAH metabolites 1-hydroxypyrene and 1-and 2-naphthol in urine of the general population in Germany: basis for validation of human biomonitoring data in environmental medicine. Int. J. Hyg Environ. Health 211 (3–4), 447–453.
World Health Organization, 1996. Trace Elements in Human Nutrition and Health. World Health Organization.
WHO/FAO (World Health Organisation/Food and Agricultural Organisation of the United Nations), 2004. Vitamin and mineral requirements in human nutrition. WHO, Geneva. Accessed April 2021. http://www.who.int/nutrition/publications/micronutrients/9241546123/en/.
WHO/UNICEF/ICCIDD (World Health Organisation/United Nations Children's Fund/International Council for Control of Iodine Deficiencies Disorders), 2007. Assessment of the Iodine Deficiency Disorders and Monitoring Their Elimination: A Guide for Programme Managers, third ed. World Health Organisation, Geneva. WHO/NDH/01.1.

International Journal of Hygiene and Environmental Health 238 (2021) 113850

Contents lists available at ScienceDirect

International Journal of Hygiene and Environmental Health

journal homepage: www.elsevier.com/locate/ijheh

Identifying psychosocial determinants of water, sanitation, and hygiene (WASH) behaviors for the development of evidence-based Baby WASH interventions (REDUCE program)

Camille Williams [a], Elizabeth D. Thomas [a], Jennifer Kuhl [a], Lucien Bisimwa [b], Nicole Coglianese [b], Sarah Bauler [b], Ruthly François [a], Ronald Saxton [a], Presence Sanvura [b], Jean Claude Bisimwa [b], Patrick Mirindi [b], Jamie Perin [a], Christine Marie George [a,*]

[a] Department of International Health, Johns Hopkins Bloomberg School of Public Health, Baltimore, MD, USA
[b] Food for the Hungry, Washington, DC, USA

ARTICLE INFO

Keywords:
Psychosocial factors
Water
Sanitation
And hygiene
Rural
Formative research
Democratic Republic of the Congo

ABSTRACT

Diarrheal disease remains a leading cause of child mortality, globally. In the Democratic Republic of the Congo (DRC), each year there are an estimated 45 million episodes of diarrhea in children under five years of age. The Reducing Enteropathy, Diarrhea, Undernutrition, and Contamination in the Environment (REDUCE) program seeks to develop theory-driven, evidence-based approaches to reduce diarrheal diseases among young children. The REDUCE prospective cohort study in Walungu Territory in Eastern DRC took guidance from the risks, attitudes, norms, abilities, and self-regulation model, the integrated behavioral model for water, sanitation, and hygiene (WASH), and other behavior change theories to identify psychosocial factors associated with WASH behaviors. Psychosocial factors were measured among 417 caregivers at baseline and caregiver responses to child mouthing of dirty fomites and handwashing with soap was assessed by 5-hour structured observation at the 6-month follow-up. Caregivers who agreed that their child could become sick if they put dirt in their mouth (perceived susceptibility) and caregivers that agreed they could prevent their child from playing with dirty things outside (self-efficacy) were significantly more likely to stop their child from mouthing a dirty fomite. Higher perceived susceptibility, self-efficacy, and disgust, and lower dirty reactivity, were associated with higher handwashing with soap behaviors. This study took a theory-driven and evidence-based approach to identify psychosocial factors to target for intervention development. The findings from this study informed the development of the REDUCE Baby WASH Modules that have been delivered to over 1 million people in eastern DRC.

1. Introduction

Globally, diarrheal disease is a leading cause of mortality for children under five years of age, resulting in nearly 450,000 deaths annually (Collaborators 2018). In the Democratic Republic of the Congo (DRC), there are an estimated 45 million episodes of diarrhea annually in children under the age of 5, resulting in 19,000 deaths (Collaborators 2017). Interventions targeting handwashing with soap before food preparation and after toileting events can reduce the risk of diarrheal disease by 23% (WHO 2014). However, only 19% of the world population washes their hands after contact with human excreta (Prüss-Ustün et al., 2014).

Diarrheal diseases are often transmitted through fecal-oral pathways through ingestion of unclean food and water, and dirty fomites, fingers, and dirt (Wagner and Lanoix 1958). However, most WASH interventions focus on sanitation, water treatment, and/or hand hygiene and often do not emphasize the risk of diarrheal diseases associated with contact with animal feces, such as mouthing dirty fomites and soil (Null et al., 2018; Pickering et al., 2019). The Global Burden of Disease (GBD) study estimated that pathogens that cross the zoonotic barrier are responsible for 28% of diarrheal deaths in children under five (Collaborators, 2016). Recent literature suggests that intervention studies should consider other transmission routes beyond traditional WASH improvements for reducing child diarrheal diseases (Budge et al., 2019; Kwong et al., 2020;

* Corresponding author. Associate Professor, Department of International Health, Program in Global Disease Epidemiology and Control, Johns Hopkins Bloomberg School of Public Health, 615 N. Wolfe Street, Room E5535, Baltimore, MD, 21205-2103, USA.
E-mail address: cmgeorge@jhu.edu (C.M. George).

https://doi.org/10.1016/j.ijheh.2021.113850
Received 17 June 2021; Received in revised form 15 September 2021; Accepted 15 September 2021
Available online 18 October 2021

Ngure et al., 2014; Prendergast et al., 2019). Multiple studies have provided evidence that enteropathogen exposure through child mouthing of dirty fomites and soil can have adverse health outcomes (Delahoy et al., 2018; George et al., 2021; Investigators 2018; Kotloff et al., 2013; Morita et al., 2017). Therefore, effective WASH interventions are needed to target these important fecal exposures pathways for young children.

WASH interventions that incorporate elements of psychosocial theory and target multiple behavioral determinants are more likely to be effective than interventions that seek to promote WASH behavior change by providing information alone (Briscoe and Aboud 2012; Curtis et al., 2011; De Buck et al., 2018). Theory-driven interventions take guidance from behavior change theories and frameworks to identify factors likely to drive, facilitate, or impede behavior change; these factors are often referred to as psychosocial determinants. Some examples of behavior change theories and theory-based approaches for WASH intervention development include protection motivation theory, the health belief model, the integrated behavioral model for water, sanitation, and hygiene (IBM-WASH), the risks, attitudes, norms, abilities, and self-regulation (RANAS) model, the Behavior Center Design (BCD) Behavior Determination Model, and the Focus, Opportunity, Ability and Motivation (FOAM) framework (Aunger and Curtis, 2019; Daniel et al., 2019; Devine et al., 2012; Dreibelbis et al., 2013; Le and Makarchev 2020; Mosler 2012; Prentice-Dunn and Rogers 1986; Rainey and Harding 2005). Identifying the psychosocial determinants of a target behavior, such as handwashing with soap, can inform intervention development through the selection of behavior change techniques to target determinants (Michie and Abraham 2004; Mosler 2012).

The objectives of the Reducing Enteropathy Undernutrition and Contamination in the Environment (REDUCE) program were to: 1) identify fecal exposure pathways that contribute to diarrheal disease, child growth, and child cognitive development in young children in the DRC and 2) develop theory-driven and evidence-based interventions to reduce child morbidity via these pathways. The REDUCE cohort study found that child mouthing of contaminated fomites, *E.coli* in soil and on child hands, and child contact with animals was associated with subsequent diarrhea, impaired child growth, and adverse child cognitive developmental outcomes (George et al., 2021b; George et al., 2021). In order to inform an intervention to address these risk factors identified during the REDUCE cohort study, the objective of this study was to identify psychosocial determinants of two target WASH behaviors: 1) handwashing with soap by caregivers at stool- and food-related events and 2) caregivers stopping a child from mouthing dirty fomites (soil and contaminated surfaces and objects).

2. Methods

2.1. Study design

This prospective cohort study of 417 caregivers of young children was conducted in the Walungu Territory, South Kivu, DRC as part of the REDUCE program. This study enrolled households with at least one child under the age of five years and followed these households for 6 months. The sample size for this analysis was based on the number of caregivers of children under five years of age that were enrolled between June 2018 and January 2019 that had WASH psychosocial factor questionnaire data at baseline and had 5-hour structured observation data available at the 6-month follow-up.

2.2. Questionnaire

At baseline, 15 research assistants, after receiving a 2 month training, administered a structured psychosocial factor questionnaire to caregivers (12 years or older) of a child under five years of age. Items (e.g., "It is difficult to watch children when they are playing outside in the dirt.") to measure psychosocial factors were informed by protection motivation theory (response efficacy), the RANAS model, IBM-WASH, and previous work done by our group on determinants of handwashing with soap (Dreibelbis et al., 2013; George et al., 2017a; Mosler 2012; Prentice-Dunn and Rogers 1986). Using the three models, we developed an approach that incorporates psychosocial factors over multiple levels of influence. All items related to child mouthing were developed for this study. To save time spent in the household, most psychosocial factors were measured with a single item. We assessed the following psychosocial factors: impediments, instrumental attitudes, descriptive norms, injunctive norms, dirt reactivity, disgust, perceived severity, perceived susceptibility, remembering, response efficacy, and self-efficacy. Definitions of each factor are in Table 1.

Psychosocial factor questionnaire items were developed in English, translated into the Bukavu dialect of Swahili, and back translated into English in two iterations. The questionnaire was piloted with 99 individuals before the cohort study and six interviews were conducted with verbal probing techniques, where participants were asked to re-explain the questions back to the interviewer to explore the comprehension of questionnaire items and reasons for a participant's responses (Willis and Artino, 2013). We then conducted a focus group discussion (FGD) with mothers of young children to further refine items and response options. Psychosocial items were modified based on piloting, interviews, and FGD findings, as well as concurrent formative research refers to Kuhl et al. (2021) ahead of inclusion in the final questionnaire for the cohort study (Kuhl et al., 2021). Response options for each item were a Likert-type scale ranging from one to five (e.g., 1 = strongly disagree, 2 = disagree, 3 = neither agree nor disagree, 4 = agree, 5 = strongly agree).

2.3. Structured observations

A trained research assistant conducted a 5-hour structured observation using a structured questionnaire form at the 6-month follow-up. Observations took place between the hours of 8:00 a.m. and 1:00 p.m. to include as many household members as possible and to ensure that timing for observations was standardized across all households. The

Table 1
Psychosocial factors in behavior change theories, including risk, attitude, norm, ability, and self-regulation (RANAS) model and integrated behavior model in WASH of behavior change and their definition.

Factors	Definition
Impediments	Anticipated barriers and distractions to a behavior (Contzen et al., 2015)
Instrumental Attitudes	Beliefs about the benefits and costs of a behavior (Fishbein and Ajzen, 1977)
Descriptive Norms	Perceptions about which behaviors are typically performed by others (Mosler, 2012)
Dirt Reactivity	Only washing hands with soap in response to dirt, feces, or smell (George et al., 2017a)
Disgust	Revulsion that is occasioned by the sight of excreta, rotten food, slime, and bugs (Curtis and Biran, 2001)
Injunctive Norms	Perceptions of which behaviors are typically approved or disapproved of by relatives, friends, or neighbors (also the dos and don'ts expressed by religious, civil or other institutional leaders) (Schultz et al., 2007)
Perceived Severity	A person's perception of the seriousness of the consequences of contracting an illness (Prentice-Dunn and Rogers, 1986)
Perceived Susceptibility	A person's perception of his or her risk of contracting diarrheal disease and other illnesses (Orbell et al., 2009)
Remembering	To perform a behavior, it has to be remembered at the right time/situation (Tobias, 2009)
Response Efficacy	Judgments about the efficacy of a preventive response that will avert the perceived threat (Prentice-Dunn and Rogers, 1986)
Self-efficacy	The belief in one's capabilities to organize and execute the courses of action required to manage prospective behaviors; the ability to deal with barriers that arise when trying to maintain the behavior (Bandura, 1997)

research assistant sat in a part of the household defined as a common living space used for cooking, sleeping, and other indoor/outdoor activities to observe household activities with minimal movement and interaction with the household members. Households were informed that research assistants were observing daily activities, without specifying WASH-related events to reduce the Hawthorne effect (Adair 1984).

Child mouthing events. For child mouthing events, research assistants recorded whether a child under five years of age put food or dirty fomites in their mouth during the structured observation period. A dirty fomite was defined as a child putting mud, soil, clay, sand, feces, or an object or surface with visible dirt to or inside their mouth. The object was considered visibly dirty if it had visible mud, soil, clay, sand, or feces on its surface. Information was also collected on whether a caregiver over the age of 12 years stopped a child from mouthing a dirty fomite during structured observation, defined as a participant: 1) physically stopping the child from putting the substance in their mouth, 2) physically stopping the child from handling the dirty fomite, 3) removing the dirty fomite from the child's mouth, or 4) removing the substance from the child's hand.

Handwashing at food- and stool-related events. During structured observation, research assistants recorded handwashing practices for caregivers 12 years of age or older at the following stool- and food-related events: (1) before preparing food, (2) before eating, (3) before serving food/feeding a child, (4) after a toileting event, defined as after use of a sanitation option (e.g., toilet or improved or unimproved latrine), after cleaning a child's anus after a defecation event, and (6) after disposal/removal of child feces.

2.4. Statistical analysis

All statistical analyses were conducted in SAS Version 9.4 (SAS Institute Inc., Cary, NC). Pearson correlations were calculated for psychosocial factors at baseline. Our handwashing with soap outcome was a binary variable defined as a caregiver washing both hands with soap during a food- or stool-related event at least once during structured observation. Our caregiver response to a child mouthing event outcome was a binary variable defined as a caregiver stopping a child from mouthing a dirty fomite at least once during the 5-h structured observation. Logistic regression models using generalized estimating equations to account for clustering within households were conducted to estimate the odds of caregivers handwashing with soap at key events and stopping a child from mouthing a dirty fomite event at least one time during 5-h structured observation at the 6-month follow-up, with psychosocial items at baseline as predictors. Responses to psychosocial items were transformed to a scale of 0–1 by dividing each Likert-type scale response by 5 for regression analyses to make odds ratios easier to interpret (e.g., observed behavior associated with the participant strongly agreeing with a psychosocial item).

2.5 Ethical approval

Informed consent was obtained by all study participants. If the participant was between 12 and 17 years old, assent was obtained along with parental permission from the child's guardian. This study was approved by the research ethical review committee of the University of Kinshasa (Protocol 043–2017) and the Johns Hopkins Bloomberg School of Public Health (Protocol 8057).

3. Results

3.1. Characteristics and demographics of study participants

From June 2018 to January 2019, 417 caregivers over the age of 12 years with at least one child under the age of five years were enrolled in the cohort study and administered the structured psychosocial factor questionnaire at baseline. There were 50 participants who did not have data at the 6-month follow-up (12% (50/417) loss to follow up). The mean age of participants was 30 years (standard deviation: 13, range 12–84) and 82% (340/417) were female. Among study participants, 67% (280/417) of caregivers had at least a primary-school level of education. There were 209 caregivers who had both handwashing at key events and child mouthing events during 5-hour structured observations. Baseline demographics and characteristics can be found in Table 2.

3.2. Analysis of psychosocial factors

The two largest Pearson correlation for psychosocial items at baseline were perceived susceptibility and dirt reactivity (Supplementary Tables 1 and 2).

3.3. Participants stopping a child mouthing a dirty fomite

Two hundred thirty-nine caregivers were present during a child mouthing event during structured observation at the 6-month follow-up. Thirty-nine percent (93/239) of these caregivers stopped a child at least once from mouthing a dirty fomite during structured observation. Caregivers who agreed that a child could become sick if they put dirt in their mouth (perceived susceptibility) were more likely to stop a child from mouthing a dirty fomite (Odds Ratio (OR) = 1.28 95% Confidence Interval (CI) = 1.02–1.61). Caregivers who were sure they could prevent their child from playing with dirty things outside were more likely to stop a child from mouthing a dirty fomite (OR = 1.21; 95% CI = 1.01–1.44) (Table 3).

3.4. Handwashing with soap at food- and stool-related events

Two hundred twenty caregivers had a stool- or food-related event during structured observations at the six-month follow-up. Fourteen percent (30/220) of these caregivers washed both of their hands with soap at least once during these events. Caregivers who felt compelled to wash their hands with soap after toileting due to disgust (OR = 1.85 (95% CI = 1.04, 3.30) (disgust) were more likely to wash both hands

Table 2
Baseline demographics and characteristics among caregivers of children under five years in Walungu, South Kivu, Democratic Republic of the Congo.

	%	n
Caregivers		417
Caregiver baseline age (years) Median SD (min-max)	30 ± 13 (12–84)	
Households		261
Children <5 years		465
Caregiver any formal education	67%	280
Gender		
Female	82%	340
Household wall type		
Mud walls	59%	154
Wood walls	7%	18
Concrete walls	4%	10
Wood and mud walls	4%	11
Biomass walls	5%	12
Brick walls	3%	8
Wood and concrete walls	1%	3
Other	20%	53
Household animal ownership	52%	135
Unimproved latrine	92%	239
Water source type		
Protected spring	62%	162
Public tap	23%	59
Unprotected spring	4%	10
Other	5%	13
Household size Median SD (min-max)	6 ± 2.4 (2–17)	

SD: standard deviation; unimproved latrine: use of pit latrines without a slab or platform, hanging latrines, or bucket latrines; any formal education: primary, secondary, or not finished secondary school.

Table 3
Logistic regression analysis of psychosocial factors (predictor) and caregivers atopping a child during a mouthing of a dirty fomite event (outcome) during 5-hour structured observation (N = 239).

Factor Category	[a]Item	M	SD	OR (95% CI)
Impediments	It is difficult to watch children when they are playing outside in the dirt	3.57	1.58	1.00 (0.85, 1.17)
Descriptive Norms	Most of (many among) the people in your village let their young children eat dirt	4.03	1.36	0.95 (0.80, 1.13)
Perceived Severity	If your child(ren) less than 2 years of age gets diarrhea, how severely would that impact your life?	4.43	1.18	1.04 (0.83, 1.29)
	[b]How likely is it that someone who develops diarrhea will die?	4.42	1.10	0.86 (0.69, 1.07)
Perceived Susceptibility	It is not harmful for a child to play outside in the dirt	2.9	1.72	0.87 (0.75, 1.01)
	It is not harmful for a child to eat dirt	2.44	1.66	0.90 (0.77, 1.06)
	It is not harmful for children to pick up used wrappers or bottles from the ground and put them in their mouths	2.42	1.63	0.94 (0.80, 1.10)
	Eating dirt is good for your child's health	1.77	1.3	0.91 (0.75, 1.10)
	Your child will become sick if they put dirt in their mouth	**4.31**	**1.18**	**1.33 (1.04, 1.69)**
	There is no need to clean up after a child defecates in the dirt	2.62	1.67	0.90 (0.78, 1.05)
	How likely is it that your child will develop diarrhea in the next month? Do you think it is unlikely or likely?	3.53	1.37	1.12 (0.93, 1.33)
Self-efficacy	[c]How sure are you that you can protect your child from getting diarrhea?	3.50	1.51	1.2 (1.00, 1.44)
	[c]How sure are you that you can prevent your child from eating dirt?	3.21	1.53	1.09 (0.91, 1.29)
	[c]How sure are you that you can prevent your child from playing with dirty things outside?	**3.24**	**1.51**	**1.21 (1.01, 1.44)**

M: Mean (Likert-scale); SD: Standard Deviation; OR: Odds Ratio; L95%CI: Lower 95% Confidence Interval, U95%CI: Upper 95% Confidence Interval; Boldface indicates significant effects $p < 0.05$; [a]Factors are ordinal and range from 1 to 5 based on responses to psychosocial questions. Answering options were as follows unless otherwide noted: 1 = strongly disagree, 2 = disagree, 3 = neither agree nor disagree, 4 = agree, 5 = strongly agree; [b]The answering options were as follows: 1 = extremely unlikely, 2 = unlikely, 3 = neither likely nor unlikely, 4 = likely, 5 extremely likely; [c]The answering options were as follows: 1 = not sure at all, 2 = not sure, 3 = neither sure nor not sure, 4 = a little sure, 5 = very sure.

Table 4
Logistic regression analysis of psychosocial factors (predictor) and handwashing with soap at a key stool- or food-related event (outcome) during 5-hour structured observation (N = 220).

Factor Category	[a]Item	M	SD	OR (95% CI)
Impediments	If you put soap near the latrine (WC) people will steal it	3.86	1.50	1.00 (0.77, 1.31)
	You have a specific place in your home to wash your hands with soap	2.64	1.75	1.17 (0.94, 1.46)
	It is hard to find water to wash hands with soap	2.27	1.47	0.98 (0.80, 1.20)
Convenience	You have too little time to wash your hands with soap	3.54	1.49	0.97 (0.73, 1.30)
Descriptive Norms	Most of (many among) your neighbors don't wash their hands with soap	3.99	1.32	0.93 (0.70, 1.24)
Dirt Reactivity	If your hands look clean, there are no germs on them	2.93	1.69	0.99 (0.75, 1.32)
	You only wash your hands with soap when they have dirt on them	3.53	1.61	0.83 (0.66, 1.04)
	You only wash your hands with soap when they are sticky (when they have sticky things on them)	3.37	1.65	0.90 (0.72, 1.13)
	You only wash your child's hands with soap when they are sticky (when they have sticky things on them)	**3.42**	**1.62**	**0.75 (0.59, 0.95)**
	You only wash your child's hands with soap when they have dirt on them	**3.43**	**1.60**	**0.76 (0.59, 0.96)**
Disgust	After toileting (using the WC), you are compelled to wash your hands with soap because you feel your hands are disgusting	**4.10**	**1.34**	**1.85 (1.04, 3.30)**
	You feel your hands are disgusting after cleaning up a child's feces	3.50	1.61	1.31 (1.00, 1.73)
Injunctive Norms	Visitors will respect you if they find a place to wash hands with soap at your home	4.38	1.09	1.05 (0.72, 1.53)
Instrumental Attitudes	It is burdensome to always wash your hands with soap (every time and every day)	3.28	1.60	0.96 (0.77, 1.21)
	Soap is too costly to use for handwashing	3.38	1.60	0.86 (0.67, 1.10)
	You do not have enough time to wash your child's hands with soap	3.38	1.48	0.99 (0.80, 1.23)
Perceived Severity	If your child(ren) less than 2 years of age gets diarrhea, how severely would that impact your life?	4.43	1.18	0.94 (0.67, 1.31)
	[b]How likely is it that someone who develops diarrhea will die?	4.42	1.10	1.15 (0.77, 1.71)
Perceived Susceptibility	[b]How likely is it that your child will develop diarrhea in the next month?	**3.53**	**1.37**	**1.43 (1.02, 2.00)**
Remembering	It is hard to remember to wash your hands with soap while preparing a meal	3.48	1.51	0.88 (0.71, 1.10)
	Washing your hands with soap after using the toilet (WC) is hard to remember	3.17	1.61	0.95 (0.73, 1.22)
	It is hard to remember to wash your child's hands with soap	3.18	1.56	1.21 (0.92, 1.57)
Response Efficacy	[b]How likely is it that your child will get diarrhea if you always (every time and every day) wash your hands with soap?	3.31	1.49	0.97 (0.78, 1.20)
Self-efficacy	[c]How sure are you that you can make soap for handwashing available for your family every day?	3.46	1.48	1.08 (0.85, 1.37)
	[c]How sure are you that you can always (every time and every day) wash your hands with soap after using the toilet (after WC)?	**3.86**	**1.35**	**1.41 (1.01, 1.98)**
	[c]How sure are you that you can always (every time and every day) wash your hands with soap before feeding your child?	**4.08**	**1.30**	**1.50 (1.02, 2.18)**
	[c]How sure are you that you can protect your child from getting diarrhea?	3.50	1.51	1.19 (0.92, 1.53)

M: Mean (Likert-scale); SD: Standard Deviation; OR: Odds Ratio; L95%CI: Lower 95% Confidence Interval, U95%CI: Upper 95% Confidence Interval; Boldface indicates significant effects $p < 0.05$; [a]Factors are ordinal and range from 1 to 5 based on responses to psychosocial questions. Answering options were as follows unless otherwide noted: 1 = strongly disagree, 2 = disagree, 3 = neither agree nor disagree, 4 = agree, 5 = strongly agree; [b]The answering options were as follows: 1 = extremely unlikely, 2 = unlikely, 3 = neither likely nor unlikely, 4 = likely, 5 extremely likely; [c]The answering options were as follows: 1 = not sure at all, 2 = not sure, 3 = neither sure nor not sure, 4 = a little sure, 5 = very sure.

with soap during key handwashing events at the 6-month follow-up. Caregivers who agreed that they could always wash their hands with soap after a toileting event were more likely to wash both hands with soap (OR = 1.41 (95% CI = 1.01–1.98)) (self-efficacy). Caregivers who agreed they could always wash their hands with soap before feeding their child were more likely to wash their hands with soap (OR = 1.50, (95% CI = 1.02–2.18)) (self-efficacy). Caregivers who agreed that they only wash their child's hands when they are sticky (OR = 0.75 (95% CI = 0.59–0.95)) or have dirt on them (OR = 0.76, 95% CI = 0.69–0.96) (dirt reactivity) were less likely to wash their own hands with soap. Caregivers who agreed their child was likely to develop diarrhea in the next month were more likely to wash their own hands with soap (OR = 1.43, (95% CI = 1.02–2.00) (Table 4).

4. Discussion

This prospective cohort study investigated the psychosocial determinants of stopping a child from mouthing a dirty fomite and handwashing with soap at stool- and food-related events among caregivers with a young child in their household in rural DRC. Caregivers who believed a child would become sick if the child put dirt in their mouth (high perceived susceptibility) and who were sure they could prevent a child from playing with dirty things outside at baseline (higher self-efficacy) were more likely to stop a child from mouthing a dirty fomite during structured observation at the 6-month follow-up. Higher baseline self-efficacy and higher perceived susceptibility around handwashing with soap at key food- and stool-related events were associated with increased handwashing with soap at the 6-month follow-up. Caregivers who said that they only washed their child's hands when they appeared dirty or sticky (high dirt reactivity) were less likely to wash their own hands with soap. However, those that felt their hands were disgusting after coming into contact with feces were more likely to wash their hands with soap at follow-up. This is the first published study, to our knowledge, investigating WASH psychosocial factors associated with caregivers' response to child mouthing behaviors. This study took a theory-driven and evidence-based approach to identify psychosocial factors to target for intervention development. These findings were applied to develop the REDUCE Baby WASH intervention modules that have been delivered to over 1 million people in South Kivu and Tanganyika provinces of DRC Kuhl et al. (2021).

Higher perceived susceptibility and higher self-efficacy related to child mouthing practices were associated with a caregiver stopping a child from mouthing a dirty fomite in our cohort study. The only other paper to our knowledge that has investigated psychosocial factors related to child mouthing behaviors is Wodnik et al., who developed items using the Capability Opportunity Motivation and Behavior (COM-B) model on provision of a safe play environment for children in Kenya (Wodnik et al., 2018). However, this previous study did not investigate the association between caregivers' responses to child mouthing behaviors and WASH psychosocial determinants. Previous studies in rural Bangladesh have found that child mouthing behavior of soil and dirty fomites is associated with environmental enteropathy and impaired growth in children under five years (Morita et al., 2017). Additionally, studies in urban Kenya and rural Ghana found an association between mouthing soil and diarrhea (Bauza et al. 2017, 2018). These findings emphasize the need for studies to identify the psychosocial determinants driving participant responses to child mouthing behaviors to develop interventions that target reducing child mouthing of dirty fomites.

The finding that perceived susceptibility and higher self-efficacy were psychosocial determinants of stopping children from mouthing dirty fomites informed the development of the REDUCE Baby WASH Child Mouthing Module. A pictorial flipbook delivered by a health promoter was developed targeting perceived susceptibility of diarrheal diseases from child mouthing practices through images of worms in the stomach of a child that mouthed dirty fomites, and a story of a child that mouthed dirt and then had to be admitted to the hospital with severe diarrhea. A locally-sourced play mat was also provided to create an enabling environment which made it easier for caregivers to keep young children off the ground to reduce child contact with contaminated soil in their environment (Kuhl et al., 2021). Caregivers reported that playmats reduced child mouthing of dirty fomites and enabled caregivers to have more ease when conducting household chores, since they knew their young child was sitting on the playmat (self-efficacy) (Kuhl et al., 2021).

Higher self-efficacy was found to be associated with handwashing with soap in our cohort study. These findings are consistent with the current literature demonstrating that perceived severity and self-efficacy are important psychosocial determinants of handwashing with soap behaviors (Contzen and Inauen 2015; Contzen et al., 2015; De Wandel et al., 2010; Scott et al., 2007). A study in Ethiopia and Haiti found that higher self-efficacy was positively associated with handwashing with soap behaviors at food- and feces-related events (Contzen and Inauen 2015; Contzen and Mosler 2015). However, this study was cross-sectional and used self-reported handwashing with soap behaviors instead of structured observation. In our recent randomized controlled trial (RCT) of the CHoBI7 WASH mobile health program, we found self-efficacy was a significant mediator of handwashing with soap habit maintenance at the 12-month follow-up (George et al., 2021a). These findings highlight the need to target self-efficacy in handwashing with soap interventions.

Our finding that disgust was significantly associated with higher handwashing with soap behaviors among caregivers is consistent with findings from Contzen et al. in Ethiopia and Haiti (Contzen and Mosler 2015). This result is also consistent with a study conducted in Kenya, which found that disgust was a motivating factor for handwashing with soap behaviors (Aunger et al., 2010). Porzig-Drummond et al. reported that disgust-based interventions were significantly more effective in increasing handwashing with soap behaviors compared to education- and technology-only hand hygiene interventions (Porzig-Drummond et al., 2009). An eleven-country review of determinants of handwashing with soap found disgust to be a key motivator of handwashing with soap behavior (Curtis et al., 2009). In our previous RCT in Bangladesh, disgust was a significant mediator of handwashing with soap habit maintenance (George et al., 2017a). These findings demonstrate the important role of disgust in facilitating handwashing with soap behaviors.

High dirt reactivity was found to reduce handwashing with soap behavior among caregivers in our cohort study. Dirt reactivity can be an important barrier for handwashing with soap, as people will only wash their hands when their hands look dirty, rather than washing them during all key handwashing events. Previous qualitative research has found that olfactory cues and feeling dirty are key contributors to handwashing with soap behaviors (Scott et al., 2007). Our findings are consistent with a study in Indonesia, where hands feeling dirty was a key motivator for handwashing with soap (Hirai et al., 2016). Our previous RCTs in Bangladesh also found high dirt reactivity to be associated with less handwashing with soap (George et al., 2017a; George et al., 2021a). Our findings suggest that reducing hand-dirt reactivity as a barrier could improve handwashing with soap at food- and stool-related events. The role of dirt reactivity on handwashing with soap behaviors should be investigated in future studies in other contexts.

High perceived susceptibility was significantly associated with higher handwashing with soap at food- and stool-events among caregivers at the 6-month follow-up. This finding is consistent with previous studies that found perceived susceptibility to be a factor in a person's decision to wash their hands with soap (Contzen et al., 2015; Scott et al., 2007). Previous WASH intervention studies have found that targeting perceived susceptibility in behavior change communication can lower this psychosocial factor because those who adhere to the intervention feel less vulnerable to diarrheal diseases (George et al., 2017b; George et al., 2021a; Inauen and Mosler 2014).

Psychosocial determinants of handwashing with soap found in this study were targeted in the development of the REDUCE Baby WASH

Handwashing with Soap Module. The Handwashing with Soap Module promoted a tippy tap to increase self-efficacy by providing an enabling technology to make handwashing with soap at stool- and food-related events easier for caregivers (Kuhl et al., 2021). A pictorial flipbook explained how to construct tippy taps (a low-cost, locally-made handwashing station) and prepare soapy water (water and detergent powder), a low-cost alternative to bar soap. Perceived susceptibility was targeted by creating stories about how severe diarrhea can be transmitted to children. In the module, the pictorial flipbook targeted dirt reactivity through stating that even hands that appeared to be clean by the eye could still have intestinal worms and germs that can make young children sick with severe diarrhea.

There are several strengths in this study. First, this study investigated psychosocial WASH factors and their association to caregivers stopping a child from mouthing a dirty fomite. This is a potential transmission route that is not often focused on in WASH interventions. Second, this study measured handwashing with soap behaviors using 5-hour structured observations. This approach enabled us to observe behaviors rather than relying on caregivers' reports. Third, we conducted a prospective analysis that measured psychosocial factors at baseline and WASH behaviors at the 6-month follow-up.

This study has some limitations. The 5-hour structured observation could be subject to the Hawthorne effect (Adair 1984). We tried to reduce this bias by not telling caregivers what we were observing, rather that we were there to observe day-to-day activities. In addition, given the long time-gap between the baseline questionnaire and the structured observation, the potential for this study to have substantial Hawthorne effect is low. Second, we were not able to distinguish between food- and stool-related handwashing events in our analysis; these events were combined to any key event to increase statistical power. Third, this analysis focused on psychosocial at the household, individual and habitual levels of IBM-WASH. Future studies should include items that measure contextual and technological factors that also influence WASH behaviors at the interpersonal, community, and structural levels.

5. Conclusion

Our findings supported the development of the REDUCE Baby WASH modules currently being delivered to over 1 million beneficiaries in South Kivu and Tanganyika provinces of DRC. This is the first study published investigating psychosocial determinants of WASH behaviors in rural DRC. This study took a theory-driven and evidence-based approach to identify psychosocial determinants of WASH behaviors, and developed intervention modules to intervene upon the identified determinants. In addition to supporting the development of targeted WASH interventions in rural DRC, these findings highlight a gap in current literature focusing on psychosocial factors that influence WASH behaviors, in particular, caregivers stopping a child from mouthing dirty fomites. Given the growing literature demonstrating that child mouthing of dirty fomites is associated with diarrheal disease, environmental enteropathy, and impaired growth, further studies are needed that investigate the behavioral determinants driving caregiver responses to child mouthing events.

Declaration of competing interest

No authors have a conflict of interest.

Acknowledgement

We thank USAID/Bureau for Humanitarian Assistance and Phil Moses and Amagana Togo at Food for the Hungry for their support. We also thank all the study participants and the following research supervisors and assistants who were crucial to the successful implementation of this study: Willy Mapendano, Eric-Yves Iragi, Pascal Tezangi, Blessing Muderhwa, Manu Kabiyo, Fraterne Luhiriri, Wivine Ntumba, Julienne Rushago, Pacifique Kitumaini, Freddy Endelea, Claudia Bazilerhe, Jean Claude Lunye Lunye, Adolophine F. Rugusha, Gisele N. Kasanzike, Brigitte Munyerenkana, Jessy T. Mukulikire, Dieudonné Cibinda, Jean Basimage, and Siloé Barhuze. These individuals were supported by funding from the USAID and declare no conflicts of interest. This material is based in part upon work supported by the USAID Bureau for Humanitarian Assistance (BHA), under a Development Food Security Activity (DFSA), led by Food for the Hungry in the Sud Kivu and Tanganyika provinces of DRC (Cooperative Agreement AID-FFP-A-16-00010). Any opinion, findings, and conclusions or recommendations expressed in this material are those of the author and do not necessarily reflect the views of partner organizations or the U.S. Government.

Appendix A. Supplementary data

Supplementary data to this article can be found online at https://doi.org/10.1016/j.ijheh.2021.113850.

References

Adair, J.G., 1984. The hawthorne effect: a reconsideration of the methodological artifact. J. Appl. Psychol. 69, 334–345.
Aunger, R., Curtis, V., 2019. Bcd Framework Behavior Change Design Resources Website.
Bauza, V., Ocharo, R.M., Nguyen, T.H., Guest, J.S., 2017. Soil ingestion is associated with child diarrhea in an urban slum of nairobi, Kenya. Am. J. Trop. Med. Hyg. 16, 0543.
Aunger, R, Schmidt, W.P., Ranpura, A, Coombes, Y, Maina, M.P., Matiko, C.N., Curtis, V., 2010. Three kinds of psychological determinants for hand-washing behaviour in Kenya. Soc. Sci. Med. 70 (3), 383–391. https://doi.org/10.1016/j.socscimed.2009.10.038.
Bandura, A., 1997. Self-efficacy: The exercise of control. W H Freeman/Times Book/Henry Holt & Co.
Bauza, V., Byrne, D.M., Trimmer, J.T., Lardizabal, A., Atiim, P., Asigbee, M.A.K., et al., 2018. Child soil ingestion in rural Ghana - frequency, caregiver perceptions, relationship with household floor material and associations with child diarrhoea. Trop. Med. Int. Health 23, 558–569.
Briscoe, C., Aboud, F., 2012. Behaviour change communication targeting four health behaviours in developing countries: a review of change techniques. Soc. Sci. Med. 75, 612–621.
Budge, S., Hutchings, P., Parker, A., Tyrrel, S., Tulu, T., Gizaw, M., et al., 2019. Do domestic animals contribute to bacterial contamination of infant transmission pathways? Formative evidence from Ethiopia. J. Water Health 17, 655–669.
Collaborators, G.B.D., 2016. Global, regional, and national life expectancy, all-cause mortality, and cause-specific mortality for 249 causes of death, 1980–2015: a systematic analysis for the global burden of disease study 2015. Lancet 388, 1459–1544.
Collaborators, G.D.D., 2017. Estimates of global, regional, and national morbidity, mortality, and aetiologies of diarrhoeal diseases: a systematic analysis for the global burden of disease study 2015. Lancet Infect. Dis. 17, 909–948.
Collaborators, G.D.D., 2018. Estimates of the global, regional, and national morbidity, mortality, and aetiologies of diarrhoea in 195 countries: a systematic analysis for the global burden of disease study 2016. Lancet Infect. Dis. 18, 1211–1228.
Contzen, N., Inauen, J., 2015. Social-cognitive factors mediating intervention effects on handwashing: a longitudinal study. J. Behav. Med. 38, 956–969.
Contzen, N., Mosler, H.-J., 2015. Identifying the psychological determinants of handwashing: results from two cross-sectional questionnaire studies in Haiti and Ethiopia. Am. J. Infect. Contr. 43, 826–832.
Contzen, N., Meili, I.H., Mosler, H.-J., 2015. Changing handwashing behaviour in southern Ethiopia: a longitudinal study on infrastructural and commitment interventions. Soc. Sci. Med. 124, 103–114.
Curtis, V., Biran, A., 2001. Dirt, disgust, and disease. Is hygiene in our genes? Perspect. Biol. Med. 44 (1), 17–31. https://doi.org/10.1353/pbm.2001.0001.
Curtis, V., Danquah, L.O., Aunger, R.V., 2009. Planned, motivated and habitual hygiene behaviour: an eleven country review. Health Educ. Res. 24, 655–673.
Curtis, V., Schmidt, W., Luby, S., Florez, R., Touré, O., Biran, A., 2011. Hygiene: new hopes, new horizons. Lancet Infect. Dis. 11, 312–321.
Daniel, D., Diener, A., Pande, S., Jansen, S., Marks, S., Meierhofer, R., et al., 2019. Understanding the effect of socio-economic characteristics and psychosocial factors on household water treatment practices in rural Nepal using bayesian belief networks. Int. J. Hyg Environ. Health 222, 847–855.
De Buck, E., Hannes, K., Cargo, M., Van Remoortel, H., Vande Veegaete, A., Mosler, H.-J., et al., 2018. Engagement of stakeholders in the development of a theory of change for handwashing and sanitation behaviour change. Int. J. Environ. Health Res. 28, 8–22.
De Wandel, D., Maes, L., Labeau, S., Vereecken, C., Blot, S., 2010. Behavioral determinants of hand hygiene compliance in intensive care units. Am. J. Crit. Care 19, 230–239.
Delahoy, M.J., Wodnik, B., McAliley, L., Penakalapati, G., Swarthout, J., Freeman, M.C., et al., 2018. Pathogens transmitted in animal feces in low- and middle-income countries. Int. J. Hyg Environ. Health 221, 661–676.

Devine, J., Karver, J., Coombes, Y., Chase, C., Hernandez, O., 2012. Global Scaling up Handwashing Project Behavioral Determinants of Handwashing with Soap Among Mothers and Caretakers: Emergent Learning from senegal and peru. Water and Sanitation Program.

Dreibelbis, R., Winch, P.J., Leontsini, E., Hulland, K.R., Ram, P.K., Unicomb, L., et al., 2013. The integrated behavioural model for water, sanitation, and hygiene: a systematic review of behavioural models and a framework for designing and evaluating behaviour change interventions in infrastructure-restricted settings. BMC Publ. Health 13, 1015.

George, C.M., Biswas, S., Jung, D., Perin, J., Parvin, T., Monira, S., et al., 2017a. Psychosocial factors mediating the effect of the chobi7 intervention on handwashing with soap: a randomized controlled trial. Health Educ. Behav. 44, 613–625.

George, C.M., Inauen, J., Perin, J., Tighe, J., Hasan, K., Zheng, Y., 2017b. Behavioral determinants of switching to arsenic-safe water wells: an analysis of a randomized controlled trial of health education interventions coupled with water arsenic testing. Health Educ. Behav. 44, 92–102.

George, C.M., Cirhuza, L.B., Kuhl, J., Williams, C., Coglianese, N., Thomas, E., et al., 2021. Child mouthing of feces and fomites and animal contact are associated with diarrhea and impaired growth among young children in the democratic republic of the Congo: a prospective cohort study (reduce program). J. Pediatr. 228, 110–116 e111.

Fishbein, M.A., Ajzen, I., 1977. Belief, attitude, intention and behaviour: An introduction to theory and research. Reading MA: Addison-Wesley.

George, C.M., Bhuyian, M.S.I., Thomas, E.D., Parvin, T., Monira, S., Zohura, F., et al., 2021a. Psychosocial factors mediating the effect of the chobi7 mobile health program on handwashing with soap and household stored water quality: a randomized controlled trial. Health Educ. Behav., 109019812098713

George, C.M., Cirhuza, L.B., Birindwa, A., Williams, C., Beck, S., Julian, T., et al., 2021b. Child hand contamination is associated with subsequent pediatric diarrhea in rural democratic republic of the Congo (reduce program). Trop. Med. Int. Health 26, 102–110.

Hirai, M., Graham, J., Mattson, K., Kelsey, A., Mukherji, S., Cronin, A., 2016. Exploring determinants of handwashing with soap in Indonesia: a quantitative analysis. Int. J. Environ. Res. Publ. Health 13, 868.

Inauen, J., Mosler, H.-J., 2014. Developing and testing theory-based and evidence-based interventions to promote switching to arsenic-safe wells in Bangladesh. J. Health Psychol. 19, 1483–1498.

Investigators, M.-E.N., 2018. Early childhood cognitive development is affected by interactions among illness, diet, enteropathogens and the home environment: findings from the mal-ed birth cohort study. BMJ Global Health 3, e000752.

Kotloff, K.L., Nataro, J.P., Blackwelder, W.C., Nasrin, D., Farag, T.H., Panchalingam, S., et al., 2013. Burden and aetiology of diarrhoeal disease in infants and young children in developing countries (the global enteric multicenter study, gems): a prospective, case-control study. Lancet 382, 209–222.

Kuhl, J., Bisimwa, L., Thomas, E.D., Williams, C., Ntakirutimana, J., Coglianese, N., et al., 2021. Formative research for the development of baby water, sanitation, and hygiene interventions for young children in the democratic republic of the Congo (reduce program). BMC Publ. Health 21.

Kwong, L.H., Ercumen, A., Pickering, A.J., Unicomb, L., Davis, J., Luby, S.P., 2020. Age-related changes to environmental exposure: variation in the frequency that young children place hands and objects in their mouths. J. Expo. Sci. Environ. Epidemiol. 30, 205–216.

Le, D.A., Makarchev, N., 2020. Latrine use practices and predictors in rural vietnam: evidence from going trom district, ben tre. Int. J. Hyg Environ. Health 228, 113554.

Michie, S., Abraham, C., 2004. Interventions to change health behaviours: evidence-based or evidence-inspired? Pyschology & Health 19.

Morita, T., Perin, J., Oldja, L., Biswas, S., Sack, R.B., Ahmed, S., et al., 2017. Mouthing of soil contaminated objects is associated with environmental enteropathy in young children. Trop. Med. Int. Health 22, 670–678.

Mosler, H.-J., 2012. A systematic approach to behavior change interventions for the water and sanitation sector in developing countries: a conceptual model, a review, and a guideline. Int. J. Environ. Health Res. 22, 431–449.

Ngure, F.M., Reid, B.M., Humphrey, J.H., Mbuya, M.N., Pelto, G., Stoltzfus, R.J., 2014. Water, sanitation, and hygiene (wash), environmental enteropathy, nutrition, and early child development: making the links. Ann. N. Y. Acad. Sci. 1308, 118–128.

Null, C., Stewart, C.P., Pickering, A.J., Dentz, H.N., Arnold, B.F., Arnold, C.D., et al., 2018. Effects of water quality, sanitation, handwashing, and nutritional interventions on diarrhoea and child growth in rural Kenya: a cluster-randomised controlled trial. The Lancet Global Health 6, e316–e329.

Orbell, S., Lidierth, P., Henderson, C., Geeraert, N., Uller, C., Uskul, A.K., Kyriakaki, M., 2009. Social-cognitive beliefs, alcohol, and tobacco use: a prospective community study of change following a ban on smoking in public places. Psychol. Health 28 (6), 753–761. https://doi.org/10.1037/a0016943.

Pickering, A.J., Null, C., Winch, P.J., Mangwadu, G.T., Arnold, B.F., Prendergast, A.J., et al., 2019. The wash benefits and shine trials: interpretation of wash intervention effects on linear growth and diarrhoea. The Lancet Global Health 7, e1139–1146.

Porzig-Drummond, R., Stevenson, R., Case, T., Oaten, M., 2009. Can the emotion of disgust be harnessed to promote hand hygiene? Experimental and field-based tests. Soc. Sci. Med. 68, 1006–1012.

Prendergast, A.J., Chasekwa, B., Evans, C., Mutasa, K., Mbuya, M.N.N., Stoltzfus, R.J., et al., 2019. Independent and combined effects of improved water, sanitation, and hygiene, and improved complementary feeding, on stunting and anaemia among hiv-exposed children in rural Zimbabwe: a cluster-randomised controlled trial. The Lancet Child & Adolescent Health 3, 77–90.

Prentice-Dunn, S., Rogers, R., 1986. Protection motivation theory and preventative health: beyond the health believe model. Health Educ. Res. 1, 153–161.

Prüss-Ustün, A., Bartram, J., Clasen, T., Colford, J.M., Cumming, O., Curtis, V., et al., 2014. Burden of disease from inadequate water, sanitation and hygiene in low- and middle-income settings: a retrospective analysis of data from 145 countries. Trop. Med. Int. Health 19, 894–905.

Rainey, R.C., Harding, A.K., 2005. Acceptability of solar disinfection of drinking water treatment in kathmandu valley, Nepal. Int. J. Environ. Health Res. 15, 361–372.

Schultz, W.P., Nolan, J.M., Cialdini, R.B., Goldstein, N.J., Griskevicius, V., 2007. The constructive, destructive, and reconstructive power of social norms. Psychol. Sci. 18 (5), 429–434. https://doi.org/10.1111/j.1467-9280.2007.01917.x.

Scott, B., Curtis, V., Rabie, T., Garbrah-Aidoo, N., 2007. Health in our hands, but not in our heads: understanding hygiene motivation in Ghana. Health Pol. Plann. 22, 225–233.

Tobias, R., 2009. Changing behavior by memory aids: a social psychological model of prospective memory and habit development tested with dynamic field data. Pyschol Rev. 116 (2), 408–438. https://doi.org/10.1037/a0015512.

Wagner, E.G., Lanoix, J.N., 1958. Excreta disposal for rural areas and small communities. In: Monograph Series. World Health Organization, Switzerland.

WHO, 2014. Preventin Diarrhoea through Better Water Sanitation and Hygiene.

Willis, Gordon B., Artino Jr., Anthony R., 2013. What Do Our Respondents Think We're Asking? Using Cognitive Interviewing to Improve Medical Education Surveys. J. Grad. Med. Educ. 5 (3), 353–356. https://doi.org/10.4300/JGME-D-13-00154.1.

Wodnik, B., Freeman, M., Ellis, A., Awino Ogutu, E., Webb Girard, A., Caruso, B., 2018. Development and application of novel caregiver hygiene behavior measures relating to food preparation, handwashing, and play environments in rural Kenya. Int. J. Environ. Res. Publ. Health 15, 1994.

International Journal of Hygiene and Environmental Health 238 (2021) 113839

Contents lists available at ScienceDirect

International Journal of Hygiene and Environmental Health

journal homepage: www.elsevier.com/locate/ijheh

Increased hospital admissions for asthma from short-term exposure to cold spells in Beijing, China

Yuxiong Chen [a], Dehui Kong [a], Jia Fu [a], Yongqiao Zhang [a], Yakun Zhao [a], Yanbo Liu [a], Zhen'ge Chang [a], Yijie Liu [a], Xiaole Liu [a], Kaifeng Xu [a], Chengyu Jiang [b], Zhongjie Fan [a,*]

[a] Department of Medicine, Peking Union Medical College Hospital, Peking Union Medical College & Chinese Academy of Medical Sciences, No.1 Shuaifuyuan Wangfujing Dongcheng District, Beijing, 100730, China

[b] State Key Laboratory of Medical Molecular Biology, Institute of Basic Medical Sciences, Chinese Academy of Medical Sciences, Department of Biochemistry, Peking Union Medical College, Beijing, 100005, China

ARTICLE INFO

Keywords:
Cold spells
Asthma
Hospital admissions
Distributed lag model

ABSTRACT

Background: There is a paucity of studies investigating extreme cold events and asthma exacerbations. This study examined whether an association exists between cold spells and daily hospital admissions for asthma in Beijing, China from 2012 to 2016.

Methods: Daily hospital admissions for asthma, meteorological variables and air quality data were collected during 2012–2016 in Beijing. A cold spell was defined as a period of at least two consecutive days with the daily mean temperature below or at the 5th percentile (−7 °C) in cold seasons (November to March) during the study period. We applied a time-series design using quasi-Poisson regression combined with a distributed lag model to estimate the risk of asthma hospital admissions associated with cold spells. Stratified analyses by gender and age groups were conducted to identify the potential susceptible subpopulations to cold spells. We also explored the effect modification by air quality by dividing the daily air quality index (AQI) into two levels (high and low) based on the median value.

Results: Cold spells increased the risk of asthma hospital admissions, with the maximum cumulative relative risk (CRR) over three weeks (Lag0-21) in the total population. The highest single-day relative risk (RR) was found on the days of cold spells (Lag0) with the RR = 1.059 (95% CI: 1.008–1.113), and the CRR at Lag0-21 was 1.333 (95% CI: 1.049–1.693). Across different gender and age groups, younger people (<65 years) were more sensitive to cold spells. No significant effect modification by AQI was detected.

Conclusion: Short-term exposure to cold spells is associated with an increased risk of hospital admissions for asthma in Beijing. During the cold spells, younger people aged <65 years were at particular risk for asthma exacerbations. Our results suggest that extreme cold events have a significant impact on asthma.

1. Introduction

Asthma is a highly prevalent chronic airway disease characterized by recurrent attacks of breathlessness and wheezing (Dharmage et al., 2019). It is a severe public health issue, affecting an estimated 358 million people worldwide in 2015 (Soriano et al., 2017). As the largest developing country with a dense population, China shoulders an enormous burden of asthma. A national cross-sectional China Pulmonary Health (CPH) study conducted during 2012–2015 showed that the overall prevalence of asthma among Chinese adults (aged≥20) was 4.2%, representing 45.7 million people (Huang et al., 2019). Because asthma is incurable with severe impacts on quality of life, it is crucial to identify risk factors leading to asthma prevalence and exacerbation for establishing effective prevention and control strategies.

Global climate changes have increased the frequency, intensity, and duration of extreme weather events, such as heatwaves and cold spells (Green et al., 2013; Yang et al., 2021). A cold spell is defined as a prolonged period of extremely low temperatures. Due to global warming, the general population may adapt to heat whereas their tolerance to cold may decrease (Chung et al., 2017; Lee et al., 2018). Additionally, the warming trend in the Arctic may increase the likelihood of severe cold spells in the mid-latitude continents (Cohen et al., 2013, 2018).

* Corresponding author.
E-mail address: Fanzhongjie@pumch.cn (Z. Fan).

https://doi.org/10.1016/j.ijheh.2021.113839
Received 18 May 2021; Received in revised form 31 August 2021; Accepted 4 September 2021
Available online 7 September 2021

Therefore, the health consequences of cold spells are of growing public concern. Studies have reported increased risks of mortality and morbidity of several diseases on cold-spell days as compared to non-cold-spell days (Cheng et al., 2019; de'Donato et al., 2013; Ma et al., 2013; Xie et al., 2013).

Asthma is a complicated respiratory disease influenced by both hereditary and environmental factors (Yang et al., 2017). As one of the major environmental factors, low temperatures play a role in aggravating chronic respiratory diseases (D'Amato et al., 2018). Epidemiological studies in different regions have also suggested that lower temperatures are significantly associated with higher risks of asthma hospital visits or admissions (Lam et al., 2016; Zhang et al., 2014). However, only a few studies have investigated the short-term effects of cold spells on asthma, and results have remained elusive. A study from Shanghai, a subtropical city in southern China, reported a positive relationship between cold spells and pediatric outpatient visits for asthma (Guo et al., 2012). Another study from Hefei, a northern city in China, also found significant associations between cold spells and admission risk for childhood asthma (Liu et al., 2021a). A nationwide study conducted in Japan reported a positive but non-significant association between cold spells and mortality from asthma (Ma et al., 2021). Nevertheless, Fitzgerald et al. found that cold spells were related to a decline in asthma hospital admissions during the winter months in New York, USA (Fitzgerald et al., 2014). The considerable heterogeneity across regions may lead to inconsistency in study results, which limits their extrapolation, leading to the need for more studies conducted in different climate regions.

Beijing, covering an area of 16410.54 km^2, is in northern China with a typical temperate and monsoonal climate with a cold, dry winter. With a resident population of over 21 million, Beijing has a high prevalence of and heavy burden of asthma (Zhang et al., 2018). The objectives of our study were to explore the association between cold spells and hospital admissions for asthma, and to further identify potentially vulnerable populations in Beijing, China from 2012 to 2016. We believe that these findings will provide additional insights into the relationship between cold spells and asthma exacerbations and help in the design and implementation of practical measures in mitigation of the adverse health effects caused by cold spells.

2. Methods

2.1. Data collection

Daily hospital admissions for asthma were obtained from the Beijing Public Health Information Center (http://www.phic.org.cn/) during the period of January 1, 2012, to December 31, 2016. The data were from the secondary and tertiary hospitals in Beijing, covering practically the entire population. Each record includes the admission and discharge date, age, sex, address, and discharge diagnoses. We selected the hospital admission records with a primary discharge diagnosis of asthma according to the codes (J45-46) defined in the International Classification of Diseases, 10th Version (ICD-10). We only included patients who lived in Beijing based on their residential addresses. Because all the records included were anonymous with no individually identifiable information for the analysis, the study was approved and was exempt from a full ethical review by the Institutional Review Board of Peking Union Medical College Hospital.

Daily meteorological data, including mean temperature (°C), mean relative humidity (%), mean atmospheric pressure (hPa), and mean wind speed (m/s) were acquired during the same period from the China Meteorological Data Sharing Service System (http://data.cma.cn/). Daily air quality index (AQI) data were retrieved from the China National Environmental Monitoring Center (http://www.cnemc.cn/). The daily AQI is a quantitative index reflecting the integrated effects of six major air pollutants (fine particulate matter, inhalable particulate matter, sulfur dioxide, nitrogen dioxide, ozone, and carbon monoxide) in real-time. We also collected information on influenza from the Chinese National Influenza Center (http://www.chinaivdc.cn/cnic/). We identified influenza epidemics (a dichotomous variable denoting a period with intense influenza episodes) as when the isolated positive proportion for influenza surpassed 30% of the maximum seasonal level. Influenza surveillance season was defined from the 27th week of the previous year to the 26th week of the following year (Cowling et al., 2006).

2.2. Study design and statistical analysis

There are no standard definitions of cold spells around the world. Diverse definitions of cold spells were used in different studies, mainly because of various climatic features in different geographic locations. A recent study of cold spells and mortality covering 31 capital cities in China reported the definition of a cold spell as $\geq$ two consecutive days with a daily mean temperature falling below the location-specific 5th percentile. This definition produced the optimal model fit performance (Chen et al., 2019). Therefore, in our primary analysis, we defined the cold spell similarly as a period of at least two consecutive days with the daily mean temperature below or at the threshold level [5th percentile (−7 °C)] in cold seasons (November to March, the five coldest months in a row) in Beijing during 2012–2016.

We employed a time-series design using quasi-Poisson regression combined with a distributed lag model (DLM) to explore the risk of asthma hospital admissions on cold spell days compared with non-cold spell days. According to the distribution of cold spells, the study period was restricted from November in the previous year to March in the following year. Confounding factors included the day of the week, seasonality, long-term trend, statutory holidays, influenza epidemics and several environmental variables, involving mean relative humidity, mean wind speed, mean atmospheric pressure and AQI. All the degrees of freedom (df) for variable terms were selected according to the quasi-Poisson Akaike information criteria (Q-AIC) value of the model. The equation is described as follows:

$$Log[E(Y_t)] = \alpha + cb(CS_t, lag, 3) + ns(RH_t,\ 3) + ns(WS_t,\ 3) + ns(AP_t, 3) + ns(AQI_t,\ 3) + ns(DOS_t,\ 3) + \delta Season_t + \lambda DOW_t + \eta Holiday_t + \gamma Influenza_t \quad (1)$$

where E (Y_t) denotes the expected daily number of asthma hospital admissions on day t. α is the intercept. CS_t is a binary variable denoting a cold spell day (0 = non-cold spell days and 1 = cold spell days). cb represents the cross-basis function combining the linear exposure-response function and a natural cubic spline with three degrees of freedom (df) for the lag-response function, with a maximum lag of 21 days to account for delayed cold effects (Liu et al., 2021b; Ma et al., 2021). ns () means the natural cubic spline function. RH_t, WS_t, AP_t, and AQI_t refer to mean relative humidity, mean wind speed, mean atmospheric pressure, and mean AQI on day t with 3 df, respectively. DOS_t with 3 df for the day of the season (from 1 to 151 or 152) is used to control for seasonality. $Season_t$ is a categorical variable for each season to control for the long-term trend. DOW_t is a categorical variable indicating the day of the week on day t. Both $Holiday_t$ and $Influenza_t$ are binary variables, representing statutory holidays (0 for non-holiday

days, 1 for holidays) and influenza epidemics (0 for days without influenza epidemics, 1 for days with influenza epidemics), respectively. β, δ, η and γ are the coefficients of the corresponding variables.

To analyze the potential lagged effects of cold spells, we calculated the single-day lag effects (from Lag0 to Lag 21) and cumulative lag effects (Lag0, Lag0-14 and Lag0-21) of cold spells on asthma hospital admissions. We performed subgroup analyses by gender (male and female) and age (65 years as a cut-off point) to identify the susceptible subpopulations. We also explored the interaction effect between cold spells and AQI. To examine effect modification by air quality, we introduced interaction terms between DLM term of cold spells and AQI strata indicators into the main model. AQI was categorized into two levels (high: AQI≥97 and low: AQI<97) based on the median value. The statistical differences of the risk estimates between the subgroups were examined by the following equation (Liu et al., 2021a):

$$(E_1 - E_2) \pm 1.96\sqrt{(SE_1{}^2 + SE_2{}^2)}$$

where E_1 and E_2 denote the effect estimates of two groups; SE_1 and SE_2 are corresponding standard errors of E_1 and E_2.

2.3. Sensitivity analysis

We conducted several sensitivity analyses to test the robustness of our findings. We altered the df of the day of the season (3–5 df), relative humidity (3–5 df), wind speed (3–5 df), atmospheric pressure (3–5 df), and AQI (3–5 df) in the model. Furthermore, we used different durations (two to four consecutive days) and intensities (daily mean temperature below or at the thresholds of 3rd, 5th or 10th percentiles during the study period) to generate eight more cold spell definitions. All statistical analyses were performed with R version 3.6.1 (R Foundation for Statistical Computing, Vienna, Austria). Statistical significance was considered as a two-sided $p < 0.05$.

3. Results

3.1. Data description

Table 1 displays the descriptive statistics of daily hospital admissions for asthma, meteorological factors, and air quality in cold seasons (November to March) in Beijing, China, 2012–2016. The total number of hospital admissions for asthma during the study period was 11,021. There were more hospital admissions for asthma in females (60.5%) than in males (39.5%). The proportion of patients younger than 65 years old was higher than that of patients aged over 65 (57.6% vs. 42.4%). The mean values of daily mean temperature, relative humidity, wind speed, atmospheric pressure, and AQI were 0.9 °C, 46.6%, 10.3 m/s, 1025.3 hPa, and 126.3, respectively.

Fig. 1 presents the daily mean temperature and daily cases of asthma hospital admissions in cold seasons in Beijing from 2012 to 2016. Table 2 shows detailed information on cold spells that occurred in Beijing during the study period. Based on the definitions of cold spells, eight cold spells ranged from 2 to 11 days with a total duration of 37 days. The average number of daily asthma hospital admissions was 16.3. The average, lowest, and highest daily mean temperatures were −8.8 °C, −16.0 °C and −7.0 °C, respectively.

3.2. Relationship between cold spells and asthma hospital admissions

Fig. 2 depicts the single-day effects from 0-day to 21-day lags of cold spells on asthma hospital admissions in the total population. Cold spells were associated with an immediate and significant increase in the risk of asthma hospital admissions from Lag0 to Lag 5, with the maximum single-day relative risk (RR) at Lag0 [RR = 1.059, 95% confidence interval (CI): 1.008–1.113]. Table 3 shows the cumulative lag effects of cold spells on asthma hospital admissions. The cumulative lag effects of cold spells on asthma hospital admissions of the total population remained significant and increased with longer cumulative lags, with the highest cumulative relative risk (CRR) at Lag0-21 [CRR = 1.333, 95% CI: 1.049–1.693].

Fig. 3 and Table 3 show the results for the subgroup analyses stratified by gender and age. The cumulative lag effects of cold spells lasted longer in males, with significant CRR appearing at Lag0-21 (CRR = 1.621, 95% CI: 1.156–2.275), whereas a significant CRR in females was only observed at Lag0-14 (CRR = 1.286, 95% CI: 1.043–1.585). However, the effects were similar but were not statistically significant (see Supplementary Materials, Table S3). In the subgroups stratified by age, the most significant single-day and cumulative lag effects for people aged <65 years old were at Lag0 (RR = 1.102, 95% CI: 1.039–1.169) and Lag0-21 (CRR = 1.453, 1.090–1.937), respectively. In contrast, no significant association was observed in those aged ≥65 years old. We also observed statistically significant differences between the two age groups at Lag0 (see Supplementary Materials, Table S3), suggesting that younger people were more vulnerable to asthma exacerbations from the effects of cold spells.

The single-day and cumulative effects of cold spells on asthma hospital admissions of the total population on days with high and low AQI levels are shown in Fig. S2 and Table S3 (see Supplementary Materials). Although the cumulative effects of cold spells were slightly higher at a high AQI level than at a low AQI level, the modification effect of AQI was not significant.

The results of sensitivity analyses were still robust by applying another eight definitions of cold spells (See Supplementary Materials, Fig. S1 and Table S2). The risk estimates did not substantially differ after

Table 1
Descriptive statistics of daily hospital admissions for asthma (counts per day), meteorological variables, and air quality in cold seasons (November to March) in Beijing, China, 2012–2016.

	Sum	Mean (SD)	Min	Percentiles			Max
				25th	50th	75th	
Total	11021	14.6 (6.5)	0.0	9.0	15.0	19.0	34.0
Gender							
Male	4358	5.8 (3.1)	0.0	3.0	6.0	8.0	16.0
Female	6663	8.8 (4.4)	0.0	5.0	8.0	12.0	22.0
Age							
<65	6345	8.4 (4.1)	0.0	5.0	8.0	11.0	22.0
≥65	4676	5.9 (3.5)	0.0	3.0	6.0	9.0	19.0
Environmental variables							
Mean temperature (°C)	/	0.9 (5.4)	−16.0	−3.0	0.0	4.0	18.0
Relative humidity (%)	/	46.6 (20.4)	8.0	30.0	43.0	61.0	98.0
Wind speed (m/s)	/	10.3 (6.1)	3.0	6.0	8.0	13.0	34.0
Atmospheric pressure (hPa)	/	1025.3 (6.5)	1005.0	1021.0	1026.0	1030.0	1044.0
Air quality index	/	126.3 (89.2)	17.0	61.0	97.0	170.0	485.0

SD, standard deviation.

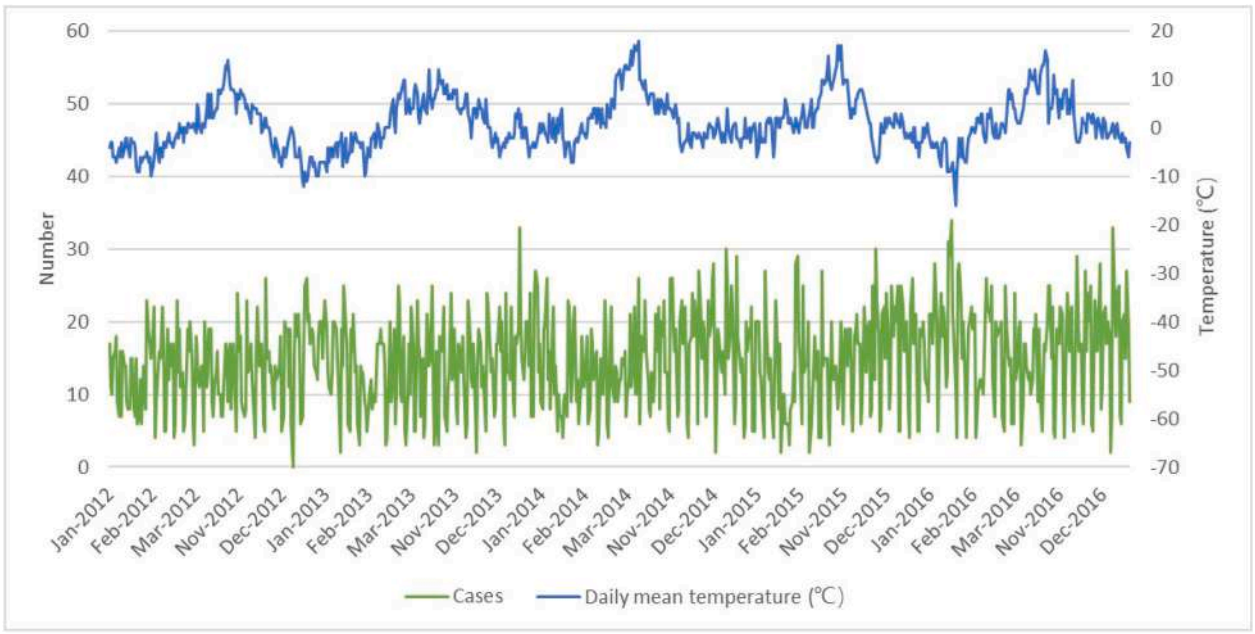

Fig. 1. Time-series plot of the daily mean temperature and daily cases of asthma hospital admissions in cold seasons (November to March) in Beijing, China, 2012–2016.

Table 2
Characteristics of cold spells in Beijing, China, 2012–2016.

Number	Period	Average number of daily asthma hospital admissions	Duration (days)	Average Tmean (°C)	Lowest Tmean (°C)	Highest Tmean (°C)
1	2012/1/21–2012/1/23	9.3	3	−8.7	−9.0	−8.0
2	2012/2/1–2012/2/2	17	2	−9.0	−10.0	−8.0
3	2012/12/23–2012/12/28	19.2	6	−10.2	−12.0	−8.0
4	2012/12/31–2013/1/10	17.5	11	−8.0	−10.0	−7.0
5	2013/2/7–2013/2/8	8.5	2	−9.5	−10.0	−9.0
6	2014/2/9–2014/2/11	13.7	3	−7.0	−7.0	−7.0
7	2016/1/17–2016/1/24	20.1	8	−9.7	−16.0	−7.0
8	2016/1/30–2016/1/31	7.5	2	−7.0	−7.0	−7.0
Total	–	16.3	37	−8.8	−16.0	−7.0

Tmean, daily mean temperature.

changing the df for confounding variables: day of the season (3–5 df), relative humidity (3–5 df), wind speed (3–5 df), atmospheric pressure (3–5 df), and AQI (3–5 df) (See Supplementary Materials, Table S1).

4. Discussion

In this study, we found that short-term exposure to cold spells was significantly associated with increased risks of asthma hospital admissions during the coldest months from 2012 to 2016 in Beijing, China. As no significant association was found in people aged 65 and older, younger people were more vulnerable to cold spells. Our findings may support controlling and preventing asthma episodes and exacerbation on extremely cold days, especially during prolonged cold weather.

The results of the positive relationship between cold spells and asthma are consistent with findings in two previous studies focusing on children in China. A time-series study conducted by Guo et al. in Shanghai showed that cold spells had a significant impact on asthma outpatient visits among children (Guo et al., 2012). Liu and colleagues found that hospital admissions for childhood asthma were significantly associated with cold spells (Liu et al., 2021a). On the contrary, in New York State of the United States, asthma hospital admissions of all ages declined during cold spells in the coldest winter seasons (December through March). Nevertheless, in the transitional months (November and April), a significant increase in hospital admissions for asthma was observed during or after cold spells (Fitzgerald et al., 2014). New York State has a much colder and snowier winter than Beijing. The average temperature during winter cold spells (December to March) was −15 °C, as compared to −6 °C and −2 °C for cold spells in November and April, respectively in New York State. Due to the very cold and snowy winters, asthmatics in New York State may change their behaviors, such as spending more time indoors and wearing a face mask or a scarf outdoors to prevent asthma exacerbations during cold spells. The winter climate in Beijing is like the transitional months (November and April) in New York State. Under a moderate climate condition, asthmatics may be less likely to alter their behaviors, leading to increased exposure to relatively cold temperatures and a higher risk of exacerbations. The discrepancy in outcomes across the studies may be related to climatic differences in various geographical locations and resulting adaptions in behaviors, study populations, statistical methods, and confounding factors controlled in the model. Hence, large-scale and multi-center studies in a range of locations should be encouraged.

Various underlying biological mechanisms have been proposed behind the association between asthma exacerbation and cold exposure. Two preclinical studies on rabbits and cats both reported that cold exposure is capable of inducing bronchoconstriction (Jammes et al., 1983, 1986). Experimental studies on asthmatic mouse models showed

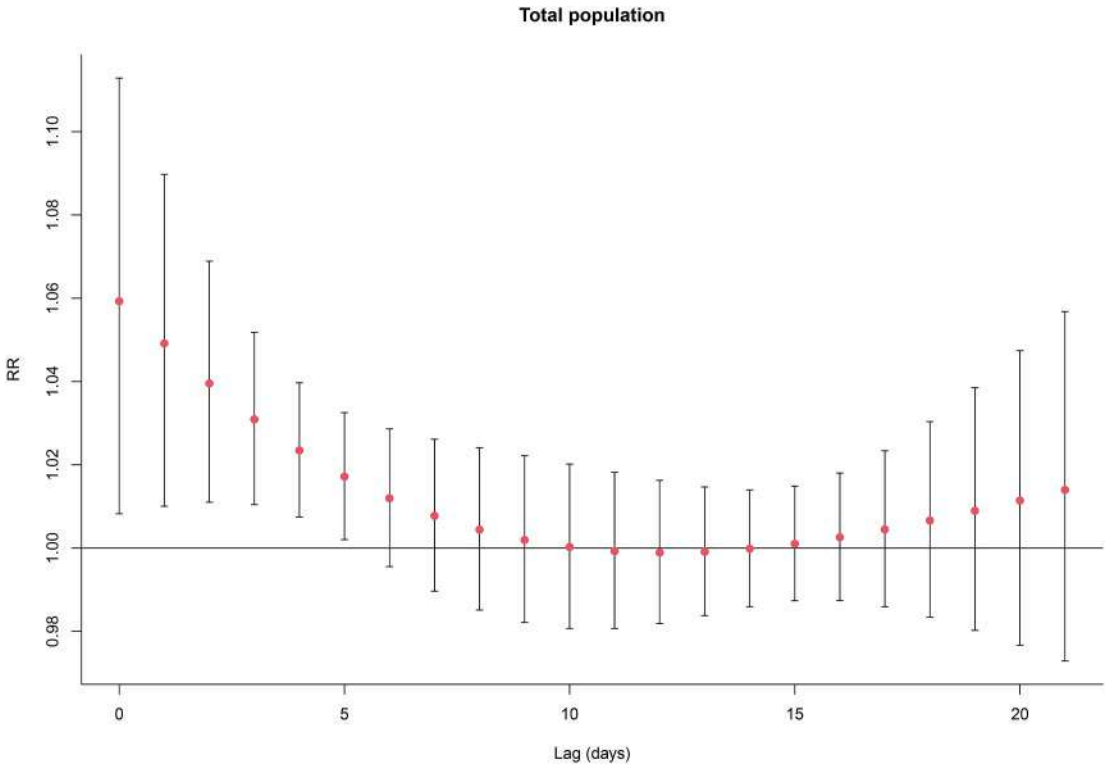

Fig. 2. Lag-response relationships between cold spells and asthma hospital admissions of the total population in Beijing, 2012–2016.

Table 3
Cumulative relative risks of cold spells on asthma hospital admissions in Beijing, 2012–2016.

	CRR (95% CI)		
	Lag0	Lag0-14	Lag0-21
Total	1.059 (1.008, 1.113)[a]	1.269 (1.063, 1.516)[a]	1.333 (1.049, 1.693)[a]
Male	1.061 (0.988, 1.138)	1.240 (0.960, 1.602)	1.621 (1.156, 2.275)[a]
Female	1.058 (0.998, 1.122)	1.286 (1.043, 1.585)[a]	1.162 (0.872, 1.547)
<65 years old	1.102 (1.039, 1.169)[a]	1.332 (1.077, 1.648)[a]	1.453 (1.090, 1.937)[a]
≥65 years old	1.004 (0.937, 1.077)	1.179 (0.920, 1.512)	1.189 (0.852, 1.661)

[a] $p < 0.05$; CRR cumulative relative risk; CI, confidence interval.

that low temperatures can aggravate airway inflammation of asthma (Deng et al., 2020; Liu et al., 2018). *In vitro* studies on human bronchial epithelial cells suggested that cold temperature can stimulate airway mucus hypersecretion (Juan et al., 2016; Li et al., 2011). Moreover, several animal models indicated that cold temperatures can lead to a state of immunosuppression and increase infection risk (LaVoy et al., 2011; Shephard and Shek, 1998). Future studies should be directed towards unraveling the specific and direct pathways behind these mechanisms.

The effect modifications by gender, age, and air quality on the correlation between cold spells and asthma have been rarely studied. Based on our subgroup analysis stratified by gender, the impact of cold spells on asthma hospital admissions was similar in men and women. Regarding the subgroup analysis stratified by age, the effects of cold spells were higher in the younger population than the elderly aged 65 years or older, with statistically significant differences at Lag0. A study from eight cities in South Korea also found a stronger association between low temperature and asthma hospital admissions among the younger age groups (0–14 and 15–64 years old) than older age groups (65–74 and ≥ 75 years old) (Son et al., 2014). One possible explanation is that younger people are more likely to have activities outdoors than the elderly, increasing their exposure to extremely cold weather. In contrast, the elderly tend to spend more time indoors during cold spells. On the other hand, the lack of statistically significant results for the elderly may be due to a smaller sample size and a lack of statistical power. Identifying the subgroups more susceptible to cold spells can aid in the development of targeted asthma prevention measures, although the results need to be validated in larger populations. In addition, the effects of cold spells on asthma hospital admissions were slightly stronger on days with a higher AQI level, whereas no significant effect modification by AQI was detected. Fang et al. reported that the impact of extreme cold temperature on childhood asthma hospital visits can be enhanced under higher-level exposure to O_3 in Beijing (Fang et al., 2021). In our analysis, the relatively short study duration with a limited number of cold spells may have led to a shortage of statistical power. The effect modification by air pollution and other environmental factors on cold spells' impact should be further explored in long-term studies.

Our findings may provide several public health implications for the prevention of asthma attacks for cold spells. Local governments can play a critical role in mitigating the health hazards of cold spells through a series of actions. Firstly, meteorological departments should improve early warning systems with the development of more timely forecasts and publication of cold spells events. Secondly, the government should guarantee adequate preparation and effective allocation of medical and health resources to mitigate the asthma burden resulting from cold spells. Thirdly, the official media should enhance public awareness of the dangers of cold spells and recommend active preventive measures (Chen et al., 2019). For individuals, a personal diary-based survey has suggested that paying more attention to personal perception of cold temperature and air quality may reduce the chance of asthma attacks (Chan et al., 2019). Moreover, wearing warm clothing and staying in warm housing can reduce overall cold-related mortality in extremely cold weather (Donaldson et al., 1998). Therefore, asthmatics should

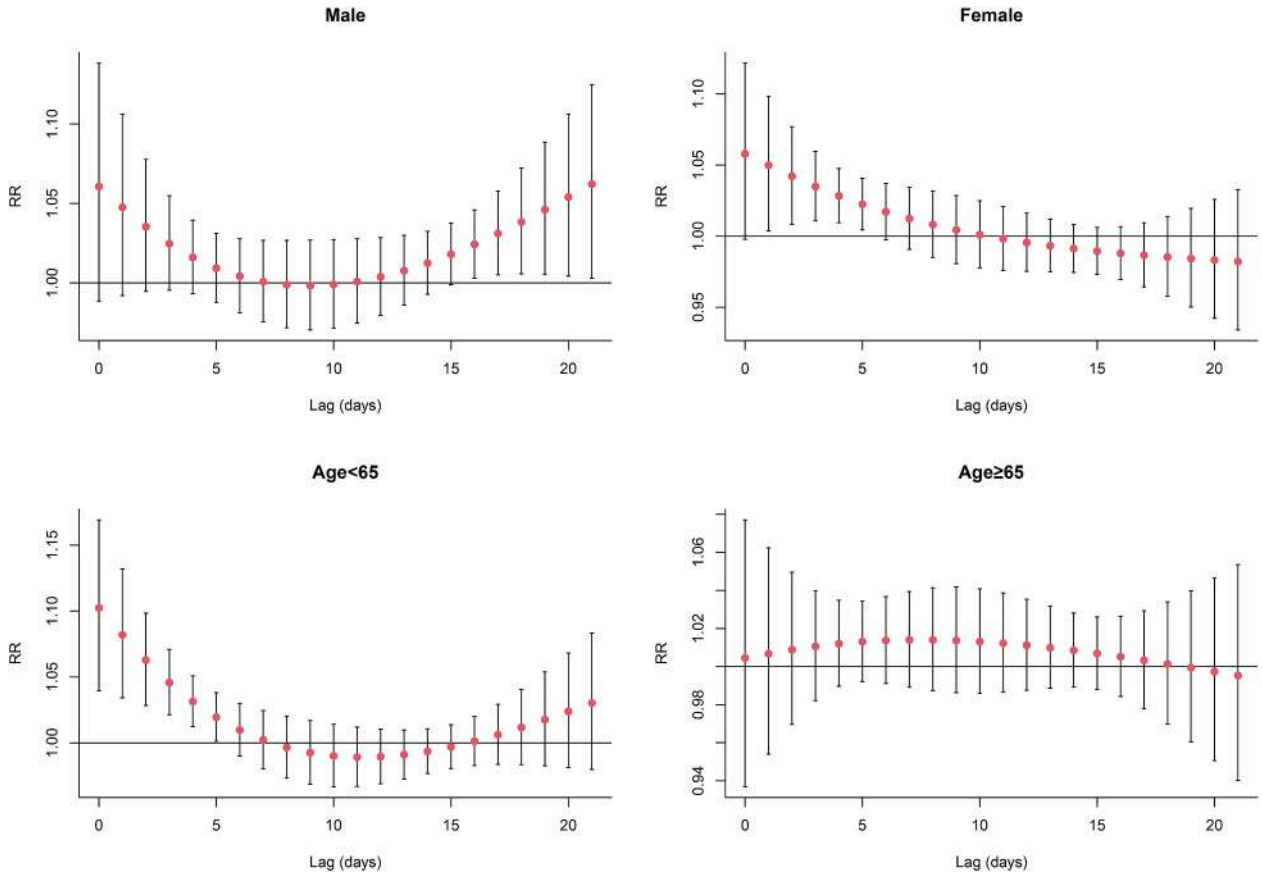

Fig. 3. Lag-response relationships between cold spells and asthma hospital admissions stratified by gender and age in Beijing, 2012–2016.

spend more time indoors, put on more clothing and a face mask or scarf to prevent asthma exacerbations associated with cold spells, especially for younger people who have more outdoor activities.

The study has several advantages. Firstly, the database used in this study maintained by the public health information center of Beijing covers almost all the hospital admissions of the entire city over a 5-year study period. Comprehensive and high-quality data improve the representativeness and reliability of our results. Secondly, we controlled for confounding factors including other meteorological factors, air quality, public holidays and influenza epidemics in our analysis to accurately determine the associations between cold spells and asthma hospital admissions. Thirdly, to assess the effects of cold spells more precisely, we categorized the records of asthma hospital admissions into gender and different age subgroups, as well as exploring the effect modification by air quality.

However, some major limitations of our study should also be noted. Firstly, as an ecological study, the results are prone to ecological fallacy (Sedgwick, 2015). We collected and aggregated meteorological and air quality data measured by fixed-site monitoring stations in the study area to roughly represent the exposure levels of the entire study population rather than individual-level measurements, which could result in exposure misclassification bias. Consequently, a more precise approach to individual exposure measurement is required for further studies to confirm the association. Due to a lack of personal information, many individual-level factors, such as medication, smoking, and time-activity patterns, could not be included in the analysis. Secondly, our data inevitably include some non-emergency hospital admissions, which are less susceptible to cold spells. Mild asthma attacks treated in the outpatient setting were not included in the study. We only examined the association between cold spells and more severe asthma attacks requiring to be hospitalized, which may underestimate the impact of cold spells to some extent. Lastly, using only one city's data implied a limited generalization of our findings to other areas with different climate or socio-economic characteristics.

5. Conclusion

The study shows that cold spells are associated with higher risks of hospital admissions for asthma in Beijing, China. The lag effect of cold spells suggests more attention should be paid during and about three weeks after cold spells to prevent asthma attacks and exacerbations of such. Younger ages (<65 years) are potentially vulnerable populations to cold spell-related asthma hospital admissions. Our findings may lead to increased awareness of asthma triggered by cold spells and contribute to tailoring precautionary guidelines for extreme cold events for patients with asthma.

Funding

This work was supported by Chinese Academy of Medical Sciences (CAMS) Initiative for Innovative Medicine [grant number 2017-I2M-2-001]; National Natural Science Foundation [grant number 91643208]; and National Key Research and Development Plan [grant number 2017YFC0211703 and 2015CB553402].

Appendix A. Supplementary data

Supplementary data to this article can be found online at https://doi.org/10.1016/j.ijheh.2021.113839.

References

Chan, T.C., Hu, T.H., Chu, Y.H., Hwang, J.S., 2019. Assessing effects of personal behaviors and environmental exposure on asthma episodes: a diary-based approach. BMC Pulm. Med. 19, 231.

Chen, J., Yang, J., Zhou, M., Yin, P., Wang, B., Liu, J., Chen, Z., Song, X., Ou, C.Q., Liu, Q., 2019. Cold spell and mortality in 31 Chinese capital cities: definitions, vulnerability and implications. Environ. Int. 128, 271–278.

Cheng, Q., Wang, X., Wei, Q., Bai, L., Zhang, Y., Gao, J., Duan, J., Xu, Z., Yi, W., Pan, R., Su, H., 2019. The short-term effects of cold spells on pediatric outpatient admission for allergic rhinitis in Hefei, China. Sci. Total Environ. 664, 374–380.

Chung, Y., Noh, H., Honda, Y., Hashizume, M., Bell, M.L., Guo, Y.L., Kim, H., 2017. Temporal changes in mortality related to extreme temperatures for 15 cities in Northeast asia: adaptation to heat and maladaptation to cold. Am. J. Epidemiol. 185, 907–913.

Cohen, J., Jones, J., Furtado, J., Tziperman, E., 2013. Warm arctic, cold continents: a common pattern related to arctic sea ice melt, snow advance, and extreme winter weather. Oceanography 26.

Cohen, J., Pfeiffer, K., Francis, J.A., 2018. Warm Arctic episodes linked with increased frequency of extreme winter weather in the United States. Nat. Commun. 9, 869.

Cowling, B.J., Wong, I.O., Ho, L.M., Riley, S., Leung, G.M., 2006. Methods for monitoring influenza surveillance data. Int. J. Epidemiol. 35, 1314–1321.

D'Amato, M., Molino, A., Calabrese, G., Cecchi, L., Annesi-Maesano, I., D'Amato, G., 2018. The impact of cold on the respiratory tract and its consequences to respiratory health. Clin. Transl. Allergy 8, 20.

de'Donato, F.K., Leone, M., Noce, D., Davoli, M., Michelozzi, P., 2013. The impact of the February 2012 cold spell on health in Italy using surveillance data. PloS One 8, e61720.

Deng, L., Ma, P., Wu, Y., Ma, Y., Yang, X., Li, Y., Deng, Q., 2020. High and low temperatures aggravate airway inflammation of asthma: evidence in a mouse model. Environmental pollution (Barking, Essex : 1987 256, 113433.

Dharmage, S.C., Perret, J.L., Custovic, A., 2019. Epidemiology of asthma in children and adults. Frontiers in pediatrics 7, 246.

Donaldson, G.C., Ermakov, S.P., Komarov, Y.M., McDonald, C.P., Keatinge, W.R., 1998. Cold related mortalities and protection against cold in Yakutsk, eastern Siberia: observation and interview study. BMJ (Clinical research ed.) 317, 978–982.

Fang, J., Song, J., Wu, R., Xie, Y., Xu, X., Zeng, Y., Zhu, Y., Wang, T., Yuan, N., Xu, H., Song, X., Zhang, Q., Xu, B., Huang, W., 2021. Association between ambient temperature and childhood respiratory hospital visits in Beijing, China: a time-series study (2013-2017). Environmental Science and Pollution Research International.

Fitzgerald, E.F., Pantea, C., Lin, S., 2014. Cold Spells and the Risk of Hospitalization for Asthma, vol. 192. USA, New York, pp. 947–954, 1991-2006. Lung.

Green, M.S., Pri-Or, N.G., Capeluto, G., Epstein, Y., Paz, S., 2013. Climate change and health in Israel: adaptation policies for extreme weather events. Isr. J. Health Pol. Res. 2, 23.

Guo, Y., Jiang, F., Peng, L., Zhang, J., Geng, F., Xu, J., Zhen, C., Shen, X., Tong, S., 2012. The association between cold spells and pediatric outpatient visits for asthma in Shanghai, China. PloS One 7, e42232.

Huang, K., Yang, T., Xu, J., Yang, L., Zhao, J., Zhang, X., Bai, C., Kang, J., Ran, P., Shen, H., Wen, F., Chen, Y., Sun, T., Shan, G., Lin, Y., Xu, G., Wu, S., Wang, C., Wang, R., Shi, Z., Xu, Y., Ye, X., Song, Y., Wang, Q., Zhou, Y., Li, W., Ding, L., Wan, C., Yao, W., Guo, Y., Xiao, F., Lu, Y., Peng, X., Zhang, B., Xiao, D., Wang, Z., Chen, Z., Bu, X., Zhang, H., Zhang, X., An, L., Zhang, S., Zhu, J., Cao, Z., Zhan, Q., Yang, Y., Liang, L., Tong, X., Dai, H., Cao, B., Wu, T., Chung, K.F., He, J., Wang, C., 2019. Prevalence, risk factors, and management of asthma in China: a national cross-sectional study. Lancet 394, 407–418.

Jammes, Y., Barthelemy, P., Delpierre, S., 1983. Respiratory effects of cold air breathing in anesthetized cats. Respir. Physiol. 54, 41–54.

Jammes, Y., Barthelemy, P., Fornaris, M., Grimaud, C., 1986. Cold-induced bronchospasm in normal and sensitized rabbits. Respir. Physiol. 63, 347–360.

Juan, Y., Haiqiao, W., Xie, W., Huaping, H., Zhong, H., Xiangdong, Z., Kolosov, V.P., Perelman, J.M., 2016. Cold-inducible RNA-binding protein mediates airway inflammation and mucus hypersecretion through a post-transcriptional regulatory mechanism under cold stress. Int. J. Biochem. Cell Biol. 78, 335–348.

LaVoy, E.C., McFarlin, B.K., Simpson, R.J., 2011. Immune responses to exercising in a cold environment. Wilderness Environ. Med. 22, 343–351.

Lee, W., Choi, H.M., Lee, J.Y., Kim, D.H., Honda, Y., Kim, H., 2018. Temporal changes in mortality impacts of heat wave and cold spell in Korea and Japan. Environ. Int. 116, 136–146.

Li, M., Li, Q., Yang, G., Kolosov, V.P., Perelman, J.M., Zhou, X.D., 2011. Cold temperature induces mucin hypersecretion from normal human bronchial epithelial cells in vitro through a transient receptor potential melastatin 8 (TRPM8)-mediated mechanism. J. Allergy Clin. Immunol. 128, 626–634 e621-625.

Liu, H., Hua, L., Liu, Q., Pan, J., Bao, Y., 2018. Cold stimuli facilitate inflammatory responses through transient receptor potential melastatin 8 (TRPM8) in primary airway epithelial cells of asthmatic mice. Inflammation 41, 1266–1275.

Liu, X., He, Y., Tang, C., Wei, Q., Xu, Z., Yi, W., Pan, R., Gao, J., Duan, J., Su, H., 2021a. Association between cold spells and childhood asthma in Hefei, an analysis based on different definitions and characteristics. Environ. Res. 195, 110738.

Liu, Y., Chen, Y., Kong, D., Liu, X., Fu, J., Zhang, Y., Zhao, Y., Chang, Z., Zhao, X., Xu, K., Jiang, C., Fan, Z., 2021b. Short-term effects of cold spells on hospitalisations for acute exacerbation of chronic obstructive pulmonary disease: a time-series study in Beijing, China. BMJ open 11, e039745.

Ma, C., Yang, J., Nakayama, S.F., Iwai-Shimada, M., Jung, C.R., Sun, X.L., Honda, Y., 2021. Cold spells and cause-specific mortality in 47 Japanese prefectures: a systematic evaluation. Environ. Health Perspect. 129, 67001.

Ma, W., Yang, C., Chu, C., Li, T., Tan, J., Kan, H., 2013. The impact of the 2008 cold spell on mortality in Shanghai, China. Int. J. Biometeorol. 57, 179–184.

Sedgwick, P., 2015. Understanding the ecological fallacy. BMJ (Clinical research ed.) 351, h4773.

Shephard, R.J., Shek, P.N., 1998. Cold exposure and immune function. Can. J. Physiol. Pharmacol. 76, 828–836.

Son, J.Y., Bell, M.L., Lee, J.T., 2014. The impact of heat, cold, and heat waves on hospital admissions in eight cities in Korea. Int. J. Biometeorol. 58, 1893–1903.

Soriano, J.B., Abajobir, A.A., Abate, K.H., Abera, S.F., Agrawal, A., Ahmed, M.B., Aichour, A.N., Aichour, I., Aichour, M.T.E., Alam, K., Alam, N., Alkaabi, J.M., Al-Maskari, F., Alvis-Guzman, N., Amberbir, A., Amoako, Y.A., Ansha, M.G., Antó, J.M., Asayesh, H., Atey, T.M., Avokpaho, E.F.G.A., Barac, A., Basu, S., Bedi, N., Bensenor, I.M., Berhane, A., Beyene, A.S., Bhutta, Z.A., Biryukov, S., Boneya, D.J., Brauer, M., Carpenter, D.O., Casey, D., Christopher, D.J., Dandona, L., Dandona, R., Dharmaratne, S.D., Do, H.P., Fischer, F., Gebrehiwot, T.T., Geleto, A., Ghoshal, A.G., Gillum, R.F., Ginawi, I.A.M., Gupta, V., Hay, S.I., Hedayati, M.T., Horita, N., Hosgood, H.D., Jakovljevic, M.B., James, S.L., Jonas, J.B., Kasaeian, A., Khader, Y.S., Khalil, I.A., Khan, E.A., Khang, Y.-H., Khubchandani, J., Knibbs, L.D., Kosen, S., Koul, P.A., Kumar, G.A., Leshargie, C.T., Liang, X., El Razek, H.M.A., Majeed, A., Malta, D.C., Manhertz, T., Marquez, N., Mehari, A., Mensah, G.A., Miller, T.R., Mohammad, K.A., Mohammed, K.E., Mohammed, S., Mokdad, A.H., Naghavi, M., Nguyen, C.T., Nguyen, G., Le Nguyen, Q., Nguyen, T.H., Ningrum, D.N.A., Nong, V. M., Obi, J.I., Odeyemi, Y.E., Ogbo, F.A., Oren, E., Pa, M., Park, E.-K., Patton, G.C., Paulson, K., Qorbani, M., Quansah, R., Rafay, A., Rahman, M.H.U., Rai, R.K., Rawaf, S., Reinig, N., Safiri, S., Sarmiento-Suarez, R., Sartorius, B., Savic, M., Sawhney, M., Shigematsu, M., Smith, M., Tadese, F., Thurston, G.D., Topor-Madry, R., Tran, B.X., Ukwaja, K.N., van Boven, J.F.M., Vlassov, V.V., Vollset, S.E., Wan, X., Werdecker, A., Hanson, S.W., Yano, Y., Yimam, H.H., Yonemoto, N., Yu, C., Zaidi, Z., El Sayed Zaki, M., Lopez, A.D., Murray, C.J.L., Vos, T., 2017. Global, regional, and national deaths, prevalence, disability-adjusted life years, and years lived with disability for chronic obstructive pulmonary disease and asthma, 1990–2015: a systematic analysis for the Global Burden of Disease Study 2015. The Lancet Respiratory Medicine 5, 691–706.

Xie, H., Yao, Z., Zhang, Y., Xu, Y., Xu, X., Liu, T., Lin, H., Lao, X., Rutherford, S., Chu, C., Huang, C., Baum, S., Ma, W., 2013. Short-term effects of the 2008 cold spell on mortality in three subtropical cities in Guangdong Province, China. Environ. Health Perspect. 121, 210–216.

Yang, I.V., Lozupone, C.A., Schwartz, D.A., 2017. The environment, epigenome, and asthma. J. Allergy Clin. Immunol. 140, 14–23.

Yang, J., Zhou, M., Ren, Z., Li, M., Wang, B., Liu, L., Ou, C.Q., Yin, P., Sun, J., Tong, S., Wang, H., Zhang, C., Wang, J., Guo, Y., Liu, Q., 2021. Projecting heat-related excess mortality under climate change scenarios in China. Nat. Commun. 12, 1039.

Zhang, H., Dong, L., Kang, Y.K., Lu, Y., Wei, H.H., Huang, J., Wang, X., Huang, K., 2018. Epidemiology of chronic airway disease: results from a cross-sectional survey in Beijing, China. J. Thorac. Dis. 10, 6168–6175.

Zhang, Y., Peng, L., Kan, H., Xu, J., Chen, R., Liu, Y., Wang, W., 2014. Effects of meteorological factors on daily hospital admissions for asthma in adults: a time-series analysis. PloS One 9, e102475.

International Journal of Hygiene and Environmental Health 238 (2021) 113855

Contents lists available at ScienceDirect

International Journal of Hygiene and Environmental Health

journal homepage: www.elsevier.com/locate/ijheh

Lead (Pb) and neurodevelopment: A review on exposure and biomarkers of effect (BDNF, HDL) and susceptibility

Claudia Gundacker [a,*], Martin Forsthuber [a,b], Tamás Szigeti [c], Réka Kakucs [c], Vicente Mustieles [d,e], Mariana F. Fernandez [d,e], Elizabeth Bengtsen [f], Ulla Vogel [f,g], Karin Sørig Hougaard [f,h], Anne Thoustrup Saber [f]

[a] Medical University of Vienna, Institute of Medical Genetics, Vienna, Austria
[b] Medical University of Vienna, Department of Environmental Health, Center for Public Health, Vienna, Austria
[c] National Public Health Center, Albert Flórián 2-6., H-1097 Budapest, Hungary
[d] University of Granada, Center for Biomedical Research (CIBM), Spain; Instituto de Investigación Biosanitaria (ibs. GRANADA), Spain
[e] Consortium for Biomedical Research in Epidemiology & Public Health (CIBERESP), Spain
[f] The National Research Centre for the Working Environment, Copenhagen, Denmark
[g] National Food Institute, Technical University of Denmark, Kgs. Lyngby, Denmark
[h] University of Copenhagen, Department of Public Health, Section of Environmental Health, Denmark

ARTICLE INFO

Keywords:
Human biomonitoring
HBM4EU
Effect biomarkers
Susceptibility biomarkers
Neurodevelopmental toxicity
Epigenetics

ABSTRACT

Lead (Pb) is a ubiquitous environmental pollutant and a potent toxic compound. Humans are exposed to Pb through inhalation, ingestion, and skin contact via food, water, tobacco smoke, air, dust, and soil. Pb accumulates in bones, brain, liver and kidney. Fetal exposure occurs via transplacental transmission. The most critical health effects are developmental neurotoxicity in infants and cardiovascular effects and nephrotoxicity in adults.

Pb exposure has been steadily decreasing over the past decades, but there are few recent exposure data from the general European population; moreover, no safe Pb limit has been set. Sensitive biomarkers of exposure, effect and susceptibility, that reliably and timely indicate Pb-associated toxicity are required to assess human exposure-health relationships in a situation of low to moderate exposure.

Therefore, a systematic literature review based on PubMed entries published before July 2019 that addressed Pb exposure and biomarkers of effect and susceptibility, neurodevelopmental toxicity, epigenetic modifications, and transcriptomics was conducted. Finally included were 58 original papers on Pb exposure and 17 studies on biomarkers. The biomarkers that are linked to Pb exposure and neurodevelopment were grouped into effect biomarkers (serum brain-derived neurotrophic factor (BDNF) and serum/saliva cortisol), susceptibility markers (epigenetic markers and gene sequence variants) and other biomarkers (serum high-density lipoprotein (HDL), maternal iron (Fe) and calcium (Ca) status). Serum BDNF and plasma HDL are potential candidates to be further validated as effect markers for routine use in HBM studies of Pb, complemented by markers of Fe and Ca status to also address nutritional interactions related to neurodevelopmental disorders. For several markers, a causal relationship with Pb-induced neurodevelopmental toxicity is likely. Results on BDNF are discussed in relation to Adverse Outcome Pathway (AOP) 13 ("Chronic binding of antagonist to N-methyl-D-aspartate receptors (NMDARs) during brain development induces impairment of learning and memory abilities") of the AOP-Wiki. Further studies are needed to validate sensitive, reliable, and timely effect biomarkers, especially for low to moderate Pb exposure scenarios.

1. Introduction

Lead (Pb) is found in the environment mainly in its inorganic form. Most Pb in the environment originates from anthropogenic activities. Human exposure occurs mainly through food, water, tobacco smoke, air, dust and soil, and exposure can occur through inhalation, ingestion and skin contact. The fetus is exposed via placental transfer (EFSA 2010; WHO 2019).

* Corresponding author. Institute of Medical Genetics Medical University of Vienna, Waehringer Strasse 10 A-1090, Vienna, Austria.
E-mail address: claudia.gundacker@meduniwien.ac.at (C. Gundacker).

https://doi.org/10.1016/j.ijheh.2021.113855
Received 14 July 2021; Received in revised form 29 September 2021; Accepted 1 October 2021
Available online 13 October 2021

Pb absorption depends on the chemical form, particle size, exposure route, diet, health and age of the individual. Humans are mainly exposed to inorganic Pb. Most ingested Pb is excreted in urine and feces. Bioavailable Pb is more strongly absorbed by children than adults. (ATSDR 2017). In blood, >90% of the Pb is present in erythrocytes, and blood-Pb constitutes the most widely used biomarker of exposure. Although blood contains only a small fraction of the total Pb body burden, the matrix reliably reflects recent exposure. The half-life in the blood of adult humans ranges between 28 and 36 days. Plasma Pb can enter soft tissue compartments with a high exchange rate and hard tissues in which Pb is more strongly bound. Pb accumulates in the brain, liver, kidney and, over time, in bones and teeth. The calcified tissues contain 94% (adults) and 73% (children) of the total Pb body burden, where the metal can be stored in inert form for decades. From here, only a small labile proportion can be exchanged with the blood. Pb in the bone can, however, be mobilized into blood, a process that increases with age, physiological stress, certain diseases, pregnancy, lactation, menopause and calcium (Ca) deficiency. Therefore, the Pb pool in bones constitutes a particular risk as it is an endogenous source which, when activated, can increase blood Pb levels long after cessation of exposure (ATSDR 2017; Klotz and Goen, 2017; EFSA 2010; WHO 2019).

Developmental neurotoxicity in infants and cardiovascular effects, and nephrotoxicity in adults constitute the most critical health effects of Pb exposure (EFSA 2010). IARC has furthermore classified inorganic Pb compounds as probably carcinogenic to humans (Group 2A), while organic Pb compounds are not classifiable (Group 3) (IARC 2006). Even low Pb levels (<5 μg/100 mL blood) are known to exert adverse health effects in children and adults (Betts 2012). The dose-response relationship between Pb exposure and intelligence quotient (IQ) of children seems nonlinear, with lower exposures of Pb resulting in relatively greater loss of IQ than higher exposures. Hence, one study observed that increase in blood Pb from <1 to 30 μg/dL was associated with a deficit of ~9 IQ points, but with the largest fraction of the deficit (~6 IQ points) occurring below 10 μg/dL (Lanphear 2017; Lanphear et al., 2005). Primarily with regard to developmental neurotoxicity, the EFSA CONTAM Panel determined the $BMDL_{01}$ to 12 μg/L (EFSA 2010) but concluded that "there is no evidence for a threshold for critical lead-induced effects" and that "protection of children against the potential risk of neurodevelopmental effects would be protective for all other adverse effects of lead, in all populations" (EFSA, 2010). ECHA's Committee for Risk Assessment (RAC) recently evaluated the occupational exposure limits for Pb and its compounds. The biological limit value (BLV) was set to 150 μg/L blood for Pb and its inorganic compounds, while no BLV was set for organic Pb compounds. RAC notes, "*Neither the proposed BLV of* 150 μg/L *blood and the proposed air limit value of* 4 μg/m^3 … *protects from developmental toxicity*" and "*it is recommended to add a qualitative statement in the Chemical Agents Directive that the exposure of fertile women to lead should be avoided or minimized in the workplace because the BLV for lead is not protective of the offspring of women of childbearing age"* (RAC, 2020). Several health authorities are currently refraining from setting guideline values for Pb exposure, as it cannot be ruled out that Pb can affect neurological development even at very low levels of exposure (ATSDR 2017).

Neurodevelopment is characterized by decisive phases in which neuronal circuits are refined by interaction with the environment. When chemicals interfere with these critical developmental processes, neurological development can be irreversibly altered. Developmental exposure to Pb can alter neural structures, synapse formation, synaptic transmission and cell survival. Out of 214 human neurotoxicants, Pb was identified as the neurotoxicant that contributed the most to dysregulation of gene expression in the brains of mice during critical periods of plasticity (Smith et al., 2018). Accumulating data show that Pb can interfere with epigenetic regulation (Khalid and Abdollahi 2019). Low socioeconomic status and certain genetic factors can increase children's susceptibility to the neurotoxic effects of Pb (Lidsky and Schneider 2003).

The European Human Biomonitoring Initiative (HBM4EU), a joint effort of 30 countries, the European Environment Agency (EEA) and the European Commission, generates evidence on EU citizens' exposure to chemicals and their potential health effects to support policy. The main objective is to create an inventory of mechanistically-based effect biomarkers of utility in HBM programs (Baken et al., 2019; Mustieles et al., 2020). Pb was prioritised because of its hazardous properties, exposure characteristics, public concern and the strong need for an up-to-date health-based EU Biological Limit Value (BLV)[1] to protect workers, women of fertile age and children (Ougier et al., 2018). Of note, women have a high employment rate in the EU (63% on average in 2019) (Eurostat, 2020), which in combination with relatively high age at child birth (29.3 years at first child) (Eurostat, 2018), increases the risk of Pb exposure prior to conception, and hence the potential for induction of neurodevelopmental toxicity.

In recent decades, a downward trend in blood Pb levels has been observed in Europe and some other developed countries, due to the introduction of effective risk management measures, e.g. decrease and subsequent phasing-out of Pb in petrol, and removal of Pb from paints, ceramics, water pipes and food cans (EFSA 2012). Atmospheric emissions of anthropogenic Pb were reduced by 68% in European countries from 2000 to 2018 (EEA 2020).

Pb levels in food have declined significantly since 2003 (EFSA, 2012), but some foods, especially when grown at contaminated sites, still constitute non-negligible sources, alongside the use of herbal and traditional medicines (including geophagy), cosmetics, and water from leaded pipes in non-renovated houses (EFSA, 2010; EFSA, 2012; Saoudi et al., 2018; Parnia et al., 2018; Gundacker et al., 2017). Overall, cereals and grain-based foods are the most important dietary sources of Pb due to their high consumption, while milk and dairy products contribute the most to infants and toddlers. In 2012, EFSA estimated dietary intakes of 1.32 and 1.03 μg/kg b.w./day for toddlers and children, respectively (EFSA, 2012). These exceeded the dietary intake level of 0.50 μg/kg b.w./day corresponding to the EFSA $BMDL_{01}$ of 12 μg/L blood Pb for developmental neurotoxicity (EFSA, 2010). A recent study reported that the average Pb intake from food and tap water for infants, toddlers and children exceeded 0.50 μg/kg b.w./day (Kirinčič, 2019). Similar conclusions were made regarding women of child-bearing age (EFSA 2012).

The low to moderate exposure of the European population furthermore requires the identification of effect and susceptibility biomarkers that are sufficiently sensitive to reliably and timely detect Pb-induced health effects and sensitive populations, respectively. *Effect biomarkers* can be defined as measurable biochemical, physiological, behavioural or other alterations that are associated with an established or possible adverse health outcome (Zare Jeddi et al., 2021). *Susceptibility markers* can be considered inherent or acquired abilities of an organism to respond to the challenge of exposure to a particular chemical substance. Finally, some *other biomarkers* that do not fall into either of these categories can still be relevant as complementary markers in HBM studies. Fig. 1 provides a general overview of how the use of exposure, effect and susceptibility biomarkers can provide insight into the exposure-disease continuum.

In the present review, we focus on biomarkers associated with neurodevelopmental adverse effects following exposure to Pb, as recent reports indicate that effects might also be induced at the lower range of the exposure continuum. For this purpose, we conducted a systematic literature review to identify publications that addressed the endpoint of neurodevelopmental toxicity. The set of identified biomarkers is discussed in relation to current Pb exposure levels in Europe. We

[1] According to Ougier et al. (2018) "The Annex II of the Chemicals Agents Directive 98/24/EC mentions that a more up to date BLV will be recommended by the Scientific Committee on Occupational Exposure Limits (SCOEL). The binding BLV for lead indicated by the Directive 98/24/EC is 70 μg/100 mL blood, whereas the recommended BLV from SCOEL is 30 μg/100 mL blood".

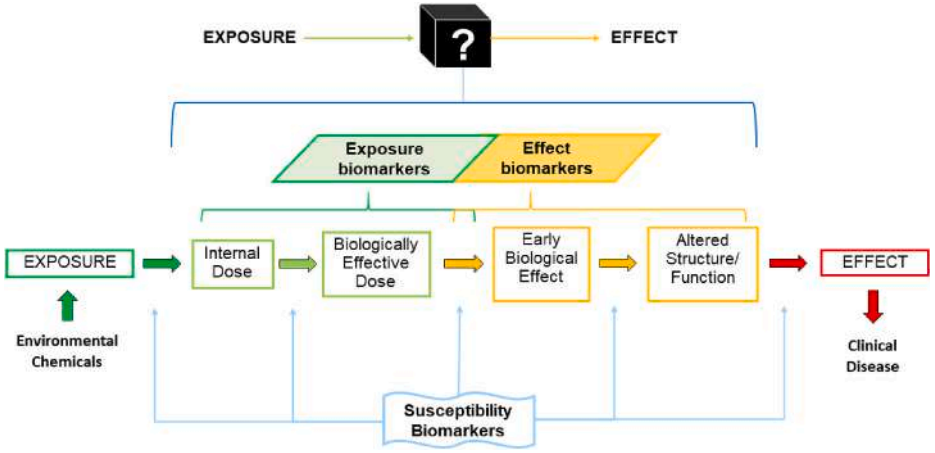

Fig. 1. Conceptual pathway representing the continuum between environmental chemical exposure and clinical disease. *Exposure biomarkers* measure the actual absorbed/excreted dose ("internal dose") and active dose at the putative target organ/tissue ("biologically effective dose"). *Effect biomarkers* measure early molecular or biochemical/cellular responses in target or non-target tissues ("early biological effect"), functional or structural changes in affected cells or tissues ("altered structure/function"), or actual clinical disease. *Susceptibility biomarkers* help to identify individuals with genetically mediated predisposition to xenobiotic-induced toxicity. Reprinted from Mustieles et al. (2020).

furthermore describe gaps in knowledge, in particular on the mechanisms of Pb-associated damage to the developing central nervous system, as well as the data needed to validate sensitive and reliable effect biomarkers in the future, with reference to existing AOPs.

2. Methods

2.1. Search history

Three literature searches in peer-reviewed journals were performed in the bibliographic database PubMed (Fig. 2). Details can be found in the search histories listed in Suppl. Table 1. The term 'biomarker' was not integrated into any of the searches, as this was found to significantly reduce the number of hits (data not shown).

2.1.1. PubMed search 1 and identification of relevant papers

2.1.1.1. Search terms. ("lead"[Title/Abstract] OR "pb"[Title/Abstract] OR lead[MeSH Terms] OR "plumbum"[Title/Abstract] OR "7439 92 1"[EC/RN Number]) AND neurodevelopment.

The elements of the search strategy (**search 1**) comprised the term *lead* combined with the term *neurodevelopment*. A preliminary search was performed using these terms. The term *lead* was searched with a combination of Medical Subject Headings (MeSH) and chemical registration numbers (EC/RN) in the title/abstract fields using AND/OR terms in Boolean logic to cover as many publications as possible. However, the term presented some challenges in order to avoid the inclusion of publications that only contained the verb *lead*. Therefore, the resulting 596 abstracts (search #1) were manually sorted to identify the articles studying the metal *lead*. The selected 160 abstracts were evaluated, and 15 references met the inclusion criteria (i.e., studies of Pb-exposed humans in relation to neurodevelopment and epigenetic changes published before July 2019). Several articles that reported associations between gene sequence variants and neurodevelopmental outcomes were also included. The 15 eligible publications selected from the PubMed search were supplemented by one review found by hand-search (Keil and Lein 2016). From this, two additional original works were identified (Wright et al., 2003; Pilsner et al., 2010) and also included (i.e., 17 papers in total; Fig. 1). Because some relevant papers were not retrieved in the first search, a second literature search was performed. The list of search terms was extended with epigenetic and OMIC terms.

2.1.2. PubMed search 2 and identification of relevant papers

2.1.2.1. Search terms. ("lead"[Title/Abstract] OR "pb"[Title/Abstract] OR "lead"[Mesh] OR "plumbum"[Title/Abstract] OR "7439 92 1"[EC/RN Number]) AND ("DNA (Cytosine-5-)-Methyltransferase 1"[Mesh] OR "DNA (Cytosine-5-)-Methyltransferases/genetics"[Mesh] OR "DNA (Cytosine-5-)-Methyltransferases*"[Mesh] OR "Epigenesis, Genetic*"[Mesh] OR "DNA Modification Methylases*"[Mesh] OR "Epigenetic*"[tiab] OR "Epigenomics*"[Mesh] OR "DNA Methylation*"[Mesh] OR "Methylation"[Mesh] OR "DNA Methylation/drug effects*"[Mesh] OR "DNA Methylation/genetics*"[Mesh] OR "Genomic Instability/genetics"[Mesh] OR "CpG Islands/genetics"[Mesh] OR "Transcriptome/drug effects"[Mesh] OR "Transcriptome/genetics*"[Mesh] OR "Metabolomics"[Mesh] OR "metabolome"[Mesh] OR "Metabolomics"[Mesh] OR "Metabolome/drug effects*"[Mesh] OR "Metabolic Diseases/genetics"[Mesh]).

In **search 2** the term *lead* was searched in the same way as in search 1. The epigenetic and OMICS terms were searched using only MeSH terms (search #43 and #44). Terms not indexed in PubMed as MeSH were omitted. As in search 1, the combination with the term *lead* resulted in an exorbitantly high number of irrelevant hits (#46). To resolve this, further terms related to "neurodevelopment" were added to the search strategy (#49). The search (#50) retrieved 105 hits. These abstracts were manually sorted to identify articles addressing the metal *lead*. This was the case in 13 articles that were further screened for relevance. Seven articles were selected. These seven references, however, were already included in the final 17 references from search 1.

2.1.3. PubMed search 3 and identification of relevant papers

2.1.3.1. Search terms. ("lead"[Title/Abstract] OR "pb"[Title/Abstract]) AND ("human biomonitoring"[Title/Abstract] OR "human exposure"[Title/Abstract] OR "environmental exposure"[Title/Abstract] OR "biomarker of exposure"[Title/Abstract]) AND ("blood"[Title/Abstract] OR "urine"[Title/Abstract] OR "breast milk"[Title/Abstract] OR "cord blood"[Title/Abstract] OR "*teeth"[Title/Abstract] OR "nail"[Title/Abstract] OR "hair"[Title/Abstract] or "placenta" [Title/Abstract]); Filter: 2000–2021.

The strategy in **search 3** comprised three preliminary searches to identify the publications in which the terms *lead* or *pb* (#1), *human biomonitoring* or *human exposure* or *environmental exposure* or *biomarker of exposure* (#2), and *blood* or *urine* or *cord blood* or *breast milk* or *teeth* or

Table 1
Comparison of Pb concentrations determined in different matrices of fetuses, children and young people in European surveys carried out in the period of 2000–2018.

Biomarker of Pb exposure	Pb concentration (population)	No. of samples	Sampling year and country	Reference
Whole blood (venous or capillary) (μg/L)	6.9[b] (6–14 yr)	14	2018, Kosovo	Dehari-Zeka et al. (2020)
- *children and young people*	11.3[a] (20–29 yr)	995	2015–2016, Germany	Lermen et al. (2021)
	8.3[c] (20–39 yr)	158	2011–2015, Norway	Fløtre et al. (2017)
	11.7[a] (20–29 yr)	986	2013–2014, Germany	Lermen et al. (2021)
	9.5[a] (14–15 yr)	204	2013–2014, Belgium	Schoeters et al. (2017)
	23[b] (6–12 yr)	53	2012–2014, Kosovo	Kutllovci-Zogaj et al. (2014)
	2.4[a] (18–40 yr)	73	2011–2014, Denmark	Rosofsky (2017)
	9.7–11.0[c] (25–35 yr female - male)	477	2004–2014, Sweden	Wennberg et al. (2017)
	16.1[a] (14–15 yr)	174	2011–2013, Slovenia	Snoj Tratnik et al. (2013)
	17.3[a] (20–35 yr)	127	2011–2013, Slovenia	Snoj Tratnik et al. (2013)
	12.3[a] (20–29 yr)	968	2011–2012, Germany	Lermen et al. (2021)
	14.6[a] (14–15 yr)	207	2007–2011, Belgium	Schoeters et al. (2017)
	12.1[a] (20–29 yr)	5765	2009–2010, Germany	Lermen et al. (2021)
	14.9[a] (1–6 yr)	3831	2008–2009, France	Etchevers et al. (2014)
	19-22[c] (8–10 yr)	n.a.	2008, Czech Republic	Cerná et al. (2012)
	17.9[a] (7–11 yr)	46	2007–2008, Croatia	Hrubá et al. (2012)
	19.4[a] (7–11 yr)	57	2007–2008, Slovakia	Hrubá et al. (2012)
	14[a] (7–11 yr)	41	2007–2008, Sweden	Hrubá et al. (2012)
	13.4[a] (7–11 yr)	42	2007–2008, Slovenia	Hrubá et al. (2012)
	16.3[a] (7–11 yr)	27	2007–2008, Poland	Hrubá et al. (2012)
	18.7[a] (18–39 yr)	579	2006–2007, France	Falq et al. (2011)
	15.1[a] (20–29 yr)	856	2005–2006, Germany	Lermen et al. (2021)
	30[a] (4–15 yr)	253	2006, Hungary	Rudnai et al. (2009)
	16.9[c] (3–14 yr)	1560	2003–2006, Germany	Schultz et al. (2009)
	22.5[a] (14–15 yr)	1659	2003–2004, Belgium	Schoeters et al. (2017)
	31[c] (8–10 yr)	333	2001–2003, Czech Republic	Batáriová et al. (2006)
	42[c] (6 yr)	202	1997–2004, Poland	Barton (2011)
- *pregnant women*	10[c] (1st trimester)	48	2016–2017, Spain	Bocca et al. (2019)
	12[c] (at delivery)	40	2016–2017, Spain	Bocca et al. (2019)
	8.5[c,d] (at delivery)	100	2010–2012, Slovakia	Gundacker et al. (2021)
	12.5[c,d] (at delivery)	98	2010–2012, Austria	Gundacker et al. (2021)
	11.1[a] (at delivery)	235	2007–2011, Belgium	Baeyens et al. (2014)
	11[a] (2nd trimester)	210	2007–2011, Poland	Polańska et al. (2014)
	7.2[a] (2nd trimester)	211	2007–2009, Norway	Hansen et al. (2011)
	11.5[c] (at delivery)	50	2006, Germany	Kopp et al. (2012)
	24.9[c] (3rd trimester)	53	2005, Austria	Gundacker et al. (2010)
- *lactating women*	8.3[a] (2nd trimester)	2982	2000–2008, Norway	Caspersen et al. (2019)
	11[c] (n.a.)	100	2002–2003, Sweden	Gerhardsson. (2010)
	16.7[a] (6th wk. postpartum)	536	2008–2014, Slovenia	Snoj Tratnik et al. (2019)
	9.2[a] (3rd d. postpartum)	211	2007–2009, Norway	Hansen et al. (2011)
	13.2[a] (6th wk. postpartum)	253	2007–2009, Norway	Hansen et al. (2011)
Cord blood (μg/L)	7.9[c] (mother BL:12)	31	2016–2017, Spain	Bocca et al. (2019)
	6.4[a] (mother BL: n.a.)	281	2012–2015, Belgium	Schoeters et al. (2017)
	8.3[a] (mother BL: n.a.)	1968	2011, France	Saoudi et al. (2018)
	4.5[c,e] (mother BL: 8.5)	100	2010–2012, Slovakia	Gundacker et al. (2021)
	7.0[c,e] (mother BL: 12.5)	100	2010–2012, Austria	Gundacker et al. (2021)
	9.6[a] (mother BL: 9.9)	594	2007–2011, Poland	Polańska et al. (2018)
	8.6[a] (mother BL: 11.1)	241	2007–2011, Belgium	Baeyens et al. (2014)
	10.3[c] (mother BL: 11.5)	50	2006, Germany	Kopp et al. (2012)
	13.7[a] (mother BL: n.a.)	1196	2002–2004, Belgium	Schoeters et al. (2017)
	13.4[c] (mother BL: 24.9)	53	2005, Austria	Gundacker et al. (2010)
	14.5[a] (mother BL: 18.3)	145	2003–2004, Spain	García-Esquinas et al. (2014)
Placenta (μg/kg)	<6.5[c]	327	2000–2008, Spain	Freire et al. (2019)
	25.8[c]	53	2005, Austria	Gundacker et al. (2010)
	45.2[c]	36	2003–2004, Croatia	Klapec et al. (2008)
	13.8[c] (non-smokers)	109	n.a., Croatia	Stasenko et al. (2010)
	17.9[c] (smokers)	99	n.a., Croatia	Stasenko et al. (2010)
	51.6[c]	23	n.a., Poland	Zagrodzki et al. (2003)
Breast milk (μg/L unless otherwise indicated)	1.74[b] (1th-8th wk. postpartum)	27	2017–2018, Hungary	Ecsedi-Angyal et al. (2020)
	1.19 μg/kg[b] (n.a.)	50	2015, Cyprus	Kunter et al. (2017)
	0.23[c] (6th-8th wk. postpartum)	353	2008–2014, Slovenia	Snoj Tratnik et al. (2019)
	5.0 μg/kg[c] (colostrum[d]) (mother BL: 7 μg/L)	20	2012–2013, Croatia	Grzunov L. et al., 2016
	2.6 μg/kg[c] (3rd-4th wk. postpartum[d])	51	2012–2013, Croatia	Grzunov L. et al., 2016
	3.3 μg/kg[c] (3rd-4th wk. postpartum[e])	20	2012–2013, Croatia	Grzunov L. et al., 2016
	6.3[b] (1st-12th mo. postpartum)	320	2010, Poland	Winiarska-M. 2014
	2.6–6[b] (n.a)	52	2008–2009, Italy	De Felip et al. (2014)
	1.5[b] (2nd-3rd wk. postpartum)	60	2002–2009, Sweden	Björklund et al. (2012)
	<0.67 μg/kg[c] (3rd-8th wk. postpartum)	300	2002–2009, Norway	Vollset et al. (2019)
	15.5[a] (3rd wk. postpartum)	107	2003–2004, Spain	García-Esquinas et al. (2011)
	1.55[b] (colostrum) (mother BL: 20 μg/L)	34	2003, Portugal	Almeida et al. (2008)
	0.94[b] (4th wk. postpartum)	19	2003, Portugal	Almeida et al. (2008)
	0.48[b] (3rd d. postpartum)	95	2001–2002, Greece	Leotsinidis et al. (2005)
	0.85–1[b] (4th-8th wk. postpartum)	39	1999–2001, Italy	Abballe et al. (2008)

(*continued on next page*)

Table 1 (*continued*)

	7.7[c] (3rd-4th d. postpartum)	143	2000, Italy	Turconi et al. (2004)
	1.63[b] (2nd-14th d. postpartum)	138	1999, Austria	Gundacker et al. (2002)
	0.15[b] µg/kg (1st wk. postpartum)	102	n.a., Portugal	Matos et al. (2009)
	13.8[b] (n.a.)	72	n.a., Spain	Falcó et al. (2006)
	4.7[b] (4th d. postpartum)	158	n.a., Slovakia	Ursinyova and Masanova (2005)
Urine (µg/g creatinine unless otherwise indicated)	1.3[c] (pregnant women)	53	2016–2017, Spain	Bocca et al. (2019)
	0.54[a] (mean age of 28.9 yr)	50	2013–2016, Belgium	Bai et al. (2019)
	0.49[a] (6th wk. postpartum)	410	2008–2014, Slovenia	Snoj Tratnik et al. (2019)
	1.16[c] (6–11 yr)	n.a.	2010–2011, Spain	Roca et al. (2016)
	1.24 µg/L[a] (5–11 yr)	n.a.	2007–2008, Italy	Protano et al. (2016)
	0.8[a] (2–17 yr)	n.a.	2005, Germany	Heitland and Köster (2006)
Hair (µg/g)	0.6–1.3 (11–12 yr)[a]	n.a.	2011–2012, Greece	Evrenoglou et al. (2013)
	0.7 (0–18 yr)[c]	n.a.	2008–2009, Spain	Llorente et al. (2017)
	1.13[a] (6 yr)	n.a.	1997–2004, Poland	Barton (2011)
	0.56[b] (11–15yr.)	n.a.	2001, Italy	Sanna et al. (2008)
	1.6[c] (mean age of 9.9 yr)	217	1994–2001, Czech Republic	Benes et al. (2003)
	1.01[b] (0–18 yr)	n.a.	n.a., Italy	Dongarrà et al. (2011)
Primary teeth (µg/g)	1.6[a] (6 yr)	284	1997–2004, Poland	Barton (2011)

Abbreviations: BL: blood level; LOD: limit of detection; n.a.: not available.
[a] geometric mean.
[b] arithmetic mean.
[c] median.
[d] Median Ery-Pb values obtained in the study (Bratislava: 17 µg/kg, Vienna: 25 µg/kg) were converted to whole blood values for comparability.
[e] Median Ery-Pb values obtained in the study (Bratislava: 9 µg/kg, Vienna: 17 µg/kg) were converted to whole blood values for comparability.

nail or *hair* or *placenta* (#3) were indicated in the title/abstract. Then these three preliminary searches were combined (#4) and articles published before year 2000 were filtered out (#5). This search had 656 hits which were manually sorted to identify publications on human biomonitoring studies focusing on children's, pregnant women's and young people's exposure to lead. In total, 58 publications from European countries were included. Some relevant publications from non-European countries were also selected for comparison (22 references). It must be noted that the selection of non-European data was not based on any predefined criteria.

2.2. Flowchart

3. Results and discussion

We conducted a systematic literature search to identify publications addressing exposure to Pb relative to neurodevelopmental toxicity, identified as the most sensitive endpoint. The biomarkers that are linked to Pb exposure and neurodevelopment were grouped into three different types: *effect biomarkers* (Table 3), *susceptibility markers* (Table 4), and *other biomarkers* (Table 5). This classification of markers is not generally applicable. Several of the biomarkers discussed here, such as high-density lipoprotein (HDL) levels or epigenetic changes, could also be caused by mutations/polymorphisms (this was not investigated in the studies included here), which would thus make them also susceptibility markers. The set of identified biomarkers is discussed in relation to current Pb exposure levels in Europe.

Table 2
Comparison of maternal peripheral blood, placental and cord blood Pb levels in surveys carried out in non-European countries after 2000.

Maternal blood (µg/L)	Placenta (µg/kg w.w.)	Cord blood (µg/L)	N. of samples	Sampling year and country	Reference
6.2[a]	-	-	1282	1999–2016, USA (NHANES)	Watson et al. (2020)
10.3[a]	-	7.1[a]	104	2013, South Korea	Kim et al. (2015)
-	2.3[b]	-	1159	2008–2013, USA	Punshon et al. (2019)
41.6[b]	-	35.0[b]	1050	2007–2011, Mexico	Sanchez-Guerra et al. (2019)
8.9[a]	-	-	211	2009–2011, USA	Sanders et al. (2012)
5.6[c]	-	7.6[c]	2000	2008–2011, Canada	Arbuckle et al. (2016)
39.7[c]	-	-	1931	2010, China, Shanghai	Li et al. (2017)
36.4[c]	7.5[c]	24.6[c]	91	2009–2010, Turkey	Tekin et al. (2012)
55.9[b]	-	-	174	2009–2010, China, Nanjing	Liu et al. (2013)
26.5[c]	-	22.5[c]	240	2007–2008, Bolivia	Barbieri et al. (2016)
595.0[b]	-	-	214	2006–2008, Nigeria	Adekunle et al. (2010)
32.6[c]	-	22.9[c]	350	2006–2007, Iraq	Al-Jawadi et al. (2009)
-	-	16.6[b]	121	2006–2007, Turkey	Dursun et al. (2016)
64.3[c]	-	35.7[c]	130	2006–2007, China, Shanghai	Wang et al. (2008)
72.4[c]	600[c] (d.w.)	43.6[c]	109	2002–2007, China, Hubei	Tian et al. (2009)
25.5[a]	390[a] (d.w.)	21.4[a]	1572	2005–2006, Saudi Arabia	Al-Saleh et al. (2011)
17.1[b]	-	12.9[b]	308	2004–2005, Taiwan	Lin et al. (2010)
21.0[b]	-	-	43,288	2003–2005, USA	Zhu et al. (2010)
48.2[b]	-	35,2[b]	365	2003–2004, Iran	Vigeh et al. (2006)
10.8[c]	11.2[c]	9.9[c]	649	2001–2003, Japan	Iwai-Shimada et al. (2019)
159.0[a]	-	-	50	n.a., Pakistan	Kayama et al. (2016)
-	300[c]	-	60	n.a., India	Singh et al. (2010)

Abbreviations: n.a.: not available; w.w.: wet weight, d.w.: dry weight.
[a] geometric mean.
[b] arithmetic mean.
[c] median.

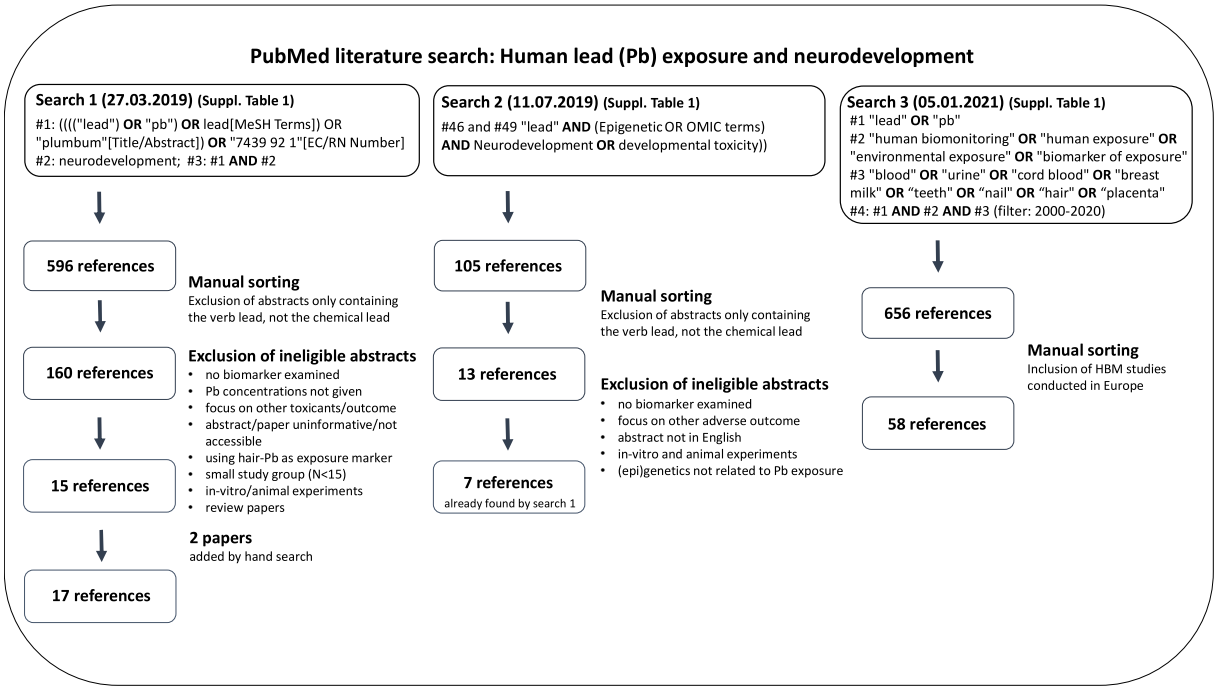

Fig. 2. The sequence of the literature search. Two PubMed searches on Pb exposure and neurodevelopment (search 1 and 2) identified 17 publications (for specific references, see Tables 3–5). PubMed search number 3 identified 58 publications focused on Pb exposure in Europe (Table 1). Several articles were reviewed in full length, if sufficiently specific information e.g., on biomarkers, was missing in the abstract.

Table 3
Summary of studies on **effect markers** linked to Pb exposure and neurodevelopment.

Author(s), Country	Marker(s) of Pb exposure	Effect Biomarker(s)	Neurodevelopmental testing	Summary
Brain derived neurotrophic factor (BDNF)				
Zhou et al., (2019) China	Whole blood, children, mean age: 5 yrs 6.7 μg/dL (6.5–7.0 μg/dL) (N = 561)	**Serum BDNF** (ELISA) 19.5 ng/mL	-	Serum BDNF negatively associated with blood Pb levels in all subjects and in boys, but not in girls. A negative interaction between blood Pb and Hg levels as well as a positive interaction between blood Pb and Al levels on serum BDNF concentrations was found in boys (not in girls).
Ren et al., (2016) China	Cord blood 7 ± 3 μg/dL[b] (low exp. group, N = 60) 13 ± 3 μg/dL[b] (high exp. group; N = 60)	**Cord serum BDNF** (ELISA) 2.5 ± 0.9 ng/mL (low exp gr) 3.5 ± 1.2 ng/mL (high exp gr)	Neonatal Behavioral Neurological Assessment (NBNA)	Cord serum BDNF positively associated with blood Pb, while NBNA sum score inversely correlated with blood Pb.
Serum cortisol				
Cai et al., (2019) China	Whole Blood (median), children, 3–6 yrs 4.9 μg/dL (Guiyu, N = 358) 3.5 μg/dL (Haojiang, N = 216)	**Children serum cortisol** (median) (Immunoassay) 452 ng/mL (Guiyu) 594 ng/mL (Haojiang)	Sensory Processing Measure-Hong Kong Chinese version (SPM-HKC). Note: Higher score means greater impairment.	Children from Guiyu (e-waste recycling town) had significantly lower concentration of serum cortisol than children in Haojiang (control site). Serum cortisol negatively correlated with blood Pb. All Sensory Processing Measure scores in Guiyu children were higher than in Haojiang children. Most sensory processing scores also positively correlated with blood Pb.
Tamayo et al., (2016) Mexico	Mat. whole blood and bone[a], N = 255 3.5 ± 2.5 μg/dL (Mat. Bl., 2nd trimester) 3.7 ± 2.9 μg/dL (Mat. Bl., 3rd trimester) 5.6 ± 5.8 μg/g (Mat. Tibia, postpartum) Maternal Pb levels refer to infants at the age of 12 months.	**Infant saliva cortisol** (Chemiluminescence assay) Cortisol levels not given	-	Early gestational Pb exposure alters diurnal cortisol rhythms of infants. Association is modified by infant age at 12 months and 18–24 months of age. Elevated prenatal Pb exposure of 12-month-old infants (2nd trim. Pb ≥ 10 μg/dL) is associated with 40% lower cortisol levels compared to infants with lower 2nd trim. Pb exposure (<5 μg/dL).

Pb concentrations are given as arithmetic or geometric mean values ± standard deviation, unless otherwise specified.
Abbreviations: exp.: exposure; Mat. Bl.: Maternal Blood; RBC: red blood cell.
[a] Bone Pb: in all studies midtibial shaft and/or patella Pb was analysed with a K-shell X-ray fluorescence instrument (KXRF).
[b] as converted from μM concentrations given in abstract.

Table 4
Summary of studies on **susceptibility markers** linked to Pb exposure and neurodevelopment.

Author(s), Country	Marker(s) of Pb exposure	Susceptibility marker(s)	Neurodevelopmental testing	Summary
Epigenetic modifications				
Wu et al., (2017) USA	Mat. RBC (2nd trimester) 1.2 ± 0.6 μg/dL (N = 268)	Cord blood leukocyte DNA (=268) ***CLEC11A DNHD1*** HumanMethylation450 Bead Chips	-	Prenatal low-level Pb exposure associated with newborn DNA methylation, particularly in female infants. CpG cg10773601, annotated to CLEC11A, showed an epigenome-wide significant negative association with maternal Pb exposure. CpG (cg24637308), which showed a strong negative association with maternal Pb exposure among girls, was annotated to DNHD1.
Pilsner et al., (2009) Mexico	Mat. bone[a], Cord blood (N = 103) 10.5 ± 8.4 μg/g (Mat. Tibia, N = 103) 12.9 ± 14.3 μg/g (Mat. Patella, N = 103)6.6 ± 2.7 μg/dL (Cord Blood)	Cord blood leukocyte DNA (N = 103) **LINE-1 methylation Alu methylation** EZ-96 DNA Methylation-Gold Kit	-	Prenatal Pb exposure (as indicated by maternal patella Pb) is inversely associated with genomic DNA methylation of the LINE-1 element. No association was found between cord blood Pb and cord genomic DNA methylation.
Candidate genes/Gene variants				
Wang et al., (2017) Bangladesh Mexico	Cord blood 5.1 ± 6.5 μg/dL (N = 390) 3.8 ± 2.7 μg/dL (N = 497)	***UNC5D SLC1A5*** Genome-wide gene-environment interaction study	Mental composite score and motor composite score (BSID-III) of infants 24 months of age	Top locus containing *UNC5D* associated with mental composite score. Two *UNC5D* SNPs had comparable main effects and GxE effects on both mental and motor composite scores in each cohort. By comparing GxE analyses and in-vitro transcriptome, glutamate transporter *SLC1A5* was identified as common gene/protein of interest with a *SLC1A5* variant being associated with mental composite score.
Wagner et al., (2017) Mexico	Mat. whole blood Pb, 2nd trimester 3.8 ± 2.6 μg/dL (N = 462)	***SPP1*** Genome-wide association study	Cognitive Development Index (CDI) score (BSID-III) of infants 24 months of age	Pb induces upregulation of SPP1 via NRF2 in human neural stem cells. *SPP1* SNP rs12641001 significantly associated with CDI score, however, no significant interaction with prenatal Pb exposure.
Wright et al., (2003) Mexico	Cord blood 6.6 ± 3.4 μg/dL (N = 311)	***APOE***	Mental Development Index (MDI) score (BSID-IIS) of infants 24 months of age	Negative effect of Pb exposure on MDI score at 24 months of age was 4-fold greater in APOE3/APOE2 carriers than in APOE4 carriers. Subjects with the E4 isoform of APOE may have advantages over those with the E2 or E3 isoforms with respect to early life neurodevelopment.
Pilsner et al., (2010) Mexico	Cord blood 6.7 ± 3.6 μg/dL (N = 255)	***MTHFR***	MDI score (BSID-IIS) of infants 24 months of age	Maternal MTHFR-677 genotype predicted MDI scores of infants at 24 months of age (BSID-IIS) but *MTHFR* genotype x Pb interaction was not observed. The maternal *MTHFR* 677T allele is an independent predictor of poorer child neurodevelopment at 24 months of age.
Liu et al., (2015) China	Whole blood, children, 3 yrs 11.3 ± 5.4 μg/dL (Guiyu, N = 120) 5.8 ± 2.5 μg/dL (ref group, N = 138)	***DRD2***	Cognitive and language scales (BSID-III)	Both scores lower in Guiyu children compared to reference group. No significant association between (DRD2) Taq IA polymorphism and neurodevelopment of Pb exposed children.

Pb concentrations are given as arithmetic or geometric mean values ± standard deviation, unless otherwise specified.
Abbreviations: Alu: Alu retrotransposons; APOE: Apolipoprotein E; BSID-III: Bayley Scales of Infant and Toddler Development, Third Edition; BSID-IIS: Spanish version of the BSID-II; CLEC11A: C-Type Lectin Domain Family 11, Member A; DNHD1: Dynein Heavy Chain Domain 1 gene; DRD2 (Dopamine receptor D2); GxE: gene-environment interaction; LINE-1: long interspersed nuclear element; Mat.: Maternal; MTHFR: Methylenetetrahydrofolate reductase; NRF2: Nuclear Factor Erythroid 2-Related Factor 2; p16: tumor suppressor gene p16; RBC: red blood cell; SLC1A5: Solute Carrier Family 1 Member 5 (alias ASCT2); SNP: Single Nucleotid Polymorphism; SPP1 (Secreted phosphoprotein 1); UNC5D: Unc-5 Netrin Receptor D.
[a] Bone Pb: in all studies midtibial shaft and/or patella Pb was analysed with a K-shell X-ray fluorescence instrument (KXRF).

3.1. Pb exposure in Europe

Whole blood Pb is the most widely used exposure parameter, as it is the most suitable indicator of the concentration of Pb in soft tissues, like the brain. There are limited recent European HBM data on Pb levels in other matrices than blood.

In the past two decades, more than 25 HBM surveys on blood Pb levels were performed in European countries, including Belgium, Czech Republic, France, Germany, Norway, Slovenia, and Spain. Nearly 20 studies included children (Table 1). The majority were carried out before 2015; thus data on the most recent exposure is lacking. As the developing central nervous system is at the highest risk for impairment due to Pb exposure, this review on the concentration of Pb in blood, placenta, breast milk, urine, hair, and teeth reflects the exposure of fetuses and children in Europe during the past two decades (Table 1). For surveys at contaminated sites, only data on the reference populations are reported. In addition, Pb levels in some populations of young adults of child-bearing age are provided as indicators of potential exposures of future fetuses.

3.1.1. Pb levels in children and young adults

The mean Pb concentrations of blood samples collected from children and young adults in European countries after the year 2000 were comparable (Table 1). Data show a decreasing trend in Pb blood levels of

Table 5
Summary of studies on **other markers** linked to Pb exposure and neurodevelopment.

Author(s), Country	Marker(s) of Pb exposure	Marker	Neurodevelopmental testing	Summary
High density lipoprotein (HDL)				
Ji et al., (2018) USA	RBC Pb, children (postnatal) 2.2 ± 1.6 μg/dL (whole gr; N = 1479) 2.1 ± 1.5 μg/dL (control gr; N = 1180) 2.4 ± 1.9 μg/dL (ADHD gr; N = 299)	**Maternal plasma HDL** (median) (nonfasting blood samples) 60.7 mg/dL (N = 1479) 61.5 mg/dL (N = 1180) 57.4 mg/dL (N = 299)	Attention Deficit Hyperactivity Disorder (ADHD) according to ICD-9 and ICD-10. Age of children's ADHD diagnosis not specified.	Mothers of children with any ADHD diagnosis had low HDL levels and high stress. 9% of the children had elevated Pb levels (5–10 μg/dL) in early childhood associated with a 66% increased risk of ADHD particularly for boys. The OR of ADHD associated with elevated Pb levels among boys was reduced by one-half if mothers had adequate HDL levels or low stress.
Iron (Fe), Calcium (Ca), Zinc (Zn), Copper Cu)				
Shah-Kulkarni et al., (2016) Korea	Whole blood (N = 765–790) 0.9 ± 1.5 μg/dL (Cord Blood) 1.3 ± 1.5 μg/dL (Mat. Blood, at delivery)	**Maternal Fe intake** (N = 891) 13 ± 4 mg/d	Mental Development Index (MDI) and Psychomotor Development Index (PDI), Korean version of Bayley Scales of Infant Development II (K-BSID-II), 6, 12, 24, and 36 months of age (N = 558–965)	Maternal Pb exposure in late pregnancy associated with lower MDI score in children 6 months of age with stronger effect in lower Fe intake group. No such associations found for Pb exposure in early pregnancy, in relation to cord blood, or PDI.
Ettinger et al., (2009) Mexico	Maternal Blood 3.8 ± 2.0 μg/dL (Ca suppl group, N = 283) 4.1 ± 2.0 μg/dL (Placebo group, N = 274)	**Maternal Ca intake**	-	Supplementation of 1200 mg dietary Ca associated with modest reductions in blood Pb (on average 11% reduction, i.e. 0.4 μg/dL) when administered during pregnancy.
Liu et al., (2014) China	Maternal Blood, 1st trimester, N = 415 3.98 ± 1.15 μg/dL	**Maternal Ca, Fe, Zn supplementation**	Neonatal behavioral neurological assessments (NBNA), postnatal day 3	Inverse associations between maternal Pb and neonatal behavioral neurological assessment (NBNA) scores. Ca, Fe, and/or Zn supplementation protects against high blood Pb levels.
Parajuli et al., (2013) Nepal	2.1 μg/dL (Cord Blood), N = 100	**Cord blood Zn**	Brazelton Neonatal Behavioral Assessment Scale (NBAS-III), postnatal day 1	Cord blood levels of Pb and As, but not Zn, showed significant inverse association with neurodevelopment of newborns (motor cluster).
Liu et al., (2018) Mexico	Maternal Blood, 2nd trimester PROGRESS (prospective prebirth cohort) study, Mexico City Metal levels (Mn, Pb, Co, Cr, Cs, Cu, As, Cd, Sb) not specified in this method paper	**Maternal blood Cu** Size of study group(s) not specified	BSID-III (cognition score, cognitive trajectories), 6, 12, 18, and 24 months after birth	Bayesian varying coefficient kernel machine regression was used to assess neurodevelopmental trajectories associated with exposure to complex metal mixtures. Positive associations between 2nd trimester exposure to Cu and cognition score at 24 months, and cognitive abilities across 6–24 months were found. Across 6–24 months, Pb was negatively associated with neurodevelopment. Overall, this resulted in negative interaction effect between 2nd trimester copper (Cu) and Pb exposures with 24-month neurodevelopment.

Pb concentrations are given as arithmetic or geometric mean values ± standard deviation.
Abbreviations: BSID-II: Bayley Scales of Infant Development, Second Edition; BSID-III: Bayley Scales of Infant Development, Third Edition; Mat. Bl.: Maternal Blood; NBAS-III: Brazelton Neonatal Behavioral Assessment Scale, Third Edition.

children and young adults after 2000. In surveys implemented before 2013, all reported mean blood Pb levels of children and young adults were above the BMDL01 of 12 μg/L set by EFSA for developmental neurotoxicity (EFSA, 2010). Moreover, a percentage of individual blood Pb concentrations exceeded this level even in populations characterized by a low mean exposure value. However, all values were substantially below the reference levels of 50 μg/L and 35 μg/L set by the CDC and the German Environmental Agency, respectively (CDC, 2010; Schulz et al., 2007). It must be noted that the risk for neurodevelopmental disorders due to Pb exposure cannot be ignored. Importantly, developmental neurotoxicity due to Pb exposure has been reported at exposures as low as 20 μg/L (Gilbert, 2006; EFSA, 2012; Rocha, 2019), and there is likely no safe threshold for Pb neurotoxicity (Lanphear et al., 2005; Skerfving et al., 2015). Although the information on Pb levels in children and young people after 2015 is limited, in some countries with regular nationwide surveys, the decreasing trend has not been observed to continue since 2010, and the concentration values levelled out at approximately 10 μg/L (Lermen et al., 2021; Wennberg et al., 2017).

3.1.2. Pb exposure of fetuses

Due to particular concern about neurodevelopmental effects, studies often included pregnant women and mother-neonate pairs. Pregnant and lactating women were investigated in at least nine European studies, and a similar number analysed cord blood with or without a sampling of maternal blood. The data show a decreasing trend in both maternal and cord blood Pb levels. In the European surveys implemented after 2005, mean maternal and cord blood Pb concentrations did not exceed the EFSA BMDL01 of 12 μg/L.

A significant correlation between maternal and cord blood Pb concentrations was found in most surveys, with ratios ranging between 0.55 and 0.97. Hence, Pb concentrations were only slightly lower in cord than in maternal blood, indicating that the placenta does not constitute a barrier for Pb transfer from the maternal to the fetal compartment. Maternal smoking and alcohol consumption were associated with enhanced maternal and cord blood Pb levels, while maternal Ca and Vitamin D intake seems to be protective against the mobilization of Pb from bones (Saoudi et al., 2018; Taylor et al., 2013; Gulson et al., 2016).

Some selected data on maternal and cord blood levels from non-European populations are listed in Table 2. The comparison shows that higher blood Pb levels were measured in developing countries (e.g. Nigeria, Pakistan) than in developed countries. Pb concentrations in maternal and cord blood observed in European surveys are similar to those reported from other high-income countries outside Europe, while they are much lower than Pb blood levels of populations living in

polluted as well as deprived areas.

3.1.3. Pb exposure of breastfed infants

Breast milk Pb level provides a direct indicator of Pb exposure of breastfeeding infants. Breast milk shows a higher variation in Pb levels than maternal blood (Table 1). In general, lower mean Pb concentrations in breast milk were measured in studies conducted after the year 2000 compared to previous studies (WHO, 1989). Due to the high variability in milk Pb levels, even within studies, this decreasing trend in breast milk Pb levels is not observed to continue after 2000. The opposite trend is even observed according to some studies (Abbale et al., 2008; De Felip et al., 2014).

Several studies showed higher breast milk Pb levels in current, passive or ever smokers than in never smokers (Gundacker et al., 2002; Grzunov Letinic et al., 2016; Winiarska-Meiczan 2014; Almeida et al., 2008). The high variation in breast milk Pb levels among the included studies suggests that besides differences in external exposures and genetic predispositions of the mothers, other individual maternal factors (e.g. age, past exposures, previous lactations and pregnancies, stage of lactation, Ca and D-vitamin intake during lactation) are also important.

The reported breast milk Pb concentrations in some studies (Winiarska-Meiczan 2014; García-Esquinas et al., 2011) suggest that infant Pb intake could approach the EFSA $BMDL_{01}$ of 0.5 μg/kg of body weight/day (EFSA 2010). Breast milk constitutes the optimal nutrition for young infants, but the potential for high Pb intake of infants via mother's milk cannot be ignored considering (i) the high Pb content of breast milk samples reported in some studies, (ii) other potential sources (e.g. complementary food or water) relevant at this period, and (iii) the fact that infants may absorb dietary Pb more efficiently than adults, especially if there is a concurrent deficit in Ca and other essential elements.

Overall, Pb exposure could still be associated with risk for developing fetuses, infants and children. Therefore, a new Pb action level for blood should be established. Larger nationwide surveys are needed to reliably assess recent exposure to Pb. To facilitate large campaigns, non-invasive sampling methods with harmonized methodology and adequate reference levels should be applied in HBM surveys among non-occupationally exposed populations, especially in the case of children (Esteban and Castano, 2009). Except for maternal and cord blood sampled in departments of obstetrics, blood is not an easily collectable biological matrix. Urinary Pb levels usually correlate with those measured in plasma as well as with the external exposure (Bai, 2019). Urine Pb therefore presents a valid and non-invasive alternative to blood Pb. Nail and hair Pb levels can serve as indicators of exposure to Pb; however, they are not considered reliable biomarkers of internal dose (Klotz and Goen, 2017; Olympio et al., 2020). Deciduous teeth Pb levels could also be easily applicable for biomonitoring of Pb exposure in children over the years of the preschool and early school period, since good correlation with blood levels has been reported (Barton, 2011). Placental tissue might be a suitable matrix for investigation of fetal exposure, although the comparability of the results requires standardization of collection, tissue preparation (e.g. washing and homogenization of whole placenta or biopsies from specific parts), and analytical methods (Esteban et al., 2012). Due to heterogeneity of the methods applied in published studies, data on placental Pb levels show great variability.

3.2. Biomarkers

Data sets from each of the 17 studies (Fig. 2) were grouped by type of marker and ranked in ascending order according to blood Pb concentrations in the populations measured for these groups of biomarkers (Tables 3–5).

3.2.1. Biomarkers of the effect associated with Pb exposure and neurodevelopment

Classical effect biomarkers of Pb exposure include markers related to heme biosynthesis and pyrimidine nucleotide metabolism (IARC 2006). However, these effects are not specifically related to neurodevelopment and have mostly been applied in settings of high (occupational) Pb exposure. The following section describes the studies found on effect biomarkers (Table 3).

3.2.1.1. Brain-derived neurotrophic factor (BDNF). As a member of the neurotrophin family of growth factors, brain-derived neurotrophic factor (BDNF) constitutes a key regulator of brain development and neural plasticity and is involved in the pathophysiology of diverse psychiatric disorders, including depression, anxiety, ADHD and autism (Kowiański et al., 2018).

We identified two studies on Pb exposure, neurodevelopment and BDNF showing apparently opposite results (Table 3). In the first study, 561 pre-school children at 5 years of age in China were assessed for blood concentrations of Pb (geometric mean of 6.7 μg/dL), Hg (0.10 μg/dL), Al (5.2 μg/dL), and Mn (1.8 μg/dL) as well as for BDNF concentration in serum (Zhou et al., 2019). Adjusted multivariable linear regression models were used to evaluate the possible interactions between metal co-exposure, taking into account several covariates. Blood Pb concentrations correlated significantly and inversely with serum BDNF concentrations in boys but not in girls. There was furthermore a negative interaction between blood Pb and Hg levels and positive interaction between blood Pb and Al levels in relation to serum BDNF concentrations in boys.

In the second study, cord blood total BDNF levels were determined in neonates from China grouped according to high (Pb > 10 μg/dL; N = 60) and low exposure (Pb < 10 μg/dL; N = 60) relative to their scores in the neonatal behavioral neurological assessment test (Ren et al., 2016). As described in the English abstract (article in Chinese), the high Pb exposure group showed significantly lower NBNA scores and higher serum levels of BDNF compared to the low Pb exposure group. Notably, higher cord serum levels of total BDNF were associated with poorer NBNA summary scores. Information on the number of male and female neonates, statistical analyses and the influence of infant sex on NBNA scores and BDNF levels missing from the abstract.

The physiology of BDNF is complex. In the brain, the precursor pro-BDNF is synthesized and stored in dendrites or axons. While pro-BDNF preferentially binds the p75 neurotrophin receptor leading to apoptosis, mature BDNF activates tyrosine kinase receptors (TrkB) to promote cell survival and synaptic plasticity (Miranda et al., 2019). Moreover, the ratio between the BDNF and its precursor may vary throughout development and hence vary between life-stages such as neonates, children, adolescents, adults and elders (Miranda et al., 2019).

Data from the paper by Ren et al. (2016) is only available from an abstract, and this obviously hampers the interpretation of data. However, the inconsistency between studies could possibly be ascribed to the different life stages of the children (neonates vs children) at the time of BDNF assessment, but it does not explain the difference in sensitivity between boys and girls at birth. Rather, these findings could be explained in terms of the BDNF isoform (pro- or mature) driving the association. The association between Pb exposure and higher serum BDNF levels thus could be explained by higher levels of the pro-BDNF isoform, which exerts proapoptotic effects, and could explain the association between higher serum BDNF levels linked to poorer neonatal development (Ren et al., 2016).

BDNF can be assessed in different biological matrices and at different levels of biological complexity. Until now, most ELISA kits have been designed to measure both pro-BDNF and mature BDNF in human serum/plasma. However, more specific measures that allow discriminating between the pro- and mature BDNF serum forms are progressively available and will facilitate the interpretation of divergent results in the

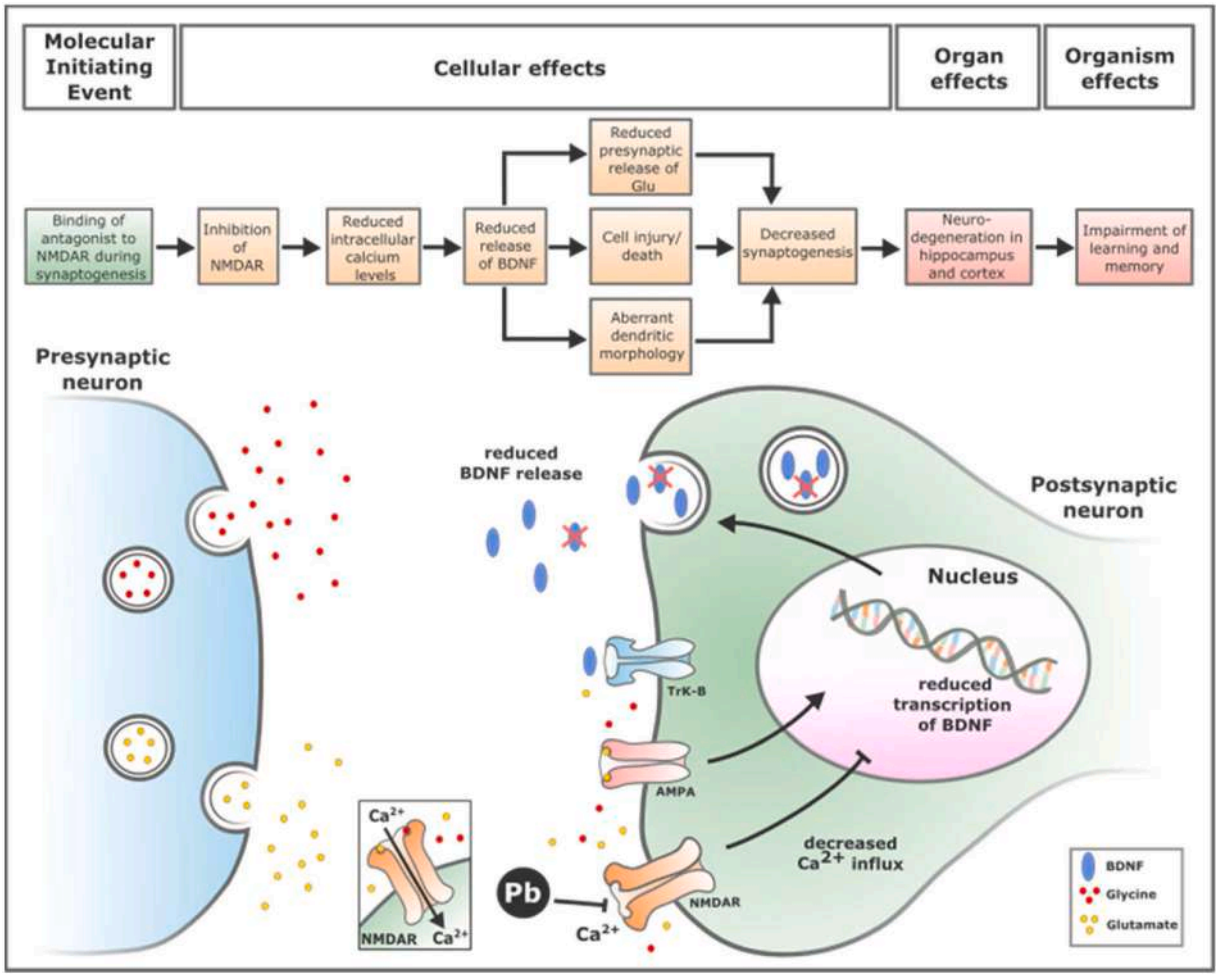

Fig. 3. Inhibition of the NMDA receptor (NMDAR) by Pb is followed by reduced Ca influx into the nucleus, which reduces transcription of BDNF. The reduced BDNF release eventually leads to neurodegeneration in the hippocampus and cortex and impairs learning and memory as described in AOP13 (https://aopwiki.org/aops/13).

literature (Bharani et al., 2020; Mizoguchi et al., 2020).

The potential for the use of BDNF biomarkers in relation to Pb exposure in HBM studies is supported by toxicological and AOP data (Fig. 3). Also, other environmental chemicals, including bisphenols, phthalates and polycyclic aromatic hydrocarbons, have been shown to interfere with BDNF signaling (Mustieles et al., 2020; Perera et al., 2015; Ponsonby et al., 2016). Therefore, there is recent interest in assessing BDNF at different levels of biological complexity (e.g. DNA methylation, gene expression, protein levels) as biomarkers of brain function with promising application in HBM studies (Mustieles et al., 2020). Indeed, epigenetic mechanisms, including DNA methylation, influence BDNF expression and regulation (Ikegame et al., 2013). Additionally, the DNA methylation status of the BDNF gene seems consistent across tissues, including the brain and blood, supporting its use as a valid and useful peripheral biomarker of psychiatric disorders (Kundakovic et al., 2015; Stenz et al., 2015). Another advantage is that peripheral blood BDNF DNA methylation could be more stable over time compared to serum/plasma BDNF protein levels, providing information on a longer period of time (Mustieles et al., under review).

Future HBM studies should ideally investigate a related set of BDNF biomarkers at different levels of biological organization, testing both pro- and mature BDNF protein isoforms in combination with infant/child neuropsychological tests to achieve the most accurate picture possible (Mustieles et al. under review).

3.2.1.2. Cortisol. Endocrine disrupting properties of Pb, one of which relates to cortisol, are thought to contribute to the metal's neurotoxicity. The stress hormone cortisol, synthesized from cholesterol, is the major glucocorticoid produced by the human adrenal cortex and the end product of the hypothalamic-pituitary-adrenal (HPA) axis. In the fetal brain, glucocorticoids are involved in several central aspects of development. The hippocampus, a known target of Pb toxicity and a central player in memory function, has the highest concentration of glucocorticoid receptors in the central nervous system (Lee et al., 2015; Tamayo et al., 2016; Graham et al., 2019).

Infant salivary cortisol was measured as an index of HPA-axis functioning in a birth cohort in Mexico City (Tamayo et al., 2016). Saliva samples were repeatedly collected over 2 days at 12 (N = 255) or 18–24 months of age (N = 150). Mixed-effects regression models were applied to account for the nonlinearity of cortisol rhythms. Several covariates were taken into account. In age-stratified models, a statistically significant negative association between maternal blood Pb and cortisol levels in 12-month-old infants and a positive association for 18–24-month-old infants were observed, although the latter was not statistically significant.

Children aged 3–6 years were studied for Pb exposure and serum cortisol in China (Cai et al., 2019). Children from Guiyu (n = 358, median Pb level: 4.9 μg/dL), a town where electronic waste is recycled, and Haojiang (n = 216, median Pb level: 3.5 μg/dL), a nearby town with no such recycling activity, were included. Serum cortisol levels were obtained from peripheral venous morning blood samples from fasting children. The children's sensory processing (relating to vision, hearing,

touch, taste and smell, body awareness, balance and motion) were assessed with the Sensory Processing Measure-Hong Kong Chinese version (SPM-HKC) home form, filled in by parents. Multiple linear regression analysis was applied to blood Pb and serum cortisol levels, taking into account several covariates. Blood Pb exceeded 5 μg/dL in 47% of the Guiyu children, and their serum cortisol concentrations were significantly lower than those of the Haojiang children. All scores of the Sensory Processing Measure were higher in Guiyu than Haojiang children, indicating greater difficulties, especially for touch, body awareness, balance and motion, and total sensory systems. Most sensory scores were also positively correlated with blood Pb.

In these studies, elevated maternal Pb exposure was associated with reduced cortisol levels in the 12 months and 3–6 year old children, whereas the cortisol curve shifted upwards in the 18–24 month old children. The normal trend in cortisol levels from 12 to 18–24 months of age is a downward shift. Pb exposure, therefore, appears to produce a cortisol rhythm pattern in 12-month-old children that is similar to the pattern normally seen at 18-24-month. It was concluded that early prenatal Pb exposure is associated with dysregulated infant HPA axis function, perhaps representing a premature HPA axis maturation (Tamayo et al., 2016). In the study from China, Pb exposure was associated with both lower cortisol levels and an increase in child sensory integration difficulties, especially regarding touch, body awareness, balance and motion, and total sensory systems. Cai et al. (2019) concluded that cortisol might be involved in touch-related sensory integration difficulties.

The most commonly used biomarkers, serum and salivary cortisol reflect levels at a single point in time. Levels are highly variable due to circadian fluctuations and fast changes in response to stressors. Effects of long-term systemic cortisol exposure are therefore complicated to assess, even if a predefined protocol is strictly adhered to (Lee et al., 2015). If basal cortisol levels are to be determined in human studies, cortisol concentrations must not only be measured several times a day to capture the large diurnal variation but also be done with non-invasive sampling to avoid acute stress (Tamayo et al., 2016). These requirements rather speak against the use of serum cortisol for routine use in HBM studies, and even salivary cortisol sampling might provoke stress in children. Hair cortisol analysis, which has been suggested as a promising technique for retrospective global assessment of chronic stress (Lee et al., 2015) may be an alternative in some settings. Another design that has been previously applied in infants is collecting salivary samples before and after a stressful stimulus (e.g. blood draw), which may provide information on the acute stress response of the child (Giesbrecht et al., 2017). Of note, it would be interesting to investigate the influence of Pb exposure on the response of the HPA-axis.

3.2.2. *Susceptibility markers associated with Pb exposure and neurodevelopment*

3.2.2.1. Epigenetic modifications. DNA methylation, a fundamental epigenetic process, modulates the level of gene expression without altering the DNA sequence. Methylation programming patterns can be modified during development. LINE-1 and Alu elements are repetitive DNA retrotransposons that constitute approximately 17% and 25% of the human genome, respectively (Baba et al., 2014; Luo et al., 2014). Therefore, the extent of LINE-1 and Alu methylation is considered a surrogate marker for global DNA methylation levels (Ruiz-Hernandez et al., 2015).

Two studies have examined DNA methylation in relation to prenatal Pb exposure, albeit without the concomitant study of markers of neurodevelopment (Table 3) (Pilsner et al., 2009; Wu et al., 2017). An epigenome-wide association study examined 268 mother-infant pairs in the USA (Wu et al., 2017). Genome-wide DNA methylation levels of infants were determined at 482,397 CpG[2] loci in umbilical cord blood nucleated cells using HumanMethylation450 Bead Chips. Maternal Pb exposure was analysed in red blood cells in the 2nd trimester (mean level: 1.2 ± 0.6 μg/dL). After adjusting for batch effects, cell types, and several covariates, robust linear regression models were used to examine associations of prenatal Pb exposure with DNA methylation in cord blood at epigenome-wide significance levels (false discovery rate <0.05). Elevated maternal Pb levels were associated with decreased DNA methylation of most CpG sites, and the methylation pattern was more frequently associated with maternal Pb levels in female than male infants (Wu et al., 2017). A CpG site annotated to *CLEC11A* showed an epigenome-wide significant negative association with maternal Pb levels. CLEC11A stimulates proliferation and differentiation of primitive hematopoietic precursor cells (RBCs, lymphocytes, granulocytes, macrophages), and Pb is known to interfere with hemoglobin synthesis (Wu et al., 2017). A second CpG site showed a negative association with prenatal Pb exposure among female infants was annotated to *DNHD1*. Little is known about its function, but it has been reported as a novel candidate gene associated with intellectual disability (Anazi et al., 2017) and early human developmental diseases (Meier et al., 2019). Of note, in another study, CpG methylation in *DNHD1* was shown to match well between blood and brain (Hannon et al., 2015), suggesting that peripheral blood cells may serve as a surrogate for the brain with respect to certain key regulatory loci.

In the study by Pilsner et al. (2009), genomic DNA methylation within CpG islands of LINE-1 and Alu retrotransposons was analysed in 103 umbilical cord blood samples. Cord blood Pb and genomic DNA methylation were not correlated, but maternal patella Pb correlated inversely with umbilical cord LINE-1 methylation, and maternal tibia Pb correlated inversely with Alu methylation. In a mixed-effects regression model, only maternal tibial Pb remained negatively associated with Alu methylation.

In a systematic review on environmental chemicals and DNA methylation in adults (Ruiz-Hernandez et al., 2015), four studies addressed Pb exposure. All studies reported a trend toward inverse associations of Pb exposure and DNA methylation. One of the studies confirms to some degree the findings of Pilsner et al. (2009), as Pb in the patella of adult men was also inversely associated with LINE-1 methylation (Wright et al., 2010). Since the method does not provide a fine epigenomic mapping of DNA methylation patterns, it remains unclear to which extent reduced global DNA methylation actually alters gene expression and in which specific chromosomal regions.

3.2.2.2. Candidate genes and gene variants. A genome-wide gene-environment interaction study (GWIS) in two birth cohorts (390 children from Mexico, 497 from Bangladesh) aimed to identify genetic loci in the child that modified the effect of prenatal Pb exposure (cord blood Pb) on

[2] CpG is the abbreviation for 5′-C-phosphate-G-3′, i.e. cytosine and guanine that are separated by only one phosphate group along its 5′ to 3′ direction. This notation is used to distinguish the single-stranded linear sequence from the CG base pairing in double-stranded sequences. CpG islands (CGIs) of vertebrates represent a class of short DNA sequences that are GC-rich, CpG-rich, and predominantly unmethylated. Silencing of CGI promoters is achieved by, among other mechanisms, dense CpG methylation. CGIs are thus generally capable of affecting local chromatin structure and facilitating regulation of gene activity (Deaton and Bird 2011).

neurodevelopment at approximately 2 years of age (Wang et al., 2017). Neurodevelopment was assessed using the motor composite scores as determined with the Bayley Scales of Infant Development. In addition, in-vitro transcriptome data were generated from Pb-exposed human neural stem cells. Univariate and multivariate regression analyses were performed to estimate the effects of covariates (child sex and age of neurologic examination, gestational age at birth, parity, maternal education, environmental tobacco smoke exposure) on neurodevelopment. The study (GWIS) provided data on several genetic polymorphisms that modified neurodevelopmental outcomes in response to prenatal Pb exposure. All candidate genes were generally related to neurodevelopment. The functional role of UNC5D is largely unclear, but involvement in neurite growth and developmentally programmed death of neurons have been demonstrated (Zhu et al., 2013; Srikanth et al., 2018). Two *UNC5D* variants had main effects on the Bayley Scales of Infant Development mental score and additionally showed a GxE interaction on the score. This was in an unexpected way, as the minor alleles of these *UNC5D* SNPs were associated with lower mental scores, but the GxE interaction was positive. It was suspected that Pb somehow counteracted the negative effects on neurodevelopment in carriers of the minor alleles. Another candidate gene, *SLC1A5*, was identified when GWIS data were combined with in-vitro transcriptomics. This solute carrier transports the neurotransmitter glutamate and is involved in synaptic function, neuronal development, and excitotoxicity. Pb, in turn, can selectively block glutamatergic synapses. Five hub genes were identified in network analysis. *CHUK* and *TWIST1* play important roles in early neurogenesis. As a physiological analogue to Ca^{2+}, Pb can directly activate Ca-dependent PKCs (α, β1, β2, and γ). *HSPA5* and *XBP1* are key genes in ER stress signalling pathways. Taken together, the network provided by the study revealed that certain genetic polymorphisms in/near oxidative stress genes and neurodevelopmental genes can modify the effects of Pb-induced oxidative stress on neurodevelopment (Wang et al., 2017).

Another GWIS aimed to identify Pb-induced transcriptomic changes in neural stem cells (NSCs) and link these changes to neurodevelopmental outcomes of 462 Pb-exposed children in a birth cohort in Mexico (Wagner et al., 2017). Human NSCs were exposed to 1 μM Pb and subjected to RNA-seq-based profiling. Prenatal Pb exposure was determined from 2nd trimester maternal blood samples. Infant neurodevelopment was assessed at 24 months of age using the Bayley Scales of Infant and Toddler Development. Nineteen genes showed significantly altered expression, several regulated by NFR2, a transcription factor largely responsible for the oxidative stress response. *SPP1* exerted a neuroprotective role by reducing Pb toxicity in hNSCs. Certain *SPP1* SNPs were associated with cognitive abilities of Pb exposed children, but significant interaction between any of the *SPP1* SNPs and Pb exposure on neurodevelopmental outcome was not found. One possible link between SPP1 and neurodevelopmental disorders may be that the etiology of neurodevelopmental disorders is associated with the dysfunction of microglia. A cluster of white matter-associated microglia express a unique signature of genes, including SPP1, which are enriched at early postnatal stages, and share molecular features with disease-associated microglia (Thion and Garel 2020).

In three other studies, Pb-exposed populations of infants and children were investigated relative to functional gene polymorphisms for *APOE* (encoding Apolipoprotein E), *MTHFR* (encoding Methylenetetrahydrofolate reductase), and *DRD2* (encoding Dopamine Receptor D2), proteins that have been related to neurodevelopment.

APOE is thought to play a role in the maintenance of lipids and cholesterol, the major components of brain myelin, with carriers of the APOE4 polymorphism showing decreased cortical gray matter volume, different distribution of white matter and myelin development, but no cognitive or behavioral differences (Dean et al., 2014). In a cohort of Pb-exposed mother-child pairs from Mexico City, 311 infants were genotyped (Wright et al., 2003). The polymorphic *APOE* gene (rs429358) leads to three isoforms that differ by one or two amino acids. The *APOE* genotypes were analysed in association with the 24-months Mental Development Index of the Bayley Scales of Infant Development (MDI). After adjustment for covariates, APOE4 carriers showed a 4.4-point higher MDI-24 score as compared to APOE3/E2 carriers. In multiple linear regression analysis stratified by *APOE* genotype, the negative effect of cord blood Pb level on the MDI-score was 4-fold greater in APOE3/APOE2 carriers than in APOE4 carriers. It was stated that the protective role of the *APOE* genotype in neurodevelopment remains to be confirmed (Wright et al., 2003).

Another study from Mexico City genotyped 255 mother-child pairs for two non-synonymous SNPs in the *MTHFR* gene (Pilsner et al., 2010), encoding a key enzyme in folate metabolism. The genetically determined reduction of MTHFR enzyme activity leads to impaired methylation and folate deficiency associated with the onset of several psychiatric disorders, autism, and ADHD (Wan et al., 2018). Perinatal Pb exposure was determined in newborns (cord blood levels) and mothers (bone Pb during the first month after birth) (Pilsner et al., 2010). The Bayley's Mental Development Index scores were examined at 24 months of age. Linear regression models were used to describe the relationship between MTHFR genotype and infant Index scores, adjusting for several covariates, including cord Pb levels. Maternal and child *MTHFR* genotypes had no impact on the MDI-scores, and *MTHFR* genotype × Pb interactions were not detected. The authors concluded that the maternal *MTHFR* 677T allele independently predicted poorer child neurodevelopment at 24 months (Pilsner et al., 2010).

DRD2 is a G-protein-coupled receptor located on postsynaptic dopaminergic neurons, centrally involved in reward-mediating mesocorticolimbic pathways, and a known target of antipsychotic drugs. The *DRD2* Taq1 polymorphism is associated with reduced receptor density in the brain (Jönsson et al., 1999; Neville et al., 2004). In the study of Liu et al. (2015), children were genotyped for *DRD2* Taq IA polymorphism (rs1800497), which had no impact on the neurodevelopment of children exposed to Pb.

3.2.3. Other markers associated with Pb exposure and neurodevelopment

3.2.3.1. Maternal high-density lipoprotein (HDL). Cholesterol and triglycerides are insoluble in water. Therefore, these lipids must be transported in conjunction with proteins. Lipoproteins are complex particles, and HDL is the plasma lipoprotein with the highest protein to lipid ratio (Feingold and Grunfeld 2000). Due to its anti-atherogenic activity, HDL has been considered as 'good cholesterol', beneficial to the whole body and especially to cardio-vascular health (Jomard and Osto 2020). Cholesterol is also essential for neuronal physiology during development. It is a major component of cell membranes, a precursor of steroid hormones, and is involved in the regulation of ion permeability, cell shape, cell–cell interaction, and transmembrane signaling (Martín et al., 2014). The brain contains about 20% of the body's cholesterol in the entire body, making it the organ with the highest cholesterol content. Most of the cholesterol in the adult brain (>70%) is found in the myelin sheaths formed by oligodendrocytes to insulate axons, with the remainder integrated into plasma membranes of astrocytes and neurons (Zhang and Liu 2015). Hereditary diseases with mutations in cholesterol-related genes result in impaired brain function during early life (Martín et al., 2014).

In a study by Ji et al. (2018), 303 children (20%) from the Boston Birth Cohort (1479 mother-infant pairs) were followed up to the age of 15 years and diagnosed for attention deficit hyperactivity disorder (ADHD) according to ICD-9 and ICD-10 codes (Ji et al., 2017). Maternal HDL levels were analysed in non-fasting blood samples obtained 24–72 h after delivery. Maternal stress during pregnancy was analysed as a binary variable (not stressed, stressed). Low maternal plasma HDL levels (≤60 mg/dL) were associated with an increased risk of ADHD in the children, particularly among boys. The same year, the group presented data that took into account postnatal Pb exposure of 299 of these

children (Ji et al., 2018). Findings from the Boston Birth Cohort showed that high maternal HDL levels and low maternal stress during pregnancy could partially counteract the increased odds of ADHD associated with early life Pb exposure in boys (Ji et al., 2018). The significance of the marker as a modulator of Pb-associated neurodevelopmental outcome is unclear. According to Fujita et al. (2008), HDL would be a dominant cholesterol carrier in fetal blood; very high HDL cholesterol could also contribute to neurodevelopment because of its close relationship with APOE levels. This may fit with the fact that mothers of growth-impaired neonates with a higher prevalence of neurodevelopmental delays had significantly lower HDL levels (Miranda et al., 2018). Regarding the association between Pb exposure and HDL levels of adults, contradictory results have been reported (e.g. Kristal-Boneh et al., 1999; Ademuyiwa et al., 2005; Buhari et al., 2020).

As HDL levels can be relatively easily implemented as a routine marker in HBM studies, this marker merits further investigation in future studies.

3.2.3.2. Nutritional markers. Five studies that measured Pb exposure addressed dietary intake of or supplementation with Fe, Ca, Zn, and Cu during pregnancy, whereof four also assessed neurodevelopment in infants and children.

In a study by Shah-Kulkarni et al. (2016), 965 pregnant women and newborns were studied in Korea (Shah-Kulkarni et al., 2016). Pb exposure was examined in relation to maternal Fe intake and infant neurodevelopment at 6, 12, 24, and 36 months of age (N = 965, 732, 655, and 558, respectively). The Korean version of the Bayley Scales of Infant Development was used, from which the Mental and the Psychomotor Development Indices were derived. Prenatal Pb exposure was determined in maternal blood during early pregnancy (before gestational week 20) and at birth and in cord blood. Maternal Pb exposure during late pregnancy was associated with lower mental developmental index levels in 6 months old children. This effect was stronger in the group with lower maternal Fe intake. The results implicate that adequate Fe intake during pregnancy might reduce Pb-associated effects on neurodevelopment. Findings from in-vitro, animal and human studies suggest an interaction between Pb and Fe. Fe can inhibit Pb uptake into human intestinal cells (Bannon et al., 2003), and iron deficiency is accompanied by higher Pb body burden in mice (Flanagan et al., 1979) and humans (e.g., Kwong et al., 2004; Wright 1999; Kim and Park, 2014). Placental transfer of Pb is also lower in women who consume iron-rich diets and have higher hemoglobin levels, as well as in hemochromatosis, a disease of systemic Fe overload (Kordas et al., 2007; Karwowski et al., 2014).

Fe is essential for many processes of brain development. It is an essential component of intracellular metabolism, for instance, as an integral component of cytochrome C oxidase. In this way, Fe deficiency can interfere with the metabolically demanding processes of brain development. Early Fe deficiency can also lead to sustained decreased metabolic activity due to alterations in gene regulation resulting from mTOR (Mechanistic Target Of Rapamycin Kinase), BDNF, and MAP2 (Microtubule Associated Protein 2) signaling. The hippocampus and the process of myelination may be particularly vulnerable to Fe deficiency. Fe is also involved in the production of dopamine, epinephrine, norepinephrine, and serotonin, which means that socio-emotional development, executive functions, and memory processes that rely on these neurotransmitters may also be affected (McCann et al., 2020). However, evidence from human studies on the role of Fe in brain development is inconclusive. In a recent systematic review, no clear relationship was found between Fe status and developmental outcomes in all included time windows from pregnancy up to 2–4 years of age (McCann et al., 2020). Another systematic review found some evidence that low Fe in pregnancy, possibly especially in the 3rd trimester, may be associated with adverse neurodevelopment. Fe supplementation during pregnancy did not appear to affect neurodevelopment in the offspring (Janbek et al., 2019).

In a study by Liu et al. (2014), 415 Pb-exposed mothers and their newborns (332 newborns with complete data sets) participated in a study undertaken to determine potential associations between Pb exposure and neurodevelopment of newborns in China, using the neonatal behavioral neurological assessment (NBNA) test scored in 20 items grouped in five clusters (behavior, passive tone, active tone, primary reflexes, general assessment) (Liu et al., 2014). An inverse association between maternal blood Pb in the first trimester and NBNA scores was observed. This was complemented by the finding that maternal supplementation of Ca, Fe, and Zn was associated with lower Pb exposure. However, the variable (Ca, Fe, or Zn supplements) was not further explained and was not used as a co-variate in regression analyses or examined for interaction with Pb. In another study from Nepal, NBNA scores were associated with Pb and As, but not with Zn, cord blood levels (Parajuli et al., 2013). In a review paper of Kordas et al. (2007), a similar finding was reported for children studied for the efficacy of supplementation of Ca, Fe alone, and Fe plus Zn. The only supplementation of Fe and Ca had some beneficial effect in lowering blood Pb levels.

Pregnancy and lactation are accompanied by physiologically upregulated bone resorption in response to Ca requirements of the developing fetus and for milk production. More than 95% of the maternal Pb is stored in bone. Mobilization of bone Pb into the bloodstream represents an endogenous source of exposure that can pose a significant risk to the fetus and infant in life after birth (Ettinger et al., 2007). Animal studies and human studies on adult women and children demonstrated a reduction in Pb concentrations when the diet was supplemented with Ca during pregnancy and lactation (Kordas et al., 2007). Finally, the aim of another study was to investigate whether Ca supplementation (1200 mg dietary Ca) can attenuate fetal Pb exposure (Ettinger et al., 2009). In a double-blind, randomized, placebo-controlled study conducted in Mexico City, 670 women were randomly assigned to receive Ca (n = 334) or placebo (n = 336) during the first trimester of pregnancy; it was found that Ca supplementation during pregnancy was associated with an average 11% reduction of maternal blood Pb (0.4 μg/dL) (Ettinger et al., 2009). Ca administration could therefore represent an important secondary preventive measure to reduce maternal Pb levels and, consequently, fetal exposure. These results agree with previous studies that showed dietary Ca supplementation to slightly reduce Pb content in the blood of lactating women (Hernandez-Avila et al., 2003) and in breast milk (Ettinger et al., 2006).

According to Liu et al. (2018), there is a lack of existing statistical models that can flexibly capture the longitudinal impact of exposure to chemical mixtures. The delineation of exposure-response relationships between mixed exposure to metals and neurodevelopment is complex, particularly in longitudinal studies. Potential interaction, correlation among mixture components, and potentially nonlinear and nonadditive mixture effects must be taken into account. Using Bayesian varying coefficient kernel machine regression, a negative interaction effect between 2nd trimester copper (Cu) and Pb exposures with neurodevelopmental scores at 24 months was found. This makes sense, as Cu is essential for myelin formation (myelin is formed by phospholipids whose synthesis depends on cytochrome C oxidase, a Cu-dependent enzyme) and is involved in ferroxidase activity and thus in Fe uptake into various tissues (González and Visentin 2016).

3.3. Selected biomarkers to be used in future HBM studies

The use of **BDNF** biomarkers in relation to Pb exposure in HBM studies is supported by toxicological/mechanistic data. AOP number 13 "Chronic binding of antagonist to N-methyl-D-aspartate receptors (NMDARs) during brain development induces impairment of learning and memory abilities" (https://aopwiki.org/aops/13) was constructed based on in-vitro and in-vivo studies, and on human data (Sachana et al., 2018). In this AOP, Pb can inhibit the N-methyl-D-aspartate (NMDA) receptor (the molecular initiating event - MIE) (Bal-Price and Meek 2017). This is followed by a cascade of key events (KEs), including

alteration of intracellular Ca homeostasis and reduced BDNF release. This, in turn favoring impairment of synaptogenesis and the neuronal network at the tissue level, leading to learning and memory problems as one possible adverse outcome (Sachana et al., 2018) (Fig. 3). The AOP has been endorsed by the OECD Task Force on Hazard Assessment/Working Group of the National Coordinators of the Test Guidelines Programme (TFHA/WNT).

Given the abundant evidence on the adverse effect of Pb on BDNF transcription and eventually decreased levels of extracellular mature BDNF, serum/plasma BDNF should be considered as a promising marker of effect (Gejl et al., 2019). Of note, Pb induced DNA methylation changes in the *BDNF* gene are consistent across some tissues, including peripheral blood and brain, in both adult rodents and in human post-mortem studies, supporting its use as a peripheral biomarker (Januar et al., 2015; Kundakovic et al., 2015; Zheleznyakova et al., 2016). Urinary BDNF protein concentrations have been investigated to a lesser extent in adult humans (Koven and Collins, 2014); therefore its use as an effect marker cannot be evaluated. Overall, the interpretation of BDNF findings should consider the biological matrix employed (serum, plasma, blood), the critical period of development (neonatal, infancy, childhood, etc.), as well as the BDNF form assessed (total, pro-BDNF or mature BDNF).

Additional information comes from a study in hippocampal neuron cultures from E18 rat embryos treated with 1 and 2 μM Pb acetate. Pb exposure was shown to decrease BDNF gene and protein expression and to alter BDNF vesicle transport to release sites, leading to decreased levels of extracellular mature BDNF. Moreover, it was shown that Pb exposure disrupted synaptic development and function by altering BDNF-TrkB transsynaptic signaling with subsequent changes in synaptic proteins and impairment of synaptic function. These effects likely alter synaptic maturation and disrupt neurodevelopmental processes that may underlie the cognitive and behavioral deficits in Pb-intoxicated children (Stansfield et al., 2012).

Cortisol levels have been shown to be inversely associated with Pb concentrations in infants and children (Tamayo et al., 2016; Cai et al., 2019); in one study, increased Pb levels in conjunction with decreased cortisol levels were also associated with reduced sensory abilities (Cai et al., 2019). However, the measurement of cortisol levels and the interpretation of the data obtained are complex, as described above. In our opinion, these requirements argue against serum cortisol for routine use in HBM studies. Hair cortisol as a marker of chronic stress could be an alternative in some situations but requires further validation. In prospective HBM cohorts with complex and repeated follow-ups, salivary cortisol, in addition to hair cortisol, may provide an important advantage.

Susceptibility markers, especially those based on genome-wide and epigenetic-wide studies, cannot be routinely examined in HBM studies. However, specific polymorphisms and targeted epigenetic measurements could be performed if sufficiently supported by the weight of evidence. (Prenatal) Pb exposure seems to reduce global DNA methylation (Pilsner et al., 2009; Ruiz-Hernandez et al., 2015), but global DNA methylation pattern provides little evidence for specific changes in gene expression. Data on Pb-induced methylation of certain loci (Wu et al., 2017) and on gene variants associated with Pb exposure (Pilsner et al., 2010; Wagner et al., 2017) or interacting with Pb to modulate neurodevelopmental outcome (Wright et al., 2003; Wang et al., 2017) increases our understanding of the complex gene-environment interrelations and may also serve as a starting point for further studies.

With respect to other markers, findings from one study in the Boston Birth Cohort showed that high maternal **HDL** levels during pregnancy could partially counteract the increased odds of ADHD associated with early life Pb exposure in boys (Ji et al., 2018). It is, therefore, possible that maternal HDL levels interact with Pb exposure in early life. It is of interest that a common *APOE* genotype (*APOE4* carriers) was shown to protect from Pb neurotoxicity during early life (Wright et al., 2003). This genotype is associated with lower HDL levels, as demonstrated in animal and human studies (Hopkins et al., 2002).

Some **nutritional markers** have been found to be associated with Pb exposure and neurodevelopment and are candidates for inclusion in studies of Pb-induced developmental neurotoxicity. Fe is essential for brain development, which may be reflected by the finding that low Fe intake during pregnancy aggravated the neurotoxic effects of Pb in children (Shah-Kulkarni et al., 2016). Because **Fe status** is comparatively easy to analyse, especially in the clinical setting, blood counts (hemoglobin, hematocrit, and other RBC parameters), serum Fe, and more specific Fe status markers (serum transferrin receptor saturation, serum ferritin along with C-reactive protein to assess inflammation) could be included in HBM studies of Pb-induced effects on neurodevelopment to identify populations at nutritional risk. A similar line of thinking applies to serum Ca. Ca supplementation have been found to reduce blood Pb levels in pregnancy (Ettinger et al., 2009; Liu et al., 2014). **Serum Ca** is easy to study and can aid the interpretation of blood Pb levels (Ettinger et al., 2007) relative to the risk for neurodevelopmental disorders.

Interestingly, Fe deficiency reduces the expression and function of BDNF and its receptor in certain areas of the brain (Estrada et al., 2014). Taken together, serum BDNF isoforms (if possible combined with targeted BDNF DNA methylation) constitute an interesting candidate to be considered as an effect marker for routine use in HBM studies of Pb exposed populations, complemented by markers of Fe and Ca status to also include nutritional risk for neurodevelopmental disorders. Further studies are needed to validate the markers, especially for the situation of moderate Pb exposure.

3.4. Literature search considerations

To simplify literature searches on publications dealing with the metal lead, it would be useful if the chemical abbreviation 'Pb' is included at least in the keywords. Our search posed a great challenge because the search term 'lead' will also retrieve all publications containing only the verb 'lead'.

4. Conclusions

A very thorough literature search revealed that relatively few biomarkers had been investigated for elucidating the potential effects of Pb exposure. In addition, the markers studied had been investigated in at most two studies, sometimes with divergent results. Based on the retrieved studies, it is therefore not possible to recommend 'mandatory' inclusion of specific effect markers in future HBM studies. However, some effect markers are highly interesting, especially when other knowledge is taken into account and merits further investigation in future HBM studies.

Evidence from mechanistic studies and molecular epidemiological studies point towards the key event of reduced BDNF release as being a potential biomarker of Pb-induced neurotoxicity that should be further studied as effective markers for routine use in future HBM studies of Pb-exposed populations. Indeed, we recommend combining BDNF biomarkers at different levels of biological organisation (serum BDNF pro- and mature isoforms, peripheral blood BDNF DNA methylation, etc.) to better map this key event. In addition, plasma HDL, Fe and Ca status are potentially very relevant markers that should be investigated not only in pregnant women but also in neonates. Further studies are needed to validate these biomarkers, especially for low to moderate Pb exposure levels.

The studies discussed here on biomarkers such as serum BDNF or

plasma HDL were conducted in populations exposed to Pb levels that may also occur in Europe. However, Pb exposure in Europe, particularly in vulnerable populations of fetuses, infants and children, and young women, has been studied only very sporadically since 2015. Standardized studies, including repeated measurements (and non-invasive methods), would be needed to investigate Pb concentrations in pregnant and lactating women and their children through adolescence. In summary, representative surveys examining both current Pb exposure in Europe and (effect) biomarkers related to neurodevelopment are undoubtedly needed to fill these knowledge gaps.

Health-based guideline values for blood and urine biomarkers are urgently needed for pregnant women, infants, and children. Since even low-level Pb exposure is associated with adverse neurodevelopmental effects, new efforts should be made to further reduce fetal and childhood exposure.

Funding

This research was supported by funding from the European Unions' Horizon 2020 research and innovation Programme under grant agreement No 733032 HBM4EU.

Author's contributions

Work conceptualization and design of search strategies: AT Saber, E Bengtsen, C Gundacker, V Mustieles, T Szigeti, R Kakucs; Articles screening and selection: AT Saber, E Bengtsen, C Gundacker, T Szigeti, R Kakucs; Data extraction: AT Saber, C Gundacker, T Szigeti, R Kakucs; Original draft preparation: C Gundacker, M Forsthuber, AT Saber, T Szigeti, R Kakucs, V Mustieles; Critical review of the manuscript, edition, and provision of important intellectual content: V Mustieles, MF Fernández, M Forsthuber, C Gundacker, U Vogel, KS Hougaard, AT Saber. Manuscript revision and final version approval: all authors.

Declaration of competing interest

The authors declare that they have no known competing financial interests or personal relationships that could have appeared to influence the work reported in this paper.

Appendix A. Supplementary data

Supplementary data to this article can be found online at https://doi.org/10.1016/j.ijheh.2021.113855.

References

Abballe, A., Ballard, T.J., Dellatte, E., et al., 2008. Persistent environmental contaminants in human milk: concentrations and time trends in Italy. Chemosphere 73 (1 Suppl. l), S220–S227. https://doi.org/10.1016/j.chemosphere.2007.12.036.

Adekunle, I.M., Ogundele, J.A., Oguntoke, O., Akinloye, O.A., 2010. Assessment of blood and urine lead levels of some pregnant women residing in Lagos, Nigeria. Environ. Monit. Assess. 170 (1–4), 467–474. https://doi.org/10.1007/s10661-009-1247-4.

Ademuyiwa, O., Ugbaja, R.N., Idumebor, F., Adebawo, O., 2005. Plasma lipid profiles and risk of cardiovascular disease in occupational lead exposure in Abeokuta, Nigeria. Lipids Health Dis. 4, 19. https://doi.org/10.1186/1476-511X-4-19.

Almeida, A.A., Lopes, C.M., Silva, A.M., Barrado, E., 2008. Trace elements in human milk: correlation with blood levels, inter-element correlations and changes in concentration during the first month of lactation. J. Trace Elem. Med. Biol. 22 (3), 196–205. https://doi.org/10.1016/j.jtemb.2008.03.007.

Al-Jawadi, A.A., Al-Mola, Z.W.A., Al-Jomard, R.A., 2009. Determinants of maternal and umbilical blood lead levels: a cross-sectional study, Mosul, Iraq. BMC Res. Notes 2 (1), 47. https://doi.org/10.1186/1756-0500-2-47.

Al-Saleh, I., Shinwari, N., Mashhour, A., Mohamed Gel, D., Rabah, A., 2011. Heavy metals (lead, cadmium and mercury) in maternal, cord blood and placenta of healthy women. Int. J. Hyg Environ. Health 214 (2), 79–101. https://doi.org/10.1016/j.ijheh.2010.10.001.

Anazi, S., Maddirevula, S., Faqeih, E., et al., 2017. Clinical genomics expands the morbid genome of intellectual disability and offers a high diagnostic yield. Mol. Psychiatr. 22 (4), 615–624. https://doi.org/10.1038/mp.2016.113.

Arbuckle, T.E., Liang, C.L., Morisset, A.S., et al., 2016. Maternal and fetal exposure to cadmium, lead, manganese and mercury: the MIREC study. Chemosphere 163, 270–282. https://doi.org/10.1016/j.chemosphere.2016.08.023.

ATSDR, 2017. Case Studies in Environmental Medicine, Lead Toxicity. https://www.atsdr.cdc.gov/csem/lead/docs/CSEM-Lead_toxicity_508.pdf. (Accessed 6 July 2021). accessed.

Baba, Y., Murata, A., Watanabe, M., Baba, H., 2014. Clinical implications of the LINE-1 methylation levels in patients with gastrointestinal cancer. Surg. Today 44 (10), 1807–1816. https://doi.org/10.1007/s00595-013-0763-6.

Baeyens, W., Vrijens, J., Gao, Y., et al., 2014. Trace metals in blood and urine of newborn/mother pairs, adolescents and adults of the Flemish population (2007-2011). Int. J. Hyg Environ. Health 217 (8), 878–890. https://doi.org/10.1016/j.ijheh.2014.06.007.

Bai, Y., Laenen, A., Haufroid, V., Nawrot, T.S., Nemery, B., 2019. Urinary lead in relation to combustion-derived air pollution in urban environments. A longitudinal study of an international panel. Environ. Int. 125, 75–81. https://doi.org/10.1016/j.envint.2019.01.044.

Baken, K.A., Lambrechts, N., Remy, S., et al., 2019. A strategy to validate a selection of human effect biomarkers using adverse outcome pathways: proof of concept for phthalates and reproductive effects. Environ. Res. 175, 235–256. https://doi.org/10.1016/j.envres.2019.05.013.

Bal-Price, A., Meek, M.E.B., 2017. Adverse outcome pathways: application to enhance mechanistic understanding of neurotoxicity. Pharmacol. Ther. 179, 84–95. https://doi.org/10.1016/j.pharmthera.2017.05.006.

Bannon, D.I., Abounader, R., Lees, P.S., Bressler, J.P., 2003. Effect of DMT1 knockdown on iron, cadmium, and lead uptake in Caco-2 cells. Am. J. Physiol. Cell Physiol. 284 (1), C44–C50. https://doi.org/10.1152/ajpcell.00184.2002.

Barbieri, F.L., Gardon, J., Ruiz-Castell, M., et al., 2016. Toxic trace elements in maternal and cord blood and social determinants in a Bolivian mining city. Int. J. Environ. Health Res. 26 (2), 158–174. https://doi.org/10.1080/09603123.2015.1061114.

Barton, H.J., 2011. Advantages of the use of deciduous teeth, hair, and blood analysis for lead and cadmium bio-monitoring in children. A study of 6-year-old children from Krakow (Poland). Biol. Trace Elem. Res. 143 (2), 637–658. https://doi.org/10.1007/s12011-010-8896-6.

Batáriová, A., Spevácková, V., Benes, B., Cejchanová, M., Smíd, J., Cerná, M., 2006. Blood and urine levels of Pb, Cd and Hg in the general population of the Czech Republic and proposed reference values. Int. J. Hyg Environ. Health 209 (4), 359–366. https://doi.org/10.1016/j.ijheh.2006.02.005.

Benes, B., Sladká, J., Spevácková, V., Smid, J., 2003. Determination of normal concentration levels of Cd, Cr, Cu, Hg, Pb, Se and Zn in hair of the child population in the Czech Republic. Cent. Eur. J. Publ. Health 11 (4), 184–186. PMID: 14768779.

Betts, K.S., 2012. CDC updates guidelines for children's lead exposure. Environ. Health Perspect. 120 (7), a268. https://doi.org/10.1289/ehp.120-a268.

Bharani, K.L., Ledreux, A., Gilmore, A., Carroll, S.L., Granholm, A.C., 2020. Serum pro-BDNF levels correlate with phospho-tau staining in Alzheimer's disease. Neurobiol. Aging 87, 49–59. https://doi.org/10.1016/j.neurobiolaging.2019.11.010.

Björklund, K.L., Vahter, M., Palm, B., Grandér, M., Lignell, S., Berglund, M., 2012. Metals and trace element concentrations in breast milk of first time healthy mothers: a biological monitoring study. Environ. Health 11, 92. https://doi.org/10.1186/1476-069X-11-92.

Bocca, B., Ruggieri, F., Pino, A., et al., 2019. Human biomonitoring to evaluate exposure to toxic and essential trace elements during pregnancy. Part A. concentrations in maternal blood, urine and cord blood. Environ. Res. 177, 108599. https://doi.org/10.1016/j.envres.2019.108599.

Buhari, O., Dayyab, F.M., Igbinoba, O., Atanda, A., Medhane, F., Faillace, R.T., 2020. The association between heavy metal and serum cholesterol levels in the US population: national Health and Nutrition Examination Survey 2009-2012. Hum. Exp. Toxicol. 39 (3), 355–364. https://doi.org/10.1177/0960327119889654.

Cai, H., Xu, X., Zhang, Y., Cong, X., Lu, X., Huo, X., 2019. Elevated lead levels from e-waste exposure are linked to sensory integration difficulties in preschool children. Neurotoxicology 71, 150–158. https://doi.org/10.1016/j.neuro.2019.01.004.

Caspersen, I.H., Thomsen, C., Haug, L.S., et al., 2019. Patterns and dietary determinants of essential and toxic elements in blood measured in mid-pregnancy: the Norwegian Environmental Biobank. Sci. Total Environ. 671, 299–308. https://doi.org/10.1016/j.scitotenv.2019.03.291.

CDC- Centers for Disease Control and Prevention, 2010. Guidelines for the Identification and Management of Lead Exposure in Pregnant and Lactating Women. http://www.cdc.gov/nceh/lead/publications/LeadandPregnancy2010.pdf. (Accessed 8 July 2021). accessed.

Cerná, M., Krsková, A., Cejchanová, M., Spěváčková, V., 2012. Human biomonitoring in the Czech Republic: an overview. Int. J. Hyg Environ. Health 215 (2), 109–119. https://doi.org/10.1016/j.ijheh.2011.09.007.

Dean 3rd, D.C., Jerskey, B.A., Chen, K., et al., 2014. Brain differences in infants at differential genetic risk for late-onset Alzheimer disease: a cross-sectional imaging study. JAMA Neurol 71 (1), 11–22. https://doi.org/10.1001/jamaneurol.2013.4544.

Deaton, A.M., Bird, A., 2011. CpG islands and the regulation of transcription. Genes Dev. 25 (10), 1010–1022. https://doi.org/10.1101/gad.2037511.

Dehari-Zeka, M., Letaj, K.R., Selimi, Q.I., Elezaj, I.R., 2020. Blood lead level (BLL), δ-aminolevulinic acid dehydratase activity (ALAD), hemoglobin (Hb) and hematocrit (hct) in primary school-children and adult residents living in smelter rural areas in Kosovo. J Environ Sci Health A Tox Hazard Subst Environ Eng 55 (10), 1179–1187. https://doi.org/10.1080/10934529.2020.1780851.

De Felip, E., Bianchi, F., Bove, C., et al., 2014. Priority persistent contaminants in people dwelling in critical areas of Campania Region, Italy (SEBIOREC biomonitoring study). Sci. Total Environ. 487, 420–435. https://doi.org/10.1016/j.scitotenv.2014.04.016.

Dongarrà, G., Lombardo, M., Tamburo, E., Varrica, D., Cibella, F., Cuttitta, G., 2011. Concentration and reference interval of trace elements in human hair from students living in Palermo, Sicily (Italy). Environ. Toxicol. Pharmacol. 32 (1), 27–34. https://doi.org/10.1016/j.etap.2011.03.003.

Dursun, A., Yurdakok, K., Yalcin, S.S., et al., 2016. Maternal risk factors associated with lead, mercury and cadmium levels in umbilical cord blood, breast milk and newborn hair. J. Matern. Fetal Neonatal Med. 29 (6), 954–961. https://doi.org/10.3109/14767058.2015.1026255.

Ecsedi-Angyal, M., Tatár, E., Óvári, M., Kurin-Csörgei, K., Záray, G., Mihucz, V.G., 2020. Determination of low-level arsenic, lead, cadmium and mercury concentration in breast milk of Hungarian women. Int. J. Environ. Anal. Chem. 100 (5), 549–566. https://doi.org/10.1080/03067319.2019.1637429.

EEA, 2020. Air Quality in Europe — 2020 Report. EEA Report No 09/2020. European Environment Agency. https://www.eea.europa.eu/publications/air-quality-in-europe-2020-report. (Accessed 6 July 2021). accessed.

EFSA, 2010. Scientific opinion on lead in food. EFSA J 8 (4), 1570. https://doi.org/10.2903/j.efsa.2010.1570.

EFSA, 2012. Lead dietary exposure in the European population. EFSA J 10 (7), 2831. https://doi.org/10.2903/j.efsa.2012.2831.

Esteban, M., Castaño, A., 2009. Non-invasive matrices in human biomonitoring: a review. Environ. Int. 35 (2), 438–449. https://doi.org/10.1016/j.envint.2008.09.003.

Esteban-Vasallo, M.D., Aragonés, N., Pollan, M., López-Abente, G., Perez-Gomez, B., 2012. Mercury, cadmium, and lead levels in human placenta: a systematic review. Environ. Health Perspect. 120 (10), 1369–1377. https://doi.org/10.1289/ehp.1204952.

Estrada, J.A., Contreras, I., Pliego-Rivero, F.B., Otero, G.A., 2014. Molecular mechanisms of cognitive impairment in iron deficiency: alterations in brain-derived neurotrophic factor and insulin-like growth factor expression and function in the central nervous system. Nutr. Neurosci. 17 (5), 193–206. https://doi.org/10.1179/1476830513Y.0000000084.

Etchevers, A., Bretin, P., Lecoffre, C., et al., 2014. Blood lead levels and risk factors in young children in France, 2008-2009. Int. J. Hyg Environ. Health 217 (4–5), 528–537. https://doi.org/10.1016/j.ijheh.2013.10.002.

Ettinger, A.S., Téllez-Rojo, M.M., Amarasiriwardena, C., et al., 2006. Influence of maternal bone lead burden and calcium intake on levels of lead in breast milk over the course of lactation. Am. J. Epidemiol. 163 (1), 48–56. https://doi.org/10.1093/aje/kwj010.

Ettinger, A.S., Hu, H., Hernandez-Avila, M., 2007. Dietary calcium supplementation to lower blood lead levels in pregnancy and lactation. J. Nutr. Biochem. 18 (3), 172–178. https://doi.org/10.1016/j.jnutbio.2006.12.007.

Ettinger, A.S., Lamadrid-Figueroa, H., Téllez-Rojo, M.M., et al., 2009. Effect of calcium supplementation on blood lead levels in pregnancy: a randomized placebo-controlled trial. Environ. Health Perspect. 117 (1), 26–31. https://doi.org/10.1289/ehp.11868.

Eurostat, 2018. Women Are Having Their First Child at an Older Age. https://ec.europa.eu/eurostat/web/products-eurostat-news/-/DDN-20200515-2. (Accessed 8 July 2021). accessed.

Eurostat, 2020. The Life of Women and Men in Europe. A STATISTICAL PORTRAIT 2020 edition. https://ec.europa.eu/eurostat/en/web/products-interactive-publications/-/ks-04-20-395. (Accessed 8 July 2021). accessed.

Evrenoglou, L., Partsinevelou, S.A., Stamatis, P., et al., 2013. Children exposure to trace levels of heavy metals at the north zone of Kifissos River. Sci. Total Environ. 443, 650–661. https://doi.org/10.1016/j.scitotenv.2012.11.041.

Falcó, G., Bocio, A., Gómez-Catalán, J., Llobet, J.M., Domingo, J.L., 2006. Arsenic, cadmium, lead and mercury dietary intake by babies from Catalonia, Spain. An evaluation of risk. Epidemiology 17 (6), S321. Poster Abstract.

Falq, G., Zeghnoun, A., Pascal, M., et al., 2011. Blood lead levels in the adult population living in France the French Nutrition and Health Survey (ENNS 2006-2007). Environ. Int. 37 (3), 565–571. https://doi.org/10.1016/j.envint.2010.11.012.

Feingold, K.R., Grunfeld, C., 2000. Introduction to Lipids and Lipoproteins. MDText.com, Inc., South Dartmouth (MA. https://europepmc.org/article/NBK/nbk305896. (Accessed 8 July 2021). accessed.

Flanagan, P.R., Hamilton, D.L., Haist, J., Valberg, L.S., 1979. Interrelationships between iron and lead absorption in iron-deficient mice. Gastroenterology 77 (5), 1074–1081. https://doi.org/10.1016/S0016-5085(79)80080-3.

Fløtre, C.H., Varsi, K., Helm, T., Bolann, B., Bjørke-Monsen, A.L., 2017. Predictors of mercury, lead, cadmium and antimony status in Norwegian never-pregnant women of fertile age. PLoS One 12 (12), e0189169. https://doi.org/10.1371/journal.pone.0189169.

Freire, C., Amaya, E., Gil, F., et al., 2019. Placental metal concentrations and birth outcomes: the Environment and Childhood (INMA) project. Int. J. Hyg Environ. Health 222 (3), 468–478. https://doi.org/10.1016/j.ijheh.2018.12.014.

Fujita, H., Okada, T., Inami, I., et al., 2008. Heterogeneity of high-density lipoprotein in cord blood and its postnatal change. Clin. Chim. Acta 389 (1–2), 93–97. https://doi.org/10.1016/j.cca.2007.11.032.

García-Esquinas, E., Pérez-Gómez, B., Fernández, M.A., et al., 2011. Mercury, lead and cadmium in human milk in relation to diet, lifestyle habits and sociodemographic variables in Madrid (Spain). Chemosphere 85 (2), 268–276. https://doi.org/10.1016/j.chemosphere.2011.05.029.

García-Esquinas, E., Aragonés, N., Fernández, M.A., et al., 2014. Newborns and low to moderate prenatal environmental lead exposure: might fathers be the key? Environ. Sci. Pollut. Res. Int. 21 (13), 7886–7898. https://doi.org/10.1007/s11356-014-2738-6.

Gejl, A.K., Enevold, C., Bugge, A., Andersen, M.S., Nielsen, C.H., Andersen, L.B., 2019. Associations between serum and plasma brain-derived neurotrophic factor and influence of storage time and centrifugation strategy. Sci. Rep. 9 (1), 9655. https://doi.org/10.1038/s41598-019-45976-5.

Gerhardsson, L., Lundh, T., 2010. Metal concentrations in blood and hair in pregnant females in southern Sweden. J. Environ. Health 72 (6), 37–41. PMID: 20104833.

Giesbrecht, G.F., Ejaredar, M., Liu, J., et al., APrON Study Team, 2017. Prenatal bisphenol a exposure and dysregulation of infant hypothalamic-pituitary-adrenal axis function: findings from the APrON cohort study. Environ. Health 16 (1), 47. https://doi.org/10.1186/s12940-017-0259-8.

Gilbert, S.G., Weiss, B., 2006. A rationale for lowering the blood lead action level from 10 to 2 microg/dL. Neurotoxicology 27 (5), 693–701. https://doi.org/10.1016/j.neuro.2006.06.008.

González, H.F., Visentin, S., 2016. Micronutrients and neurodevelopment: an update. Micronutrientes y neurodesarrollo: actualización. Arch. Argent. Pediatr. 114 (6), 570–575. https://doi.org/10.5546/aap.2016.eng.570.

Graham, A.M., Rasmussen, J.M., Entringer, S., et al., 2019. Maternal cortisol concentrations during pregnancy and sex-specific associations with neonatal Amygdala Connectivity and emerging internalizing behaviors. Biol. Psychiatr. 85 (2), 172–181. https://doi.org/10.1016/j.biopsych.2018.06.023.

Grzunov Letinić, J.G., Matek Sarić, M., Piasek, M., et al., 2016. Use of human milk in the assessment of toxic metal exposure and essential element status in breastfeeding women and their infants in coastal Croatia. J. Trace Elem. Med. Biol. 38, 117–125. https://doi.org/10.1016/j.jtemb.2016.08.002.

Gulson, B., Mizon, K., Korsch, M., Taylor, A., 2016. Revisiting mobilisation of skeletal lead during pregnancy based on monthly sampling and cord/maternal blood lead relationships confirm placental transfer of lead. Arch. Toxicol. 90 (4), 805–816. https://doi.org/10.1007/s00204-015-1515-8.

Gundacker, C., Pietschnig, B., Wittmann, K.J., et al., 2002. Lead and mercury in breast milk. Pediatrics 110 (5), 873–878. https://doi.org/10.1542/peds.110.5.873.

Gundacker, C., Fröhlich, S., Graf-Rohrmeister, K., 2010. Perinatal lead and mercury exposure in Austria. Sci. Total Environ. 408 (23), 5744–5749. https://doi.org/10.1016/j.scitotenv.2010.07.079.

Gundacker, C., Kutalek, R., Glaunach, R., Deweis, C., Hengstschläger, M., Prinz, A., 2017. Geophagy during pregnancy: is there a health risk for infants. Environ. Res. 156, 145–147. https://doi.org/10.1016/j.envres.2017.03.028.

Gundacker, C., Graf-Rohrmeister, K., Gencik, M., et al., 2021. Gene variants determine placental transfer of perfluoroalkyl substances (PFAS), mercury (Hg) and lead (Pb), and birth outcome: findings from the UmMuKi bratislava-vienna study. Front. Genet. 12, 664946. https://doi.org/10.3389/fgene.2021.664946.

Hannon, E., Lunnon, K., Schalkwyk, L., Mill, J., 2015. Interindividual methylomic variation across blood, cortex, and cerebellum: implications for epigenetic studies of neurological and neuropsychiatric phenotypes. Epigenetics 10 (11), 1024–1032. https://doi.org/10.1080/15592294.2015.1100786.

Hansen, S., Nieboer, E., Sandanger, T.M., et al., 2011. Changes in maternal blood concentrations of selected essential and toxic elements during and after pregnancy. J. Environ. Monit. 13 (8), 2143–2152. https://doi.org/10.1039/c1em10051c.

Heitland, P., Köster, H.D., 2006. Biomonitoring of 30 trace elements in urine of children and adults by ICP-MS. Clin. Chim. Acta 365 (1–2), 310–318. https://doi.org/10.1016/j.cca.2005.09.013.

Hernandez-Avila, M., Gonzalez-Cossio, T., Hernandez-Avila, J.E., et al., 2003. Dietary calcium supplements to lower blood lead levels in lactating women: a randomized placebo-controlled trial. Epidemiology 14 (2), 206–212. https://doi.org/10.1097/01.EDE.0000038520.66094.34.

Hopkins, P.C., Huang, Y., McGuire, J.G., Pitas, R.E., 2002. Evidence for differential effects of apoE3 and apoE4 on HDL metabolism. J. Lipid Res. 43 (11), 1881–1889. https://doi.org/10.1194/jlr.m200172-jlr200.

Hrubá, F., Strömberg, U., Černá, M., et al., 2012. Blood cadmium, mercury, and lead in children: an international comparison of cities in six European countries, and China, Ecuador, and Morocco. Environ. Int. 41, 29–34. https://doi.org/10.1016/j.envint.2011.12.001.

IARC, 2006. IARC Monographs on the Evaluation of Carcinogenic Risks to Humans, vol. 87. Inorganic and Organic Lead Compounds, Lyon.

Ikegame, T., Bundo, M., Murata, Y., Kasai, K., Kato, T., Iwamoto, K., 2013. DNA methylation of the BDNF gene and its relevance to psychiatric disorders. J. Hum. Genet. 58 (7), 434–438. https://doi.org/10.1038/jhg.2013.65.

Iwai-Shimada, M., Kameo, S., Nakai, K., et al., 2019. Exposure profile of mercury, lead, cadmium, arsenic, antimony, copper, selenium and zinc in maternal blood, cord blood and placenta: the Tohoku Study of Child Development in Japan. Environ. Health Prev. Med. 24 (1), 35. https://doi.org/10.1186/s12199-019-0783-y.

Janbek, J., Sarki, M., Specht, I.O., Heitmann, B.L., 2019. A systematic literature review of the relation between iron status/anemia in pregnancy and offspring neurodevelopment, 2019 Eur. J. Clin. Nutr. 73 (12), 1561–1578. https://doi.org/10.1038/s41430-019-0400-6.

Januar, V., Ancelin, M.L., Ritchie, K., Saffery, R., Ryan, J., 2015. BDNF promoter methylation and genetic variation in late-life depression. Transl. Psychiatry 5 (8), e619. https://doi.org/10.1038/tp.2015.114.

Ji, Y., Riley, A.W., Lee, L.C., et al., 2017. A prospective birth cohort study on maternal cholesterol levels and offspring attention deficit hyperactivity disorder: new insight on sex differences. Brain Sci. 8 (1) https://doi.org/10.3390/brainsci8010003.

Ji, Y., Hong, X., Wang, G., et al., 2018. A prospective birth cohort study on early childhood lead levels and attention deficit hyperactivity disorder: new insight on sex differences. J. Pediatr. 199, 124–131. https://doi.org/10.1016/j.jpeds.2018.03.076 e8.

Jomard, A., Osto, E., 2020. High density lipoproteins: metabolism, function, and therapeutic potential. Front Cardiovasc Med 7, 39. https://doi.org/10.3389/fcvm.2020.00039.

Jönsson, E.G., Nöthen, M.M., Grünhage, F., et al., 1999. Polymorphisms in the dopamine D2 receptor gene and their relationships to striatal dopamine receptor density of healthy volunteers. Mol. Psychiatr. 4 (3), 290–296. https://doi.org/10.1038/sj.mp.4000532.

Karwowski, M.P., Just, A.C., Bellinger, D.C., et al., 2014. Maternal iron metabolism gene variants modify umbilical cord blood lead levels by gene-environment interaction: a birth cohort study. Environ. Health 13, 77. https://doi.org/10.1186/1476-069X-13-77.

Kayama, F., Fatmi, Z., Ikegami, A., et al., 2016. Exposure assessment of lead from food and airborne dusts and biomonitoring in pregnant mothers, their fetus and siblings in Karachi, Pakistan and Shimotsuke, Japan. Rev. Environ. Health 31 (1), 33–35. https://doi.org/10.1515/reveh-2015-0046.

Keil, K.P., Lein, P.J., 2016. DNA methylation: a mechanism linking environmental chemical exposures to risk of autism spectrum disorders? Environ Epigenet 2 (1), dvv012. https://doi.org/10.1093/eep/dvv012.

Khalid, M., Abdollahi, M., 2019. Epigenetic modifications associated with pathophysiological effects of lead exposure. J Environ Sci Health C 37 (4), 235–287. https://doi.org/10.1080/10590501.2019.1640581.

Kim, Y.M., Chung, J.Y., An, H.S., et al., 2015. Biomonitoring of lead, cadmium, total mercury, and methylmercury levels in maternal blood and in umbilical cord blood at birth in South Korea. Int. J. Environ. Res. Publ. Health 12 (10), 13482–13493. https://doi.org/10.3390/ijerph121013482.

Kim, Y., Park, S., 2014. Iron deficiency increases blood concentrations of neurotoxic metals in children. Korean J Pediatr 57 (8), 345–350. https://doi.org/10.3345/kjp.2014.57.8.345.

Kirinčič, S., Šömen Joksić, A., Zupan, M., et al., 2019. Lead and Cadmium in Foods/drinking Water from Slovenian Market/taps: Estimation of Overall Chronic Dietary Exposure and Health Risks [published Correction Appears in Food Addit Contam Part A Chem Anal Control Expo Risk Assess, 2019 Oct;36(10):1584-1588]. Food Addit Contam Part A Chem Anal Control Expo Risk Assess. 2019, vol. 36, pp. 1522–1537. https://doi.org/10.1080/19440049.2019.1628355, 10.

Klapec, T., Cavar, S., Kasac, Z., Rucević, S., Popinjac, A., 2008. Selenium in placenta predicts birth weight in normal but not intrauterine growth restriction pregnancy. J. Trace Elem. Med. Biol. 22 (1), 54–58. https://doi.org/10.1016/j.jtemb.2007.10.004.

Klotz, K., Göen, T., 2017. Human biomonitoring of lead exposure. /books/9783110434330/9783110434330-006/9783110434330-006.xml Met Ions Life Sci 17. https://doi.org/10.1515/9783110434330-006.

Kopp, R.S., Kumbartski, M., Harth, V., Brüning, T., Käfferlein, H.U., 2012. Partition of metals in the maternal/fetal unit and lead-associated decreases of fetal iron and manganese: an observational biomonitoring approach. Arch. Toxicol. 86 (10), 1571–1581. https://doi.org/10.1007/s00204-012-0869-4.

Kordas, K., Lönnerdal, B., Stoltzfus, R.J., 2007. Interactions between nutrition and environmental exposures: effects on health outcomes in women and children. J. Nutr. 137 (12), 2794–2797. https://doi.org/10.1093/jn/137.12.2794.

Koven, N.S., Collins, L.R., 2014. Urinary brain-derived neurotrophic factor as a biomarker of executive functioning. Neuropsychobiology 69 (4), 227–234. https://doi.org/10.1159/000362242.

Kowiański, P., Lietzau, G., Czuba, E., Waśkow, M., Steliga, A., Moryś, J., 2018. BDNF: a key factor with multipotent impact on brain signaling and synaptic plasticity. Cell. Mol. Neurobiol. 38 (3), 579–593. https://doi.org/10.1007/s10571-017-0510-4.

Kristal-Boneh, E., Coller, D., Froom, P., Harari, G., Ribak, J., 1999. The association between occupational lead exposure and serum cholesterol and lipoprotein levels. Am J Public Health 89 (7), 1083–1087. https://doi.org/10.2105/ajph.89.7.1083.

Kundakovic, M., Gudsnuk, K., Herbstman, J.B., Tang, D., Perera, F.P., Champagne, F.A., 2015. DNA methylation of BDNF as a biomarker of early-life adversity. Proc. Natl. Acad. Sci. U. S. A. 112 (22), 6807–6813. https://doi.org/10.1073/pnas.1408355111.

Kunter, İ., Hürer, N., Gülcan, H.O., Öztürk, B., Doğan, İ., Şahin, G., 2017. Assessment of Aflatoxin M1 and heavy metal levels in mothers breast milk in Famagusta, Cyprus. Biol. Trace Elem. Res. 175 (1), 42–49. https://doi.org/10.1007/s12011-016-0750-z.

Kutllovci-Zogaj, D., Krasniqi, S., Elezaj, I., et al., 2014. Correlation between blood lead level and hemoglobin level in mitrovica children. Med. Arch. 68 (5), 324–328. https://doi.org/10.5455/medarh.2014.68.324-328.

Kwong, W.T., Friello, P., Semba, R.D., 2004. Interactions between iron deficiency and lead poisoning: epidemiology and pathogenesis. Sci. Total Environ. 330 (1–3), 21–37. https://doi.org/10.1016/j.scitotenv.2004.03.017.

Lanphear, B.P., 2017. Low-level toxicity of chemicals: No acceptable levels? PLoS Biol. 15 (12), e2003066 https://doi.org/10.1371/journal.pbio.2003066.

Lanphear, B.P., Hornung, R., Khoury, J., et al., 2005. Low-level environmental lead exposure and children's intellectual function: an international pooled analysis. published correction appears in Environ Health Perspect. 2019 Sep;127(9):99001 Environ. Health Perspect. 113 (7), 894–899. https://doi.org/10.1289/ehp.7688.

Lee, D.Y., Kim, E., Choi, M.H., 2015. Technical and clinical aspects of cortisol as a biochemical marker of chronic stress. BMB Rep 48 (4), 209–216. https://doi.org/10.5483/bmbrep.2015.48.4.275.

Leotsinidis, M., Alexopoulos, A., Kostopoulou-Farri, E., 2005. Toxic and essential trace elements in human milk from Greek lactating women: association with dietary habits and other factors. Chemosphere 61 (2), 238–247. https://doi.org/10.1016/j.chemosphere.2005.01.084.

Lermen, D., Weber, T., Göen, T., et al., 2021. Long-term time trend of lead exposure in young German adults - evaluation of more than 35 Years of data of the German Environmental Specimen Bank. Int. J. Hyg Environ. Health 231, 113665. https://doi.org/10.1016/j.ijheh.2020.113665.

Li, S., Xu, J., Liu, Z., Yan, C.H., 2017. The non-linear association between low-level lead exposure and maternal stress among pregnant women. Neurotoxicology 59, 191–196. https://doi.org/10.1016/j.neuro.2016.07.005.

Lidsky, T.I., Schneider, J.S., 2003. Lead neurotoxicity in children: basic mechanisms and clinical correlates. Brain 126 (1), 5–19. https://doi.org/10.1093/brain/awg014.

Lin, C.M., Doyle, P., Wang, D.L., Hwang, Y.H., Chen, P.C., 2010. The role of essential metals in the placental transfer of lead from mother to child. Reprod. Toxicol. 29 (4), 443–446. https://doi.org/10.1016/j.reprotox.2010.03.004.

Liu, K.S., Mao, X.D., Hao, J.H., Shi, J., Dai, C.F., Chen, W.J., 2013. Towards prenatal biomonitoring in Nanjing, China: lead and cadmium levels in the duration of pregnancy. Chin. Med. J. 126 (16), 3107–3111. PMID: 23981621.

Liu, J., Gao, D., Chen, Y., Jing, J., Hu, Q., Chen, Y., 2014. Lead exposure at each stage of pregnancy and neurobehavioral development of neonates. Neurotoxicology 44, 1–7. https://doi.org/10.1016/j.neuro.2014.03.003.

Liu, L., Xu, X., Yekeen, T.A., Lin, K., Li, W., Huo, X., 2015. Assessment of association between the dopamine D2 receptor (DRD2) polymorphism and neurodevelopment of children exposed to lead. Environ. Sci. Pollut. Res. Int. 22 (3), 1786–1793. https://doi.org/10.1007/s11356-014-2565-9.

Liu, S.H., Bobb, J.F., Claus Henn, B., et al., 2018. Bayesian varying coefficient kernel machine regression to assess neurodevelopmental trajectories associated with exposure to complex mixtures. Stat. Med. 37 (30), 4680–4694. https://doi.org/10.1002/sim.7947.

Llorente Ballesteros, M.T., Navarro Serrano, I., Izquierdo Álvarez, S., 2017. Reference levels of trace elements in hair samples from children and adolescents in Madrid, Spain. J. Trace Elem. Med. Biol. 43, 113–120. https://doi.org/10.1016/j.jtemb.2016.12.010.

Luo, Y., Lu, X., Xie, H., 2014. Dynamic Alu methylation during normal development, aging, and tumorigenesis. BioMed Res. Int. 2014, 784706. https://doi.org/10.1155/2014/784706.

Martín, M.G., Pfrieger, F., Dotti, C.G., 2014. Cholesterol in brain disease: sometimes determinant and frequently implicated. EMBO Rep. 15 (10), 1036–1052. https://doi.org/10.15252/embr.201439225.

Matos, C., Moutinho, C., Balcão, V., et al., 2009. Total antioxidant activity and trace elements in human milk: the first 4 months of breast-feeding. Eur. Food Res. Technol. 230 (2), 201–208. https://doi.org/10.1007/s00217-009-1157-2.

McCann, S., Perapoch Amadó, M., Moore, S.E., 2020. The role of iron in brain development: a systematic review. Nutrients 12 (7), 2001. https://doi.org/10.3390/nu12072001.

Meier, N., Bruder, E., Lapaire, O., et al., 2019. Exome sequencing of fetal anomaly syndromes: novel phenotype-genotype discoveries. Eur. J. Hum. Genet. 27 (5), 730–737. https://doi.org/10.1038/s41431-018-0324-y.

Miranda, J., Simões, R.V., Paules, C., et al., 2018. Metabolic profiling and targeted lipidomics reveals a disturbed lipid profile in mothers and fetuses with intrauterine growth restriction. Sci. Rep. 8 (1), 13614. https://doi.org/10.1038/s41598-018-31832-5.

Miranda, M., Morici, J.F., Zanoni, M.B., Bekinschtein, P., 2019. Brain-derived neurotrophic factor: a key molecule for memory in the healthy and the pathological brain. Front. Cell. Neurosci. 13, 363. https://doi.org/10.3389/fncel.2019.00363.

Mizoguchi, Y., Yao, H., Imamura, Y., Hashimoto, M., Monji, A., 2020. Lower brain-derived neurotrophic factor levels are associated with age-related memory impairment in community-dwelling older adults: the Sefuri study. Sci. Rep. 10 (1), 16442. https://doi.org/10.1038/s41598-020-73576-1.

Mustieles, V., D'Cruz, S.C., Couderq, S., et al., 2020. Bisphenol A and its analogues: a comprehensive review to identify and prioritize effect biomarkers for human biomonitoring. Environ. Int. 144, 105811. https://doi.org/10.1016/j.envint.2020.105811.

Mustieles V, Rodríguez-Carrillo A, Vela-Soria F, et al. BDNF as a potential mediator between childhood BPA exposure and behavioral function in adolescent boys from the INMA-Granada cohort. Sci. Total Environ. (Under review).

Neville, M.J., Johnstone, E.C., Walton, R.T., 2004. Identification and characterization of ANKK1: a novel kinase gene closely linked to DRD2 on chromosome band 11q23.1. Hum. Mutat. 23 (6), 540–545. https://doi.org/10.1002/humu.20039.

Olympio, K., Ferreira, A., Rodrigues, M., et al., 2020. Are fingernail lead levels a reliable biomarker of lead internal dose? J. Trace Elem. Med. Biol. 62, 126576. https://doi.org/10.1016/j.jtemb.2020.126576.

Ougier, E., Lecoq, P., Rousselle, C., Ormsby, J.-N., 2018. Second List of HBM4EU Priority Substances and Chemical Substance Group Leaders for 2019-2021. Ref. Ares 4423297 - 28/08/2018.

Parajuli, R.P., Fujiwara, T., Umezaki, M., Watanabe, C., 2013. Association of cord blood levels of lead, arsenic, and zinc with neurodevelopmental indicators in newborns: a birth cohort study in Chitwan Valley, Nepal. Environ. Res. 121, 45–51. https://doi.org/10.1016/j.envres.2012.10.010.

Parnia, A., Chakravartty, D., Wiseman, C.L.S., et al., 2018. Environmental factors associated with blood lead among newcomer women from South and East Asia in the Greater Toronto Area. Sci. Total Environ. 624, 558–566. https://doi.org/10.1016/j.scitotenv.2017.11.336.

Perera, F., Phillips, D.H., Wang, Y., et al., 2015. Prenatal exposure to polycyclic aromatic hydrocarbons/aromatics, BDNF and child development. Environ. Res. 142, 602–608. https://doi.org/10.1016/j.envres.2015.08.011.

Pilsner, J.R., Hu, H., Ettinger, A., et al., 2009. Influence of prenatal lead exposure on genomic methylation of cord blood DNA. Environ. Health Perspect. 117 (9), 1466–1471. https://doi.org/10.1289/ehp.0800497.

Pilsner, J.R., Hu, H., Wright, R.O., et al., 2010. Maternal MTHFR genotype and haplotype predict deficits in early cognitive development in a lead-exposed birth cohort in Mexico City. Am. J. Clin. Nutr. 92 (1), 226–234. https://doi.org/10.3945/ajcn.2009.28839.

Polańska, K., Hanke, W., Sobala, W., et al., 2014. Predictors of environmental lead exposure among pregnant women - a prospective cohort study in Poland. Ann. Agric. Environ. Med. 21 (1), 49–54. PMID: 24738496.

Polańska, K., Hanke, W., Pawlas, N., et al., 2018. Sex-dependent impact of low-level lead exposure during prenatal period on child psychomotor functions. Int. J. Environ. Res. Publ. Health 15 (10), 2263. https://doi.org/10.3390/ijerph15102263.

Ponsonby, A.L., Symeonides, C., Vuillermin, P., Mueller, J., Sly, P.D., Saffery, R., 2016. Epigenetic regulation of neurodevelopmental genes in response to in utero exposure to phthalate plastic chemicals: how can we delineate causal effects? Neurotoxicology 55, 92–101. https://doi.org/10.1016/j.neuro.2016.05.011.

Protano, C., Astolfi, M.L., Canepari, S., Vitali, M., 2016. Urinary levels of trace elements among primary school-aged children from Italy: the contribution of smoking habits of family members. Sci. Total Environ. 557–558, 378–385. https://doi.org/10.1016/j.scitotenv.2016.03.073.

Punshon, T., Li, Z., Jackson, B.P., Parks, W.T., Romano, M., Conway, D., Baker, E.R., Karagas, M.R., 2019. Placental metal concentrations in relation to placental growth, efficiency and birth weight. Environ. Int. 126, 533–542. https://doi.org/10.1016/j.envint.2019.01.063.

RAC, 2020. RAC Opinion 'Evaluation of Occupational Exposure Limits (OELs) for Lead and its Compounds'. https://echa.europa.eu/de/rac-opinions-on-scientific-evaluations-of-oels. (Accessed 9 July 2021). accessed.

Ren, L.H., Mu, X.Y., Chen, H.Y., Yang, H.L., Qi, W., 2016. [Prenatal lead exposure related to cord blood brain derived neurotrophic factor (BDNF) levels and impaired neonatal neurobehavioral development]. Zhonghua Yufang Yixue Zazhi 50 (6), 514–518. https://doi.org/10.3760/cma.j.issn.0253-9624.2016.06.008.

Roca, M., Sánchez, A., Pérez, R., Pardo, O., Yusà, V., 2016. Biomonitoring of 20 elements in urine of children. Levels and predictors of exposure. Chemosphere 144, 1698–1705. https://doi.org/10.1016/j.chemosphere.2015.10.008.

Rocha, A., Trujillo, K.A., 2019. Neurotoxicity of low-level lead exposure: History, mechanisms of action, and behavioral effects in humans and preclinical models. Neurotoxicology 73, 58–80. https://doi.org/10.1016/j.neuro.2019.02.021.

Rosofsky, A., Janulewicz, P., Thayer, K.A., et al., 2017. Exposure to multiple chemicals in a cohort of reproductive-aged Danish women. Environ. Res. 154, 73–85. https://doi.org/10.1016/j.envres.2016.12.011.

Rudnai, P, Varró, M, Rudnai, T, et al., 2009. Associations between children's blood lead level and their health status. Epidemiology 20 (6), pS260. https://doi.org/10.1097/01.ede.0000362869.64255.7b.

Ruiz-Hernandez, A., Kuo, C.C., Rentero-Garrido, P., et al., 2015. Environmental chemicals and DNA methylation in adults: a systematic review of the epidemiologic evidence. Clin. Epigenet. 7 (1), 55. https://doi.org/10.1186/s13148-015-0055-7.

Sachana, M., Rolaki, A., Bal-Price, A., 2018. Development of the Adverse Outcome Pathway (AOP): chronic binding of antagonist to N-methyl-d-aspartate receptors (NMDARs) during brain development induces impairment of learning and memory abilities of children. Toxicol. Appl. Pharmacol. 354, 153–175. https://doi.org/10.1016/j.taap.2018.02.024.

Sanders, A.P., Flood, K., Chiang, S., Herring, A.H., Wolf, L., Fry, R.C., 2012. Towards prenatal biomonitoring in North Carolina: assessing arsenic, cadmium, mercury, and lead levels in pregnant women. PLoS One 7 (3), e31354. https://doi.org/10.1371/journal.pone.0031354.

Sanna, E., Floris, G., Vallascas, E., 2008. Town and gender effects on hair lead levels in children from three Sardinian towns (Italy) with different environmental backgrounds. Biol. Trace Elem. Res. 124 (1), 52–59. https://doi.org/10.1007/s12011-008-8122-y.

Sanchez-Guerra, M., Peng, C., Trevisi, L., et al., 2019. Altered cord blood mitochondrial DNA content and pregnancy lead exposure in the PROGRESS cohort. Environ. Int. 125, 437–444. https://doi.org/10.1016/j.envint.2019.01.077.

Saoudi, A., Dereumeaux, C., Goria, S., et al., 2018. Prenatal exposure to lead in France: cord-blood levels and associated factors: results from the perinatal component of the French Longitudinal Study since Childhood (Elfe). Int. J. Hyg Environ. Health 221 (3), 441–450. https://doi.org/10.1016/j.ijheh.2018.01.007.

Schoeters, G., Govarts, E., Bruckers, L., et al., 2017. Three cycles of human biomonitoring in Flanders - time trends observed in the Flemish environment and health study. Int. J. Hyg Environ. Health 220 (2 Pt A), 36–45. https://doi.org/10.1016/j.ijheh.2016.11.006.

Schulz, C., Angerer, J., Ewers, U., Kolossa-Gehring, M., 2007. The German human biomonitoring Commission. Int. J. Hyg Environ. Health 210 (3–4), 373–382. https://doi.org/10.1016/j.ijheh.2007.01.035.

Schulz, C., Angerer, J., Ewers, U., Heudorf, U., Wilhelm, M., 2009. Human Biomonitoring Commission of the German Federal Environment Agency (2009) Revised and new reference values for environmental pollutants in urine or blood of children in Germany derived from the German environmental survey on children 2003-2006 (GerES IV). Int. J. Hyg Environ. Health 212 (6), 637–647. https://doi.org/10.1016/j.ijheh.2009.05.003.

Shah-Kulkarni, S., Ha, M., Kim, B.M., et al., 2016. Neurodevelopment in Early Childhood Affected by Prenatal Lead Exposure and Iron Intake [published correction appears in Medicine (Baltimore) 95(10):e077f. Kim's, Young Ju [Corrected to Kim, Young Ju]]. Medicine (Baltim.) 95 (4), e2508. https://doi.org/10.1097/MD.0000000000002508.

Smith, M.R., Yevoo, P., Sadahiro, M., et al., 2018. Integrative bioinformatics identifies postnatal lead (Pb) exposure disrupts developmental cortical plasticity. Sci. Rep. 8 (1), 16388. https://doi.org/10.1038/s41598-018-34592-4.

Skerfving, S., Löfmark, L., Lundh, T., Mikoczy, Z., Strömberg, U., 2015. Late effects of low blood lead concentrations in children on school performance and cognitive functions. Neurotoxicology 49, 114–120. https://doi.org/10.1016/j.neuro.2015.05.009.

Singh, J., Singh, V., Anand, M., Kumar, P., Siddiqui, M., 2010. Placental lead and its interaction with some essential metals among women from Lucknow, India. Asian J. Med. Sci. 1 (2), 32–36. https://doi.org/10.3126/ajms.v1i2.3199.

Snoj Tratnik, J., Mazej, D., Miklavčič, A., et al., 2013. Biomonitoring of selected trace elements in women, men and children from Slovenia. E3S Web of Conferences 1, 26001. https://doi.org/10.1051/e3sconf/20130126001.

Snoj Tratnik, J., Falnoga, I., Mazej, D., et al., 2019. Results of the first national human biomonitoring in Slovenia: trace elements in men and lactating women, predictors of exposure and reference values. Int. J. Hyg Environ. Health 222 (3), 563–582. https://doi.org/10.1016/j.ijheh.2019.02.008.

Srikanth, P., Lagomarsino, V.N., Pearse 2nd, R.V., et al., 2018. Convergence of independent DISC1 mutations on impaired neurite growth via decreased UNC5D expression. Transl. Psychiatry 8 (1), 245. https://doi.org/10.1038/s41398-018-0281-9.

Stansfield, K.H., Pilsner, J.R., Lu, Q., Wright, R.O., Guilarte, T.R., 2012. Dysregulation of BDNF-TrkB signaling in developing hippocampal neurons by Pb(2+): implications for an environmental basis of neurodevelopmental disorders. Toxicol. Sci. 127 (1), 277–295. https://doi.org/10.1093/toxsci/kfs090.

Stasenko, S., Bradford, E.M., Piasek, M., et al., 2010. Metals in human placenta: focus on the effects of cadmium on steroid hormones and leptin. J. Appl. Toxicol. 30 (3), 242–253. https://doi.org/10.1002/jat.1490.

Stenz, L., Zewdie, S., Laforge-Escarra, T., et al., 2015. BDNF promoter I methylation correlates between post-mortem human peripheral and brain tissues. Neurosci. Res. 91, 1–7. https://doi.org/10.1016/j.neures.2014.10.003.

Tamayo Y Ortiz, M., Téllez-Rojo, M.M., Wright, R.J., Coull, B.A., Wright, R.O., 2016. Longitudinal associations of age and prenatal lead exposure on cortisol secretion of 12-24 month-old infants from Mexico City. Environ. Health 15, 41. https://doi.org/10.1186/s12940-016-0124-1.

Taylor, C.M., Golding, J., Hibbeln, J., Emond, A.M., 2013. Environmental factors predicting blood lead levels in pregnant women in the UK: the ALSPAC study. PLoS One 8 (9), e72371. https://doi.org/10.1371/journal.pone.0072371.

Tekin, D., Kayaaltı, Z., Söylemezoğlu, T., 2012. The effects of metallothionein 2A polymorphism on lead metabolism: are pregnant women with a heterozygote genotype for metallothionein 2A polymorphism and their newborns at risk of having higher blood lead levels? Int. Arch. Occup. Environ. Health 85 (6), 631–637. https://doi.org/10.1007/s00420-011-0711-y.

Thion, M.S., Garel, S., 2020. Microglial ontogeny, diversity and neurodevelopmental functions. Curr. Opin. Genet. Dev. 65, 186–194. https://doi.org/10.1016/j.gde.2020.06.013.

Tian, L.L., Zhao, Y.C., Wang, X.C., et al., 2009. Effects of gestational cadmium exposure on pregnancy outcome and development in the offspring at age 4.5 years. Biol. Trace Elem. Res. 132 (1–3), 51–59. https://doi.org/10.1007/s12011-009-8391-0.

Turconi, G., Guarcello, M., Livieri, C., et al., 2004. Evaluation of xenobiotics in human milk and ingestion by the newborn–an epidemiological survey in Lombardy (Northern Italy). Eur. J. Nutr. 43 (4), 191–197. https://doi.org/10.1007/s00394-004-0458-2.

Ursinyova, M., Masanova, V., 2005. Cadmium, lead and mercury in human milk from Slovakia. Food Addit. Contam. 22 (6), 579–589. https://doi.org/10.1080/02652030500135201.

Vigeh, M., Yokoyama, K., Ramezanzadeh, F., et al., 2006. Lead and other trace metals in preeclampsia: a case–control study in Tehran, Iran. Environ. Res. 100 (2), 268–275. https://doi.org/10.1016/j.envres.2005.05.005.

Vollset, M., Iszatt, N., Enger, Ø., Gjengedal, E.L.F., Eggesbø, M., 2019. Concentration of mercury, cadmium, and lead in breast milk from Norwegian mothers: association with dietary habits, amalgam and other factors. Sci. Total Environ. 677, 466–473. https://doi.org/10.1016/j.scitotenv.2019.04.252.

Wagner, P.J., Park, H.R., Wang, Z., et al., 2017. In vitro effects of lead on gene expression in neural stem cells and associations between up-regulated genes and cognitive scores in children. Environ. Health Perspect. 125 (4), 721–729. https://doi.org/10.1289/EHP265.

Wan, L., Li, Y., Zhang, Z., Sun, Z., He, Y., Li, R., 2018. Methylenetetrahydrofolate reductase and psychiatric diseases. Transl. Psychiatry 8 (1), 242. https://doi.org/10.1038/s41398-018-0276-6.

Wang, P., Tian, Y., Shi, R., et al., 2008. [Study on maternal-fetal status of Pb, As, Cd, Mn and Zn elements and the influence factors]. Chin. J. Prev. Med. 42, 722–726. PMID: 19178832.

Wang, Z., Henn, B.C., Wang, C., et al., 2017. Genome-wide gene by lead exposure interaction analysis identifies UNC5D as a candidate gene for neurodevelopment. Environ. Health 16, 81. https://doi.org/10.1186/s12940-017-0288-3.

Watson, C.V., Lewin, M., Ragin-Wilson, A., et al., 2020. Characterization of trace elements exposure in pregnant women in the United States, NHANES 1999-2016. Environ. Res. 183, 109208. https://doi.org/10.1016/j.envres.2020.109208.

Wennberg, M., Lundh, T., Sommar, J.N., Bergdahl, I.A., 2017. Time trends and exposure determinants of lead and cadmium in the adult population of northern Sweden 1990-2014. Environ. Res. 159, 111–117. https://doi.org/10.1016/j.envres.2017.07.029.

WHO, 1989. Minor and Trace Elements in Breast Milk: Report of a Joint WHO/IAEA Collaborative Study. https://apps.who.int/iris/handle/10665/39678. (Accessed 9 July 2021). accessed.

WHO, 2019. Exposure to Lead: a Major Public Health Concern. https://apps.who.int/iris/bitstream/handle/10665/329953/WHO-CED-PHE-EPE-19.4.7-eng.pdf?ua=1. (Accessed 9 July 2021). accessed.

Winiarska-Mieczan, A., 2014. Cadmium, lead, copper and zinc in breast milk in Poland. Biol. Trace Elem. Res. 157 (1), 36–44. https://doi.org/10.1007/s12011-013-9870-x.

Wright, R.O., 1999. The role of iron therapy in childhood plumbism. Curr. Opin. Pediatr. 11 (3), 255–258. https://doi.org/10.1097/00008480-199906000-00016.

Wright, R.O., Hu, H., Silverman, E.K., et al., 2003. Apolipoprotein E genotype predicts 24-month bayley scales infant development score. Pediatr. Res. 54 (6), 819–825. https://doi.org/10.1203/01.PDR.0000090927.53818. DE.

Wright, R.O., Schwartz, J., Wright, R.J., et al., 2010. Biomarkers of lead exposure and DNA methylation within retrotransposons. Environ. Health Perspect. 118 (6), 790–795. https://doi.org/10.1289/ehp.0901429.

Wu, S., Hivert, M.F., Cardenas, A., et al., 2017. Exposure to low levels of lead in utero and umbilical cord blood DNA methylation in project viva: an epigenome-wide association study. Environ. Health Perspect. 125 (8), 087019 https://doi.org/10.1289/EHP1246.

Zagrodzki, P., Zamorska, L., Borowski, P., 2003. Metal (Cu, Zn, Fe, Pb) concentrations in human placentas, 2003 Cent. Eur. J. Publ. Health 11 (4), 187–191. PMID: 14768780.

Zare Jeddi, M., Hopf, N.B., Viegas, S., et al., 2021. Towards a systematic use of effect biomarkers in population and occupational biomonitoring. Environ. Int. 146, 106257. https://doi.org/10.1016/j.envint.2020.106257.

Zhang, J., Liu, Q., 2015. Cholesterol metabolism and homeostasis in the brain. Protein & Cell 6 (4), 254–264. https://doi.org/10.1007/s13238-014-0131-3.

Zheleznyakova, G.Y., Cao, H., Schiöth, H.B., 2016. BDNF DNA methylation changes as a biomarker of psychiatric disorders: literature review and open access database analysis. Behav. Brain Funct. 12 (1), 17. https://doi.org/10.1186/s12993-016-0101-4.

Zhou, C.C., Gao, Z.Y., He, Y.Q., et al., 2019. Effects of lead, mercury, aluminium and manganese co-exposure on the serum BDNF concentration of pre-school children in Taizhou, China. Chemosphere 217, 158–165. https://doi.org/10.1016/j.chemosphere.2018.11.028.

Zhu, M, Fitzgerald, EF, Gelberg, KH, et al., 2010. Maternal low-level lead exposure and fetal growth. Environmental Health Perspectives 118, 10. https://doi.org/10.1289/ehp.0901561.

Zhu, Y., Li, Y., Haraguchi, S., et al., 2013. Dependence receptor UNC5D mediates nerve growth factor depletion-induced neuroblastoma regression. J. Clin. Invest. 123 (7), 2935–2947. https://doi.org/10.1172/JCI65988.

International Journal of Hygiene and Environmental Health 238 (2021) 113853

Contents lists available at ScienceDirect

International Journal of Hygiene and Environmental Health

journal homepage: www.elsevier.com/locate/ijheh

Levels and determinants of urinary phthalate metabolites in New Zealand children and adults

Andrea 't Mannetje *, Jonathan Coakley, Jeroen Douwes

Research Centre for Hauora and Health, Massey University, Wellington, New Zealand

ARTICLE INFO

Keywords:
Biomonitoring
Urine
Phthalates
New Zealand
Children
Adults

ABSTRACT

Background: This first national biomonitoring survey of urinary phthalate metabolites in the New Zealand population aimed to provide baseline data, identify exposure determinants, and make comparisons with health-based exposure guidance values.

Methods: The survey conducted in 2014–2016 involved the collection of morning-void urine from 298 children (5–18 years) and 302 adults (20–65 years), 33% of Māori ethnicity. A questionnaire collected information on demographic factors and diet. Urine was analysed for creatinine, specific gravity, and 10 phthalate metabolites through liquid chromatography tandem-mass spectrometry (MMP; MEP; MBP iso+n; MBzP; MCHP; MEHP; MEOHP; MEHHP; MCPP; and MiNP). Determinants of exposure were assessed using multivariable linear regression.

Results: Detection frequencies exceeded 95% for metabolites of DEP, DEHP and DBP. The highest GM was observed for the DBP metabolite MBP iso+n (36.1 μg/L adults; 60.5 μg/L children), followed by the sum of three DEHP metabolites (MEHP+MEOHP+MEHHP: 19.0 μg/L adults; 37.0 μg/L children), and the DEP metabolite MEP (19.1 μg/L adults; 12.0 μg/L children). For most phthalate metabolites New Zealand levels were in the mid-range of internationally reported levels, while for DEP they were in the low range. Māori and non-Māori had similar levels. Children had higher GMs than adults for most metabolites, except for MEP. A proportion of children and adults exceeded the biomonitoring equivalents of health-based guidance values for DBP (0–16% and 0–3% respectively), and DEHP (0–0.7% and 0–0.3% respectively). Eating warm meals from plastic containers ≥2 times/week was associated with higher levels of DEHP metabolites, MBP iso+n, and MBzP.

Conclusion: Phthalate exposure is omnipresent in both children and adults in New Zealand. Exceedances of the biomonitoring equivalents for DBP and DEHP indicate that potential health effects from exposure to these phthalates cannot be excluded with sufficient certainty.

1. Introduction

Phthalates, diesters of phthalic acid, are widely used in plastics to make them flexible and durable, and as additives in a range of consumer products (Wang et al., 2019). The wide range of products that may contain phthalates include building materials (e.g. vinyl flooring, PVC pipes, cable, wire, paints); plastics used in the food supply chain (e.g. food production conveyor belts, tubing used in e.g. milking, plastic greenhouses (Zhang et al., 2019); plastic and cardboard containers/wrappings); children's products (e.g. plastic toys, teethers, school supplies) (Ashworth and Chappell, 2015; Babich et al., 2020); medical products (e.g. blood bags, intravenous lines, respiratory support equipment, pill covering); clothing (Li et al., 2019; Tang et al., 2020); furniture; and personal care products (e.g. shampoo, soap, deodorant, perfume, nail polish, hair spray, feminine hygiene products (Gao et al., 2020), and tattoo inks (Lehner et al., 2011)).

Phthalates easily migrate from products through leaching, evaporation and abrasion, and have been measured in food (Giuliani et al., 2020), water (Gonsioroski et al., 2020), air (Darbre, 2018), soil (Gao and Wen, 2016) and house dust (Bi et al., 2018), with exposure occurring through oral, dermal, intravenous and respiratory routes (Giovanoulis et al., 2018). Phthalates are rapidly (within 24 h) metabolised and excreted from the body (Koch et al., 2012), but are nonetheless considered pseudo-persistent due to their ubiquitous and continuous presence.

While phthalates have a low order of toxicity in experimental animals following oral administration, links between phthalate exposure

* Corresponding author.
E-mail address: a.mannetje@massey.ac.nz (A. 't Mannetje).

https://doi.org/10.1016/j.ijheh.2021.113853
Received 2 May 2021; Received in revised form 23 September 2021; Accepted 29 September 2021
Available online 9 October 2021

Abbreviations

BBzP	butyl benzyl phthalate
BE	biomonitoring equivalent
DBP iso+n	dibutyl phthalate iso+n
DCHP	dicyclohexyl phthalate
DEHP	di (2-ethylhexyl) phthalate
DEP	diethyl phthalate
DiDP	di-iso-decyl phthalate
DINCH	1,2-cyclohexane dicarboxylic acid diisononyl ester
DiNP	di-iso-nonyl phthalate
DMP	dimethyl phthalate
DnOP	di-n-octyl phthalate
GM	geometric mean
$HBM\text{-}GV_{GenPop}$	human biomonitoring guidance value for the general population
LC-MS/MS	liquid chromatography tandem-mass spectrometry
LOD	limit of detection
MBP iso+n	monobutyl phthalate iso+n
MBzP	monobenzyl phthalate
MCHP	mono-cyclohexyl phthalate
MCPP	mono-(3-carboxypropyl) phthalate
MEHHP	mono-(2-ethyl-5-hydroxyhexyl) phthalate
MEHP	mono-2-ethylhexyl phthalate
MEOHP	mono-(2-ethyl-5-oxohexyl) phthalate
MEP	monoethyl phthalate
MiNP	mono-iso-nonyl phthalate
MMP	monomethyl phthalate
RfD	reference dose
TDI	tolerable daily intake

and several health effects have been described. In particular, phthalates' endocrine disrupting properties are now well recognised (De Falco et al., 2015), and associations with male and female reproductive outcomes (Radke et al., 2018), metabolic effects (Ko et al., 2019; Radke et al., 2019), allergies and asthma (Hoppin et al., 2013), blood pressure (Zhang et al., 2018), heart rate variability (Jaimes et al., 2017), autism (Oulhote et al., 2020), and decreased motor function (Daniel et al., 2020) have been reported.

Biomonitoring surveys have revealed humans to be ubiquitously exposed to phthalates, with marked differences between populations and between different time points (Wang et al., 2019) resulting from variations in phthalate use and regulations. While the European Union and the USA have introduced some legislative measures to restrict the use of phthalates (Kamrin, 2009), in New Zealand such regulations are not in place (Ashworth et al., 2018) and human biomonitoring studies of phthalates have not been conducted. Here we present the first national biomonitoring survey of urinary phthalate metabolites in the New Zealand population, to provide baseline data to monitor future trends, identify determinants of exposure, and make comparisons with other countries and health-based exposure guidance values.

2. Material and methods

2.1. Subject recruitment

The biological monitoring programme included a cross-section of adult and school-age (5–18 years) New Zealanders. This cross-sectional study used stratified random sampling, stratifying on age, gender, region, and ethnicity, to ensure that all main demographic groups were represented, as previously described ('t Mannetje et al., 2018). For adults the 2014 New Zealand Electoral Roll was used to randomly invite, by mail, men and women in four age groups (i.e. 19-24, 25–34, 35–49, 50–64 years), from four geographic regions (Northland/Auckland, Waikato/Bay of Plenty, Lower North Island, South Island), and of both Māori (the indigenous population of New Zealand) and non-Māori ethnicity. For children we contacted primary, intermediate, and high schools and recruited at public events such as science fairs and sports clubs. We aimed for a total of 300 adults and 300 children with approximately equal numbers in each of the gender/-age/geographical/ethnic sub-groups.

Study participation involved providing a urine sample, a blood sample (results reported elsewhere), and the completion of a 15 min questionnaire including questions on demographic and lifestyle factors.

The study received approval from the Health and Disabilities Ethics Committees (HDEC), reference 14/CEN/44. Informed consent was provided by all study participants or their guardians.

2.2. Urine sampling and analyses

First-void morning urine samples were self-collected (instructions aimed to limit contamination were provided) into 60 mL sterile, pre-labelled polypropylene urine collection containers, with samples stored in the participant's home freezer (-20 °C) until they were sent to our laboratory using a pre-paid insulated postal envelope with frozen gel pack allowing samples to be kept cold during transit.

All samples were shipped on dry ice to Canterbury Health Laboratories (www.chl.co.nz/) where the analyses for creatinine and specific gravity was conducted. Creatinine was measured using the colorimetric end-point Jaffe method. The specific gravity of the urine samples was determined with a refractometer.

Sample aliquoting was conducted at Canterbury Health Laboratories after which 1 mL urine aliquots were shipped on dry ice to Axys Analytical Services in Sidney, Canada (www.axysanalytical.com/) who conducted the analyses for phthalate metabolites, including: MMP; MEP; MBP iso+n; MBzP; MCHP; MEHP; MEOHP; MEHHP; MCPP; and MiNP. Concentrations were determined using liquid chromatography tandem-mass spectrometry (LC-MS/MS; accredited method ID: SGS AXYS MLA-059; Method Detection Limit protocol: Federal Register 40 CFR Part 136, Appendix B, no iteration), based on previously described methods (Kato et al., 2005). Isotope ^{13}C dilution quantification procedures provided recovery corrected results. Blank matrix samples (synthetic urine), fortified with known amounts of authentic analytes, were used to demonstrate analytical accuracy. Aqueous lab blanks were included with each batch of samples (n = 32), which were below the limit of detection for all analytes, except for MBP detected in one lab blank (1.7 μg/L). MBP concentrations for this batch were lab blank corrected.

2.3. Statistical analyses

Urinary concentrations were expressed unadjusted for urine dilution (in μg/L) as well as adjusted for creatinine (in μg/g creatinine) and specific gravity (in μg/L specific gravity adjusted). Summary statistics of urine phthalate metabolite concentrations, including geometric means (GM) and 95% confidence intervals were calculated separately for adults and children, and by age group and gender. For analytical results below the limit of detection, half the limit of detection was used in further calculations. Linear regression on log-transformed urine concentrations was used to assess associations with a range of demographic and lifestyle factors. The exponentiated regression coefficients represent an exposure ratio (e.g. an exponentiated coefficient of 2 for males indicating a 2 times higher exposure for males compared to females). Initial models included the individual variables adjusting for age and gender. Individual variables included ethnicity (Māori, other), highest achieved education (adults only), body mass index (BMI, adults only), smoking

(adults only), living with a smoker, alcohol consumption (adults only), age of dwelling, type of water supply of dwelling, water filter at dwelling, rural/urban residency, consumption of tap water, consumption of bottled water, and a short list of dietary items (including the frequency of eating hot meals that have been stored, cooked, or reheated in plastic containers). If the variable was associated with phthalate metabolite urine concentrations ($p < 0.05$) in these initial models, the variable was then included in a multivariable model together with other variables that were associated with the phthalate metabolite ($p < 0.05$) in the initial models (whilst also adjusting for age and gender).

2.4. International comparison

Human biomonitoring studies conducted in other countries reporting on general population urinary phthalate metabolite levels were identified through a literature search. Studies included in the international comparison were restricted to those that: (i) had urine samples collected within 5 years of the New Zealand study collection period, i.e. within the period 2009–2020; (ii) included both males and females; (iii) reported geometric means; and (iv) reported urinary concentrations in μg/L as this was the most commonly reported unit. For studies reporting on MiBP and MnBP separately, GMs were added to enable a comparison with MBP iso+n. The same approach was used for the DEHP metabolites MEHP+MEOHP+MEHHP.

3. Results

For a total of 600 participants (298 children and 302 adults, 29% and 38% of which Māori, 33% overall), urinary phthalate metabolite concentrations were determined. Of the 10 phthalate metabolites measured in urine (Table 1), 7 were detected in the majority of samples (MEP, MBP iso+n, MBzP, MEHP, MEOHP, MEHHP, MCPP). The highest GM was observed for MBP iso+n (37.0 μg/L for adults and 60.5 μg/L for children), followed by the sum of three DEHP metabolites (MEHP+MEOHP+MEHHP: 19.0 μg/L for adults and 35.5 μg/L for children), MEP (19.0 μg/L for adults and 13.0 μg/L for children), and MBzP (4.2 μg/L for adults and 7.7 μg/L for children). More summary statistics, and levels adjusted for urine dilution, are provided in Supplementary Table 1.

Concentrations of the three metabolites of DEHP were strongly correlated with each other as well as with their summed values (Supplementary Table 2), with Pearson coefficients ranging between 0.65 and 0.97 ($p < 0.0001$). Strong correlations were also observed among DEHP metabolites, MBP, MBzP and MCPP, with Pearson coefficients ranging between 0.26 and 0.60 ($p < 0.0001$). MEP, on the other hand, was not strongly correlated with any of the other metabolites, with Pearson coefficients ranging between 0.08 and 0.13.

Geometric mean concentrations of phthalate metabolites, by age group and gender, are provided in Fig. 1, for the metabolites detected in the majority of samples. Children had higher GMs compared to the older age groups for MBP iso+n, DEHP metabolites, MBzP and MCPP. The pattern was reversed for MEP, for which children had lower levels. The differences between age groups depended on the type of adjustment made to normalise the urinary concentrations (Supplementary Fig. 1). Creatinine adjustment increased differences between children and adults, and decreased differences for the 20+ age groups, while unadjusted concentrations suggested a more gradual trend by age. Specific gravity adjustment tended to reduce differences in metabolite concentrations between age groups, while showing the same increasing age trend observed for the unadjusted urinary concentrations.

Overall, there were few differences in phthalate metabolite levels between males and females. Whether gender differences were observed depended to some extent on whether adjustment for creatinine or specific gravity was applied (Supplementary Fig. 1). For example, the GM for MEP for 40-60-year-old women were significantly higher than for men when creatinine or specific gravity adjustments were applied, but this difference reduced for unadjusted concentrations.

When considering exposure to the overall sum of the phthalate metabolites (Fig. 2), the youngest age group (age 5–10) had the highest exposure to phthalates, which was independent of the type of adjustment made (Supplementary Fig. 2). For all age and gender groups, the largest contributor to the summed value of phthalate metabolites was MBP iso+n (>40% for most groups). With higher age, MEP contributed

Table 1
Urinary phthalate metabolite concentrations (μg/L) in New Zealand children (n = 298) and adults (n = 302), 2014–2016.

metabolite measured in urine **(precursor phthalate)**	**population group**	**detection frequency (%)**[a]	**50th %ile**	**95th %ile**	**GM**	**(95%CI) GM**
MMP **(DMP)**	children	10	<LOD	13.6	<LOD	–
	adults	4	<LOD	2.9	<LOD	–
MEP **(DEP)**	children	94	12.0	109.5	13.0	(11.4–14.8)
	adults	96	19.1	147.7	19.0	(16.6–21.9)
MBP iso+n[b] (DBP iso+n[c])	children	100	60.5	198.5	60.5	(55.7–65.7)
	adults	100	36.1	147.2	37.0	(33.4–40.9)
MBzP **(BBzP)**	children	93	7.4	50.6	7.7	(6.7–8.8)
	adults	82	4.6	32.7	4.2	(3.6–4.8)
MCHP **(DCHP)**	children	0	<LOD	<LOD	<LOD	–
	adults	1	<LOD	<LOD	<LOD	–
MEHP **(DEHP)**	children	90	2.8	11.3	2.7	(2.5–3.0)
	adults	75	2.1	10.1	2.0	(1.8–2.2)
MEOHP **(DEHP)**	children	100	14.3	47.0	14.2	(13.1–15.4)
	adults	99	7.0	25.9	7.0	(6.4–7.7)
MEHHP **(DEHP)**	children	98	18.6	68.2	17.6	(15.9–19.4)
	adults	96	9.6	38.9	9.0	(8.0–10.1)
MEHP+MEOHP+MEHHP	children	100	37.0	122.4	35.5	(32.5–38.7)
	adults	100	19.0	76.1	19.0	(17.2–20.9)
MCPP[d] **(DnOP)**	children	77	3.0	11.8	3.3	(3.0–3.7)
	adults	64	2.0	18.3	2.4	(2.1–2.7)
MiNP[e] (**DiNP**)	children	0	<LOD	<LOD	<LOD	–
	adults	1	<LOD	<LOD	<LOD	–

[a] Limit of detection was 1 μg/L for MMP, MBP, MBzP, MEHP, MEOHP, MEHHP, MCHP, MiNP; 2 μg/L for MEP, MCPP.
[b] Mono-n-butyl phthalate and mono-iso-butyl phthalate were measured together.
[c] MnBP is also a minor metabolite of butyl benzyl phthalate (BBzP) (Johns et al., 2015)
[d] MCPP is thought to be the main metabolite of DnOP (Calafat et al., 2006)
[e] Oxidative metabolites of DiNP were not determined as part of this study, MiNP is considered to be only a minor metabolite of DiNP(Frederiksen et al., 2007)

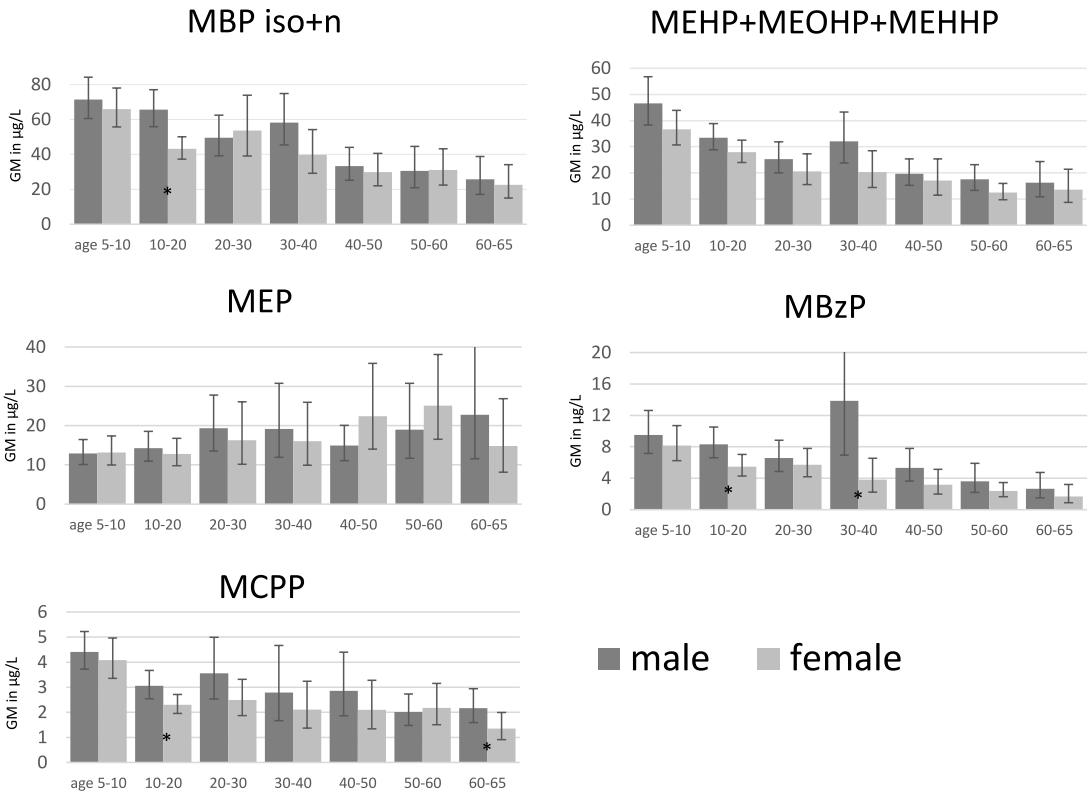

Fig. 1. Geometric means and 95%CI of phthalate metabolite urine concentrations (µg/L) by age and gender (*p < 0.05 for difference between males and females).

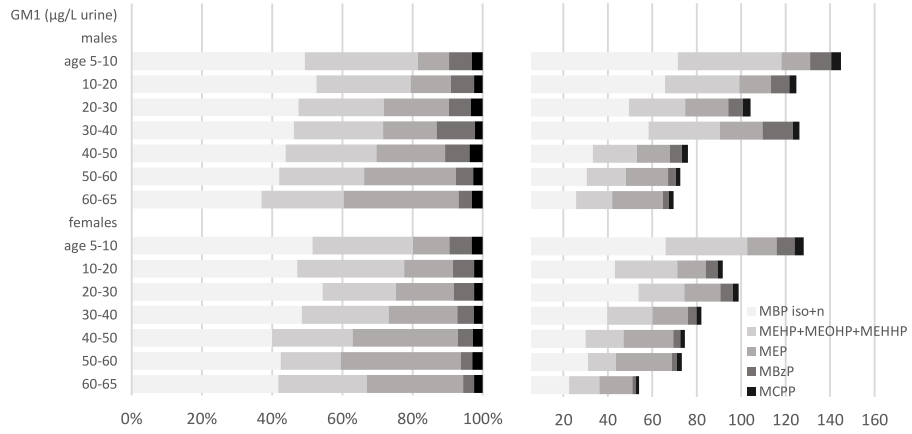

Fig. 2. Sum of GMs of phthalate metabolites (in % of total and in µg/L), by age and gender.

relatively more (ranging from 10% to >30%) to the sum of phthalate metabolites.

Multivariable linear regression showed that specific gravity-adjusted phthalate metabolite concentrations were not associated with ethnicity (Māori/non-Māori), rural/urban residency, highest achieved education (adults only) or specific dietary items. BMI (only available for adults) was inversely associated with both MEP and MBzP metabolite concentrations (Table 2), with a BMI>35 associated with an approximately 40–50% lower urinary concentrations compared to those with a BMI of 17–25. Eating warm meals from plastic containers >2 times/week was associated with higher levels of MBP iso+n (for adults), MEHP+MEOHP+MEHHP (for children and adults), and MBzP (for children) (Table 2). These associations were similar when different urinary dilution adjustments were applied (Supplementary Table 3).

Fig. 3 compares the GMs observed in this study with those reported internationally. This indicates that New Zealand levels are in the middle of the international range for MBP iso+n, MEHP+MEOHP+MEHHP and MBzP, while levels of MEP were relatively low. Supplementary Fig. 3 provides an additional comparison of the New Zealand data with time trends reported for the USA (CDC, 2021), showing that New Zealand urinary concentrations for MBP iso+n are higher than those reported for the USA at any time since 1999.

Health-based exposure guidance values and biomonitoring equivalents (BE) are available for several phthalate metabolites assessed in this

Table 2
Linear regression on urine concentrations of phthalate metabolites (specific gravity adjusted and log-transformed) for New Zealand children and adults.

		MBP iso+n	MEHP+ MEOHP+ MEHHP	MEP	MBzP	MCPP
	n	exposure ratio (ER)	exposure ratio (ER)	exposure ratio (ER)	exposure ratio (ER)	exposure ratio (ER)
adults						
BMI						
17-25	114	ref	ref	ref	ref	ref
25-30	92	1.0	0.9	0.9	0.7	0.8
30-35	44	0.8	0.9	0.8	0.9	0.7
35+	41	0.9	0.9	**0.5***	**0.6***	1.0
meals from plastic[a]						
never	35	ref	ref	ref	ref	ref
<1 times/week	87	1.1	1.0	0.9	0.9	0.8
1-2 times/week	99	1.3	1.1	0.7	1.1	0.9
>2 times/week	70	**1.4***	1.3	0.7	1.2	1.0
children						
meals from plastic[a]						
never	44	ref	ref	ref	ref	ref
<1 times/week	140	1.1	**1.3***	1.0	1.1	1.0
1-2 times/week	72	1.1	1.2	1.1	1.1	0.9
>2 times/week	37	1.2	**1.4***	0.9	**1.7***	1.0

ER: exposure ratio (exponentiated regression coefficient).
BMI: body mass index based on self-reported weight and height.
Adjustment: all models were adjusted for gender (male/female) and age (years).
*$p < 0.05$.
Ref: reference.
[a] Based on the question: How often do you/does your child eat hot meals that have been stored, cooked, or re-heated in plastic containers (e.g. take-away meal, ready-made meal, leftovers heated or stored in plastic containers)?.

study (Table 3). Exceeding the BE suggests that adverse health effects cannot be excluded with sufficient certainty (Schwedler et al., 2020). The GMs for the New Zealand study population (Table 1) were generally far below these BEs. For DBP and DEHP, some individual urinary concentrations exceeded the BE, for both children (up to 16%) and adults (up to 3%). Because in this study MnBP and MiBP were not determined individually, and these two metabolites have different Biomonitoring Equivalents, a comparison was not straight forward. Only HBM-GV provides a BE for both MiBP and MnBP, with MiBP having a higher BE than MnBP. The percentage of exceedances among children therefore ranged between 9.1% (assuming all MBP is MiBP) and 16.4% (assuming all MBP is MnBP). The percentage of exceedances among adults ranged between 2.6% (assuming all MBP is MiBP) and 3.3% (assuming all MBP is MnBP). Urinary concentrations of DEP and BBzP metabolites never exceeded the BEs.

4. Discussion

This study shows that exposure to phthalate plasticisers in the New Zealand population is widespread, and that New Zealand levels are in the mid-range when compared to other countries with recent data available. In contrast, levels of DEP, used in personal care products rather than as a plasticiser, were relatively low in New Zealand.

This study did not include all relevant phthalates or phthalate metabolites. While low molecular weight phthalates metabolise predominantly to their simple monoesters, high molecular weight phthalates can metabolise to a range of oxidised metabolites, with only a small fraction excreted as the simple monoester. The only metabolite of DiNP analysed in this study was its simple monoester, thus underestimating exposure to DiNP. It is likely that New Zealanders have substantial exposure to DiNP, given that among 14 phthalates analysed in New Zealand food items, DiNP was most frequently detected (Pearson and van den Beuken, 2017). DEHP has increasingly been replaced by DiNP, for which the relevant metabolites were not included in this study, and by DiDP which was also not included. Future studies on phthalate exposure in New Zealand will therefore need to consider replacements of previously widely used phthalates, including non-phthalate replacement plasticisers such as DINCH.

For this population, the highest levels were measured for metabolites of DBP. The analytical methods used did not distinguish between MnBP and MiBP and only the summed urinary concentrations were obtained (MBP iso+n). Historically MnBP has been dominant, but in the USA urinary levels of MnBP have decreased over time, while that of MiBP have increased (Zota and Woodruff, 2014). MBP iso+n was detected at levels substantially higher than those reported for the USA at any time since the start of phthalate biomonitoring in 1999, with some individual levels among adults and children exceeding the BE. This is of concern, given that DBP has been shown to be a skin irritant, a suspected reproduction toxicant (Xie et al., 2019), and may aggravate asthma (Zhou et al., 2020). The use of DBP in toys and children's products has been restricted in the USA and EU, but not in New Zealand (Ashworth et al., 2018).

DEHP was the second highest phthalate measured here, at levels higher than the most recent NHANES data. Many manufacturers have discontinued use of DEHP in their products due to potential health concerns, and for the USA substantial reductions in exposure over time have been reported (CDC, 2019). It is therefore likely that New Zealand exposures to DEHP were higher in the past because many goods containing DEHP are imported from the USA and other countries. Exceedances of the BE for DEHP metabolites did occur in our study population, albeit rarely (<1%).

MEP, a metabolite of DEP, was measured at the third highest level in this population. Levels were lower than reported for several other countries including the USA, where urinary MEP levels have reduced substantially over time, likely reflecting reductions in the use of DEP in personal care products. None of the participants in this study exceeded the BE for MEP, with even the highest measured levels at least 10 times below the BE. MEP was not strongly correlated with any of the other phthalate metabolites, suggesting a different exposure source from those of other phthalates. MEP was also the only metabolite that was higher in adults compared to children, and higher among females compared to males in the 40–60-year age group. These patterns are consistent with personal care products as a dominant source of exposure to DEP in the New Zealand population.

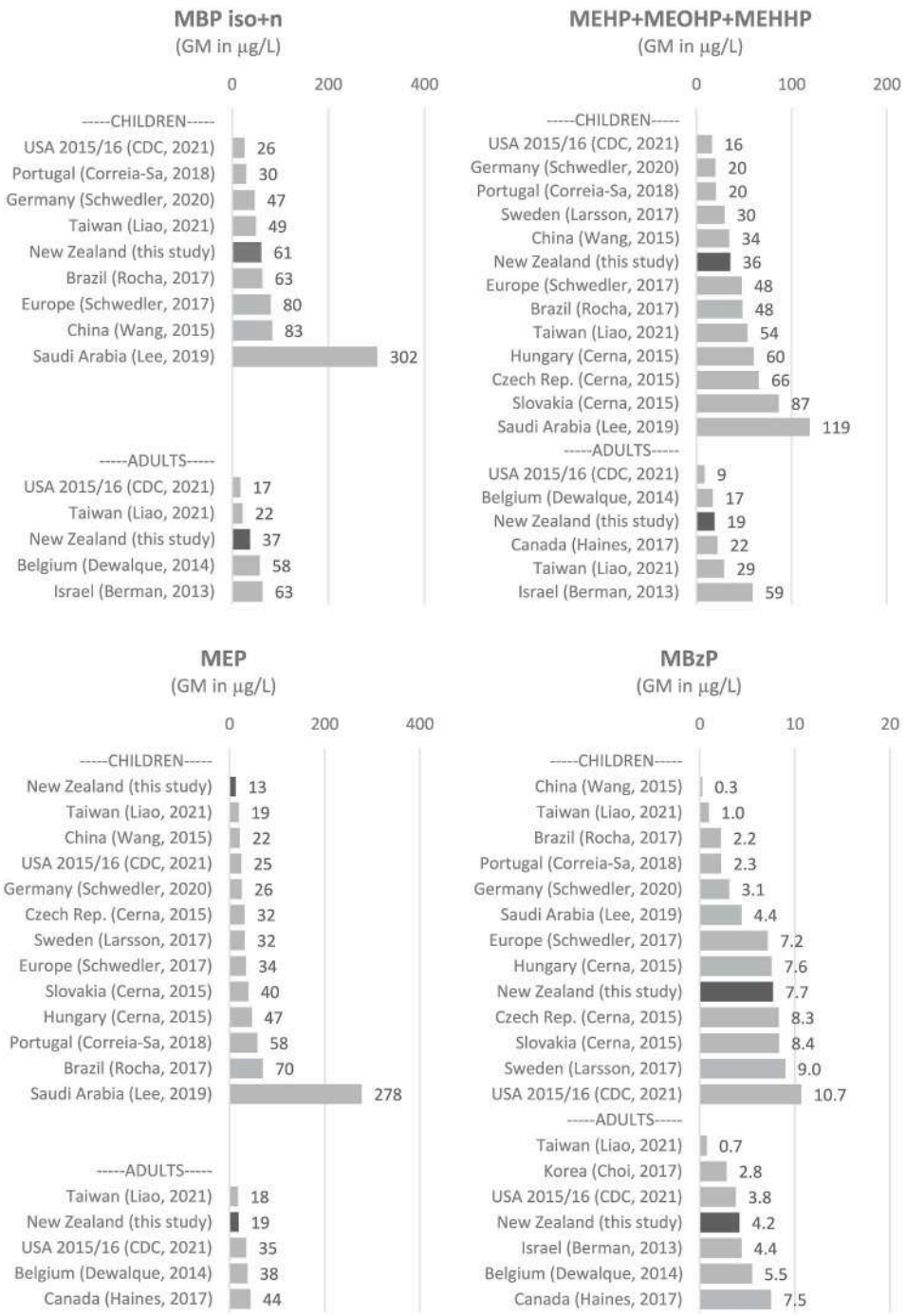

Fig. 3. Urinary phthalate metabolite concentrations (GM in µg/L) for New Zealand children and adults (2014–2016), compared to internationally reported levels (studies conducted ≥2009) (Berman et al., 2013; Cerna et al., 2015; Choi et al., 2017; Correia-Sa et al., 2018; Dewalque et al., 2014; Haines et al., 2017; Hartmann et al., 2015; Huang et al., 2015; Larsson et al., 2017; Lee et al., 2019; Liao et al., 2021; Rocha et al., 2017; Schwedler et al., 2017; Wang et al., 2015).

Our study did not identify associations with specific dietary items, which is not surprising given the large number of sources and routes of phthalate exposure, and the limitations of the short dietary questionnaire used in this study. Fasting studies have identified diet as a principal route of exposure to many phthalates, in particular high molecular weight phthalates. In a 48-h fasting study among 5 adults in Germany (Koch et al., 2013), concentrations of metabolites of high molecular weight phthalates (DEHP, DiNP and DiDP) showed a rapid decline within 24 h of fasting, rising again after food consumption resumed. By contrast, for metabolites of the low molecular weight phthalates including DMP, DEP, BBzP, DnBP and DiBP, only a weak influence of fasting was observed. For several phthalate metabolites we found that eating hot meals from plastic containers was associated with higher levels, including DEHP metabolites, MBP iso+n, and MBzP. Food packaging is a known source of DEHP exposure (Rudel et al., 2011) and limiting consumption of foods packaged and prepared in plastics and cans has been shown to significantly reduce urinary DEHP metabolites, with an increase shown after resuming packaged food consumption (Rudel et al., 2011). Both DEHP and DBP have been found to migrate from polypropylene food containers, particularly under acidic conditions and after longer heating time (Fang et al., 2017). These results suggest that phthalate reductions in food packaging and storage

Table 3
Health-based exposure guidance values for selected phthalate metabolites and exceedances of biomonitoring equivalents in New Zealand children and adults.

phthalate	metabolites	Biomonitoring Equivalent (BE)[1)] in μg/L		Health based guidance value the BE was based on		Exceedances in 298 children		Exceedances in 302 adults	
		children	adults			n	%	n	%
DnBP	MnBP	120	190	HBM-GV_{GenPop}	*Scenario 1*	49	16.4%	10	3.3%
					Scenario 2	10	3.4%	3	1.0%
		200	200	EFSA TDI	*Scenario 1*	15	5.0%	9	3.0%
					Scenario 2	2	0.7%	3	1.0%
		1400	1400	Health Canada TDI		0		0	
		2700	2700	USEPA RfD		0		0	
DiBP	MiBP	160	230	HBM-GV_{GenPop}	*Scenario 3*	27	9.1%	8	2.6%
DEHP	MEOHP+MEHHP	340	500	HBM-GV_{GenPop}		0		0	
	MEHP+MEOHP+MEHHP	260	260	USEPA RfD		2	0.7%	1	0.3%
		660	660	EFSA TDI		0		0	
DEP	MEP	18000	18000	USEPA RfD		0		0	
BBzP	MBzP	2000	3000	HBM-GV_{GenPop}		0		0	
		3800	3800	USEPA RfD		0		0	
		12000	12000	EFSA TDI		0		0	
		31000	31000	Health Canada TDI		0		0	

Biomonitoring Equivalents (BE) were extracted from (Aylward et al., 2009a, b; Lange et al., 2021).
Scenario 1: assuming all MBP is MnBP; Scenario 2: assuming 50% of MBP is MnBP.
Scenario 3: assuming all MBP is MiBP.

materials could present an effective strategy to reduce exposure for the New Zealand population, in particular for those phthalates for which biomonitoring equivalents were exceeded and therefore of greatest health concern (i.e., DBP and DEHP).

We observed an inverse association between BMI and urinary MEP and MBzP levels. Inconsistent associations between BMI and urinary phthalate metabolites have been reported in the literature (Goodman et al., 2014). A recent review of 18 studies reported predominantly positive but also inverse associations between BMI and phthalate levels (Ribeiro et al., 2020). This inconsistency among populations suggest that the association does not necessarily indicate a direct link between phthalate exposure and obesity, but instead may be mediated by certain lifestyle factors (i.e., diet, use of personal care products) in a population-specific way. For example, the inverse association observed here between BMI and MEP could be the result of a lower use of personal care products in those with a higher BMI in this population, although our questionnaire did not collect the information needed to verify this hypothesis. Alternatively, a lower body surface area to volume ratio associated with higher BMI may lead to a lower dermal uptake of personal care products relative to body volume. An additional complication in studying the association between BMI and phthalates is the differential impact the type of urinary dilution adjustment can have on the association (Lee et al., 2021), although we note that in our study BMI was inversely associated with urinary MEP and MBzP independent of the type of adjustment applied. Also, both causality (phthalates have been suggested to act as obesogens (Grun and Blumberg, 2009)) and reverse causality (BMI could impact on phthalate storage and metabolism) may play a role, but this cannot be confirmed or excluded in cross-sectional studies such as these. To fully elucidate the link between phthalates and BMI, longitudinal studies are needed that consider these complexities.

In this study we observed no difference in urinary phthalate metabolite levels between Māori and non-Māori. In the US NHANES study (Silva et al., 2004) ethnic differences were also not observed for most phthalate metabolites, but significantly higher concentrations of MEP were observed for non-Hispanic blacks compared to Mexican Americans and non-Hispanic whites, particularly among children. The authors speculated that these differences may be due to the use of certain beauty and hair care products specifically marketed for this population, often beginning at a young age. Our results suggest that such ethnic differences in the use of certain phthalate containing personal care products do not appear to be relevant for the New Zealand population.

A consistent finding among phthalate biomonitoring studies, including this study, is the higher phthalate metabolite urinary levels for children compared to adults (except for MEP). This negative association with age was observed irrespective of the type of urinary dilution adjustment applied, indicating that this trend is not an artefact of dilution adjustment. This consistent difference could be explained by children consuming a higher proportion of food compared to body size (Varshavsky et al., 2018), and other exposure sources that are particularly relevant for children. Children's toys have been a source of phthalate exposure: a study of phthalates in 49 children's toys in New Zealand (Ashworth and Chappell, 2015; Ashworth et al., 2018) reported that exceedances of the EU regulatory limit of 0.1% phthalate by weight of the material occurred for DiDP (20 samples), DEHP (17 samples), DiNP (14 samples), DiBP (7 samples), DnBP (4 samples), and DnOP (2 samples), with particularly high levels (up to 54% w/w) of DEHP. Children also play on the floor and engage more in hand-to-mouth activity, resulting in more exposure to phthalates that accumulate in house dust and leach from vinyl flooring. In a study from Germany, phthalate biomarker concentrations in urine were positively associated with the levels of the respective phthalate in house dust (Schwedler et al., 2020). A study from the USA (Hammel et al., 2019) showed that dermal contact and hand-to-mouth behaviours are important sources of exposure to phthalates. Children who lived in homes with 100% vinyl flooring had urinary concentrations of MBzP that were 15 times higher than those of children who lived in homes with no vinyl flooring (Hammel et al., 2019). These results emphasise the need for phthalate-exposure-reduction-strategies that include exposure sources that are particularly relevant to children.

5. Conclusions

Phthalate exposure is omnipresent in both children and adults in New Zealand, with the highest urinary levels observed for DBP and DEHP metabolites. Exceedances of the biomonitoring equivalents of health-based guidance values for DBP and DEHP in a small proportion of children and adults indicate that health effects from current phthalate exposure levels cannot be excluded with confidence.

Acknowledgements

The authors gratefully acknowledge the vital contribution of Michelle Gray, Tracey Whaanga, and Jean Feary McKenzie to the study

recruitment.

Appendix A. Supplementary data

Supplementary data to this article can be found online at https://doi.org/10.1016/j.ijheh.2021.113853.

Funding

This work was supported by the New Zealand Ministry of Health. The funder had no role in study design, in the collection, or in the analysis and interpretation of data.

References

Ashworth, M., Chappell, A., 2015. Health Risk Assessment of Selected Phthalates Reported from a Local Survey of Children's Plastic Toys in Christchurch, New Zealand. Institute Of Environmental Science And Research Limited.
Ashworth, M.J., Chappell, A., Ashmore, E., Fowles, J., 2018. Analysis and assessment of exposure to selected phthalates found in children's toys in christchurch, New Zealand. Int. J. Environ. Res. Publ. Health 15.
Aylward, L.L., Hays, S.M., Gagne, M., Krishnan, K., 2009a. Derivation of Biomonitoring Equivalents for di-n-butyl phthalate (DBP), benzylbutyl phthalate (BzBP), and diethyl phthalate (DEP). Regul. Toxicol. Pharmacol. 55, 259–267.
Aylward, L.L., Hays, S.M., Gagne, M., Krishnan, K., 2009b. Derivation of Biomonitoring Equivalents for di(2-ethylhexyl)phthalate (CAS No. 117-81-7). Regul. Toxicol. Pharmacol. 55, 249–258.
Babich, M.A., Bevington, C., Dreyfus, M.A., 2020. Plasticizer migration from children's toys, child care articles, art materials, and school supplies. Regul. Toxicol. Pharmacol. 111, 104574.
Berman, T., Goldsmith, R., Goen, T., Spungen, J., Novack, L., Levine, H., Amitai, Y., Shohat, T., Grotto, I., 2013. Urinary concentrations of environmental contaminants and phytoestrogens in adults in Israel. Environ. Int. 59, 478–484.
Bi, C., Maestre, J.P., Li, H., Zhang, G., Givehchi, R., Mahdavi, A., Kinney, K.A., Siegel, J., Horner, S.D., Xu, Y., 2018. Phthalates and organophosphates in settled dust and HVAC filter dust of U.S. low-income homes: association with season, building characteristics, and childhood asthma. Environ. Int. 121, 916–930.
Calafat, A.M., Silva, M.J., Reidy, J.A., Earl Gray, L., Samander, E., Preau, J.L., Herbert, A. R., Needham, L.L., 2006. Mono-(3-carboxypropyl) phthalate, a metabolite of di-n-octyl phthalate. J. Toxicol. Environ. Health A 69, 215–227.
CDC, 2019. Fourth National Report on Human Exposure to Environmental Chemicals. U. S. Department of Health and Human Services. Centres for Disease Control and Prevention. Updated Tables, January 2019, Volume One.
CDC, 2021. Fourth National Report on Human Exposure to Environmental Chemicals Updated Tables, March 2021. Volume Two: NHANES 2011-2016. U.S. Department of Health and Human Services. Centers for Disease Control and Prevention.
Cerna, M., Maly, M., Rudnai, P., Kozepesy, S., Naray, M., Halzlova, K., Jajcaj, M., Grafnetterova, A., Krskova, A., Antosova, D., Forysova, K., Den Hond, E., Schoeters, G., Joas, R., Casteleyn, L., Joas, A., Biot, P., Aerts, D., Angerer, J., Bloemen, L., Castano, A., Esteban, M., Koch, H.M., Kolossa-Gehring, M., Gutleb, A.C., Pavlouskova, J., Vrbik, K., 2015. Case study: possible differences in phthalates exposure among the Czech, Hungarian, and Slovak populations identified based on the DEMOCOPHES pilot study results. Environ. Res. 141, 118–124.
Choi, W., Kim, S., Baek, Y.W., Choi, K., Lee, K., Kim, S., Yu, S.D., Choi, K., 2017. Exposure to environmental chemicals among Korean adults-updates from the second Korean National Environmental Health Survey (2012-2014). Int. J. Hyg Environ. Health 220, 29–35.
Correia-Sa, L., Kasper-Sonnenberg, M., Palmke, C., Schutze, A., Norberto, S., Calhau, C., Domingues, V.F., Koch, H.M., 2018. Obesity or diet? Levels and determinants of phthalate body burden - a case study on Portuguese children. Int. J. Hyg Environ. Health 221, 519–530.
Daniel, S., Balalian, A.A., Whyatt, R.M., Liu, X., Rauh, V., Herbstman, J., Factor-Litvak, P., 2020. Perinatal phthalates exposure decreases fine-motor functions in 11-year-old girls: results from weighted Quantile sum regression. Environ. Int. 136, 105424.
Darbre, P.D., 2018. Overview of air pollution and endocrine disorders. Int. J. Gen. Med. 11, 191–207.
De Falco, M., Forte, M., Laforgia, V., 2015. Estrogenic and anti-androgenic endocrine disrupting chemicals and their impact on the male reproductive system. Front Env Sci-Switz 3.
Dewalque, L., Pirard, C., Charlier, C., 2014. Measurement of urinary biomarkers of parabens, benzophenone-3, and phthalates in a Belgian population. BioMed Res. Int. 2014, 649314.
Fang, H.Q., Wang, J., Lynch, R.A., 2017. Migration of di(2-ethylhexyl)phthalate (DEHP) and di-n-butylphthalate (DBP) from polypropylene food containers. Food Control 73, 1298–1302.
Frederiksen, H., Skakkebaek, N.E., Andersson, A.M., 2007. Metabolism of phthalates in humans. Mol. Nutr. Food Res. 51, 899–911.
Gao, D.W., Wen, Z.D., 2016. Phthalate esters in the environment: a critical review of their occurrence, biodegradation, and removal during wastewater treatment processes. Sci. Total Environ. 541, 986–1001.
Gao, C.J., Wang, F., Shen, H.M., Kannan, K., Guo, Y., 2020. Feminine hygiene products-A neglected source of phthalate exposure in women. Environ. Sci. Technol. 54, 930–937.
Giovanoulis, G., Bui, T., Xu, F., Papadopoulou, E., Padilla-Sanchez, J.A., Covaci, A., Haug, L.S., Cousins, A.P., Magner, J., Cousins, I.T., de Wit, C.A., 2018. Multi-pathway human exposure assessment of phthalate esters and DINCH. Environ. Int. 112, 115–126.
Giuliani, A., Zuccarini, M., Cichelli, A., Khan, H., Reale, M., 2020. Critical review on the presence of phthalates in food and evidence of their biological impact. Int. J. Environ. Res. Publ. Health 17.
Gonsioroski, A., Mourikes, V.E., Flaws, J.A., 2020. Endocrine disruptors in water and their effects on the reproductive system. Int. J. Mol. Sci. 21.
Goodman, M., Lakind, J.S., Mattison, D.R., 2014. Do phthalates act as obesogens in humans? A systematic review of the epidemiological literature. Crit. Rev. Toxicol. 44, 151–175.
Grun, F., Blumberg, B., 2009. Endocrine disrupters as obesogens. Mol. Cell. Endocrinol. 304, 19–29.
Haines, D.A., Saravanabhavan, G., Werry, K., Khoury, C., 2017. An overview of human biomonitoring of environmental chemicals in the Canadian Health Measures Survey: 2007-2019. Int. J. Hyg Environ. Health 220, 13–28.
Hammel, S.C., Levasseur, J.L., Hoffman, K., Phillips, A.L., Lorenzo, A.M., Calafat, A.M., Webster, T.F., Stapleton, H.M., 2019. Children's exposure to phthalates and non-phthalate plasticizers in the home: the TESIE study. Environ. Int. 132, 105061.
Hartmann, C., Uhl, M., Weiss, S., Koch, H.M., Scharf, S., Konig, J., 2015. Human biomonitoring of phthalate exposure in Austrian children and adults and cumulative risk assessment. Int. J. Hyg Environ. Health 218, 489–499.
Hoppin, J.A., Jaramillo, R., London, S.J., Bertelsen, R.J., Salo, P.M., Sandler, D.P., Zeldin, D.C., 2013. Phthalate exposure and allergy in the U.S. population: results from NHANES 2005-2006. Environ. Health Perspect. 121, 1129–1134.
Huang, P.C., Tsai, C.H., Liang, W.Y., Li, S.S., Pan, W.H., Chiang, H.C., 2015. Age and gender differences in urinary levels of eleven phthalate metabolites in general Taiwanese population after a DEHP episode. PLoS One 10, e0133782.
Jaimes, R., Swiercz, A., Sherman, M., Muselimyan, N., Marvar, P.J., Posnack, N.G., 2017. Plastics and cardiovascular health: phthalates may disrupt heart rate variability and cardiovascular reactivity. Am J Physiol-Heart C 313, H1044–H1053.
Johns, L.E., Cooper, G.S., Galizia, A., Meeker, J.D., 2015. Exposure assessment issues in epidemiology studies of phthalates. Environ. Int. 85, 27–39.
Kamrin, M.A., 2009. Phthalate risks, phthalate regulation, and public health: a review. J. Toxicol. Environ. Health B Crit. Rev. 12, 157–174.
Kato, K., Silva, M.J., Needham, L.L., Calafat, A.M., 2005. Determination of 16 phthalate metabolites in urine using automated sample preparation and on-line preconcentration/high-performance liquid chromatography/tandem mass spectrometry. Anal. Chem. 77, 2985–2991.
Ko, N.Y., Lo, Y.C., Huang, P.C., Huang, Y.C., Chang, J.L., Huang, H.B., 2019. Changes in insulin resistance mediate the associations between phthalate exposure and metabolic syndrome. Environ. Res. 175, 434–441.
Koch, H.M., Christensen, K.L., Harth, V., Lorber, M., Bruning, T., 2012. Di-n-butyl phthalate (DnBP) and diisobutyl phthalate (DiBP) metabolism in a human volunteer after single oral doses. Arch. Toxicol. 86, 1829–1839.
Koch, H.M., Lorber, M., Christensen, K.L., Palmke, C., Koslitz, S., Bruning, T., 2013. Identifying sources of phthalate exposure with human biomonitoring: results of a 48h fasting study with urine collection and personal activity patterns. Int. J. Hyg Environ. Health 216, 672–681.
Lange, R., Apel, P., Rousselle, C., Charles, S., Sissoko, F., Kolossa-Gehring, M., Ougier, E., 2021. The European Human Biomonitoring Initiative (HBM4EU): human biomonitoring guidance values for selected phthalates and a substitute plasticizer. Int. J. Hyg Environ. Health 234, 113722.
Larsson, K., Lindh, C.H., Jonsson, B.A., Giovanoulis, G., Bibi, M., Bottai, M., Bergstrom, A., Berglund, M., 2017. Phthalates, non-phthalate plasticizers and bisphenols in Swedish preschool dust in relation to children's exposure. Environ. Int. 102, 114–124.
Lee, I., Alakeel, R., Kim, S., Al-Sheikh, Y.A., Al-Mandeel, H., Alyousef, A.A., Kho, Y., Choi, K., 2019. Urinary phthalate metabolites among children in Saudi Arabia: occurrences, risks, and their association with oxidative stress markers. Sci. Total Environ. 654, 1350–1357.
Lee, I., Park, Y.J., Kim, M.J., Kim, S., Choi, S., Park, J., Cho, Y.H., Hong, S., Yoo, J., Park, H., Cheon, G.J., Choi, K., Moon, M.K., 2021. Associations of urinary concentrations of phthalate metabolites, bisphenol A, and parabens with obesity and diabetes mellitus in a Korean adult population: Korean National Environmental Health Survey (KoNEHS) 2015-2017. Environ. Int. 146.
Lehner, K., Santarelli, F., Vasold, R., Konig, B., Landthaler, M., Baumler, W., 2011. Black tattoo inks are a source of problematic substances such as dibutyl phthalate. Contact Dermatitis 65, 231–238.
Li, H.L., Ma, W.L., Liu, L.Y., Zhang, Z., Sverko, E., Zhang, Z.F., Song, W.W., Sun, Y., Li, Y. F., 2019. Phthalates in infant cotton clothing: occurrence and implications for human exposure. Sci. Total Environ. 683, 109–115.
Liao, K.W., Chang, W.H., Chou, W.C., Huang, H.B., Waits, A., Chen, P.C., Huang, P.C., 2021. Human biomonitoring reference values and characteristics of Phthalate exposure in the general population of Taiwan: taiwan Environmental Survey for Toxicants 2013-2016. Int. J. Hyg Environ. Health 235, 113769.
Oulhote, Y., Lanphear, B., Braun, J.M., Webster, G.M., Arbuckle, T.E., Etzel, T., Forget-Dubois, N., Seguin, J.R., Bouchard, M.F., MacFarlane, A., Ouellet, E., Fraser, W., Muckle, G., 2020. Gestational exposures to phthalates and folic acid, and autistic traits in Canadian children. Environ. Health Perspect. 128, 27004.

Pearson, A., van den Beuken, J., 2017. Occurrence and risk characterisation of migration of packaging chemicals in New Zealand foods. Ministry for Primary Industries (MPI). Technical Paper No: 2017/61.

Radke, E.G., Braun, J.M., Meeker, J.D., Cooper, G.S., 2018. Phthalate exposure and male reproductive outcomes: a systematic review of the human epidemiological evidence. Environ. Int. 121, 764–793.

Radke, E.G., Galizia, A., Thayer, K.A., Cooper, G.S., 2019. Phthalate exposure and metabolic effects: a systematic review of the human epidemiological evidence. Environ. Int. 132, 104768.

Ribeiro, C.M., Beserra, B.T.S., Silva, N.G., Lima, C.L., Rocha, P.R.S., Coelho, M.S., Neves, F.A.R., Amato, A.A., 2020. Exposure to endocrine-disrupting chemicals and anthropometric measures of obesity: a systematic review and meta-analysis. BMJ Open 10, e033509.

Rocha, B.A., Asimakopoulos, A.G., Barbosa Jr., F., Kannan, K., 2017. Urinary concentrations of 25 phthalate metabolites in Brazilian children and their association with oxidative DNA damage. Sci. Total Environ. 586, 152–162.

Rudel, R.A., Gray, J.M., Engel, C.L., Rawsthorne, T.W., Dodson, R.E., Ackerman, J.M., Rizzo, J., Nudelman, J.L., Brody, J.G., 2011. Food packaging and bisphenol A and bis (2-ethyhexyl) phthalate exposure: findings from a dietary intervention. Environ. Health Perspect. 119, 914–920.

Schwedler, G., Seiwert, M., Fiddicke, U., Issleb, S., Holzer, J., Nendza, J., Wilhelm, M., Wittsiepe, J., Koch, H.M., Schindler, B.K., Goen, T., Hildebrand, J., Joas, R., Joas, A., Casteleyn, L., Angerer, J., Castano, A., Esteban, M., Schoeters, G., Den Hond, E., Sepai, O., Exley, K., Bloemen, L., Knudsen, L.E., Kolossa-Gehring, M., 2017. Human biomonitoring pilot study DEMOCOPHES in Germany: contribution to a harmonized European approach. Int. J. Hyg Environ. Health 220, 686–696.

Schwedler, G., Rucic, E., Lange, R., Conrad, A., Koch, H.M., Palmke, C., Bruning, T., Schulz, C., Schmied-Tobies, M.I.H., Daniels, A., Kolossa-Gehring, M., 2020. Phthalate metabolites in urine of children and adolescents in Germany. Human biomonitoring results of the German Environmental Survey GerES V, 2014-2017. Int. J. Hyg Environ. Health 225, 113444.

Silva, M.J., Barr, D.B., Reidy, J.A., Malek, N.A., Hodge, C.C., Caudill, S.P., Brock, J.W., Needham, L.L., Calafat, A.M., 2004. Urinary levels of seven phthalate metabolites in the U.S. Population from the national health and nutrition examination survey (NHANES) 1999-2000. Environ. Health Perspect. 112 (3), 331–338.

Tang, Z., Chai, M., Wang, Y., Cheng, J., 2020. Phthalates in preschool children's clothing manufactured in seven Asian countries: occurrence, profiles and potential health risks. J. Hazard Mater. 387, 121681.

Varshavsky, J.R., Morello-Frosch, R., Woodruff, T.J., Zota, A.R., 2018. Dietary sources of cumulative phthalates exposure among the U.S. general population in NHANES 2005-2014. Environ. Int. 115, 417–429.

Wang, B., Wang, H., Zhou, W., Chen, Y., Zhou, Y., Jiang, Q., 2015. Urinary excretion of phthalate metabolites in school children of China: implication for cumulative risk assessment of phthalate exposure. Environ. Sci. Technol. 49, 1120–1129.

Wang, Y., Zhu, H., Kannan, K., 2019. A review of biomonitoring of phthalate exposures. Toxics 7.

Xie, F., Chen, X., Weng, S., Xia, T., Sun, X., Luo, T., Li, P., 2019. Effects of two environmental endocrine disruptors di-n-butyl phthalate (DBP) and mono-n-butyl phthalate (MBP) on human sperm functions in vitro. Reprod. Toxicol. 83, 1–7.

Zhang, S.H., Shen, Y.X., Li, L., Fan, T.T., Wang, Y., Wei, N., 2018. Phthalate exposure and high blood pressure in adults: a cross-sectional study in China. Environ. Sci. Pollut. Res. Int. 25, 15934–15942.

Zhang, Y., Huang, B., Sabel, C.E., Thomsen, M., Gao, X., Zhong, M., Chen, Z., Feng, P., 2019. Oral intake exposure to phthalates in vegetables produced in plastic greenhouses and its health burden in Shaanxi province, China. Sci. Total Environ. 696, 133921.

Zhou, S.Y., Han, M., Ren, Y.L., Yang, X., Duan, L.J., Zeng, Y., Li, J.Q., 2020. Dibutyl phthalate aggravated asthma-like symptoms through oxidative stress and increasing calcitonin gene-related peptide release. Ecotoxicol. Environ. Saf. 199.

Zota, A.R., Woodruff, T.J., 2014. Changing trends in phthalate exposures: zota and Woodruff respond. Environ. Health Perspect. 122, A264–A265.

't Mannetje, A., Coakley, J., Douwes, J., 2018. Report on the Biological Monitoring of Selected Chemicals of Concern Results of the New Zealand Biological Monitoring Programme, 2014-2016. Centre for Public Health Research Massey University, Wellington, New Zealand. Technical report number 2017-1. http://publichealth.massey.ac.nz/assets/Uploads/SOCs-Report-FINAL-06032018.pdf.

International Journal of Hygiene and Environmental Health 238 (2021) 113851

Contents lists available at ScienceDirect

International Journal of Hygiene and Environmental Health

journal homepage: www.elsevier.com/locate/ijheh

Low SARS-CoV-2 infection rates and high vaccine-induced immunity among German healthcare workers at the end of the third wave of the COVID-19 pandemic

Thomas Theo Brehm [a,b], Michelle Thompson [a], Felix Ullrich [a], Dorothee Schwinge [a], Marylyn M. Addo [a,b], Anthea Spier [c], Johannes K. Knobloch [b,c], Martin Aepfelbacher [c], Ansgar W. Lohse [a,b], Marc Lütgehetmann [b,c,1], Julian Schulze zur Wiesch [a,b,1,*]

[a] I. Department of Internal Medicine, University Medical Center Hamburg-Eppendorf, Martinistraße 52, 20246, Hamburg, Germany
[b] German Center for Infection Research (DZIF), Partner Site Hamburg-Lübeck-Borstel-Riems, Germany
[c] Institute of Medical Microbiology, Virology and Hygiene, University Medical Center Hamburg-Eppendorf, Martinistraße 52, 20246, Hamburg, Germany

ARTICLE INFO

Keywords:
SARS-CoV-2
COVID-19
Healthcare workers
Seroprevalence
Vaccination
Immunity
Antibody titers

ABSTRACT

In this longitudinal cohort study, we assessed the severe acute respiratory syndrome coronavirus type 2 (SARS-CoV-2) seroconversion rates and analyzed the coronavirus disease 2019 (COVID-19) vaccine-induced immunity of 872 hospital workers at the University Medical Center Hamburg-Eppendorf between May 11 and May 31, 2021. The overall seroprevalence of anti–NC–SARS-CoV-2 antibodies was 4.7% (n = 41), indicating low SARS-CoV-2 infection rates and persistent effectiveness of hospital-wide infection control interventions during the second and third wave of the pandemic. In total, 92.7% (n = 808) out of the entire study cohort, 98.2% (n = 325) of those who had been vaccinated once and all 393 individuals who had been vaccinated twice had detectable anti-S1-RBD-SARS-CoV-2 antibody titers and no significant differences in vaccine-induced immune response were detected between male and female individuals and between different age groups. Vaccinated study participants with detectable anti–NC–SARS-CoV-2 antibody titers (n = 30) developed generally higher anti-S1-RBD-SARS-CoV-2 antibody titers compared to anti–NC–SARS-CoV-2 negative individuals (n = 694) (median titer: 7812 vs. 345 BAU/ml, $p < 0.0001$). Furthermore, study participants who received heterologous vaccination with AZD1222 followed by an mRNA vaccine showed markedly higher anti-S1-RBD-SARS-CoV-2 antibody titers than individuals who received two doses of an mRNA vaccine or two doses of AZD1222 (median titer: AZD1222/AZD1222: 1069 BAU/ml, mRNA/mRNA: 1388 BAU/ml, AZD1222/mRNA: 9450 BAU/ml; $p < 0.0001$). Our results indicate that infection control interventions were generally effective in preventing nosocomial transmission of SARS-CoV-2 and that COVID-19 vaccines can elicit strong humoral responses in the majority of a real-world cohort of hospital workers.

1. Introduction

We have previously reported the first results of our severe acute respiratory syndrome coronavirus type 2 (SARS-CoV-2) seroprevalence project and could demonstrate low anti-S1-SARS-CoV-2 seroprevalence in 1253 hospital workers at the University Medical Center Hamburg-Eppendorf during the first wave of the coronavirus disease 2019 (COVID-19) epidemic up until July 2020 (Brehm et al., 2021c). As the epidemic in Germany evolved, an exponential increase in COVID-19 cases occurred during a second wave in autumn 2020 with incidence peaks with a 7-day incidence of more than 200 per 100,000 inhabitants in December and January 2020 and again during a third wave which peaked in April 2021 with more than 150 per 100,00 inhabitants (Robert-Koch-Institut, 2021a). At our center, the majority of COVID-19 patients were hospitalized during the second and third waves of the pandemic (Brehm et al., 2021a). Various infection control interventions such as universal masking, visitor restrictions, universal reverse transcription polymerase chain reaction (RT-PCR) admission screening of

* Corresponding author. I. Department of Internal Medicine, University Medical Center Hamburg-Eppendorf, Martinistraße 52, 20246 Hamburg, Germany.
E-mail address: j.schulze-zur-wiesch@uke.de (J. Schulze zur Wiesch).
[1] contributed equally.

https://doi.org/10.1016/j.ijheh.2021.113851
Received 27 June 2021; Received in revised form 19 September 2021; Accepted 23 September 2021
Available online 25 September 2021

patients, and regular RT-PCR screening of asymptomatic healthcare workers (HCW) were rapidly implemented at our tertiary care center and repeatedly adapted throughout the epidemic. By June 2021, more than 150.000 SARS-CoV-2 RT-PCR tests were conducted among hospital employees, and a total of 111 infections were detected, the majority of which were classified as not work-related. However, it is not clear how many infections have been missed despite these screening efforts. Since both infection with SARS-CoV-2 and vaccination with the now licensed COVID-19 vaccines elicit antibodies directed against the receptor binding domain (RBD) of the viral spike protein (S) , we adapted our strategy to detect resolved infections by screening for antibodies directed against the viral nucleocapsid (NC), which are only present after natural infection. By June 2021, the European Medicines Agency (EMA) has granted conditional marketing authorizations for the two mRNA COVID-19 vaccines BNT162b2 (Comirnaty, Biontech/Pfizer) (EMA, 2021a), mRNA-1273 (Moderna/NIAID) (EMA, 2021b), and the viral vector-based vaccines AZD1222 (Vaxzevria, AstraZeneca) (EMA, 2021c), and Ad26.COV2.S (Janssen) (EMA, 2021d). The respective phase 3 trials reported high efficacy in priming neutralizing anti-spike-SARS-CoV-2 antibodies and preventing symptomatic SARS-CoV-2 infections after a single dose (AZD1222) (Sadoff et al., 2021) or two doses administered three (BNT162b2) (Polack et al., 2020), four (mRNA-1273) (Baden et al., 2021) or 12 weeks (AZD1222) (Voysey et al., 2021) apart. However, vaccine efficacy may differ in different populations, and vaccine regimens may vary depending on availability, national guidelines, and findings of post-marketing surveillance. Since the administration of AZD1222 was suspended in individuals below 60 years in Germany after the occurrence of vaccine-induced immune thrombotic thrombocytopenia in March 2021 (Greinacher et al., 2021; Schultz et al., 2021), heterologous booster vaccination with an mRNA vaccine was recommended in this group of vaccinees. As evidence on the quality and quantity of short and mid-term immune responses to these different COVID-19 vaccine regimens is currently limited, real-world studies are urgently needed to develop rational and efficient vaccination schedules for the long-term protection of both hospital employees and their patients. As part of our seroprevalence project, we performed another study visit in May 2021 to determine the number of hospital employees who were knowingly or unknowingly infected with SARS-CoV-2 as well as to assess the vaccine-induced humoral immunity to different COVID-19 vaccine regimens.

2. Materials and methods

2.1. Study design

Participants of our ongoing SARS-CoV-2 seroprevalence study were recruited by informing employees of the University Medical Center Hamburg-Eppendorf via email about the possibility to participate at the current study visit and written informed consent was obtained by all study participants before recruitment. For the present study visit, participants were invited to provide a serum sample between May 11 and May 31, 2021. Demographic and occupational characteristics, prior SARS-CoV-2 infections, and vaccination status were assessed using an online REDcap electronic data capture tool specifically designed for the present study. The two licensed mRNA vaccines, BNT162b2 and mRNA-1273, were subsequently subsumed to one category. The study protocol was reviewed and approved by the Ethics Committee of the Medical Council of Hamburg (PV 7298).

2.2. Serology

The humoral immune response to COVID-19 vaccination and/or SARS-CoV-2 infection was assessed by the quantitative anti-S1-RBD-SARS-CoV-2 assay (Elecsys Anti-SARS-CoV-2 Spike, Roche, Mannheim, Germany; cut off 0.8 U/ml), which RB has a reported sensitivity of 99.8% and specificity of 100% (Roche 2021a). To differentiate between past infection and vaccine-induced immune response, the qualitative anti–NC–SARS-CoV-2 Ig assay was used (Elecsys Anti-SARS-CoV-2, Roche, Mannheim Germany; cut off ≥1 COI/ml). The reported sensitivity (in patients ≥14 days after infection) and specificity of this assay are 99.5% and 99.8%, respectively (Roche 2021b). Both electrochemiluminescence immunoassays (Cobas e411, Roche; Mannheim, Germany) use a double-antigen sandwich assay format that detects IgA, IgM, and IgG. Samples with titers above 250 U/ml were manually diluted 1:100 in dilution buffer according to the manufacturer's recommendations to increase the linear range to 25000 U/ml. A mathematical transposition of Elecsys anti-S1-RBD-SARS-CoV-2 specific U/ml to the World Health Organization (WHO) standard BAU/ml was performed using the following equation: U/ml = 0.972 x BAU/ml (Resman Rus et al., 2021). It has been previously demonstrated that an anti-S1-RBD-SARS-CoV-2 antibody concentration of more than 133 BAU/ml predicts the presence of neutralizing antibodies after natural infection (Resman Rus et al., 2021). It may thus be a potential surrogate for high protection from COVID-19 after vaccination, so we specifically calculated the percentage of different subgroups of our study cohort with antibody titers above this threshold.

2.3. Statistical analyses

A two-tailed Mann–Whitney *U* test was used to analyze the median antibody titers between subgroups. In addition, linear regression analysis was performed to assess the correlation between age and antibody titers. P-values lower than 0.05 were considered statistically significant. Statistical analyses were performed using GraphPad Prism, version 9 for macOS (GraphPad Software, La Jolla, California, USA).

3. Results

3.1. Characterization of the study population

A total of 872 individuals participated in the current study visit, representing around 8% of all employees of the University Medical Center Hamburg-Eppendorf. The median age was 38 years (IQR 30–49 years), and 78.0% (n = 680) of the study population were women (Table 1). The majority of study participants were HCW (81.7%, n = 712) directly involved in patient care at different departments of our tertiary care center: 36.0% were nurses (n = 314), 20.1% physicians (n = 175), 10.1% medical technicians (n = 88) and 15.5% had other professions (n = 135). Information on prior SARS-CoV-2 infections and

Table 1
Characterization of the study cohort.

	n	%
Study participants, total	872	100
Age*		
Median (years)	38	
IQR (years)	30–49	
Not provided	11	1.3
Sex		
female	680	78.0
male	183	21.0
diverse	9	1.0
Healthcare worker		
yes	712	81.7
no	149	17.1
unknown	11	1.3
Profession		
nurse	314	36.0
physician	175	20.1
medical technician	88	10.1
other healthcare worker	135	15.5
non-healthcare worker	149	17.1
unknown	11	1.3

vaccination status was provided by the majority of study participants (90.6%, n = 790) (Supplemental Table 1). Of those, 41.9% (n = 331) had received one dose of a COVID-19 vaccine (AZD1222: n = 267, mRNA: n = 64). Another 49.7% (n = 393) had received two COVID-19 vaccine doses (AZD1222/AZD1222: n = 25; AZD1222/mRNA: n = 106; mRNA/mRNA: n = 261) at the time of the study visit. Thirty-one individuals (3.9%) reported that they had been diagnosed with SARS-CoV-2 in the past.

3.2. Serological results

At the current study visit, 4.7% (n = 41) of the study population had detectable anti-NC-antibodies indicating prior infection with SARS-CoV-2. Of those, 31 (76%) had been knowingly infected with SARS-CoV-2 in the past, while 12 (29%) did not report a previous infection. In total, 92.7% (n = 808) out of the entire study cohort, 98.2% (n = 325) of those who had been vaccinated once and all 393 individuals who had been vaccinated twice had detectable anti-S1-RBD-SARS-CoV-2 antibody titers. Among all vaccinated study participants, those with detectable anti–NC–SARS-CoV-2 antibody titers (n = 30) developed generally higher anti-S1-RBD-SARS-CoV-2 antibody titers compared to anti–NC–SARS-CoV-2 negative individuals (n = 694) (median titer: 7812 vs. 345 BAU/ml, p < 0.0001). Among individuals who had received one vaccine dose with AZD1222, those who were anti–NC–SARS-CoV-2 positive (median titer: 7797 BAU/ml) had significantly higher anti-S1-RBD-SARS-CoV-2 antibody titers than those who were anti–NC–SARS-CoV-2 negative (median titer: 61 BAU/ml; p < 0,0001) (Fig. 1). Likewise, anti-S1-RBD-SARS-CoV-2 antibody titers were higher amongst individuals with detectable anti–NC–SARS-CoV-2 antibodies compared to those without detectable anti–NC–SARS-CoV-2 antibodies both in the subgroup of individuals who had received one dose of an mRNA vaccine (median titer: 15269 BAU/ml vs 109 BAU/ml; p < 0.0001) and the subgroup that had received two doses of an mRNA vaccine (median titer; 4725 BAU/ml vs 1333 BAU/ml; p = 0.0003). In the subgroups with other vaccination regimens (AZD122/AZD122, AZD122/mRNA), the number of individuals with detectable anti–NC–SARS-CoV-2 antibodies was too small for detailed statistical analysis. Since the interval between the first and the second vaccine at our center was generally six weeks for mRNA vaccines and 12 weeks for AZD1222, the duration after the first vaccine dose at the time of the study visit was generally longer amongst study participants who had received one dose of AZD1222 (median duration: AZD1222: 80 days, mRNA: 28 days, p < 0.0001), but anti-S1-RBD-SARS-CoV-2 antibody titers were higher among individuals who had received an mRNA vaccine (median titer: AZD1222: 63 BAU/ml, mRNA: 122 BAU/ml; p = 0.005) (Fig. 2A and B). Among study participants who had already received two vaccine doses, the duration after the second dose was markedly longer amongst those who had received two doses of an mRNA vaccine since those vaccines were licensed and available earlier compared to AZD1222 (median duration: AZD1222/AZD1222: 9 days, mRNA/mRNA: 106 days, AZD1222/mRNA: 9 days; p < 0.001) (Fig. 2 C and 2D). Of note, the study participants who received vaccination with AZD1222 followed by an mRNA vaccine showed significantly higher anti-S1-RBD-SARS-CoV-2 antibody titers than individuals who had received two doses of an mRNA vaccine or two doses of AZD1222 (median titer: AZD1222/AZD1222: 1069 BAU/ml, mRNA/mRNA: 1388 BAU/ml, AZD1222/mRNA: 9450 BAU/ml; p < 0.0001). Anti-S1-RBD-SARS-CoV-2 antibody concentrations above the cut-off of 133 BAU/ml, which has been shown to predict the presence of neutralizing antibodies after natural SARS-CoV-2 infections (Resman Rus et al., 2021), were detected in 28.7% (n = 95) of those who received one vaccine dose and 93.6% (n = 368) who received two vaccine doses. COVID-19 vaccinees are generally regarded as fully vaccinated two weeks after the second vaccination (Keehner et al., 2021), at which time all but two study participants (99.3%, n = 287) had antibody titers above 133 BAU/ml (Supplemental Fig. 1. Linear regression analysis did not demonstrate a significant correlation between age and anti-S1-RBD-SARS-CoV-2 titers amongst study participants who had received one (R^2 = 0.02) or two (R^2 = 0.001) vaccine doses (Supplemental Fig. 2). Median anti-S1-RBD-SARS-CoV-2 antibody titers did not significantly differ between male and female study participants after the first (median titer: 52 BAU/ml vs. 74 BAU/ml; p = 0.07) and the second (1456 BAU/ml vs. 1705 BAU/ml; P = 0.98) vaccine dose.

4. Discussion

Here we describe the prevalence and titers of anti-S1-RBD-SARS-

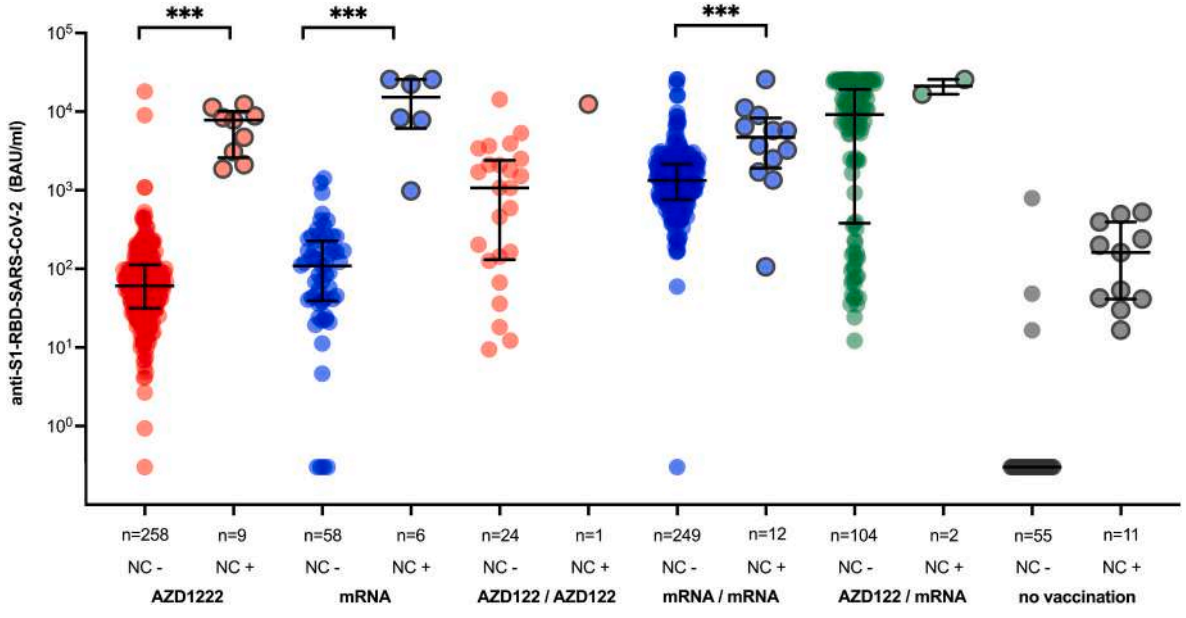

Fig. 1. Anti-S1-RBD-SARS-CoV-2 antibody titers based on infection status and different vaccination regimens.
Legend: Anti-S1-RBD-SARS-CoV-2 antibody titers on a logarithmic scale among study participants with (NC+) and without (NC-) detectable anti–NC–SARS-CoV-2 based on their vaccination status. Individual data points are shown as an aligned dot plot with lines showing the median with the interquartile range. Significant differences were determined by the two-tailed Mann–Whitney *U* test (***P < 0.001; **P < 0.01; *P < 0.05).

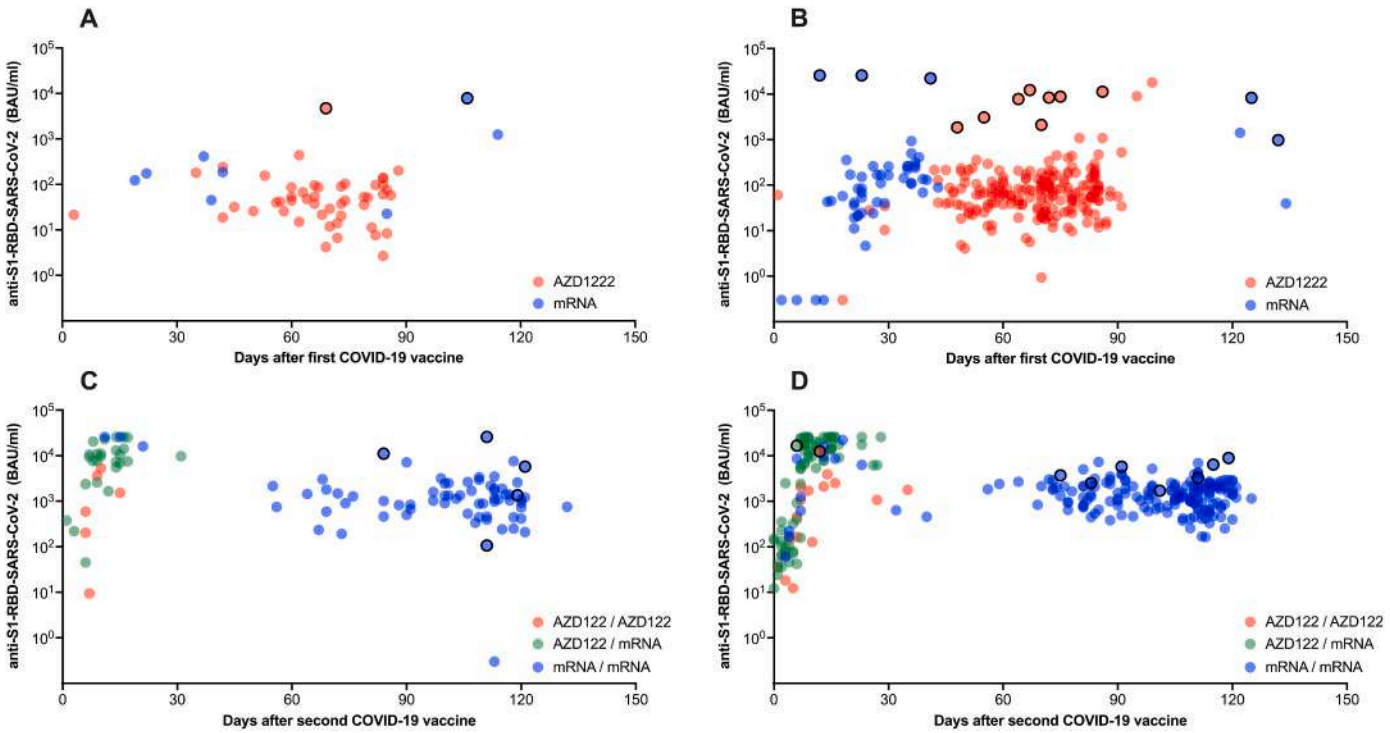

Fig. 2. Anti-S1-RBD-SARS-CoV-2 antibody titers based on sex, vaccination status, and duration after vaccination.
Legend: Anti-S1-RBD-SARS-CoV-2 antibody titers on a logarithmic scale among male (A, C) and female (B, D) study participants with (dots with black edging) and without (dots without black edging) detectable anti–NC–SARS-CoV-2 plotted against the duration after administration after the first (A, B) and second (B, C) COVID-19 vaccine dose.

CoV-2 and anti–NC–SARS-CoV-2 antibodies in 872 employees of a German tertiary care center in May 2021 based on their vaccination and infection status.

We have previously reported an anti-S1-SARS-CoV-2 seroprevalence of 1.8% among a cohort of hospital workers at our center by the end of the first wave in early July 2020 (Brehm et al., 2021c). One of the main findings of the current study visit was that only 4.7% of the hospital employees had detectable anti–NC–SARS-CoV-2 antibodies, indicating persistently low nosocomial SARS-CoV-2 transmission rates throughout the second and third wave of the COVID-19 epidemic. Since the official rate of recovered COVID-19 patients among inhabitants of the city-state of Hamburg was 4.2% in June 2021 and further unidentified cases have to be assumed, the infection rate among hospital employees appears to be not increased compared to the general population. The fact that only a few infections in hospital workers occurred during the second and third wave of the COVID-19 pandemic despite a large number of patients treated at our center (Brehm et al., 2021a) indicate a persistent effectiveness of the progressive infection control interventions that included universal RT-PCR admission screening of patients and regular RT-PCR screening of HCW. These findings are reassuring since, despite increasing vaccination coverage, both hospital workers and vulnerable patient groups will have to be protected from nosocomial SARS-CoV-2 transmission in the upcoming months.

Another important finding of our study is the fact that the vast majority of our study cohort developed anti-S1-RBD-SARS-CoV-2 antibody titers after COVID-19 vaccination that have been shown to correlate with neutralizing activity after natural infection (Resman Rus et al., 2021) after the second vaccine dose irrespective of age, sex, and respective vaccine regimen. While these observations are reassuring, the transferability of humoral immune responses in patients after natural infection to individuals after COVID-19 vaccination is limited and a reliable absolute antibody threshold for individual protection from COVID-19 may not exist. Importantly, infections may occur even in the presence of neutralizing antibodies (Brehm et al., 2021b). However, population-based correlates for immunity appear attainable and need to be identified by large prospective studies in the future (Jin et al., 2021). All study participants obtained their serological results as well as the results of the entire study cohort and were given a chance to discuss these findings with the scientific study team. We feel that these interactions provided reassurance to the hospital employees about the generally high potency of COVID-19 vaccines on the one hand and the limited predictive value of individual antibody titers for the level of protection from SARS-CoV-2 on the other hand.

Strikingly, study participants receiving a heterologous prime-boost vaccination regimen with AZD1222 vaccine followed by an mRNA vaccine developed significantly higher antibody titers than individuals receiving homologous vaccination regimens. This finding adds to preliminary data indicating that heterologous vaccination regimens may be more immunogenic than homologous vaccine regimens and have comparable reactogenicity profiles (Hillus et al., 2021; Schmidt et al., 2021; Borobia et al., 2021). While these results still need further confirmation in larger cohorts, they may have implications for future vaccine strategies against COVID-19 and other pathogens.

It has been previously demonstrated that the humoral immune response to a single COVID-19 vaccine dose in individuals primed by natural infection may provide antibody titers at least comparable to those found in non-infected individuals after the second vaccine dose (Blain et al., 2021; Havervall et al., 2021; Krammer et al., 2021; Reynolds et al., 2021; Saadat et al., 2021). In our study cohort, unvaccinated participants with detectable anti–NC–SARS-CoV-2 antibodies indicating prior infection had lower anti-S1-RBD-SARS-CoV-2 antibody titers compared to anti–NC–SARS-CoV-2 negative individuals who were vaccinated twice, indicating that booster vaccination is indeed needed for those recovered patients. However, anti–NC–SARS-CoV-2 positive individuals developed markedly higher anti-S1-RBD-SARS-CoV-2 antibody titers after both one and two vaccine doses compared to anti–NC–SARS-CoV-2 negative individuals regardless of the vaccine regimen. While Germany's official public health institute currently

recommends the administration of only a single dose of any of the COVID-19 vaccines for individuals with prior SARS-CoV-2 infection (Robert-Koch-Institut, 2021b), the duration of protection as well as the optimal timing of booster doses and selection of the most effective vaccine regimen yet need to be determined.

Our study has important limitations, most of which are inherent to the cross-sectional character of our study. First, we only provide vaccine-induced antibody titers for individual time points and are not able to assess longitudinal data or serological kinetics. Also, since different COVID-19 vaccines were licensed and distributed to hospital workers at different points in time, we are not able to compare immune responses elicited by different vaccines at the same post-vaccination interval. Second, while our longitudinal study was initiated before COVID-19 vaccines could be anticipated, and study participants were recruited across all age groups and occupations, we did not recruit a strictly representative sample of hospital employees at our tertiary care center, which limits the overall generalizability of results. Study participants with a positive attitude towards COVID-19 vaccines in general and those who have been vaccinated in particular may be more likely to participate in our study which may represent an important selection bias. Third, anti–NC–SARS-CoV-2 titers after infection with SARS-CoV-2 wane over time (Van Elslande et al., 2021) and may theoretically not be detectable some months after SARS-CoV-2 infection in some individuals, especially in those with mild or asymptomatic disease course. However, healthcare workers at our institution were regularly tested for SARS-CoV-2 infection bi-weekly RT-PCR so it is rather unlikely that a substantial number of infections were not detected. Fourth, while underlying comorbidities and immunocompromising medications may have an impact on humoral immune responses to COVID-19 vaccination and SARS-CoV-2 infection, we do not have any information on the immune status of the study participants. Fifth, the number of study participants, especially those with anti–NC–SARS-CoV-2 antibodies, was relatively small in some subgroups, and our findings need to be confirmed by larger cohort studies.

While the COVID-19 pandemic evolves and the overall vaccination coverage increases, prospective longitudinal studies will be necessary to get a better understanding of the kinetics humoral and cellular immune responses to different COVID-19 vaccines, to identify correlates of protection against SARS-CoV-2, and to determine the duration and quality of infection- and vaccine-induced immunity. Considering the increasing occurrence of variants of concern, it will be important to determine how different vaccination regimens may influence protection against COVID-19.

5. Conclusion

At our tertiary care center, the number of SARS-CoV-2 infections among exposed hospital employees appears to have remained low throughout the second and third waves of the pandemic. Anti-S1-RBD-SARS-CoV-2 antibody titers show a high rate of strong humoral response to COVID-19 vaccines regardless of age, sex, and vaccine regimens and indicate a high level of protection from SARS-CoV-2 infections in our real-world cohort. Significantly higher anti-S1-RBD-SARS-CoV-2 antibody titers among individuals receiving heterologous prime-boost vaccination regimens with AZD1222 followed by an mRNA vaccine may suggest even higher efficacy than homologous regimens.

Declarations of competing interest

None.

Acknowledgments

We thank Nils Dittberner, Sabrina Kreβ and Martina Fahl for excellent technical assistance. We thank all study participants and departments of the University Medical Center Hamburg-Eppendorf for their active participation in the study.

Appendix A. Supplementary data

Supplementary data to this article can be found online at https://doi.org/10.1016/j.ijheh.2021.113851.

References

Baden, L.R., El Sahly, H.M., Essink, B., Kotloff, K., Frey, S., Novak, R., Diemert, D., Spector, S.A., Rouphael, N., Creech, C.B., McGettigan, J., Khetan, S., Segall, N., Solis, J., Brosz, A., Fierro, C., Schwartz, H., Neuzil, K., Corey, L., Gilbert, P., Janes, H., Follmann, D., Marovich, M., Mascola, J., Polakowski, L., Ledgerwood, J., Graham, B.S., Bennett, H., Pajon, R., Knightly, C., Leav, B., Deng, W., Zhou, H., Han, S., Ivarsson, M., Miller, J., Zaks, T., 2021. Efficacy and safety of the mRNA-1273 SARS-CoV-2 vaccine. N. Engl. J. Med. 384, 403–416.

Blain, H., Tuaillon, E., Gamon, L., Pisoni, A., Miot, S., Picot, M.C., Bousquet, J., 2021. Spike antibody levels of nursing home residents with or without prior COVID-19 3 Weeks after a single BNT162b2 vaccine dose. Jama.

Borobia, A.M., Carcas, A.J., Pérez Olmeda, M.T., Castaño, L., Jesús Bertrán, M., García-Pérez, J., Campins, M., Portolés, A., Gonzalez-Perez, M., García Morales, M.T., Arana, E., Aldea Novo, M., Díez-Fuertes, F., Fuentes-Camps, I., Ascaso, A., Lora, D., Imaz-Ayo, N., Baron-Mira, L.E., Agustí, A., Pérez-Ingidua, C., Gómez de la Cámara, A., Arribas, J.R., Ochando, J., Alcamí Pertejo, J., Belda-Iniesta, C., Frías, J., CombiVacS Study Group, Reactogenicity and Immunogenicity of BNT162b2 in Subjects Having Received a First Dose of ChAdOx1s: Initial Results of a Randomised, Adaptive, Phase 2 Trial (CombiVacS), https://doi.org/10.2139/ssrn.3854768. (accessed 26.06.2021).

Brehm, T.T., Heyer, A., Roedl, K., Jarczak, D., Nierhaus, A., Nentwich, M.F., van der Meirschen, M., Schultze, A., Christner, M., Fiedler, W., Kröger, N., Huber, T.B., Klose, H., Sterneck, M., Jordan, S., Kreuels, B., Schmiedel, S., Addo, M.M., Huber, S., Lohse, A.W., Kluge, S., Schulze Zur Wiesch, J., 2021a. Patient characteristics and clinical course of COVID-19 patients treated at a German tertiary center during the first and second waves in the year 2020. J. Clin. Med. 10.

Brehm, T.T., Pfefferle, S., von Possel, R., Kobbe, R., Nörz, D., Schmiedel, S., Grundhoff, A., Olearo, F., Emmerich, P., Robitaille, A., Günther, T., Braun, P., Andersen, G., Knobloch, J.K., Addo, M.M., Lohse, A.W., Aepfelbacher, M., Fischer, N., Schulze Zur Wiesch, J., Lütgehetmann, M., 2021b. SARS-CoV-2 reinfection in a healthcare worker despite the presence of detectable neutralizing antibodies. Viruses 13.

Brehm, T.T., Schwinge, D., Lampalzer, S., Schlicker, V., Küchen, J., Thompson, M., Ullrich, F., Huber, S., Schmiedel, S., Addo, M.M., Lütgehetmann, M., Knobloch, J.K., Schulze Zur Wiesch, J., Lohse, A.W., 2021c. Seroprevalence of SARS-CoV-2 antibodies among hospital workers in a German tertiary care center: a sequential follow-up study. Int. J. Hyg Environ. Health 232, 113671.

EMA 2021a, https://www.ema.europa.eu/en/news/ema-recommends-first-covid-19-vaccine-authorisation-eu (accessed 26.06.2021).

EMA 2021b, https://www.ema.europa.eu/en/news/ema-recommends-covid-19-vaccine-moderna-authorisation-eu (accessed 26.06.2021).

EMA 2021c, https://www.ema.europa.eu/en/news/ema-recommends-covid-19-vaccine-astrazeneca-authorisation-eu (accessed 26.06.2021).

EMA 2021d, https://www.ema.europa.eu/en/news/ema-recommends-covid-19-vaccine-janssen-authorisation-eu (accessed 26.06.2021).

Greinacher, A., Thiele, T., Warkentin, T.E., Weisser, K., Kyrle, P.A., Eichinger, S., 2021. Thrombotic thrombocytopenia after ChAdOx1 nCov-19 vaccination. N. Engl. J. Med. 384, 2092–2101.

Havervall, S., Marking, U., Greilert-Norin, N., Ng, H., Salomonsson, A.-C., Hellström, C., Pin, E., Blom, K., Mangsbo, S., Phillipson, M., Klingström, J., Åberg, M., Hober, S., Nilsson, P., Thålin, C., 2021. Antibody responses after a single dose of ChAdOx1 nCoV-19 vaccine in healthcare workers previously infected with SARS-CoV-2. medRxiv, 2021.2005.2008.21256866.

Hillus, D., Schwarz, T., Tober-Lau, P., Hastor, H., Thibeault, C., Kasper, S., Helbig, E.T., Lippert, L.J., Tscheak, P., Schmidt, M.L., Riege, J., Solarek, A., Kalle, C.v., Dang-Heine, C., Kopankiewicz, P., Suttorp, N., Drosten, C., Bias, H., Seybold, J., Conrad, C., Steuer, D., Gläser, U., Sinnigen, A.-S., Rubisch, C., Olk, N., Hasler, L., Sanchez-Rezza, A., Kronenberg, P., Horn, A., Koch, W., Stubbemann, P., Gabelich, J.-A., Münn, F., Tesch, J., Mackeldanz, P., Bergfeld, L., Bleicker, T., Beheim-Schwarzbach, J.I., Hiller, A., Brumhard, S., Bardtke, L., Pohl, K., Wendisch, D., Georg, P., Treue, D., Briesemeister, D., Schlesinger, J., Hetey, A., Kegel, L., Richter, A., Al-Rim, B., Maeß, B., Behn, K., Lysi, M., Zvorc, S., Rönnefarth, M., Schmidt, S., Krannich, A., Schellenberger, I., Schwanitz, G., Schenkel, V., Bethke, N., Hülso, C., Dieckmann, S., Peiser, C., Kurth, F., Corman, V.M., Sander, L.E., 2021. Safety, reactogenicity, and immunogenicity of homologous and heterologous prime-boost immunisation with ChAdOx1-nCoV19 and BNT162b2: a prospective cohort study. medRxiv, 2021.2005.2019.21257334.

Jin, P., Li, J., Pan, H., Wu, Y., Zhu, F., 2021. Immunological surrogate endpoints of COVID-2019 vaccines: the evidence we have versus the evidence we need. Signal Transduct Target Ther 6, 48.

Keehner, J., Horton, L.E., Pfeffer, M.A., Longhurst, C.A., Schooley, R.T., Currier, J.S., Abeles, S.R., Torriani, F.J., 2021. SARS-CoV-2 infection after vaccination in health care workers in California. N. Engl. J. Med. 384, 1774–1775.

Krammer, F., Srivastava, K., Alshammary, H., Amoako, A.A., Awawda, M.H., Beach, K.F., Bermúdez-González, M.C., Bielak, D.A., Carreño, J.M., Chernet, R.L., Eaker, L.Q.,

Ferreri, E.D., Floda, D.L., Gleason, C.R., Hamburger, J.Z., Jiang, K., Kleiner, G., Jurczyszak, D., Matthews, J.C., Mendez, W.A., Nabeel, I., Mulder, L.C.F., Raskin, A. J., Russo, K.T., Salimbangon, A.T., Saksena, M., Shin, A.S., Singh, G., Sominsky, L.A., Stadlbauer, D., Wajnberg, A., Simon, V., 2021. Antibody responses in seropositive persons after a single dose of SARS-CoV-2 mRNA vaccine. N. Engl. J. Med. 384, 1372–1374.

Polack, F.P., Thomas, S.J., Kitchin, N., Absalon, J., Gurtman, A., Lockhart, S., Perez, J.L., Pérez Marc, G., Moreira, E.D., Zerbini, C., Bailey, R., Swanson, K.A., Roychoudhury, S., Koury, K., Li, P., Kalina, W.V., Cooper, D., Frenck Jr., R.W., Hammitt, L.L., Türeci, Ö., Nell, H., Schaefer, A., Ünal, S., Tresnan, D.B., Mather, S., Dormitzer, P.R., Şahin, U., Jansen, K.U., Gruber, W.C., 2020. Safety and efficacy of the BNT162b2 mRNA covid-19 vaccine. N. Engl. J. Med. 383, 2603–2615.

Resman Rus, K., Korva, M., Knap, N., Avšič Županc, T., Poljak, M., 2021. Performance of the rapid high-throughput automated electrochemiluminescence immunoassay targeting total antibodies to the SARS-CoV-2 spike protein receptor binding domain in comparison to the neutralization assay. J. Clin. Virol. 139, 104820.

Reynolds, C.J., Pade, C., Gibbons, J.M., Butler, D.K., Otter, A.D., Menacho, K., Fontana, M., Smit, A., Sackville-West, J.E., Cutino-Moguel, T., Maini, M.K., Chain, B., Noursadeghi, M., Brooks, T., Semper, A., Manisty, C., Treibel, T.A., Moon, J.C., Valdes, A.M., McKnight, Á., Altmann, D.M., Boyton, R., 2021. Prior SARS-CoV-2 infection rescues B and T cell responses to variants after first vaccine dose. Science.

Robert-Koch-Institut, 2021a. COVID-19-Dashboard. https://experience.arcgis.com/experience/478220a4c454480e823b17327b2bf1d4/page/page_1/. (Accessed 26 June 2021). accessed.

Robert-Koch-Institut, 2021b. Epidemiologisches Bulletin 17/2021. https://www.rki.de/DE/Content/Infekt/EpidBull/Archiv/2021/Ausgaben/16_21.pdf?_blob=publicationFile. (Accessed 26 June 2021). accessed.

Roche 2021a. https://diagnostics.roche.com/content/dam/diagnostics/Blueprint/en/pdf/cps/Elecsys-Anti-SARS-CoV-2-S-factsheet-SEPT-2020-2.pdf (accessed 18.09.2021).

Roche 2021b. https://diagnostics.roche.com/content/dam/diagnostics/Blueprint/en/pdf/cps/Elecsys-Anti-SARS-CoV-2-factsheet-2020-JUL.pdf (accessed 18.09.2021).

Saadat, S., Rikhtegaran Tehrani, Z., Logue, J., Newman, M., Frieman, M.B., Harris, A.D., Sajadi, M.M., 2021. Binding and neutralization antibody titers after a single vaccine dose in health care workers previously infected with SARS-CoV-2. Jama 325, 1467–1469.

Sadoff, J., Gray, G., Vandebosch, A., Cárdenas, V., Shukarev, G., Grinsztejn, B., Goepfert, P.A., Truyers, C., Fennema, H., Spiessens, B., Offergeld, K., Scheper, G., Taylor, K.L., Robb, M.L., Treanor, J., Barouch, D.H., Stoddard, J., Ryser, M.F., Marovich, M.A., Neuzil, K.M., Corey, L., Cauwenberghs, N., Tanner, T., Hardt, K., Ruiz-Guiñazú, J., Le Gars, M., Schuitemaker, H., Van Hoof, J., Struyf, F., Douoguih, M., 2021. Safety and efficacy of single-dose Ad26.COV2.S vaccine against covid-19. N. Engl. J. Med.

Schmidt, T., Klemis, V., Schub, D., Mihm, J., Hielscher, F., Marx, S., Abu-Omar, A., Schneitler, S., Becker, S.L., Gärtner, B.C., Sester, U., Sester, M., 2021. Immunogenicity and reactogenicity of a heterologous COVID-19 prime-boost vaccination compared with homologous vaccine regimens. medRxiv, 2021.2006.2013.21258859.

Schultz, N.H., Sørvoll, I.H., Michelsen, A.E., Munthe, L.A., Lund-Johansen, F., Ahlen, M. T., Wiedmann, M., Aamodt, A.H., Skattør, T.H., Tjønnfjord, G.E., Holme, P.A., 2021. Thrombosis and thrombocytopenia after ChAdOx1 nCoV-19 vaccination. N. Engl. J. Med. 384, 2124–2130.

Van Elslande, J., Oyaert, M., Ailliet, S., Van Ranst, M., Lorent, N., Vande Weygaerde, Y., André, E., Lagrou, K., Vandendriessche, S., Vermeersch, P., 2021. Longitudinal follow-up of IgG anti-nucleocapsid antibodies in SARS-CoV-2 infected patients up to eight months after infection. J. Clin. Virol. 136, 104765.

Voysey, M., Clemens, S.A.C., Madhi, S.A., Weckx, L.Y., Folegatti, P.M., Aley, P.K., Angus, B., Baillie, V.L., Barnabas, S.L., Bhorat, Q.E., Bibi, S., Briner, C., Cicconi, P., Collins, A.M., Colin-Jones, R., Cutland, C.L., Darton, T.C., Dheda, K., Duncan, C.J.A., Emary, K.R.W., Ewer, K.J., Fairlie, L., Faust, S.N., Feng, S., Ferreira, D.M., Finn, A., Goodman, A.L., Green, C.M., Green, C.A., Heath, P.T., Hill, C., Hill, H., Hirsch, I., Hodgson, S.H.C., Izu, A., Jackson, S., Jenkin, D., Joe, C.C.D., Kerridge, S., Koen, A., Kwatra, G., Lazarus, R., Lawrie, A.M., Lelliott, A., Libri, V., Lillie, P.J., Mallory, R., Mendes, A.V.A., Milan, E.P., Minassian, A.M., McGregor, A., Morrison, H., Mujadidi, Y.F., Nana, A., O'Reilly, P.J., Padayachee, S.D., Pittella, A., Plested, E., Pollock, K.M., Ramasamy, M.N., Rhead, S., Schwarzbold, A.V., Singh, N., Smith, A., Song, R., Snape, M.D., Sprinz, E., Sutherland, R.K., Tarrant, R., Thomson, E.C., Török, M.E., Toshner, M., Turner, D.P.J., Vekemans, J., Villafana, T.L., Watson, M.E. E., Williams, C.J., Douglas, A.D., Hill, A.V.S., Lambe, T., Gilbert, S.C., Pollard, A.J., 2021. Safety and efficacy of the ChAdOx1 nCoV-19 vaccine (AZD1222) against SARS-CoV-2: an interim analysis of four randomised controlled trials in Brazil, South Africa, and the UK. Lancet 397, 99–111.

International Journal of Hygiene and Environmental Health 238 (2021) 113859

Contents lists available at ScienceDirect

International Journal of Hygiene and Environmental Health

journal homepage: www.elsevier.com/locate/ijheh

Persisting antibiotic resistance gene pollution and its association with human sewage sources in tropical marine beach waters

Prasert Makkaew [a,d], Akechai Kongprajug [b], Natcha Chyerochana [b], Montakarn Sresung [b], Nopadol Precha [a,d], Skorn Mongkolsuk [b,c], Kwanrawee Sirikanchana [b,c,*]

[a] Department of Environmental Health and Technology, School of Public Health, Walailak University, Nakhon Si Thammarat, 80160, Thailand
[b] Research Laboratory of Biotechnology, Chulabhorn Research Institute, Bangkok, 10210, Thailand
[c] Center of Excellence on Environmental Health and Toxicology EHT, Ministry of Education, Bangkok, 10400, Thailand
[d] One Health Research Center, Walailak University, Nakhon Si Thammarat, 80160, Thailand

ARTICLE INFO

Keywords:
Antibiotic resistance genes
Microbial source tracking
Fecal pollution
Southeast asia
Seawater
Quantitative PCR
crAssphage

ABSTRACT

Antibiotic-resistant bacteria (ARB) and antibiotic resistance genes (ARGs) are pollutants of worldwide concern that threaten human health and ecosystems. Anthropogenic activities and wastewater could be ARB and ARG pollution sources; however, research on ARG abundance and microbial source tracking (MST) of contamination in tropical marine waters is limited. This study examined spatiotemporal variations of six ARGs (bla_{NDM}, bla_{TEM}, bla_{VIM}, *mcr-1*, *sul1*, and *tetQ*) against the widely used antibiotic groups and a class 1 integron-integrase gene (*intI1*) at two Thai tropical recreational beaches (n = 41). Correlations between ARGs and sewage-specific MST markers (i.e., crAssphage and human polyomaviruses [HPyVs]) and fecal indicator bacteria (i.e., total coliforms, fecal coliforms, and enterococci) were also investigated. Bla_{TEM}, *intI1*, *sul1*, and *tetQ* were ubiquitous at both beaches (85.4–100% detection rate); *intI1* was the most abundant (3–6 orders in $\log_{10}$ copies/100 mL), followed by bla_{TEM} (2–4 orders), *sul1* (2–3 orders), and *tetQ* (2–4 orders). Bla_{NDM} was found in 7.3% (up to 4 orders), and no *mcr-1* was detected. Interestingly, bla_{VIM} was prevalent at one beach (2–5 orders; n = 17), but found in only one sample at the other (4 orders). Temporal, but not spatial, differences were noticed; bla_{TEM} was at higher levels in the wet season. *IntI1* correlated with *sul1* and *tetQ* (Spearman's rho = 0.47–0.97), suggesting potential horizontal gene transfer. CrAssphage, but not HPyVs, correlated with *intI1*, *sul1*, and *tetQ* (Spearman's rho = 0.50–0.74). Higher numbers of ARGs tended to co-occur in samples with higher crAssphage concentrations, implying sewage contribution to the marine water, with a persisting ARG background. This study provides insight into the ARG pollution status of tropical coastal waters and suggests crAssphage as a proxy for ARG pollution, which could facilitate effective management policies to minimize ARG dissemination in marine environments.

1. Introduction

Antibiotics are effective life-saving drugs approved for therapeutic use in humans and animals and for therapeutic and preventive use or growth promotion in plant agriculture, livestock production, and aquaculture (FAO, 2016; World Health Organization, 2015). However, imprudent use in these settings results in selective pressure on bacteria, leading to the development of antibiotic-resistant bacteria (ARB) that reduce the efficacy of antibiotic treatment (Andersson and Hughes, 2014). With the realization of the importance of antimicrobial resistance (AMR), global surveillance action has been initiated via the Global Antimicrobial Resistance Surveillance System (GLASS) to collect evidence of ARB prevalence and abundance, primarily from bacterial isolates retrieved from clinical specimens (WHO, 2017). In addition to the human sector, emphasis has been placed on the environmental sector through the adoption of the One Health perspective, which underlines the relationships between the human, animal, and environmental sectors for AMR management and control (Booton et al., 2021; European Commission, 2017; Veterinary Medicines Directorate, 2019). ARB and antibiotic resistance genes (ARGs) have been recognized as emerging pollutants in the environment that could pose a threat to human health due to the release of resistant pathogens, as well as the introduction of

* Corresponding author. Research Laboratory of Biotechnology, Chulabhorn Research Institute, Bangkok, 10210, Thailand.
E-mail address: kwanrawee@cri.or.th (K. Sirikanchana).

https://doi.org/10.1016/j.ijheh.2021.113859
Received 5 July 2021; Received in revised form 25 September 2021; Accepted 5 October 2021
Available online 14 October 2021

ARGs to health-relevant microorganisms through horizontal gene transfer (Amarasiri et al., 2020; WHO, 2014). However, there is insufficient information available on the prevalence and abundance of AMR and ARGs in the environment, locally and globally (Ministry of Public Health and Ministry of Agriculture and Cooperatives, 2020; World Health Organization, 2015). Therefore, increasing the monitoring of, and consequently the amount of data on, AMR and ARGs in the environment will help fill current gaps and support both national and global action plans to curb AMR dissemination (Ministry of Public Health and Ministry of Agriculture and Cooperatives, 2020; Singer et al., 2016; World Health Organization, 2015).

Marine and coastal environments are impacted by human activities, with approximately 40% of the global population living within 100 km of the coastline (United Nations, 2017). Hence, marine waters could be hotspots for ARGs, as they receive domestic wastewater that harbors ARB and ARGs (Guo et al., 2017; Le et al., 2018; Ng et al., 2018b; Pärnänen et al., 2019; Rodríguez et al., 2021; Wang et al., 2020). The occurrence and distribution of ARB and ARGs in the marine waters of many geographical areas have been reported (Griffin et al., 2020; Mann et al., 2020; Oliveira and Pinhata, 2008; Zheng et al., 2021; Zhu et al., 2017). On a global scale, the marine waters of low- and middle-income countries are more likely to be contaminated with antibiotics at higher levels than high-income countries (Zheng et al., 2021). Interestingly, ARG contamination levels in environmental waters were comparable between low-/middle- and high-income countries, but dependent on latitudinal location. This may be due to different ARB having different optimal temperatures for growth (Zheng et al., 2021). Notably, there have been fewer studies on ARG prevalence and abundance conducted in regions of lower latitudes (near the equator) than in regions more distant from the equator (Zheng et al., 2021).

To alleviate the ARG pollution problem, it is essential to identify the occurrence, transport, and sources of ARGs in the environment, and to develop an indicator for occurrence and concentration (Amarasiri et al., 2020; WHO, 2014). Although ARB and ARGs can evolve due to selective pressure and resistance gene transfer in the environment (Andersson and Hughes, 2014; Jutkina et al., 2018; Singer et al., 2019; Stanton et al., 2020; von Wintersdorff et al., 2016), it has been found that in certain situations, ARGs are mainly derived from fecal pollution (Chu et al., 2018; Karkman et al., 2019). Therefore, developing methods to detect and address the fecal pollution of environmental water is critical. Because wastewater also contains pollutants (e.g., antibiotics, metals, and organic matter), the identification of fecal pollution and wastewater sources will also facilitate the management of co-occurring contaminants that could adversely induce and co-select ARB and ARGs in the environment. One method used to discriminate fecal pollution sources in environmental water is microbial source tracking (MST). It detects microbial markers present in the gastrointestinal tracts of humans or specific animal species (Harwood et al., 2014; Zhang et al., 2019). CrAssphage, a bacteriophage first discovered in human fecal metagenomes (Dutilh et al., 2014) and reportedly specific to human sewage pollution, has been suggested for use as a human-specific MST marker in many geographical regions (Ahmed et al., 2018a; Bivins et al., 2020; Chen et al., 2021; Crank et al., 2020; Sala-Comorera et al., 2021; Stachler et al., 2017; Ward et al., 2020). Human polyomaviruses BK and JC (HPyVs), the etiological agents of kidney nephritis and progressive multifocal leukoencephalopathy, have also been used to indicate human sewage contamination (Ahmed et al., 2010; Haramoto et al., 2010; Kirs et al., 2016; McQuaig et al., 2009; Rachmadi et al., 2016). CrAssphage and HPyVs have been characterized for their performance (sensitivity and specificity) and their applicability validated in Thailand's freshwater and seawater (Kongprajug et al., 2019, 2020, 2021a, 2021b; Petcharat et al., 2020; Sangkaew et al., 2021). While MST markers, such as crAssphage, have been shown to correlate with ARGs in more polluted environments, such as wastewater or impacted urban freshwater and sediments (Ahmed et al., 2021b; Chen et al., 2021; Stachler et al., 2019), our understanding of their applicability in recreational marine environments is still limited.

In this study, ARGs that confer resistance to the following commonly used antibiotics were selected: beta-lactams (bla_{NDM}, bla_{TEM}, and bla_{VIM}), colistin (*mcr-1*), sulfonamides (*sul1*), and tetracycline (*tetQ*). These genes have been shown to be significant in estuarine and marine environments (Li et al., 2020; Zheng et al., 2021). *IntI1*, a class 1 integron-integrase gene, was included because it indicates potential gene transfer by mobile genetic elements and has been suggested as an indicator of anthropogenic pollution (Gillings et al., 2015).

The objectives of this study were to investigate the spatial and temporal distributions of ARGs and *intI1* in tropical coastal waters, and to assess correlations between the ARGs and *intI1* and the MST markers and fecal indicator bacteria (FIB). We hypothesized that a portion of ARG pollution originated from human sewage, and therefore, human-specific MST marker could serve as an indicator of ARG pollution. The FIB being regulated as part of Thailand's coastal water quality standards comprises total coliforms, fecal coliforms, and enterococci (National Environment Board, 2017). For comparison, the crAssphage, HPyVs, and FIB groups measured in a previous study were used due to similarities in the sample sets (Kongprajug et al., 2021a). The findings from this study could reveal the ARG pollution levels at tropical recreational beaches and suggest an indicator of ARG pollution, which could assist in monitoring marine water quality to reduce risks to human and ecosystem health.

2. Materials and methods

2.1. DNA samples

ARGs were detected in 41 archived DNA samples collected from Bangsaen beach (Beach BS) and Pattaya beach (Beach PT), Chonburi Province, from seven sampling stations (Stations A–C at Beach BS and D–G at Beach PT; Table S1) and at six time points (Dec 2018, Feb 2019, Mar 2019, Apr, 2019; Jun 2019, and Jul/Aug 2019), as described elsewhere (Kongprajug et al., 2021a). Briefly, a water sample (10 L) was pH adjusted to 3.5 ± 0.2 prior to membrane filtration using seven HAWP membrane filters (0.45 μm pore size; Merck Darmstadt, Germany). DNA was extracted from each membrane separately using a Quick DNA Fecal Soil Microbe Miniprep Kit (Zymo Research, Irvine, CA). Then, DNA extracts from the same water sample were mixed before the concentration was measured using a NanoDrop 2000 Spectrophotometer (Thermo Fisher Scientific, Waltham, MA). Samples were stored at −80 °C.

2.2. ARG qPCR assay

Seven gene targets (bla_{NDM}, bla_{TEM}, bla_{VIM}, *intI1*, *mcr-1*, *sul1*, and *tetQ*) were assessed using a QuantStudio3 Real-Time PCR System (Applied Biosystems, Thermo Fisher Scientific, Waltham, MA) following the Minimum Information for Publication of Quantitative Real-Time PCR Experiments (MIQE) guidelines (Bustin et al., 2009). The qPCR mixture (20 μL total) was composed of forward primer, reverse primer, and hydrolysis probe, as specified in Table S2. The remaining components were extracted DNA (2 μL), 2X Luna® Universal Probe qPCR Master Mix (10 μL; New England Biolabs, Ipswich, MA), and bovine serum albumin (1 μg/μL). The qPCR cycle steps were as follows: initial denaturation at 95 °C for 3 min, 40 cycles of denaturation at 95 °C for 20 s, and combined annealing and elongation at the temperature indicated in Table S2 for 1 min. Each sample was run in duplicate, and the average C_q was determined using QuantStudio Design & Analysis software (Applied Biosystems, Thermo Fisher Scientific, Waltham, MA) with an automatic baseline and manual adjustment of the threshold values (Table S2). When the standard deviation of C_q was more than 1, an additional run was performed. The triplicate of no-template controls (NTCs) as a negative control and the DNA standard at a concentration of 5×10^4 to 5×10^5 copies/reaction as a calibration control were added in

each instrumental run. The gene copy number was calculated according to a mixed model (Kongprajug et al., 2020; Sivaganesan et al., 2010).

2.3. Standard curve characteristics

Standard curves used for target gene quantification were generated using synthetic plasmid standards containing each ARG marker sequence (Macrogen, Seoul, South Korea). The standard curves were obtained from four replicates of individual instrumental runs according to the mixed model method (Kongprajug et al., 2020; Sivaganesan et al., 2010), by running a triplicate of six 10-fold concentrations, ranging from 5×10^1 to 5×10^6 copies/reaction. The assay limit of detection (ALOD) was defined by testing 10 standard replicates of the lowest concentration in copies/reactions that showed all positive detection with a standard deviation of $C_q < 1$. The assay limit of quantification (ALOQ) was the lowest concentration in the standard curve. The method limit of quantification (MLOQ) was calculated for each sample as copies/100 mL using the sample's filtration volume and DNA extracted volume. The standard curve performance characteristics, qPCR efficiencies, ALOD, and ALOQ for this study are shown in Table S3. No inhibition was confirmed by testing the GenBac3 assay using the dilution method previously described (Kongprajug et al., 2021a). It was also determined that there was no cross-contamination during the field and laboratory processes for these archived DNA samples (Sangkaew et al., 2021); this was further evaluated using the *tetQ* assay in four field blanks and 18 method blanks. Reproducibility was assessed using five field duplicate samples tested with all seven genes.

2.4. Statistical analyses

Statistical analyses were conducted using the R program (R Core Team, 2019). The normality test was performed using the Shapiro–Wilk test. Two-group comparisons were tested using a *t*-test for the normal data and the Mann–Whitney *U* test for the non-normal data. For the paired test between two samples, a parametric paired *t*-test and the nonparametric Wilcoxon signed-rank test were used. The statistical difference of multiple comparisons was conducted using one-way analysis of variance, with Tukey's multiple comparisons for the normal data, and the Kruskal–Wallis test with Dunn's multiple comparisons for the non-normal data.

A nonparametric survival analysis procedure was used for the data sets containing censored data, or non-detects (Helsel, 2012). Descriptive statistics were calculated using Kaplan–Meier estimates with Efron bias correction. The significance of the differences was tested using the paired Prentice–Wilcoxon test for paired comparisons and the generalized Wilcoxon test with Holm's correction for multiple comparisons. A correlation analysis was performed using Spearman's rho on U-Score rank. The multivariate analysis was analyzed by model-based clustering, which was based on parameterized finite Gaussian mixture models. Models were estimated by the expectation-maximization (EM) algorithm initialized by hierarchical model-based agglomerative clustering. The optimal model was then selected according to the Bayesian information criterion (BIC) value.

3. Results

3.1. The qPCR standard curve characteristics, limits, and controls

The standard curves for bla_{NDM}, bla_{TEM}, bla_{VIM}, *intI1*, *mcr-1*, *sul1*, and *tetQ* were characterized, and the PCR efficiencies ranged from 89.67 to 99.91% (Table S3). The ALOD ranged from 10 copies/reaction (*tetQ*) to 100 copies/reaction (bla_{VIM}). For six genes, the ALOQ was 50 copies/reaction; for bla_{VIM} it was 100 copies/reaction. The MLOQ ranged from 1.94 to 3.00 $\log_{10}$ copies/100 mL. The laboratory reproducibility was determined when all seven qPCR assays were analyzed in field duplicates. The acceptable coefficients of variation in five representative samples were 0.76–25.45% (Table S4). Furthermore, all of the field blanks and method blanks were negative in the *tetQ* assay, confirming no field and laboratory cross-contamination.

3.2. Prevalence and concentrations of the ARGs

Among the seven genes, *intI1* and bla_{TEM} were detected in all samples at 3.50–6.25 and 2.08–4.12 $\log_{10}$ copies/100 mL, respectively. *Sul1* was detected at concentrations up to 3.97 $\log_{10}$ copies/100 mL (97.6% positive detection), and *tetQ* had a maximum concentration of 4.57 $\log_{10}$ copies/100 mL (85.4% positive detection) (Fig. 1 and Table S5). *Mcr-1* was not detected in all samples, while bla_{NDM} was found in 7.3% of samples at up to 4.36 $\log_{10}$ copies/100 mL. Interestingly, bla_{VIM} was detected in all samples at Beach BS (n = 17) at 2.80–5.02 $\log_{10}$ copies/100 mL, but was observed in only one sample at Beach PT at 4.67 $\log_{10}$ copies/100 mL. Bla_{NDM}, *intI1*, and *sul1* were at significantly higher levels at Beach BS compared to Beach PT, and *tetQ* was at significantly higher levels at Beach PT compared to Beach BS ($p < 0.05$; Fig. 1 and Table S6). *IntI1* was the most abundant gene at Beach BS, followed by bla_{VIM}, a tie of bla_{TEM} and *sul1*, *tetQ*, and bla_{NDM}, respectively (Table S7). At Beach PT, *intI1* was also dominant, followed by a tied group of bla_{TEM}, *sul1*, and *tetQ*.

3.3. The spatiotemporal distribution of the ARGs

ARG contamination was equally distributed among sites at the same beach; that is, no significant spatial variation was observed for any of the genes (Table S8). However, there were differences in temporal distribution between certain sampling events for bla_{TEM} (highest in Jul), *intI1* (highest in Feb and Apr), *sul1* (highest in Apr), and *tetQ* (highest in Feb) (Table S9). Wet weather sampling was reported only for the Mar, Apr, and Jul events, with 24-h accumulated rainfall of 2, 7, and 0.5 mm, respectively. These light rainfalls did not have any observed explicit effect on ARG levels. When categorized into the locally defined dry (Dec, Feb, and Mar) and wet (Apr, Jun, and Jul/Aug) seasons in Thailand, only bla_{TEM} showed significantly higher concentrations in the wet season; no differences were observed for the other genes (Table S10).

3.4. Correlation among ARGs, MST markers, and FIB indicators

Correlation analysis was performed using the concentrations of all seven genes (ARGs and *intI1*) and the previously reported MST markers (crAssphage and HPyVs) and FIB indicators (total coliforms, fecal coliforms, and enterococci) (Kongprajug et al., 2021a). More parameter pairs were significantly correlated, and generally with higher correlation coefficients, at Beach BS than at Beach PT (Fig. 2). *Sul1* strongly

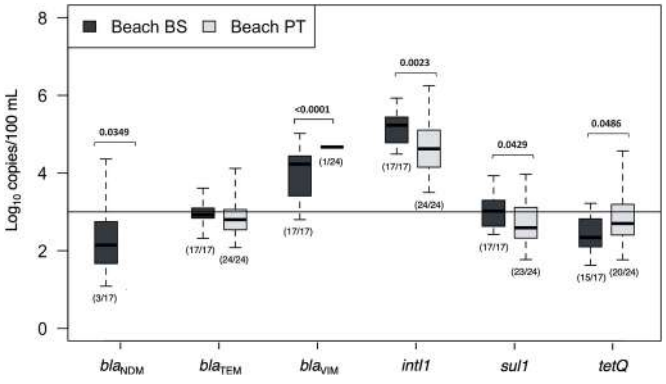

Fig. 1. Box plots of ARG concentrations at Beaches BS and PT. The numbers in parentheses denote the number of positive samples/total samples. The solid lines represent the highest method limit of quantification (MLOQ) at 3.00 $\log_{10}$ copies/100 mL. The p-values indicate significant differences between the two beaches.

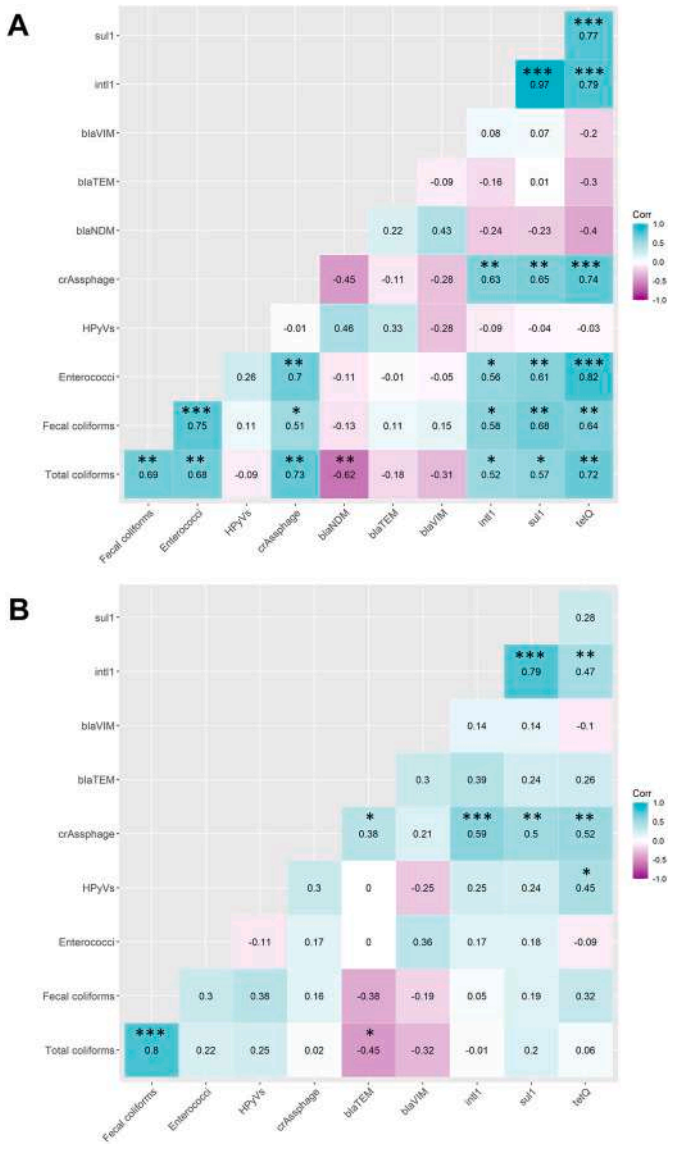

Fig. 2. Spearman's rho correlation analysis for ARG and *intI1* parameters, MST markers, and FIB indicators for Beach BS (a) and Beach PT (b). The colors and numbers represent Spearman's correlation coefficients. Asterisks indicate significant difference, where * denotes $p < 0.05$, ** denotes $p < 0.01$, and *** denotes $p < 0.001$. (For interpretation of the references to color in this figure legend, the reader is referred to the Web version of this article.)

correlated with *tetQ* at Beach BS (rho = 0.77). At both beaches, *intI1* was significantly associated with *sul1* and *tetQ* (rho = 0.79–0.97 for Beach BS and 0.47–0.79 for Beach PT), and crAssphage correlated with *intI1*, *sul1*, and *tetQ* (rho = 0.63–0.74 for Beach BS and 0.50–0.59 for Beach PT). At Beach PT, moderate correlations were observed for crAssphage and bla_{TEM} (rho = 0.38) and for HPyVs and *tetQ* (rho = 0.45). At Beach BS, all three FIB indicators also correlated with crAssphage, *intI1*, *sul1*, and *tetQ* (rho = 0.51–0.82), while only total coliforms was inversely associated with bla_{NDM} (rho = −0.62). Total coliforms was also only inversely correlated with bla_{TEM} at Beach PT (rho = −0.45). Model-based clustering categorized 11 parameters into nine optimal clusters for each beach (Fig. 3). The clustering results substantiated the strong correlations between crAssphage and *tetQ* and between *intI1* and *sul1*.

Due to the explicit association between the concentrations of the human-specific marker crAssphage and those of *intI1*, *sul1*, and *tetQ* (Fig. 2), the ARG co-occurrences in the samples were further investigated in relation to crAssphage levels (Fig. 4). In samples with no detectable crAssphage, there were still at least four and two ARGs co-occurring at Beaches BS and PT, respectively. These results indicated that there could be background levels of ARGs present in the beach water, and that concentrations of ARGs were enhanced by human sewage input, as indicated by the crAssphage marker.

4. Discussion

4.1. Occurrence of and correlation among integron-associated and antibiotic resistance genes in environmental water

This study revealed a wide range of concentrations of different ARGs and *intI1* at two recreational beaches in Thailand. The dominant genes in the beach water included bla_{TEM}, *intI1*, *sul1*, and *tetQ*. Furthermore, correlations among these genes, except bla_{TEM}, were observed (rho = 0.47–0.97).

Other studies have found *intI1* and *sul1* to be the most prevalent genes in rivers downstream of wastewater treatment plants at levels similar to and two to three orders higher than those found in this study, respectively (Cacace et al., 2019; Calero-Caceres et al., 2017; Harnisz et al., 2020; Koczura et al., 2016). *IntI1*, *sul*, and *tet* genes have also been reported to be more prevalent in wastewater-impacted coastal water (Lu et al., 2020; Niu et al., 2016) than in this study's samples, reaching levels of up to 9, 8, and 7 orders (log_{10} copies/100 mL), respectively (Zhang et al., 2020). *Sul* and *tet* genes were also dominant in sediments in coastal areas impacted by wastewater treatment plant effluents and mariculture (Chen et al., 2020; Gao et al., 2018; Ng et al., 2018a). *Sul1* and bla_{TEM} genes were ubiquitous, while *tetQ* and *intI1* were slightly less abundant, from coastal aquaculture farm effluent directly released to the coast (Jang et al., 2018). Overall, the four most abundant genes detected in Thailand's beach water in this study concurred with reports on freshwater and coastal water in other geographical regions, raising global concerns about these ARG pollutants in environmental waters. The dominance of these ARGs in the environment could be due to their high resistance to environmental conditions (e.g., pH and temperature) and disinfection (Calero-Caceres and Muniesa, 2016; Liu et al., 2018).

Bla_{TEM} has been reported to be prevalent in rivers impacted by wastewater effluent (Calero-Caceres et al., 2017; Harnisz et al., 2020), at three orders higher than what was observed in this study of coastal water. Bla_{TEM}, *tet*, and *sul* genes were also ubiquitous in *Escherichia coli* isolated from estuarine water (Divya and Hatha, 2019). ARGs in urban marine water were studied using a metagenomic approach, and bla_{TEM} was the most prevalent, while no *tetQ* nor *sul1* was observed (Fresia et al., 2019). Regarding the less abundant genes, there are fewer reports on bla_{VIM} and bla_{NDM} genes in coastal environments when compared to other *bla*-like genes. Bla_{VIM} has been reported in wastewater (Hiller et al., 2019; Rizzo et al., 2013) and public beach sand (Furlan et al., 2020). This is the first report of bla_{VIM} in marine water in Thailand. Interestingly, bla_{VIM} was detected in all samples in Beach BS (n = 17; 2.80–5.02 log_{10} copies/100 mL), but in only one sample in Beach PT (4.67 log_{10} copies/100 mL).

Mcr-1 was not found in any of the samples, while bla_{NDM} was detected in 7.3% of the samples (up to 4.36 log_{10} copies/100 mL). The bla_{VIM}, bla_{NDM}, and *mcr-1* genes were all found in the influent and effluent of the municipal wastewater treatment facility near both beaches (our unpublished data), implying a dilution effect of these genes in environmental water from wastewater sources. Other studies have detected bla_{NDM} in a wastewater-impacted river (Ahammad et al., 2014; Lekunberri et al., 2017) and sediments (Subirats et al., 2017). The plasmid-mediated colistin resistance gene, *mcr-1*, has been detected in environmental water, including recreational beach water, which could pose a threat to tourists (Anyanwu et al., 2020; Drali et al., 2018; Fernandes et al., 2017; Nguyen et al., 2020).

Correlations between *intI1*, *sul1,* and *tetQ* in this study also corroborated the trends observed in other studies of estuarine and coastal waters (Jang et al., 2018; Lu et al., 2020; Niu et al., 2016), and sediments

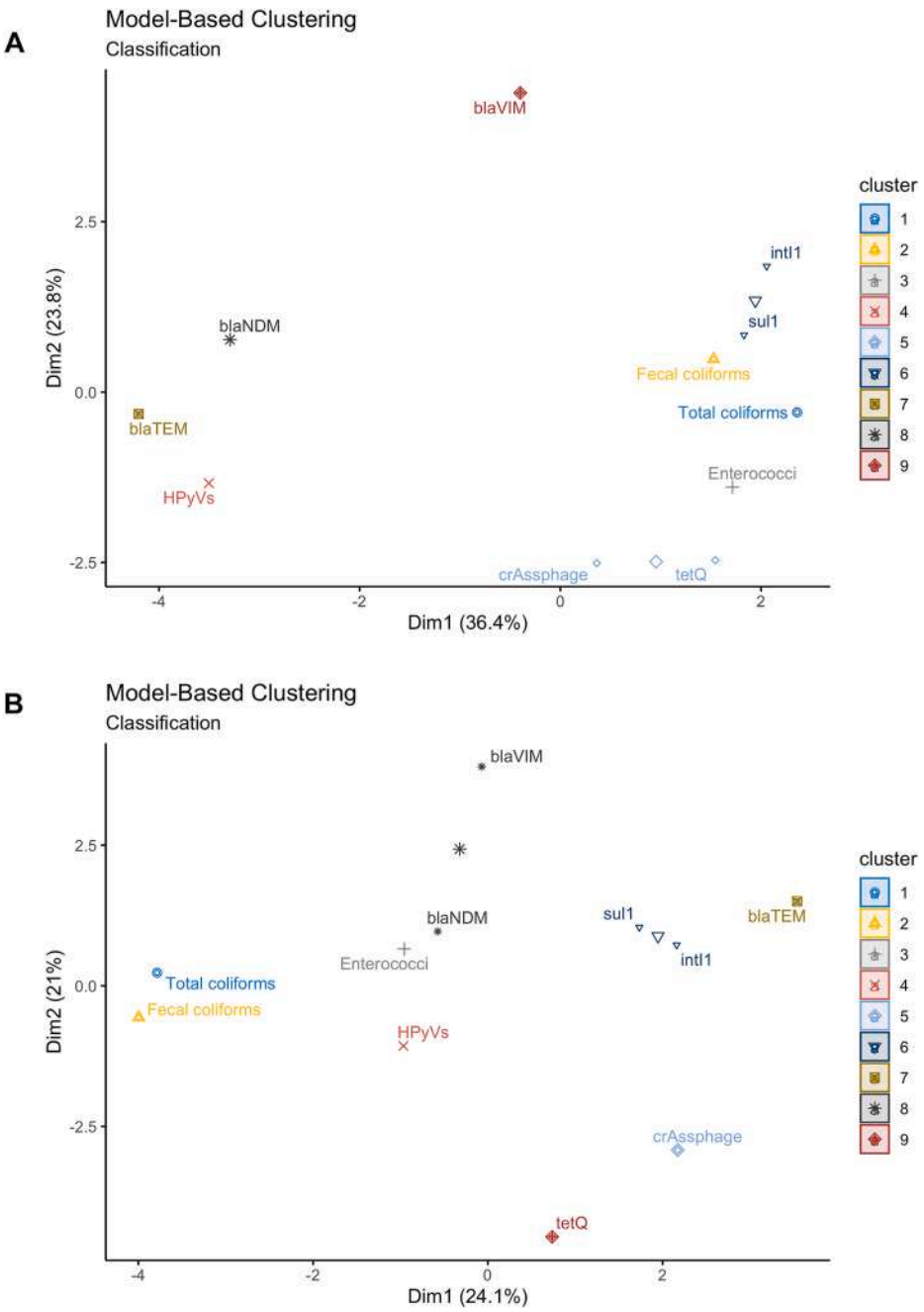

Fig. 3. Model-based clustering of ARGs, MST markers, and FIB indicators for Beach BS (a) and Beach PT (b).

(Chen et al., 2020; Leng et al., 2020; Zhu et al., 2017). The prevalence of *intI1* and the associations between *intI1* and the ARGs imply that integron (part of the mobile genetic elements) supports horizontal gene transfer, which is a main mechanism driving ARG diversity (Amarasiri et al., 2020; Mazhar et al., 2021). Association between *sul* and *tet* genes may imply that they originated from the same pollution sources, as co-presence of both genes was reported in wastewater treatment plants, aquaculture and livestock farms (Gao et al., 2012; McKinney et al., 2010; Nguyen et al., 2021). Cross-selection of antibiotics to ARGs was also evident in water and sediment where concentrations of sulfonamide antibiotics were significantly correlated not only with their corresponding *sul* genes, but also with *tet* genes. (McKinney et al., 2010; Niu et al., 2016). Vice versa, the tetracycline antibiotics were associated with both corresponding *tet* genes and *sul* genes (McKinney et al., 2010; Niu et al., 2016).

4.2. Potential sources of ARG pollution in tropical beach water

This study demonstrated a significant correlation between concentrations of the human-specific marker crAssphage and *intI1*, *sul1*, and *tetQ* at two tropical beaches (rho = 0.50–0.74). The FIB group (i.e., total coliforms, fecal coliforms, and enterococci) was also associated with *intI1*, *sul1*, and *tetQ* at Beach BS (0.52–0.82). Significant correlations between the MST marker or FIB group and the ARGs have been previously reported, primarily in sewage-impacted and polluted environments. For example, crAssphage and *E. coli* showed a significant correlation with ARGs in urban rivers in Australia (Ahmed et al., 2021b) and a polluted urban stream in the USA (Stachler et al., 2019). CrAssphage and HF183 MST markers also correlated with ARGs in stormwater runoff in the USA, which received point and non-point source pollution (Ahmed et al., 2018b). CrAssphage was also indicated by the

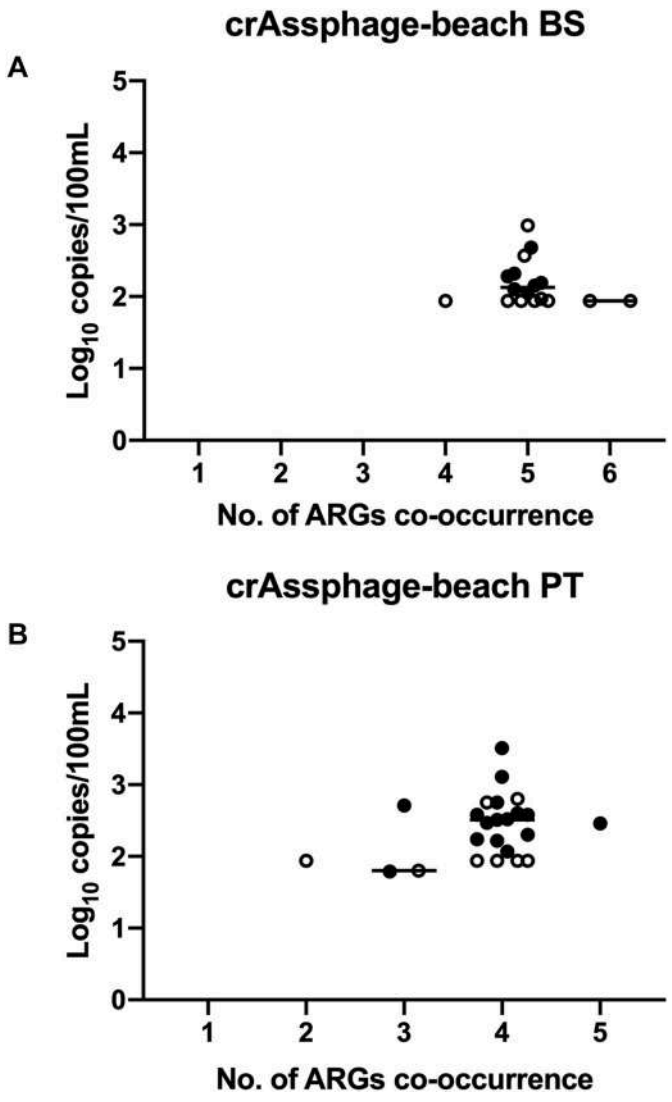

Fig. 4. CrAssphage concentrations in samples with numbers of co-occurring ARGs at Beach BS (a) and Beach PT (b). The medians are shown in solid lines. Dark circles indicate quantifiable crAssphage results and white circles indicate the crAssphage's method limit of quantification (MLOQ) of non-detect results.

metagenomic approach for its correlation with ARGs in anthropogenically impacted river waters and sediments (Chen et al., 2021; Davis et al., 2020; Karkman et al., 2019). Several human MST markers, including crAssphage, HF183, and HPyV, were detected in a set of samples from a sewage-impacted freshwater stream; all of these markers correlated with ARGs (Stachler et al., 2018, 2019).

However, few studies have compared the capability of different human-specific MST markers to indicate ARG abundance in marine water. Although this study showed that crAssphage correlated well with the most prevalent genes (i.e., *intI1*, *sul1*, and *tetQ*), interestingly, another human sewage marker, HPyVs, did not correlate with any of the ARGs. Consequently, this study underlines the importance of evaluating several markers to find the appropriate one for ARG indication in tropical marine environments. One study has demonstrated no correlation between ARGs and the human MST marker HF183 in urban streams or urban bathing waters, suspectedly due to fecal pollution dynamics, the sporadic nature of fecal pollution, and decay factors (Reynolds et al., 2020). Association among different gene markers and ARGs could also be affected by different decay rates in environmental sediments and water that were influenced by factors such as gene types, soil texture, water matrix (e.g., seawater and freshwater) and environmental conditions, as reported previously (Ahmed et al., 2019; Brown et al., 2020; Macedo et al., 2020). Moreover, sample matrices and laboratory protocols have been shown to affect recoveries of ARGs, and bacterial and viral genomes at various extents, which could influence the correlation between sewage markers and ARGs (Ahmed et al., 2021a; Haramoto et al., 2018; Liang et al., 2021). Both crAssphage and HPyVs have been validated for their high performance (very specific and sensitive) as human sewage indicators and for their capability in freshwater and seawater in Thailand (Kongprajug et al., 2019; Sangkaew et al., 2021). Thus, we hypothesize that the different decay characteristics of crAssphage and HPyVs in seawater in a tropical climate have an impact. As previously discussed (Sangkaew et al., 2021), in the same set of marine water samples, there were no correlations between the two markers, and a lower rate of crAssphage (56.1%) compared to the HPyVs (92.7%). However, crAssphage was shown to be significantly higher than HPyVs in human sewage and tropical freshwater (Sangkaew et al., 2021). This suggests that crAssphage has a higher decay rate than the HPyVs in seawater (Ahmed et al., 2019; Ballesté et al., 2018, 2019).

ARGs could enter marine water as a result of anthropogenic activities, for example, via wastewater treatment plants, sewage discharge, and leaking sewer pipelines, or non-human activities, such as riverine runoff, coastal aquaculture, and wildlife (Zheng et al., 2021). The municipal wastewater treatment facilities that receive sewage from the Beaches BS and PT areas discharge the treated effluent into canals that run into adjacent beaches on the other side of the coves (approximately 7 km away), so it is less likely that effluent reaches the studied beaches. However, non-human sources have not yet been identified and could be additional sources of ARGs. There have been reports stating that gulls and shorebirds may disseminate ARGs by carrying ARBs and ARGs from coastal wetlands (Antilles et al., 2021; Navedo et al., 2021). At the studied beaches, pigeons, and stray dogs have been sporadically observed. No aquaculture or shellfish farming was seen in the area during the study period. It is worth noting that coastal sediment resuspension has been reported as an ARG source in coastal water (Gao et al., 2018; Zhu et al., 2017). ARGs could also be naturally present in environmental water (Allen et al., 2010; D'Costa et al., 2011; Perron et al., 2015). Regrowth of fecal bacteria, especially ARB, could be promoted in the environment by various factors, such as temperature, pH, salinity, nutrients, organic pollutants, and the microbial community (Zheng et al., 2021). Factors contributing to the co-selection of ARB and ARGs also include heavy metals (Mazhar et al., 2021), biocides (Pal et al., 2015), phytoplankton and zooplankton in aquatic ecosystems (Xue et al., 2021), and organic contaminants (Wang et al., 2017). This study detected at least three ARGs in most samples, with two co-occurring ARGs in one sample. The presence of several ARGs indicates persisting ARG pollution of the beach water that could be caused by multiple sources and complicated environmental pathways. The results of this study emphasize that crAssphage can be utilized as an ARG pollution indicator for the better management of tropical marine waters. Not all microbial indicators act in a similar manner; thus, there is a need to evaluate multiple markers to find a suitable proxy for ARG pollution.

5. Conclusion

This study investigated integron-associated and antibiotic resistance genes in recreational beach water in Thailand and assessed their correlation with human-sewage MST markers and FIB indicators. The results showed high prevalence and levels of the *intI1*, bla_{TEM}, *sul1*, and *tetQ* genes. Significant correlation between *intI1* and *sul1* and *tetQ* genes suggests horizontal gene transfer as a crucial mechanism for ARG dissemination in environmental water. The human-specific marker crAssphage also correlated well with *intI1*, *sul1*, and *tetQ*, indicating that human sewage could be one source of ARG pollution. CrAssphage was therefore suggested as a proxy for ARG contamination in tropical beach water. Samples were found to contain co-occurring ARGs, even in

crAssphage-negative samples. These high ARG background levels imply that ARGs have been persisting in beach water, potentially reaching the water via non-human sources or environmental pathways. Another human-specific MST marker, HPyVs, surprisingly showed no correlation with ARGs, highlighting the need to evaluate a set of microbial indicators to define an appropriate indicator for ARG pollution. This study provides a better understanding of how ARGs circulate in the environment and the relationships between ARGs and other microbial parameters in tropical beach water, which could facilitate future intervention to reduce antibiotic resistance by targeting the environment sector as part of the One Health approach.

CRediT authorship contribution statement

Prasert Makkaew: Conceptualization, Methodology, Investigation, Writing – original draft, Funding acquisition. **Akechai Kongprajug:** Investigation, Formal analysis, Visualization, Writing – original draft. **Natcha Chyerochana:** Investigation, Formal analysis, Visualization. **Montakarn Sresung:** Investigation, Formal analysis, Visualization. **Nopadol Precha:** Investigation, Writing – original draft. **Skorn Mongkolsuk:** Conceptualization, Supervision, Funding acquisition. **Kwanrawee Sirikanchana:** Conceptualization, Supervision, Writing – original draft, Writing – review & editing.

Declaration of competing interest

The authors declare that they have no known competing financial interests or personal relationships that could have appeared to influence the work reported in this paper.

Acknowledgements

This study was financially supported by Walailak University (Grant No. WU-IRG-63-025) and Chulabhorn Research Institute (Grant No. 312/3057).

Appendix A. Supplementary data

Supplementary data to this article can be found online at https://doi.org/10.1016/j.ijheh.2021.113859.

References

Ahammad, Z.S., Sreekrishnan, T.R., Hands, C.L., Knapp, C.W., Graham, D.W., 2014. Increased waterborne blaNDM-1 resistance gene abundances associated with seasonal human pilgrimages to the Upper Ganges River. Environ. Sci. Technol. 48, 3014–3020.

Ahmed, W., Wan, C., Goonetilleke, A., Gardner, T., 2010. Evaluating sewage-associated JCV and BKV polyomaviruses for sourcing human fecal pollution in a coastal river in Southeast Queensland, Australia. J. Environ. Qual. 39, 1743–1750. https://doi.org/10.2134/jeq2010.0062.

Ahmed, W., Payyappat, S., Cassidy, M., Besley, C., Power, K., 2018a. Novel crAssphage marker genes ascertain sewage pollution in a recreational lake receiving urban stormwater runoff. Water Res. 145, 769–778. https://doi.org/10.1016/j.watres.2018.08.049.

Ahmed, W., Zhang, Q., Lobos, A., Senkbeil, J., Sadowsky, M.J., Harwood, V.J., Saeidi, N., Marinoni, O., Ishii, S., 2018b. Precipitation influences pathogenic bacteria and antibiotic resistance gene abundance in storm drain outfalls in coastal sub-tropical waters. Environ. Int. 116, 308–318. https://doi.org/10.1016/j.envint.2018.04.005.

Ahmed, W., Zhang, Q., Kozak, S., Beale, D., Gyawali, P., Sadowsky, M.J., Simpson, S., 2019. Comparative decay of sewage-associated marker genes in beach water and sediment in a subtropical region. Water Res. 149, 511–521. https://doi.org/10.1016/j.watres.2018.10.088.

Ahmed, W., Bivins, A., Simpson, S.L., Smith, W.J.M., Metcalfe, S., McMinn, B., Symonds, E.M., Korajkic, A., 2021a. Comparative analysis of rapid concentration methods for the recovery of SARS-CoV-2 and quantification of human enteric viruses and a sewage-associated marker gene in untreated wastewater. Sci. Total Environ. 799, 149386. https://doi.org/10.1016/j.scitotenv.2021.149386.

Ahmed, W., Gyawali, P., Hamilton, K.A., Joshi, S., Aster, D., Donner, E., Simpson, S.L., Symonds, E.M., 2021b. Antibiotic resistance and sewage-associated marker genes in untreated sewage and a river characterized during baseflow and Stormflow. Front. Microbiol. 12, 1–13. https://doi.org/10.3389/fmicb.2021.632850.

Allen, H.K., Donato, J., Wang, H.H., Cloud-hansen, K.A., Davies, J., Handelsman, J., 2010. Call of the wild: antibiotic resistance genes in natural environments Heather. Nat. Rev. Microbiol. 8, 251–259. https://doi.org/10.1038/nrmicro2312.

Amarasiri, M., Sano, D., Suzuki, S., 2020. Understanding human health risks caused by antibiotic resistant bacteria (ARB) and antibiotic resistance genes (ARG) in water environments: current knowledge and questions to be answered. Crit. Rev. Environ. Sci. Technol. 50 https://doi.org/10.1080/10643389.2019.1692611, 2016–2059.

Andersson, D.I., Hughes, D., 2014. Microbiological effects of sublethal levels of antibiotics. Nat. Rev. Microbiol. 1–14. https://doi.org/10.1038/nrmicro3270.

Antilles, N., García-Bocanegra, I., Alba-Casals, A., López-Soria, S., Pérez-Méndez, N., Saco, M., González-Solís, J., Cerdà-Cuéllar, M., 2021. Occurrence and antimicrobial resistance of zoonotic enteropathogens in gulls from southern Europe. Sci. Total Environ. 763, 1–10. https://doi.org/10.1016/j.scitotenv.2020.143018.

Anyanwu, M.U., Jaja, I.F., Nwobi, O.C., 2020. Occurrence and characteristics of mobile colistin resistance (mcr) gene-containing isolates from the Environment : a review. Int. J. Environ. Res. Publ. Health 17, 1–38.

Ballesté, E., García-Aljaro, C., Blanch, A.R., 2018. Assessment of the decay rates of microbial source tracking molecular markers and faecal indicator bacteria from different sources. J. Appl. Microbiol. https://doi.org/10.1111/jam.14058.

Ballesté, E., Pascual-Benito, M., Martín-Díaz, J., Blanch, A.R., Lucena, F., Muniesa, M., Jofre, J., García-Aljaro, C., 2019. Dynamics of crAssphage as a human source tracking marker in potentially faecally polluted environments. Water Res. 155, 233–244. https://doi.org/10.1016/j.watres.2019.02.042.

Bivins, A., Crank, K., Greaves, J., North, D., Wu, Z., Bibby, K., 2020. Cross-assembly phage and pepper Mild Mottle virus as viral water quality monitoring tools – potential, research gaps, and way forward. Curr. Opin. Environ. Sci. Heal. 16, 54–61. https://doi.org/10.1016/j.coesh.2020.02.001.

Booton, R.D., Meeyai, A., Alhusein, N., Buller, H., Feil, E., Lambert, H., Mongkolsuk, S., Pitchforth, E., Reyher, K.K., Sakcamduang, W., Satayavivad, J., Singer, A.C., Sringernyuang, L., Thamlikitkul, V., Vass, L., Avison, M.B., Turner, K.M.E., 2021. One Health drivers of antibacterial resistance : quantifying the relative impacts of human , animal and environmental use and transmission. One Heal 12, 100220.

Brown, P.C., Borowska, E., Peschke, R., Schwartz, T., Horn, H., 2020. Decay of elevated antibiotic resistance genes in natural river sediments after sedimentation of wastewater particles. Sci. Total Environ. 705, 1–9. https://doi.org/10.1016/j.scitotenv.2019.135861.

Bustin, S.A., Benes, V., Garson, J.A., Hellemans, J., Huggett, J.F., Kubista, M., Mueller, R. D., Nolan, T., Pfaffl, M.W., Shipley, G.L., Vandesompele, J., Wittwer, C.T., 2009. The MIQE guidelines: Minimum information for publication of quantitative real-time PCR experiments. Clin. Chem. 55, 611–622. https://doi.org/10.1373/clinchem.2008.112797.

Cacace, D., Fatta-Kassinos, D., Manaia, C.M., Cytryn, E., Kreuzinger, N., Rizzo, L., Karaolia, P., Schwartz, T., Alexander, J., Merlin, C., Garelick, H., Schmitt, H., de Vries, D., Schwermer, C.U., Meric, S., Ozkal, C.B., Pons, M.-N., Kneis, D., Berendonk, T.U., 2019. Antibiotic resistance genes in treated wastewater and in the receiving water bodies: a pan-European survey of urban settings. Water Res. 162, 320–330. https://doi.org/10.1016/j.watres.2019.06.039.

Calero-Caceres, W., Muniesa, M., 2016. Persistence of naturally occurring antibiotic resistance genes in the bacteria and bacteriophage fractions of wastewater. Water Res. 95, 11–18. https://doi.org/10.1016/j.watres.2016.03.006.

Calero-Caceres, W., Mendez, J., Martin-Diaz, J., Muniesa, M., 2017. The occurrence of antibiotic resistance genes in a Mediterranean river and their persistence in the riverbed sediment. Environ. Pollut. 223, 384–394. https://doi.org/10.1016/j.envpol.2017.01.035.

Chen, J., Zhang, Z., Lei, Z., Shimizu, K., Yao, P., Su, Z., Wen, D., 2020. Occurrence and distribution of antibiotic resistance genes in the coastal sediments of effluent-receiving areas of WWTPs, China. Bioresour. Technol. Reports 11, 100511. https://doi.org/10.1016/j.biteb.2020.100511.

Chen, H., Liu, C., Li, Y., Teng, Y., 2021. Integrating metagenomic and bayesian analyses to evaluate the performance and confidence of CrAssphage as an indicator for tracking human sewage contamination in China. Environ. Sci. Technol. 55, 4992–5000. https://doi.org/10.1021/acs.est.1c00071.

Chu, B.T.T., Petrovich, M.L., Chaudhary, A., Wright, D., Murphy, B., Wells, G., Poretsky, R., 2018. Metagenomics reveals the impact of wastewater treatment plants on the dispersal of microorganisms and genes in aquatic sediments. Appl. Environ. Microbiol. 84, 17 e02168.

Crank, K., Li, X., North, D., Ferraro, G.B., Iaconelli, M., Mancini, P., Rosa, G. La, Bibby, K., 2020. CrAssphage abundance and correlation with molecular viral markers in Italian wastewater. Water Res. 184, 116161. https://doi.org/10.1016/j.watres.2020.116161.

Davis, B.C., Riquelme, M.V., Ramirez-toro, G., Bandaragoda, C., Garner, E., Rhoads, W.J., Vikesland, P., Pruden, A., 2020. Demonstrating an integrated antibiotic resistance gene surveillance approach in Puerto Rican watersheds post-Hurricane Maria. Environ. Sci. Technol. 54, 15108–15119. https://doi.org/10.1021/acs.est.0c05567.

Divya, S.P., Hatha, A.A.M., 2019. Screening of tropical estuarine water in south-west coast of India reveals emergence of ARGs-harboring hypervirulent Escherichia coli of global significance. Int. J. Hyg Environ. Health 222, 235–248. https://doi.org/10.1016/j.ijheh.2018.11.002.

Drali, R., Berrazeg, M., Zidouni, L.L., Hamitouche, F., Abbas, A.A., Deriet, A., Mouffok, F., 2018. Emergence of mcr-1 plasmid-mediated colistin-resistant Escherichia coli isolates from seawater. Sci. Total Environ. 642, 90–94. https://doi.org/10.1016/j.scitotenv.2018.05.387.

Dutilh, B.E., Cassman, N., McNair, K., Sanchez, S.E., Silva, G.G.Z., Boling, L., Barr, J.J., Speth, D.R., Seguritan, V., Aziz, R.K., Felts, B., Dinsdale, E.A., Mokili, J.L., Edwards, R.A., 2014. A highly abundant bacteriophage discovered in the unknown

sequences of human faecal metagenomes. Nat. Commun. 5, 1–11. https://doi.org/10.1038/ncomms5498.
D'Costa, V.M., King, C.E., Kalan, L., Morar, M., Sung, W.W.L., Schwarz, C., Froese, D., Zazula, G., Calmels, F., Debruyne, R., Golding, G.B., Poinar, H.N., Wright, G.D., 2011. Antibiotic resistance is ancient. Nature 477, 457–461. https://doi.org/10.1038/nature10388.
European Commission, 2017. One Health Action Plan against Antimicrobial Resistance (AMR).
FAO, 2016. The FAO Action Plan on Antimicrobial Resistance 2016-2020. https://doi.org/10.1016/S2213-2600(19)30031-1.
Fernandes, M.R., Sellera, F.P., Esposito, F., Sabino, C.P., Cerdeira, L., Lincopan, N., 2017. Colistin-resistant mcr-1-positive Escherichia coli on public beaches, an infectious threat emerging in recreational waters. Antimicrob. Agents Chemother. 61, 7–10.
Fresia, P., Antelo, V., Salazar, C., Giménez, M., D'Alessandro, B., Afshinnekoo, E., Mason, C., Gonnet, G.H., Iraola, G., 2019. Urban metagenomics uncover antibiotic resistance reservoirs in coastal beach and sewage waters. Microbiome 7, 1–9. https://doi.org/10.1186/s40168-019-0648-z.
Furlan, J.P.R., dos Santos, L.D.R., Ramos, M.S., Gallo, I.F.L., Stehling, E.G., 2020. Presence of colistin resistance mcr-4 gene and clinically relevant antimicrobial resistance genes in sand samples from a public beach. Water. Air. Soil Pollut. 231 https://doi.org/10.1007/s11270-020-04707-7.
Gao, P., Mao, D., Luo, Y., Wang, L., Xu, B., Xu, L., 2012. Occurrence of sulfonamide and tetracycline-resistant bacteria and resistance genes in aquaculture environment. Water Res. 46, 2355–2364. https://doi.org/10.1016/j.watres.2012.02.004.
Gao, Q., Li, Y., Qi, Z., Yue, Y., Min, M., Peng, S., Shi, Z., Gao, Y., 2018. Diverse and abundant antibiotic resistance genes from mariculture sites of China's coastline. Sci. Total Environ. 630, 117–125. https://doi.org/10.1016/j.scitotenv.2018.02.122.
Gillings, M.R., Gaze, W.H., Pruden, A., Smalla, K., Tiedje, J.M., Zhu, Y.G., 2015. Using the class 1 integron-integrase gene as a proxy for anthropogenic pollution. ISME J. 9, 1269–1279. https://doi.org/10.1038/ismej.2014.226.
Griffin, D.W., Banks, K., Gregg, K., Shedler, S., Walker, B.K., 2020. Antibiotic resistance in marine microbial communities proximal to a Florida sewage outfall system. Antibiotics 9, 1–8.
Guo, J., Li, J., Chen, H., Bond, P.L., Yuan, Z., 2017. Metagenomic analysis reveals wastewater treatment plants as hotspots of antibiotic resistance genes and mobile genetic elements. Water Res. 123, 468–478. https://doi.org/10.1016/j.watres.2017.07.002.
Haramoto, E., Kitajima, M., Katayama, H., Ohgaki, S., 2010. Real-time PCR detection of adenoviruses, polyomaviruses, and torque teno viruses in river water in Japan. Water Res. 44, 1747–1752. https://doi.org/10.1016/j.watres.2009.11.043.
Haramoto, E., Kitajima, M., Hata, A., Torrey, J.R., Masago, Y., Sano, D., Katayama, H., 2018. A review on recent progress in the detection methods and prevalence of human enteric viruses in water. Water Res. 135, 168–186. https://doi.org/10.1016/j.watres.2018.02.004.
Harnisz, M., Kiedrzyńska, E., Kiedrzyński, M., Korzeniewska, E., Czatzkowska, M., Koniuszewska, I., Jóźwik, A., Szklarek, S., Niestępski, S., Zalewski, M., 2020. The impact of WWTP size and sampling season on the prevalence of antibiotic resistance genes in wastewater and the river system. Sci. Total Environ. 741 https://doi.org/10.1016/j.scitotenv.2020.140466.
Harwood, V.J., Staley, C., Badgley, B.D., Borges, K., Korajkic, A., 2014. Microbial source tracking markers for detection of fecal contamination in environmental waters: relationships between pathogens and human health outcomes. FEMS Microbiol. Rev. 38, 1–40. https://doi.org/10.1111/1574-6976.12031.
Helsel, D.R., 2012. Statistics for Censored Environmental Data Using Minitab and R, second. John Wiley & Sons, Inc., Hoboken, New Jersey, United States.
Hiller, C.X., Hübner, U., Fajnorova, S., Schwartz, T., Drewes, J.E., 2019. Antibiotic microbial resistance (AMR) removal efficiencies by conventional and advanced wastewater treatment processes: a review. Sci. Total Environ. 685, 596–608. https://doi.org/10.1016/j.scitotenv.2019.05.315.
Jang, H.M., Kim, Y.B., Choi, S., Lee, Y., Shin, S.G., Unno, T., Kim, Y.M., 2018. Prevalence of antibiotic resistance genes from effluent of coastal aquaculture, South Korea. Environ. Pollut. 233, 1049–1057. https://doi.org/10.1016/j.envpol.2017.10.006.
Jutkina, J., Marathe, N.P., Flach, C., Larsson, D.G.J., 2018. Antibiotics and common antibacterial biocides stimulate horizontal transfer of resistance at low concentrations. Sci. Total Environ. 616–617, 172–178. https://doi.org/10.1016/j.scitotenv.2017.10.312.
Karkman, A., Pärnänen, K., Larsson, D.G.J., 2019. Fecal pollution can explain antibiotic resistance gene abundances in anthropogenically impacted environments. Nat. Commun. 10, 1–8. https://doi.org/10.1101/341487.
Kirs, M., Caffaro-filho, R.A., Wong, M., Harwood, V.J., Moravcik, P., Fujioka, S., 2016. Human-associated Bacteroides spp. and human polyomaviruses as microbial source tracking markers in Hawaii. Appl. Environ. Microbiol. 82, 6757–6767. https://doi.org/10.1128/AEM.01959-16.
Koczura, R., Mokracka, J., Taraszewska, A., Łopacinska, N., 2016. Abundance of class 1 integron-integrase and sulfonamide resistance genes in river water and sediment is affected by anthropogenic pressure and environmental factors. Microb. Ecol. 72, 909–916. https://doi.org/10.1007/s00248-016-0843-4.
Kongprajug, A., Mongkolsuk, S., Sirikanchana, K., 2019. CrAssphage as a potential human sewage marker for microbial source tracking in Southeast Asia. Environ. Sci. Technol. Lett. 6, 159–164. https://doi.org/10.1021/acs.estlett.9b00041.
Kongprajug, A., Chyerochana, N., Mongkolsuk, S., Sirikanchana, K., 2020. Effect of quantitative polymerase chain reaction data analysis using sample amplification efficiency on microbial source tracking assay performance and source attribution. Environ. Sci. Technol. 54, 8232–8244.
Kongprajug, A., Chyerochana, N., Rattanakul, S., Denpetkul, T., Sangkaew, W., Somnark, P., Patarapongsant, Y., Tomyim, K., Sresang, M., Mongkolsuk, S., Sirikanchana, K., 2021a. Integrated analyses of fecal indicator bacteria , microbial source tracking markers , and pathogens for Southeast Asian beach water quality assessment. Water Res. 203, 117479.
Kongprajug, A., Denpetkul, T., Chyerochana, N., Mongkolsuk, S., Sirikanchana, K., 2021b. Human fecal pollution and associated microbial risks in a coastal industrial-residential mixed use watershed. Front. Microbiol. 12 https://doi.org/10.3389/fmicb.2021.647602.
Le, T., Ng, C., Tran, N.H., Chen, H., Gin, K.Y., 2018. Removal of antibiotic residues, antibiotic resistant bacteria and antibiotic resistance genes in municipal wastewater by membrane bioreactor systems. Water Res. https://doi.org/10.1016/j.watres.2018.08.060.
Lekunberri, I., Villagrasa, M., Balcázar, J.L., Borrego, C.M., 2017. Contribution of bacteriophage and plasmid DNA to the mobilization of antibiotic resistance genes in a river receiving treated wastewater discharges. Sci. Total Environ. 601–602, 206–209. https://doi.org/10.1016/j.scitotenv.2017.05.174.
Leng, Y., Xiao, H., Li, Z., Wang, J., 2020. Tetracyclines, sulfonamides and quinolones and their corresponding resistance genes in coastal areas of Beibu Gulf. China. Sci. Total Environ. 714, 136899. https://doi.org/10.1016/j.scitotenv.2020.136899.
Li, L.G., Huang, Q., Yin, X., Zhang, T., 2020. Source tracking of antibiotic resistance genes in the environment — challenges, progress, and prospects. Water Res. 185, 116127. https://doi.org/10.1016/j.watres.2020.116127.
Liang, C., Wei, D., Zhang, S., Ren, Q., Shi, J., Liu, L., 2021. Removal of antibiotic resistance genes from swine wastewater by membrane filtration treatment. Ecotoxicol. Environ. Saf. 210, 111885. https://doi.org/10.1016/j.ecoenv.2020.111885.
Liu, S.-S., Qu, H.-M., Yang, D., Hu, H., Liu, W.-L., Qiu, Z.-G., Hou, A.-M., Guo, J., Li, J.-W., Shen, Z.-Q., Jin, M., 2018. Chlorine disinfection increases both intracellular and extracellular antibiotic resistance genes in a full-scale wastewater treatment plant. Water Res. 136, 131–136. https://doi.org/10.1016/j.watres.2018.02.036.
Lu, J., Zhang, Y., Wu, J., 2020. Continental-scale spatio-temporal distribution of antibiotic resistance genes in coastal waters along coastline of China. Chemosphere 247, 125908. https://doi.org/10.1016/j.chemosphere.2020.125908.
Macedo, G., Hernandez-leal, L., Maas, P. Van Der, Heederik, D., Mevius, D., Schmitt, H., 2020. The impact of manure and soil texture on antimicrobial resistance gene levels in farmlands and adjacent ditches. Sci. Total Environ. 737, 139563. https://doi.org/10.1016/j.scitotenv.2020.139563.
Mann, D., Jaafar, H., Kassem, I., 2020. Dissemination of multidrug-resistant Escherichia coli harboring the mobile colistin resistance gene mcr-1.1 on transmissible plasmids in the Mediterranean Sea. J. Glob. Antimicrob. Resist. 22, 84–86. https://doi.org/10.1016/j.jgar.2020.05.007.
Mazhar, S.H., Li, X., Rashid, A., Su, Junming, Xu, J., Daniel, A., Su, Jian-qiang, Wu, Y., Zhu, Y., Gui, S., Feng, R., Rensing, C., 2021. Co-selection of antibiotic resistance genes , and mobile genetic elements in the presence of heavy metals in poultry farm environments. Sci. Total Environ. 755, 142702. https://doi.org/10.1016/j.scitotenv.2020.142702.
McKinney, C.W., Loftin, K.A., Meyer, M.T., Davis, J.G., Pruden, A., 2010. Tet and sul antibiotic resistance genes in livestock lagoons of various operation type, configuration, and antibiotic occurrence. Environ. Sci. Technol. 44, 6102–6109. https://doi.org/10.1021/es9038165.
McQuaig, S.M., Scott, T.M., Lukasik, J.O., Paul, J.H., Harwood, V.J., 2009. Quantification of human polyomaviruses JC virus and BK virus by TaqMan quantitative PCR and comparison to other water quality indicators in water and fecal Samples. Appl. Environ. Microbiol. 75, 3379–3388. https://doi.org/10.1128/AEM.02302-08.
Ministry of Public Health Ministry of Agriculture and Cooperatives, 2020. National Strategic Plan on Antimicrobial Resistance 2017-2021 Thailand: at a Glance.
National Environment Board, 2017. Notification of the national environmental board, No. 134/288, B.E. 2560 (2017) entitled coastal water quality standards (in Thai). R. Gov. Gaz. 134, 28–37.
Navedo, J.G., Araya, V., Verdugo, C., 2021. Upraising a silent pollution: antibiotic resistance at coastal environments and transference to long-distance migratory shorebirds. Sci. Total Environ. 777, 146004. https://doi.org/10.1016/j.scitotenv.2021.146004.
Ng, C., Chen, H., Goh, S.G., Haller, L., Wu, Z., Charles, F.R., Trottet, A., Gin, K., 2018a. Microbial water quality and the detection of multidrug resistant E. coli and antibiotic resistance genes in aquaculture sites of Singapore. Mar. Pollut. Bull. 135, 475–480. https://doi.org/10.1016/j.marpolbul.2018.07.055.
Ng, C., Tay, M., Tan, B., Le, T.H., Haller, L., Chen, H., Koh, T.H., Barkham, T.M.S., Thompson, J.R., Gin, K.Y.H., 2018b. Characterization of metagenomes in urban aquatic compartments reveals high prevalence of clinically relevant antibiotic resistance genes in wastewaters. Front. Microbiol. 9, 1–12. https://doi.org/10.3389/fmicb.2018.00175.
Nguyen, N.T., Liu, M., Katayama, H., Takemura, T., Kasuga, I., 2020. Association of the colistin resistance gene mcr-1 with faecal pollution in water environments in Hanoi. Vietnam. Lett. Appl. Microbiol. 1–8 https://doi.org/10.1111/lam.13421.
Nguyen, A.Q., Vu, H.P., Nguyen, L.N., Wang, Q., Djordjevic, S.P., Donner, E., Yin, H., Nghiem, L.D., 2021. Monitoring antibiotic resistance genes in wastewater treatment: current strategies and future challenges. Sci. Total Environ. 783, 146964. https://doi.org/10.1016/j.scitotenv.2021.146964.
Niu, Z.G., Zhang, K., Zhang, Y., 2016. Occurrence and distribution of antibiotic resistance genes in the coastal area of the Bohai Bay, China. Mar. Pollut. Bull. 107, 245–250. https://doi.org/10.1016/j.marpolbul.2016.03.064.
Oliveira, A.J.F.C. de, Pinhata, J.M.W., 2008. Antimicrobial resistance and species composition of Enterococcus spp . isolated from waters and sands of marine recreational beaches in Southeastern Brazil. Water Res. 42, 2242–2250. https://doi.org/10.1016/j.watres.2007.12.002.

Pal, C., Bengtsson-Palme, J., Kristiansson, E., Larsson, D.G.J., 2015. Co-occurrence of resistance genes to antibiotics, biocides and metals reveals novel insights into their co-selection potential. BMC Genom. 16, 964. https://doi.org/10.1186/s12864-015-2153-5.

Pärnänen, K.M.M., Narciso-da-rocha, C., Kneis, D., Berendonk, T.U., Cacace, D., Do, T.T., Elpers, C., Fatta-kassinos, D., Henriques, I., Jaeger, T., Karkman, A., Martinez, J.L., Michael, S.G., Michael-kordatou, I., Sørum, H., Stedtfeld, R.D., Tiedje, J.M., Varela, S., Giustina, D., 2019. Antibiotic resistance in European wastewater treatment plants mirrors the pattern of clinical antibiotic resistance prevalence. Sci. Adv. 5, 1–10.

Perron, G.G., Whyte, L., Turnbaugh, P.J., Goordial, J., Hanage, P., Dantas, G., Desai, M. M., 2015. Functional characterization of bacteria isolated from ancient Arctic soil exposes Diverse resistance mechanisms to modern antibiotics. PLoS One 10, e0069533. https://doi.org/10.1371/journal.pone.0069533.

Petcharat, T., Kongprajug, A., Chyerochana, N., Sangkaew, W., Mongkolsuk, S., Sirikanchana, K., 2020. Assessing human-specific CrAssphage recovery after acidification-filtration concentrating method in environmental water. Water Environ. Res. 92, 35–41. https://doi.org/10.1002/wer.1209.

R Core Team, 2019. R: A Language and Environment for Statistical Computing. R Found. Stat. Comput., Vienna, Austria. https://www.R-project.org/.

Rachmadi, A.T., Torrey, J.R., Kitajima, M., 2016. Human polyomavirus : Advantages and limitations as a human-specific viral marker in aquatic environments. Water Res. 105, 456–469. https://doi.org/10.1016/j.watres.2016.09.010.

Reynolds, L.J., Sala-Comorera, L., Martin, N.A., Nolan, T.M., Stephens, J.H., Gitto, A., O'Hare, G.M.P., O'Sullivan, J.J., Meijer, W.G., 2020. Correlation between antimicrobial resistance and faecal contamination in small urban streams and bathing waters. Sci. Total Environ. 739, 140242. https://doi.org/10.1016/j.scitotenv.2020.140242.

Rizzo, L., Manaia, C., Merlin, C., Schwartz, T., Dagot, C., Ploy, M.C., Michael, I., Fatta-kassinos, D., 2013. Urban wastewater treatment plants as hotspots for antibiotic resistant bacteria and genes spread into the environment : a review. Sci. Total Environ. 447, 345–360.

Rodríguez, E.A., Ramirez, D., Balcázar, J.L., Jiménez, J.N., 2021. Metagenomic analysis of urban wastewater resistome and mobilome: a support for antimicrobial resistance surveillance in an endemic country. Environ. Pollut. https://doi.org/10.1016/j.envpol.2021.116736.

Sala-Comorera, L., Reynolds, L.J., Martin, N.A., Pascual-Benito, M., Stephens, J.H., Nolan, T.M., Gitto, A., O'Hare, G.M.P., O'Sullivan, J.J., Garcia-Aljaro, C., Meijer, W. G., 2021. crAssphage as human molecular marker to evaluate temporal and spatial variability in faecal contamination of urban marine bathing waters. Sci. Total Environ. 789, 147828. https://doi.org/10.1016/j.scitotenv.2021.147828.

Sangkaew, W., Kongprajug, A., Chyerochana, N., Ahmed, W., Rattanakul, S., Denpetkul, T., Mongkolsuk, S., Sirikanchana, K., 2021. Performance of viral and bacterial genetic markers for sewage pollution tracking in tropical Thailand. Water Res. 190, 116706. https://doi.org/10.1016/j.watres.2020.116706 WR 116706.

Singer, A.C., Shaw, H., Rhodes, V., Hart, A., 2016. Review of antimicrobial resistance in the environment and its relevance to environmental regulators. Front. Microbiol. 7, 1–22. https://doi.org/10.3389/fmicb.2016.01728.

Singer, A.C., Xu, Q., Keller, V.D.J., 2019. Translating antibiotic prescribing into antibiotic resistance in the environment : a hazard characterisation case study. PLoS One.

Sivaganesan, M., Haugland, R.A., Chern, E.C., Shanks, O.C., 2010. Improved strategies and optimization of calibration models for real-time PCR absolute quantification. Water Res. 44, 4726–4735. https://doi.org/10.1016/j.watres.2010.07.066.

Stachler, E., Kelty, C., Sivaganesan, M., Li, X., Bibby, K., Shanks, O.C., 2017. Quantitative crAssphage PCR assays for human fecal pollution measurement. Environ. Sci. Technol. 51, 9146–9154. https://doi.org/10.1021/acs.est.7b02703.

Stachler, E., Akyon, B., Aquino De Carvalho, N., Ference, C., Bibby, K., 2018. Correlation of crAssphage-based qPCR markers with culturable and molecular indicators of human fecal pollution in an impacted urban watershed. Environ. Sci. Technol. 52, 7505–7512. https://doi.org/10.1021/acs.est.8b00638.

Stachler, E., Crank, K., Bibby, K., 2019. Co-occurrence of crAssphage with antibiotic resistance genes in an impacted urban watershed. Environ. Sci. Technol. Lett. 6, 216–221. https://doi.org/10.1021/acs.estlett.9b00130.

Stanton, I.C., Murray, A.K., Zhang, L., Snape, J., Gaze, W.H., 2020. Evolution of antibiotic resistance at low antibiotic concentrations including selection below the minimal selective concentration. Commun. Biol. 3, 1–11. https://doi.org/10.1038/s42003-020-01176-w.

Subirats, J., Royo, E., Balcázar, J.L., Borrego, C.M., 2017. Real-time PCR assays for the detection and quantification of carbapenemase genes (bla KPC, bla NDM, and bla OXA-48) in environmental samples. Environ. Sci. Pollut. Res. 24, 6710–6714. https://doi.org/10.1007/s11356-017-8426-6.

United Nations, 2017. Factsheet: People and Oceans. The Ocean Conference. United Nation, New York, 5-9 June 2017.

Veterinary Medicines Directorate, 2019. UK One Health Report: Joint Report on Antibiotic Use and Antibiotic Resistance, 2013 - 2017. Veterinary Medicines Directorate., New Haw, Addlestone.

von Wintersdorff, C.J.H., Penders, J., van Niekerk, J.M., 2016. Dissemination of antimicrobial resistance in microbial ecosystems through horizontal gene transfer. Front. Microbiol. 7, 1–10. https://doi.org/10.3389/fmicb.2016.00173.

Wang, J., Chu, L., Wojnárovits, L., Takács, E., 2020. Occurrence and fate of antibiotics, antibiotic resistant genes (ARGs) and antibiotic resistant bacteria (ARB) in municipal wastewater treatment plant: an overview. Sci. Total Environ. 744, 140997. https://doi.org/10.1016/j.scitotenv.2020.140997.

Wang, J., Wang, J., Zhao, Z., Chen, J., Lu, H., Liu, G., Zhou, J., Guan, X., 2017. PAHs accelerate the propagation of antibiotic resistance genes in coastal water microbial community. Environ. Pollut. 231, 1145–1152. https://doi.org/10.1016/j.envpol.2017.07.067.

Ward, L.M., Ghaju Shrestha, R., Tandukar, S., Sherchand, J.B., Haramoto, E., Sherchan, S.P., 2020. Evaluation of CrAssphage marker for tracking fecal contamination in river water in Nepal. Water. Air. Soil Pollut 231, 4–10. https://doi.org/10.1007/s11270-020-04648-1.

WHO, 2014. Antimicrobial Resistance: an Emerging Water, Sanitation and Hygiene Issue Briefing Note. https://doi.org/10.13140/RG.2.2.24776.32005. WHO/FWC/WSH/14.07.

WHO, 2017. Global antimicrobial resistance surveillance system (GLASS) report. Who. https://doi.org/10.1016/ISBN.978-92-4-151344-9.

World Health Organization, 2015. Global Action Plan on Antimicrobial Resistance. World Health Organisation.

Xue, X., Wang, L., Xing, H., Zhao, Y., Li, X., Wang, G., Wang, Z., 2021. Characteristics of phytoplankton-zooplankton communities and the roles in the transmission of antibiotic resistance genes under the pressure of river contamination. Sci. Total Environ. 780, 146452. https://doi.org/10.1016/j.scitotenv.2021.146452.

Zhang, Q., Gallard, J., Wu, B., Harwood, V.J., Sadowsky, M.J., Hamilton, K.A., Ahmed, W., 2019. Synergy between quantitative microbial source tracking (qMST) and quantitative microbial risk assessment (QMRA): a review and prospectus. Environ. Int. 130, 1–10. https://doi.org/10.1016/j.envint.2019.03.051.

Zhang, Y., Wang, J., Lu, J., Wu, J., 2020. Antibiotic resistance genes might serve as new indicators for wastewater contamination of coastal waters: spatial distribution and source apportionment of antibiotic resistance genes in a coastal bay. Ecol. Indicat. 114, 106299. https://doi.org/10.1016/j.ecolind.2020.106299.

Zheng, D., Yin, G., Liu, M., Chen, C., Jiang, Y., Hou, L., Zheng, Y., 2021. A systematic review of antibiotics and antibiotic resistance genes in estuarine and coastal environments. Sci. Total Environ. 777, 146009. https://doi.org/10.1016/j.scitotenv.2021.146009.

Zhu, Y., Zhao, Y., Li, B., Huang, C., Zhang, S., Yu, S., Chen, Y., Zhang, T., Gillings, M.R., Su, J., 2017. Continental-scale pollution of estuaries with antibiotic resistance genes. Nat. Microbiol. 2, 1–7. https://doi.org/10.1038/nmicrobiol.2016.270.

International Journal of Hygiene and Environmental Health 238 (2021) 113862

Contents lists available at ScienceDirect

International Journal of Hygiene and Environmental Health

journal homepage: www.elsevier.com/locate/ijheh

Predicting childhood lead exposure at an aggregated level using machine learning

G.P. Lobo *, B. Kalyan, A.J. Gadgil

Department of Civil and Environmental Engineering, University of California, Berkeley, 94720, United States

ARTICLE INFO

Keywords:
Lead poisoning
Machine learning
Lead
Environmental exposure
Aggregated data

ABSTRACT

Childhood lead exposure affects over 500,000 children under 6 years old in the US; however, only 14 states recommend regular universal blood screening. Several studies have reported on the use of predictive models to estimate lead exposure of individual children, albeit with limited success: lead exposure can vary greatly among individuals, individual data is not easily accessible, and models trained in one location do not always perform well in another. We report on a novel approach that uses machine learning to accurately predict elevated Blood Lead Levels (BLLs) in large groups of children, using aggregated data. To that end, we used publicly available zip code and city/town BLL data from the states of New York (n = 1642, excluding New York City) and Massachusetts (n = 352), respectively. Five machine learning models were used to predict childhood lead exposure by using socioeconomic, housing, and water quality predictive features. The best-performing model was a Random Forest, with a 10-fold cross validation ROC AUC score of 0.91 and 0.85 for the Massachusetts and New York datasets, respectively. The model was then tested with New York City data and the results compared to measured BLLs at a borough level. The model yielded predictions in excellent agreement with measured data: at a city level it predicted elevated BLL rates of 1.72% for the children in New York City, which is close to the measured value of 1.73%. Predictive models, such as the one presented here, have the potential to help identify geographical hotspots with significantly large occurrence of elevated lead blood levels in children so that limited resources may be deployed to those who are most at risk.

1. Introduction

Childhood lead exposure is a problem that affects over 500,000 children under 6 years of age in the US (Hauptman et al., 2017). There is no safe level of lead in the bloodstream (Vorvolakos et al., 2016) and even lead levels of 1 μg dL^{-1} have been linked to permanent and irreversible cognitive damage in children under age 6 (Lanphear et al., 2000; Schwartz, 1994). Elevated Blood Lead Levels (BLLs) in US children often result from exposure to lead in paint, soil, dust, and water (Gould, 2009; Mielke and Reagan, 1998; Roy and Edwards, 2019). However, children with elevated BLLs are not evenly distributed in society: those living below the poverty line are four times more likely to have elevated BLLs than their richer counterparts (Vivier et al., 2011). Non-Hispanic Black children are particularly at risk (Whitehead and Buchanan, 2019).

The lifetime social cost of childhood lead exposure (lead blood levels over 1 μg dL^{-1}) is estimated to be $50,000 USD per child (Muennig, 2009). This cost includes all medical costs, loss in IQ, special education, and increased crime rates, among other consequences of low-level lead exposure. However, this estimate does not include the cost of other adverse effects, including immune, cardiovascular, renal, and developmental effects (U.S. Department of Health and Human Services, 2012). Thus, childhood lead exposure in the US is a $25 billion problem (cumulative cost) that not only permanently hinders the livelihood of thousands of children, but is also a preventable, yet persistent, matter of social and environmental justice (Ettinger et al., 2019).

Identifying children at risk is challenging because data on housing with lead-based paint and plumbing components, or with lead-contaminated soils and dust are scarce (Cattle et al., 2002; Mielke, 1999; Triantafyllidou and Edwards, 2012). Instead, socioeconomic features are often used as predictors of elevated BLLs as they account for the unfortunate fact that poor minorities are more likely to live in older housing with multiple lead sources (lead paint and plumbing were commonly used in housing prior to 1978) (Marshall et al., 2020).

These socioeconomic features have been integrated into statistical models meant to predict the risk of lead exposure of individuals and

* Corresponding author. 410 O'Brien Hall, Berkeley, CA, 94720, United States.
E-mail address: gplobo@berkeley.edu (G.P. Lobo).

https://doi.org/10.1016/j.ijheh.2021.113862
Received 12 July 2021; Received in revised form 8 October 2021; Accepted 13 October 2021
Available online 18 October 2021

communities; however, their success has been limited. For instance, Taylor et al. (2013) found that, while socioeconomic factors are correlated to elevated BLLs in pregnant women, using a logistic regression to predict their individual exposure risk did not provide accurate results ($R^2 = 0.1$). Bierkens et al. (2011) concluded that even if environmental lead concentrations in air, soil, and water are known, linear regressions are not suited to estimate the average risk of lead exposure of select EU countries. This is due to the multifactorial, non-linear, and region-specific nature of the problem, compounded by the lack of available data (Lanphear et al., 1998).

Machine learning is particularly well-suited for complex nonlinear problems in which traditional statistical methods fail. Machine learning has been used to predict lead concentrations in air (Sethi and Mittal, 2019), water (Chojnacki et al., 2017), and soil (Zhang et al., 2020), as well as the likelihood of housing hazards, including lead paint (Ye et al., 2019). However, this approach has seldom been tested to predict the risk of childhood lead exposure. To the best of our knowledge, only two machine learning models have been reported in literature for this purpose. Potash et al. (2015) developed a gradient boosting model using 2.5 million BLL tests from Chicago, IL, and household characteristics, including year of construction, physical condition, and number of housing units, among others. Socio-demographic characteristics were also included. Their best performing model resulted in a precision of 0.39 and a recall of 0.42 for individual children, (see section 2.4 for technical definitions of the terms precision and recall). Another study by Potash et al. (2020) used a random forest model to predict childhood elevated BLLs. Their best-performing model had a ROC AUC of 0.69 (see section 2.4 for a technical definition of ROC AUC). The performance of these two pioneering machine learning models for childhood BLL predictions is better than that of traditional statistical methods; however, it is still below of that of other models used in other public health applications (Dos Santos et al., 2019). This is likely explained by the high resolution of the predictions, in which the risk of lead exposure of each individual child is predicted. Childhood lead exposure usually involves many environmental factors specific to each child that are difficult to measure (Lanphear et al., 2002), thus, predicting individual lead blood levels is challenging. Moreover, access to individual-based datasets is often limited, particularly for healthcare, where data are protected by patients' privacy laws (Wojtusiak and Baranova, 2011). This makes it hard not only to validate existing models, but to extend their use to locations outside of individual cities where these models are usually trained and tested.

In the context of designing strategies to prevent childhood lead exposure, such as large-scale lead blood testing or source removal programs, using individual-based models with modest predictive power to allocate resources might not provide optimal results. These programs often involve conducting lead blood tests and source removal at a neighborhood scale, and not on an individual basis (Billings and Schnepel, 2017; Magavern, 2018; Zahran et al., 2020). Thus, a model meant to allocate resources for lead blood testing and removal programs should be able to accurately identify geographical areas at risk rather than much less accurately identify individuals at risk (of course, accurately identifying all individuals with elevated BLLs would be even more preferable; however, no model is currently capable of this).

We hypothesize that using spatially aggregated data (e.g., zip code or city) could significantly improve the performance of existing models meant to predict elevated BLL in children, while still being valuable for designing strategies to prevent childhood lead exposure at a geographically large scale. This is because aggregated data often convey population trends that smoothen out the variability among individuals living under similar conditions, decreasing the noise of individual-based datasets (Rushton, 2003). Moreover, aggregated datasets are often public and readily available (Wojtusiak and Baranova, 2011), increasing data access, transparency, and restrictions on publishing results. Of course, the aggregation level should be relevant for the problem at hand: using a model that predicts city-wide risk of childhood lead exposure might not be as useful as a model that predicts zip codes at risk when designing a program meant to identify neighborhoods where children have elevated BLLs.

To date, there are no published studies that have attempted to process relevant features of aggregated BLL data to predict geographical areas at risk of childhood lead exposure. Thus, to our knowledge, prior literature is unclear whether BLL data aggregation increases the accuracy of childhood BLL predictive models at a spatially aggregated scale.

We report here on the use of machine learning to predict the risk of elevated BLLs in children at a spatially aggregated level. Using zip code and community-level socioeconomic and environmental data, we predicted the risk of childhood lead exposure for the states of New York and Massachusetts. This statistical model is *not* meant to provide a mechanistic understanding of how children are exposed to lead, but to help identify areas where they might be exposed to lead so that limited resources may be allocated more effectively.

2. Materials and methods

2.1. Study sites

New York and Massachusetts were chosen as study sites because they are two of the few states with publicly available BLL surveys in the US. The percentage of children under 6 years of age with elevated BLLs were obtained for 1642 zip codes in New York from the New York State Department of Health for the year 2015 (New York State Department of Health, 2015). These data were missing for all 178 zip codes in New York City because this city belongs to a separate health jurisdiction, NYC Health. In this study we used the Centers for Disease Control and Prevention (CDC) reference value of 5 μg dL^{-1} to determine whether children had elevated BLLs or not. We chose this value because it is the current CDC guideline and because the datasets provided by both states report only the number of children with BLL between 0 and 5, 5–10 and over 10 μg dL^{-1}. This reference value of 5 μg dL^{-1} was adopted in 2012 by the CDC based on the 97.5th percentile of the National Health and Nutrition Examination Survey (NHANES) blood lead distribution in children ages 1–5 years (CDC, 2021). Although more recent lead blood data suggest that this 97.5th percentile is closer to 3.5 μg dL^{-1} (Tsoi et al., 2016), the CDC has not yet updated their guideline value of 5 μg dL^{-1}. In the case of Massachusetts, the percentage of children with elevated BLLs were obtained for all 352 town/cities (also referred to as communities) in the state from the Massachusetts Department of Public Health, also for 2015 (Massachusetts Department of Public Health, 2021a).

We note that not all children within a community or zip code were tested for lead. In this study we assumed that the tested children were representative of all at-risk children within their respective zip codes or cities. BLL testing for children under 3 is mandatory in Massachusetts, after which BLLs are monitored only for children living in at-risk areas (Massachusetts Department of Public Health, 2021). In contrast, New York children are only tested if they are considered to be at risk (New York State Department of Health, 2021). Thus, the datasets used likely overrepresent children with elevated BLLs, which is desirable given the large social cost of failing to identify children at risk of having elevated BLLs.

While other states do report BLLs in children, many of them do so at a county level. Given that the robustness of machine learning models is often dictated by the amount of data used during training, working at a county level will likely not provide enough datapoints per state to develop a robust model. Furthermore, the low resolution of county-level BLLs cannot facilitate narrowly targeted intervention and mitigation strategies.

2.2. Data acquisition

Socioeconomic data for New York and Massachusetts were obtained

from the 2015 American Community Survey (US Census Bureau, 2016). These data include, for each census tract, average income, percentage below the poverty line, percentage of property ownership, race, and ethnicity, among others. These socioeconomic features have been linked to elevated BLLs in numerous studies (Schultz et al., 2017; Trimble, 2016).

The 2015 Housing Price Indices (HPI) for each zip code were also obtained from the Federal Housing Finance Agency. HPIs represent the average price changes in repeat sales or refinancings on the same properties. We included HPI in the model because this index reflects, among many other things, housing construction year, which is an important feature given that old housings are more likely to have lead paint and plumbing (Whitehead and Buchanan, 2019). Housing construction year data were publicly available only for Massachusetts from the Massachusetts Department of Public Health, but not for New York.

Lead levels in drinking water were also obtained for each school in New York and Massachusetts from the New York State Department of Health and the Massachusetts Department of Public Health, respectively. Lead in drinking water in schools is an important source of lead exposure in children (Doré et al., 2018); however, it does not provide information on exposure in children under 4 or 5 years of age (children often start going to school at age 5). To the best of our knowledge, no household lead levels in drinking water at a state level are publicly available.

2.3. Data processing

A schematic overview of the steps taken to process the data and implement the machine learning model, described herein, is shown in Fig. 2. The data described in section 2.3 were combined with the BLL data using Geographic Information Systems (GIS). In the case of the New York dataset, the socioeconomic data were converted from a census tract scale to a zip code level by averaging the tract data within each zip code. The lead water levels in schools were first converted to average values per school district and then each zip code was assigned to a school district based on distance. This was done because not all zip codes have schools. Thus, the New York dataset consisted of 1643 datapoints, where each point corresponded to a zip code and all the associated data (percentage of elevated BLLs and socioeconomic, housing and lead water data, among others) with that geolocation. A total of 46 features were associated with each datapoint.

In the case of the Massachusetts dataset, the socioeconomic data were aggregated from a census tract level to a town/city level by taking the weighted average by population density. The HPI index was aggregated from a zip code level to a town/city level also using a weighted average. On the other hand, lead in drinking water levels in schools were averaged for all schools within a town/city. Thus, the Massachusetts dataset consisted of 352 points, all of which corresponded to towns/cities and their corresponding socioeconomic, demographic and water quality data. A total of 38 features were associated with each datapoint.

Both datasets were further processed by first one-hot-encoding (turning into binary values) all categorical features and by normalizing every feature so that all values range from 0 to 1. Missing values were filled in by using the mean value of each feature (e.g. missing income values were filled in using the average income of every city or zip code). Less than 5% of the data were missing for both New York and Massachusetts datasets.

The BLL data was also binarized by using a variable threshold T and the 5 μg dL^{-1} reference value established by the CDC. In the case of the Massachusetts dataset, a 1% threshold ($T = 1\%$) was established: if over 1% children within a town/city had elevated BLLs (over 5 μg dL^{-1}), then the value was set to 1; otherwise, it was set to 0. In the case of the New York dataset, a 6% threshold ($T = 6\%$) was established: if over 6% children within a zip code had BLLs over 5 μg dL^{-1}, then the value was set to 1; otherwise, it was set to 0. We binarized both datasets differently because of the different resolutions of the data and because the percentage of children with high BLLs per zip code in New York are much higher than the percentage per city in Massachusetts, as shown in Fig. 1.

2.4. Model implementation

Five machine learning models were implemented, and their performance compared using the processed Massachusetts and New York datasets: Random Forest, Logistic Regression, k-Nearest Neighbor (kNN), Decision Trees, and Support Vector Machine (SVM). These models were implemented using the Python *sklearn* package and their hyperparameters (model parameters) optimized using 10-fold cross validation (described below). The process of hyperparameter optimization consisted of iterating through multiple combinations of hyperparameters and finding those that provided the highest cross validation scores. A short description of each of the models, and their optimized hyperparameters are provided in the S.I.

We briefly introduce a method and five metrics used to evaluate machine learning models:

(1) K-fold cross validation is a commonly used method to test how a predictive model will perform in practice. Predictive models are typically calibrated with a "training" data set, and their performance must be tested against data from outside this training set. In cross validation, the original data is separated into k independent (i.e., non-overlapping) subsets and then the model is trained with only k-1 subsets. The trained model is then tested using the withheld subset. This process is repeated k times by successively withholding a different subset for testing each time, effectively creating k instances of the model that is trained and tested using k different training and testing datasets.

(2) The "Receiver Operating Characteristic Area Under the Curve" (ROC AUC) metric, was briefly introduced in Section 1. This metric ranges from 0.5 to 1, is commonly used to evaluate the ability of the model to distinguish between True Positives (TP) and False Positives (FP) for different probability thresholds. Thus, ROC AUC values close to 1 indicate that the model can perfectly distinguish between TP and FP, while values close to 0.5 indicate that the model is no better than random selection. TPs in our case mean that the model predicts that a zip code or town/city has more than T% of children with elevated BLLs, and the measured value for that zip code or town/city is indeed over T%. FP are those cases in which the model predicts that a zip code or town/city has more than T% of children with elevated BLLs, while the actual (measured) value for that zip code or town/city is below T %

(3) The "Precision Recall Area Under the Curve" (PR AUC) metric, which ranges from 0.5 to 1, is typically used to evaluate the ability of the model to distinguish between TP and False Negatives (FN) for different probability thresholds. PR AUC values close to 1 indicate that the model can perfectly distinguish between TPs and FNs, while values close to 0.5 indicate that the model is no better than random selection. FNs are those cases in which the model predicts that a zip code or town/city has less than T% of children with elevated BLLs, while the measured value for that zip code or town/city is under T%.

(4) The F1 metric is the harmonic mean of Precision and Recall, which are defined as follows:

$$Precision = \frac{TP}{TP + FP} \tag{1}$$

$$Recall = \frac{TP}{TP + FN} \tag{2}$$

Thus, the F1 metric accounts for the ability of the model to distinguish between TP and FN for a specific probability threshold (0.5 in our

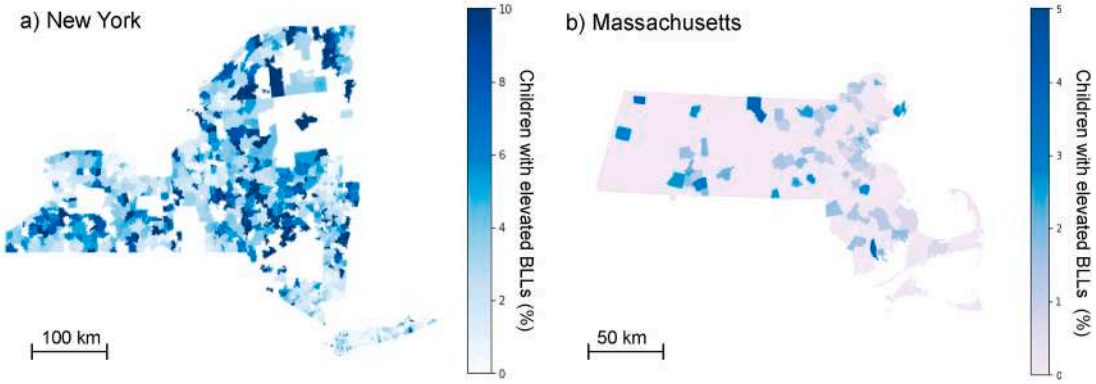

Fig. 1. Heat maps of the study sites showing the percentage of children with elevated BLLs (over 5 μg dL^{-1}) within (a) zip codes in New York (n = 1642) and (b) each community (city/town) in Massachusetts (n = 353). There is missing data for some zip codes the in New York dataset; these are shown in white. Note that the color scale in each map is different. New York has a larger percentage of children with elevated BLLs (more than 5 μg dL^{-1}) than Massachusetts. (For interpretation of the references to color in this figure legend, the reader is referred to the Web version of this article.)

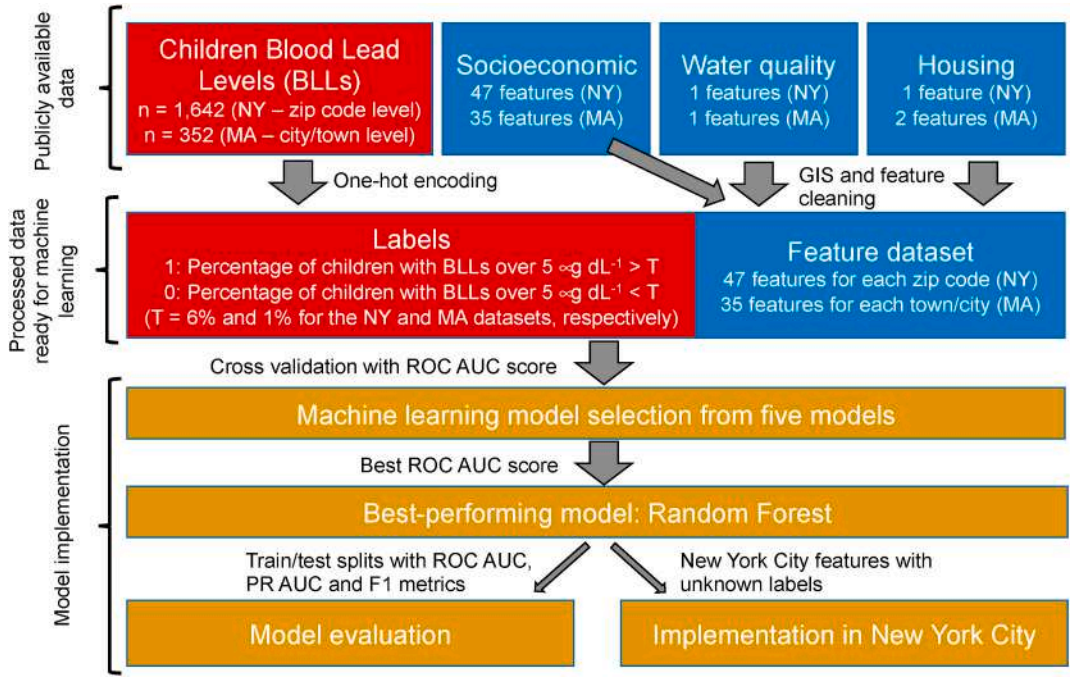

Fig. 2. Schematic overview of the steps taken to process the data and implement the machine learning models. Note that each datapoint corresponds to the percentage of children within each zip code or town/city with Blood Lead Levels (BLLs) over 5 μg dL^{-1} in New York and Massachusetts, respectively, and all its associated features (socioeconomic, chemical, and housing). BLLs are encoded as binary variables, where 1 and 0 represent that a zip code or town/city has over or under T% of children with elevated BLLs, respectively, where T% is 6% for NY and 1% for MA datasets.

case).

The five tested models were compared in terms of their mean ROC AUC score obtained with a 10-fold cross-validation. The best-performing model was tested further by splitting the data randomly into a 70% training and a 30% testing dataset by using the *train_test_split* function in the Python *scikit-learn* package. The data was split 1000 times, and the ROC AUC, PR AUC and F1 score were then calculated for the test data in each split. Given the importance of accurately identifying locations where children might have elevated BLLs and the unbalanced nature of our dataset (only about 20% of the datapoints have BLLs above the chosen threshold for each State), the PR AUC and F1 metrics provide insights into the ability of the model to accurately predict the minority class labels and to avoid predicting FNs.

2.5. Model implementation in New York city

The best-performing model was implemented with data from New York City to predict, for each zip code, the likelihood that over 6% of the children have elevated BLLs. These results were compared to measured childhood BLLs in New York City, which were obtained at a borough level for the year 2015 (New York City Department of Health and Mental Hygiene, 2020). To compare these data to our modeled results, we first calculated the modeled expected number of children with elevated BLLs for each zip code using the following equation:

$$E(Ch) = T * P(T) * Pop \quad (3)$$

Where *E(Ch)* is the expected number of children with BLLs exceeding 5 μg dL^{-1} within each zip code, *P(T)* is the modeled probability that over *T*% of the children have elevated BLLs (T = 6% for the New York model)

and *Pop* is the population of children under 6 years old residing in each zip code. The values of *E(Ch)* were then aggregated for all zip codes within each borough in New York City and the results compared to the measured data. We note that Eq. (3) would underestimate the number of children with elevated BLLs in zip codes where more than 6% of the children have elevated BLLs. However, this threshold is far from the 1.73% average of children with elevated BLLs in New York City in 2015 (New York City Department of Health and Mental Hygiene, 2020).

The compiled datasets used in this study, as well as the code used to implement the machine learning models may be found in our Github repository (Lobo et al., 2021).

3. Results and discussion

3.1. Model selection

The best-performing model for both the New York and Massachusetts datasets was a Random Forest (RF), as shown in Fig. 3 (these results were obtained after model hyperparameter optimization). The hyperparameters used in the model for each dataset are shown in Table 1, while the hyperparameters of the other models are shown in the S.I. The RF model outperformed all other models in terms of the average ROC AUC score, demonstrating that it provides more TP and less FP than the other models. Moreover, this model resulted in less variability among the folds, as shown by the lower standard deviations among the folds during cross validation. Thus, the RF model was selected for further testing with data from the study sites and New York City.

We note that all the tested models provided good results during cross validation. Even the logistic regression model, which has been used unsuccessfully in previous studies for similar purposes (Taylor et al., 2013) resulted in high ROC AUC values (0.84 and 0.87 for the New York and Massachusetts datasets, respectively). This supports our hypothesis that predicting elevated BLLs at a geospatially aggregated level (zip codes or towns/cities) is more feasible than predicting BLLs at an individual person-scale, as other studies have attempted.

3.2. Model performance

The optimized RF model was further tested by randomly splitting the datasets into train and test sets 1000 times and by calculating the ROC AUC, PR AUC and F1 scores. These results are shown in Fig. 4. As a reference, the average F1 score reported in the study by Potash et al. (2015) was 0.40 (we calculated this value using the harmonic mean of their average precision and recall of 0.39 and 0.42, respectively). In contrast, our geospatially aggregated model provided an average F1 score of 0.78 and 0.80 for the New York and Massachusetts datasets, respectively. Another model developed by Potash et al. (2020) resulted in an average ROC AUC score of 0.69, while our model's average ROC AUC was 0.87 and 0.91 for the New York and Massachusetts datasets, respectively. It is likely that the difference in performance between our model and those previously reported in literature results from the lower resolution of our datasets. Most of the models reported in literature use socioeconomic and environmental features to predict elevated BLLs of individuals in specific locations. In contrast, our model predicts elevated BLLs in relatively large populations (on the scale of zip codes and cities/towns) at a state level using aggregated data. The aggregated data helps smoothen the variability among individual children, which allows identifying spatial trends.

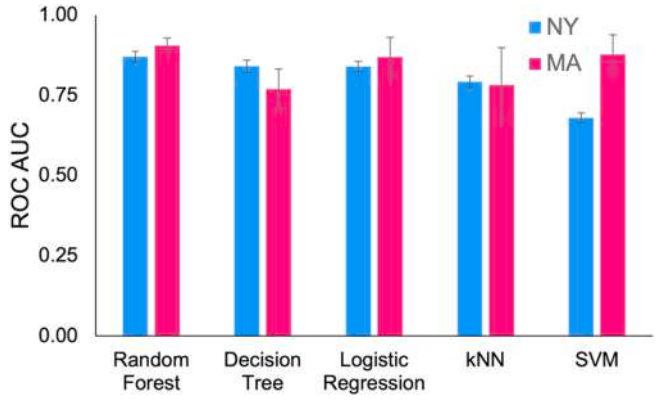

Fig. 3. 10-fold cross validation score of 5 optimized machine learning models using the ROC AUC score for the New York and Massachusetts datasets. The bars represent the mean ROC AUC scores, and the error bars the standard deviation. Random forest outperformed all other models in terms of attaining the highest average ROC AUC score, and demonstrating the smallest value for the standard deviation among the folds.

Table 1
Best combination of hyperparameters for the random forest model implemented using the New York and Massachusetts datasets.

	NY	MA
Number of trees	1000	500
Maximum features	4	6
Maximum depth	12	9

Despite the good average performance of the RF model, significant variations in performance were observed among the 1000 splits for both datasets, as shown in Fig. 2. The variability for all three metrics, F1 score, ROC AUC and PR AUC, was higher when using the Massachusetts dataset. The worst-performing model instance in the Massachusetts dataset had an F1 score of 0.55, a ROC AUC of 0.73 and a PR AUC of 0.62. It is likely that this performance was a product of overfitting, as models trained using small datasets are more likely to overfit the data (Ying, 2019). However, the worst-performing model still has a higher ROC AUC than other models found in literature.

As also shown in Fig. 4, the New York RF model tended to have larger PR AUC than ROC AUC values. This means that this model overestimates the positive label (when over 6% of children within zip codes have elevated BLLs), sacrificing accuracy for precision. This is desirable from a public health perspective, as the cost of predicting FPs are lower than those of predicting FNs (it is more desirable to falsely predict that a zip code has a high risk of childhood lead exposure than to falsely predict that it does not have a high risk of lead exposure). However, the opposite is true for the Massachusetts model: ROC AUC values were greater that PR AUC values. This suggests that the model tends to underestimate the positive label, indicating that it will predict more FNs than FPs. This problem may be addressed by decreasing the probability threshold used to decide the model's outcomes so that more positive predictions (those where the model predicts that over *T*% of the children have elevated BLLs) are made.

3.3. Feature importance analysis using random forest

The features in the New York and Massachusetts RF models were ranked by their Gini score, which represents the loss in entropy (statistical dispersion) resulting from adding each feature to the model (see Fig. 5). We note here that the way RF models work, only the magnitude of reduction in entropy (impact on prediction) is measurable, but not the direction in which the feature impacts the prediction. In both RF models, poverty and race-related features are most important when predicting childhood lead exposure, which aligns with previous studies (Hauptman et al., 2017). In the case of the Massachusetts model, the most important feature corresponds to the percentage of children under 6 living in each zip code or town/city. We have two hypotheses to explain this: 1) It may be the case that not enough BLL tests were performed or that testing was not done randomly, making the results in each zip code or city unrepresentative of the population. This could explain why the model's outcome changes as the number of children tested increases (areas with

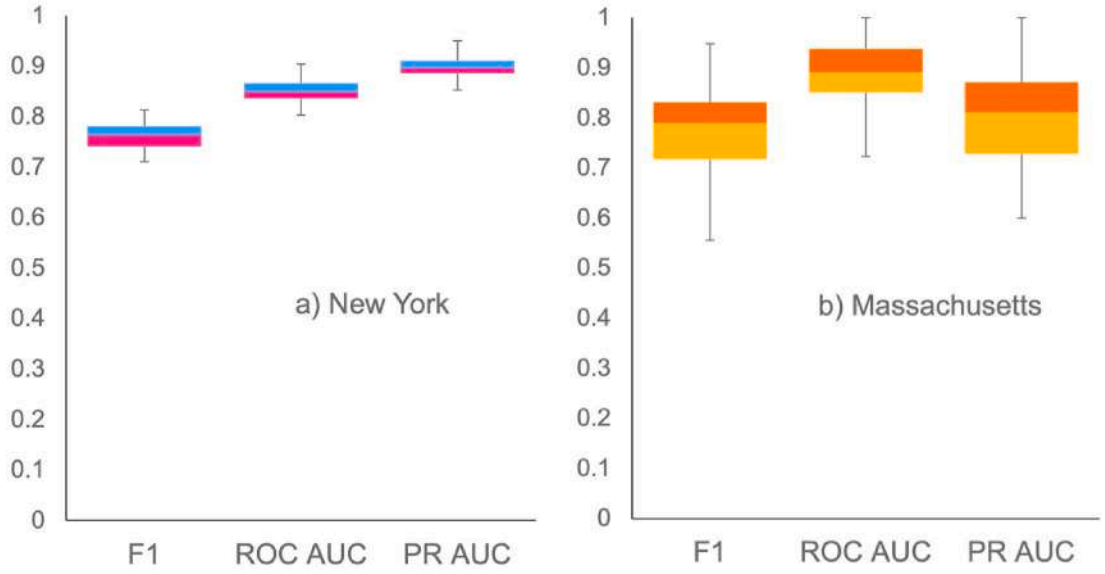

Fig. 4. Box plot of the F1 score and the Area Under the Receiver Operating Characteristic (ROC AUC) and Precision-Recall (PR AUC) curves for 1000 instances of the model using the (a) New York and (b) Massachusetts datasets. The performance of the model is excellent for both the New York and Massachusetts datasets; however, more variability is observed when using the Massachusetts dataset, for reasons discussed in the text.

more children have greater number of tests). 2) Low-income minorities tend to have higher fertility rates (Baughman and Dickert-Conlin, 2009) and this population disproportionally suffers from elevated BLLs (Hauptman et al., 2017). Thus, it may be the case that a town/city with more children is more likely to have more cases of elevated childhood BLLs because more children might indicate less wealth and the presence of minority communities.

Other important features in both random forest models include housing metrics. These results were expected and have been proven to correlate to childhood elevated BLLs in multiple studies. In the case of the Massachusetts RF model, the percentage of pre-1978 housing units is an important feature, which was also expected because old housing is more likely to have lead plumbing and lead paint, two major sources of lead exposure. In the case of the New York model, we did not have access to housing construction year; however, we used Housing Price Index (HPI) as a proxy. As shown in Fig. 5, this index is an important source of information gain in the New York model, indicating that it might be a useful variable for predicting elevated childhood BLLs. Finally, lead levels in schools' drinking water were not an important feature according to the Gini index. This might be because drinking water is not usually the main source of lead exposure in children (Dignam et al., 2019) and because school water quality does not directly impact children under 4 or 5 years of age. These children usually consume water in their homes; however, there are no available public records of lead-levels in household water supplies. It is likely that the housing data used in the model (housing construction date and HPI) indirectly provides information of lead exposure from drinking water at a household level. This is because old buildings are more likely to have lead pipes (Abernethy et al., 2018), which is the main source of lead in drinking water.

3.4. Feature importance analysis using a logistic regression

Even though the Gini index provides information about the importance of each feature, it does not inform on how each of them affect the outcome of the model in terms of magnitude and sign. Given that the logistic regression model provided good results in both datasets during cross validation (see Fig. 3), we ranked the features based on the magnitude of the regression coefficients to gain insights into how each feature affects the outcome of the model but presented our results to also differentiate them by the direction (color-coded for positive or negative) of the influence on the final resulting prediction. These results are shown in Fig. 6.

As seen in the figure, and just like in the random forest model, housing information (HPI and pre-1798 housing) is a very important feature. As expected from prior more narrow studies, HPI is negatively related to childhood elevated BLLs, while pre-1798 housing is positively related to it. Prior literature strongly suggests that older houses, which usually have a lower HPI index, may be sources of lead exposure. In both models, race-related features also behave as expected from prior narrower literature: the percentage of White and Black populations are negatively and positively related to childhood lead exposure, respectively. Furthermore, the prior known fact emerges from both models that low-income communities are disproportionately exposed to toxic levels of environmental lead. Prior researchers have documented in the literature that low-income minority groups tend to have higher rates of childhood lead exposure (Sampson and Winter 2016). Finally, both models agree that lead in school drinking water is less important than other features for children of age 4–5 years (in the New York model this feature is even negatively related to lead exposure). However, the importance of lead in drinking water as a source of childhood lead exposure cannot be disregarded based on these results as we do not have direct information on household water quality.

3.5. Illustrative example of model implementation in New York city

The zip code-level RF model, previously trained with data from the entire State of New York, excluding New York City, was used to predict the probability that over 6% of the children residing in each zip code in New York City have elevated BLLs (BLLs >5 μg dL^{-1}). The resulting probabilities are shown in Fig. 7. As seen in the figure, our model predicted that most zip codes in New York City are not at risk of having over 6% of children with elevated BLLs. This is consistent with the average 1.73% of children 2015 with elevated BLLs in New York City (New York City Department of Health and Mental Hygiene, 2020). However, the map shown in Fig. 7 has two high risk areas (shown in orange) which are located in the Brooklyn and Queens boroughs. These two boroughs account for most of the cases of elevated BLLs in New York City children, as measured by NYC Environment & Health (New York City Department of Health and Mental Hygiene, 2020). Furthermore, the neighborhoods in

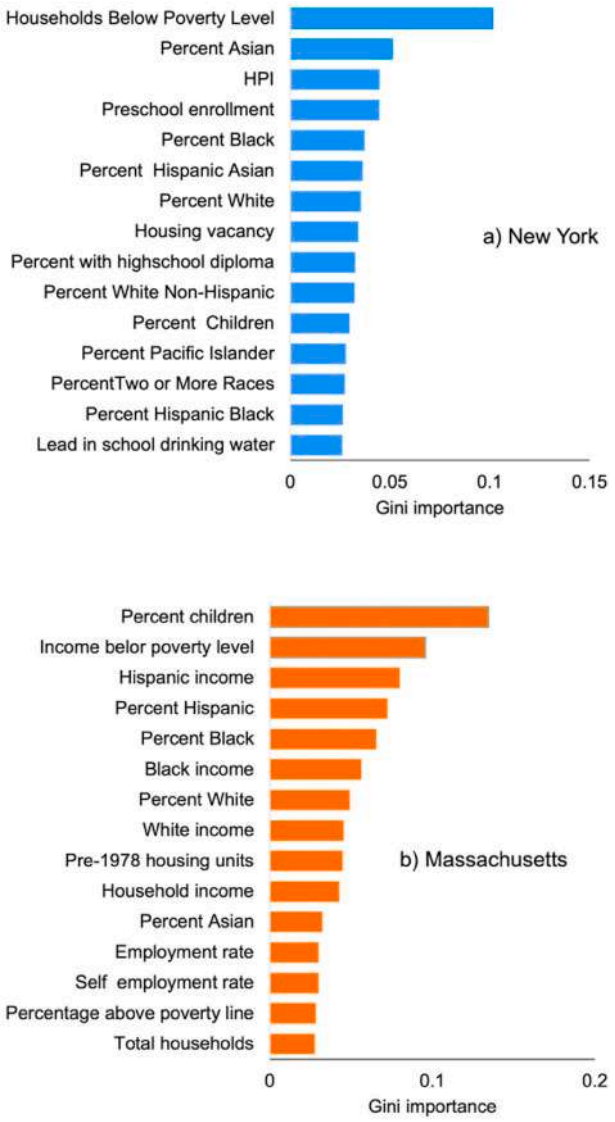

Fig. 5. Top 15 most important features ranked according to the Gini Index when using the optimized random forest model with the a) New York and b) Massachusetts datasets. Race-related features are among the most important predictors of childhood lead exposure.

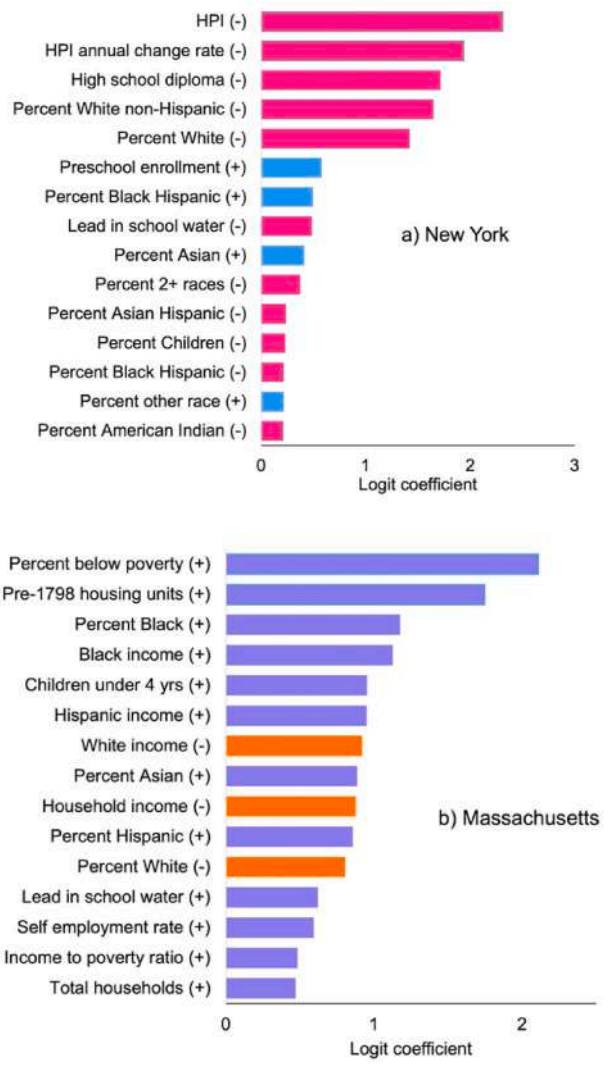

Fig. 6. Top 15 most important features ranked according to the absolute value of the logistic regression coefficients when using the a) New York and b) Massachusetts datasets. The symbols placed in parentheses next to the feature names represent the positive (+) or negative (−) influence of the regression coefficients. As in the random forest model, income and racial features have the largest weights; however, water quality and housing construction date are also important. All features were normalized before the regression so that their magnitudes can be compared.

Brooklyn and Queens with the highest rate of children with elevated BLLs in 2015 were Clinton Hill and Jamaica, respectively (New York City Department of Health and Mental Hygiene, 2020), both of which are contained within the orange areas shown in Fig. 7.

Using Eq. (3) for every zip code, we estimated the expected childhood elevated BLL exposure rates, expressed as cases per 1000 children, for every borough in New York City. These modeled results, as well as the measured childhood elevated BLL exposure rates are shown in Fig. 8. As seen in the figure, the modeled results are within the standard error of every borough. The mean values between measured and modeled data are also similar, except for the Staten Island borough. However, the reported childhood elevated BLL exposure rates in this borough are likely unrepresentative of the population given the small sample size, which explains the large standard error. In fact, the data from two of the sampled neighborhoods in Staten Island have the following warning: "Estimate is based on small numbers so should be interpreted with caution".

It is worth noting that our model provided accurate BLL estimates for New York City even though this city has taken aggressive measures to combat childhood lead exposure (recall that the model was trained with state data, excluding New York City). In 2015, 2.8% of the children residing in the State of New York, excluding New York City, had BLLs over 5 μg dL^{-1}, one of the largest exposure rates in the US (Centers for Disease Control and Prevention, 2019). In contrast, on the same year, only 1.73% of the children residing in New York City had BLLs over 5 μg dL^{-1} (New York Health, 2021). This is likely a result of wealth distribution: New York City is the wealthiest city in the State of New York (United States Census Bureau, 2011); thus, it has more resources to invest in the removal of potential lead sources. This effect was captured by our model, as wealth is one of the most important features for the model implemented with data from New York State (see Fig. 3).

Of course, the map shown in Fig. 7 does not show any new information given that New York City already tests children for BLLs. However, given that our modeled results closely match those reported in lead blood tests, we expect that this model may be trained with data from other states and then applied to cities within those same states where BLL testing data is lacking.

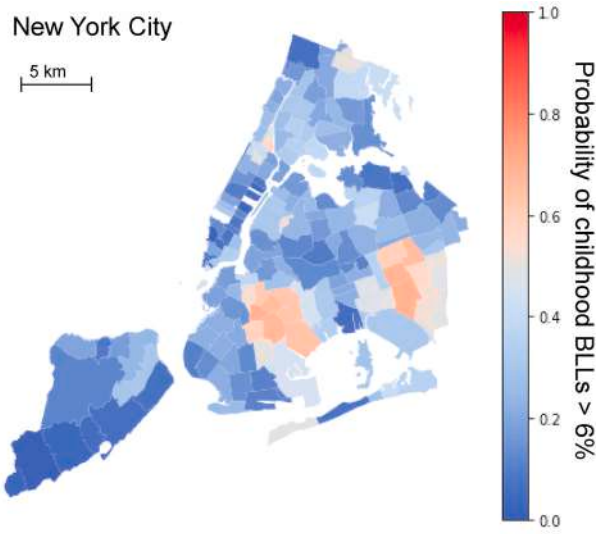

Fig. 7. Predicted probabilities of childhood lead exposure (BLLs over 5 μg dL^{-1}) exceeding 6% in each New York City zip code. The areas with the highest modeled risk are in the Brooklyn and Queens boroughs.

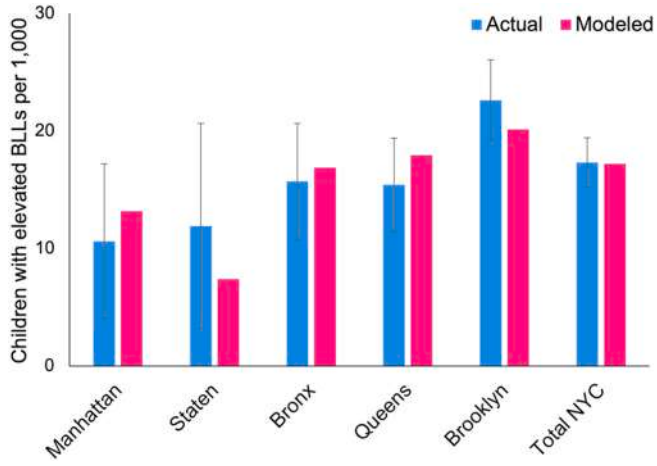

Fig. 8. Modeled and measured childhood elevated BLL exposure rate, expressed as cases per 1000 children, for every borough in New York City in 2015. Standard error bars are shown for the measured data to account for differences in the number of children tested in each borough. The modeled results are within the standard error margins of every borough.

3.6. Model limitations

The RF models presented thus far were implemented by establishing an arbitrary exposure threshold T (1% and 6% for Massachusetts communities and New York zip codes, respectively) and the current CDC reference value of 5 μg dL^{-1}. It is likely that these models may be applied elsewhere and using different values for the threshold T; however, in all cases they must be retrained to account for socioeconomic differences and their effect on lead exposure rates. We hypothesize that other reference values for determining whether children have elevated BLLs or not may also be used; however, this remains untested given that the datasets used only report the number of children with BLLs exceeding 5 μg dL^{-1}. Given that the models rely heavily on socioeconomic features, we do not expect that a model trained with data from one state will be directly applicable to another state or country because different locations have different policies to address childhood lead exposure. However, training the model with partial data, like in the case of the state of New York, may provide useful insights into locations where BLLs have not been measured so that targeted testing and mitigation strategies may be implemented.

Another disadvantage of relying on socioeconomic data is that the model does not directly reflect the mechanisms by which children ingest lead. Ideally, a model to predict childhood lead exposure will rely exclusively on environmental variables, such as lead in air, soil and drinking water. However, those variables are rarely measured, thus, socioeconomic features are needed because, unfortunately, they correlate with lead exposure. We hope that environmental justice efforts will make models like the one presented in this study obsolete (income and race should not be related to BLLs); however, at present they constitute useful tools for predicting, and thus, preventing childhood lead exposure.

While the model accurately predicts the risk of childhood lead exposure for a given area (zip code or community), it does not provide information regarding the variability within each area. This might limit its applicability in large and heterogenous communities where aggregated data fails to accurately describe the population.

Finally, the current version of our model is also limited by the lack of publicly available data. For instance, water utilities in the US test for lead in drinking water in several locations yearly; however, they are only required to report the 90th percentile lead level, per the Lead and Copper Rule. Knowing the locations where high lead water levels were detected would provide invaluable information to models such as the ones presented in this study. Not only would this benefit modeling the impacts of lead in drinking water on childhood lead exposure, but it would also increase the transparency and accountability of water distribution systems. Good quality BLL data is also scarce, as, to the best of our knowledge, only New York and Massachusetts have published data at a high enough resolution to be useful. Other states have published data at a county or state level, which are unsuitable for data science applications or even for people interested in knowing if their children are likely to have elevated BLLs or not. Making high quality BLL data public and easily accessible is not only key for the development of models like the one presented in this study but will also increase transparency and accountability of local authorities.

4. Conclusions

Even though this work focused on developing a machine learning model to predict elevated BLLs at an aggregate level in the states of New York and Massachusetts, we envision future applications in states that do not routinely monitor childhood BLLs. Only 14 states currently recommend universal screening (Michel et al., 2020), thus, this model has the potential to fill in the gaps in the other 36 states that perform partial screening. By testing a fraction of children in these states, this modeling approach may help identify areas at the state level where children are at high risk of having elevated BLLs so that targeted testing and mitigation strategies may be adopted. Moreover, the data collected can be can then be added to the training data, successively improving its accuracy. We believe that modelling approaches using machine learning have the potential to help identify and mitigate childhood lead exposure, a preventable heath crisis that affects the most vulnerable members of our communities.

Acknowledgements

The authors are grateful for key funding support that enabled this work. This includes support from the Fulbright Program, the Hellman Foundation, Prof. Gadgil's Rudd Chair funds and a gift from the Barbara and Gerson Bakar Foundation. We thank Joseph Mella and David Sanchez, undergraduate students at UC Berkeley, for participation in data mining and analysis. Some of the effort for this work was enhanced by the InFEWS program at UC Berkeley, supported by the National Science Foundation under Grant No. DGE-1633740.

Appendix A. Supplementary data

Supplementary data to this article can be found online at https://doi.org/10.1016/j.ijheh.2021.113862.

References

Abernethy, J., Chojnacki, A., Farahi, A., Schwartz, E., Webb, J., 2018. Active Remediation: the search for lead pipes in Flint, Michigan. Proc. ACM SIGKDD Int. Conf. Knowl. Discov. Data Min. 5–14 https://doi.org/10.1145/3219819.3219896.

Baughman, R., Dickert-Conlin, S., 2009. The earned income tax credit and fertility. J. Popul. Econ. 22, 537–563. https://doi.org/10.1007/s00148-007-0177-0.

Bierkens, J., Smolders, R., Van Holderbeke, M., Cornelis, C., 2011. Predicting blood lead levels from current and past environmental data in Europe. Sci. Total Environ. 409, 5101–5110. https://doi.org/10.1016/j.scitotenv.2011.08.034.

Billings, S.B., Schnepel, K.T., 2017. The value of a healthy home: lead paint remediation and housing values. J. Publ. Econ. 153, 69–81. https://doi.org/10.1016/j.jpubeco.2017.07.006.

Cattle, J.A., McBratney, A.B., Minasny, B., 2002. Kriging method evaluation for assessing the spatial distribution of urban soil lead contamination. J. Environ. Qual. 31, 1576–1588. https://doi.org/10.2134/jeq2002.1576.

CDC, 2021. Blood lead reference value. accessed 10.4.21. https://www.cdc.gov/nceh/lead/data/blood-lead-reference-value.htm.

Centers for Disease Control and Prevention, 2019. Blood Lead Levels (μg/dL) Among U.S. Children < 72 Months of Age, by State, Year, and Blood Lead Level (BLL) Group Year State.

Chojnacki, A., Dai, C., Farahi, A., Shi, G., Webb, J., Zhang, D.T., Abernethy, J., Schwartz, E., 2017. A data science approach to understanding residential water contamination in flint. Proc. ACM SIGKDD Int. Conf. Knowl. Discov. Data Min. Part F1296, 1407–1416. https://doi.org/10.1145/3097983.3098078.

Dignam, T., Kaufmann, R.B., LeStourgeon, L., Brown, M.J., 2019. Control of lead sources in the United States, 1970-2017. J. Publ. Health Manag. Pract. 25 https://doi.org/10.1097/phh.0000000000000889. S13–S22.

Doré, E., Deshommes, E., Andrews, R.C., Nour, S., Prévost, M., 2018. Sampling in schools and large institutional buildings: implications for regulations, exposure and management of lead and copper. Water Res. 140, 110–122. https://doi.org/10.1016/j.watres.2018.04.045.

Dos Santos, B.S., Steiner, M.T.A., Fenerich, A.T., Lima, R.H.P., 2019. Data mining and machine learning techniques applied to public health problems: a bibliometric analysis from 2009 to 2018. Comput. Ind. Eng. 138, 106120. https://doi.org/10.1016/j.cie.2019.106120.

Ettinger, A.S., Ruckart, P.Z., Dignam, T., 2019. Lead poisoning prevention: the unfinished agenda. J. Publ. Health Manag. Pract. 25, S1–S2. https://doi.org/10.1097/PHH.0000000000000902.

Gould, E., 2009. Childhood lead poisoning: conservative estimates of the social and economic benefits of lead hazard control. Environ. Health Perspect. 117, 1162–1167. https://doi.org/10.1289/ehp.0800408.

Hauptman, M., Bruccoleri, R., Woolf, A., 2017. An update on childhood lead poisoning. Clin. Pediatr. Emerg. Med. 18, 181–192. https://doi.org/10.1117/12.2549369.Hyperspectral.

Lanphear, B.P., Burgoon, D.A., Rust, S.W., Eberly, S., Galke, W., 1998. Environmental exposures to lead and urban children's blood lead levels. Environ. Res. 76, 120–130. https://doi.org/10.1006/enrs.1997.3801.

Lanphear, B.P., Dietrich, K., Auinger, P., Cox, C., 2000. Cognitive deficits associated with blood lead concentrations < 10 μg/dL in US children and adolescents. Publ. Health Rep. 115, 521–529. https://doi.org/10.1093/phr/115.6.521.

Lanphear, B.P., Hornung, R., Ho, M., Howard, C.R., Eberle, S., Knauf, K., 2002. Environmental lead exposure during early childhood. J. Pediatr. 140, 40–47. https://doi.org/10.1067/mpd.2002.120513.

Lobo, G.P., Kalyan, B., Gadgil, A.J., 2021. Childhood BLL model data and code. GitHub. https://github.com/gadgil-group/childhood_BLL_model.git.

Magavern, S., 2018. Policies to reduce lead exposure: lessons from buffalo and rochester. Int. J. Environ. Res. Publ. Health 15. https://doi.org/10.3390/ijerph15102197.

Marshall, A.T., Betts, S., Kan, E.C., Mcconnell, R., Lanphear, B.P., Sowell, E.R., 2020. Association of lead-exposure risk and family income with childhood brain outcomes. Nat. Med. 26, 91–97. https://doi.org/10.1038/s41591-019-0713-y.Association.

Massachusetts Department of Public Health, 2021a. PHIT data: childhood lead poisoning. accessed 8.7.21. https://www.mass.gov/guides/phit-data-childhood-lead-poisoning.

Massachusetts Department of Public Health, 2021. Learn about lead screening and reporting requirements. accessed 10.4.21. https://www.mass.gov/service-details/learn-about-lead-screening-and-reporting-requirements.

Michel, J.J., Erinoff, E., Tsou, A.Y., 2020. More Guidelines than states: variations in U.S. lead screening and management guidance and impacts on shareable CDS development. BMC Publ. Health 20, 1–10. https://doi.org/10.1186/s12889-020-8225-8.

Mielke, H.W., 1999. Lead in the inner cities. Am. Sci. 87, 62–73. https://doi.org/10.1511/1999.1.62.

Mielke, H.W., Reagan, P.L., 1998. Soil is an important pathway of human lead exposure. Environ. Health Perspect. 106, 217–229. https://doi.org/10.1289/ehp.98106s1217.

Muennig, P., 2009. The social costs of childhood lead exposure in the post-lead regulation era. Arch. Pediatr. Adolesc. Med. 163, 844–849. https://doi.org/10.1001/archpediatrics.2009.128.

New York City Department of Health and Mental Hygiene, 2020. Environment & health data portal. accessed 8.7.21. http://a816-dohbesp.nyc.gov/IndicatorPublic/Subtopic.aspx?theme_code=2,3&subtopic_id=108.

New York Health, 2021. Childhood Blood Lead Level Surveillance Quarters 1-3 2020.

New York State Department of Health, 2021. Childhood lead poisoning prevention. accessed 10.4.21. https://www.health.ny.gov/environmental/lead/.

New York State Department of Health, 2015. Childhood blood lead testing and elevated incidence by zip code: beginning 2000. accessed 8.7.21. https://health.data.ny.gov/Health/Childhood-Blood-Lead-Testing-and-Elevated-Incidenc/d54z-enu8.

Potash, E., Brew, J., Loewi, A., Majumdar, S., Reece, A., Walsh, J., Rozier, E., Jorgensen, E., Mansour, R., Ghani, R., 2015. Predictive modeling for public health: preventing childhood lead poisoning. Proc. ACM SIGKDD Int. Conf. Knowl. Discov. Data Min. https://doi.org/10.1145/2783258.2788629, 2039–2047.

Potash, E., Ghani, R., Walsh, J., Jorgensen, E., Lohff, C., Prachand, N., Mansour, R., 2020. Validation of a machine learning model to predict childhood lead poisoning. JAMA Netw. open 3, e2012734. https://doi.org/10.1001/jamanetworkopen.2020.12734.

Roy, S., Edwards, M.A., 2019. Preventing another lead (Pb) in drinking water crisis: lessons from the Washington D.C. and Flint MI contamination events. Curr. Opin. Environ. Sci. Heal. 7, 34–44. https://doi.org/10.1016/j.coesh.2018.10.002.

Rushton, G., 2003. Public health, GIS, and spatial analytic tools. Annu. Rev. Publ. Health 24, 43–56. https://doi.org/10.1146/annurev.publhealth.24.012902.140843.

Sampson, R.J., Winter, A.S., 2016. The racial of lead poisoning: toxic inequality in Chicago neighborhoods, 1995-2013. Du. Bois Rev. 13, 261–283. https://doi.org/10.1017/S1742058X16000151.

Schultz, B.D., Morara, M., Buxton, B.E., Weintraub, M., 2017. Predicting blood-lead levels among U.S. Children at the census tract level. Environ. Justice 10, 129–136. https://doi.org/10.1089/env.2017.0005.

Schwartz, J., 1994. Low-level lead exposure and Children's IQ: a metaanalysis and search for a threshold. Environ. Res. https://doi.org/10.1006/enrs.1994.1020.

Sethi, J.K., Mittal, M., 2019. A new feature selection method based on machine learning technique for air quality dataset. J. Stat. Manag. Syst. 22, 697–705. https://doi.org/10.1080/09720510.2019.1609726.

Taylor, C.M., Golding, J., Hibbeln, J., Emond, A.M., 2013. Environmental factors predicting blood lead levels in pregnant women in the UK: the ALSPAC study. PLoS One 8, 1–8. https://doi.org/10.1371/journal.pone.0072371.

Triantafyllidou, S., Edwards, M., 2012. Lead (Pb) in tap water and in blood: implications for lead exposure in the United States. Crit. Rev. Environ. Sci. Technol. 42, 1297–1352. https://doi.org/10.1080/10643389.2011.556556.

Trimble, D., 2016. Measuring the Efficacy of Lead Interventions. Millvale, Pennsylvania.

Tsoi, M.F., Cheung, C.L., Cheung, T.T., Cheung, B.M.Y., 2016. Continual decrease in blood lead level in Americans: United States National health Nutrition and Examination survey 1999-2014. Am. J. Med. 129, 1213–1218. https://doi.org/10.1016/j.amjmed.2016.05.042.

U.S. Department of Health and Human Services, 2012. Health effects of low-level lead. Natl. Toxicol. Progr. Monogr.

United States Census Bureau, 2011. Demographic profile with geos summary file dataset. accessed 8.7.21. https://www.census.gov/programs-surveys/decennial-census/data/datasets.html.

US Census Bureau, 2016. American community survey 2015 data profiles. accessed 8.7.21. https://www.census.gov/acs/www/data/data-tables-and-tools/data-profiles/2018/.

Vivier, P.M., Hauptman, M., Weitzen, S.H., Bell, S., Quilliam, D.N., Logan, J.R., 2011. The important health impact of where a child lives: neighborhood characteristics and the burden of lead poisoning. Matern. Child Health J. 15, 1195–1202. https://doi.org/10.1007/s10995-010-0692-6.

Vorvolakos, T., Arseniou, S., Samakouri, M., 2016. There is no safe threshold for lead exposure: a literature review. Psychiatriki 27, 204–214. https://doi.org/10.1177/1461444810365020.

Whitehead, L.S., Buchanan, S.D., 2019. Childhood lead poisoning: a perpetual environmental justice issue? J. Publ. Health Manag. Pract. 25, S115–S120. https://doi.org/10.1097/PHH.0000000000000891.

Wojtusiak, J., Baranova, A., 2011. Model learning from published aggregated data. Stud. Comput. Intell. 375, 369–384. https://doi.org/10.1007/978-3-642-22913-8_17.

Ye, T., Johnson, R., Fu, S., Copeny, J., Donnelly, B., Freeman, A., Lima, M., Walsh, J., Ghani, R., 2019. Using machine learning to help vulnerable tenants in New York City. COMPASS 2019 - Proc. 2019 Conf. Comput. Sustain. Soc. 248–258. https://doi.org/10.1145/3314344.3332484.

Ying, X., 2019. An overview of overfitting and its solutions. J. Phys. Conf. Ser. 1168 https://doi.org/10.1088/1742-6596/1168/2/022022.

Zahran, S., Mushinski, D., McElmurry, S.P., Keyes, C., 2020. Water lead exposure risk in Flint, Michigan after switchback in water source: implications for lead service line replacement policy. Environ. Res. 181, 108928. https://doi.org/10.1016/j.envres.2019.108928.

Zhang, H., Yin, S., Chen, Y., Shao, S., Wu, J., Fan, M., Chen, F., Gao, C., 2020. Machine learning-based source identification and spatial prediction of heavy metals in soil in a rapid urbanization area, eastern China. J. Clean. Prod. 273, 122858. https://doi.org/10.1016/j.jclepro.2020.122858.

International Journal of Hygiene and Environmental Health 238 (2021) 113840

Contents lists available at ScienceDirect

International Journal of Hygiene and Environmental Health

journal homepage: www.elsevier.com/locate/ijheh

Psychological impairment and extreme weather event (EWE) exposure, 1980–2020: A global pooled analysis integrating mental health and well-being metrics

C. Chique [a,b], P. Hynds [c,d], M.M. Nyhan [e,f], S. Lambert [g], M. Boudou [d], J. O'Dwyer [a,b,c,*]

[a] School of Biological, Earth and Environmental Science (BEES), University College Cork, Cork, Ireland
[b] Environmental Research Institute, University College Cork, Cork, Ireland
[c] Irish Centre for Research in Applied Geoscience, University College Dublin, Dublin, Ireland
[d] Environmental Sustainability and Health Institute (ESIH), Technological University Dublin, Dublin, Ireland
[e] School of Engineering & Architecture, MaREI Centre for Energy, Climate & Marine & Environmental Research Institute, University College Cork, Ireland
[f] Harvard TH Chan School of Public Health, Harvard University, Boston, United States
[g] School of Applied Psychology Research, University College Cork, Cork, Ireland

ARTICLE INFO

Keywords:
Extreme weather events
Mental health
Psychological disorder
Psychological impairment
Well-being

ABSTRACT

Extreme Weather Events (EWEs) impose a substantial health and socio-economic burden on exposed populations. Projected impacts on public health, based on increasing EWE frequencies since the 1950s, alongside evidence of human-mediated climatic change represents a growing concern. To date, the impacts of EWEs on mental health remain ambiguous, largely due to the inherent complexities in linking extreme weather phenomena with psychological status. This exploratory investigation provides a new empirical and global perspective on the psychological toll of EWEs by exclusively focusing on psychological morbidity among individuals exposed to such events. Morbidity data collated from a range of existing psychological and well-being measures have been integrated to develop a single ("holistic") metric, namely, psychological impairment. Morbidity, and impairment, were subsequently pooled for key disorders-, specifically PTSD, anxiety and depression. A "composite" (any impairment) post-exposure pooled-prevalence rate of 23% was estimated, with values of 24% calculated for depression and ~17% for both PTSD and anxiety. Notably, calculated pooled odds ratios (pOR = 1.9) indicate a high likelihood of any negative psychological outcome (+90%) following EWE exposure. Pooled analyses of reported risk factors ($p < 0.05$) highlight the pronounced impacts of EWEs among individuals with higher levels of event exposure or experienced stressors (14.5%) and socio-demographic traits traditionally linked to vulnerable sub-populations, including female gender (10%), previous history (i.e., pre-event) of psychological impairment (5.5%), lower socio-economic status (5.5%), and a lower education level (5.2%). Inherent limitations associated with collating mental health data from populations exposed to EWEs, and key knowledge gaps in the field are highlighted. Study findings provide a robust evidence base for developing and implementing public health intervention strategies aimed at ameliorating the psychological impacts of extreme weather among exposed populations.

1. Introduction

Extreme Weather Events (EWEs) have a substantial global public health and socio-economic burden, equating to an estimated 6 million deaths and 50 million injured since 1950, with economic losses of US $640 billion between 1970 and 2019 also projected (CRED, 2020; IFRC, 2020; WMO et al., 2020). The myriad interactions between EWEs and human health are complex, with impacts generally classified into two main categories: (*i*) direct, due to finite physical climatic manifestations (e.g., storms, floods), and (*ii*) indirect, often caused by changes in biogeophysical processes influenced by climatic phenomena (e.g., water quality, land-use change) (Watts et al., 2015; Forzieri et al., 2017). These two impact categories actively interact with social factors (e.g., demographic profile), and potentially modify (e.g., amplify, mitigate) the

* Corresponding author. School of Biological, Earth and Environmental Science (BEES), University College Cork, Cork, Ireland.
E-mail address: jean.odwyer@ucc.ie (J. O'Dwyer).

https://doi.org/10.1016/j.ijheh.2021.113840
Received 30 June 2021; Received in revised form 19 August 2021; Accepted 10 September 2021
Available online 17 September 2021

intensity of subsequent impacts, ultimately influencing mental health and well-being (Watts et al., 2015).

Current evidence suggests that the frequency and intensity of EWEs has increased significantly since the 1950s in concurrence with a ~0.8 °C global temperature rise (IPCC et al, 2021). While evidence explicitly linking anthropogenic climate change with EWE frequency and/or intensity varies with respect to phenomena type, indicators suggest human-mediated global warming has *likely* resulted in an increase in compound EWEs since the 1950s (IPCC et al, 2012; 2018; 2019; 2021). A recent report from the Centre of Epidemiology of Disasters (CRED) indicates a ten-fold increase in the number of climate-mediated disaster events recorded in the last ~70 years (CRED, 2020), with events associated with a climatic origin accounting for ~79% of all disaster typologies (e.g., technological, conflict-related) over the last 50 years (IFRC, 2020).

Since 2016, an annual, global, multi-disciplinary effort to track the links between climate change and public health, including monitoring of key "progress" indicators, has been led by The *Lancet* Countdown (https://www.lancetcountdown.org/), a taskforce seeking to provide policy-makers with evidence-based feedback relating the impacts of climate change on public health. While initially identified as a key emerging public health concern, a series of limitations have precluded successful integration of climate-associated mental health indicators into progress metrics (Watts et al., 2015, 2018, 2019, 2020). Similar constraints apply to the integration of EWEs and mental health fields, with main obstacles ranging from ambiguity regarding attribution (i.e., cause-effect, psychological disorders potentially exhibiting compounded and distal origins), to the inherent complexity of psychological disorders, including co-morbidity, and symptom variability as a product of "resilience" and life-course epidemiology (Kuh et al., 2003; Goldman and Galea, 2014; Watts et al., 2018). Additional constraints include under-reporting and differing diagnostic standards depending on geographical location and socio-demographic background (Watts et al., 2015, 2021; Berry et al., 2018; Hayes et al., 2018; Habrok et al., 2020). Accordingly, to date, much of the research emphasis in the context of EWEs and mental health has been placed in exploring associations between temperature extremes and metrics associated with mental health at a (macro-) population level (Watts et al., 2019). While informative, this approach precludes identification of direct links between individual exposure and mental health outcomes. This lack of research focus contrasts with mounting evidence for increased risk of psychological impairment in response to extreme weather, potentially amplified by increasing event frequency, duration and intensity, and concurrently, projected estimates of a substantial, widespread, and cumulative psychological burden (Trombley et al., 2017; Obradovich et al., 2018; Clayton 2020, 2021; Liu et al., 2021).

Notwithstanding the aforementioned difficulties, key quantitative insights into the psychological burden associated with EWEs may be obtained from the disaster-psychopathology literature. Hydro-meteorological events, which can be tentatively associated with climatic change (e.g., floods, storms, droughts), are frequently linked with an increased risk of developing psychopathological disorders (Bourque and Willox, 2014; Trombley et al., 2017; Habrok et al., 2020; Palinkas and Wong, 2020). However, to date, much of the disaster literature has focused in evaluating PTSD, with a need for a more "holistic" approach aiming to incorporate different mental health metrics (Goldman and Galea, 2014). As such, mental health morbidity data derived from an iterative, pooled or meta-analytical approach, which aims to condense psychological/well-being data in response to extreme weather events, may prove particularly insightful. As of yet, no empirical literature review has focused exclusively on EWEs at a global scale, with available studies often regionally-specific, adopting an overarching approach towards "public health impacts" (both physical and mental) or the concept of disaster and thus including non-climatic natural events (Rubonis and Bickman, 1991; Norris et al., 2002; Galea et al., 2005; Neria et al., 2008; Rataj et al., 2016; Lowe et al., 2019; Cruz et al., 2020; Weilnhammer et al., 2021).

Within this context, the current study represents the first empirical attempt to collate, integrate, and analyse psychological morbidity data from populations exposed to EWEs. Key geographical and socio-economic factors interacting with (modifying) the cause (EWE) and effect (psychological disorder) relationship are extracted and analysed, thus enabling a greater understanding of the associations between extreme weather exposure and mental health disparities and inequity. Ultimately, study findings seek to provide an evidence base for policy-makers and other stakeholders for designing and improving intervention and/or mitigation strategies, aimed to guide resource allocation efforts before and following extreme weather events.

2. Methodology

2.1. Review Scope and bibliographic databases

Given the exploratory and multi-disciplinary scope of target literature, the literature identification protocol employed was adapted from the Population/Concept/Context (PCC) Framework for "scoping" literature reviews (Peters et al., 2020). Additionally, a range of published scoping reviews and pooled analyses, focusing on topics related to public health, (social-)epidemiology, and disaster-psychopathology (e.g., Rubonis and Bickman, 1991; Norris et al., 2002; Galea et al., 2005; Sargeant et al., 2006), were consulted to inform the review process. The following research question was developed to direct the literature identification process:

> "*What was the global prevalence of psychological impairment among populations exposed to Extreme Weather Events during the period 1980–2020 and what risk factors were associated with impairment?*"

Literature searches (conducted July 1st, 2020) were confined to Scopus, Web of Science and PubMed bibliographic databases. Notably, the review was potentially restricted in scope in terms of database searches, with an exclusive focus on the three databases deemed to be most pertinent in the context of EWEs. Additional and potentially relevant databases (e.g., PsycInfo) were omitted from the review protocol. Employed literature search terms (Table A1; See Appendix) followed pre-established classifications derived from the Population-Agent-Outcome Model (PAO) model used for previous scoping reviews (e.g., Hynds et al., 2014). Search terms relate to the two primary (in-)direct impact classifications of EWEs (e.g., direct = "hurricane"; indirect = "water quality"), and the primary psychological outcomes associated with population exposure to EWEs (e.g., PTSD, anxiety, depression). All database searches used Boolean positional operators (e.g., "AND", "OR").

2.2. Eligibility criteria, article Screening and data extraction

A total of 1218 records were identified through bibliographic database searches with de-duplication reducing this to 923 (Phase 1–2; Fig. 1). All records were initially screened for suitability based on article title and abstract content, with forward-selected articles subject to full-text screening ($n = 321$) (Phase 2–3). At each stage, article screening and inclusion followed a set of pre-established suitability criteria (Table A2). A senior postdoctoral fellow led the review (CC). PH and JOD independently assessed all abstracts for suitability/relevance, where a disagreement arose, the authors (CC, JOD, PH and SL) conferred to reach agreement (i.e., majority vote). A central objective of the review was to quantify the psychological and well-being impacts of EWEs on exposed populations. The concept of EWE is inclusive of extreme weather and climatic events, which can be grouped under the term "climate extremes", and follows IPCC terminology, i.e., *an abnormal, above-below threshold, and (temporally) irregular weather/climatic phenomena* (IPCC et al, 2012). Exposure was predicated on respondent direct (or

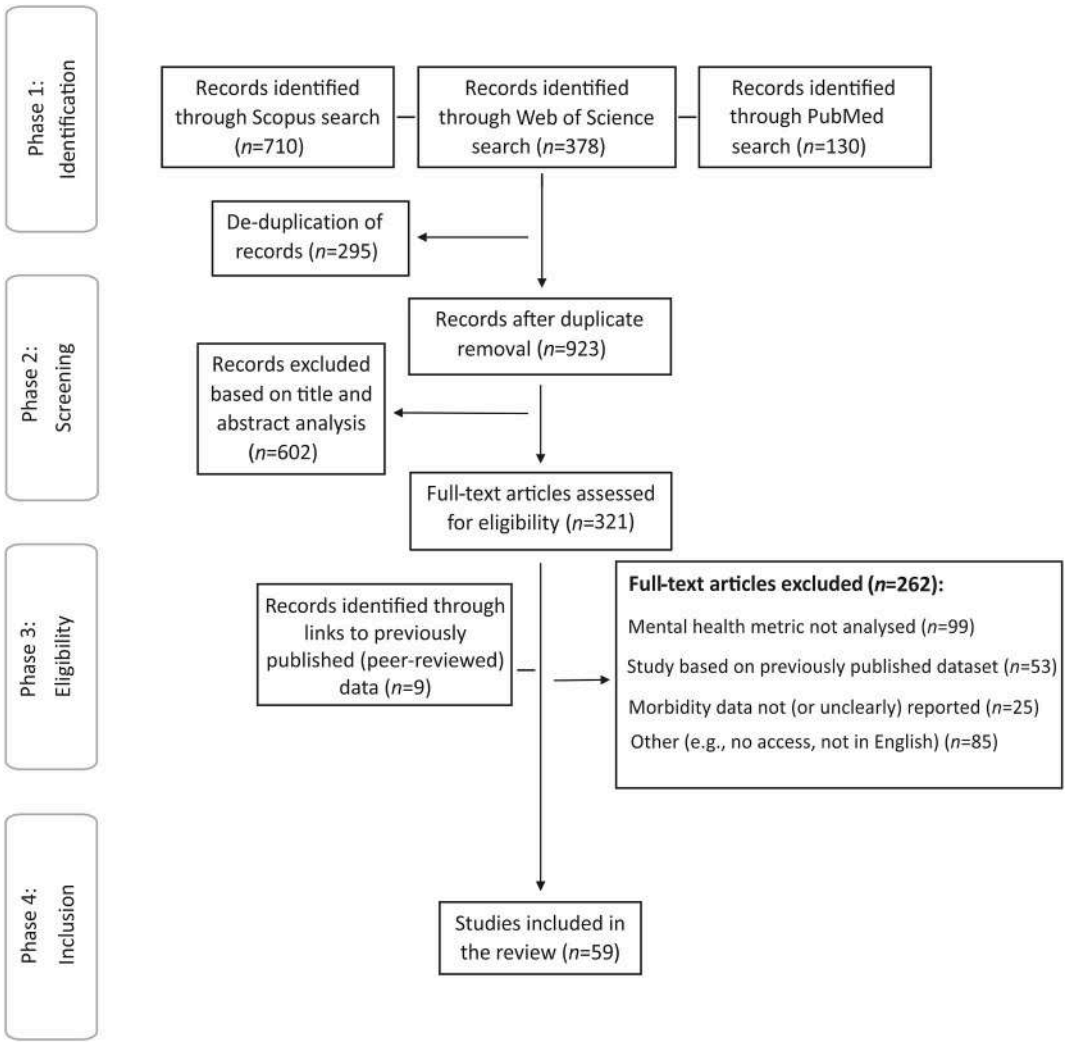

Fig. 1. Schematic of the systematic literature review protocol employed.

"lived-in") EWE(s) experience. Importantly, exposure was dependent on individual study design, with a degree of spatio-temporal ambiguity in relation to individual EWE exposure, particularly in the context of large-scale and distance-based studies (e.g., online, mail surveys). Event types were grouped into four main categories to facilitate analysis with further details provided in Appendices B-C. Specifically, "quantification" refers to a psychological diagnosis (individual case/outcome), and/or evidence for well-being impairment (or lack thereof) among evaluated population samples. Both the term psychological impairment (cf. Rubonis and Bickman, 1991), and the data presented within, incorporate a range of pre-established (non-)clinical and study-specific (or "generic") psychopathological, mental health and well-being measures. Thus, literature inclusion was not constrained to investigations employing standardised psychological disorders (e.g., DSM, ICD-10). The underlining criteria and rationale employed for article inclusion and established data extraction field (sub-)categories are outlined in Appendices B-D.

2.3. Quantifying psychological impairment

All included investigations provided a number or percentage of the population meeting predetermined criteria deemed sufficient to attribute psychological impairment. Thresholds were determined and followed the discretion of individual authors. In an effort to integrate all data into a single "composite" metric representative of (overall) psychological impairment, reported psychological disorders were condensed into four nosological domains outlined by the Diagnostic and Statistical Manual of Mental Disorders (DSM-IV, 4th Edition) (viz. Rubonis and Bickman, 1991), as follows: (*i*) PTSD (including other "stress" measures), (*ii*) Depression, (*iii*) Anxiety and (*iv*) Substance Use Disorder. Additionally, a fifth domain classification, denoted as "Additional Distress", was used to amalgamate disorders (and domains) not frequently encountered ($n < 3$) among identified studies (e.g., Somatization, Schizophrenia). The outlined approach enabled calculation of one composite and five domain-specific estimates of psychological impairment with emphasis given to data estimated at a composite level and for PTSD, anxiety and depression; the latter representative of the three main psychopathological domains in the disaster-psychopathology literature (cf. Norris et al., 2002; Neria et al., 2009; Goldman and Galea, 2014). In the case of longitudinal studies, i.e., investigations based on psychological evaluation at multiple points (post-event) in time (or waves), all impairment data extracted and pooled were restricted to the first evaluation. Additional details on the extraction of impairment data and pooling categories are provided in Appendices B-E.

2.4. Reported risk factors

Where reported, all variables (i.e., potential confounders and/or modifiers) statistically associated ($p < 0.05$, irrespective of employed statistical test/method) with psychological impairment within

individual studies were extracted and collated. Due to the large (cumulative) number of risk factors investigated across studies, where possible, risk factors were nested into one of three main risk categories commonly employed in the disaster-psychopathology literature (Maguen et al., 2009; Goldman and Galea, 2014), namely "pre-event", or intrinsic risk factors (primarily socio-demographics); "peri-event", or variables pertaining (and confined to) a specific event and its timeframe (e.g., perceived intensity, stressors); and "post-event", i.e., variables associated with conditions and settings following exposure to extreme weather (e.g., access to aid/relief).

2.5. Study-Specific and pooled odds ratio calculations

Odds ratios (ORs) were calculated as a relative measure to evaluate the strength of association between EWE exposure and psychological impairment. Study-specific ORs were estimated for each domain including composite data, with a "pooled" (or adjusted) OR (pOR) calculated using the Mantel-Haenszel method (Mantel and Haenszel, 1959). pOR, which represents a weighted metric for aggregating study-specific (non-)exposed populations and standard deviations, provides an overall measure of association between EWE exposure and specific domains. OR calculation relied on availability of case-control data and was therefore restricted to those investigations employing independent control groups ($n = 12$). Only one investigation reporting "actual pre-post" (i.e., pre- and post-event) control data met the criteria allowing OR calculation. This investigation was treated separately from those employing independent control groups in terms of pOR calculation. Investigations reporting retrospective pre-post data were also excluded from calculations. Subject to adequate data reporting, ORs were calculated for studies reporting composite ($n = 7$) and domain-specific impairment ($n = 8$). The latter was only calculated for the three main disorder domains, i.e., PTSD ($n = 7$), anxiety ($n = 7$) and depression ($n = 8$).

3. Results

3.1. Key dataset characteristics

Overall, 59 relevant articles were identified, assessed and incorporated for data extraction and pooled analyses (Fig. 1). A descriptive summary and geographical distribution of all studies are presented in Table A3 and Fig. 2, respectively. Bibliographic details and selected data fields for each reviewed investigation are provided in Appendix F. Extractions comprise psychological impairment data from 61,443 EWE-exposed individuals. A majority were assessed for PTSD (77.4%), followed by depression (40.3%), and anxiety (23.4%). Reviewed articles span a publication period of twenty years (2000–2020) and report data pertaining to EWEs occurring between 1992 and 2014 (Table A3). Geographically, over half of investigations (and associated populations) originated from North America (31/59; 52.5%), of which 30 studies (50.9%) derived from the USA (Fig. 2), with the remainder of investigations primarily derived from Asia (17/59; 28.8%). Consequently, most investigations were associated with categorically high-income settings (38/59; 64.4%), followed by those allocated to the lower income classification (16/59; 27.1%). Approximately 56% (33/59) of studied populations were classified by age as occurring within the adult

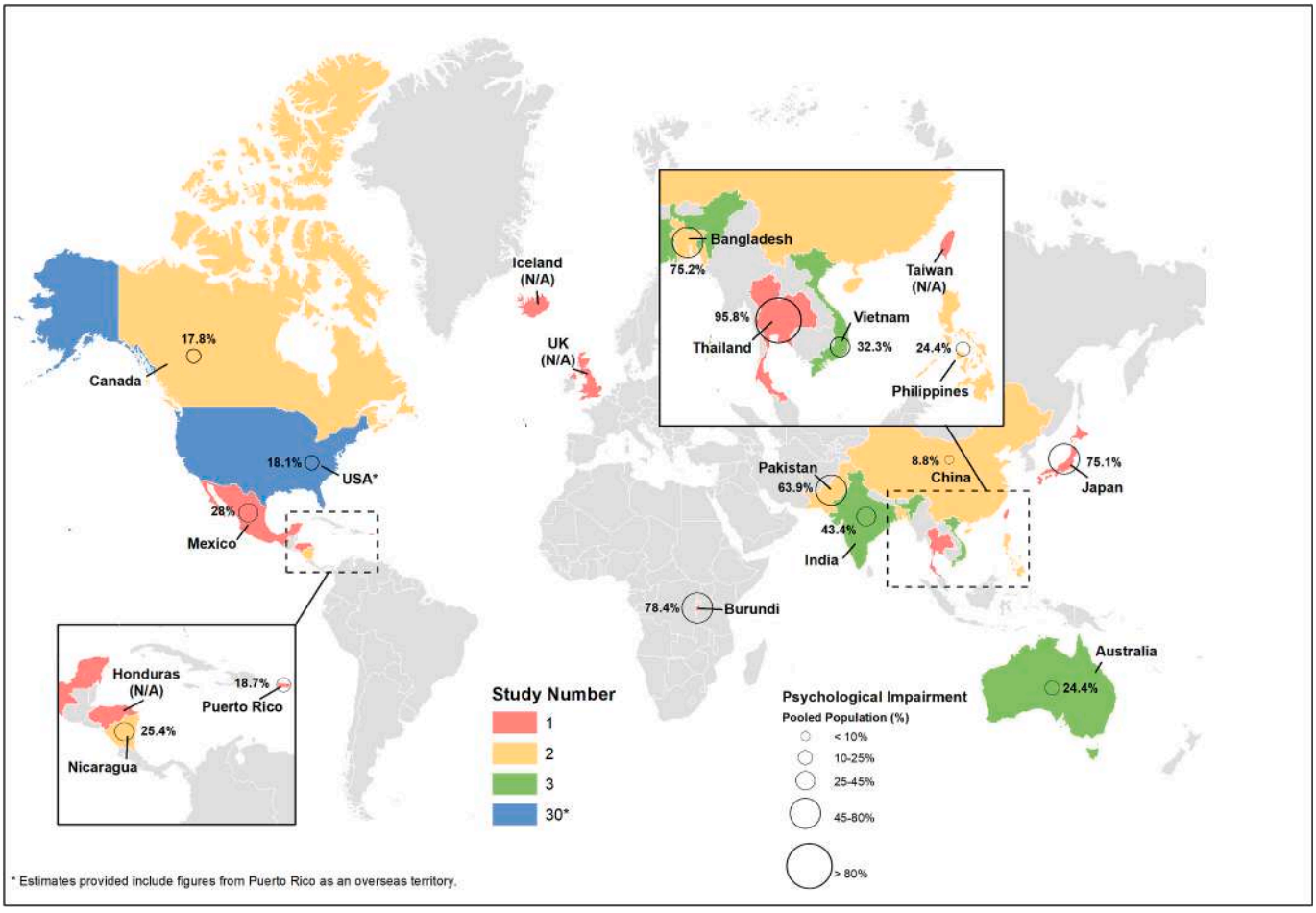

Fig. 2. Global distribution of reviewed investigations. The number of articles per country of origin and the composite metric for psychological impairment are also provided. N/A = Not Available.

(31–50) (19/59; 32.2%) and child (<15) (14/59; 23.7%) sub-populations (Table A3). Investigations with population samples dominated by female gender (17/59; 28.8%) and racial/ethnic minorities (12/59; 20.3%) represented 16.6% and 9.8% of the total dataset population, respectively (Table A3).

3.2. Event Types and study methodology

Most articles focused on extreme weather phenomena associated with "storm" (39/59; 66.1%) and "flood" (15/5; 25.4%) event categories, with "drought/heat" and "wildfire" events infrequently studied ($n \leq 3$) (Table A3). Reviewed investigations almost entirely comprised population samples exposed to "acute" (or fast-onset) phenomena, defined within as "weather" events (see Appendix C) (56/59; 94.9%), compared with "climatic" (gradual or sub-acute) phenomena represented by studies focusing on heat waves and droughts (3/59; 5.1%).

Cross-sectional study types, i.e., investigations based on evaluation at a single point in time, dominated the dataset (51/59; 86.4%). Among the few longitudinal studies identified (8/59; 13.6%), a majority were confined to only two waves of psychological evaluation (7/8; 87.5%). Importantly, the reported time lag between EWE exposure and (post-event) psychological evaluation was highly comparable between investigations employing cross-sectional and longitudinal study designs (Appendix F). While most investigations were based on non-representative sample selection criteria (34/59; 57.6%), i.e., a study sample not reflective of the general population, several incorporated representative (or random) sampling designs (26/59; 44.1%) (Table A3). Diagnostic methods generally consisted of self-reported measures, accounting for 71.8% of the total examined population, with clinically established cases less common (23.5%). A substantial number of investigations lacked a control population (41/59; 69.5%) with just 12/59 (20.3%) studies employing independent control criteria, while 7/59 (11.9%) reported pre- and post-event impairment data. The latter included four studies reporting retrospectively acquired pre-event data. Overall, 75.2% ($n = 45{,}576$) of respondent impairment data lacked any control parallel.

3.3. Estimates of psychological impairment

Comprehensive summaries of pooled psychological impairment data, i.e., morbidity data extracted and collated (specifically) at a sub-category level, for both composite (any impairment) and domain-specific categories are provided in Table 1–3Summary statistics for key (sub-)categories are presented in Figs. 3–4, with pooled data at a national level presented in Table A4. Additional impairment data are presented separately in Table A5. Overall, a composite (post-event) psychological impairment rate of 23.2% (10,052/43,385) was estimated (Table 1). However, a considerable proportion of investigations failed to provide sufficient data to derive composite impairment (20/59; 33.9%). Lack of reporting of co-morbidity data among studies employing multiple measures represented a recurrent limitation in the calculation of composite values. Highest rates of impairment were estimated for depression (24%), with lower values calculated for PTSD and anxiety (~17%) (Table 1). Compiled data also enabled the determination of composite values solely based on standardised psychopathology (e.g., DSM), with a composite (i.e., PTSD, anxiety, depression) prevalence rate of

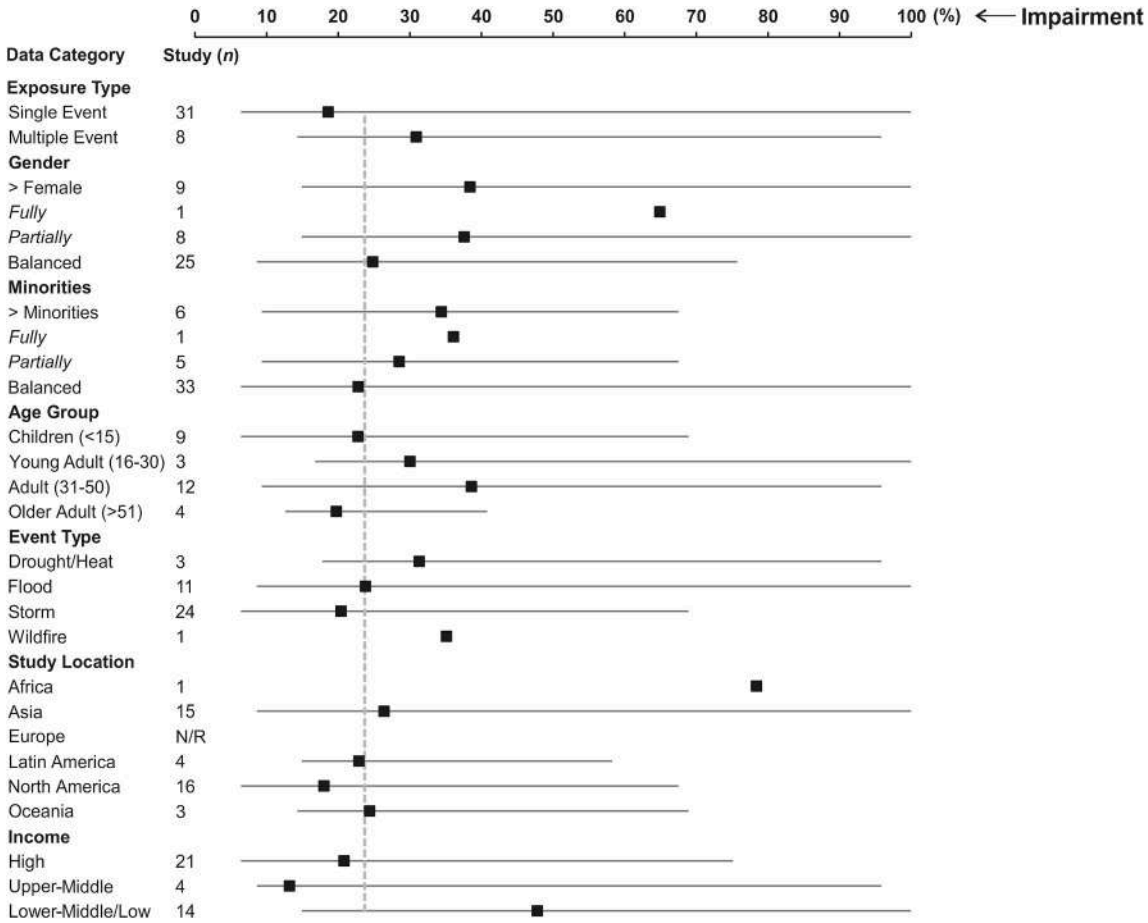

Fig. 3. Plot of composite psychological impairment values stratified by key data sub-categories. The number of reporting studies (n) in each sub-category is also provided. Black squares indicate the mean value estimated per sub-category with horizontal black lines providing value range. The vertical dashed grey line indicates the "global" mean value. N/R = Not Reported.

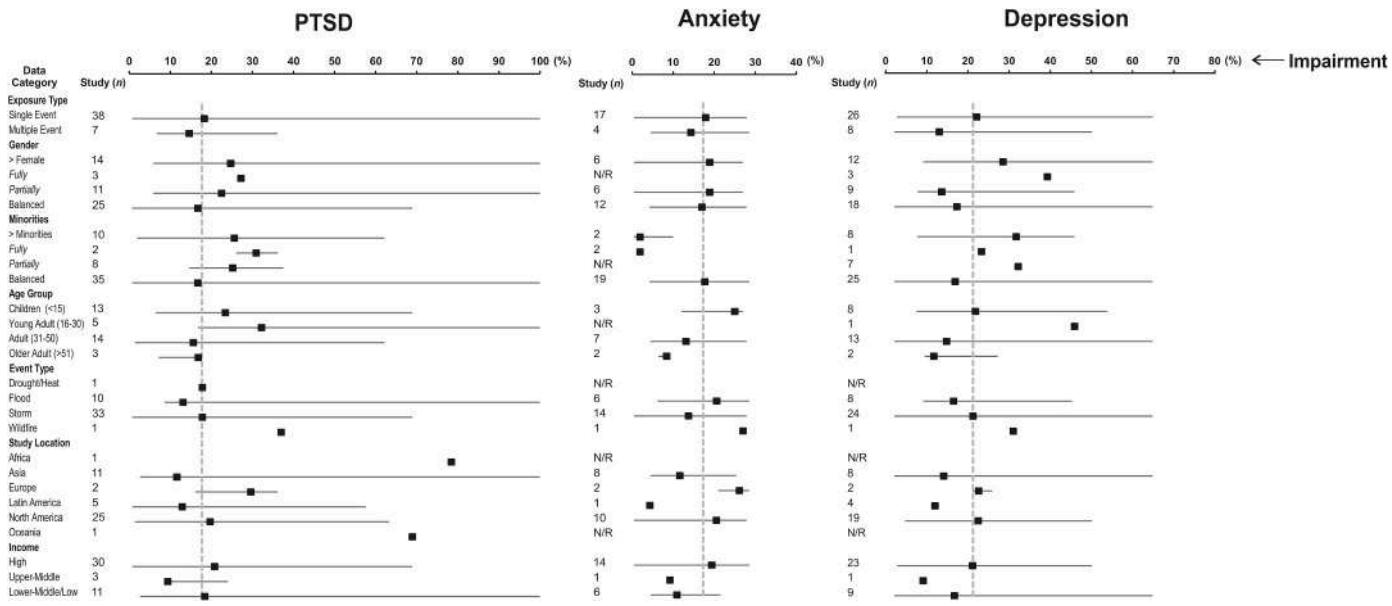

Fig. 4. Plot of psychological impairment values by key data sub-categories per domain (PTSD, anxiety, depression). The number of reporting studies (*n*) in each sub-category is also provided. Black squares indicate the mean value estimated per sub-category with horizontal black lines providing value range. The vertical dashed grey line indicates the "global" mean value. N/R = Not Reported.

Table 1
Estimated psychological impairment values at composite and domain-specific levels. The total population subject to psychological diagnosis (*N*) and corresponding number of positive cases (*n*) per category are also provided.[1] Values excluding data derived from non-standardised mental health measures contained within the "Additional Distress" domain. *Estimates presented are subject to accurate (full) study co-morbidity reporting and thus differ from domain-specific values.

Domain	Impairment % (*N*/*n*)	Impairment Range (%)	Study *n* (%)
PTSD	17.7 (8144/46,075)	0.7–100	45 (76.3)
Anxiety	17.3 (2477/14,355)	0.5–28.5	21 (35.6)
Depression	24 (5737/23,924)	2.1–64.9	34 (57.6)
Substance Use Disorder	17.4 (1388/7963)	1.8–39.9	8 (13.6)
Additional Distress	33.9 (4726/13,934)	4.9–95.8	15 (25.4)
Composite	23.2 (10,052/43,385)	6.4–100*	39 (66.1)
Composite[1]	18.6 (5889/31,613)	6.4–100*	29 (49.2)

18.6% (5889/31,613) calculated. Estimated psychological impairment exhibited marked variability among identified studies, with the largest range reported for PTSD (0.7%–100%) (Table 1).

Regionally, Asian countries were characterized by higher prevalence, particularly Bangladesh (75.2%), Pakistan (63.9%) and India (43.4%) (Fig. 2; Table A4). Observed regional/national trends were at least partially mirrored with respect to income category and impairment estimates were highest across studies in lower income regions (47.8%) in comparison to middle- or high-income settings (≤20%) (Fig. 3). Residents of rural areas exhibited higher composite impairment (38.8%) relative to their (peri-)urban counterparts (≤30%).

Populations exposed to events classified as "wildfires" (35.1%) and "drought/heat" (31.3%) exhibited the highest composite prevalence rates (Fig. 3). Respondents experiencing events within the "storm" and "flood" categories exhibited comparable prevalence rates (20.4%–23.8%). Populations exposed to "multiple" (more than a single event) weather events also reported higher composite prevalence (30.9%) in comparison to those experiencing single ("one-off") events (18.6%) (Fig. 3). Temporally, composite impairment rates exhibited a decadal monotonic increase (11.1%–39.5%; cf. event year in Table 2). Higher values were also observed for individuals evaluated within one-month post-event, particularly at a composite level (49.6%) (Tables 2-3). The estimated recency and relevance of shorter-term sequelae may be supported by a higher prevalence observed among individuals recruited from relief centres (81.9%), with diagnoses in these settings generally generated within a two-month window (Tables 2-3).

Composite estimates suggest that study populations primarily comprised of adults aged 31–50 exhibited higher rates of psychological impairment relative to other populations (38.6%; Fig. 3). Overall, impairment was lowest among older adults (>51 years). Population samples dominated by minorities (34.4%) and female gender (38.4%) exhibited higher impairment rates than those with more balanced socio-demographics (~ 23%) (Fig. 3).

3.4. Reported risk factors

As shown (Table 4), over half of reported risk variables occurred within the pre-event risk category (156/290; 53.9%). Here, female gender was most frequently associated with risk of psychological impairment (29/156; 18.9%). Specifically, female gender was often linked with increased occurrence of PTSD (15/73; 20.5%) and anxiety (6/23; 26.1%). Additional (frequent) risk factors included lower socio-economic status and reports of previous mental health symptoms/disorders; each accounting for 10.3% (16/155) among pre-event risk factors. Within the peri-event category, event exposure was the variable most commonly associated with any type of psychopathology (42/69; 60.9%) with levels of fear/perceived threat and (in-)direct experience of physical injuries or somatic conditions (i.e., personally or through family members) identified as common risk factors for PTSD (Table 4). Event exposure was also the most important risk factor across the three adopted risk typologies (42/257; 14.5%) (Table 4). In relation to post-event factors, respondents experiencing property damage/loss and financial stress were most at risk of developing psychological impairment (~ 20%).

3.5. Pooled odds ratios

Odd ratios calculated from reported composite data are provided in Fig. 5, with domain-specific estimates presented in Figs. 6–8. Key

Table 2
Estimated values for composite psychological impairment stratified by selected data sub-categories. The study *n* column provides the number of investigations (among sub-category total) with adequate (full) data reporting to derive pooled values.

Data Category	Study *n* (%)	Impairment (%)	Data Category	Study *n* (%)	Impairment (%)
Study Location			Sampling Strategy		
Africa	1/1 (100)	78.4	Representative	8/12 (66.7)	21.2
Asia	15/17 (88)	26.4	Non-representative	31/47 (66)	28.9
Europe	N/R	N/R	**Population Pool**		
Latin America	4/5 (80)	22.9	Educational Institution	10/14 (71.4)	21.3
North America	16/31 (52)	18	General Population	25/37 (67.6)	23
Oceania	3/3 (100)	24.4	Healthcare Centre	1/3 (33.3)	14.9
Income Level			Relief Centre	3/5 (60)	81.9
High	21/38 (55.3)	20.8	**Racial Composition**		
Upper-Middle	4/4 (100)	13.2	> Minorities	6/12 (50)	34.4
Lower-Middle/Low	14/16 (87.5)	47.8	*Fully*	1/1 (100)	36.1
N/A	N/R	N/R	*Partially*	5/11 (45.5)	28.5
Local Setting			Balanced/Low	33/47 (70.2)	22.8
Rural	6/10 (60)	38.8	**Gender Composition**		
Urban	13/19 (68.4)	27.5	> Female	9/19 (47.4)	38.4
Mixed	5/7 (71.4)	30.3	*Fully*	1/4 (25)	64.9
N/R	15/23 (65.2)	13.5	*Partially*	8/11 (72.7)	37.6
Climate			Balanced/Low	25/33 (75.8)	24.8
Arid	1/1 (100)	51.6	N/R	4/6 (66.7)	12.9
Tropical	15/17 (88)	34.7	**Event Lag (months)**		
Temperate	19/34 (56)	18.3	<1	4/6 (66.7)	49.6
Cold/Polar	1/4 (25)	7.2	2–6	12/17 (70.6)	22.2
Unknown	3/3 (100)	17.4	7–12	7/13 (53.8)	32
Event Type			>13	12/18 (66.7)	12.5
Drought/Heat	3/3 (100)	31.3	N/A	4/5 (80)	38
Flood	11/14 (78.6)	23.8	**Event Year**		
Storm	24/38 (63.2)	20.4	1990–2000	9/13 (69.2)	11.1
Wildfire	1/2 (50)	35.1	2001–2010	21/31 (67.7)	29.9
Age Group			2011–2020	9/15 (60)	39.5
Children (<15)	9/14 (64.3)	22.8	**Exposure Type**		
Young Adult (16–30)	3/5 (60)	30	Single Event	31/47 (66)	18.6
Adult (31–50)	12/19 (63.2)	38.6	Multiple Events	8/12 (66.7)	30.9
Older Adult (>51)	4/5 (80)	19.7	**Impact Type**		
N/R	11/16 (68.8)	17.7	Weather (Acute)	36/56 (64.3)	22
Diagnosis Type			Climatic (Sub-Acute)	3/3 (100)	31.3
Clinical Evaluation	6/8 (75)	11			
Evaluation/Self-report	1/4(25)	22.7			
Self-report	32/47 (68.1)	28			

characteristics for investigations incorporating control groups are also provided in Table A6. Inconsistent reporting of co-morbidity data precluded (composite) OR calculation in 5/12 (41.7%) studies (Table A6). Similarly, at a domain-specific level, two investigations failed to provide morbidity data necessary for pooled OR calculation.

Overall, the odds of developing any psychological impairment were approximately 90% higher among individuals exposed to extreme weather events in comparison to control populations (pOR = 1.9; CI = 1.7–2; Fig. 5). At a domain level, odds were highest for PTSD development (pOR = 4.8), with a population sample exposed to hurricanes (cf. Kar et al., 2007; Tucker et al., 2017) reporting the highest probability of PTSD development (OR = 7.4–7.8) (Fig. 6; Table A6). Similarly, pORs indicate exposed populations were approximately twice as likely to exhibit depressive symptomology (pOR = 2.04) (Fig. 7). Anxiety was the only domain exhibiting a negative calculated association with EWE exposure (pOR = 0.6) (Fig. 8). Here, it is important to note that estimates are particularly influenced by control group data provided from Brown et al. (2019) with higher odds of anxiety diagnosis in contrast to those exposed to extreme weather (Fig. 8). Brown et al. (2019) reports data from school children exposed to wildfires, with an explicit study caveat represented by introduction of a post-event (and pre-measure) school-wide student mental health support programme. As such, reported anxiety data were possibly influenced by a successful intervention.

4. Discussion

4.1. Composite estimates of psychological impairment and odds ratios

To the authors' knowledge, this represents the first global collation and empiric integration of mental health and well-being data exclusively from populations exposed to extreme weather events. Calculated ORs indicate a high probability (+90%) for development of any form of psychological impairment following exposure to weather/climatic phenomena (pOR = 1.9; Fig. 5), providing strong evidence for the detrimental effects of EWEs on human health. Notwithstanding, estimates presented, particularly pertaining pooled data, need to be interpreted cautiously due to a number of inherent methodological limitations which are discussed in detail in the limitation and recommendation section below.

Accounting for potential limitations, comparisons of prevalence data with available mental health "baselines" may prove particularly insightful in ascertaining the relevance of pooled estimates presented. For example, data recently curated by the Institute for Health Metrics and Evaluation (IHME), indicate a global prevalence rate for mental disorders of ~ 13% (GDB, 2019). This is considerably lower than estimated composite impairment rates within the current study (18.6%–23.2%) (Table 1), representing the potential severity of EWEs on mental health. Likewise, global (12-month) prevalence rates for mental disorders provided by Steel et al. (2014) (~ 17%), may be indicative of a

Table 3
Estimated psychological impairment values per domain (PTSD, anxiety, depression) stratified by data sub-categories. The study *n* column provides the number of investigations (among sub-category total) providing adequate (full) data reporting to derive pooled values.

Data Category	PTSD		Anxiety		Depression		Data Category	PTSD		Anxiety		Depression	
Study Location	Study *n* (%)	Impairment (%)	Study *n* (%)	Impairment (%)	Study *n* (%)	Impairment (%)	**Sampling Strategy**	Study *n* (%)	Impairment (%)	Study *n* (%)	Impairment (%)	Study *n* (%)	Impairment (%)
Africa	1 (2.2)	78.4	N/A	N/A	N/A	N/A	Representative	18 (40)	15	10 (47.6)	16.6	14 (42.4)	11.4
Asia	11 (24.4)	11.6	8 (38.1)	11.6	8 (24.2)	14.1	Non-representative	27 (60)	22.1	11 (52.4)	17.6	19 (57.6)	24.2
Europe	2 (4.4)	29.6	2 (9.5)	26.1	2 (6.1)	22.6	**Population Pool**						
Latin America	5 (11.1)	12.9	1 (4.8)	4.3	4 (12.1)	12	Educational Institution	13 (28.9)	25.8	3 (14.3)	25	7 (21.2)	28.3
North America	25 (55.6)	19.7	10 (47.6)	20.5	19 (57.6)	22.5	General Population	26 (57.8)	13.2	18 (85.7)	14.8	23 (69.7)	12.3
Oceania	1 (2.2)	68.9	N/A	N/A	N/A	N/A	Healthcare Centre	3 (6.7)	22.4	N/A	N/A	2 (6.1)	38.4
Country Income Level							Relief Centre	3 (6.7)	81.9	N/A	N/A	1 (3)	50.1
High	30 (66.7)	20.8	14 (66.7)	19.4	23 (69.7)	21.1	**Racial Composition**						
Upper-Middle	3 (6.7)	9.4	1 (4.8)	9.2	1 (3)	9.1	> Minorities	10 (20.2)	25.6	2 (9.5)	1.9	8 (24.2)	31.7
Lower-Middle/Low	11 (24.4)	18.4	6 (28.6)	10.9	9 (27.3)	16.7	*Fully*	2 (4.4)	30.9	2 (9.5)	1.9	1 (3)	23.3
N/A	1 (2.2)	25.8	N/A	N/A	N/A	N/A	*Partially*	8 (17.8)	25.2	N/A	N/A	7 (21.2)	32.2
Local Setting							Balanced/Low	35 (77.8)	16.7	19 (90.5)	17.7	25 (75.8)	16.9
Rural	7 (15.6)	29	4 (19)	19.6	5 (15.2)	22.2	**Gender Composition**						
Urban	15 (33.3)	22.5	4 (19)	23.4	11 (33.3)	20.3	> Female	14 (31.1)	24.7	6 (28.6)	18.9	12 (36.4)	28.5
Mixed	3 (6.7)	13.1	2 (9.5)	10.2	3 (9.1)	8.9	*Fully*	3 (6.7)	27.2	N/A	N/A	3 (9.1)	39.3
N/R	20 (44.4)	13	11 (52.4)	14.9	14 (42.4)	22	*Partially*	11 (24.4)	22.5	6 (28.6)	18.9	9 (27.3)	13.6
Climate							Balanced/Low	25 (55.6)	16.7	12 (57.1)	17.3	18 (54.5)	17.3
Arid	N/A	N/A	N/A	N/A	N/A	N/A	N/R	6 (13.3)	13.4	3 (14.3)	17	3 (9.1)	12.4
Tropical	13 (28.9)	14.9	7 (33.3)	9.2	10 (30.3)	13.8	**Event Lag (months)**						
Temperate	27 (60)	16	12 (57.1)	17.9	19 (57.6)	21	<1	4 (8.9)	26	1 (4.8)	27	N/A	N/A
Cold/Polar	3 (6.7)	26.3	2 (9.5)	26.5	3 (9.1)	26.1	2–6	13 (28.9)	22	3 (14.3)	11	10 (30.3)	21.2
Unknown	2 (4.4)	40.4	N/A	N/A	1 (3)	9.1	7–12	10 (22.2)	24.8	6 (28.6)	18.6	9 (27.3)	19
Event Type							>13	15 (33.3)	13.6	10 (47.6)	20.6	12 (36.4)	22.4
Drought/Heat	1 (2.2)	17.8	N/A	N/A	N/A	N/A	N/A	3 (6.7)	14.5	1 (4.8)	4.5	2 (6.1)	8.5
Flood	10 (22.2)	13.1	6 (28.6)	20.6	8 (24.2)	16.5	**Event Year**						
Storm	33 (73.3)	17.8	14 (66.7)	13.7	24 (72.7)	21.2	1990–2000	9 (20.5)	9.7	5 (23.8)	9.3	7 (21.2)	14
Wildfire	1 (2.2)	37	1 (4.8)	27	1 (3)	31	2001–2010	25 (56.8)	23.5	14 (66.7)	9	20 (60.6)	21
Age Group							2011–2020	10 (22.7)	23.1	2 (9.5)	26.7	6 (18.2)	22
Children (<15)	13 (28.9)	23.4	3 (14.3)	25	8 (24.2)	21.8	**Exposure Type**						
Young Adult (16–30)	5 (11.1)	32.2	N/A	N/A	1 (3)	45.9	Single Event	38 (84.4)	18.3	17 (81)	17.9	26 (76.5)	22.1
Adult (31–50)	14 (31.1)	15.6	7 (33.3)	13.1	13 (39.4)	14.8	Multiple Events	7 (15.6)	14.6	4 (19)	14.3	8 (23.5)	13
Older Adult (>51)	3 (6.7)	16.8	2 (9.5)	8.4	2 (6.1)	11.7	**Impact Type**						
N/R	10 (22.2)	11.4	9 (42.9)	17.3	9 (27.3)	14.1	Weather (Acute)	44 (97.8)	17.6	21 (100)	17.4	33 (100)	20
Diagnosis Type							Climatic (Sub-Acute)	1 (2.2)	19.2	N/A	N/A	N/A	N/A
Clinical Evaluation	8 (17.8)	9.6	4 (19)	12.2	5 (15.2)	11.6							
Evaluation/Self-report	4 (8.9)	11.3	2 (9.5)	6.6	3 (9.1)	8.3							
Self-report	33 (73.3)	22.2	15 (71.4)	19.4	25 (75.8)	23.2							

Table 4
Incidence of identified risk factors among composite and domain-specific classifications. *Pre-event variable (obtained pre-event or retrospectively). °The composite category incorporates risk factors from domains not shown in table. +Risk factor categories follow Maguen et al. (2009).

Risk Factor Classification Group+	Harmonised Risk Factor Categories	Domain-Specific Risk Factor Incidence			
		PTSD *n* (%)	Anxiety *n* (%)	Depression *n* (%)	Composite° *n* (%)
Pre-Event	Age (younger)	3 (2.2)	1 (2.4)	2 (3.1)	9 (3.1)
	Age (older)	4 (2.9)	2 (4.8)	3 (4.7)	11 (3.8)
	Legal Status (widowed/divorced/single)	1 (0.7)	2 (4.8)	N/A	3 (1)
	Socio-Economic Status (lower)	7 (5.1)	1 (2.4)	5 (7.8)	16 (5.5)
	Education Level (lower)	8 (5.8)	3 (7.1)	2 (3.1)	15 (5.2)
	Employment Status (unemployed)	4 (2.9)	1 (2.4)	4 (6.3)	11 (3.8)
	Racial/Ethnic Minority	7 (5.1)	1 (2.4)	2 (3.1)	12 (4.1)
	Religion	1 (0.7)	1 (2.4)	2 (3.1)	4 (1.4)
	Female	15 (10.9)	6 (14.3)	3 (4.7)	29 (10)
	Trauma Exposure *	6 (4.4)	2 (4.8)	5 (7.8)	14 (4.8)
	Mental Health Symptom/Disorder *	8 (5.8)	1 (2.4)	3 (4.7)	16 (5.5)
	Physical Injury/Somatic Condition *	2 (1.5)	N/A	1 (1.6)	5 (1.7)
	General Health Status (lower)	1 (0.7)	1 (2.4)	1 (1.6)	3 (1)
	Other	6 (4.4)	1 (2.4)	1 (1.6)	8 (2.9)
	Sub-total n (%)	*73 (53.2)*	*23 (55)*	*34 (53.2)*	*156 (53.9)*
Peri-Event	Family Death/Injury	4 (2.9)	N/A	2 (3.1)	7 (2.4)
	Physical Injury/Somatic Condition (higher)	5 (3.6)	N/A	3 (4.7)	10 (3.5)
	Level of Event Exposure/Stressors (higher)	21 (15.3)	5 (11.9)	9 (14.1)	42 (14.5)
	Fear and Perceived Threat (higher)	6 (4.4)	1 (2.4)	2 (3.1)	10 (3.4)
	Sub-total n (%)	*36 (26.3)*	*6 (14.3)*	*16 (25)*	*69 (23.9)*
Post-Event	Displacement/Evacuation	4 (2.9)	1 (2.4)	N/A	6 (2.1)
	Financial Stress	4 (2.9)	2 (4.8)	2 (3.1)	12 (4.1)
	Property Damage/Loss	7 (5.1)	2 (4.8)	3 (4.7)	13 (4.5)
	Restricted Access to Food/Water	1 (0.7)	1 (2.4)	2 (3.1)	4 (1.4)
	Restricted Access to Medical Facilities/Treatment	3 (2.2)	2 (4.8)	2 (3.1)	9 (3.1)
	Utility Disruption	2 (1.5)	2 (4.8)	2 (3.1)	6 (2.1)
	Level of Social Support (lower)	5 (3.6)	2 (4.8)	2 (3.1)	9 (3.1)
	Other	2 (1.5)	1 (2.4)	1 (1.6)	4 (1.4)
	Sub-Total n (%)	*28 (20.5)*	*13 (31.2)*	*14 (21.8)*	*63 (21.7)*
	Total *n* (%)	**137 (100)**	**42 (100)**	**64 (100)**	**290 (99.5)**

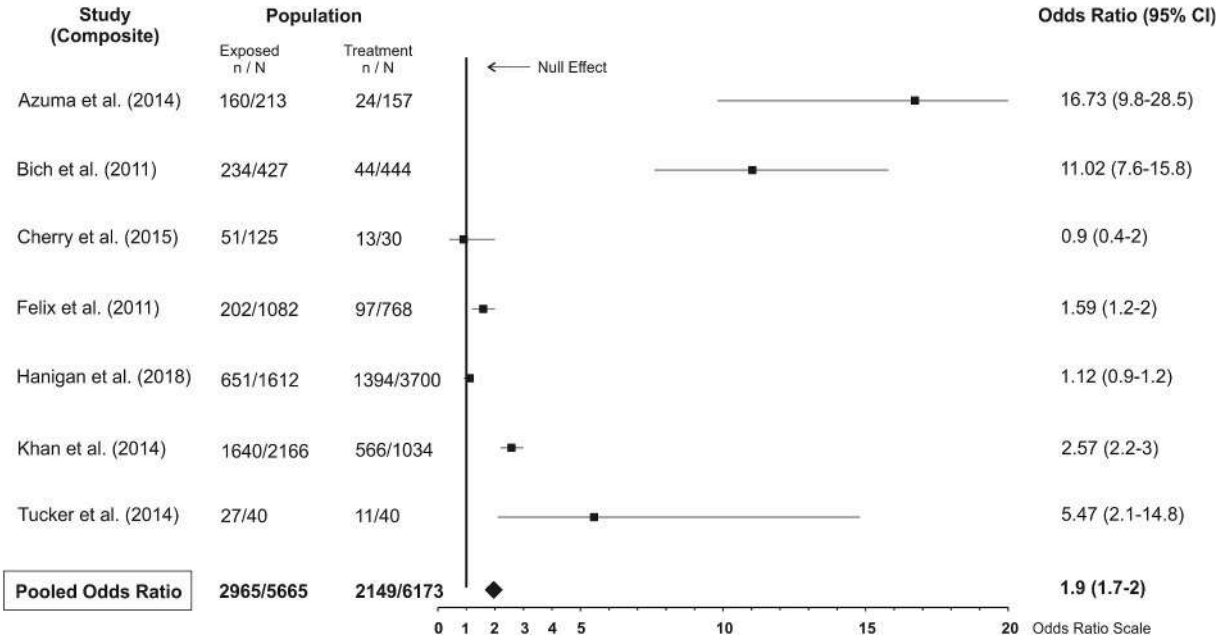

Fig. 5. Forest plot showing calculated ORs for studies reporting composite psychological impairment. The population column provides the total number of positive cases (n) among exposed and control groups (N). Black squares indicate ORs which are also provided at the right along with 95% confidence intervals. The pOR is provided at the bottom of the plot. The vertical black lines indicates the point (or threshold) of null effect.

"background" burden. Overall, mental health estimates vary significantly in the literature (e.g., Norris et al., 2002; Rataj et al., 2016; Lowe et al., 2019); a factor clearly represented among observed domain ranges (Table 1). Arguably, comparisons with pertinent "baselines" from the disaster literature could provide more relevant standards for direct comparison. Here, estimated composite values (18.6%–23.2%) are

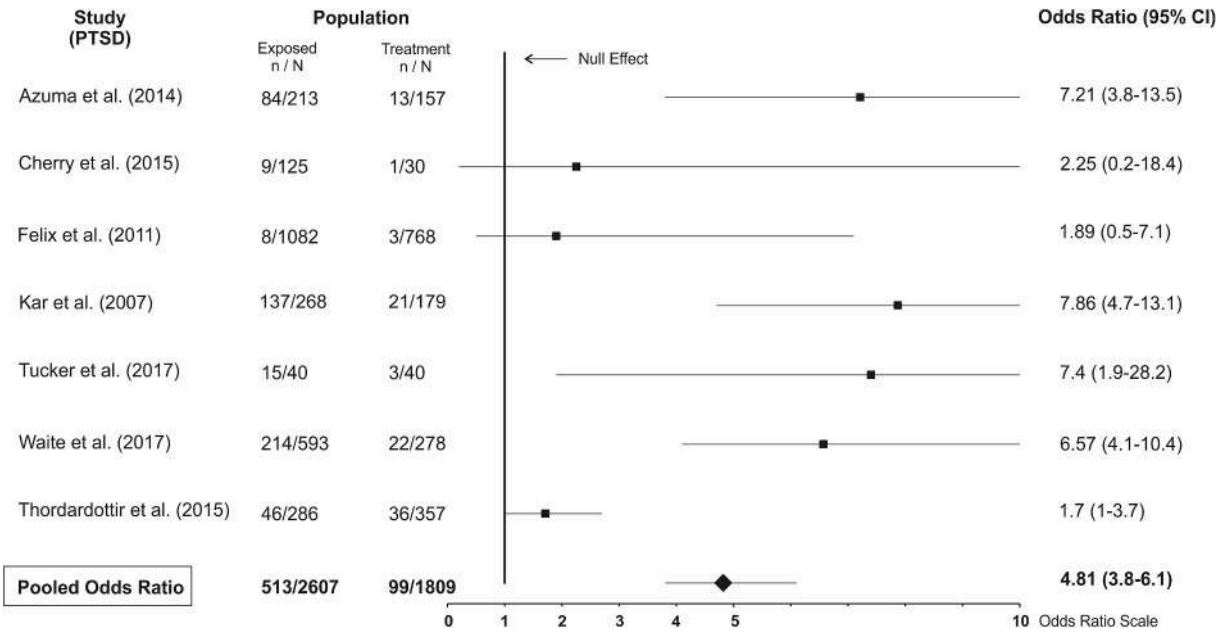

Fig. 6. Forest plot showing calculated ORs based on PTSD studies. The population column provides the total number of positive cases (n) among exposed and control groups (N). Black squares indicate ORs which are also provided at the right along with 95% confidence intervals. The pOR is provided at the bottom of the plot. The vertical black lines indicates the point (or threshold) of null effect.

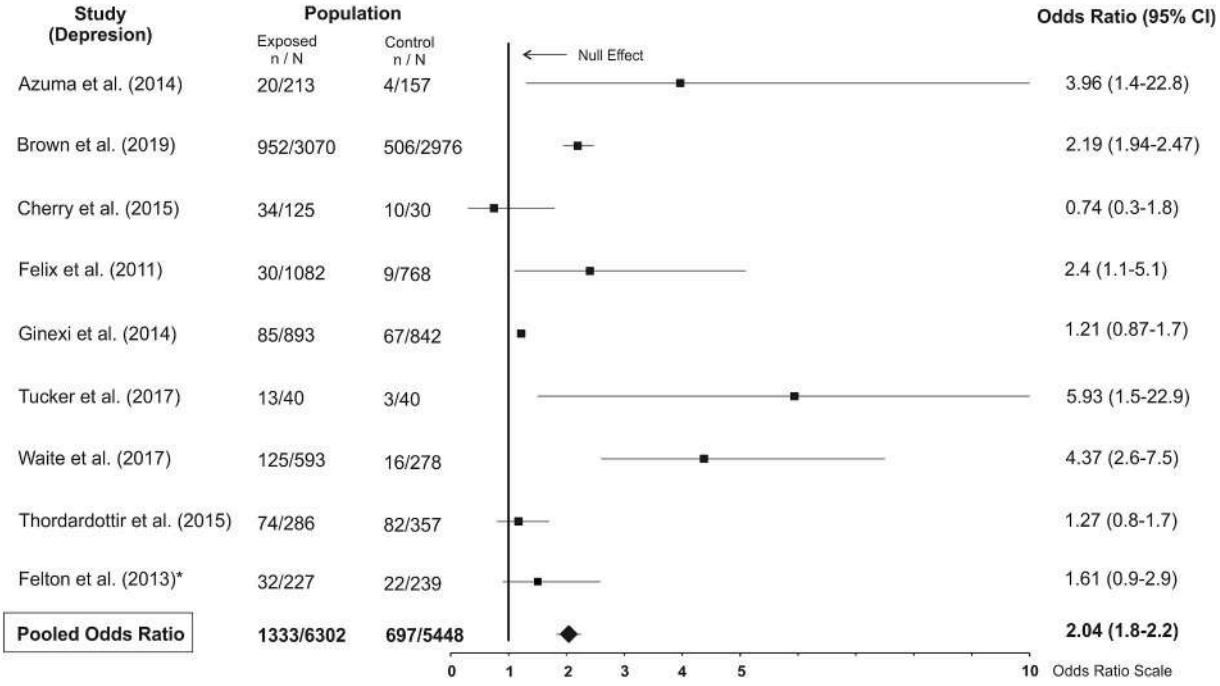

Fig. 7. Forest plot showing calculated ORs based on depression studies. *Study based on pre-post control data and not included into pOR calculation. The population column provides the total number of positive cases (n) among exposed and control groups (N). Black squares indicate ORs which are also provided at the right along with 95% confidence intervals. The pOR is provided at the bottom of the plot. The vertical black lines indicates the point (or threshold) of null effect.

analogous with reported "general" population estimates of psychological impairment following EWE exposure (~ 20%) (Clayton 2021), supporting the presented prevalence rates. Following WHO baselines for disorder prevalence following natural (i.e., (non-)climatic) disasters in general (6%–11%) (Berry et al., 2010), the estimated composite rates are indicative of (*i*) a significant impact which can be specifically attributed to extreme weather, or (*ii*) an underestimate of previous baselines. In either case, these highlight the relevance of the presented prevalence data, in improving our understanding of the psychological burden of EWEs.

4.2. Psychological impairment and domains

PTSD is the only assessed psychological disorder requiring exposure to a trauma, and thus is less likely to be methodologically constrained in terms of population, exposure level, and background (pre-event) impairment (Lowe et al., 2019). This conveys a degree of support for pooled PTSD estimates (Tables 1–3); comparisons with reported

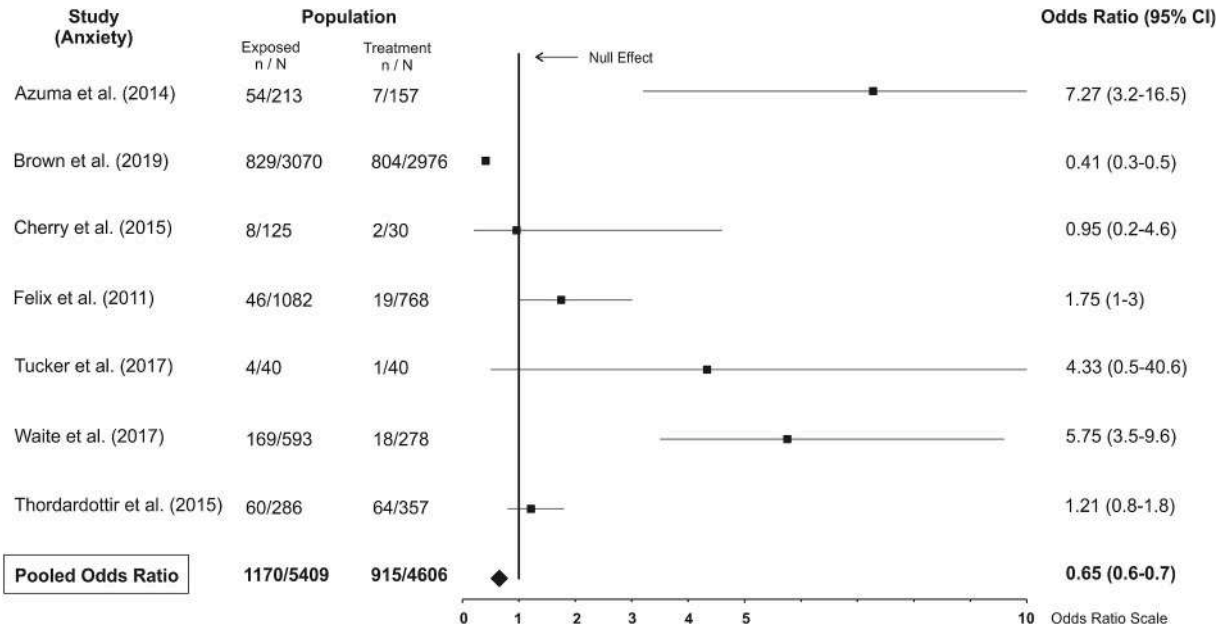

Fig. 8. Forest plot showing calculated ORs based on anxiety studies. The population column provides the total number of positive cases (n) among exposed and control groups (N). Black squares indicate ORs which are also provided at the right along with 95% confidence intervals. The pOR is provided at the bottom of the plot. The vertical black lines indicates the point (or threshold) of null effect.

(background) epidemiological figures may prove more particularly pertinent in the context of PTSD. For example, comparison of PTSD figures (17.7%) with general population estimates (2%–10%) (Kessler et al., 1995, 2005; Galea et al., 2005; Atwoli et al., 2015) indicate significantly increased rates of PTSD following EWE exposure, with this finding further emphasized by high estimated ORs (pOR = 4.8; Fig. 6).

While PTSD featured as the most frequently encountered psychopathological measure, depression exhibited a higher prevalence (24%) among pooled cohorts (Table 1). Observed trends concur with recent findings reported by Lowe et al. (2019), with depression cases generally higher than PTSD among 20/26 (76.9%) peer-reviewed investigations focusing on populations exposed to "environmental" disasters. Once again, comparison with epidemiological data, which have placed the global prevalence of depression disorders between 3% and 12% (Kessler et al., 2009; Steel et al., 2014; GBD, 2019), are indicative of an elevated (domain-specific) burden linked with EWE exposure. Nonetheless, depression is one of the most prevalent mental health disorders among the general public, and consequently, the possibility of empiric inflation by pre-event morbidity should be highlighted (Kessler et al., 2012; Goldman and Galea, 2014). For anxiety disorders, potential baselines of 4%–11% have been reported among the general public (Kessler et al., 2009; Steel et al., 2014; GBD, 2019), thus indicating a potentially significant impact within the context of EWEs (17.3%; Table 1).

4.3. Socio-economic, geographical and temporal trends

Analyses indicate two main regional trends, namely, higher impairment among residents of low-income regions at a composite level (47.8%; Fig. 3), and conversely, a higher proportion of EWE-related anxiety (19.4%) and depression (21.1%) in high-income settings (Table 3; Fig. 4). In low-income regions, a combination of key drivers including high poverty levels, increased exposure to extreme weather, and restricted access to "recovery" resources are likely associated with higher risks of psychological impairment following EWEs (McFarlane and Williams, 2012; Rataj et al., 2016; Berry et al., 2018; Morganstein and Ursano, 2020). The relevance of lower socio-economic status, as inferred from prevalence data obtained from investigations based on low-income countries, is also reinforced by its recurrence among (pre--event) risk factors identified in the literature (Table 4). Importantly, associations between low socio-economic background, extreme weather, and a higher risk of psychological impairment, were reported in both high- and low-income settings (e.g., Galea et al., 2007; Bandla et al., 2019) highlighting its importance at (inter-)national scales irrespective of regional income.

The higher prevalence of anxiety and depression disorders in high-income settings mirrors recurrent trends (Kessler et al., 2009; Witchen et al., 2011; Kessler and Bromet, 2013), linked to typically "western" cultural traits (Koplewicz et al., 2009). For example, Kessler et al. (2005, 2012) estimate epidemiological anxiety baselines between 18% and 25% in the USA. These values are considerably higher than calculated estimates (Table 1), emphasizing the potential bias introduced by regional trends. However, calculated ORs did not demonstrate any particular geographical trends (Figs. 5–8; Table A6), with the caveat that only one investigation reported control data from a typically non-Western setting (Felix et al., 2011). Anxiety was the only domain exhibiting a negative (OR) association with extreme weather exposure (Fig. 8), this highlighting the complexity of interpreting mental health data.

Globally, Asia consistently experiences the highest proportion of major hydro-meteorological hazards, including (event) incidence, associated mortality and economic loses (CRED, 2020; IFRC, 2020; WMO et al., 2020). This was reflected in the current study, with Asian populations exhibiting the highest pooled psychological impairment rates (Table 1 and A5; Fig. 3). Similarly, Asian studies were characterised by the highest composite ORs (Fig. 5; Table A6). This has been attributed to elevated regional population density, with the potential to exacerbate the effects of EWE exposure (Watts et al., 2015; Stephenson, 2008; Forzieri et al., 2017; IFRC, 2020). In this context, presented data may demonstrate the reported (cumulative) spatio-temporal impacts of EWEs at a global scale (IPCC et al, 2012; Goldman and Galea, 2014; WMO et al., 2020), with a higher event frequency and gradual (global) population expansion reflected in the monotonic temporal increase of prevalence rates (cf. event year intervals; Tables 2-3). However, the latter may also be an artefact of improving psychopathological diagnoses resulting in increasingly reliable case detection (Aboraya et al., 2006). Identified trends also provide key insights into (post-event) psychological impairment and the effects of recency, with marked impacts among cohorts with immediate (<1 month) EWE exposure

(49.6%; Table 2). The importance of short-term impacts, which are also reflected via higher impairment among respondents from relief centres (81.9%; Table 2), highlight the need for swift and efficient mental health intervention following EWEs. Collated data tend to concur with the literature suggesting psychological disorder symptomology typically peaks within 12 months following EWE exposure (Table 2) (Goldman and Galea, 2014). Conversely, some investigations did identify long-term sequelae (>16 years) (Thordardottir et al., 2016; Dai et al., 2017), indicating efforts towards providing long-term recovery resources also merit consideration. However, investigations evaluating cohorts over extended timeframes were relatively rare (4/59; 6.9%), representing a critical focus area for future research.

A higher prevalence rate among respondents from rural settings (38.8%; Table 2) points to the influence of "location" on mental health outcomes. Several investigations have focused on the impacts of EWEs in rural settings (e.g., Morrisey and Reser, 2007; Berry et al., 2008; Vins et al., 2015; Ellis and Albrecht, 2017; Hayes et al., 2018; Hrabok et al., 2020). Here, a number of archetypal factors of rural populations, linked to community culture and health perception, and which are often compounded by limited access to aid, may lead to impaired health-seeking behaviour and (post-event) adaptation capacity. These include rural stoicism, self-reliance, and prevailing stigmas associated with psychological disorders (Morrisey and Reser, 2007; Allen et al., 2012; Vins et al., 2015; Hrabok et al., 2020). Furthermore, isolation or lack of awareness around (or the benefits of) recovery resources is prevalent in rural and remote locations (Berry et al., 2008; Vins et al., 2015). Pooled data suggest rural populations are particularly prone to PTSD (Table 3), potentially underscoring issues with access to immediate emergency relief and/or mental intervention following EWEs, and/or impaired social support (due to isolation) in rural or remote locations (Goldman and Galea, 2014; Vins et al., 2015). Reported results contrast with baseline epidemiological evidence indicating a higher psychological burden in urban areas (Peen et al., 2010; Allen et al., 2012), suggesting rural inhabitants are particularly vulnerable to the impacts of extreme weather.

4.4. Socio-demographics – role of gender, ethnicity and age

The predominance of pre-event risk factors (156/290; 53.9%) (Table 4), emphasizes the crucial link between intrinsic socio-demographic factors and a predisposition to psychological impairment following EWEs. Generally, a higher mental health burden is associated with "marginalized" population groups which often lack the resources to adequately cope with traumatic events (Galea et al., 2005; Cianconi et al., 2020; Hrabok et al., 2020; Clayton, 2021). The concept of "allostatic" (over-)load, i.e., accumulation of chronic stress and life events (Guidi et al., 2021), can help elucidate the role of lower social standing, predisposition towards psychological vulnerability, and likelihood of impairment following environmental challenges. The latter is clearly reflected among risk factors identified in reviewed investigations (Table 4), as lower educational attainment, previous history of mental health impairment and/or trauma, and a (overall) lower socio-economic status are frequently reported. A marked gender imbalance was also found. Female gender has been consistently associated with a higher risk of psychological impairment following EWEs (WHO, 2014; Berry et al., 2018; Obradovich et al., 2018; Lowe et al., 2019). This has been attributed to a combination of cultural, socio-economic, and physiological factors, which can result in a gendered "disadvantaged" status, often irrespective of income (Norris et al., 2002; Kessler et al., 2005; Lopez et al., 2006; Tang et al., 2014; Watts et al., 2015). Specific factors linked to higher impairment rates among females vary substantially and may include reduced access to education and aid resources (e.g., pre- and post-EWE), poor nutrition in contrast to male counterparts (both generally and during periods of food scarcity), stress/burden associated with a traditional caregiver social role (e.g., wife, mother), and likelihood of experiencing post-disaster violence (Norris et al., 2002; Kimerling et al., 2009; WHO, 2014; Watts et al., 2015).

Evidence also suggests females perceive and react more negatively to natural disasters and are considered more susceptible to the effects of these events (Norris et al., 2002; Bonano and Gupta, 2009; Tang et al., 2014). While interpretations remain tentative, the composite prevalence rates presented, which monotonically increase with sample female representation (Figs. 3–4), indicate a higher burden among female gender with potential domain-specific implications (cf. depression, PTSD; Fig. 4). As expected, the role of gender is also predicated by its recurrence among risk factors (29/290; 10%) (Table 4), second only to levels of event exposure. Conversely, just two investigations reported male gender as a risk factor (2/290; 0.7%) representing a high level of gender disparity. Overall, females represent a critical sub-population in the implementation of pre- and post-EWE mental health intervention strategies (e.g., counselling, outreach) and recovery resource allocation, all of which can play a key role in ameliorating the psychological burden of disaster events (Cohen 2002; Morganstein and Ursano, 2020).

Identifying as a racial/ethnic minority was also a recurrent risk factor linking EWE exposure and psychological impairment (Norris et al., 2002; Galea et al., 2005; Goldman and Galea, 2014; Lowe et al., 2019). The importance of racial background is reflected in higher estimated composite and PTSD prevalence rates (Figs. 4–5). Similarly, belonging to a minority was a frequently identified risk factor (4.1%; Table 4). A higher likelihood of impairment among minorities has been attributed to disadvantaged social standing and associated vulnerability to trauma (Norris et al., 2002; Galea et al., 2005; Berry et al., 2010; Hayes et al., 2018; Lowe et al., 2019). Assessment of racial/ethnic background as a potential risk factor was exclusive to US-based investigations ($n = 30$), and thus, not representative of wider global risks associated with individuals from minority backgrounds.

A degree of subjectivity in relation to age and impairment is mirrored in the comparable recurrence of young and old age among risk factor typologies (Table 4). The results highlight a degree of ambiguity in the nexus of disaster events, age, and mental health sequelae, which is likely driven by locally-specific cultural and socio-economic attributes (Kohn et al., 2005; Cook and Elmore, 2009; Parker et al., 2016; Lowe et al., 2019). For example, several previous studies report that older (particularly elderly) populations exhibit high resilience in the face of natural disasters (Norris et al., 2002; Kohn et al., 2005; Cook and Elmore, 2009); a trend tentatively supported by prevalence rates among older adults (>51) found in the current study (Figs. 3–4). Here, cumulative (past or pre-event) life experience may confer a degree of protection from stresses imparted by EWEs (Knight et al., 2000), with children conversely yet to develop coping mechanisms to counteract stressful situations (Goldman and Galea, 2014). Notably, the data reported by Kar et al. (2007), resulting in the highest PTSD OR (Fig. 6), derives exclusively from a sample of school children exposed to the cyclone Orissa. However, calculated prevalence rates were highest for the adult (31–59) sub-category (38.6%; Fig. 3), representing a key age sub-group for consideration in the context of mental health intervention. Overall, the results support evidence of middle-aged individuals being particularly vulnerable in post-disaster settings, attributed to high levels of life stress and responsibility burden (e.g., dependents) (Norris et al., 2002; Goldman and Galea, 2014).

5. Limitations and recommendations

The authors consider that a number of inherent impediments exist which require careful consideration in the interpretation of presented pooled estimates. Importantly, a number of methodological limitations stem from the comprehensive approach towards EWEs and individual exposures necessary to produce a comprehensive "scoping" review. Data akin to a meta-analytical or systematic review were not attainable given the wide range of EWE types, levels of exposure, variations in sample size, and range of mental health outcomes analysed. Additionally, due to the study design associated with some investigations, and particularly

the lack of participant controls, it was not possible to calculate study-specific effect size(s) for several studies. Crucially, extracted psychological impairment data (Tables 1–3) more closely represent "prevalence" rates, i.e., positive cases at a single (post-event) point in time, than longitudinal "incidence", or a finite metric of psychological impairment linked to EWEs (pre- and post-event). As such, few studies have established a "direct" temporal link between EWE exposure and adverse mental health outcomes, representing a key knowledge gap with respect to our current understanding of the intersect between socio-epidemiological mechanisms in the aftermath of climatic extremes. Most disaster-focused investigations lack pre-event ("background") mental status data, or refrain from incorporating independent control groups to measure or predict the trajectory of outcomes (Norris 2006; Yzermans et al., 2009). These factors, and concomitant limitations, are clearly reflected in the compiled dataset with a majority of investigations lacking any control criterion (69.5%; Table A3). The uniform distribution of event-evaluation time lag characterizing the pooled dataset (Table A3; Appendix F) also highlights potential issues associated with "resilience", temporal variability of symptoms, and the nature of diagnosis (Norris et al., 2002; Norris 2006; McFarlane et al., 2009). In conjunction with a paucity of longitudinal studies, the temporal trajectory of mental health sequelae in the aftermath of EWEs represents a critical knowledge gap and focus area for further research.

The accuracy of presented estimates is also potentially influenced by the spatial adjacency of studied EWEs relative to affected (or targeted) study populations, with impacts and outcomes ultimately proportional to levels of event exposure (i.e., dose-response) (Norris et al., 2002; Goldman and Galea, 2014; Harville et al., 2015). The importance of event exposure and experienced stressors is clearly reflected in its predominance (14.5%) among reported risk factor typologies (Table 4). Additional peri- and post-event risk factors linked to levels of event "exposure", including perceived threat/fear, injury/somatic conditions, and property damage, all commonly associated with PTSD (Norris et al., 2002; Neria et al., 2008; Goldman and Galea, 2014), were also frequently reported in the reviewed literature (Table 4). Notably, disaster victims tend to report higher somatic conditions and concerns in comparison to non-exposed counterparts, potentially highlighting important links between psychological and physiological stress in the aftermath of EWEs (Norris et al., 2002; Ursano et al., 2009; Yzermans et al., 2009).

Further, psychological measures are also invariably constrained by the range of diagnostic criteria employed, and the potential incorporation of cultural bias subject to their regional origin, which may limit cross-cultural application (Galea et al., 2005; McFarlane et al., 2009; Lowe et al., 2019; WMO, 2020; Moore et al., 2020). Inevitably, compiled data will also be subject to variability according to study-specific geographical, cultural and socio-economic variables. In this context, efforts should be directed towards (*i*) implementation of culturally-relevant psychological and well-being measures and (*ii*) generation of data at a regional level facilitating comparisons among samples with similar socio-demographic backgrounds.

The need for clear, detailed, and homogeneous data reporting of pertinent study aspects (e.g., methods, outcomes) is critical, and highlighted by the proportion of investigations failing to fully report co-morbidity data (20/59; 33.9%), and those providing insufficient information for OR calculation. Further, pooled analysis inevitably relied on integration of morbidity data from disparate events in terms of intensity, forecasting and (pre- and post-event) risk communication levels. Both forecasting and risk communication strategy can be determinant for event preparedness and influence psychological outcomes (Ellis and Albrecht, 2017; Morganstein and Ursano, 2020). For example, a higher composite impairment in "wildfire" (35%) and (possibly) "drought/heat" (31%) event categories (Table 2), could be related to their relative unpredictability and temporal ambiguity with lower associated levels of event anticipation and preparation. However, given the range of spatio-temporal impediments potentially influencing EWE exposure levels and resulting "impairment", comparisons of calculated estimates for individual EWEs categories are challenging. As previously outlined, this represents a key methodological limitation of the comprehensive "scoping" approach necessary to produce an all-encompassing metric of psychological impairment. In this context, forthcoming investigations can provide additional insights through the implementation of a "focused" set of eligibility criteria in terms of (EWE) individual exposure, diagnosis, space and time.

A key limitation of the review is also represented by the low number of investigations focusing on "climatic" (gradual or sub-acute) event types identified (Table A3). Characterized by higher prevalence rates (Table 2), data extracted from these studies may support indicators of a higher (and more complex) public health and socio-economic burden associated with slow-onset in contrast to acute (or fast-onset) climatic phenomena (Vins et al., 2015; Watts et al., 2015; Obradovich et al., 2018; Morganstein and Ursano, 2020). However, the limited number of reviewed studies focusing on sub-acute events prevents further insights. Similarly, few identified investigations focused on "wildfires" events (Fig. 3), a factor potentially affecting applicability of the results for EWEs with increased frequency and intensity in recent years. Given the paucity of research in concurrence with an increasing global frequency, this is a key area for further research and which would benefit from a similar empirical approach employed within.

6. Conclusion

The pooled analyses presented in this study provide a concise empirical link between individual extreme weather exposures and adverse psychological impacts. This comprehensive "scoping" review serves as a framework for future systematic reviews focusing on specific EWE types and mental health outcomes while elucidating knowledge gaps and limitations. Despite inevitable methodological limitations, the prevalence rates presented in this study provide (novel) global, regional, domain- and category-specific "standards", representing highly relevant reference points for forthcoming investigations. Crucially, psychological impairment estimates presented tend to be above available epidemiological baselines, demonstrating the psychological toll associated with extreme weather exposure. Overall, a prevalence of pre-event risk factors, identified from both individual studies and through collective pooled data, and which often relate to socio-demographic variables linked to marginalized groups, highlights the need for stakeholders to adopt and/or improve bespoke anticipation and preparation interventions. Further, sub-populations which should be prioritized in the context of pre- and post-disaster intervention and recovery resource allocation are outlined.

Acknowledgments

The authors wish to thank the Environmental Protection Agency (EPA) for providing research funding for this project (2018-W-DS- 21) under the remit of the EPA Research Programme 2014–2020.

Appendix A. Supplementary data

Supplementary data to this article can be found online at https://doi.org/10.1016/j.ijheh.2021.113840.

References

Aboraya, A., Rankin, E., France, C., El-Missiry, A., John, C., 2006. The reliability of psychiatric diagnosis revisited: the clinician's guide to improve the reliability of psychiatric diagnosis. Psychiatry 3 (1), 41–50.

Allen, J., Inder, K.J., Lewin, R.J., Attia, J., Kelly, B.J., 2012. Social support and age influence distress outcomes differentially across urban, regional and remote Australia: an exploratory study. BMC Publ. Health 12 (928).

Atwoli, L., Stein, D.J., Koenen, K.C., McLaughlin, K.A., 2015. Epidemiology of posttraumatic stress disorder: prevalence, correlates and consequences. Curr. Opin. Psychiatr. 28 (4), 307–311.

Bandla, S., Nappinnai, N.R., Gopalasamy, S., 2019. Psychiatric morbidity in December 2015 flood-affected population in Tamil Nadu, India. Int. J. Soc. Psychiatr. 65 (4), 338–344.
Berry, H.L., Kelly, B.J., Hanigan, I.C., Coates, J.H., McMichael, A.J., Welsh, J.A., Kjellstrom, T., 2008. Rural Mental Health Impacts of Climate Change. Garnault Climate Change Review. Australian National University, Canberra.
Berry, H.L., Bowen, K., Kjellstrom, T., 2010. Climate change and mental health: a causal pathways framework. Int. J. Publ. Health 55 (2), 123–132.
Berry, H.L., Waite, T.D., Dear, K.B.G., Capon, A.G., Murray, V., 2018. The case for systems thinking about climate change and mental health. Nat. Clim. Change 8 (4), 282–290.
Bonano, G.A., Gupta, S., 2009. Resilience after Disasters. In: Neria, Y., Galea, S., Norris, F.H. (Eds.), Mental Health and Disasters. Cambridge University Press, Cambridge.
Bourque, F., Willox, A.C., 2014. Climate change: the next challenge for public mental health? Int Rev Psychiatry 26 (4), 415–422.
Brown, M.R.G., Agyapong, V., Greenshaw, A.J., Cribben, I., Brett-MacLean, P., Drolet, J., McDonald-Harker, C., Omeje, J., Mankowsi, M., Noble, S., Kitching, D., Silverstone, P.H., 2019. After the Fort McMurray wildfire there are significant increases in mental health symptoms in grade 7-12 students compared to controls. BMC Psychiatr. 19 (1), 18.
Cianconi, P., Betro, S., Janiri, L., 2020. The impact of climate change on mental health: a systematic descriptive review. Front. Psychiatr. 11, 74.
Cook, J.A., Elmore, D.L., 2009. Disaster Mental Health in Older Adults: Symptoms, Policy, and Planning. In: Neria, Y., Galea, S., Norris, F.H. (Eds.), Mental Health and Disasters. Cambridge University Press, Cambridge.
Clayton, S., 2020. Climate anxiety: psychological responses to climate change. J. Anxiety Disord. 74, 102263.
Clayton, S., 2021. Climate change and mental health. Curr Environ Health Rep.
Cohen, R.E., 2002. Mental health services for victims of disasters. World Psychiatr. 1 (3), 149–152.
CRED, 2020. Natural Disasters 2019. CRED, Brussels. https://emdat.be/sites/default/files/adsr_2019.pdf.
Cruz, J., White, P.C.L., Bell, A., Coventry, P.A., 2020. Effect of extreme weather events on mental health: a narrative synthesis and meta-analysis for the UK. Int. J. Environ. Res. Publ. Health 17, 8581.
Dai, W., Kaminga, A.C., Tan, H., Wang, J., Lai, Z., Wu, X., Liu, A., 2017. Long-term psychological outcomes of flood survivors of hard-hit areas of the 1998 Dongting Lake flood in China: prevalence and risk factors. PloS One 12 (2), e0171557.
Ellis, N.R., Albrecht, G.A., 2017. Climate change threats to family farmer's sense of place and mental wellbeing: a case study from the Western Australian Wheatbelt. Soc. Sci. Med. 175, 161–168.
Felix, E., Hernandez, L.A., Bravo, M., Ramirez, R., Cabiya, J., Canino, G., 2011. Natural disaster and risk of psychiatric disorders in Puerto Rican children. J. Abnorm. Child Psychol. 39 (4), 589–600.
Forzieri, G., Cescatti, A., e Silva, F.B., Feyen, L., 2017. Increasing risk over time of weather-related hazards to the European population: a data-driven prognostic study. The Lancet Planetary Health 1 (5), 200–208.
Galea, S., Nandi, A., Vlahov, D., 2005. The epidemiology of post-traumatic stress disorder after disasters. Epidemiol. Rev. 27, 78–91.
Galea, S., Brewin, C.R., Gruber, M., Russell, T.J., King, D.W., King, L.A., McNally, R.J., Ursano, R.J., Petukhova, M., Kessler, R.C., 2007. Exposure to hurricane-related stressors and mental illness after hurricane katrina. Arch. Gen. Psychiatr. 64 (12), 1427–1434.
GBD, 2019. GBD data visualizations. IHME. http://www.healthdata.org/gbd/data-visualizations.
Goldmann, E., Galea, S., 2014. Mental health consequences of disasters. Annu. Rev. Publ. Health 35, 169–183.
Guidi, J., Lucente, M., Sonino, N., Fava, G.A., 2021. Allostatic load and its impact on health: a systematic review. Psychother. Psychosom. 90, 11–27.
Harville, E.W., Jacobs, M., Boynton-Jarrett, R., 2015. When is exposure to a natural disaster traumatic? Comparison of a trauma questionnaire and disaster exposure inventory. PloS One 10, e0123632.
Hayes, K., Blashki, G., Wiseman, J., Burke, S., Reifels, L., 2018. Climate change and mental health: risks, impacts and priority actions. Int. J. Ment. Health Syst. 12, 28.
Hrabok, M., Delorme, A., Agyapong, V.I.O., 2020. Threats to mental health and well-being associated with climate change. J. Anxiety Disord. 76, 102295.
Hynds, P.D., Thomas, M.K., Pintar, K.D., 2014. Contamination of groundwater systems in the US and Canada by enteric pathogens, 1990-2013: a review and pooled-analysis. PloS One 9.
IPCC, 2012. In: Field, C.B., Barros, T.F., Stocker, D., Qin, D., Dokken, D.J., Ebi, K.L., Mastrandrea, M.D., Mach, K.J., Plattner, G.K., Allen, S.K., Tignor, M., Midgley, P.M. (Eds.), Managing the Risks of Extreme Events and Disasters to Advance Climate Change Adaption A Special Report of Working Groups I and II of the Intergovernmental Panel on Climate Change. Cambridge University Press, Cambridge.
IPCC, 2018. Global Warming of 1.5°C an IPCC special report on the impacts of global warming of 1.5 °C above pre-industrial levels and related global greenhouse gas emission pathways. In: Masson-Delmotte, V., Zhai, P., Pörtner, H.O., Roberts, D., Skea, J., Shukla, P.R., Pirani, A., Moufouma-Okia, W., Péan, C., Pidcock, R., Connors, S., Matthews, J.B.R., Chen, Y., Zhou, X., Gomis, M.I., Lonnoy, E., Maycock, T., Tignor, M., Waterfield, T. (Eds.), The Context of Strengthening the Global Response to the Threat of Climate Change, Sustainable Development, and Efforts to Eradicate Poverty (in press).
IPCC, 2019. In: Pörtner, O., Roberts, D.C., Masson-Delmotte, P.Z., Tignor, M., Poloczanska, E., Mintenbeck, K., Alegria, A., Nicolai, M., Okem, A., Petzold, J., Rama, B., Weyer, N.M. (Eds.), IPCC Special Report on the Ocean and Cryosphere in a Changing Climate (in press).
IPCC, 2021. In: Masson-Delmotte, V., Zhai, P., Pirani, A., Connors, S.L., Péan, C., Berger, S., Caud, N., Chen, Y., Goldfarb, L., Gomis, M.I., Huang, M., Leitzell, K., Lonnoy, E., Matthews, J.B.R., Maycock, T.K., Waterfield, T., Yelekçi, O., Yu, R., Zhou, B. (Eds.), Climate Change 2021: the Physical Science Basis. Contribution of Working Group I to the Sixth Assessment Report of the Intergovernmental Panel on Climate Change. Cambridge University Press (in press).
IFRC, 2020. World Disasters Report 2020. IFRC, Geneva. https://media.ifrc.org/ifrc/world-disaster-report-2020/.
Kar, N., Mohapatra, P.K., Nayak, K.C., Pattanaik, P., Swain, S.P., Kar, H.C., 2007. Post-traumatic stress disorder in children and adolescents one year after a super-cyclone in Orissa, India: exploring cross-cultural validity and vulnerability factors. BMC Psychiatr. 7, 8.
Kessler, R.C., Sonnega, A., Bromet, E.J., Hughes, M., Nelson, C.B., 1995. Posttraumatic stress disorder in the national comorbidity survey. Arch. Gen. Psychiatr. 52, 1048–1060.
Kessler, R.C., Chiu, W.T., Demler, O., Merikangas, K.R., Walters, E.E., 2005. Prevalence, severity, and comorbidity of 12-month DSM-IV disorders in the national comorbidity survey replication. Arch. Gen. Psychiatr. 62 (6), 617–627.
Kessler, R.C., Aguilar-Gaxiola, S., Alonso, J., Chatterji, S., Lee, S., Ormel, J., Ustun, T.B., Wang, S.P., 2009. The global burden of mental disorders: an update from the WHO World Mental Health (WMH) Surveys. Epidemiol Psichatr Soc 18 (1), 23–33.
Kessler, R.C., Petukhova, M., Sampson, N.A., Zaslavsky, A.M., Wittchen, H.U., 2012. Twelve-month and lifetime prevalence and lifetime morbid risk of anxiety and mood disorders in the United States. Int. J. Methods Psychiatr. Res. 21 (3), 169–184.
Kessler, R.C., Bromet, E.J., 2013. The epidemiology of depression across cultures. Annu. Rev. Publ. Health 34, 119–138.
Kohn, R., Levav, I., Garcia, I.D., Machuca, M.E., Tamashiro, R., 2005. Prevalence, risk factors and aging vulnerability for psychopathology following a natural disaster in a developing country. Int. J. Geriatr. Psychiatr. 20, 835–841.
Koplewicz, H.S., Gurian, A., Williams, K., 2009. The era of affluence and its discontents. J. Am. Acad. Child Adolesc. Psychiatry 48 (11), 1053–1055.
Knight, B.G., Gatz, M., Heller, K., Bengtson, V.L., 2000. Age and emotional response to the Northridge Earthquake: a longitudinal analysis. Psychol. Aging 15, 627–634.
Kuh, D., Ben-Shlomo, Y.B., Lynch, J., Hallqvist, J., Power, C., 2003. Life Course Epidemiology J Epidemiol Community Health, pp. 778–781.
Liu, J., Varghese, B.M., Hansen, A., Xiang, J., Zhang, Y., Dear, K., Gourley, M., Driscoll, T., Morgan, G., Capon, A., Bi, P., 2021. Is there an association between hot weather and poor mental health outcomes? A systematic review and meta-analysis. Environ. Int. 153, 106533.
Lopez, A.D., Mathers, C.D., Ezzatim, M., Jamison, D.T., Murray, C.J.L., 2006. In: Lopez, A.D., Mathers, C.D., Ezzatim, M., Jamison, D.T., Murray, C.J.L. (Eds.), Global Burden of Disease and Risk Factors. The World Bank/Oxford University Press, Washington DC.
Lowe, S.R., Bonumwezi, J.L., Valdespino-Hayden, Z., Galea, S., 2019. Posttraumatic stress and depression in the aftermath of environmental disasters: a review of quantitative studies published in 2018. Curr Environ Health Rep 6 (4), 344–360.
Maguen, S., Neria, Y., Conoscenti, L.M., Litz, B.T., Galea, S., Norris, F.H., 2009. In: Neria, Y., Galea, S., Norris, F.H. (Eds.), Depression and Prolonged Grief in the Wake of Disasters. Mental Health and Disasters. Cambridge University Press, Cambridge.
Mantel, N., Haenszel, W., 1959. Statistical aspects of the analysis of data from retrospective studies of disease. Journal or the National Cancer Institute 22 (4), 719–748.
McFarlane, A.C., Van Hooff, M., Goodhew, F., 2009. In: Neria, Y., Galea, S., Norris, F.H. (Eds.), Anxiety Disorders and PTSD. Mental Health and Disasters. Cambridge University Press, Cambridge.
McFarlane, A.C., Williams, R., 2012. Mental health services required after disasters: learning from the lasting effects of disasters. Depress Res Treat 2012, 970194.
Moore, A., van Loenhout, J.A.F., de Almeida, M.M., Smith, P., Guha-Sapir, D., 2020. Measuring mental health burden in humanitarian settings: a critical review of assessment tools. Glob. Health Action 13 (1), 1783957.
Morganstein, J.C., Ursano, R.J., 2020. Ecological disasters and mental health: causes, consequences, and interventions. Front. Psychiatr. 11, 1.
Morrissey, S.A., Reser, J.P., 2007. Natural disasters, climate change and mental health considerations for rural Australia. Aust. J. Rural Health 15 (2), 120–125.
Neria, Y., Nandi, A., Galea, S., 2008. Post-traumatic stress disorder following disasters: a systematic review. Psychol. Med. 38 (4), 467–480.
Neria, Y., Galea, S., Norris, F.H., 2009. In: Neria, Y., Galea, S., Norris, F.H. (Eds.), Disaster Mental Health Research: Exposure, Impact and Response. Mental Health and Disasters. Cambridge University Press, Cambridge.
Norris, F.H., 2006. Disaster research methods: past progress and future directions. J. Trauma Stress 19 (2), 173–184.
Norris, F.H., Friedman, M.J., Watson, P.J., Byrne, C.M., Diaz, E., Kaniasty, K., 2002. 60,000 disaster victims speak: Part I. An empirical review of the empirical literature, 1981-2001. Psychiatry 65 (3), 207–239.
Obradovich, N., Migliorini, R., Paulus, M.P., Rahwan, I., 2018. Empirical evidence of mental health risks posed by climate change. Proc. Natl. Acad. Sci. U. S. A. 115 (43), 10953–10958.
Palinkas, L.A., Wong, M., 2020. Global climate change and mental health. Curr Opin Psychol 32, 12–16.
Parker, G., Lie, D., Siskind, D.J., Martin-Khan, M., Raphael, B., Crompton, D., Kisely, S., 2016. Mental health implications for older adults after natural disasters–a systematic review and meta-analysis. Int. Psychogeriatr. 28 (1), 11–20.
Peen, J., Schoevers, R.A., Beekman, A.T., Dekker, J., 2010. The current status of urban-rural differences in psychiatric disorders. Acta Psychiatr. Scand. 121 (2), 84–93.

Peters, M.D.J., Godfrey, C., McInerney, P., Munn, Z., Tricco, A.C., Khalil, H., 2020. In: Aromataris, E., Munn, Z. (Eds.), Chapter 11: Scoping Reviews. https://doi.org/10.46658/JBIMES-20-12. JBI Manual for Evidence Synthesis.

Rataj, E., Kunzweiler, K., Garthus-Niegel, S., 2016. Extreme weather events in developing countries and related injuries and mental health disorders - a systematic review. BMC Publ. Health 16 (1), 1020.

Rubonis, A.V., Bickman, L., 1991. Psychological impairment in the wake of disaster: the disaster-psychopathology relationship. Psychol. Bull. 109 (3), 384–399.

Sargeant, J.M., Rajic, A., Rad, S., Ohlsson, A., 2006. The process of systematic review and its application in agri-food public health. Prev. Vet. Med. 75 (3), 141–151.

Steel, Z., Marnane, C., Iranpour, C., Chey, T., Jackson, J.W., Patel, V., Silove, D., 2014. The global prevalence of common mental disorders: a systematic review and meta-analysis 1980-2013. Int. J. Epidemiol. 43 (2), 476–493.

Tang, B., Liu, X., Liu, Y., Xue, C., Zhang, L., 2014. A meta-analysis of risk factors for depression in adults and children after natural disasters. BMC Publ. Health 14 (623), 1–12.

Thordardottir, E.B., Hansdottir, I., Shipherd, J.C., Valdimarsdottir, U.A., Resnick, H., Elklit, A., Gudmundsdottir, R., Gudmundsdottir, B., 2016. Risk factors for posttraumatic stress symptoms among avalanche survivors: a 16-year follow-up. J. Nerv. Ment. Dis. 204 (4), 298–305.

Trombley, J., Chalupka, S., Anderko, L., 2017. Climate change and mental health. Am. J. Nurs. 117 (4), 44–52.

Tucker, P., Pfefferbaum, B., Nitiema, P., Khan, Q., Aggarwal, R., Walling, E.E., 2017. Possible link of Interleukin-6 and Interleukin-2 with psychiatric diagnosis, ethnicity, disaster or BMI. Cytokine 96, 247–252.

Ursano, R.J., Fullerton, C.S., Benedek, D.M., 2009. In: Neria, Y., Galea, S., Norris, F.H. (Eds.), What Is Psychopathology after Disasters? Considerations about the Nature of the Psychological and Behavioural Consequences of Disasters. Mental Health and Disasters. Cambridge University Press, Cambridge.

Vins, H., Bell, J., Saha, S., Hess, J.J., 2015. The mental health outcomes of drought: a systematic review and causal process diagram. Int. J. Environ. Res. Publ. Health 12 (10), 13251–13275.

Watts, N., Adger, W.N., Agnolucci, P., Blackstock, J., Byass, P., Cai, W., Chaytor, S., Colbourn, T., Collins, M., Cooper, A., Cox, P.M., Depledge, J., Drummond, P., Ekins, P., Galaz, V., Grace, D., Graham, H., Grubb, M., Haines, A., Hamilton, I., Hunter, A., Jiang, X., Li, M., Kelman, I., Liang, L., Lott, M., Lowe, R., Luo, Y., Mace, G., Maslin, M., Nilsson, M., Oreszczyn, T., Pye, S., Quinn, T., Svensdotter, M., Venevsky, S., Warner, K., Xu, B., Yang, J., Yin, Y., Yu, C., Zhang, Q., Gong, P., Montgomery, H., Costello, A., 2015. Health and climate change: policy responses to protect public health. Lancet 386, 1861–1914.

Watts, N., Amann, M., Ayeb-Karlsson, S., Belesova, K., Bouley, T., Boykoff, M., Byass, P., Cai, W., Campbell-Lendrum, D., Chambers, J., Cox, P.M., Daly, M., Dasandi, N., Davies, M., Depledge, M., Depoux, A., Dominguez-Salas, P., Drummond, P., Ekins, P., Flahault, A., Frumkin, H., Georgeson, L., Ghanei, M., Grace, D., Graham, H., Grojsman, R., Haines, A., Hamilton, I., Hartinger, S., Johnson, A., Kelman, I., Kiesewetter, G., Kniveton, D., Liang, L., Lott, M., Lowe, R., Mace, G., Odhiambo Sewe, M., Maslin, M., Mikhaylov, S., Milner, J., Latifi, A.M., Moradi-Lakeh, M., Morrissey, K., Murray, K., Neville, T., Nilsson, M., Oreszczyn, T., Owfi, F., Pencheon, D., Pye, S., Rabbaniha, M., Robinson, E., Rocklöv, J., Schütte, S., Shumake-Guillemot, J., Steinbach, R., Tabatabaei, M., Wheeler, N., Wilkinson, P., Gong, P., Montgomery, H., Costello, A., 2018. The Lancet Countdown on health and climate change: from 25 years of inaction to a global transformation for public health. Lancet 391 (10120), 581–630.

Watts, N., Amann, M., Arnell, N., Ayeb-Karlsson, S., Belesova, K., Boykoff, M., Byass, P., Cai, W., Campbell-Lendrum, D., Capstick, S., Chambers, J., Dalin, C., Daly, M., Dasandi, N., Davies, M., Drummond, P., Dubrow, R., Ebi, K.L., Eckelman, M., Ekins, P., Escobar, L.E., Fernandez Montoya, L., Georgeson, L., Graham, H., Haggar, P., Hamilton, I., Hartinger, S., Hess, J., Kelman, I., Kiesewetter, G., Kjellstrom, T., Kniveton, D., Lemke, B., Liu, Y., Lott, M., Lowe, R., Sewe, M.O., Martinez-Urtaza, J., Maslin, M., McAllister, L., McGushin, A., Jankin Mikhaylov, S., Milner, J., Moradi-Lakeh, M., Morrissey, K., Murray, K., Munzert, S., Nilsson, M., Neville, T., Oreszczyn, T., Owfi, F., Pearman, O., Pencheon, D., Phung, D., Pye, S., Quinn, R., Rabbaniha, M., Robinson, E., Rocklöv, J., Semenza, J.C., Sherman, J., Shumake-Guillemot, J., Tabatabaei, M., Taylor, J., Trinanes, J., Wilkinson, P., Costello, A., Gong, P., Montgomery, H., 2019. The 2019 report of the Lancet Countdown on health and climate change: ensuring that the health of a child born today is not defined by a changing climate. Lancet 394 (10211), 1836–1878.

Watts, N., Amann, M., Arnell, N., Ayeb-Karlsson, S., Beagley, J., Belesova, K., Boykoff, M., Byass, P., Cai, W., Campbell-Lendrum, D., Capstick, S., Chambers, J., Coleman, S., Dalin, C., Daly, M., Dasandi, N., Dasgupta, S., Davies, M., Di Napoli, C., Dominguez-Salas, P., Drummond, P., Dubrow, R., Ebi, K.L., Eckelman, M., Ekins, P., Escobar, L.E., Georgeson, L., Golder, S., Grace, D., Graham, H., Haggar, P., Hamilton, I., Hartinger, S., Hess, J., Hsu, S.-C., Hughes, N., Jankin Mikhaylov, S., Jimenez, M.P., Kelman, I., Kennard, H., Kiesewetter, G., Kinney, P.L., Kjellstrom, T., Kniveton, D., Lampard, P., Lemke, B., Liu, Y., Liu, Z., Lott, M., Lowe, R., Martinez-Urtaza, J., Maslin, M., McAllister, L., McGushin, A., McMichael, C., Milner, J., Moradi-Lakeh, M., Morrissey, K., Munzert, S., Murray, K.A., Neville, T., Nilsson, M., Sewe, M.O., Oreszczyn, T., Otto, M., Owfi, F., Pearman, O., Pencheon, D., Quinn, R., Rabbaniha, M., Robinson, E., Rocklöv, J., Romanello, M., Semenza, J.C., Sherman, J., Shi, L., Springmann, M., Tabatabaei, M., Taylor, J., Triñanes, J., Shumake-Guillemot, J., Vu, B., Wilkinson, P., Winning, M., Gong, P., Montgomery, H., Costello, A., 2021. The 2020 report of the Lancet Countdown on health and climate change: responding to converging crises. Lancet 397 (10269), 129–170.

Weilnhammer, V., Schmid, J., Mittermeier, I., Scheiber, F., Jiang, L., Pastuhovic, V., Herr, C., Heinze, S., 2021. Extreme weather events in Europe and their health consequence – a systematic review. Int. J. Hyg Environ. Health 233, 113688.

WHO, 2014. Gender, Climate Change and Health. WHO, Geneva. https://www.who.int/globalchange/publications/reports/gender_climate_change/en/.

WMO, 2020. In: Cullman, J., Dilley, M., Egerton, P., Fowler, J., Grasso, V.F., Honore, C., Lucio, F., Luterbacher, J., Nullis, C., Power, M., Rea, A., Repnik, M., Stander, J. (Eds.), 2020 State of Climate Services - Risk Information and Early Warning Systems (Geneva).

Yzermans, C.J., van de Berg, B., Dirkzwager, A.J.E., 2009. In: Neria, Y., Galea, S., Norris, F.H. (Eds.), Physical Health Problems after Disasters. Mental Health and Disasters. Cambridge University Press, Cambridge.

International Journal of Hygiene and Environmental Health 238 (2021) 113858

Contents lists available at ScienceDirect

International Journal of Hygiene and Environmental Health

journal homepage: www.elsevier.com/locate/ijheh

The association between long-term exposure to ambient fine particulate matter and glaucoma: A nation-wide epidemiological study among Chinese adults

Xueli Yang [a,b,1], Ze Yang [a,b,1], Yuanyuan Liu [c,d], Xi Chen [a,b], Baoqun Yao [c,d], Fengchao Liang [e], Anqi Shan [a,b], Fangchao Liu [f,g], Song Chen [c], Xiaochang Yan [h], Jianfeng Huang [f,g], Shaoye Bo [i], Yang Liu [j], Naijun Tang [a,b], Dongfeng Gu [e,f,g], Hua Yan [c,d,*]

[a] Department of Occupational and Environmental Health, School of Public Health, Tianjin Medical University, Tianjin, 300070, China
[b] Tianjin Key Laboratory of Environment, Nutrition, and Public Health, Tianjin Medical University, Tianjin, 300070, China
[c] Department of Ophthalmology, Tianjin Medical University General Hospital, Tianjin, 300052, China
[d] Tianjin Medical University, Tianjin, 300070, China
[e] School of Public Health and Emergency Management, Southern University of Science and Technology, Shenzhen, 518055, China
[f] Key Laboratory of Cardiovascular Epidemiology, Chinese Academy of Medical Sciences, Beijing, 100037, China
[g] Department of Epidemiology, Fuwai Hospital, National Center for Cardiovascular Diseases, Chinese Academy of Medical Sciences and Peking Union Medical College, Beijing, 100037, China
[h] National School of Development, Peking University, Beijing, 100871, China
[i] China Foundation for Disabled Persons, Dongcheng District, Beijing, 100006, China
[j] Gangarosa Department of Environmental Health, Rollins School of Public Health, Emory University, Atlanta, GA, 30322, USA

ARTICLE INFO

Keywords:
$PM_{2.5}$
Eye
Satellite-based model

ABSTRACT

Background: A growing body of evidence has confirmed the association between fine particulate matter ($PM_{2.5}$) and ocular diseases, but little is known on the effect of long-term $PM_{2.5}$ exposure on glaucoma.
Methods: A national cross-sectional study of the Rural Epidemiology for Glaucoma was conducted in 10 provinces of China, and 33,701 adults aged 40 years or more were included. A satellite-based model at 1-km resolution level was used to estimate $PM_{2.5}$ concentrations which were assigned to each participant according to geocoded home addresses. Logistic regression model was performed to investigate associations of long-term $PM_{2.5}$ exposure with glaucoma and its subtypes.
Results: Estimated $PM_{2.5}$ concentrations ranged from 28.0 to 96.4 μg/m^3. For each 10 μg/m^3 increment in $PM_{2.5}$, the adjusted odds ratios (ORs) were 1.07 (95% CI: 1.00–1.15) and 1.14 (95% CI: 1.02–1.26) for glaucoma and primary angle-closure glaucoma (PACG), respectively. A positive but non-significant association (OR = 1.05, 95% CI: 0.92–1.18) was detected between long-term exposure to $PM_{2.5}$ and odds of primary open-angle glaucoma. The middle aged residents and non-smokers were more sensitive to the adverse effects of $PM_{2.5}$.
Conclusions: Long-term $PM_{2.5}$ exposure was associated with glaucoma and PACG in Chinese adults, which provided new insights on adverse ophthalmic effect of $PM_{2.5}$.

1. Introduction

Ambient fine particulate matter ($PM_{2.5}$) has posed a serious threat to public health worldwide as the global fifth-ranking risk factor of mortality (Cohen et al., 2017). Long-term exposure to air pollution increased risks of respiratory diseases (Liu et al., 2021), cardiovascular disease (Liang et al., 2020a) and cancer (Hvidtfeldt et al., 2020). In addition, the eye is one of the few organs directly exposed to ambient pollutants (Lin et al., 2019), and biological evidence has illustrated that air pollution can induce intraocular inflammation, corneal cell apoptosis, and oxidative stress on eyes (Jung et al., 2018; Torricelli et al., 2011). Population-based studies have already observed associations between

* Corresponding author. Department of Ophthalmology, Tianjin Medical University General Hospital, Tianjin, 300052, China.
E-mail address: zyyyanhua@tmu.edu.cn (H. Yan).
[1] These authors contribute equally to this work.

https://doi.org/10.1016/j.ijheh.2021.113858
Received 23 June 2021; Received in revised form 2 October 2021; Accepted 4 October 2021
Available online 8 October 2021

$PM_{2.5}$ exposure and ocular diseases, such as conjunctivitis (Aik et al., 2020; Mimura et al., 2014), presbyopia (Lin et al., 2019), dry eye disease (Mo et al., 2019) and visual impairment in children (Yang et al., 2020).

Glaucoma is a multifactorial neurodegenerative disease leading to the loss of retinal ganglion cells and visual field defects (Okamoto et al., 2020). The Global Burden of Disease Study estimated that 3.6 million patients aged 50 years or older were blind due to glaucoma in 2020, which has ranked as the second leading cause of blindness worldwide (GBD 2019 Blindness and Vision Impairment Collaborators, 2021). Epidemiological studies have found some risk determinants of glaucoma such as elderly, women, as well as several modifiable factors including elevated intraocular pressure (IOP), diabetes and hypertension (Flammer et al., 2013; Jonas et al., 2017). To our best knowledge, three studies investigated the adverse effects of $PM_{2.5}$ exposure on glaucoma (Chua et al., 2019; Grant et al., 2021; Sun et al., 2021). Chua et al. (2019) and Grant et al. (2021) explored the association between $PM_{2.5}$ and glaucoma using data from the UK Biobank and Canadian Longitudinal Study on Aging, respectively, but their levels of $PM_{2.5}$ concentrations were much lower than that in China. Another study in Taiwan, China found increased $PM_{2.5}$ exposure was associated with primary open-angle glaucoma (POAG), one subtype of glaucoma, but it did not assess for total glaucoma (Sun et al., 2021). Although it is plausible biologically, human evidence on association of long-term $PM_{2.5}$ exposure with glaucoma and each subtype remained scarce, especially in China and other countries with challenges of both aging population and $PM_{2.5}$ pollution from rapid industrialization.

It is estimated that the global number of individuals with glaucoma will increase to 111.8 million by 2040 (Tham et al., 2014). Given air pollution as an ongoing challenge for global health, if evidence on glaucoma linked to high $PM_{2.5}$ exposure was obtained, it would provide a modifiable risk factor of glaucoma and highlight novel health benefits potentially gained from reduction in air pollution. Based on an established spatiotemporal model at 1-km resolution level (Huang et al., 2019; Liang et al., 2020a), the study is aimed to combine satellite-based estimates of $PM_{2.5}$ level with a nation-wide survey data to investigate associations between odds of glaucoma and long-term $PM_{2.5}$ exposure. Furthermore, it will identify individuals susceptible to $PM_{2.5}$ exposure and glaucoma among Chinese adults, underlying a wide concentration gradient of $PM_{2.5}$ pollution.

2. Methods

2.1. Study population

The Rural Epidemiology for Glaucoma in China (REG-China) study is a nation-wide cross-sectional survey of glaucoma and related ocular diseases in rural Chinese populations, which is aimed to investigate the regional distributions and risk factors for epidemic of glaucoma. The details of study design were described elsewhere (Shan et al., 2021). Briefly, a multi-stage stratified cluster sampling procedure was used to enroll a nationally representative sample of study participants. First, ten provinces or municipalities were identified from Eastern China (Liaoning, Shandong and Jiangsu), Central China (Heilongjiang, Henan, Shaanxi and Shanxi) and Western China (Ningxia Hui Autonomous Region, Sichuan and Chongqing) (eFigure 1 in the Supplement). Second, a large city and a midsize city were selected from each province at random, and then two rural townships were randomly identified from each city. Last, one rural community was selected from each township at random. A total of 52,041 individuals aged 6 years or more were invited to participant in the project of REG-China, and 48,398 local residents completed the survey with a response rate of 93%, and 36,081 participants aged ≥40 years were involved in the study. Finally, 33,701 participants without missing exposure and health data were included in the further analysis (Fig. 1). The study protocol was approved by Institute Review Board of Tianjin Medical University, and written informed consents were obtained from participants before survey.

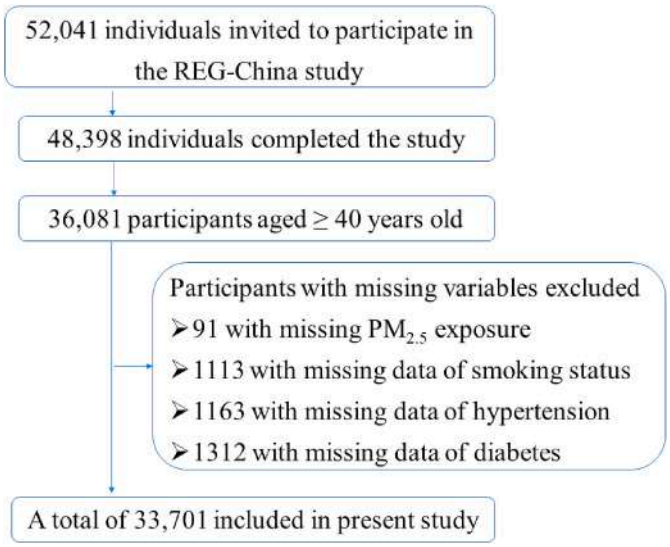

Fig. 1. The flowchart for inclusion and exclusion of study participants.

2.2. Eye examinations and definition of outcome

Each participant underwent eye examinations, including measurements of visual acuity (VA), limbal anterior chamber depth (LACD), IOP and optic disk. A standard logarithmic VAE chart (Tianjin ZhengDa Medical Care Equipment Factory, Tianjin, China) was given at a distance of 5 m to measure the VA. LACD was assessed using results of slit-lamp microscopy. The IOP was measured with non-contact tonometry (NCT; Type-NIDEK NT-2000 and Type-NIDEK NT-510, NIDEK CO, LTD, Japan). Direct ophthalmoscopy and slit-lamp biomicroscopy with a 90D convex lens were done to obtain vertical cup-to-disc ratio (VCDR) without pupil dilation. Further examinations were tested among patients classified as suspect for glaucoma, including fundus photography, Goldmann applanation tonometry, visual field and gonioscopy. Details in eye examination were described in eAppendix 1 in the Supplement.

The diagnosis of glaucoma was made by ophthalmologists according to three levels of evidence, claimed by the International Society for Geographical and Epidemiological Ophthalmology (ISGEO) (eAppendix 2 in the Supplement) (Foster et al., 2002). Furthermore, cases of primary glaucoma were divided into primary angle-closure glaucoma (PACG) and POAG based on the gonioscopic finding of a narrow angle after excluding secondary factors.

2.3. Long-term $PM_{2.5}$ exposure assessment

An established satellite-based spatiotemporal model was used to estimate $PM_{2.5}$ concentrations at 1-km spatial resolution, and detailed procedures have been described elsewhere (Liang et al., 2020b; Xiao et al., 2018). Briefly, the aerosol optical depth (AOD) product retrieved by the Multi-Angle Implementation of Atmospheric Correction (MAIAC) algorithm was derived from the US National Aeronautics and Space Administration (NASA) Moderate Resolution Imaging Spectrometer (MODIS) satellite. A machine learning algorithm was used to link AOD with other predictors of meteorology, road network, land cover index and air pollution emissions to estimate $PM_{2.5}$ concentrations. The cross validation showed a highly agreement between predicted historical $PM_{2.5}$ concentrations with available ground monitoring data at the annual level (prediction $R^2 = 0.80$). Afterwards, the estimated $PM_{2.5}$ concentrations were assigned to individual home address that has been encoded as longitude and latitude data. The annual $PM_{2.5}$ concentrations from 2000 to 2016 were available, and the 17-year mean value was calculated as long-term $PM_{2.5}$ exposure level used in the association analyses.

2.4. Covariates collection

Each participant was required to answer a standardized questionnaire to obtain information on sociodemographic characteristic, medical history and lifestyle factors. Participants who smoked at least one cigarette daily over 1 year were defined as smokers. Physician-diagnosed hypertension and/or diabetes was self-reported by participant. Data of disposable income per capita was obtained from National Bureau of Statistics (http://www.stats.gov.cn/).

2.5. Statistical analysis

Baseline characteristics of participants were displayed for continuous variables using means with corresponding standard deviations and for categorical variables using percentages. Logistic regression models were used to explore the potential association of long-term $PM_{2.5}$ exposure with glaucoma and the subtypes. We reported odds ratios (ORs) with corresponding 95% confidence intervals (95% CIs) for each 10 $\mu g/m^3$ increment in $PM_{2.5}$ concentration, after multivariable adjustments for sex, age, region (Eastern China, Central China vs Western China), disposable income per capita (RMB Yuan), smoking (yes vs no), hypertension (yes vs no), IOP (mmHg) and lowering-IOP treatment (yes vs no). ORs (95% CI) for glaucoma, PACG, and POAG were also estimated according to quarters of exposure to $PM_{2.5}$ with a trend test. In addition, the relationship between IOP levels and $PM_{2.5}$ concentrations was also tested by generalized linear regression model with covariates above except IOP.

We further did subgroup analyses stratified by sex, age, smoking and hypertension to assess the potential modification effect of covariates on the association between long-term $PM_{2.5}$ exposure and odds of glaucoma as well as its subtypes. Furthermore, because the treatment of cataract could potentially affect the progression of glaucoma (Sun et al., 2017), sensitivity analyses by excluding residents with cataract were performed to test the robustness of our results.

All statistical analyses were done using IBM SPSS Statistics for Windows (version 24.0, IBM Corp, USA) and R software (version 4.0.3, R Foundation for Statistical Computing, Vienna, Austria). The two-side $P < 0.05$ was considered as statistical significance.

3. Results

3.1. Descriptive results

The demographic characteristics of all participants are shown in Table 1 and summarized by each region in eTable 1 in the Supplement. Overall, the mean age of all participants was 62.3 years and 60.7% were female. Approximately 24.7% of participants were smokers. The screening study identified a total of 713 participants suffered from glaucoma, of which 328 cases were PACG and 247 cases were POAG. There were 343 patients, less than 50% among diagnosed glaucoma cases, having received treatment of lowering IOP. In addition, general characteristics of the included participants and the excluded individuals due to missing data are described in eTable 2 in the Supplement.

3.2. Associations between long-term $PM_{2.5}$ exposure and glaucoma

The 17-year average concentration of ambient $PM_{2.5}$ that the study participants were exposed to was 62.4 $\mu g/m^3$, ranging from 28.0 $\mu g/m^3$ to 96.4 $\mu g/m^3$. All participants were exposed to higher $PM_{2.5}$ than the World Health Organization recommended criteria (5 $\mu g/m^3$). In the regression analyses after multi-variable adjustment (Table 2), there were significant associations of glaucoma and PACG with each 10 $\mu g/m^3$ increment in $PM_{2.5}$. For example, in the Model 3 with full adjustment of age, sex, region, disposable income per capita, smoking, hypertension, IOP and lowering-IOP treatment, the odds of glaucoma increased with an OR of 1.07 (95% CI: 1.00–1.15) per 10 $\mu g/m^3$ increment in $PM_{2.5}$. For the major subtypes of glaucoma, each 10 $\mu g/m^3$ increment in $PM_{2.5}$ increased odds of PACG by 14% (95% CI: 2%–26%), and a positive but non-significant association was found between $PM_{2.5}$ exposure and POAG.

In addition, the effects of quartile exposures were also examined for each glaucomatous outcome with 3 quartile cutoff points of 51.4 $\mu g/m^3$, 59.8 $\mu g/m^3$, and 72.0 $\mu g/m^3$ in eTable 3 in the supplement. Compared with the first exposure quartile, ORs of glaucoma associated with the second to fourth exposure quartiles of $PM_{2.5}$ were 0.96 (95% CI: 0.74–1.26), 1.70 (95% CI: 1.27–2.26), and 1.48 (95% CI: 1.10–2.01), respectively, underlying a significant trend test ($P = 0.025$). A similar trend was only found for PACG but not for POAG (eTable 3 in the Supplement).

The relationship between long-term $PM_{2.5}$ exposure and IOP was also tested in a linear regression, but the effect estimation was rather mild with an increase of 0.14 mmHg per 10 $\mu g/m^3$ increment in $PM_{2.5}$, which inferred that glaucoma linked to long-term $PM_{2.5}$ exposure might not be mediated through the pathway of IOP elevation (eTable 4 in the Supplement).

3.3. Subgroup and sensitivity analyses

The results of stratified analyses described in Fig. 2 have indicated the effect modification of age and smoking status on the $PM_{2.5}$-glaucoma association. For a 10 $\mu g/m^3$ increase of $PM_{2.5}$, the estimated effects on odds of glaucoma were 1.25 (95% CI: 1.12–1.39) and 0.94 (95% CI: 0.85–1.04) for individuals aged 40–65 years and those aged over 65 years, respectively, which suggested the middle-aged adults would be more susceptible to long-term exposure to fine particulate pollutants than the elderly (P for interaction = 0.001). Furthermore, compared with smokers, the effects of $PM_{2.5}$ on glaucoma were strengthened among non-smokers with a significant interaction term tested by $PM_{2.5}$ exposure and smoking status (P for interaction = 0.008). Similarly, we found the association between long-term $PM_{2.5}$ exposure and PACG could be modified by both age and smoking status (eFigure 2 in the Supplement).

Table 1
Baseline characteristics of the study participants.

	Total	Male	Female
Participants, N	33701	13249	20452
Age, years	62.3 ± 11.3	62.6 ± 11.4	62.0 ± 11.2
Smoking, N (%)	8332 (24.7)	6218 (46.9)	2114 (10.3)
Hypertension, N (%)	8499 (25.2)	3114 (23.5)	5385 (26.3)
IOP, mmHg	14.4 ± 2.9	14.4 ± 2.9	14.4 ± 2.8
Lowering-IOP treatment, N (%)	343 (1.0)	110 (0.8)	233 (1.1)
Glaucoma, N (%)	713 (2.1)	283 (2.1)	430 (2.1)
PACG, N (%)	328 (1.0)	118 (0.9)	210 (1.0)
POAG, N (%)	247 (0.7)	115 (0.9)	132 (0.6)

IOP: intraocular pressure; PACG: primary angle-closure glaucoma; POAG, primary open-angle glaucoma.

Table 2
Odds ratios (95% CI) for glaucoma associated with each 10 $\mu g/m^3$ increase in $PM_{2.5}$.

	Odds ratios (95% CI)		
	Glaucoma	PACG	POAG
Model 1	1.00 (0.95, 1.06)	1.11 (1.03, 1.19)	0.92 (0.84, 1.00)
Model 2	1.06 (1.00, 1.14)	1.10 (1.00, 1.20)	1.06 (0.94, 1.20)
Model 3	1.07 (1.00, 1.15)	1.14 (1.02, 1.26)	1.05 (0.92, 1.18)

PACG, primary angle-closure glaucoma; POAG, primary open-angle glaucoma.
Model 1, adjusted for sex and age.
Model 2, Model 1 + adjusted for region, disposable income per capita, smoking and hypertension.
Model 3, Model 2 + adjusted for IOP and lowering-IOP treatment.

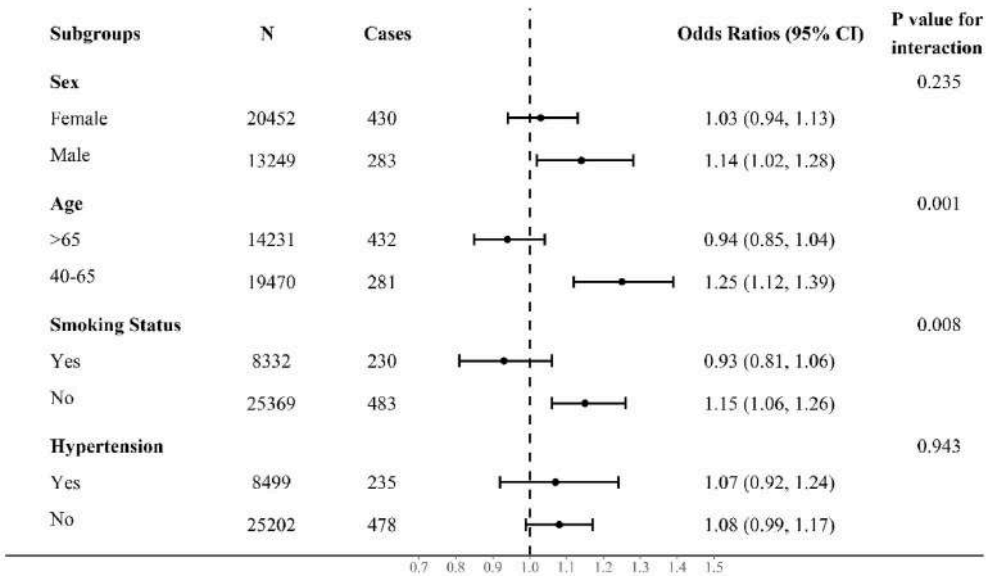

Fig. 2. Odds ratios (95% CI) for associations of glaucoma with each 10 μg/m^3 increase of $PM_{2.5}$ by subgroups. Results from subgroup analyses stratified by sex, age, smoking, and hypertension after multivariable adjustments using the Model 3.

In addition, results of sensitivity analyses after excluding the 3928 participants with cataract showed that the estimated effects of $PM_{2.5}$ on glaucoma and its subtypes were comparable to those in the main analyses (Table 3), although the ORs for associations of long-term exposure to $PM_{2.5}$ with PACG changed slightly higher.

4. Discussion

Based on multi-center population-based data in rural China covering a wide range of ambient $PM_{2.5}$ concentrations, our findings first identified that long-term $PM_{2.5}$ exposure was associated with increased odds of glaucoma in high pollution settings, and indicated that PACG seemed more sensitive to ambient $PM_{2.5}$ exposure rather than POAG in Chinese adults, which provided new evidence on adverse effect of $PM_{2.5}$ on ophthalmic damage. It was also observed that people aged 40–65 years or non-smokers might be susceptible populations to long-term $PM_{2.5}$ exposure contributing to risk of glaucoma. Although further validations from independent studies are needed, the current findings suggest the long-term exposure to fine particulate pollutant could be an important modifiable risk factor for epidemic of glaucoma beyond some well-known risk factors such as aging and elevated IOP, at least for some susceptible individuals living in high pollution environment.

To the best of our knowledge, limited studies have investigated the effect of long-term $PM_{2.5}$ exposure on glaucoma and its subtypes worldwide. Loss of retinal ganglion cells is one of the common features of all glaucoma subtypes (Jonas et al., 2017). Thinner retinal nerve fiber layer and decreased retinal thickness were observed in residents exposed to higher $PM_{2.5}$ pollution (Chua et al., 2020, 2021). Chua et al. identified a link between $PM_{2.5}$ and self-reported glaucoma using a land use regression model for exposure assessment in the UK Biobank participants, with an OR of 1.06 (95% CI: 1.01–1.12) per IQR (1.07 μg/m^3) increment in $PM_{2.5}$ (Chua et al., 2019). However, the annual average level of $PM_{2.5}$ exposure in the UK biobank data was approximately 9.9 μg/m^3 with the lower and upper quartile of 9.38 μg/m^3 and 10.45 μg/m^3, which was much lower than the average level of $PM_{2.5}$ as well as its interquartile range in this study. Similarly, increased $PM_{2.5}$ (per IQR) was also associated with glaucoma (OR = 1.14; 95% CI, 1.01–1.29) in Canadian Longitudinal Study on Aging (Grant et al., 2021), underlying the lower mean $PM_{2.5}$ concentration (6.5 μg/m^3). The aforementioned studies did not investigate the subtypes of glaucoma linked to $PM_{2.5}$ exposure (Chua et al., 2019, 2020, 2021; Grant et al., 2021). Recently, a nested case-control study in Taiwan, China, based on Longitudinal Health Insurance Database, found that increased $PM_{2.5}$ exposure was associated with POAG among elder participants aged over 65 years (Sun et al., 2021). We only obtain a positive but non-significant association between $PM_{2.5}$ and POAG in the study. Several potential explanations for the inconsistent results might include differences in study designs, methods for assessment of exposure, and participants' demographic characteristics.

The current study was a multi-center survey conducted in 10 provinces of the mainland China for epidemic of glaucoma among 33,701 participants aged over 40 years. It had broader distributions in regions and age groups of study participants, compared with the study in Taiwan province. Another strength in the study is the use of established spatiotemporal model at 1-km resolution level to improve the measurement quality of ambient $PM_{2.5}$ exposure at individual level (Liang et al., 2020b). Additionally, the proportion of PACG among glaucoma patients was 46.0% in the study, which was close to reports derived from regional surveys in China (Song et al., 2011; Zhong et al., 2012). Using the nation-wide data, it is the first time to identify a significant association of long-term $PM_{2.5}$ exposure with PACG among adults in high pollution regions. In future, independent studies with prospective study design and more accumulated cases of glaucoma will be warranted to further investigate whether differences would exist in the adverse effect of $PM_{2.5}$ exposure on PACG and POAG.

In addition, a wide gradient of $PM_{2.5}$ concentration in the multiple study centers strengthened the power to obtain a robust result. The range of $PM_{2.5}$ exposure among participants was 28.0 μg/m^3 to 96.4 μg/

Table 3
Sensitivity analyses on associations of glaucoma and the subtypes with each 10 μg/m^3 increase in $PM_{2.5}$ by excluding participants with cataract.

	Odds ratios (95% CI)		
	Glaucoma	PACG	POAG
Model 1	1.01 (0.95, 1.07)	1.14 (1.04, 1.24)	0.90 (0.81, 1.00)
Model 2	1.06 (0.98, 1.15)	1.12 (1.01, 1.25)	1.07 (0.93, 1.24)
Model 3	1.10 (1.01, 1.20)	1.25 (1.10, 1.41)	1.06 (0.91, 1.22)

PACG, primary angle-closure glaucoma; POAG, primary open-angle glaucoma.
Model 1, adjusted for sex and age.
Model 2, Model 1 + adjusted for region, disposable income per capita, smoking and hypertension.
Model 3, Model 2 + adjusted for IOP and lowering-IOP treatment.

m^3 with the mean level of 62.4 μg/m^3, which was much higher than the recommended level of 5 μg/m^3 from World Health Organization Air Quality Guideline. In 2017, the annual average of global $PM_{2.5}$ concentration was 46 μg/m^3, and population-weighted $PM_{2.5}$ ranged from 7 μg/m^3 in the United States to 91 μg/m^3 in India among the 10 largest countries by population (Turner et al., 2020). The $PM_{2.5}$ concentrations in the study covered much of global high-pollution levels, which was beneficial to capture the exposure-response relationship within a broader exposure gradient of $PM_{2.5}$.

In the subgroup analyses, we identified that middle-aged adults and non-smokers had stronger effects of $PM_{2.5}$ exposure on both glaucoma and PACG, after interaction terms of $PM_{2.5}$ and several potential risk factors were tested. As a usually asymptomatic and chronic disease, glaucoma was associated with aging and IOP elevation (Jonas et al., 2017; Quigley 2011). However, after control multiple risk factors including age and IOP, we obtained significant association of $PM_{2.5}$ with glaucoma and PACG among people aged 40–65 years, and it was inferred that glaucomatous optic nerve damage could be sensitive to $PM_{2.5}$ exposure at the middle age or even earlier. In addition, for the heterogeneous results stratified by smoking status, previous studies also proved a stronger effect of $PM_{2.5}$ on other deleterious outcomes (e.g., atherosclerosis and cardiovascular disease) in non-smokers (Künzli et al., 2005; Liang et al., 2020a). It was recorded that $PM_{2.5}$ and cigarette smoking may share similar pathogenic pathways of increased oxidative stress and inflammation, and additional exposure to $PM_{2.5}$ among smokers may not further enhance damages through competitive bio-pathways (Künzli et al., 2005).

It has not been illustrated very clearly in biological mechanisms for glaucoma associated with long-term $PM_{2.5}$ exposure. The increase of IOP was associated with occluded aqueous humor outflow due to crowded ocular anatomy or angle closure (Nongpiur et al., 2011). Since elevated IOP can interfere with optic nerve axon transport, it was considered as one of major modifiable risk factors of glaucoma (Jonas et al., 2017; Maddineni et al., 2020). However, a significant but weak association between $PM_{2.5}$ and IOP was detected in our study (eTable 4 in the Supplement), as is supported by similar findings in the UK biobank population (Chua et al., 2019). It suggested that other biological mechanisms beyond the pathway of IOP elevated might be involved in the high odds of glaucoma linked to long-term $PM_{2.5}$ exposure, considering the $PM_{2.5}$-glaucoma association obtained from multivariable regression after adjusting for IOP level and treatment of IOP. It has been demonstrated that $PM_{2.5}$ exposure was related to increased levels of pro-inflammatory factors and oxidative stress (Münzel et al., 2018; Xia et al., 2019). And some epidemiological studies observed that inflammatory cytokines and oxidative stress markers were elevated in aqueous humor and serum of patients with glaucoma (Chua et al., 2012; Huang et al., 2014; Li et al., 2020; Takai et al., 2012; Takayanagi et al., 2020). Additional evidence showed that trabecular meshwork dysfunction may be mediated by oxidative stress and inflammation (Baudouin et al., 2020), which could lead to the obstruction of the circulation of aqueous humor. It was also recorded that reactive oxygen species and oxidative mitochondrial DNA may lead to apoptosis of retinal ganglion cells (Baudouin et al., 2020). Moreover, $PM_{2.5}$-related endothelial dysfunction could lead to imbalance of endothelium-derived contracting (e.g., endothelin) and relaxing (e.g., nitric oxide) factors (Calderón-Garcidueñas et al., 2015; Wauters et al., 2013; Xia et al., 2019), which might affect the circulation of ophthalmic blood and aqueous humor (Cavet et al., 2014; Haefliger et al., 2001). Although the evidence above provides some perspectives in inflammation, oxidative stress, and endothelial dysfunction, more researches with careful design is needed to explore specific biomechanisms linking the risk of glaucoma and long-term exposure to $PM_{2.5}$.

Several limitations must be addressed to interpret the study findings with caveats in mind. First, the health data derived from an epidemiological observational design made it impossible to establish causality between $PM_{2.5}$ exposure and glaucoma. Second, the relatively small sample size of POAG limited the statistical power in testing the association between POAG and $PM_{2.5}$ exposure, although the direction of effect estimation supported that long-term exposure to $PM_{2.5}$ would increase odds of POAG in the study. Epidemiological data showed that risk of developing PACG had a greater prevalence in Asian populations than those of European and African descent (He et al., 2006). More studies considering both genetic and environment factors will be warranted to illustrate whether biological differences would exist in harmful effects of $PM_{2.5}$ on PACG and POAG in diverse populations. Third, information about indoor air pollution and time-activity patterns were not collected in the survey, which might result in bias of health effect estimation. Forth, we did not consider the co-exposure effects of mixed pollutants such as ozone and nitrogen oxides since reliable gaseous exposure data at 1-km resolution was unavailable in the study. Fifth, the current data on smoke (yes or no) cannot be further classified into never, former, or current smoke due to the limitation of questionnaire. However, an additional analysis for association between $PM_{2.5}$ exposure and glaucoma showed ORs of 1.07 (95% CI: 1.00–1.15) for glaucoma, 1.13 (95% CI: 1.02–1.26) for PACG, and 1.04 (95% CI: 0.92–1.18) for POAG, after excluding the smoke status from the covariates in Model 3. The results similar to the main analysis suggested that potential misclassification of smoke status would less bias the association estimation in the study. Last, 2380 participants were excluded in the study due to missing information in $PM_{2.5}$ and several covariates (Fig. 1). Although the excluded people had a lower percentage of women and were slightly younger compared with the people included, the prevalence of glaucoma and average level of IOP showed similar between the included and excluded, which suggested estimations of $PM_{2.5}$-glaucoma association might not be affected substantially by the excluded people due to missing data.

5. Conclusions

In this large-scale population-based study, long-term $PM_{2.5}$ exposure was associated with higher odds of glaucoma across a wider range of $PM_{2.5}$ concentrations, which added to novel evidence for the $PM_{2.5}$-induced adverse health effects. The findings may provide pivotal reference for estimation of glaucoma burdens attributable to long-term $PM_{2.5}$ pollution, and support insights on improvement of air quality being helpful in prevention of glaucoma especially in highly polluted regions.

Declaration of competing interest

Authors declare no actual or potential competing financial interests.

Acknowledgement

This work was supported by the National Natural Science Foundation of China (grant numbers, 82020108007, 81830026), Beijing-Tianjin-Hebei Special Project (grant number, 19JCZDJC64300(Z)), and National Key Research and Development Program of China (grant numbers, 2016YFC0206503, 2017YFC0211605). The work of Y. Liu was supported by the National Institute of Environmental Health Sciences of the National Institutes of Health (Award #1R01ES032140). The content is solely the responsibility of the authors and does not necessarily represent the official views of the National Institutes of Health.

Appendix A. Supplementary data

Supplementary data to this article can be found online at https://doi.org/10.1016/j.ijheh.2021.113858.

References

Aik, J., Chua, R., Jamali, N., Chee, E., 2020. The burden of acute conjunctivitis attributable to ambient particulate matter pollution in Singapore and its

exacerbation during South-East Asian haze episodes. Sci. Total Environ. 740, 140129.
Baudouin, C., Kolko, M., Melik-Parsadaniantz, S., Messmer, E.M., 2020. Inflammation in Glaucoma: from the back to the front of the eye, and beyond. Prog. Retin. Eye Res. 100916.
Calderón-Garcidueñas, L., Franco-Lira, M., D'Angiulli, A., et al., 2015. Mexico City normal weight children exposed to high concentrations of ambient $PM_{2.5}$ show high blood leptin and endothelin-1, vitamin D deficiency, and food reward hormone dysregulation versus low pollution controls. Relevance for obesity and Alzheimer disease. Environ. Res. 140, 579–592.
Cavet, M.E., Vittitow, J.L., Impagnatiello, F., Ongini, E., Bastia, E., 2014. Nitric oxide (NO): an emerging target for the treatment of glaucoma. Invest. Ophthalmol. Vis. Sci. 55, 5005–5015.
Chua, J., Vania, M., Cheung, C.M., et al., 2012. Expression profile of inflammatory cytokines in aqueous from glaucomatous eyes. Mol. Vis. 18, 431–438.
Chua, S.Y.L., Khawaja, A.P., Dick, A.D., et al., 2020. Ambient air pollution associations with retinal morphology in the UK Biobank. Invest. Ophthalmol. Vis. Sci. 61, 32.
Chua, S.Y.L., Khawaja, A.P., Morgan, J., et al., 2019. The relationship between ambient atmospheric fine particulate matter ($PM_{2.5}$) and glaucoma in a large community cohort. Invest. Ophthalmol. Vis. Sci. 60, 4915–4923.
Chua, S.Y.L., Warwick, A., Peto, T., et al., 2021. Association of ambient air pollution with age-related macular degeneration and retinal thickness in UK Biobank. Br. J. Ophthalmol. https://doi.org/10.1136/bjophthalmol-2020-316218.
Cohen, A.J., Brauer, M., Burnett, R., et al., 2017. Estimates and 25-year trends of the global burden of disease attributable to ambient air pollution: an analysis of data from the Global Burden of Diseases Study 2015. Lancet 389, 1907–1918.
Flammer, J., Konieczka, K., Bruno, R.M., Virdis, A., Flammer, A.J., Taddei, S., 2013. The eye and the heart. Eur. Heart J. 34, 1270–1278.
Foster, P.J., Buhrmann, R., Quigley, H.A., Johnson, G.J., 2002. The definition and classification of glaucoma in prevalence surveys. Br. J. Ophthalmol. 86, 238–242.
GBD 2019 Blindness and Vision Impairment Collaborators, 2021. Trends in prevalence of blindness and distance and near vision impairment over 30 years: an analysis for the Global Burden of Disease Study. Lancet Glob. Health 9, e130–e143.
Grant, A., Leung, G., Aubin, M.J., Kergoat, M.J., Li, G., Freeman, E.E., 2021. Fine particulate matter and age-related eye disease: the canadian longitudinal study on aging. Invest. Ophthalmol. Vis. Sci. 62, 7.
Haefliger, I.O., Flammer, J., Bény, J.L., Lüscher, T.F., 2001. Endothelium-dependent vasoactive modulation in the ophthalmic circulation. Prog. Retin. Eye Res. 20, 209–225.
He, M., Foster, P.J., Ge, J., et al., 2006. Prevalence and clinical characteristics of glaucoma in adult Chinese: a population-based study in Liwan District, Guangzhou. Invest. Ophthalmol. Vis. Sci. 47, 2782–2788.
Huang, K., Liang, F., Yang, X., et al., 2019. Long term exposure to ambient fine particulate matter and incidence of stroke: prospective cohort study from the China-PAR project. BMJ 367, l6720.
Huang, W., Chen, S., Gao, X., et al., 2014. Inflammation-related cytokines of aqueous humor in acute primary angle-closure eyes. Invest. Ophthalmol. Vis. Sci. 55, 1088–1094.
Hvidtfeldt, U.A., Severi, G., Andersen, Z.J., et al., 2020. Long-term low-level ambient air pollution exposure and risk of lung cancer - a pooled analysis of 7 European cohorts. Environ. Int. 146, 106249.
Jonas, J.B., Aung, T., Bourne, R.R., Bron, A.M., Ritch, R., Panda-Jonas, S., 2017. Glaucoma. Lancet 390, 2183–2193.
Jung, S.J., Mehta, J.S., Tong, L., 2018. Effects of environment pollution on the ocular surface. Ocul. Surf. 16, 198–205.
Künzli, N., Jerrett, M., Mack, W.J., et al., 2005. Ambient air pollution and atherosclerosis in Los Angeles. Environ. Health Perspect. 113, 201–206.
Li, S., Shao, M., Li, Y., et al., 2020. Relationship between oxidative stress biomarkers and visual field progression in patients with primary angle closure glaucoma. Oxid. Med. Cell. Longev. 2020, 2701539.
Liang, F., Liu, F., Huang, K., et al., 2020a. Long-term exposure to fine particulate matter and cardiovascular disease in China. J. Am. Coll. Cardiol. 75, 707–717.
Liang, F., Xiao, Q., Huang, K., et al., 2020b. The 17-y spatiotemporal trend of PM(2.5) and its mortality burden in China. Proc. Natl. Acad. Sci. U. S. A. 117, 25601–25608.
Lin, H., Guo, Y., Ruan, Z., et al., 2019. Ambient $PM_{2.5}$ and O_3 and their combined effects on prevalence of presbyopia among the elderly: a cross-sectional study in six low- and middle-income countries. Sci. Total Environ. 655, 168–173.
Liu, S., Jørgensen, J.T., Ljungman, P., et al., 2021. Long-term exposure to low-level air pollution and incidence of asthma: the ELAPSE project. Eur. Respir. J. 57, 2003099.
Maddineni, P., Kasetti, R.B., Patel, P.D., et al., 2020. CNS axonal degeneration and transport deficits at the optic nerve head precede structural and functional loss of retinal ganglion cells in a mouse model of glaucoma. Mol. Neurodegener. 15, 48.
Mimura, T., Ichinose, T., Yamagami, S., et al., 2014. Airborne particulate matter ($PM_{2.5}$) and the prevalence of allergic conjunctivitis in Japan. Sci. Total Environ. 487, 493–499.
Mo, Z., Fu, Q., Lyu, D., et al., 2019. Impacts of air pollution on dry eye disease among residents in Hangzhou, China: a case-crossover study. Environ. Pollut. 246, 183–189.
Münzel, T., Gori, T., Al-Kindi, S., et al., 2018. Effects of gaseous and solid constituents of air pollution on endothelial function. Eur. Heart J. 39, 3543–3550.
Nongpiur, M.E., He, M., Amerasinghe, N., et al., 2011. Lens vault, thickness, and position in Chinese subjects with angle closure. Ophthalmology 118, 474–479.
Okamoto, Y., Akagi, T., Suda, K., et al., 2020. Longitudinal changes in superficial microvasculature in glaucomatous retinal nerve fiber layer defects after disc hemorrhage. Sci. Rep. 10, 22058.
Quigley, H.A., 2011. Glaucoma. Lancet 377, 1367–1377.
Shan, A., Chen, X., Yang, X., et al., 2021. Association between long-term exposure to fine particulate matter and diabetic retinopathy among diabetic patients: a national cross-sectional study in China. Environ. Int. 154, 106568.
Song, W., Shan, L., Cheng, F., et al., 2011. Prevalence of glaucoma in a rural northern China adult population: a population-based survey in kailu county, inner Mongolia. Ophthalmology 118, 1982–1988.
Sun, H.Y., Luo, C.W., Chiang, Y.W., et al., 2021. Association between $PM_{2.5}$ exposure level and primary open-angle glaucoma in Taiwanese adults: a nested case-control study. Int. J. Environ. Res. Publ. Health 18, 1714.
Sun, X., Dai, Y., Chen, Y., et al., 2017. Primary angle closure glaucoma: what we know and what we don't know. Prog. Retin. Eye Res. 57, 26–45.
Takai, Y., Tanito, M., Ohira, A., 2012. Multiplex cytokine analysis of aqueous humor in eyes with primary open-angle glaucoma, exfoliation glaucoma, and cataract. Invest. Ophthalmol. Vis. Sci. 53, 241–247.
Takayanagi, Y., Takai, Y., Kaidzu, S., Tanito, M., 2020. Evaluation of redox profiles of the serum and aqueous humor in patients with primary open-angle glaucoma and exfoliation glaucoma. Antioxidants 9, 1305.
Tham, Y.C., Li, X., Wong, T.Y., Quigley, H.A., Aung, T., Cheng, C.Y., 2014. Global prevalence of glaucoma and projections of glaucoma burden through 2040: a systematic review and meta-analysis. Ophthalmology 121, 2081–2090.
Torricelli, A.A., Novaes, P., Matsuda, M., Alves, M.R., Monteiro, M.L., 2011. Ocular surface adverse effects of ambient levels of air pollution. Arq. Bras. Oftalmol. 74, 377–381.
Turner, M.C., Andersen, Z.J., Baccarelli, A., et al., 2020. Outdoor air pollution and cancer: an overview of the current evidence and public health recommendations. CA A Cancer J. Clin. https://doi.org/10.3322/caac.21632.
Wauters, A., Dreyfuss, C., Pochet, S., et al., 2013. Acute exposure to diesel exhaust impairs nitric oxide-mediated endothelial vasomotor function by increasing endothelial oxidative stress. Hypertension 62, 352–358.
Xia, B., Zhou, Y., Zhu, Q., et al., 2019. Personal exposure to $PM_{2.5}$ constituents associated with gestational blood pressure and endothelial dysfunction. Environ. Pollut. 250, 346–356.
Xiao, Q., Chang, H.H., Geng, G., Liu, Y., 2018. An ensemble machine-learning model to predict historical $PM_{2.5}$ concentrations in China from satellite data. Environ. Sci. Technol. 52, 13260–13269.
Yang, B.Y., Guo, Y., Zou, Z., et al., 2020. Exposure to ambient air pollution and visual impairment in children: a nationwide cross-sectional study in China. J. Hazard Mater. 407, 124750.
Zhong, H., Li, J., Li, C., et al., 2012. The prevalence of glaucoma in adult rural Chinese populations of the Bai nationality in Dali: the Yunnan Minority Eye Study. Invest. Ophthalmol. Vis. Sci. 53, 3221–3225.

International Journal of Hygiene and Environmental Health 238 (2021) 113856

Contents lists available at ScienceDirect

International Journal of Hygiene and Environmental Health

journal homepage: www.elsevier.com/locate/ijheh

The European Human Biomonitoring Initiative (HBM4EU): Human biomonitoring guidance values (HBM-GVs) for the aprotic solvents *N*-methyl-2-pyrrolidone (NMP) and *N*-ethyl-2-pyrrolidone (NEP)

Madlen David *, Antje Gerofke, Rosa Lange, Marike Kolossa-Gehring, Petra Apel

German Environment Agency (UBA), Corrensplatz 1, 14195 Berlin, Germany

ARTICLE INFO

Keywords:
Aprotic solvents
N-ethyl-2-pyrrolidone (NEP)
N-methyl-2-pyrrolidone (NMP)
Human biomonitoring guidance value (HBM-GV)
HBM4EU
Risk assessment

ABSTRACT

Toxicologically and/or epidemiologically derived guidance values referring to the internal exposure of humans are a prerequisite for an easy to use health-based interpretation of human biomonitoring (HBM) results. The European Joint Programme HBM4EU derives such values, named human biomonitoring guidance values (HBM-GVs), for priority substances which could be of regulatory relevance for policy makers and have been identified by experts of the participating countries, ministries, agencies and stakeholders at EU and national level. NMP and NEP are such substances for which unresolved policy relevant issues should be clarified by targeted research. Since widespread exposure of the general population in Germany to NMP and NEP was shown for the age groups 3–17 years and 20–29 years, further investigations on exposure to NMP and NEP in other European countries are warranted. The HBM-GVs derived for both solvents focus on developmental toxicity as decisive endpoint. They amount for the sum of the two specific urinary NMP metabolites 5-HNMP and 2-HMSI and likewise of the two specific urinary NEP metabolites 5-HNEP and 2-HESI to 10 mg/L for children and 15 mg/L for adolescents/adults. The values were determined following a consultation process on the value proposals within HBM4EU. A health-based risk assessment was performed using the newly derived HBM-GV_{GenPop} and exposure data from two recent studies from Germany. The risk assessment revealed that even when considering the combined exposure to both substances by applying the Hazard Index approach, the measured concentrations are below the HBM-GV_{GenPop} in all cases investigated (i.e., children, adolescents and young adults).

1. Introduction

Human biomonitoring (HBM) is the most established tool to determine human internal exposure to environmental toxicants in matrices such as blood, urine and hair. To gain further insight into the exposure of the European population to environmental pollutants and to use this information for policy advice, HBM4EU was launched. It is a joint initiative of 30 countries and the European Environment Agency (EEA). One of the overarching goals of HBM4EU is to harmonize and quality assure the tools and methods required for HBM studies, to set priorities for relevant substances to be monitored in humans (Ougier et al., 2021a) and to promote the generation of comparable data within the EU. Health-related human biomonitoring guidance values (HBM-GVs) are key evaluation instruments intended for direct comparison with the measured values. They are defined as the concentration of a substance or its specific metabolite(s) in human matrices at and below which adverse human health effects are, according to current knowledge, not expected. The HBM-GVs for the general population (HBM-GV_{GenPop}) are per definition equivalent to the HBM-I values derived by the German HBM Commission (Apel et al., 2017; German HBM Commission, 2007a, b;

Abbreviations: 2-HESI, 2-hydroxy-N-ethylsuccinimide; 2-HMSI, 2-hydroxy-N-methylsuccinimide; 5-HNEP, 5-hydroxy-*N*-ethyl-2-pyrrolidone; 5-HNMP, 5-hydroxy-N-methyl-2-pyrrolidone; DNEL, Derived No-Effect Level; ECHA, European Chemicals Agency; EEA, European Environment Agency; GC-EI-MS/MS, gas chromatography-electron ionization-mass spectrometry; GC-MS, gas chromatography-mass spectrometry; *GD*, *gestational day*; HBM, Human Biomonitoring; HBM4EU, European Human Biomonitoring Initiative; HBM-GV, Human Biomonitoring Guidance Value; NEP, N-ethyl-2-pyrrolidone; NMP, N-methyl-2-pyrrolidone; NMSI, N-methylsuccinimide; NOAEC, no observed adverse effect concentration; NOAEL, no observed adverse effect level; POD, point of departure; RAC, Risk Assessment Committee; REACH, Registration, Evaluation and Authorisation of Chemicals; RIVM, National Institute for Public Health and the Environment of the Netherlands; SCCS, Scientific Committee on Consumer Safety; SVHC, Substances of very high concern; TRV, Toxicity Reference Value.

* Corresponding author.
E-mail address: madlen.david@uba.de (M. David).

https://doi.org/10.1016/j.ijheh.2021.113856
Received 18 June 2021; Received in revised form 1 October 2021; Accepted 2 October 2021
Available online 5 October 2021

Schulz et al., 2011) and similar to the Biomonitoring Equivalents (BE) introduced by Summit Toxicology (Angerer et al., 2011; Aylward, 2018; Hays et al., 2007, 2008). Since health risks cannot be ruled out if these values are exceeded, this is a 'strong signal for monitoring the health status of the population, the identification of possible sources of exposure and the assessment of whether and how exposure can be reduced by risk management measures ' (Apel et al., 2020). So far, the concept for the derivation of HBM-GVs and also HBM-GVs for cadmium, selected phthalates and DINCH as well as BPA were derived under HBM4EU (Apel et al., 2020; Lamkarkach et al., 2021; Lange et al., 2021; Ougier et al., 2021b). Further HBM-GVs were derived for BPS and the mycotoxin Deoxynivalenol (DON) and are under preparation for publication.

In the present paper, the derivation of HBM-GVs for NMP (CAS no. 872-50-4) and NEP (CAS no. 2687-91-4) for non-occupationally exposed adults, adolescents and children (HBM-GV_{GenPop}) are presented. NMP and NEP are aprotic solvents that are used due to their solvent properties and water solubility in many technical applications and consumer products. In the context of the European chemicals regulation (REACH) both substances are classified as toxic to reproduction (category 1B) and as causing serious eye irritation (ECHA, 2020a, b). NMP is furthermore classified as a skin and respiratory irritant and is on the candidate list for authorisation under REACH. Despite similar effects, NEP is still not included in the EU candidate list. A call for evidence is under preparation for NEP to gather recent information for the preparation of a restriction dossier under Annex XV of REACH. Some uses of NMP, on the other hand, are restricted already under Annex XVII of REACH and consequently NMP shall not be manufactured, or used, as a substance on its own or in mixtures in a concentration equal to or greater than 0.3% after 9 May 2020 unless manufacturers and downstream users take the appropriate risk management measures and provide the appropriate operational conditions to ensure that exposure of workers is below the DNELs (14.4 mg/m^3 for exposure by inhalation and 4.8 mg/kg/day for dermal exposure). Additionally, NMP and NEP are forbidden in cosmetic products (Annex II, Regulation 1223/2009/EC on Cosmetic Products, as amended by Regulation, 2019/1966/EU, 28 November 2019) and other chemical legislations, e.g. construction product regulation, medical devices directive and different workers regulations are in place. Exposure of the general population to NEP is to be expected through the use of e.g. anti-freezing products, coating products, lubricants and greases, adhesives and sealants, air care products, non-metal-surface treatment products, inks and toners, leather treatment products, polishes, waxes and cleaning products (ECHA, 2020a). For NMP, ECHA has no current data whether or in which consumer products NMP might be used as the restriction of NMP has only recently entered into force (ECHA, 2020b). Dermal and inhalation exposure are the main routes of exposure of the general population to NMP and NEP and might occur especially from spray products, paints, cleaners and toners (Akrill et al., 2002; Anundi et al., 2000; RIVM, 2013a). HBM findings from the population representative German Environmental Survey V (GerES V, 2014–2017) and results from time trend analysis using samples from the German Environmental Specimen Bank (ESB) provide evidence of a wide-spread exposure of the non-occupationally exposed population at least in Germany (Schmied-Tobies et al., 2021; Ulrich et al., 2018). The HBM-GVs for NMP and NEP derived within the framework of the HBM4EU project enable the interpretation of internal exposure data and thus allow a straightforward health-based risk assessment to be carried out. The prerequisite for an appropriate evaluation is that the biomarkers that are used are identical and that the analytical methods are comparable and have been quality assured.

2. Methodology for deriving HBM-GVs for NMP and NEP

The general methodology for deriving HBM-GVs for the general population and/or workers, commonly agreed upon under HBM4EU, is described in Apel et al. (2020). It is based on earlier work of the German HBM Commission (German HBM Commission, 1996; 2007a, b, 2014), Summit Toxicology (Hays et al., 2007, 2008) and the French Agency for Food, Environmental and Occupational Health & Safety (ANSES, 2014) inter alia. Following this concept, NMP and NEP, for which German HBM values have already existed since 2015, were also re-evaluated, taking into account current literature and comments obtained during the consultation. As a result, the HBM Commission's approach for NMP and the selected key study (Saillenfait et al., 2002) was confirmed. In relation to NEP, a slightly different approach was taken with a different key study (Saillenfait et al., 2007 instead of Kaspers et al., 2006), but this resulted in the same numerical values for the HBM-GVs compared to the HBM values. In brief, for the derivation of HBM-GVs for NMP and NEP the available toxicokinetic studies were reviewed to select the most appropriate exposure biomarker(s) for NMP and NEP and to identify their respective molar urinary fraction in percent of the total dose. Furthermore, toxicity studies were reviewed to select critical endpoints for each substance, to identify the relevant key studies and PODs on which the final calculation of the HBM-GVs was based. Assessment factors to extrapolate information from animal studies to humans were applied according to generally accepted rules (ECHA, 2012). Epidemiological studies could not be found in the literature search. Levels of confidence (LoC) were assigned to give an evaluation of the quality and reliability of the data on which the derivation of the HBM-GVs is based. Finally, these newly derived HBM-GVs were used for a health-based risk assessment considering exposure data from two studies from Germany (Schmied-Tobies et al., 2021; Ulrich et al., 2018) for different age groups (children, adolescents and adults).

3. Results

3.1. Selection of biomarkers of exposure for NMP and NEP

NMP is rapidly metabolized in the liver by gradual oxidation of the pyrrolidone ring. Based on the similar chemical structure of NEP compared to NMP, metabolism is assumed to follow the same routes (Koch et al., 2014). Independent of the exposure route, 5-HNMP (5-hydroxy-N-methyl-2-pyrrolidone, CAS 41194-00-7) and 2-HMSI (2-hydroxy-N-methylsuccinimide, CAS 104612-35-3) for NMP (CAS 872-50-4) and 5-HNEP (5-hydroxy-N-ethyl-2-pyrrolidone, CAS not available) and 2-HESI (2-hydroxy-N-ethylsuccinimide, CAS 63467-80-1) for NEP (CAS 2687-91-4) were identified as the main metabolites both in rats and humans (Åkesson and Jönsson, 1997; Koch et al., 2014; RIVM, 2013a). Experimental animals as well as humans excrete NMP mainly via the kidneys (80% via urine over 24 h in rats and 65% via urine in humans), primarily in form of the abovementioned metabolites and the parent compound (Åkesson and Jönsson, 1997; Sitarek and Kilanowicz, 2006). Regarding the ratios of metabolites in urine, NMP is found in rats and also humans mainly as 5-HNMP (~70%), and around 30% as 2-HMSI; only around 1–2% consists of NMSI and the parent compound (Åkesson and Jönsson, 1997; Deutsche Forschungsgemeinschaft (DFG), 2008). Half-lives in humans were after inhalation exposure to 40 mg/m^3 NMP under resting conditions 3.9 h for NMP, 7.5 h for 5-HNMP and 28 h for 2-HMSI, respectively (Bader et al., 2007). The observed half-lives after oral exposure of humans were 4 h for 5-HNMP, 8 h for NMSI, and 17 h for 2-HMSI (Åkesson and Jönsson, 1997). No glucuronide or sulfate conjugates of the metabolites were identified. Mean urinary excretion fractions (F_{UE}) in humans were 44% for 5-HNMP (F_{UE}: 0.44) and 20% for 2-HMSI (F_{UE}: 0.20). Regarding the elimination half-life of NEP in humans, 7 h for 5-HNEP and 22–27 h for 2-HESI were determined after oral exposure (Koch et al., 2014). After 96 h, the metabolites of NEP were detected in all urine samples analysed and mean urinary excretion fractions were 28.9% for 5-HNEP (F_{UE} (96 h): 0.289) and 21.6% for 2-HESI (F_{UE} (96 h): 0.216). The described main metabolites 5-HNMP and 2-HMSI for NMP as well as 5-HNEP and 2-HESI for NEP are each substance-specific for the parent compound (Deutsche Forschungsgemeinschaft (DFG), 2008; Käfferlein et al., 2013; Meier et al., 2013) and thus suitable as exposure biomarkers. The simultaneous

determination of the two main metabolites of NMP and NEP offers the advantage of being able to investigate two biomarkers with different elimination behaviour. While 5-HNMP and 5-HNEP reach their maximum excretion values shortly after the end of exposure and have half-lives of 4–7.5 h (depending on exposure route) and 7 h respectively, 2-HMSI and 2-HESI have half-lives of about 17–28 h and 22–27 h respectively, indicating the accumulation of the substance over several days. Due to the longer elimination, it is to be expected that 2-HMSI and 2-HESI will level short-term peak exposures and thus allow for a more representative exposure estimate (Bader et al., 2007, 2008; Koch et al., 2014) also when measuring spot or morning urine samples, even if 24-h urine samples are indicated as the matrix of first choice when comparing to HBM-GV_{GenPop} (Apel et al., 2020).

Transfer of solvents to human breast milk has been reported (Anderson and Wolff, 2000), but for NMP and NEP further studies are missing. Physico-chemical properties such as molecular weight, lipophilicity and protein binding efficiency are relevant to estimate the possibility for entering in human breast milk. Due to the low log P_{ow} of NMP and NEP and their relatively short half-lives, the accumulation in fat is not very likely and the possibility of a transfer into human milk fat is reduced (Breitzka et al., 1997). But as both NMP and NEP as well as their metabolites have a very small molecular weight and through their solvent properties, it cannot be excluded that they may pass the human membranes into human breast milk via aqueous pores according to their concentration gradient (Kustrin et al., 2002), but at the moment no studies exist to confirm this hypothesis.

Due to the reproductive toxicity and classification as SVHC of NMP and the chemical analogy to its substitute NEP, the German cooperation on human biomonitoring between the Federal Ministry for the Environment, Nature Conservation and Nuclear Safety and the German Chemical Industry Association (VCI) saw the necessity to develop appropriate analytical methods to monitor NMP and its substitute NEP in urine of the general population. The cooperation was established to develop new sensitive analytical methods for those substances in human matrices to which the population may have increased exposure or which are of special toxicological relevance (Kolossa-Gehring et al., 2017). For this purpose, two analytical methods have been developed that consist of a stable isotope dilution analysis using solid phase extraction followed by derivatization (silylation) and GC–EI–MS/MS. The limit of quantification (LoQ) is for both metabolites 5-HNMP and 5-HNEP 2.5 μg/L and for 2-HMSI and 2-HESI each 2 μg/L (Schindler et al., 2012; Ulrich et al., 2018).

3.2. Selection of the critical toxicity endpoint for NMP and NEP

The HBM database for both solvents is not sufficient to derive a respective HBM-GV based on the relationship between human internal concentration of the biomarker(s) and related health effects. Furthermore, no toxicologically justified reference value from established bodies (e.g. a TDI value from EFSA) suitable for the derivation of HBM-GVs for the general population is available. Therefore, the derivation of HBM-GVs was based on results of toxicity studies in animals. Critical effects considered relevant for the derivation of HBM-GVs for NMP are effects like the reduced body weight (gain) of dams and offspring, and the embryo/foetotoxic and teratogenic effects observed in studies on reproductive toxicity (RAC and SCOEL, 2016; RIVM, 2013a, b).

Regarding the adverse effects of NEP, ECHA's Risk Assessment Committee (RAC) also highlighted effects on the foetus weight of rabbits after oral exposure and of rats after dermal and oral exposure (ECHA/RAC, 2011). Also, NEP showed effects on post-implantation losses and led to late resorptions in rats after oral exposure. Moreover, teratogenic effects were highlighted in rabbits after dermal and oral and in rats after oral administration of NEP. Skeletal malformations were noted in both species after oral administration, as well as rare cardiovascular malformations in rats after oral administration and in rabbits after dermal and oral administration. For an overview of the relevant studies for the derivation of HBM-GVs see Table 1. It can be concluded that the developmental toxic effects of NEP, especially the incidence of malformations in rats after oral administration are comparable to those of NMP. RAC emphasized that the developmental toxic effects and malformations were specific and not a consequence of maternal toxicity. These effects were regarded as the most critical endpoints for the further derivation of HBM-GVs (ECHA/RAC, 2011).

3.3. Choice of the key studies, PODs, and assessment factors

According to the strategy paper to derive HBM-GVs (Apel et al., 2020) the selection of a key study shall include the exposure pathway that is also considered as the relevant exposure pathway for humans. NMP may enter the human body via the skin, via inhalation or orally and is rapidly distributed in the whole body. Due to the good skin permeability for NMP on the one hand and the low vapour pressure of NMP under standard conditions on the other hand, it can be assumed that the dermal route of exposure is more relevant for the general population than the inhalation route (SCCS, 2011). Whether inhalation exposure occurs as vapour, an aerosol or a mixture of both may also depend on temperature and relative humidity in air (Deutsche Forschungsgemeinschaft (DFG), 1998). Due to the areas of application of NMP, the oral pathway is secondary. However, a conceivable derivation of HBM-GVs on the basis of animal studies with dermal administration is considered too uncertain because of the difficulties in extrapolation, especially with regard to the differences in dermal absorption in rodents and humans. Furthermore, even in the available studies with whole-body inhalation exposure, uncertainties exist regarding the amount of additional dermal and oral intake, so that results from studies with oral exposure were considered more appropriate to derive HBM-GVs. For NMP the oral developmental toxicity study from Saillenfait et al. (2002) on rats was chosen as key study and in addition the study from Sitarek et al. (2012) as supporting study. The oral rat study of Sitarek et al. (2012) refers to reproductive toxicity and shows effects on dams (reduced body weight) and offspring (reduced survival rate) at all doses tested. The study of Saillenfait et al. (2002) resulted in a NOAEL of 125 mg/kg bw/d for maternal and developmental effects, that was only slightly below the 150 mg/kg bw/d that showed already maternal and developmental effects in the study of Sitarek et al. (2012) (see Table 1). Because no NOAEL was identified from the study by Sitarek et al. (2012) and the LOAEL is of the same order of magnitude as the identified NOAEL from the study by Saillenfait et al. (2002), an assessment factor (AF) of 3 was considered appropriate for application to the NOAEL of 125 mg/kg bw/d from the study by Saillenfait et al. (2002) to account for uncertainties in the underlying database, thus leading to a value of 42 mg/kg bw/d. In order to account for inter- and intraspecies differences further AFs of 10 each were applied resulting in a TRV-like value of 0.42 mg/kg bw/d. The TRV (toxicity reference value)-like value is a value for external exposure guidance, calculated according to generally accepted rules, e.g. ECHA (2012) Chapter R.8.

For NEP it can also be assumed that dermal exposure is the most relevant exposure route followed by the inhalation exposure, as already described for NMP. For the reasons given above, the derivation of HBM-GVs dealt with here also considers animal studies with oral exposure, but additionally findings from "head-nose only" inhalation studies documented in the registrant summaries in the registration dossier from ECHA (see Table 1). The selected key study is a developmental toxicity study in rats with a LOAEL of 250 mg/kg bw/d and a NOAEL of 50 mg/kg bw/d (Saillenfait et al., 2007), supported by a further developmental toxicity study in rabbits with a LOAEL of 200 mg/kg bw/d and a NOAEL of 60 mg/kg bw/d (BASF, 2007). Application of inter- and intraspecies assessment factors of 10 each resulted in a TRV-like value of 0.5 mg/kg bw/d. Regarding a comparison with the inhalation route of exposure to NEP, the database is not very broad and allows only a rough estimation of the body dose having no effects. A study with subchronic exposure of rats (head-nose only) has been conducted and the summary is available

Table 1
Summary of the selected key studies and the supplementary studies of NMP and NEP for the derivation of HBM-GVs.

Substance	Species, strain, sex and number/ dose	Route, Duration	Dose (mg/kg bw/d)	NOAEL (mg/kg bw/ d)	LOAEL (mg/kg bw/ d)	Effects at LOAEL	Reference
NMP	Rat, Sprague-Dawley, 21-25 f	Oral (gavage) GD 6-20	0, 125, 250, 500 or 750	125 (maternal and developmental)	250 (maternal and developmental)	bwg↓ and bw↓ (dams and offspring), external soft-tissue and skeletal malformations of the offspring	Saillenfait et al. (2002)
	Supplementary study						
	Rat, Wistar, 22-28 f	Oral (gavage) 2 weeks before mating until end of lactation phase, 5 d/w	0, 150, 450 or 1000	–	150 (lowest dose)	Dams: bw↓ from GD 6, offspring: survival rate↓	Sitarek et al. (2012)
NEP	Rat, Sprague-Dawley, 19–24 f	Oral (gavage) GD 6-20	0, 50, 250, 500 or 750	50 (developmental)	250 (developmental)	bwg↓ of foetuses, variations of the skeleton	Saillenfait et al. (2007)
	Supplementary studies						
	Rat, Wistar, f/m, 10/10	Inhala-tion, 13 weeks, 6 h/d, 5 d/week, "head-nose only", as vapour	0, 30, 60, 200 mg/ m^3	60 mg/m^3 (local) 200 mg/m^3 (systemic)	200 mg/m^3 (local)	200 mg/m^3: degeneration/ regeneration of the olfactory epithelium, no systemic effects ≤60 mg/m^3: no local or systemic effects	(ECHA registration dossier, 2013)
	Rabbit, Himalayan, 25f	Oral (gavage) GD 6-28	0, 20, 60, 200	60	200 (maternal and developmental)	Dams: bwg↓ and reduced food consumption, relative liver and kidney weights↑; fetuses: skeletal malformations↑	BASF, 2007 (included in ECHA/RAC, 2011)

m: male, f: female, bw: body weight, bwg: body weight gain, GD: gestational day, d: days, h: hours.

in the registration dossier from ECHA (ECHA registration dossier, 2013). In this study, local effects on the mucous membranes of the nose were observed at the highest applied vapour concentration of 200 mg/m^3, but no systemic toxic effects were observed. Thus, the highest dose tested in this study, 200 mg/m^3, is regarded as the NOAEC for systemic effects. Extrapolation of this value regarding study duration and exposure conditions (200 mg/m^3: 2 × 6/24 × 5/7 = 17.86 mg/m^3) and extrapolation to body dose per 24 h (17.86 mg/m^3 x 1.15 (ECHA, 2012) = 20.5 mg/kg bw/d) would lead to a lower dose compared with the NOAEL of the key oral developmental study (50 mg/kg bw/d), but it should be kept in mind that higher concentrations have not been tested so far and we also have no information on a LOAEC for systemic effects via the inhalation path.

3.4. Calculation of HBM-GVs for NMP and NEP for the general population

By using the mass balance equation, assuming steady-state conditions (see formula 1), an HBM-GV_{GenPop} for NMP of 15 mg/L for adolescents/adults (rounded value) and 10 mg/L for children (rounded value) is calculated for the sum of the selected urinary exposure biomarkers 5-HNMP und 2-HMSI.

Main urinary excretion fractions used are 44% for 5-HNMP (F_{UE}: 0.44) and 20% for 2-HMSI (F_{UE}: 0.20) (Åkesson and Jönsson, 1997). As shown by Åkesson and Jönsson (1997) a nearly complete excretion within 24 h can be assumed as parent compound or its metabolites (80% of the dose administered within 24 h). In addition, as the TRV-like value is given in relation to body weight, the amount of urine excreted per day had to be adjusted to the body weight. As estimated by the German HBM Commission and included in the concept paper of HBM4EU (Apel et al., 2020), the daily urine volume adjusted to the body weight is assumed to be 0.02 L/kg bw/d for adolescents and adults (including women of child-bearing age) and 0.03 L/kg bw/d for children.

Formula 1: Mass balance equation for the derivation of an HBM-GV for two exposure biomarkers based on an established TRV or based on a TRV-like value.

$$\text{General formula}: \frac{\frac{[MW(\text{Metabolite1}).Fu(\text{Metabolite2})Fue(\text{Metabolite2})]}{MW(\text{Substance})}}{\text{Daily urinary flow rate adjusted to the BW}} \quad (1)$$

TRV = toxicity reference value; MW = molecular weight; MW (NMP) = 99,1 g/mol; MW (5-HNMP) = 115,1 g/mol; MW (2-HMSI) = 129,1 g/mol; MW (NEP) = 113,2 g/mol; MW (5-HNEP) = 129,2 g/mol; MW (2-HESI) = 143,2; F_{UE} = fractional urinary excretion coefficient; bw = body weight. Average daily urinary flow rates adjusted to bodyweight of 0.03 and 0.02 L/kg bw/d for children and adolescents/adults, respectively.

Regarding NEP, an HBM-GV_{GenPop} of 15 mg/L for adolescents/adults and 10 mg/L for children was calculated for the sum of the selected urinary exposure biomarkers 5-HNEP and 2-HESI. The TRV-like value used for the calculation is 0.5 mg/kg bw/d and the urinary excretion fractions are 28,9% for 5-HNEP (F_{UE} (96 h): 0.289) and 21,6% for 2-HESI (F_{UE} (96 h): 0.216) (Koch et al., 2014). In addition, as the TRV-like value is given in relation to body weight, the daily urinary flow rate had to be adjusted to body weight (0.02 L/kg bw/d for adolescents and adults and 0.03 L/kg bw/d for children).

3.5. Level of confidence attributed to the HBM-GV_{GenPop}

The information on the level of confidence (LoC) is useful to highlight possible data gaps and to address them to the scientific community. The LoC considers the various uncertainties underlying the derivation of the HBM-GV (e.g. reliability of the key study used to derive the TRV-like value, uncertainties related to the extrapolations leading to the TRV-like value, to toxicokinetic data on the substance of interest, and to the calculation of the final HBM-GV). The overall LoC attributed to the HBM-GV_{GenPop} is set to '**medium**' for NMP and "**medium/low**" for NEP. Details regarding single criteria are described in the Appendix. However, a low level of confidence does not necessarily mean a low level of protection, because the HBM-GV derivation is based on very conservative scenarios and default assumptions (Apel et al., 2020).

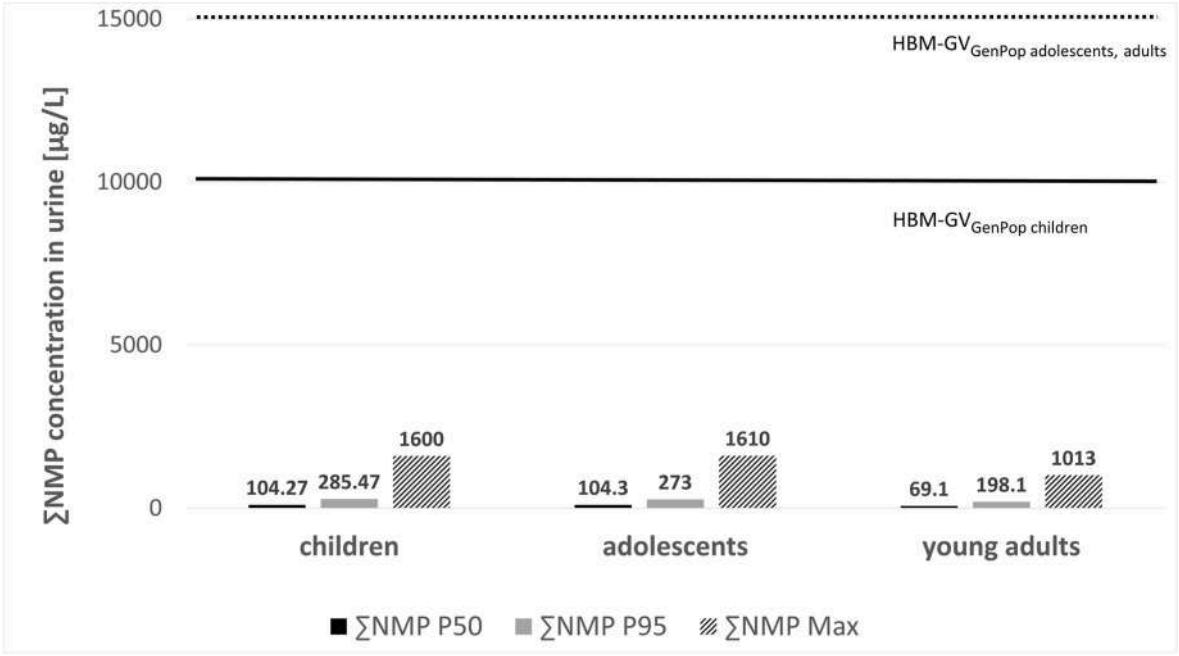

Fig. 1. Comparison of exposure data for the sum of NMP metabolites (∑NMP) from GerES V (Schmied-Tobies et al., 2021) and ESB (Ulrich et al., 2018) with the newly derived HBM-GV_{GenPop} values. P50, P95 and maximum values for children aged 3–13 years, adolescents aged 14–17 years and young adults aged 20–29 years for ∑NMP are displayed. The solid black line indicates the HBM-GV_{GenPop} for children whereas the dotted black line indicates the HBM-GV_{GenPop} for adolescents, adults for NMP.

3.6. Risk assessment (RA) based on the newly derived HBM-GV_{GenPop}

3.6.1. Comparison of exposure to NMP or NEP with their derived HBM-GV_{GenPop}

In the following, a risk assessment (RA) is presented which was performed using the exposure data (P50, P95 and maximum values) from two studies from Germany, i.e.: the German Environmental Survey V (GerES V) (Schmied-Tobies et al., 2021) and samples from the German Environmental Specimen Bank (ESB) (Ulrich et al., 2018), and comparing them with the newly derived HBM-GV_{GenPop} for NMP and NEP. Three age groups were considered: children (3–13 years), adolescents (14–17 years) and young adults (20–29 years). For this purpose, the GerES data have been reprocessed to enable the comparison with the respective age groups defined in the derived HBM-GV_{GenPop} for children and the HBM-GV_{GenPop} for adolescents/adults, respectively. The results of this comparison are presented in Figs. 1 and 2.

In all cases considered, even when considering maximum values, the reported exposures (for children and adolescents by Schmied-Tobies et al., 2021; for young adults by Ulrich et al., 2018) are lower than the corresponding HBM-GV_{GenPop} for both NMP and NEP (see Figs. 1 and 2).

The maximum concentration found by Schmied-Tobies et al. (2021) for children from 3 to 13 years, when analysing data from GerES V for ∑NMP was 1600 µg/L (for the age group 11–13 years). This is a factor of 6 below the newly derived HBM-GV_{GenPop} of 10 mg/L for children. The maximum concentration for ∑NEP for children was 1520 µg/L (for the age group 6–10 years) which is a factor of 7 below the HBM-GV_{GenPop} of 10 mg/L for children.

The maximum concentration found by Schmied-Tobies et al. (2021) for adolescents (14–17 years) was 1610 µg/L for the ∑NMP, which is a factor of 9 below the newly derived HBM-GV_{GenPop} of 15 mg/L for adolescents and adults. For ∑NEP the maximum value found for adolescents was 3140 µg/L which is a factor of 5 below the newly derived HBM-GV_{GenPop} for adolescents and adults.

The maximum concentration found by Ulrich et al. (2018) by analysing data from the ESB on students aged 20–29 for ∑NMP was 1013 µg/L. This is a factor of 15 below the newly derived HBM-GV_{GenPop} of 15 mg/L for adolescents and adults. The maximum concentration for ∑NEP was 1912 µg/L which is a factor of 8 below the HBM-GV_{GenPop} of 15 mg/L for adolescents and adults.

3.6.2. Assessing the risk of combined exposure – hazard index (HI) approach

Since in real life a simultaneous exposure to both NMP and NEP is possible and both substances exhibit very similar toxicological profiles, the combined effects of the two substances have to be considered (German HBM Commission, 2015).

In order to assess the cumulative risk of NMP and NEP, the hazard index (HI) approach was applied. Therefore, the HI was calculated as the sum of the hazard quotients (HQs) calculated for NMP and NEP. The HQ for each substance is calculated from the ratio between the sum of 2-HMSI and 5-HNMP concentrations (for NMP) and the sum of 2-HESI and 5-HNEP concentrations (for NEP), respectively, and the corresponding newly derived HBM-GV_{GenPop}. A HI < 1 indicates that the exposure is below the newly derived HBM-GV_{GenPop} when considering combined exposure to NMP and NEP (see formula 2).

Formula 2:

$$\frac{Concentration\ in\ urine\ (mg\ NMP\ metabolites/L)}{HBM-GV_{GenPop}\ (mg\ NMP\ metablites/L\ )}+\frac{Concentration\ in\ urine\ (mg\ NEP\ metabolites/L)}{HBM-GV_{GenPop}\ (mg\ NEP\ metablites/L)}\leq 1 \quad (2)$$

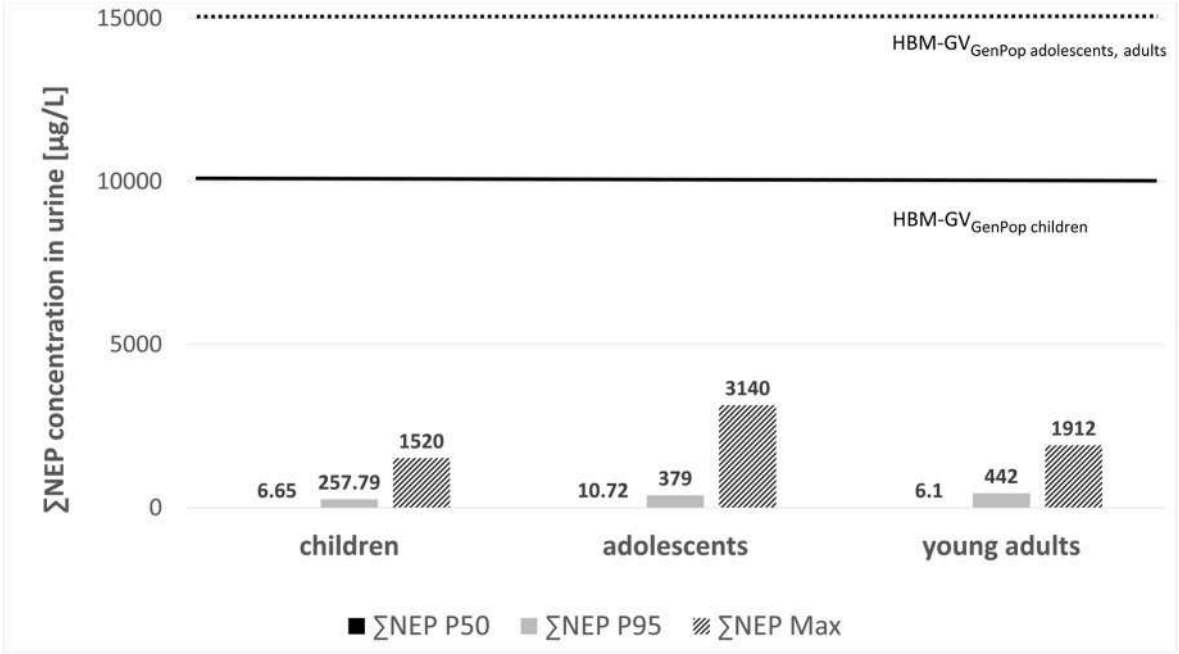

Fig. 2. Comparison of exposure data for the sum of NEP metabolites (∑NEP) from GerES V (Schmied-Tobies et al., 2021) and ESB (Ulrich et al., 2018) with the newly derived HBM-GV_{GenPop} values. P50, P95 and maximum values for children aged 3–13 years, adolescents aged 14–17 years and young adults aged 20–29 years for ∑NEP are displayed. The solid black line indicates the HBM-GV_{GenPop} for children whereas the dotted black line indicates the HBM-GV_{GenPop} for adolescents, adults for NEP.

Table 2
Hazard Index (HI) for NMP and NEP calculated for the respective age groups.

age groups (years of age); study	children (3–13); GerES V	adolescents (14–17); GerES V	adults (20–29); ESB
HI (P50)	0.01	0.01	0.01
HI (P95)	0.05	0.04	0.04
HI (max)	0.3	0.3	0.2

GerES V: German Environmental Survey V (Schmied-Tobies et al., 2021); ESB: German Environmental Specimen Bank (Ulrich et al., 2018).

In Table 2 the resulting HIs are shown for both studies and for the different age groups investigated, i.e., children (3–13 years), adolescents (14–17 years) and young adults (20–29 years).

The HI based on the newly derived HBM-GV_{GenPop} for NMP and NEP when considering co-exposure of these solvents has a maximum of 0.3 [maximum HQs: 0.1 (NMP) and 0.2 (NEP)] using the data from Schmied-Tobies et al. (2021), for children aged 3–13 and adolescents aged 14–17. The calculated HI using the data produced by Ulrich et al. (2018), for young adults aged 20–29 years are in a similar range. The maximum HI was 0.2 [maximum HQs: 0.07 for NMP and 0.1 for NEP] for the young adults.

4. Discussion and conclusion

HBM-GVs are an easy to handle health-related risk assessment tool for the interpretation of internal chemical burden. For the general population, HBM-GVs were derived for the sum of the major metabolites of the aprotic solvents NMP and NEP, respectively, which are 10 mg/L for children and 15 mg/L for adolescents/adults. The HBM-GVs have been derived under inclusion of remarks and advice from national experts coordinated via the National Hubs in the HBM4EU partner countries. Expert comments on the first proposal of HBM-GV derivation led to a different choice of key study for NEP, based on the importance of developmental effects compared with grip strength for instance. In the end, however the derived HBM-GVs equal to the HBM-I values from the German HBM Commission, although, as mentioned above, under HBM4EU another key study (Saillenfait et al., 2007) was selected for NEPs value derivation compared to the key study and endpoint/POD (grip strength/$BMDL_{05}$) selected by the German HBM Commission (Kaspers et al., 2006). The Kaspers' study was also used as basis for the derivation of the oral DNEL for systemic chronic effects under REACH. In the case of the DNEL derivation, the overall no observed adverse effect level (NOAEL) of the Kaspers' study is based on the endpoints body weight and liver effects. To derive the DNEL, an overall assessment factor of 200 was used (ECHA registration dossier, 2020).

One issue that needs further consideration, especially because NMP and NEP are developmental toxicants, are possible differences in human toxicokinetics during pregnancy compared with non-pregnancy. For example, a toxicokinetic study on plasma elimination of NEP after oral exposure of rats showed a much slower transformation in metabolites and also a decrease in metabolites' elimination rate in pregnant rats compared to non-pregnant rats, also efficient placental transfer of NEP was noted (Bury et al., 2019). This raises the question of whether exposure to NMP and NEP during pregnancy may lead to higher plasma concentration levels and may increase the possibility for health effects. However, there is no information on this from pregnant women to assess the risk. Due to this uncertainty it might be relevant to make use of an additional safety factor when considering women of child-bearing age, but this needs further discussion and agreement.

A literature search revealed that for NMP and NEP, only limited HBM data for the general population are available. HBM data from the German Environmental Specimen Bank show that NMP metabolites 5-HNMP and 2-HMSI could be quantified in 98% and 99.6% of the urine samples and NEP metabolites 5-HNEP and 2-HESI could be quantified in 34.8% and 75.7% of the urine samples of young not occupationally exposed adults. These results clearly indicate that the investigated population is exposed to both NMP and NEP. Median NMP metabolite levels were 30.3 µg/L 5-HNMP as well as 38.8 µg/L 2-HMSI and median NEP metabolite levels were < LOQ for 5-HNEP as well as 6.1 µg/L 2-HESI. 95th percentiles were higher for NEP (5-HNEP: 212 µg/L, 2-HESI: 230 µg/L) than for NMP (5-HNMP: 98.1 µg/L, 2-HMSI: 100 µg/L) (Ulrich et al., 2018).

HBM data for children (3–13 years old, 1530–1557 urine samples) and adolescents (14–17 years old, 634–656 urine samples) from the German Environmental Survey (GerES V) were reprocessed for the respective age groups and compared with the derived HBM-GVs. Results show high frequencies of quantification for NMP (100% for 5-HNMP and 2-HMSI) and NEP (32% for 5-HNEP and 87% for 2-HESI) (Schmied--Tobies et al., 2021). Geometric mean concentrations were 104.0 μg/L (5-HNMP: 56.69 μg/L, 2-HMSI: 45.34 μg/L) for the sum of NMP metabolites for children and 100.7 μg/L (5-HNMP: 54.43 μg/L, 2-HMSI: 44.46 μg/L) for adolescents. For the sum of NEP metabolites geometric mean concentrations of 10.22 μg/L (5-HNEP: 2.71 μg/L, 2-HESI: 6.51 μg/L) for children and 16.97 μg/L (5-HNEP: 4.09 μg/L, 2-HESI: 10.86) for adolescents were determined.

A health-based risk assessment (RA) was performed using the newly derived HBM-GV_{GenPop} and comparing them to exposure data from the two aforementioned studies from Germany for three age groups (i.e., children: 3–13 years, adolescents: 14–17 years and young adults: 20–29 years). The RA revealed that the reported exposure was in all considered cases below the corresponding HBM-GV_{GenPop}, even when maximum values were used for this assessment.

Even when the combined exposure to both NMP and NEP was considered by applying the Hazard Index approach, the corresponding HBM-GV_{GenPop} were not exceeded in all considered cases (i.e., children 3–13 years, adolescents 14–17 years, and young adults 20–29 years). Thus, according to current knowledge the exposure reported in the two studies from Germany following a substance-oriented approach does not give an indication of health concern, even when the exposure to both NMP and NEP is considered. Nevertheless, this paper shows widespread exposure of German children, adolescents and young adults to NMP and NEP, as NMP and NEP metabolites could nearly be detected in all investigated samples. It is also important to keep in mind that in real life other reprotoxic substances might also be present, leading to combined exposure which may increase the risk for common effects (Kortenkamp and Faust, 2018). Assessing individual chemicals in isolation, without considering risks associated with combined exposures, is increasingly considered insufficient (Martin et al., 2021). Efforts have already been undertaken to identify pathways that converge at critical nodal points to produce down-stream adverse effects, so called adverse outcome pathways (AOPs) (Kortenkamp, 2020). NMP and NEP should also be included in such considerations to avoid potential underestimation of risk.

As the HBM exposure data from Germany indicate a widespread exposure of the general population to NMP and NEP, it would be of interest to obtain HBM data from other European countries and to evaluate whether country differences regarding possible health risks exist. This would also help to create a more complete picture of exposure to NMP and NEP.

Funding

The authors received funding from the EU Horizon 2020 Framework Project, HBM4EU, Grant number 733032.

Declaration of competing interest

The authors declare that they have no known competing financial interests or personal relationships that could have appeared to influence the work reported in this paper.

Acknowledgments

We would like to thank our partners within Task 5.2, Christophe Rousselle and Matthieu Meslin from the French Agency for Food, Environmental and Occupational Health & Safety (ANSES), and also the partners from HBM4EU who commented on our draft proposal for the HBM-GVs.

Appendix A. Supplementary data

Supplementary data to this article can be found online at https://doi.org/10.1016/j.ijheh.2021.113856.

References

Åkesson, B., Jönsson, B.A.g., 1997. Major metabolic pathway for N-Methyl-2-Pyrrolidone in humans. Drug Metabol. Dispos. 25, 267–269.
Akrill, P., Cocker, J., Dixon, S., 2002. Dermal exposure to aqueous solutions of N-methyl pyrrolidone. Toxicol. Lett. 134, 265–269.
Anderson, H.A., Wolff, M.S., 2000. Environmental contaminants in human milk. J. Expo. Anal. Environ. Epidemiol. 10, 755–760.
Angerer, J., Aylward, L.L., Hays, S.M., Heinzow, B., Wilhelm, M., 2011. Human biomonitoring assessment values: approaches and data requirements. Int. J. Hyg Environ. Health 214, 348–360.
ANSES, 2014. Reference Document for the Derivation and the Measurement of Exposure Limit Values for Chemical Agents in the Workplace (OELs), French Agency for Food, Environmental and Occupational Health & Safety (ANSES). https://www.anses.fr/en/system/files/VLEP2009sa0339RaEN.pdf.
Anundi, H., Langworth, S., Johanson, G., Lind, M.L., Akesson, B., Friis, L., Itkes, N., Soderman, E., Jonsson, B.A., Edling, C., 2000. Air and biological monitoring of solvent exposure during graffiti removal. Int. Arch. Occup. Environ. Health 73, 561–569.
Apel, P., Angerer, J., Wilhelm, M., Kolossa-Gehring, M., 2017. New HBM values for emerging substances, inventory of reference and HBM values in force, and working principles of the German Human Biomonitoring Commission. Int. J. Hyg Environ. Health 220, 152–166.
Apel, P., Rousselle, C., Lange, R., Sissoko, F., Kolossa-Gehring, M., Ougier, E., 2020. Human biomonitoring initiative (HBM4EU) - strategy to derive human biomonitoring guidance values (HBM-GVs) for health risk assessment. Int. J. Hyg Environ. Health 230, 113622.
Aylward, L.L., 2018. Integration of biomonitoring data into risk assessment. Curr. Opin. Toxicol. 9, 14–20.
Bader, M., Wrbitzky, R., Blaszkewicz, M., Schäper, M., Van Thriel, C., 2008. Human volunteer study on the inhalational and dermal absorption of N-methyl-2-pyrrolidone (NMP) from the vapour phase. Arch. Toxicol. 82, 13–20.
Bader, M., Wrbitzky, R., Blaszkewicz, M., van Thriel, C., 2007. Human experimental exposure study on the uptake and urinary elimination of N-methyl-2-pyrrolidone (NMP) during simulated workplace conditions. Arch. Toxicol. 81, 335–346.
BASF, 2007. N-ethyl-2-pyrrolidone. Prenatal Developmental Toxicity Study in Himalayan Rabbits. Oral administration (gavage). Project Number: 40R0033/04058, included in ECHA/RAC, 2011, pp. 15-39. https://echa.europa.eu/documents/10162/b9c2a03a-b46d-448e-7a52-b8b7f89347eb.
Breitzka, R.L., Sandritter, T.L., Hatzopoulos, F.K., 1997. Principles of drug transfer into breast milk and drug disposition in the nursing infant. J. Hum. Lactation 13, 155–158.
Bury, D., Käfferlein, H.U., Brüning, T., Koch, H.M., Saillenfait, A.M., Marquet, F., 2019. Toxicokinetics of N-ethyl-2-pyrrolidone and its metabolites in blood, urine and amniotic fluid of rats after oral administration. Arch. Toxicol. 93, 921–929.
Deutsche Forschungsgemeinschaft (DFG), 1998. Occupational toxicants: critical data evaluation for MAK values and classification of Carcinogens: Volume 10, N-methyl-2-pyrrolidone (vapour).
Deutsche Forschungsgemeinschaft (DFG), 2008. N-methyl-2-pyrrolidon. In: Greim, H. (Ed.), Grenzwerte in Biologischem Material. Wiley-VCH, Weinheim, pp. 1–13.
ECHA, 2012. Guidance on Information Requirements and Chemical Safety Assessment. Chapter R.8: Characterisation of dose [concentration]-response for human health. Version: 2.1. https://echa.europa.eu/documents/10162/13632/information_requirements_r8_en.pdf/e153243a-03f0-44c5-8808-88af66223258.
ECHA, 2020a. Substance Information on 1-Ethylpyrrolidin-2-One. https://echa.europa.eu/de/substance-information/-/substanceinfo/100.018.409. (Accessed 15 August 2020).
ECHA, 2020b. Substance Information on 1-Methyl-2-Pyrrolidone. https://echa.europa.eu/de/substance-information/-/substanceinfo/100.011.662. (Accessed 4 August 2020).
ECHA registration dossier, 2013. N-Ethyl-2-pyrrolidone: 90-day Inhalation Study in Wistar Rats, Vapour Exposure. 5010033/041036. Unpublished, BASF SE, Ludwigshafen. https://echa.europa.eu/de/registration-dossier/-/registered-dossier/13618/7/6/3/?documentUUID=ab9fb144-a97d-4509-b234-ad87b083225a.
ECHA registration dossier, 2020. N-ethylpyrrolidin-2-one: Toxicological Summary - Workers - Hazard via Inhalation Route. https://echa.europa.eu/de/registration-dossier/-/registered-dossier/13618/7/1.
ECHA/RAC, 2011. Annex 1 Background Document to the Opinion Proposing Harmonised Classification and Labelling at Community Level of N-Ethyl-2-Pyrrolidone (NEP). ECHA/RAC/CLH-O-0000002192-83-01/F. https://echa.europa.eu/documents/10162/1c8a16a7-d82e-108a-3451-1c826a164a99.
German HBM Commission, 1996. Aufgaben, Beurteilungswerte, Stoffmonographien, Mitteilungen, Mitglieder und sonstige Mitwirkende. Umweltmed. Forsch. Prax. 1 (2), 106.
German HBM Commission, 2007a. Ableitung von Human-Biomonitoring-(HBM)-Werten auf der Basis tolerabler Aufnahmemengen - Teil I. Bundesgesundheitsblatt - Gesundheitsforsch. - Gesundheitsschutz 50 (2), 249–250.

German HBM Commission, 2007b. Ableitung von Human-Biomonitoring-(HBM)-Werten auf der Basis tolerabler Aufnahmemengen - Teil II. Bundesgesundheitsblatt - Gesundheitsforsch. - Gesundheitsschutz 50 (2), 251–254.

German HBM Commission, 2014. Grundsatzpapier zur Ableitung von HBM-Werten. Bundesgesundheitsblatt - Gesundheitsforsch. - Gesundheitsschutz 57, 138–147.

German HBM Commission, 2015. Stoffmonographie für N-Ethyl-2-pyrrolidon (NEP) und Human-Biomonitoring (HBM)-Werte für die Metaboliten 5-Hydroxy-NEP (5-HNEP) und 2-Hydroxy-N-ethylsuccinimid (2-HESI) im Urin: Stellungnahme der Kommission Human-Biomonitoring des Umweltbundesamtes. Bundesgesundheitsblatt Gesundheitsforschung Gesundheitsschutz 58, 1041–1052. https://doi.org/10.1007/s00103-015-2210-x.

Hays, S.M., Aylward, L.L., LaKind, J.S., Bartels, M.J., Barton, H.A., Boogaard, P.J., Brunk, C., DiZio, S., Dourson, M., Goldstein, D.A., Lipscomb, J., Kilpatrick, M.E., Krewski, D., Krishnan, K., Nordberg, M., Okino, M., Tan, Y.M., Viau, C., Yager, J.W., Biomonitoring Equivalents Expert, W.,, 2008. Guidelines for the derivation of biomonitoring equivalents: report from the biomonitoring equivalents expert workshop. Regul. Toxicol. Pharmacol. 51, S4–S15.

Hays, S.M., Becker, R.A., Leung, H.W., Aylward, L.L., Pyatt, D.W., 2007. Biomonitoring equivalents: a screening approach for interpreting biomonitoring results from a public health risk perspective. Regul. Toxicol. Pharmacol. 47, 96–109.

Käfferlein, H.U., Meier, S., Koslitz, S., Weiß, T., Koch, H.M., Ronge, T., Brüning, T., 2013. Exposition gegenüber entwicklungstoxischen N-Alkyl-2-pyrrolidonen. IPA-J. 01, 14–17. https://www.ipa-dguv.de/medien/ipa/publikationen/ipa-journale/ipa-journale2013/documents/ipa-journal_1301.pdf.

Kaspers, U., Strauss, V., Kaufmann, W., Fabian, E., 2006. N-Ethyl-2-pyrrolidone: Repeated Dose 90-day Oral Toxicity Study in Wistar Rats. Administration in the Diet. BASF AG, Report No. 50S0033/04072, Ludwigshafen unpublished in Registration Dossier ECHA.

Koch, H.M., Bader, M., Weiß, T., Koslitz, S., Schütze, A., Käfferlein, H.U., Brüning, T., 2014. Metabolism and Elimination of N-Ethyl-2-Pyrrolidone (NEP) in Human Males after Oral Dosage.

Kolossa-Gehring, M., Fiddicke, U., Leng, G., Angerer, J., Wolz, B., 2017. New human biomonitoring methods for chemicals of concern—the German approach to enhance relevance. Int. J. Hyg Environ. Health 220, 103–112.

Kortenkamp, A., 2020. Which chemicals should be grouped together for mixture risk assessments of male reproductive disorders? Mol. Cell. Endocrinol. 499, 110581.

Kortenkamp, A., Faust, M., 2018. Regulate to reduce chemical mixture risk. Science 361, 224–226.

Kustrin, S., Ling, L., Tham, S.Y., Alany, R., 2002. Molecular descriptors that influence the amount of drugs transfer into human breast milk. J. Pharmaceut. Biomed. Anal. 29, 103–119.

Lamkarkach, F., Ougier, E., Garnier, R., Viau, C., Kolossa-Gehring, M., Lange, R., Apel, P., 2021. Human biomonitoring initiative (HBM4EU): human biomonitoring guidance values (HBM-GVs) derived for cadmium and its compounds. Environ. Int. 147, 106337.

Lange, R., Apel, P., Rousselle, C., Charles, S., Sissoko, F., Kolossa-Gehring, M., Ougier, E., 2021. The European Human Biomonitoring Initiative (HBM4EU): human biomonitoring guidance values for selected phthalates and a substitute plasticizer. Int. J. Hyg Environ. Health 234, 113722.

Martin, O., Scholze, M., Ermler, S., McPhie, J., Bopp, S.K., Kienzler, A., Parissis, N., Kortenkamp, A., 2021. Ten years of research on synergisms and antagonisms in chemical mixtures: a systematic review and quantitative reappraisal of mixture studies. Environ. Int. 146.

Meier, S., Schindler, B.K., Koslitz, S., Koch, H.M., Weiss, T., Käfferlein, H.U., Brüning, T., 2013. Biomonitoring of exposure to N-methyl-2-pyrrolidone in workers of the automobile industry. Ann. Occup. Hyg. 57, 766–773.

Ougier, E., Ganzleben, C., Lecoq, P., Bessems, J., David, M., Schoeters, G., Lange, R., Meslin, M., Uhl, M., Kolossa-Gehring, M., Rousselle, C., Vicente, J.L., 2021a. Chemical prioritisation strategy in the European human biomonitoring initiative (HBM4EU) – development and results. Int. J. Hyg Environ. Health 236, 113778.

Ougier, E., Zeman, F., Antignac, J.P., Rousselle, C., Lange, R., Kolossa-Gehring, M., Apel, P., 2021b. Human biomonitoring initiative (HBM4EU): human biomonitoring guidance values (HBM-GVs) derived for bisphenol A. Environ. Int. 154, 106563.

RAC, SCOEL, 2016. Joint Opinion to Resolve Differences in Scientific Opinion as Regards Exposure Levels for N-Methyl-2-Pyrrolidone (NMP). Committee for Risk Assessment (RAC) and Scientific Committee on Occupational Exposure Limits (SCOEL), European Chemicals Agency (ECHA). https://echa.europa.eu/documents/10162/13579/rac_joint_nmp_opinion_en.pdf/e4b4f43b-a3bd-a7c0-08be-16c3886593e7.

RIVM, 2013a. Annex XV restriction report. Proposal for a restriction. Substance Name: N-methyl-2-pyrrolidone (NMP). National Institute for Public Health and the Environment. http://echa.europa.eu/documents/10162/ee4c88a9-d26f-4872-98fd-fb41646cc9e1. Version number 2.0.

RIVM, 2013b. CLH Report. Proposal for Harmonized Classification and Labelling Based on Regulation (EC) No 1272/2008, Annex VI, Part 2, Bureau REACH (Ed.). http://echa.europa.eu/documents/10162/9a6bb3e4-6265-41d2-b963-00e37f95a20e.

Saillenfait, A.M., Gallissot, F., Langonné, I., Sabaté, J.P., 2002. Developmental toxicity of N-methyl-2-pyrrolidone administered orally to rats. Food Chem. Toxicol. 40, 1705–1712.

Saillenfait, A.M., Gallissot, F., Sabate, J.P., 2007. Developmental toxic effects of N-ethyl-2-pyrrolidone administered orally to rats. J. Appl. Toxicol. 27, 491–497.

SCCS, 2011. Opinion on N-Methyl-2-pyrrolidone. In: Scientific Committee on Consumer Safety SCCS/1413/11, -.E. (Ed.), European Commission on Health & Consumers, Unit D3 - Risk Assessment. https://ec.europa.eu/health/scientific_committees/consumer_safety/docs/sccs_o_050.pdf.

Schindler, B.K., Koslitz, S., Meier, S., Belov, V.N., Koch, H.M., Weiss, T., Brüning, T., Käfferlein, H.U., 2012. Quantification of four major metabolites of embryotoxic N-methyl- and N-Ethyl-2-pyrrolidone in human urine by cooled-injection gas chromatography and isotope dilution mass spectrometry. Anal. Chem. 84, 3787–3794.

Schmied-Tobies, M.I.H., Murawski, A., Rucic, E., Schwedler, G., Bury, D., Kasper-Sonnenberg, M., Koslitz, S., Koch, H.M., Brüning, T., Kolossa-Gehring, M., 2021. Alkyl pyrrolidone solvents N–methyl–2–pyrrolidone (NMP) and N–ethyl–2–pyrrolidone (NEP) in urine of children and adolescents in Germany – human biomonitoring results of the German Environmental Survey 2014–2017 (GerESV). Environ. Int. 146, 106221.

Schulz, C., Wilhelm, M., Heudorf, U., Kolossa-Gehring, M., 2011. Update of the reference and HBM values derived by the German human biomonitoring commission. Int. J. Hyg Environ. Health 215, 26–35.

Sitarek, K., Kilanowicz, A., 2006. Tissue distribution and excretion of N-methyl-2-pyrrolidone in male and female rats. Int. J. Occup. Med. Environ. Health 19, 142–148.

Sitarek, K., Stetkiewicz, J., Wąsowicz, W., 2012. Evaluation of reproductive disorders in female rats exposed to N-methyl-2-pyrrolidone. Birth Defects Res B Dev Reprod Toxicol 95, 195–201.

Ulrich, N., Bury, D., Koch, H.M., Rüther, M., Weber, T., Käfferlein, H.U., Weiss, T., Brüning, T., Kolossa-Gehring, M., 2018. Metabolites of the alkyl pyrrolidone solvents NMP and NEP in 24-h urine samples of the German Environmental Specimen Bank from 1991 to 2014. Int. Arch. Occup. Environ. Health 91, 1073–1082.